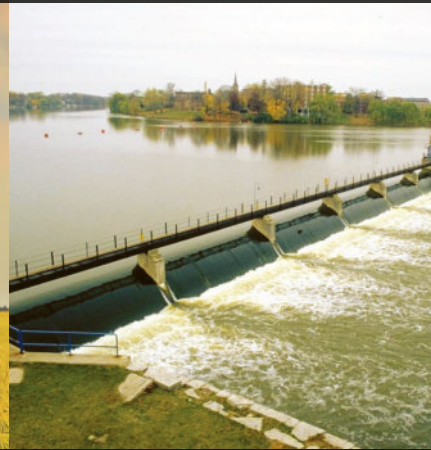


Electric Energy

An Introduction
Third Edition



Mohamed A. El-Sharkawi



CRC Press
Taylor & Francis Group

www.Techbooksyard.com

Electric Energy

An Introduction

Third Edition

POWER ELECTRONICS AND APPLICATIONS SERIES

Muhammad H. Rashid, Series Editor
University of West Florida

PUBLISHED TITLES

Advanced DC/DC Converters

Fang Lin Luo and Hong Ye

Alternative Energy Systems: Design and Analysis with Induction
Generators, Second Edition

M. Godoy Simões and Felix A. Farret

Complex Behavior of Switching Power Converters

Chi Kong Tse

DSP-Based Electromechanical Motion Control

Hamid A. Toliyat and Steven Campbell

Electric Energy: An Introduction, Third Edition

Mohamed A. El-Sharkawi

Electrical Machine Analysis Using Finite Elements

Nicola Bianchi

Modern Electric, Hybrid Electric, and Fuel Cell Vehicles:
Fundamentals, Theory, and Design

Mehrdad Eshani, Yimin Gao, Sebastien E. Gay, and Ali Emadi

Uninterruptible Power Supplies and Active Filters

Ali Emadi, Abdolhosein Nasiri, and Stoyan B. Bekiarov

Electric Energy

An Introduction

Third Edition

Mohamed A. El-Sharkawi



CRC Press

Taylor & Francis Group

Boca Raton London New York

CRC Press is an imprint of the
Taylor & Francis Group, an **informa** business

CRC Press
Taylor & Francis Group
6000 Broken Sound Parkway NW, Suite 300
Boca Raton, FL 33487-2742

© 2013 by Taylor & Francis Group, LLC
CRC Press is an imprint of Taylor & Francis Group, an Informa business

No claim to original U.S. Government works
Version Date: 20120627

International Standard Book Number-13: 978-1-4665-0431-8 (eBook - PDF)

This book contains information obtained from authentic and highly regarded sources. Reasonable efforts have been made to publish reliable data and information, but the author and publisher cannot assume responsibility for the validity of all materials or the consequences of their use. The authors and publishers have attempted to trace the copyright holders of all material reproduced in this publication and apologize to copyright holders if permission to publish in this form has not been obtained. If any copyright material has not been acknowledged please write and let us know so we may rectify in any future reprint.

Except as permitted under U.S. Copyright Law, no part of this book may be reprinted, reproduced, transmitted, or utilized in any form by any electronic, mechanical, or other means, now known or hereafter invented, including photocopying, microfilming, and recording, or in any information storage or retrieval system, without written permission from the publishers.

For permission to photocopy or use material electronically from this work, please access www.copyright.com (<http://www.copyright.com/>) or contact the Copyright Clearance Center, Inc. (CCC), 222 Rosewood Drive, Danvers, MA 01923, 978-750-8400. CCC is a not-for-profit organization that provides licenses and registration for a variety of users. For organizations that have been granted a photocopy license by the CCC, a separate system of payment has been arranged.

Trademark Notice: Product or corporate names may be trademarks or registered trademarks, and are used only for identification and explanation without intent to infringe.

Visit the Taylor & Francis Web site at
<http://www.taylorandfrancis.com>

and the CRC Press Web site at
<http://www.crcpress.com>

This textbook is dedicated to my wife, Fatma, and my sons, Adam and Tamer.

*The book is also dedicated to all engineers, without
whom we would still be living in caves.*

*A special dedication goes to the founders of our electric
power systems: Nikola Tesla and Thomas Edison.*

Contents

Preface.....	xv
Author	xix
List of Acronyms	xxi
Chapter 1 History of Power Systems	1
1.1 Thomas A. Edison (1847–1931).....	5
1.2 Nikola Tesla (1856–1943)	7
1.3 Battle of AC versus DC	8
1.4 Today’s Power Systems.....	13
Exercises.....	14
Chapter 2 Basic Components of Power Systems.....	17
2.1 Power Plants	17
2.1.1 Turbines	18
2.1.2 Generators	20
2.2 Transformers.....	20
2.3 Transmission Lines.....	20
2.4 Distribution Lines.....	22
2.5 Conductors.....	23
2.5.1 Bundled Conductor.....	24
2.5.2 Static (Shield) Wire	26
2.6 Substations.....	26
2.6.1 Potential Transformer.....	28
2.6.2 Current Transformer.....	29
2.6.3 Circuit Breaker	31
2.6.4 Disconnecting Switches	33
2.6.5 Surge Arrester	34
2.7 Control Centers.....	35
2.8 Worldwide Standards for Household Voltage and Frequency.....	37
2.8.1 Voltage Standard	38
2.8.2 Frequency Standard.....	38
2.8.2.1 Frequency of Generating Plants	38
2.8.2.2 Frequency of Power Grids	39
Exercises.....	39
Chapter 3 Energy Resources.....	41
3.1 Fossil Fuel.....	44
3.1.1 Oil.....	45
3.1.2 Natural Gas	47
3.1.3 Coal	48
3.2 Nuclear Fuel.....	50
Exercises.....	51

Chapter 4	Power Plants	53
4.1	Hydroelectric Power Plants	53
4.1.1	Types of Hydroelectric Power Plants	53
4.1.2	Impoundment Hydroelectric Power Plants.....	55
4.1.2.1	Impulse Turbine.....	57
4.1.2.2	Reaction Turbine.....	62
4.1.2.3	Reservoir.....	65
4.1.2.4	Penstock.....	66
4.1.2.5	Power Flow	68
4.2	Fossil Fuel Power Plants.....	70
4.2.1	Thermal Energy Constant	71
4.2.2	Description of Thermal Power Plant.....	72
4.3	Nuclear Power Plants.....	75
4.3.1	Nuclear Fuel	75
4.3.2	Uranium Enrichment.....	76
4.3.3	Fission Process	76
4.3.4	Fission Control	80
4.3.5	Boiling Water Reactor.....	81
4.3.6	Pressurized Water Reactor.....	82
4.3.7	CANDU Reactor	82
4.3.8	Safety Features in Nuclear Power Plants	84
4.3.9	Disposal of Nuclear Waste	85
4.3.9.1	Wet Storage.....	85
4.3.9.2	Dry Storage.....	85
4.3.9.3	Permanent Storage	85
	Exercises.....	86
Chapter 5	Environmental Impact of Power Plants	89
5.1	Environmental Concerns Related to Fossil Fuel Power Plants	90
5.1.1	Sulfur Oxides	90
5.1.2	Nitrogen Oxides	92
5.1.3	Ozone.....	92
5.1.4	Acid Rain.....	93
5.1.5	Carbon Dioxide	94
5.1.6	Ashes	95
5.1.7	Legionnaires' Disease and Cooling Towers.....	95
5.2	Environmental Concerns Related to Hydroelectric Power Plants.....	96
5.2.1	Case Study: The Aswan Dam	96
5.3	Environmental Concerns Related to Nuclear Power Plants	97
5.3.1	Radioactive Release During Normal Operation.....	97
5.3.2	Loss of Coolant	97
5.3.3	Disposal of Radioactive Waste.....	98
	Exercises.....	98
Chapter 6	Renewable Energy	99
6.1	Solar Energy	99
6.1.1	Passive Solar Energy System	103
6.1.2	Active Solar Energy System (Photovoltaic)	104
6.1.2.1	Ideal PV Model.....	108

	6.1.2.2	Effect of Irradiance and Temperature on Solar Cells.....	117
	6.1.2.3	PV Module.....	119
	6.1.2.4	Real Model of PV.....	124
	6.1.2.5	Daily Power Profile of PV Array.....	127
	6.1.2.6	Photovoltaic System Integration.....	128
	6.1.2.7	Evaluation of PV Systems.....	131
6.2		Wind Energy.....	133
	6.2.1	Kinetic Energy of Wind.....	133
	6.2.2	Wind Turbine.....	136
	6.2.3	Aerodynamic Force.....	137
	6.2.4	Angle-of-Attack.....	139
	6.2.5	Pitch Angle.....	141
	6.2.6	Coefficient of Performance and Turbine Efficiency.....	142
	6.2.7	Operating Range of Wind Turbine.....	143
	6.2.8	Tip Speed Ratio.....	143
	6.2.9	Feathering.....	147
	6.2.10	Classifications of Wind Turbines.....	147
	6.2.10.1	Alignment of Rotating Axis.....	147
	6.2.10.2	Types of Generators.....	149
	6.2.10.3	Speed of Rotation.....	150
	6.2.11	Types of Wind Turbine.....	150
	6.2.11.1	Type 1 Wind Turbine.....	151
	6.2.11.2	Type 2 Wind Turbine.....	151
	6.2.11.3	Type 3 Wind Turbine.....	152
	6.2.11.4	Type 4 Wind Turbine.....	152
	6.2.12	Wind Farm Performance.....	153
	6.2.13	Evaluation of Wind Energy.....	154
6.3		Hydrokinetic Systems.....	158
	6.3.1	Small Hydro Systems.....	158
	6.3.1.1	Main Components of Small Hydro System.....	158
	6.3.1.2	Effective Head.....	160
	6.3.1.3	System Efficiency.....	162
	6.3.1.4	Site Calculations.....	163
	6.3.1.5	Evaluation of Small Hydro Systems.....	165
	6.3.2	Tidal and Stream Energy System.....	165
	6.3.2.1	Barrage System.....	165
	6.3.2.2	Water Stream Energy.....	169
	6.3.2.3	Evaluation of Tidal and Stream Energy.....	172
	6.3.3	Wave Energy System.....	173
	6.3.3.1	Buoyant Moored System.....	174
	6.3.3.2	Hinged Contour System.....	175
	6.3.3.3	Oscillating Water Column System.....	176
	6.3.3.4	Evaluation of Wave Energy.....	178
6.4		Geothermal Energy.....	178
	6.4.1	Heat Pump.....	181
	6.4.2	Geothermal Electricity.....	181
	6.4.2.1	Geothermal Reservoir.....	181
	6.4.2.2	Hot Dry Rock.....	182
	6.4.3	Geothermal Power Plants.....	182
	6.4.3.1	Evaluation of Geothermal Energy.....	185
6.5		Biomass Energy.....	186

6.6	Fuel Cell	187
6.6.1	Hydrogen Fuel	188
6.6.2	Types of Fuel Cells	189
6.6.2.1	Proton Exchange Membrane Fuel Cell	189
6.6.2.2	Alkaline Fuel Cell	191
6.6.2.3	Phosphoric Acid Fuel Cell	192
6.6.2.4	Solid Oxide Fuel Cell	193
6.6.2.5	Molten Carbonate Fuel Cell	193
6.6.2.6	Direct Methanol Fuel Cell	194
6.6.3	Hydrogen Economy	195
6.6.4	Modeling of Ideal Fuel Cells	197
6.6.4.1	Thermal Process of Fuel Cells	197
6.6.4.2	Electrical Process of Fuel Cells	198
6.6.5	Modeling of Actual Fuel Cells	199
6.6.5.1	Polarization Characteristics of Fuel Cells	199
6.6.6	Evaluation of Fuel Cells	201
6.6.7	Fuel Cells and the Environment	202
6.6.7.1	Generation of Hydrogen	202
6.6.7.2	Safety of Hydrogen	202
6.7	Intermittency of Renewable Systems	203
6.8	Energy Storage Systems	204
6.8.1	Pumped Hydro Storage	204
6.8.2	Compressed Air Energy Storage	205
6.8.3	Batteries	207
6.8.4	Flywheels	208
	Exercises	209
Chapter 7	Alternating Current Circuits	213
7.1	Alternating Current Waveform	213
7.2	Root Mean Square	214
7.3	Phase Shift	216
7.4	Concept of Phasors	218
7.5	Complex Number Analysis	219
7.6	Complex Impedance	222
7.6.1	Series Impedance	223
7.6.2	Parallel Impedance	225
7.7	Electric Power	227
7.7.1	Real Power	230
7.7.2	Reactive Power	230
7.7.3	Complex Power	231
7.7.4	Summary of AC Phasors	232
7.7.5	Power Factor	233
7.7.6	Problems Related to Reactive Power	233
7.7.7	Power Factor Correction	238
7.8	Electric Energy	242
	Exercises	244
Chapter 8	Three-Phase Systems	247
8.1	Generation of Three-Phase Voltages	247

8.2 Connections of Three-Phase Circuits..... 250

8.2.1 Wye-Connected Balanced Source..... 251

8.2.2 Delta-Connected Balanced Source 255

8.2.3 Wye-Connected Balanced Load..... 256

8.2.4 Delta-Connected Balanced Load 259

8.2.5 Circuits with Mixed Connections 262

8.2.6 Wye-Delta Transformation..... 265

8.3 Power Calculations of Balanced Three-Phase Circuits..... 268

8.3.1 Three-Phase Power of Balanced Wye Loads 269

8.3.2 Three-Phase Power of Balanced Delta Loads..... 269

Exercises..... 271

Chapter 9 Electric Safety 273

9.1 Electric Shock..... 273

9.1.1 Current Limits of Electric Shocks..... 274

9.1.2 Factors Determining the Severity of Electric Shocks 275

9.1.2.1 Effect of Voltage 275

9.1.2.2 Effect of Current..... 276

9.1.2.3 Effect of Body Resistance..... 276

9.1.2.4 Effect of Current Pathway 277

9.1.2.5 Effect of Shock Duration 277

9.1.2.6 Effect of Frequency 277

9.1.2.7 Effect of Ground Resistance..... 278

9.2 Ground Resistance..... 280

9.2.1 Ground Resistance of Objects 280

9.2.2 Measuring Ground Resistance of Objects..... 284

9.2.3 Ground Resistance of People 284

9.3 Touch and Step Potentials..... 286

9.3.1 Touch Potential..... 286

9.3.2 Step Potential..... 290

9.4 Electric Safety at Home..... 293

9.4.1 Neutral versus Ground 294

9.4.1.1 Grounding Chassis..... 295

9.4.1.2 Bonding Chassis to Neutral 297

9.4.1.3 Grounding Chassis and Bonding Ground to Neutral 299

9.4.2 Dwelling Distribution Circuits 302

9.4.3 Ground Fault Circuit Interrupter 304

9.4.4 Neutral Integrity 306

9.4.5 World’s Residential Grounding Practices..... 309

9.5 Low Frequency Magnetic Field and Its Health Effects..... 310

9.5.1 Low-Frequency Magnetic Fields..... 311

9.5.2 Biological Effects of Magnetic Field..... 312

9.5.3 Standards for Magnetic Field 313

Exercises..... 314

Chapter 10 Power Electronics 317

10.1 Power Electronic Devices..... 318

10.1.1 Solid-State Diodes..... 318

10.1.2 Transistors 319

10.1.2.1	Bipolar Junction Transistor	320
10.1.2.2	Metal Oxide Semiconductor Field Effect Transistor	324
10.1.3	Thyristors	325
10.1.3.1	Silicon-Controlled Rectifier	325
10.1.3.2	Silicon Diode for Alternating Current	326
10.1.4	Hybrid Power Electronic Devices	327
10.1.4.1	Darlington Transistor	327
10.1.4.2	Insulated Gate Bipolar Transistor	328
10.2	Solid-State Switching Circuits	328
10.2.1	AC/DC Converters	328
10.2.1.1	Rectifier Circuits	330
10.2.1.2	Voltage-Controlled Circuits	333
10.2.1.3	Constant-Current Circuits	336
10.2.1.4	Three-Phase Circuits	339
10.2.2	DC/DC Converters	344
10.2.2.1	Buck Converter	344
10.2.2.2	Boost Converter	345
10.2.2.3	Buck–Boost Converter	348
10.2.3	DC/AC Converters	351
10.2.3.1	Single-Phase DC/AC Converter	351
10.2.3.2	Three-Phase DC/AC Converter	352
10.2.3.3	Pulse Width Modulation	356
10.2.4	AC/AC Converters	358
	Exercises	360
Chapter 11	Transformers	363
11.1	Theory of Operation	363
11.1.1	Voltage Ratio	365
11.1.2	Current Ratio	367
11.1.3	Reflected Load Impedance	367
11.1.4	Transformer Ratings	369
11.2	Multi-Winding Transformer	370
11.3	Autotransformer	372
11.4	Three-Phase Transformer	375
11.4.1	Three-Phase Transformer Ratings	375
11.4.1.1	Wye–Wye Transformer	376
11.4.1.2	Delta–Delta Transformer	378
11.4.1.3	Wye–Delta Transformer	380
11.4.2	Transformer Bank	382
11.5	Actual Transformer	383
11.5.1	Analysis of Actual Transformer	386
11.5.2	Transformer Efficiency	390
11.5.3	Voltage Regulation	391
	Exercises	392
Chapter 12	Electric Machines	395
12.1	Rotating Magnetic Field	395
12.2	Rotating Induction Motor	399
12.2.1	Rotation of Induction Motor	401

12.2.2	Equivalent Circuit of Induction Motor	403
12.2.3	Power Analysis	407
12.2.4	Speed–Torque Relationship	410
12.2.5	Starting Torque and Starting Current.....	413
12.2.6	Maximum Torque	414
12.2.7	Starting Methods	415
	12.2.7.1 Voltage Reduction.....	416
	12.2.7.2 Insertion of Resistance.....	417
12.3	Linear Induction Motor	419
	12.3.1 Wheeled Linear Induction Motor.....	420
	12.3.2 Magnetically Levitated Induction Motor	426
12.4	Induction Generator.....	427
12.5	Synchronous Generator	432
	12.5.1 Synchronous Generator Connected to Infinite Bus.....	439
	12.5.1.1 Power of Synchronous Generator	440
	12.5.2 Synchronous Generator Connected to Infinite Bus through a Transmission Line.....	444
	12.5.3 Increase Transmission Capacity	448
	12.5.3.1 Increasing Transmission Capacity by Using Series Capacitor.....	448
	12.5.3.2 Increasing Transmission Capacity by Using Parallel Lines.....	449
12.6	Synchronous Motor	451
	12.6.1 Power of Synchronous Motor.....	454
	12.6.2 Reactive Power Control and Synchronous Condenser	454
	12.6.3 Motor Torque	456
12.7	Direct Current Motor.....	457
	12.7.1 Theory of Operation of DC Motor.....	459
	12.7.2 Starting of DC Motor	461
	12.7.3 Speed Control of DC Motor	462
12.8	Stepper Motor	464
	12.8.1 Variable Reluctance Stepper Motor	465
	12.8.2 Permanent Magnet Stepper Motor	467
	12.8.3 Hybrid Stepper Motor	468
	12.8.4 Holding State of Stepper Motor	468
	12.8.5 Rotating Stepper Motor.....	471
12.9	Single-Phase Motors.....	472
	12.9.1 Split-Phase Motors	472
	12.9.2 Capacitor Starting Motors.....	475
	12.9.3 Shaded-Pole Motors	476
	Exercises.....	476
Chapter 13	Power Quality.....	481
	13.1 Voltage Problems.....	481
	13.1.1 Voltage Flickers.....	484
	13.1.2 Voltage Sag.....	488
	13.2 Harmonic Problems.....	496
	13.2.1 Harmonic Distortion of Electric Loads.....	499
	13.2.2 Resonance due to Harmonics	504
	13.2.3 Effect of Harmonics on Transmission Lines and Cables	507

13.2.4	Effect of Harmonics on Capacitor Banks	507
13.2.5	Effect of Harmonics on Electric Machines	508
13.2.6	Effect of Harmonics on Electric Power.....	509
13.2.7	Effect of Harmonics on Communications.....	512
	Exercises.....	512
Chapter 14	Power Grid and Blackouts	515
14.1	Topology of Power Systems.....	517
14.1.1	Enhancing Power System Reliability by Adding Transmission Lines.....	518
14.1.2	Enhancing Power System Reliability by Adding Generation	518
14.2	Analysis of Power Networks	519
14.3	Electric Energy Demand	523
14.4	Trading Electric Energy	526
14.5	World Wide Web of Power	528
14.6	Anatomy of Blackouts	529
14.6.1	Balance of Electric Power	530
14.6.2	Balance of Electrical and Mechanical Powers.....	531
14.6.2.1	Control Actions for Decreased Demand.....	534
14.6.2.2	Control Actions for Increased Demand.....	534
14.7	Blackout Scenarios	536
14.7.1	Great Northeast Blackout of 1965	537
14.7.2	Great Blackout of 1977.....	537
14.7.3	Great Blackout of 2003	538
	Exercises.....	539
Chapter 15	Future Power Systems	541
15.1	Smart Grid.....	541
15.1.1	Intelligent Monitoring	545
15.1.2	Smart House	548
15.1.3	Self-Diagnosis and Self-Healing	549
15.2	Electric and Hybrid Electric Vehicles	550
15.3	Alternative Resources.....	553
15.4	Less Polluting Power Plants	553
15.5	Distributed Generation	554
15.6	Power Electronics	554
15.7	Enhanced Reliability	555
15.8	Intelligent Operation, Maintenance, and Training	555
15.9	Space Power Plants.....	555
	Exercises.....	557
Appendix A:	Units and Symbols.....	559
Appendix B:	Conversions	561
Appendix C:	Key Parameters	563
Appendix D:	Inductors.....	565
Appendix E:	Key Integrals.....	567

Preface

The first course on electric energy in engineering schools is traditionally taught as an energy conversion course. This was justified during most of the last century, as power was the main topic of electrical engineering. Nowadays, the field includes a number of new specializations such as digital systems, computer engineering, communications, imaging, and networks. With the field being so widespread, energy conversion turned into a topic for students specializing only in power. Consequently, a large number of schools have decided to move their energy conversion courses from the core curricula to the elective curricula. Other schools with limited resources have dropped the energy conversion courses altogether.

In recent years, renewed interest in electric energy has emerged due to several important reasons. Among them are the ongoing search for renewable energy and smart grid, the societal impact of blackouts, the environmental impact of generating electricity, and the lack of knowledge by most electrical engineers in fundamental subjects such as electric safety and power plants. In addition, the new ABET criteria in the United States encourages the development of curricula that underline broad education in engineering, contemporary engineering, and the impact of engineering solutions in a global and societal context. All these requirements can be met by restructuring the introductory electric energy course and making it relevant to all electrical engineering and most mechanical engineering students. This is the main objective of this textbook.

The book is authored to assist schools that wish to establish a course with a wider view of electric energy while maintaining high levels of depth. Most of the topics in this book are related to issues encountered daily and, therefore, should be of great interest to all engineering students. The majority of the chapters in the book are structured to be stand-alone topics; instructors can thus pick and choose the chapters they want to teach. They can also select the sequence in which they prefer to teach the chapters. Most of the examples in the book are from real systems and with real data to make the course relevant to all students.

Among the topics covered in this third edition are energy resources, renewable energy, power plants and their environmental impacts, electric safety, power quality, power market, blackouts, and future power systems. In addition, the topics of electromechanical conversion, transformers, power electronics, and three-phase systems are included in the book to address the needs of some schools for teaching these important topics. However, these traditional topics have been made more relevant to students. For example, the section on electric motors includes linear and levitated motors as well as stepper motors.

Chapter 1 is dedicated to the history of developing the electric energy system. The innovations started with the Greek philosopher Thales of Miletus around 600 BC, passing through William Gilbert (1544–1603), Alessandro Guiseppe Antonio Anastasio Volta (1745–1827), André-Marie Ampère (1775–1836), Georg Simon Ohm (1789–1854), Michael Faraday (1791–1867), Hippolyte Pixii (1808–1835), Antonio Pacinotti (1841–1912), Thomas Alva Edison (1847–1931), and Nikola Tesla (1856–1943). In addition, the chapter includes key inventors in power electronics such as John Ambrose Fleming (1849–1945) and Julius Edgar Lilienfeld (1881–1963). The chapter analyzes the merits and demerits between the direct current (dc) and alternate current (ac) systems that were promoted by Thomas Edison and Nikola Tesla, respectively.

In Chapter 2, the modern power system is described and its main components are discussed. The system is divided into three distinct parts: generation, transmission, and distribution. In the generation part, the main types of turbines are summarized. In the transmission systems, key components are presented, including transformers, transmission lines, insulators, conductors, bundled conductors, static wires, and substations. In this third edition, substation and distribution equipment are

added including current and voltage transformers, circuit breakers, disconnecting switches, reclosers, sectionalizers, and surge arresters. The chapter includes a brief description of control centers. At the consumer voltage level, the chapter addresses the frequency and voltage standards worldwide and gives reasons for the differences among the various standards.

Chapter 3 deals with energy resources, which are often divided into three categories: fossil fuel, nuclear fuel, and renewable resources. Fossil fuels include oil, coal, and natural gas. Renewable energy resources include hydrokinetic, wind, solar, hydrogen, biomass, and geothermal energy. All these resources are also classified as primary and secondary resources. Primary resources include fossil fuel, nuclear fuel, and hydroelectric energy. Secondary resources include all renewable energy apart from hydroelectricity. The chapter discusses the known reserves as well as the world consumptions of the primary resources. In this third edition, all data are updated with 2009 or 2010 statistics.

Chapter 4 covers primary resource power plants. It describes various designs, the main components of power plants, the theory of operation, and their modeling and analyses. It provides several examples of key calculations for hydroelectric, fossil fuel, and nuclear plants. For the hydropower plant, impulse and reaction turbines have been added, explained, and modeled in the third edition. For the nuclear power plant, the enrichment process of uranium and the CANDU reactors have been added.

Chapter 5 deals with the environmental impact of generating electricity. Each of the primary resources is associated with some type of air, water, or land pollution. Although there is no pollution-free method for generating electricity, the primary resources are often thought to be responsible for most of the negative environmental impacts. In this chapter, the various pollution problems associated with the generation of electricity are presented, discussed, and put into perspective.

Chapter 6 describes renewable energy methods. “Renewable energy” is a loosely used term to describe energy generated in any manner from resources other than fossil or nuclear fuels. They include hydrokinetic systems; wind, solar, and geothermal energy; and fuel cell. The chapter describes these technologies, their main components, the merits and demerits of each technology, the mathematical modeling, and the energy calculations of key systems. In this third edition, several enhancements have been made. In the section on wind energy, aerodynamic principles, coefficient of performance dependency on pitch angles, classification of wind turbines, and the various types of existing systems have been added. The hydrokinetic systems have been expanded to include modeling and analysis for wave, tidal, and stream systems. In the section on geothermal energy, the dry rock system has been added. The chapter also discusses the intermittency of renewable resources and the impact of its integration into power grids. As a solution, energy storage systems such as pumped hydro, compressed air, battery, and flywheel systems have been added.

Chapter 7 is a review of the ac circuit analysis that is required for subsequent chapters. Usually, the topics in this chapter are covered in earlier courses. However, for convenience, they are also included in this book.

Chapter 8 discusses three-phase systems. In addition to mathematical analysis, it discusses the reasons for using three-phase systems and the various connections in power systems.

Chapter 9 deals with electric safety, a topic often overlooked by most engineering schools. Students will learn what constitutes harmful levels of currents and their biological effects. They will also learn about primary and secondary shocks and how they are affected by various variables such as currents, voltages, frequencies, and pathways. Body and ground resistance calculations are studied as well as their effects on step and touch potentials. The impact of ground resistance on the level of electric shock is explained by various common safety scenarios. In this edition, electric safety at homes has been expanded to include discussions on the need for neutral and ground conductors. Various world safety standards for neutral and ground are discussed and justifications for three-prong plugs and outlets are made. Furthermore, safety equipment for household applications such as the ground fault interrupter are presented. The practices in most parts of the world with

regard to neutral and ground wires are explained and their safety is analyzed. Magnetic field and its biological effects are also discussed.

Chapter 10 deals with various power electronic devices and circuits. Because of the power electronic revolution, the boundary between dc and ac is becoming invisible. Besides the main solid state devices such as the silicon-controlled rectifier, insulated gate bipolar transistor, and metal oxide semiconductor field effect transistor, the chapter analyzes four types of converters: ac/dc, dc/dc, dc/ac, and ac/ac. For each of these converters, at least one circuit is discussed and analyzed in detail using waveforms and mathematical models. In this edition, the dc/ac converter has been expanded to include three-phase systems and the pulse width modulation technique.

Chapter 11 provides an introduction to transformers and includes single- and three-phase transformers as well as autotransformers and transformer banks. Detailed analyses for ideal and actual transformers are also given.

Chapter 12 discusses essential electric machines such as induction machines, synchronous machines, single-phase motors, dc motors, and stepper motors. All these machines are addressed in the context of their applications to make the theory more relevant to all students. For example, linear and magnetically levitated trains are used as applications to induction machine, while hard disk drives and printers are associated with stepper motors. Besides basic machine modeling, students can also analyze application scenarios such as a train powered by a linear induction motor traveling under certain road and wind conditions. In this edition, a section on induction generator, which is widely used in wind energy systems, has been added.

Chapter 13 deals with the imperfection of the ac waveform. It includes analyses of voltage problems such as flicker and sag as well as frequency problems. Besides the analyses, the chapter identifies the impact of imperfect waveforms on other system components as well as methods to alleviate the problems associated with power quality.

Chapter 14 covers the operation of the power system. It describes secure and insecure operations as well as stable and unstable conditions of the power system. The difference between radial and network structures as related to power system reliability is addressed. The effect of a power imbalance on the power system stability is studied. The concepts of power angle, system capacity, and transmission limits are introduced. Energy demand and energy trade between utilities are addressed as an economic necessity as well as a reliability obligation. The concept of spinning reserve and its impact on system reliability is explained. The various conditions that could lead to outages and blackouts are addressed; major blackout scenarios are also described.

Chapter 15 deals with future directions in power system research. It includes smart grids, smart houses, self-diagnosis and healing, phasor measurement units, electric and hybrid vehicles, alternative resources, distributed generation, and many more.

Author

Mohamed A. El-Sharkawi is a fellow of the IEEE. He received his PhD in electrical engineering from the University of British Columbia in 1980 and joined the University of Washington as a faculty member the same year. He is presently a professor of electrical engineering in the energy area. He has also served as the associate chair and the chairman of graduate studies and research.

Professor El-Sharkawi served as the vice president for technical activities of the IEEE Computational Intelligence Society. He founded and chaired the IEEE Power and Energy Society's subcommittee on renewable energy machines and systems. He is the founder and cofounder of several international conferences and the founding chairman of numerous IEEE task forces, working groups, and subcommittees. He has organized and chaired numerous panels and special sessions in IEEE and other professional organizations. He has also organized and taught several international tutorials on power systems, renewable energy, electric safety, induction voltage, and intelligent systems.

Professor El-Sharkawi is an associate editor and a member of the editorial boards of several engineering journals. He has published over 250 papers and book chapters in his research areas. He has authored two textbooks—*Fundamentals of Electric Drives* and *Electric Energy: An Introduction*. He also authored and coauthored five research books in the area of intelligent systems and power systems. He holds five licensed patents in the area of renewable energy VAR management and minimum arc sequential circuit breaker switching.

For more information, please visit El-Sharkawi's website at <http://cialab.ee.washington.edu>

List of Acronyms

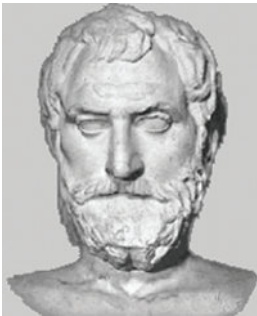
AAAC	All aluminum alloy conductors
AAC	All aluminum conductors
AC	Alternating current
ACSR	Aluminum conductors steel reinforced
BJT	Bipolar junction transistor
BM	Buoyant moored
BTU	British thermal unit
BWR	Boiling water reactor
CAES	Compressed air energy storage
CANDU	Canada Deuterium Uranium
CB	Circuit breaker
CGS	Centimeter-gram-second
COx	Carbone oxide
Cp	Coefficient of performance
CT	Current transformer
DC	Direct current
DFIG	Doubly-fed induction generator
Diac	Bilateral diode
DMFC	Direct methanol fuel cell
DS	Disconnecting switch
DT	Darlington transistor
EF	Electric field
EGC	Equipment grounding conductor
EMF	Electromagnetic field
EPA	Environmental Protection Agency
EV	Electric vehicle
FACTS	Flexible alternating current transmission system
FC	Fuel cell
FET	Field effect transistor
GFCI	Ground fault circuit interrupter
GPR	Ground potential rise
GSU xfm	Generation step-up transformer
GTO	Gate turn-off SCR
HAWT	Horizontal axis wind turbine
HC	Hinged contour
HEV	Hybrid electric vehicle
HSM	Hybrid stepper motor
HV	High voltage
ICEV	Internal combustion engine vehicle
IEEE	Institute of Electrical and Electronics Engineers
IGBT	Insulated gate bipolar transistor
IHD	Individual harmonic distortion
IM	Induction motor

ISCCS	Integrated solar combined cycle system
KE	Kinetic energy
LEO	Low Earth orbit
LIM	Linear induction motor
MagLev	Magnetically levitated
MCFC	Molten carbonate fuel cell
MF	Magnetic field
MOSFET	Metal oxide semiconductor field effect transistor
MOV	Metal oxide varistors
MPE	Maximum permissible exposure
NAAQS	National Ambient Air Quality Standards
NASA	National Aeronautics and Space Administration
NERC	North American Electric Reliability Corporation
NO _x	Nitrogen oxide
NRC	Nuclear Regulatory Commission
OHW	Overhead ground wire
OSHA	Occupational Safety and Health
OWC	Oscillating water column
P	Real power
PE	Potential energy
PEM	Proton exchange membrane
pH	Potential of hydrogen
PHS	Pumped hydro storage
PMSM	Permanent magnet stepper motor
PMU	Phasor measurement unit
PT	Potential transformer
Pu	Plutonium
PV	Photovoltaic
PWM	Pulse width modulation
PWR	Pressurized water reactor
Q	Reactive power (in ac circuits)
REM	Radiation equivalent man
rms	Root mean square
rpm	Revolutions per minute
S	Complex power, apparent power
SCR	Silicon-controlled rectifier
SCRAM	Safety control rod axe man
SF ₆	Sulfur hexafluoride
SIDAC	Silicon diode for alternating current
SO _x	Sulfur oxide
SOFC	Solid oxide fuel cell
TEC	Thermal energy constant
THD	Total harmonic distortion
TL	Transmission line
TSR	Tip speed ratio
U	Uranium
UCTE	Union for the Co-ordination of Transmission of Electricity
UPS	Uninterruptible power supply
VAWT	Vertical axis wind turbine
VF	Voltage fluctuation

VRSM	Variable reluctance stepper motor
WHO	World Health Organization
WLIM	Wheeled linear induction motor
WS	Water stream
WT	Wind turbine
xfm	Transformer

1 History of Power Systems

A large number of great scientists created wonderful innovations that led to the electric power systems as we know them today. Although electricity was discovered around 600 BC, it was not until the end of the nineteenth century that we could have electric energy on demand by flipping a switch at every home, school, office, or factory. Today, dependence on electric power is so entrenched in our societies that we cannot imagine our life without electricity. We indeed take electricity for granted, so when we experience an outage, we realize how our life is dependent on electricity. This dependency creates a formidable challenge to engineers to make the power system the most reliable and efficient complex system ever built by man.



The road to creating an electric power system began when the Greek philosopher Thales of Miletus discussed electric charge around 600 BC. The Greeks observed that when rubbing fur on amber, an electric charge would build up on the amber. The charge would allow the amber to attract light objects such as hair. However, the first scientific study of the electric and magnetic phenomena was done by the English physician William Gilbert (1544–1603). He was the first to use the term *electric*, which is derived from the Greek word for amber (ηλεκτρον). The word amber itself was derived from the Arabic word *Anbar*. Indeed, several volumes are needed to justifiably credit the geniuses behind the creation of our marvelous power system. Unfortunately, because of the lack of space, we shall only highlight the milestone developments.



A good beginning point in history would be the middle of the eighteenth century when the Italian scientist, Alessandro Guiseppe Antonio Anastasio Volta (1745–1827), showed that galvanism occurred whenever a moist substance was placed between two different metals. This discovery eventually led to the first battery in 1800. Figure 1.1 shows a model of Volta's battery that is displayed in the U.S. Smithsonian Museum in Washington, DC. The battery was the source of energy used in subsequent developments to create magnetic fields and electric currents. Today we use the unit *volt* for electric potential in honor of this great Italian inventor.



When the Danish Professor Hans Christian Oersted (1777–1851) was working on an experiment that involved the use of battery, he noticed that a compass needle had deflected from its normal heading of the magnetic north. This was the first reported discovery of electromagnetic force created by electric current. This discovery is the basis for the design of electromechanical devices such as motors and actuators. This important relationship between electricity and magnetism was not interpreted by Oersted, but was later explained by André-Marie Ampère. In honor of Oersted, his name is used as a unit for the magnetic field intensity in the centimeter–gram–second (CGS) system.



FIGURE 1.1 Model of Volta's battery. (Courtesy of the Smithsonian Museum, Washington, DC.)



The next scientist is the French mathematician and physicist André-Marie Ampère (1775–1836). He was the first to explain the ambiguous link between magnetism and electric currents that Oersted could not rationalize. His work is known as *Ampère's law*, which relates the magnetic field to electric current. Ampère's law eventually led to the development of electromagnetic devices such as motors, generators, and transformers. Today we use *ampere* as the unit of electric current in honor of this French scientist.



The German scientist Georg Simon Ohm (1789–1854) was the first to discover electrical resistance. He noticed that the current passing through a wire increased when the cross section of the wire increased and was reduced when the length of the wire increased. By this discovery, Ohm explained the fundamental relationship between the electric current, the electromotive force, and the resistance. His theory is known as *Ohm's law*. Although simple, the theory opened the door for all electrical circuit analysis and designs. We use *ohm* as the unit for resistance (or impedance) in his honor.



The English chemist and physicist Michael Faraday (1791–1867) was a superb matriculate experimentalist who laid the foundations for the electromechanical theories that we use today. Faraday, through experimentation, demonstrated the relationships between the electric current, magnetic field, and mechanical force. In 1821, Faraday built a device that produced a continuous circular motion, which was the basis for the first alternating current (ac) motor. He published his electromagnetic work in three volumes entitled *Experimental Researches in Electricity* from 1839 to 1855. These classical books have been reprinted several times and are still available in specialized bookstores. Faraday's work inspired the Scottish physicist James Clerk Maxwell (1831–1879) to develop the vector relationships of the electric current, magnetic field, and mechanical force, which



FIGURE 1.2 Pixii's generator. (Courtesy of the Smithsonian Museum, Washington, DC.)

are known today as *Maxwell's equations*. The unit of capacitance, farad, is named in memory of Michael Faraday.

The next inventor is probably the least known, but had enormous impact on power systems. Hippolyte Pixii (1808–1835) was a French instrument maker who built the first generator (or dynamo). His machine consisted of a magnet rotated by a hand crank and surrounded by a coil. Pixii found that the rotation of the magnet induced voltage across the coil. Pixii's machine, which was named magnetolectric by him, was later developed into the electrical generator we use today. Figure 1.2 shows one of the early models of Pixii's generators.



The Italian inventor Antonio Pacinotti (1841–1912) invented a device that had two sets of windings wrapped around a common core. The windings were electrically isolated from the core and from one another. When an alternating voltage was applied across one winding, an induced voltage was observed across the second winding. The induced voltage had similar shape to the applied voltage but with different magnitude. This was the invention of the transformer we use today. Westinghouse further developed the transformer and had several early models, among them are the Gaulard and Gibbs transformer developed in 1883, shown in Figure 1.3, and the Stanley transformer developed in 1886.



John Ambrose Fleming (1849–1945) was an English electrical engineer and physicist. In 1904, he invented the first electronic device that consisted of two electrodes inside a vacuum tube. One electrode was a heated filament (cathode) that emitted electrons and the other (anode) collected them. This way, the vacuum tube allowed the electrons to pass only in one direction, thus creating the first diode. His invention inspired others to create different types of vacuum tubes. One of them is the American scientist Lee DeForest, who wrapped a thin grid of wires around the cathode. By applying a small

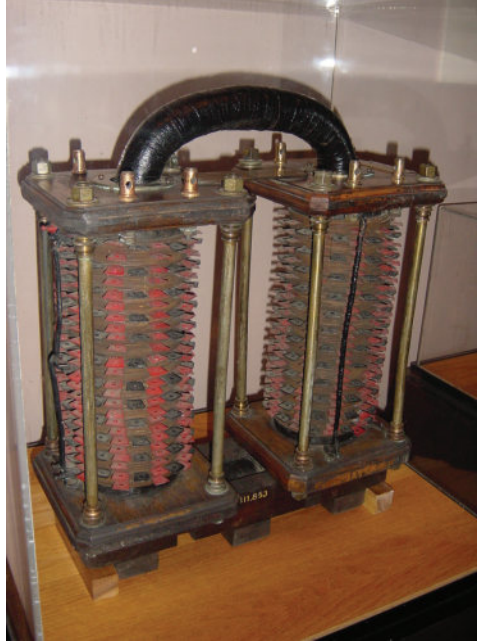


FIGURE 1.3 Gaulard and Gibbs transformer. (Courtesy of the Smithsonian Museum, Washington, DC.)

negative voltage to the grid, he managed to control the amount of electrons reaching the anode, thus controlling the electrical current. The vacuum tubes were then called *valves* as they act as a water valve where the flow of current can be reduced to zero by applying high enough negative voltage to the grid. This is the basic principle behind amplifiers. So it is not surprising that the vacuum tubes, Figure 1.4, led to the invention of the radio, television, and phone communications. The current ratings of these vacuum tubes were made high enough to allow their use in power applications. For example, the first generations of direct current (dc) lines were based on the vacuum tube technology. The vacuum tubes were used in all electronic equipment for decades until solid-state technology materialized in the 1950s.



Julius Edgar Lilienfeld (1881–1963) was born in Lemberg in Ukraine. He did his graduate studies in Germany and obtained his habilitation in 1910. He became a professor of physics at the University of Leipzig in Germany. Lilienfeld immigrated to the United States in 1927. In 1926, he discovered the field effect principle of the transistor, which was first disclosed in a U.S. patent in 1930. Later, he filed several other patents that describe the construction and operation of layered semiconductor materials. Although, there is no evidence that Lilienfeld built a working transistor based on his discoveries, his patents describe many key theories for the bipolar transistors. The first practical bipolar-junction

transistor was later developed in 1947 by Bell Laboratories' physicists Walter Houser Brattain (1902–1987), John Bardeen (1908–1991), and William Bradford Shockley (1910–1989). These scientists shared the Nobel Prize in physics in 1956 for their transistor. The invention of the transistor opened the door wide to a range of semiconductor inventions such as the field effect transistor (FET) in 1952 and the metal–oxide–semiconductor field-effect transistor (MOSFET) in 1963. In 1957, General Electric developed the silicon-controlled rectifier (SCR), which is one of the most

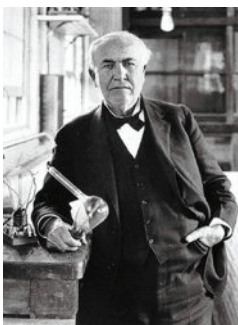


FIGURE 1.4 Vacuum tube.

important power electronic devices. The semiconductor inventions led to what is known as the *power electronics revolution*. Because of these devices, we can now build electric equipment with new capabilities and better performance while drastically reducing their sizes, costs, and losses. The power capabilities of these devices range from the milliwatt to the gigawatt, making them usable in low-power applications such as household chargers to high-power applications such as transmission line converters. Today, it is almost impossible to find electric equipment without a power electronic device.

Most of these marvelous innovations inspired two great scientists who are considered by many to be the fathers of electric power systems: Thomas Alva Edison and Nikola Tesla. Before we discuss their work, let us first summarize their biographies.

1.1 THOMAS A. EDISON (1847–1931)



Thomas Alva Edison was born on February 11, 1847, in Milan, Ohio, and died in 1931 at the age of 84. Early in his life, Edison showed brilliance in mathematics and science and was a very resourceful inventor with a wealth of ideas and knowledge. In addition to his engineering brilliance, Edison was also a businessman, although not highly successful by today's standards. During his career, he had a large number of patents (total of 1093 patents) issued under his name. His first patent was granted at the age of 21 in 1868, and his last one was at the age of 83. This makes him one of the most productive inventors ever with an average of about 1.5 patents per month. Of course, most of his patents were due to the teamwork with his research assistants.

His first patent was on an electric voting machine that tallied voting results fairly quickly. He tried to convince the Massachusetts Legislatures to adapt his machine instead of the tedious manual

process used at that time, but did not succeed. The politicians did not like his invention because the slow process at that time gave them a chance to influence, and perhaps change, the voting results.

From 1862 to 1868, Edison worked as a telegrapher in several places, including New England which was the Silicon Valley of that time; all the new and interesting innovations were made in New England. During this period, he invented a telegraphic repeater, duplex telegraph, and message printer. However, Edison could not financially gain from these inventions, so he decided to move to New York City in 1869. While there, the Wall Street stock trade was disrupted by a failure in the stock ticker machine. Coincidentally, Edison was in the area and managed to fix the machine. This landed him a high-paying job that allowed him to continue with his innovations during his off-working hours.

In 1874, at the age of 27, Edison opened his first research and development laboratory in Newark, New Jersey. In 1876, he moved the facility to a bigger laboratory at Menlo Park, New Jersey. These facilities were among the finest research and development laboratories in the world. Great scientists worked in his laboratories such as Tesla, Lewis Howard Latimer (an African-American who worked on carbon filaments), Jonas Aylsworth (who pioneered plastics), Reginald Fessenden (a radio pioneer), William K.L. Dickson (movie developments), Walter Miller (sound recording), John Kruesi (phonograph), and Francis R. Upton (dynamo). At that time, the innovations and productivities of Edison's laboratories were unmatched by any other research facility in the world. By today's jargons, these laboratories were the core of the Silicon Valley of the nineteenth century. Because of his success with various innovations, Edison expanded his research and development laboratory in 1887 and moved it to West Orange, New Jersey. There, he created the Edison General Electric Company, which in 1892 became the famous General Electric Corporation.

The large number of inventions that Edison made includes the silent movie, alkaline storage battery, electrical generator, ore separator, printer for stock ticker, printer for telegraph, electric locomotive, motion picture camera, loudspeakers telephone, microphone, mimeograph, and the telegraph repeater.

Edison was a highly competitive scientist who was willing and able to compete with great scientists in several areas at the same time. Among his innovations is the carbon transmitter, which ultimately was developed into the telephone. However, Alexander Graham Bell was also working on the same invention, and he managed to beat Edison to the telephone patent in 1876. This specific event upset Edison tremendously, but did not slow him down. He worked on the phonograph, which was one of Bell's projects, but this time Edison patented the phonograph in 1878 before Bell could apply for his own patent. One of Edison's most important inventions was the electric lightbulb. This simple device is probably one of his everlasting inventions. The first incandescent lightbulb was tested in Edison's laboratories in 1878 (see the photo in Figure 1.5). Although the filament of the bulb burned up quickly, Edison was very aesthetic about the commercial prospects of his invention. Several developments were later made to produce filaments with longer lifetimes.

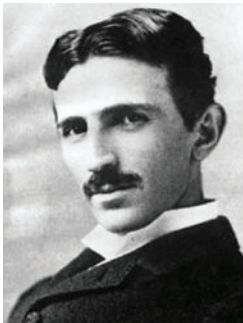
Before the invention of the electric lightbulb, New York streets were illuminated by oil lamps. So when Edison invented his bulb, the technology was resisted by Rockefeller, who was an oil tycoon. But soon after realizing that oil would be used to generate electricity, Rockefeller accepted this new technology and was among its promoters.

Edison received the U.S. Congressional Gold Medal for Career Achievements in 1928. When he died in 1931, people worldwide dimmed their lights in honor of his achievements. Initially it was suggested that the proper action would be to turn off the electricity completely for a few minutes, but the suggestion was quickly ruled out because of its impracticality; the power systems worldwide would have to shut down and restart, which was considered to be an inconceivable task. Today, a number of museums around the world have sections dedicated to Edison and his inventions. Among the best in the United States are the Edison National Historic Sites in West Orange, New Jersey, and Menlo Park in Edison, New Jersey. Also, the National Museum of American History has a section dedicated to Thomas Edison.



FIGURE 1.5 Edison's lightbulbs. (Courtesy of the Smithsonian Museum, Washington, DC.)

1.2 NIKOLA TESLA (1856–1943)



Nikola Tesla was born in Smiljan, Croatia, on July 9, 1856. Tesla was a gifted person with an extraordinary memory and highly analytical mind. He had his formal education at the Polytechnic School of Gratz, Austria, and the University of Prague in the areas of mathematics, physics, and mechanics. In addition to his strength in science and mathematics, Tesla spoke six languages. During his career, Tesla had more than 800 patents. Although lesser in number than Edison's record, his patents were mostly the direct result of his own work. Furthermore, unlike Edison, Tesla was broke most of his life and could not afford the cost of patent applications. Actually, his most resourceful era was his last 30 years, but because of his poor financial condition, he managed to apply for very few patents.

Tesla moved from Europe to the United States in 1884 and worked for Edison in his laboratory as a research assistant. This was during the time Edison patented the lightbulb and was looking for a way to bring electricity to homes, offices, and factories. He needed a reliable system to distribute electricity and Tesla was hired to help in this area.

Among Tesla's inventions are the ac motor shown in Figure 1.6, the hydroelectric generator, the radio, x-rays, vacuum tubes, fluorescent lights, microwaves, radar, the Tesla coil, the automobile ignition system, the speedometer, and the electronic microscope.

In the opinion of many scientists, historians, and engineers, Tesla invented the modern world. This is because he developed the concept of the power system we use today. By today's business standards, Tesla should have been among the richest in the world. But because of his unfortunate business failures, Tesla was broke when he died at the age of 86 on July 7, 1943. Among the honors given to Tesla was the IEEE Edison Medal in 1917, the most coveted prize in electrical engineering in the United States. Tesla was inducted into the Inventor's Hall of Fame in 1975. He received honorary degrees from institutions of higher learning, including Columbia University, Yale University, University of Belgrade, and the University of Zagreb. He also received the Elliott Cresson Medal of the Franklin Institute. In 1956, *tesla* was adopted as the unit of magnetic flux density in the meter-kilo-second-amp (MKSA) system in his honor. In 1975, the IEEE Power Engineering Society



FIGURE 1.6 Tesla's ac motor. (Courtesy of the Smithsonian Museum, Washington, DC.)

established the Nikola Tesla Award for outstanding contributions in the field of electric power in his honor. Among the best museums for Tesla are the Nikola Tesla Museum in Belgrade and the Nikola Tesla Museum of Science and Industry in Colorado Springs, Colorado.

1.3 BATTLE OF AC VERSUS DC

Edison continued to develop the lightbulb and made it reliable enough for commercial use by the end of the nineteenth century. He powered his bulbs by dc sources that were commonly used at that time. The voltage and current of a dc source are unchanging with time; an example is shown in Figure 1.7. The battery is an excellent example of a dc source.

The people in the northeast of the United States were very eager to use this marvelous electrical bulb in their homes because, unlike oil lamps, electrical bulbs did not emit horrible fumes. Edison, who was also a businessman, decided to build a dc power system and sell electricity to these eager customers. He erected poles and extended wires (conductors) above the city streets. In September 1882, his Pearl Street plant in lower Manhattan started operation as the world's first commercial electric lighting power station. One of the most significant events in technological history took place in 1883 when Edison electrified the city of Brockton, Massachusetts. The center of the city was the first place on earth to be fully electrified by a central power station.

Edison's dc generators were low voltage (100 V) machines. As a result of the increasing demand for electricity, the wires carried larger currents causing larger voltage drops across the wires, thus reducing the voltage at the customers' sites. To understand these relationships, consider the simple representation of Edison's system shown in Figure 1.8. The voltage across the load V_{load} can be expressed by Equation 1.1

$$V_{load} = V_S - IR_{wire}$$

$$V_{load} = IR = \frac{V_S}{R + R_{wire}} R = \frac{V_S}{1 + \left(\frac{R_{wire}}{R}\right)} \quad (1.1)$$

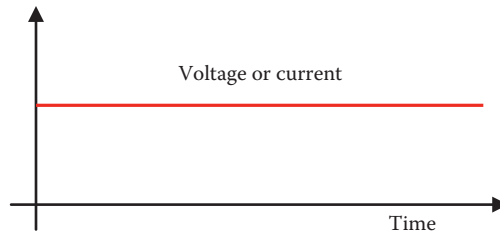


FIGURE 1.7 Direct current waveforms.

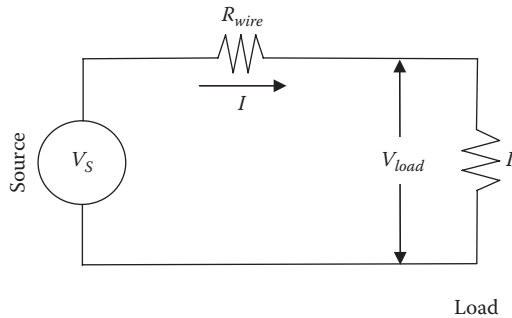


FIGURE 1.8 Simple representation of Edison's dc system.

where

V_S is the voltage of the dc source (100 V)

R is the load resistance (large number of bulbs for large number of homes)

R_{wire} is the resistance of the wire (conductor) connecting the source to the load

Because more customers mean more load resistances are added in parallel, the total load resistance R decreases when more customers are added to the system. As you can see from Equation 1.1, higher loads (i.e., more customers and smaller R) lead to lower voltage at the customers' end of the line V_{load} .

Example 1.1

Assume $V_S = 100$ V, $R = 1$ Ω , and $R_{wire} = 0.5$ Ω . Compute the following:

- Voltage at the load side
- Percentage of the load voltage with respect to the source voltage
- Energy consumed by the load during a 10 h period
- Maximum load (minimum resistance) if the load voltage cannot be reduced by more than 10% of the source voltage
- Energy consumed by the new load during a 10 h period

Solution

- By direct substitution in Equation 1.1, we can compute the voltage at the load side:

$$V_{load} = \frac{V_S}{1 + \left(\frac{R_{wire}}{R}\right)} = \frac{100}{1 + \left(\frac{0.5}{1}\right)} = 66.67 \text{ V}$$

This low voltage at the load side may not be high enough to shine the lightbulbs:

b.
$$\frac{V_{load}}{V_s} = 66.67\%$$

c. The energy is the power multiplied by time. Hence, the energy consumed by the load is

$$E = Pt = \frac{V_{load}^2}{R} t = \frac{66.67^2}{1} 10 = 44.444 \text{ kWh}$$

d. If the minimum load voltage is 90% of the source voltage, the load resistance can be computed from Equation 1.1 as

$$\frac{V_{load}}{V_s} = \frac{1}{1 + \left(\frac{R_{wire}}{R}\right)}$$

$$0.9 = \frac{1}{1 + \left(\frac{0.5}{R}\right)}$$

$$R = 4.5 \Omega$$

Notice that the new load resistance is 4.5 times the original load resistance. This means that fewer customers are connected, and less energy is consumed by the load:

$$E = Pt = \frac{V_{load}^2}{R} t = \frac{(0.9 \times 100)^2}{4.5} 10 = 18.0 \text{ kWh}$$

This is less energy than the one computed in step c.

As seen in Example 1.1, the load voltage V_{load} is reduced when more customers are added. The main reason is because the conductor resistance R_{wire} and the load current I cause a voltage drop across the conductor, thus reducing the voltage across the load resistance as given in Equation 1.1. The wire resistance increases when the length of the wire increases or the cross section of the wire decreases, as given in the following equation:

$$R_{wire} = \rho \frac{l}{A} \tag{1.2}$$

where

ρ is the resistivity of the conductor in $\Omega\text{-m}$ which is a function of the conductor's material

A is the cross section of the wire

l is the length of the wire

Example 1.2

Assume $V_s = 100$ V and the load resistance $R = 1 \Omega$. Compute the length of the wire that would not result in load voltage reduction by more than 10%. Assume the wire is made of copper and the diameter of its cross section is 3 cm.

Solution

From Equation 1.1, we can compute the wire resistance:

$$\frac{V_{load}}{V_s} = \frac{1}{1 + \left(\frac{R_{wire}}{R}\right)}$$

$$0.9 = \frac{1}{1 + \left(\frac{R_{wire}}{1}\right)}$$

$$R_{wire} = 0.111 \Omega$$

From the table of units in Appendix C, the resistivity of copper is $1.673 \times 10^{-8} \Omega\cdot\text{m}$. Hence, the length of the wire can be computed by using Equation 1.2.

$$l = \frac{AR_{wire}}{\rho} = \frac{(\pi r^2)R_{wire}}{\rho} = \frac{(\pi \times (0.015)^2)0.111}{1.673 \times 10^{-8}} = 4.69 \text{ km}$$

A wire with length longer than 4.69 km will result in lower voltage across the load than needed.

As seen in Equation 1.2 and Example 1.2, long wires cause low voltage across the load. Because of this reason, the limit of Edison's system was about 3 miles, beyond which the wire resistance would be high enough to render the lightbulbs useless. To address this problem, Edison considered the following three solutions:

1. Reduce the wire resistance by increasing its cross section. This solution was expensive because
 - a. Conductors with bigger cross sections are more expensive
 - b. Bigger conductors are heavier and would require higher poles to be placed at shorter spans
2. Have several wires feeding areas with high demands. This was also an expensive solution as it would require adding more wires for long miles.
3. Place electrical generators at every neighborhood. This was also an impractical and expensive solution.

Edison was faced with the first real technical challenge in power system planning and operation. He looked at all possible solutions from anyone who could help. That was probably why he hired Tesla in his laboratory and promised him lucrative bonuses if he could solve this problem. Tesla knew

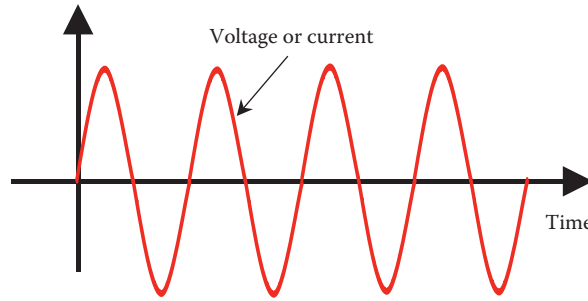


FIGURE 1.9 Alternating current waveform.

the problem was related to the low voltage (100 V) Edison was using in his dc system. The viable alternative was to increase the supply voltage so the current could be reduced and, consequently, the voltage drop across the wire could be reduced as well. Since the power consumed by the load is the multiplication of voltage by current (as given in Equation 1.3), an increase in the source voltage results in a decrease in current. If the current decreases, the voltage drop across the wire IR_{wire} is reduced, and the load voltage $V_{load} = V_S - IR_{wire}$ becomes a higher percentage of the source voltage. Although logical, adjusting the voltage of the dc systems was an unknown technology at that time.

$$P = VI \tag{1.3}$$

Instead of the dc system, Tesla promoted a totally different concept. Earlier in his life, Tesla conceived the idea of the *alternating current* (ac) whose waveform is shown in Figure 1.9. The ac is a sinusoidal waveform changing from positive to negative and back to positive in one cycle. Tesla wanted to use the ac to produce a rotating magnetic field that can spin motors (see Chapter 12). While working at the Continental Edison Company in Paris, Tesla actually built the first motor running on ac. The machine was later named the *induction motor* (see Chapter 12).

Tesla was also aware of the device invented by Pacinotti in 1860 that could adjust the ac voltages. This device was further developed by Tesla and became the transformer we use today (see Chapter 11). The transformer requires alternating magnetic field to couple its two separate windings. Therefore, it is designed for ac waveforms and is ineffective in dc systems.

Tesla molded these various technologies into a new design for the power system based on the ac as shown in Figure 1.10. The voltage source of the proposed system was ac at generally low voltage. *Transformer 1* was used to step-up (increase) the voltage at the wire side of the transformer to a high level. The high voltage of the wire resulted in lower current inside the wire. Thus, the voltage drop across the wire IR_{wire} was reduced. At the customers' sites, the high voltage of the wire was stepped down (reduced) by *transformer 2* to a safe level for home use.

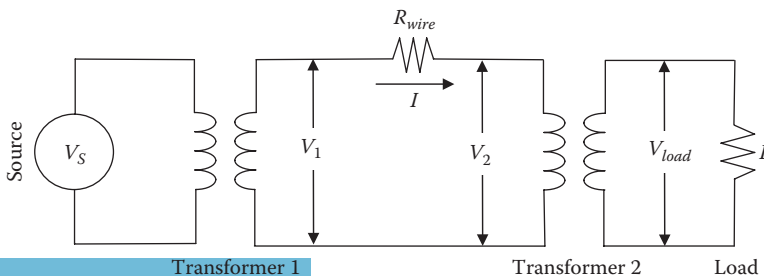


FIGURE 1.10 Tesla's proposed system.

Tesla stated three main advantages for his ac system:

1. Power can be transmitted over long distances with little voltage drop across its wires.
2. Generating plants need not be installed at residential areas as suggested by Edison for his dc system.
3. Rotating magnetic fields can be created for electric motors.

Edison was not impressed by Tesla's ac system because of its unsafe high-voltage wires that would pass through residential areas. However, most historians believe that Edison's rejection to the ac system was because he had too much money invested in the dc infrastructure. This disagreement created an irreparable rift between these two great scientists. Tesla and Edison continued to disagree on various other issues, and Tesla left Edison's laboratory and eventually worked for Westinghouse.

The dc versus ac battle started between Edison and General Electric, on one side, and Tesla and Westinghouse, on the other. Edison used unconventional methods to convince the public that Tesla's high-voltage ac system was too dangerous. He made live demonstrations where he used high voltage to deliberately electrocute animals such as puppies, cats, horses, and even elephants. Edison went so far as to convince the state of New York to use an electric chair powered by high voltage ac system to execute condemned inmates on death row. Most historians believe that his real motive was to further tarnish the safety of the ac system. Sure enough, New York City executed its condemned inmates by the proposed electric chair, and Edison captured the occasion by referring to the execution process as "Westinghoused," a clear reference to the ac system promoted by Tesla and Westinghouse. When Tesla signed a contract with Westinghouse to erect ac wires, posters were put on the power poles to warn residents from the danger of being "Westinghoused." In addition to the negative publicity, Westinghouse ran into financial trouble, and Tesla's contract with Westinghouse was terminated before the ac system was fully implemented. Instead of becoming the world's richest man, Tesla died broke. Despite all the negative publicity created by Edison, the advantages of the ac systems were overwhelming. In fact, Edison later admitted that ac is superior to dc for power distribution and was quick to exploit the economical advantages of the ac system through several inventions. Once when Edison met with George Stanley, the son of the William Stanley who developed the transformer for Westinghouse, he told him "tell your father I was wrong." Tesla was considered by many historians to be the inventor of the new world. This is probably true since social scientists use energy consumption as a measure of the advancement of modern societies.

1.4 TODAY'S POWER SYSTEMS

The great scientists mentioned in this chapter, and many more, have provided us with the power systems we know today. The power engineers made use of the various innovations to deliver electricity safely and reliably to each home, commercial building, and factory. Indeed, it is hard to imagine our life without electricity.

In 2009, the world produced over 20 PWh (20×10^{15} Wh) of electric energy as shown in Figure 1.11. In about 10 years, the world generated 40% more electric energy. This awesome amount of energy is the main reason for the highly developed societies we enjoy today. To deliver this amount of power to the consumers, power engineers constructed several millions of transmission lines, power plants, and transformers. It is overwhelming to fathom how such a massive system is controlled and operated on a continuous basis.

National Aeronautics and Space Administration (NASA) often publishes a fascinating panoramic photo of the earth at night; one of them is shown in Figure 1.12. The photo shows the earth's man-made lights and comprises of hundreds of pictures generated by the orbiting Defense Meteorological Satellites Program (DMSP). As you see in the photo, man-made lights make it quite

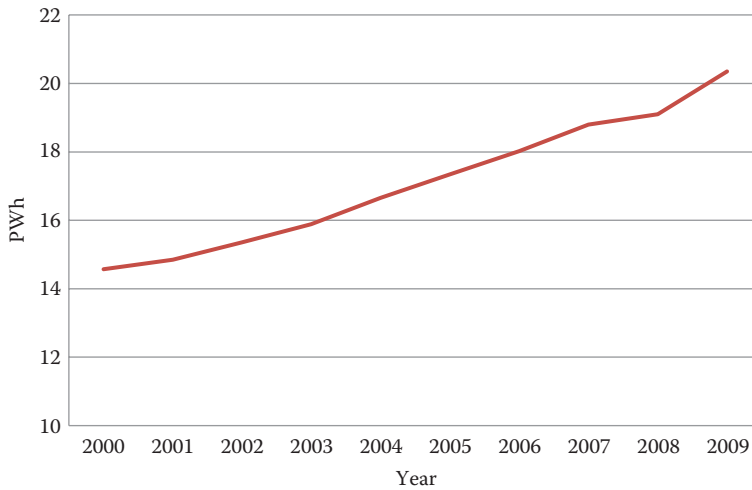


FIGURE 1.11 World's electric energy capacity. (From British Petroleum statistical review of world energy, 2007.)



FIGURE 1.12 Earth at night. (Courtesy of NASA, Washington, DC.)

possible to identify the borders of cities and countries. Note that the developed or populated areas of the earth, such as Europe, eastern United States, and Japan, are quite bright, reflecting their high consumption of electric energy. Also, for countries with high populations around rivers, such as Egypt, the path of the rivers can be traced by following the light trails. The dark areas, such as in Africa, Australia, Asia, and South America, reflect low consumption of electricity or unpopulated regions. In North Africa, you can identify the great Sahara desert by the dark and expanded region. Similarly, you can identify the unpopulated outback region in Australia.

EXERCISES

- 1.1** In your opinion, identify 10 of the most important innovations in electrical engineering and name the inventors of these innovations.
- 1.2** Thomas Alva Edison has several innovative inventions. Select one of them and write an essay on the history of its development and the impact of the invention on society.

- 1.3 Nikola Tesla has several innovative inventions. Select one of them and write an essay on the history of its development and the impact of the invention on society.
- 1.4 The transformer is one of the major inventions in power systems. Why cannot we use it in dc systems?
- 1.5 State the advantages and disadvantages of using low-voltage transmission lines.
- 1.6 State the advantages and disadvantages of using high-voltage transmission lines.
- 1.7 In your opinion, what are the major developments in future power systems?
- 1.8 A simple power system consists of a dc generator connected to a load center via a transmission line. The load resistance is $10\ \Omega$. The transmission line is 50 km copper wire of 3 cm in diameter. If the voltage at the generator terminals is 400 V, compute the following:
 - a. Voltage across the load
 - b. Voltage drop across the line
 - c. Line losses
 - d. System efficiency
- 1.9 A simple power system consists of a dc generator connected to a load center via a transmission line. The load power is 100 kW. The transmission line is 100 km copper wire of 3 cm diameter. If the voltage at the load side is 400 V, compute the following:
 - a. Voltage drop across the line V_{line}
 - b. Voltage at the source side V_{source}
 - c. Percentage of the voltage drop V_{line}/V_{source}
 - d. Line losses
 - e. Power delivered by the source
 - f. System efficiency
- 1.10 Repeat the previous problem assuming that the transmission line voltage at the load side is 10 kV.
- 1.11 Identify 10 household appliances that use power electronic devices and circuits. Discuss the advantages of using power electronics in two of these appliances.

2 Basic Components of Power Systems

Modern power networks are made up of three distinct systems: generation, transmission, and distribution. Figure 2.1 shows a sketch of a typical power system. The generation system includes the main parts of the power plants such as turbines and generators. The energy resources used to generate electricity in most power plants are combustible, nuclear, or hydropower. The burning of fossil fuels or a nuclear reaction generates heat that is converted into mechanical motion by the thermal turbines. In hydroelectric systems, the flow of water through the turbine converts the potential or kinetic energy of the water into rotating mechanical energy. These turbines rotate the electromechanical generators that convert the mechanical energy into electric energy.

The generated electricity is transmitted to all customers by a complex network of transmission systems composed mainly of transmission lines, transformers, and protective equipments. The transmission lines are the links between power plants and load centers. Transformers are used to increase (step up) or decrease (step down) the voltage. At the power plant, a transmission substation with step-up transformers increases the voltage of the transmission lines to very high values (220–1200 kV). This is done to reduce the current through the transmission lines, thus reducing the cross section of the transmission wires and consequently reducing the overall cost of the transmission system. At the load centers, the voltage of the transmission lines is reduced by step-down transformers to lower values (15–25 kV) for the distribution of power within city limits. At the consumer sites, the voltage is further reduced to values from 100 to 240 V for household use depending on the standards of the country.

Transmission lines are classified by their voltage levels. There are generally four classes: low, medium, high, and extra high. Figure 2.2 shows the general classification used by utilities. Since there is no clear border between classes, they may overlap. For example, 500 kV is considered by some utilities to be high voltage and by others to be extra high voltage.

The power system is extensively monitored and controlled. It has several levels of protections to minimize the effect of any damaged component on the system's ability to provide safe and reliable electricity to all customers. A number of key devices and equipment used in power systems are covered in this chapter.

2.1 POWER PLANTS

At the power plant, energy resources such as coal, oil, gas, hydropower, or nuclear power are converted into electricity as shown in Figure 2.3. The main parts of the power plant are the burner (in fossil plants), the reactor (in nuclear power plants), the dam (in a hydroelectric plant), the turbine, and the generator. The power plants can be huge in size and capacity. For example, the Itaipu hydroelectric power plant located at the Brazilian–Paraguayan border produces 75 TWh annually (Figure 2.3b). China is building the largest nuclear power plant in the southern province of Guangdong with a capacity of 6 GW.

Although power plants are enormous in mass, they are delicately controlled. A slight imbalance between the input power of the turbine and the output electric power of the generator may cause a blackout unless rapidly corrected. To avoid blackouts, the massive amount of water or steam inside

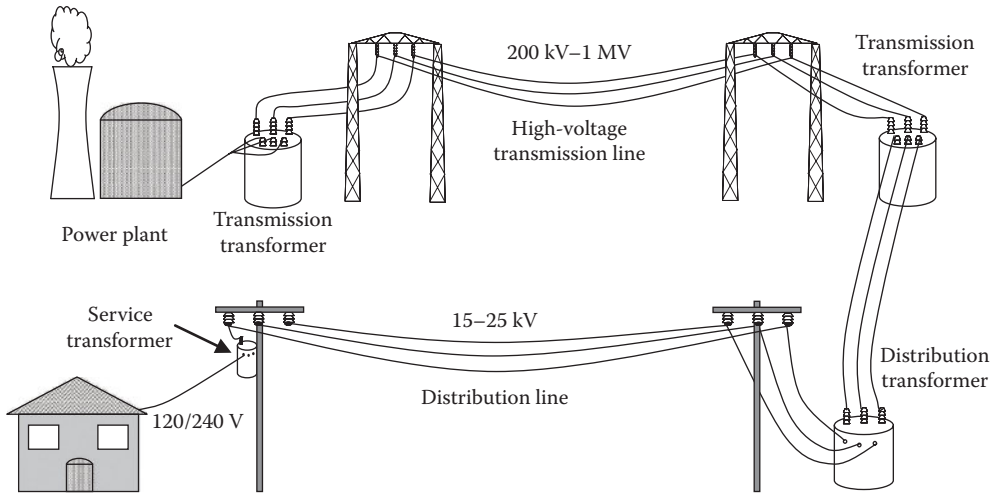


FIGURE 2.1 Main components of power systems.

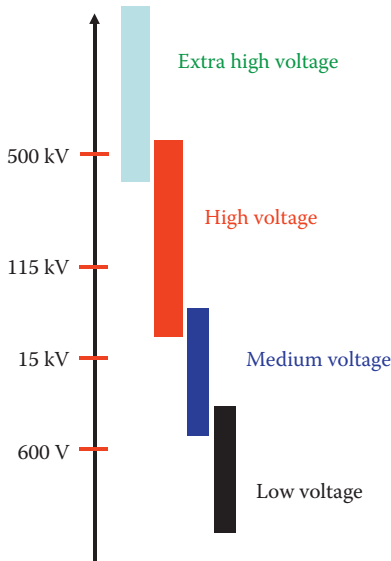


FIGURE 2.2 Categorization of transmission lines.

the plant must be tightly controlled at all times, which is an enormous challenge to mechanical, electrical, and structural engineers.

2.1.1 TURBINES

The function of the turbine is to rotate the electrical generator by converting the thermal energy of the steam or water into rotating mechanical energy. There are two types of turbines in conventional power plants: thermal and hydroelectric. Figure 2.4 shows a model of a hydroelectric turbine. It consists of blades mounted on a rotating shaft and curved to capture the maximum energy from water. The angle of the blade can be adjusted in some types of turbines for better control on its output mechanical power.



FIGURE 2.3 Power plants (a) nuclear, (b) hydro, (c) thermal.



FIGURE 2.4 Model of hydroelectric turbine.

In thermal power plants, fossil fuels or nuclear reactions are used to produce steam at high temperatures and pressures. The steam is passed through the blades of the thermal turbine and causes the turbine to rotate. The steam flow is controlled by several valves at critical locations to ensure that the turbine rotates at a precise speed.

A typical hydroelectric power plant consists of a dam that holds the water upstream at high elevations with respect to the turbine. The difference in height between the water surface behind the dam

and the turbine blades is called *head*. The larger the head, the more potential energy is stored in the water behind the dam. When electricity is needed, the water is allowed to pass to the turbine blades through pipes called *penstocks*. The turbine then rotates, and the valve of the penstock regulates the flow of water, thus controlling the speed of the turbine.

Since the generator is mounted on the shaft of the turbine, the generator rotates with the turbine and electricity is generated. To ensure that the voltage of the generator is at a constant frequency, the turbine must run at a precise and constant speed. This is not a simple task as we shall see later in Chapter 14.

2.1.2 GENERATORS

The generator used in all power plants is the *synchronous* machine (see Chapter 12). The invention of the synchronous generator goes back to Hippolyte Pixii (1808–1835), who was the first to build a dynamo. The synchronous machine has a magnetic field circuit mounted on its *rotor* and is firmly connected to the turbine. The stationary part of the generator, called a *stator*, has windings wrapped around the core of the stator. When the turbine rotates, the magnetic field moves inside the machine in a circular motion. As explained by Faraday, the relative speed between the stator windings and the magnetic field induces voltage across the stator windings. When an electrical load is connected across the stator windings, the load is energized as explained by Ohm's law. The output voltage of the generator (5–22 kV) is not high enough for the efficient transmission of power. Higher voltage generators are not practical to build as they require more insulation, making the generator unrealistically large in size. Instead, the output voltage of the generators is increased by using step-up transformers.

2.2 TRANSFORMERS

The main function of the transformer is to increase (step up) or decrease (step down) the voltage (see Chapter 11). As explained in Chapter 1, the voltage of the transmission line must be high enough to reduce the current in the transmission line. When electric power is delivered to the load centers, the voltage is stepped down for safer distribution over city streets as seen in Figure 2.1. When the power reaches customers' homes, the voltage is further stepped down to the household level of 100–240 V, depending on the various standards worldwide.

2.3 TRANSMISSION LINES

Power lines (conductors) deliver electrical energy from the generating plant to customers as shown in Figure 2.1. The bulk power of the generating plant is transmitted to load centers over long distance lines called *transmission lines*. The lines that distribute the power within city limits are called *distribution lines*. There are several other categories such as *subtransmission lines*, but these are fine distinctions that we should not worry about at this stage. In the United States alone, there is about 300,000 km of transmission lines rated 110 kV or above. This is equivalent to at least 7.5 times the circumference of the earth. The construction of such an immense grid, and maintaining the flow of power through it is one of the hardest tasks for power system engineers.

The transmission lines are high-voltage wires (220–1200 kV) mounted on tall towers to prevent them from touching the ground, humans, animals, buildings, or equipment. High-voltage towers are normally 25–45 m in height; one of these towers is shown in Figure 2.5. The higher the voltage of the wire, the taller is the tower.

High-voltage towers are normally made of galvanized steel to achieve the strength and durability needed in harsh environments. Since steel is electrically conductive, high-voltage wires cannot be attached directly to the steel tower. Instead, insulators made of nonconductive material mounted on the tower are used to hold the conductors away from the tower structure. The insulators withstand

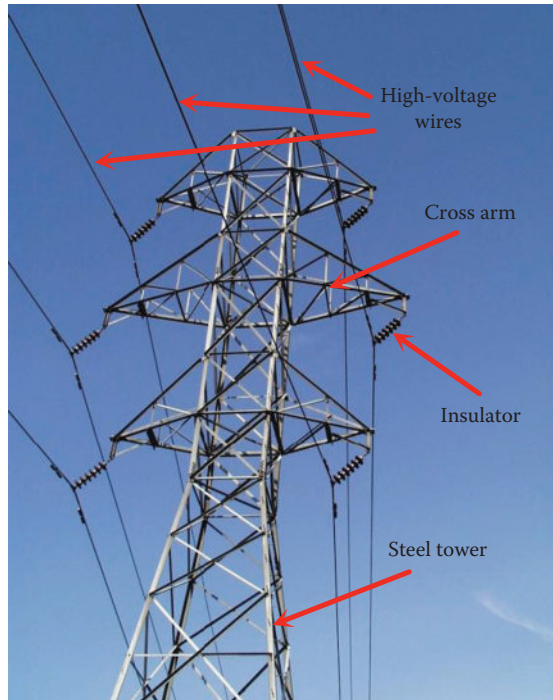


FIGURE 2.5 Transmission line tower.

the static and dynamic forces exerted on the conductor during windstorms, freezing rain, or earth movements. Insulators come in various shapes and designs; one of them is shown in Figure 2.6a. It consists of mounting ends and insulated central rod with several disk-shaped insulating materials. In some types of insulators, the disk has a slightly conical shape, where the top diameter is slightly smaller than the bottom diameter as shown in Figure 2.6b. The top end of the central rod is attached to the tower, and the lower end is attached to the conductor. The disks have two main functions:

1. They increase the flashover distance between the tower and the conductor (called *creepage* distance).
2. When it rains, the insulators are automatically cleaned since the disks are conical shaped or are slightly bent toward the earth.

An electrical discharge between any two metals having different potentials depends on the potential difference and the separation between the two metals. If an insulator is placed between two metals, a flashover may occur along the surface of the insulator if the potential difference between the two metals is high enough or the length of the insulator is small enough. To protect against the flashover in high-voltage transmission lines, the insulators must be unrealistically long. However, if a disk-shaped insulator is used, the distance between the tower and the conductor over the surface of the insulator is more than the actual length of the insulator. This is explained in Figure 2.6c, where the jagged arrow shows the flashover path which is longer than the actual height of the insulator. The flashover path is called the *creepage* distance and is defined as the shortest distance along the surface of the insulation material. But why are the disks slightly bent toward the ground or have their upper radii smaller than their lower radii? The simple answer is to make it easy to clean the insulators. When it rains, the salt and dust deposited on the insulator are washed away. If it were to be mounted upside down, there would still be pockets where dust would be trapped, thus reducing the insulation capability of the insulators.

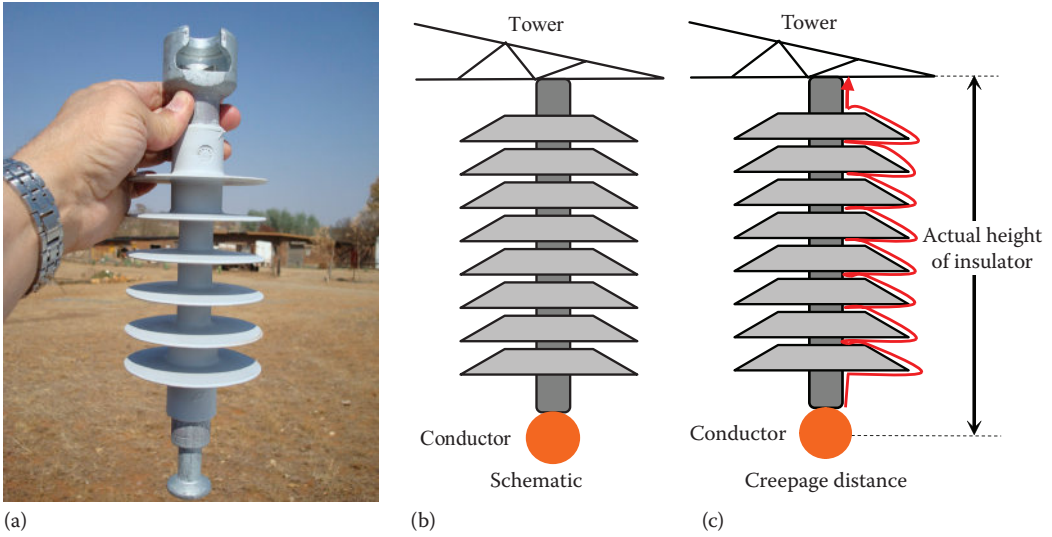


FIGURE 2.6 (a) Insulator, (b) schematic, and (c) flashover path.

2.4 DISTRIBUTION LINES

The conductors of the distribution lines are lower in voltage and are either buried underground or mounted on poles or towers. In most cities, the distribution network is mainly underground for esthetic and safety reasons. However, it is also common to have overhead distribution lines; one of these is shown in Figure 2.7.

Since the voltage of the distribution lines is much lower than that for the transmission lines, the distribution towers are shorter and their insulators are smaller. The distribution towers are often made of steel, wood, concrete, or composite materials. Most of the commercial and industrial plants have direct access to the distribution network, and they use their own transformers to step down the voltage to the levels needed by their various equipment. In residential areas, utilities install transformers in vaults or on towers to reduce the distribution line voltage to any value between 100 and 240 V, depending on the standard of the country.

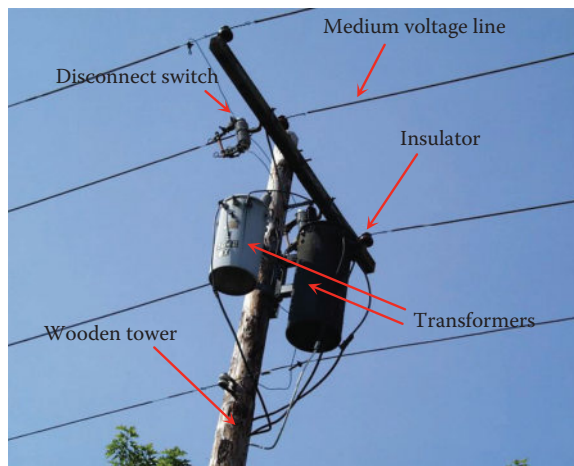


FIGURE 2.7 Distribution line tower.

2.5 CONDUCTORS

In the early days, transmission line conductors were made of copper. With the expansion of the transmission grid, copper was replaced by aluminum because of two main reasons: (1) aluminum conductors are much cheaper than copper and (2) aluminum is lighter than copper, which allows the use of longer spans between towers. The conductors used in transmission lines are not solid wires. This is because solid conductors are not flexible enough to curve and bend during transportation, storage, and the stringing of the conductors. Instead, conductors are made of a group of smaller conductors called strands that are spiraled as shown in Figure 2.8. If more than two layers of aluminum strands are used, the layers are spiraled in opposite directions to prevent unwinding. Since aluminum is a relatively soft metal and can easily break under tension (its tensile strength is relatively low), reinforcement steel alloy strands can be placed at the core of the conductor. The cross-section area of most conductors ranges from 12 to 800 mm². For cables, the conductors are also made of strands, but the conductor is encapsulated by insulation material to provide the needed isolation from the surrounding ground.

The power industry uses several types of conductors; the most common ones are the following three:

1. *All aluminum conductors (AAC)*: This conductor has one or more strands of aluminum alloy without reinforcement strands. AAC is used when the span between towers is short (urban areas). In coastal areas, where corrosion is a problem, AAC conductors are used.
2. *Aluminum conductors steel reinforced (ACSR)*: To increase the strength of the aluminum conductors, the ACSR has steel strands at its core surrounded by one or more layers of aluminum strands. The steel of the core is often galvanized steel (zinc coated). The ACSR are used when the span between towers is long. Even though the steel is galvanized, it can still be corroded over a period of time, especially in coastal areas.
3. *All aluminum alloy conductors (AAAC)*: This is an alloy conductor made of aluminum, magnesium, and silicon. The AAAC has excellent tension characteristics and superior corrosion resistance.

The industry gives bird names to the type and size of conductors. Among the names are hen, eagle, squab, etc. The conductor is also represented by an alphanumeric code such as ACSR 24/7, which means aluminum conductors steel reinforced with 24 aluminum strands and 7 reinforcement strands.

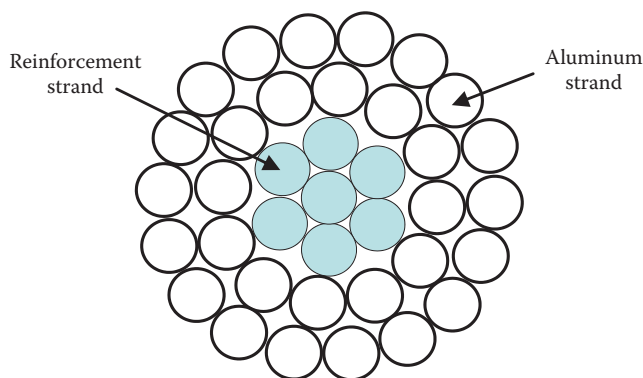


FIGURE 2.8 Transmission line conductor.

2.5.1 BUNDLED CONDUCTOR

Very-high-voltage transmission lines have their conductors split into subconductors bonded together electrically, but are separated from each other. This type of conductors is called *bundled conductor*, and is shown in Figure 2.9. But why do we bundle the conductors? After all bundling conductors is more expensive. The reason is related to the corona effect as explained next.

An object with high electric field ionizes the air surrounding it. This ionization is a form of leakage current and is called *corona*. The presence of the corona is highly undesirable for several reasons:

- Over time, corona damages the conductor; the leakage current creates spotted burns on the surface of the conductor.
- Corona produces electromagnetic fields with wide frequency spectrum that interferes with wired and wireless communications.
- Corona is a form of leakage current that causes energy losses.

The corona is intensified with the increase in the electric field strength (E) at the surface of the conductor. This electric field is

$$E = \frac{V}{d} \quad (2.1)$$

where

V is the voltage of the conductor

d is the diameter of the conductor

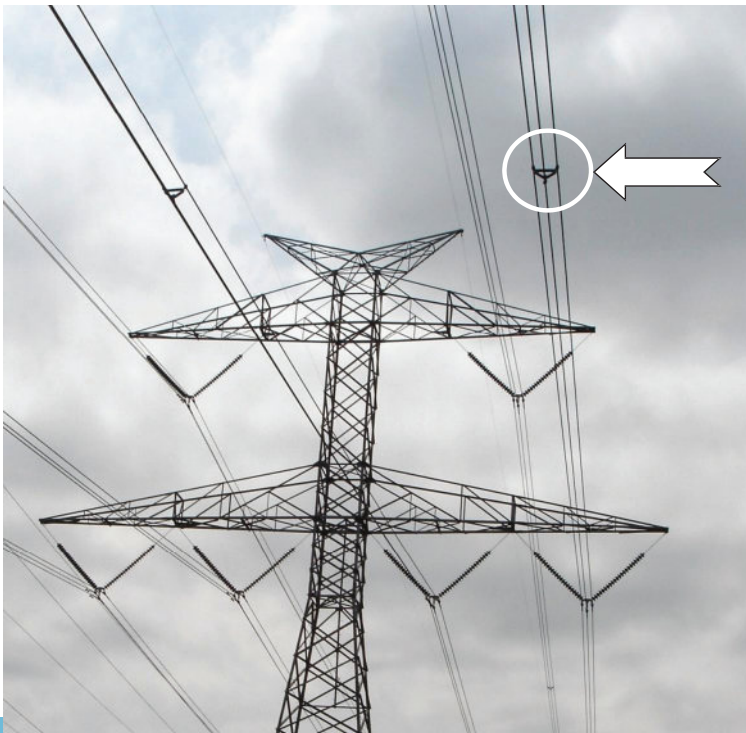


FIGURE 2.9 Bundled conductors.

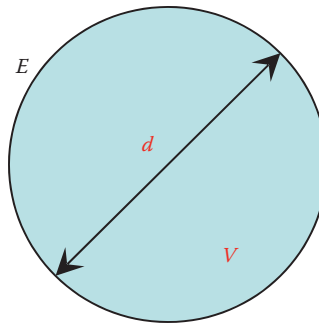


FIGURE 2.10 Electric field at surface of conductor.

Figure 2.10 shows a conductor with a voltage V and a diameter d . If the electric field at the surface of the conductor is high enough to cause corona, then we have basically two choices: reduce the voltage or increase the diameter of the conductor. The first choice is not desirable because high voltage allows us to transmit more power. The second choice has a few challenges:

- We must use more material to transmit the needed current; hence, the current density of the conductor is unnecessarily reduced.
- Conductors become more expensive.
- Conductors become heavy and difficult to string.
- Towers will have to be placed at shorter spans making the construction of the transmission line expensive.

To increase the diameter of the conductor without adding more material (i.e., maintain the same cross-section area), engineers have two options: (1) to use hollow conductors or (2) to bundle the conductors. Figure 2.11 shows these two options. In Figure 2.11a, the solid conductor with the needed cross section is shown. Assume that the voltage of this conductor is high enough to cause corona. In Figure 2.11b, a hollow conductor that has a large diameter, but with the same cross-section area, is shown. This option is not practical as the conductor becomes weak and can collapse under the pressure exerted on it during the stringing process, or due to the dynamic forces of winds. The option in Figure 2.11c is known as bundled conductor. It is composed of several subconductors with total area equal to that in Figure 2.11a. All subconductors are spaced from each other and their voltages are equalized. To maintain their space and to equalize the voltage of all subconductors,

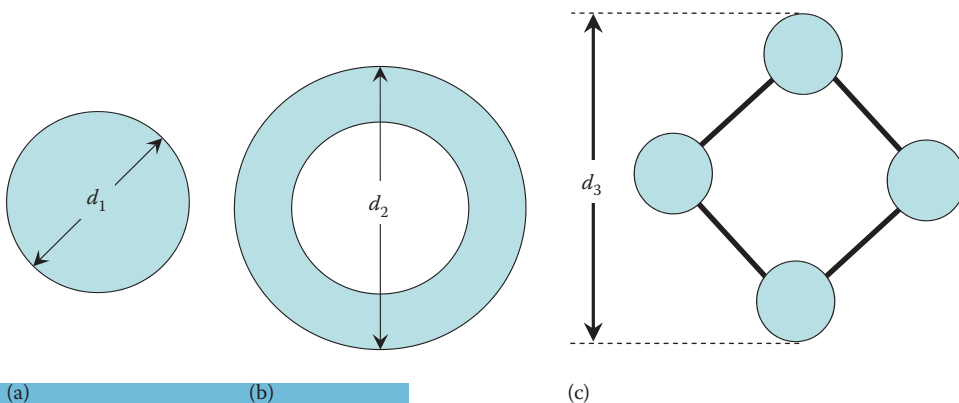


FIGURE 2.11 Options to reduce electric field strength: (a) solid conductor, (b) hollow, and (c) bundled.

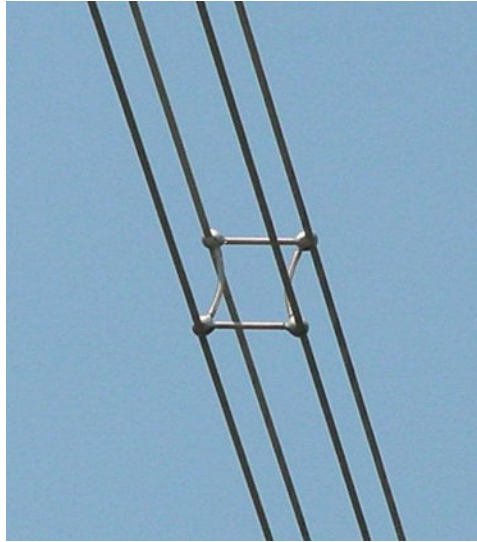


FIGURE 2.12 Bundled line with four sub-conductors.

conductive spacers are used at short distances along the transmission line. In this case, the electric field at the surface of the bundled conductor is reduced without the need to reduce the line voltage. This is because $d_3 > d_1$. Bundled conductors are typically used for transmission lines rated at or higher than 340 kV. Figure 2.12 shows a four-subconductor bundle. The spacer in the figure is repeated every few meters.

2.5.2 STATIC (SHIELD) WIRE

In some transmission lines, you can see one or two thin wires installed at the top of the tower. These wires are known as static, shield wire, or overhead ground wire (OHGW). The term *static* is used because the conductor does not carry current under normal conditions and is grounded along the transmission line and at the substations. The term *shield* is used because it protects the transmission line against lightning strikes. Figure 2.13 shows a tower with two static wires. In areas with little or no lightning storms, you may not find the static wire.

Because lightning often hits the highest point with the lowest potential, the static wire that is the highest wire at ground potential will attract the lightning strike. But why do we want to attract the lightning strike? The answer is simple; if we do not, the lightning may hit the conductors or the towers and the damage could be severe. If the line is hit, the strike could damage the insulators, rendering the transmission line unusable until the insulator is replaced. Because the buildup energy in the cloud often be dissipated through lightning strikes, engineers have decided to dissipate the energy through the static wire and protect the towers. The static wire is therefore bonded to all metal tower structures and at substations. In this way, the static wire dissipates the lightning energy throughout all ground paths along the transmission line.

The photo in Figure 2.13 shows two static wires. This is because the tower is windy and one wire may not be enough to protect all conductors.

2.6 SUBSTATIONS

The substation is where the voltage is adjusted, circuits are switched, system is monitored, and equipment is protected. A typical substation includes

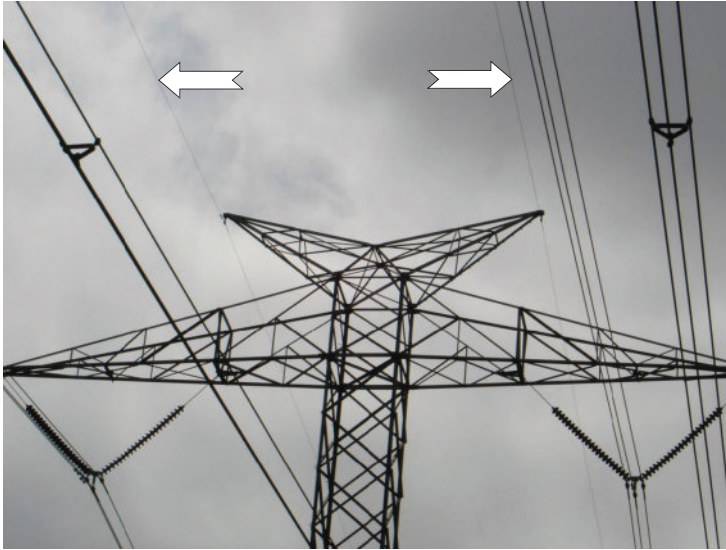


FIGURE 2.13 Static wires.

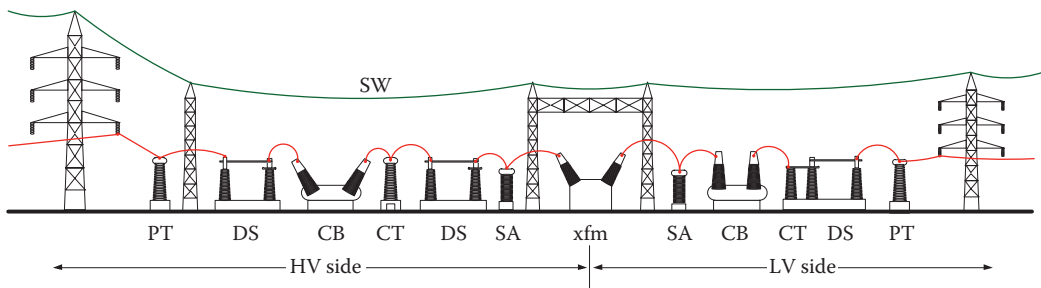


FIGURE 2.14 Main parts of a substation.

- Transformers
- Switching equipment
- Protection equipment
- Measuring devices
- Control systems

A schematic of a substation is shown in Figure 2.14. The substation steps up or steps down the voltage of the incoming power. In the figure, we assumed the high-voltage side is on the left of the graph. The incoming line reaches the substation, and its voltage is measured by a potential transformer (PT). Next, a disconnecting switch (DS) is placed to isolate a section of the substation when needed. A circuit breaker (CB) is connected to the DS to open the circuit when faults occur. A current transformer (CT) then measures the line current of the high-voltage side. Another DS is placed after the CB. When the CB is being serviced, the two adjacent DSs are opened to isolate the CB from any energized part. Before going to the transformer (xfm), a surge arrester (SA) is installed. This device is designed to dissipate any lightning or surge transients from reaching and damaging the transformer. The transformer steps down the voltage to lower levels. The low-voltage side of the transformer has another surge arrester to protect the xfm from the surges or lightning strikes that may come from the low-voltage side. Next are lower-voltage CBs, CTs, DSs, and PTs.

2.6.1 POTENTIAL TRANSFORMER

A photo of a PT is shown in Figure 2.15. To measure the voltage of the line V_1 , we can use the capacitor divider in Figure 2.16. If we make $C_2 \gg C_1$, the voltage across C_2 will be much smaller than transmission line voltage, allowing us to use low-voltage voltmeter. In this case, the current through the capacitors is

$$I = V_1 \left[2\pi f \left(\frac{C_1 C_2}{C_1 + C_2} \right) \right] = V_2 (2\pi f C_2) \quad (2.2)$$



FIGURE 2.15 Potential transformer.

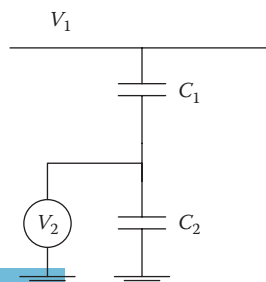


FIGURE 2.16 Capacitor divider.

where f is the frequency of the system. Equation 2.2 can be written as

$$V_1 = V_2 \left(1 + \frac{C_2}{C_1} \right) \quad (2.3)$$

By measuring the low-voltage V_2 , we can compute the high-voltage V_1 of the line.

Example 2.1

Design a capacitor divider to measure the voltage of 289 kV line.

Solution

The first step is to select the capacitors that limit the current through them to say 1 A. Also, select the voltage V_2 to be 200 V. This is low enough voltage to measure. Hence,

$$x_{c2} = \frac{V_2}{I} = \frac{200}{1} = 200 \, \Omega$$

$$C_2 = \frac{1}{\omega x_{c2}} = \frac{1}{2\pi \times 60 \times 200} = 13.26 \, \mu\text{F}$$

C_1 can be obtained by Equation 2.3.

$$V_1 = V_2 \left(1 + \frac{C_2}{C_1} \right)$$

$$289 \times 10^3 = 200 \left(1 + \frac{13.26 \times 10^{-6}}{C_1} \right)$$

$$C_1 = 9.18 \, \text{nF}$$

2.6.2 CURRENT TRANSFORMER

A CT in a distribution network is shown in Figure 2.17; its main parts are shown in Figure 2.18 and the circuit diagram is shown in Figure 2.19. The CT is a special type of transformer where the primary winding is replaced by the conductor whose current is to be measured. The secondary winding is wrapped around an iron core and has hundreds or thousands of turns. The secondary windings are shorted by an ammeter. If we ignore the leakage flux, we can use the ampere-turn theory to estimate the secondary current I_2

$$I_1 N_1 = I_2 N_2 \quad (2.4)$$

where

I_1 is the current in the transmission line conductor

I_2 is the current in the secondary winding of the CT

N_1 is the number of turns of the transmission line conductor, which is equal to 1

N_2 is the number of turns of the secondary windings



FIGURE 2.17 Current transformer.

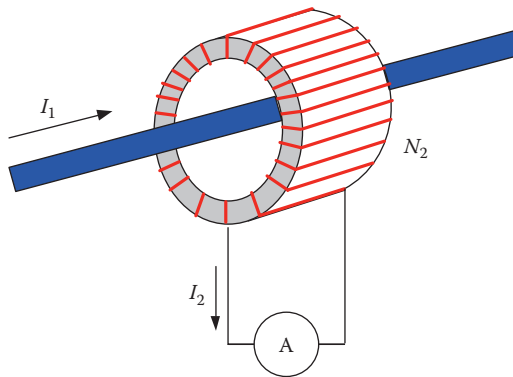


FIGURE 2.18 Main parts of CT.

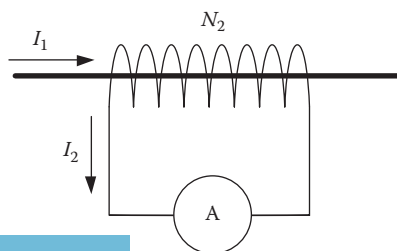


FIGURE 2.19 Circuit diagram of CT.

Hence, if we measure the current I_2 , we can compute the line current I_1 :

$$I_1 = I_2 N_2 \quad (2.5)$$

The rated secondary current I_2 is standardized at 1–5 A.

The CT must have its secondary windings shorted. This is done by the ammeter connected between its terminals. If the secondary winding is accidentally opened, the CT will be damaged. This is because the voltage per turn ratio is almost constant in the primary and secondary windings

$$\frac{V_1}{N_1} = \frac{V_2}{N_2} \quad (2.6)$$

or

$$V_2 = N_2 V_1 \quad (2.7)$$

Because N_2 and V_1 are high values, V_2 is extremely high and will cause insulation failures and arcing to force the current to pass through the secondary windings.

Example 2.2

A CT is designed to measure 10 kA in a 13.8 kV conductor; compute the turn ratio of its secondary windings.

Estimate the voltage across the secondary winding if its terminals are opened.

Solution

CTs are designed to have 1–5 A in its secondary windings. Let us select 2 A. Using Equation 2.5,

$$N_2 = \frac{I_1}{I_2} = \frac{10^4}{2} = 5000 \text{ turns}$$

When the secondary winding is open circuited, the voltage across it is

$$V_2 = 5000 \times 13.8 = 69 \text{ MV}$$

This level of voltage will certainly damage the CT.

2.6.3 CIRCUIT BREAKER

The CB is a high-voltage switching device designed to interrupt the flow of current even during faults. To operate the CB, supporting components such as the ones shown in Figure 2.20 are needed. The switching of the CBs is often by solenoids that are activated by a controller. For intentional switching, the controller receives the activation command from the control center operator. For fault clearing, the CB is automatically opened when the current exceeds predetermined values. This could be done as fast as a fraction of an alternating current (ac) cycle.

Because the energy of any inductors in the system cannot be permanently stored, all inductors must return the energy to the source when the breaker initiates the opening action. When the blades of the breaker starts to separate, an arc is developed to allow the inductors energy to return to the source. If the arc is not quickly quenched, the current keeps flowing even after the inductors' energy is fully returned to the source. Arc is a form of fire with high temperature that can easily damage the CB itself. Therefore, the arc must be quenched very quickly. To do that, the CB is immersed in

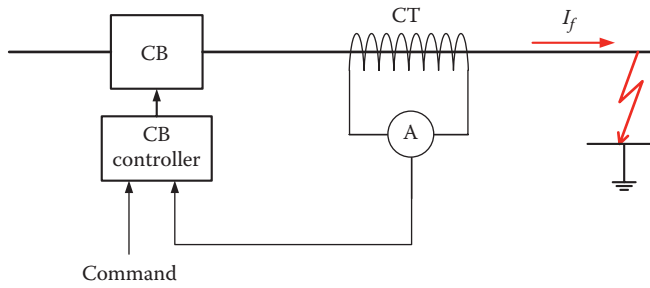


FIGURE 2.20 CB operation.



FIGURE 2.21 SF₆ CB.

a medium without oxygen and with good cooling property. Among these medium are oil and sulfur hexafluoride (SF₆). SF₆ is a colorless, odorless, nontoxic, non-flammable gas. It is not soluble in water and is higher in density than air. This is the most popular medium used today. A photo of an SF₆ breaker is shown in Figure 2.21. Other CBs, especially the ones used in distribution networks, are placed in vacuum containers to starve the arc from oxygen. Older models of CBs use air blast to blow high speed air through the arc. This prolongs the path of the arc, causing the arc to break.

The CB has two main settings: *tap setting* and *time dial setting*. The tap setting determines the level of current above which the CB is to open. Since most faults are temporary and can be cleared by themselves, the breakers are designed to wait a while before they initiate the opening. This delay time is the time dial setting. Because of all its complex features and the level of energy it can handle, the CB is among the most expensive equipment in the power grid. The power grid uses tens of thousands of CBs in the United States.

Another type of CB commonly used in distribution networks is the *recloser*. Reclosers are less expensive types of CBs with lower current ratings and slower action than substation CBs. They can interrupt fault currents and can automatically reclose after a momentary outage. However, if the fault is permanent, the recloser locks itself in the open positive after a preset number of reclosing operations occur.

Since most faults in the distribution networks are temporary, reclosers serve a very important role by automatically closing the circuit after a preset period of time. You probably have noticed its operation after an outage and have seen the power coming back and then go away again. This is a recloser closing the circuit then interrupting it again because the fault is still there.

2.6.4 DISCONNECTING SWITCHES

DSs are automatic or manually operating devices. In either case, they are not designed to interrupt a fault current and are less precise than CBs. They are normally used to isolate sections of the network. Take, for example, the case in Figure 2.22. The CB has one DS on each side. This is to allow workers to perform maintenance on the CB. The CB is first opened to interrupt the current. Then, the two DS are opened to isolate the CB from the grid. A photo of a disconnect switch is shown in Figure 2.23.

Another type of DS is the sectionalizer. This device is more sophisticated than the DS described earlier. Sectionalizers do not interrupt fault currents and are often used in conjunction with reclosers. They have counters that keep track of the number of times a recloser operates and can isolate sections of the network when the power is off. An example of operation is shown in Figure 2.24. The figure shows a recloser after the distribution transformer. Loads 1–3 are served by the recloser. A sectionalizer is installed between Loads 2 and 3. Assume that the recloser is designed to operate twice (two counts) and the sectionalizer is designed to operate once (one count). Assume a fault occurs in the line between Loads 2 and 3. The fault causes the recloser to open. The sectionalizer notices that the recloser is open. Assume that the fault is not cleared and the recloser is closed into the fault. The recloser will quickly open again as the fault is still there. The sectionalizer will know that the recloser is opened the second time. This is when the sectionalizer opens its contacts.

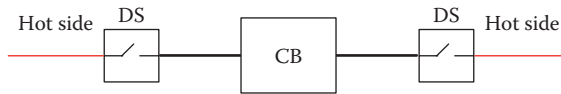


FIGURE 2.22 An application of DS.



FIGURE 2.23 Disconnect switch.

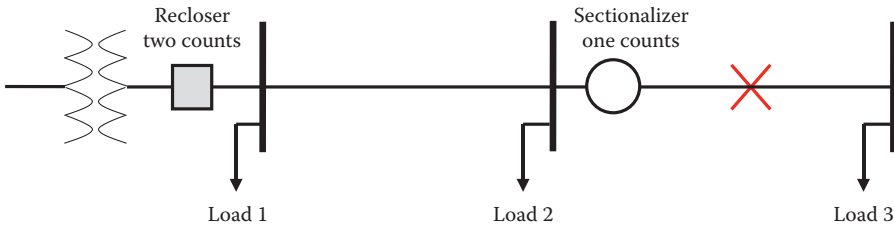


FIGURE 2.24 Operation of recloser and sectionalizer.

The next time the recloser closes the circuit, there is no fault seen by the recloser and Loads 1 and 2 are served. Because of this coordination, when the fault is permanent, we can isolate the section of the network with the fault and serve the rest of the customers.

2.6.5 SURGE ARRESTER

Switching of power lines and lightning strikes can cause excessive and sudden increase in voltage at the substations. This can lead to extensive damage to the insulation material inside expensive equipment such as transformers, insulators, CTs, and PTs. It can also cause arcing between components, leading to equipment failures. When a lightning strike reaches oil-immersed equipment, the heat produced by the lightning energy increases the pressure inside its housing. If the pressure reaches a high enough level, the housing could burst and an incredible fire could follow.

What makes this problem more severe is the fact that lightning is a wave that travels along the line at the speed of light. So when it is detected, it is often too late to react. To protect the vulnerable equipment, surge (or lightning) arresters are used in substations. These devices operate very similarly to the zener diode whose resistance is inversely proportional to the applied voltage as shown in Figure 2.25.

The surge arrester used in substations is often made of metal-oxide disks inside porcelain housing and is called metal-oxide varistor (MOV). The term “varistor” is a combination of two words: variable and resistor. The operation of the surge arrester is shown in Figures 2.26 and 2.27. The top end of the MOV is connected to the high-voltage terminal of the equipment to be protected. The lower end is connected to a good grounding system. During normal operations (see Figure 2.26), the arrester is seen as an open circuit due to its extremely high resistance at the nominal voltage. The line current in this case continues along the line as if the arrester does not exist. However, when

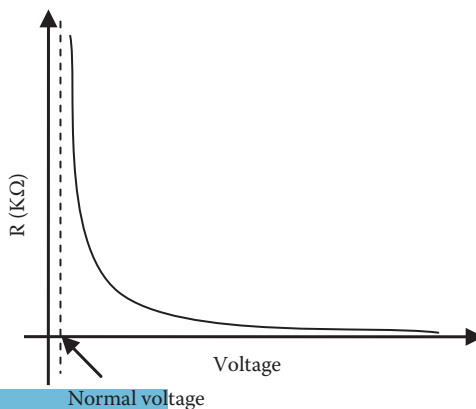


FIGURE 2.25 Resistance of surge arrester as function of applied voltage.

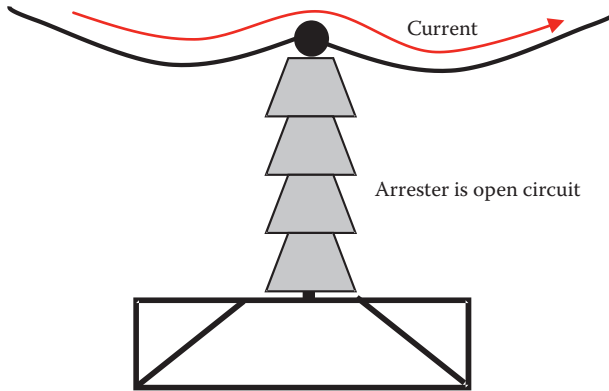


FIGURE 2.26 Surge arrester during normal voltage.

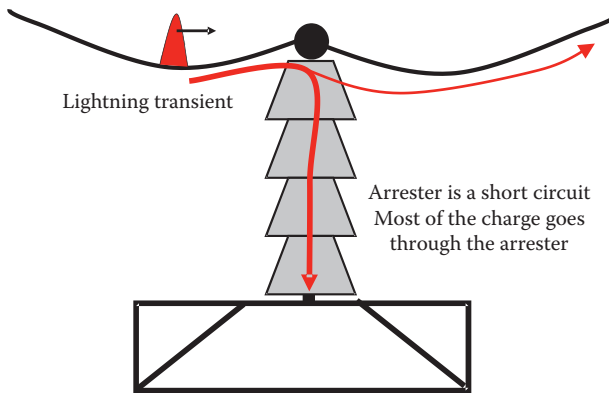


FIGURE 2.27 Surge arrester during surges.

lightning hits (see Figure 2.27), the excessive voltage of the bolt causes the resistance of the arrester to drop substantially making the surge arrester a short circuit path for the lightning current, thus dispersing almost all the energy of the bolt into ground and protecting all devices downstream from the lightning arrester.

In some cases, the surge arrester is mounted at the entrance of the transformer winding as shown in the photo in Figure 2.28. In areas with potentials for lightning storms, you may find the surge arrester installed on pole transformers.

2.7 CONTROL CENTERS

The stability and security of the power system must be maintained at all times to avoid any interruption of service to the customers or the collapse of the power system. The system must also be protected from being damaged due to the failure of any of its components or equipment. In addition, it must operate efficiently and economically to ensure the best rates to the customers. These are enormous tasks whose responsibility lies mainly with electrical engineers.

To effectively operate and control the power system, it must be extensively monitored at all times. All mechanical and electrical functions inside the power plants are monitored, evaluated, and controlled mostly in real time. All major equipment, such as substation transformers and transmission lines, are also extensively monitored and controlled. The various CBs in the network that switch the various lines and components as well as protecting the equipment during fault conditions are

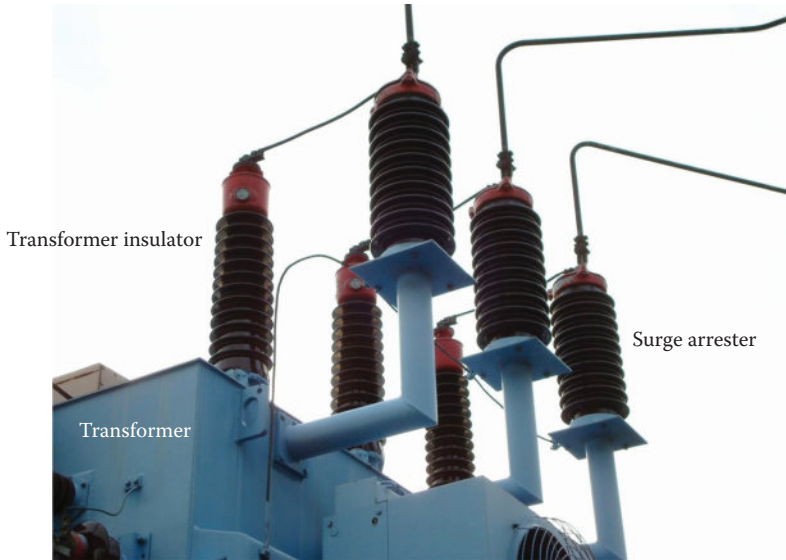


FIGURE 2.28 Surge arrester mounted on transformer.



FIGURE 2.29 Control center. (Image courtesy of Alstom Grid, Redmond, Washington.)

continuously checked for their status and their operations are often controlled remotely. Besides the extensive monitoring, engineers continuously evaluate the operation of the system, predict the future demand, and establish favorable energy trade conditions between utilities. These functions require the use of sophisticated algorithms that optimize the operation of the power system.

All these tasks are managed in the control center, which is the brain of the electric power system. One of these control centers is shown in Figure 2.29. It has a large mimic board, representing the main components of the power system such as transmission lines and CBs. The mimic board displays the current condition of the system such as the power flow in all lines and the status of each CB. Several operators (called system operators) are present at all times to monitor the power system and implement corrective actions should a problem arise. They also shift flows on transmission lines and circuits to ensure that all power system components operate within their specified voltage and

current ranges. When the system operates under normal conditions, system operators run several software to optimize the operation of the system, predict future demand and power flows, assess system stability, schedule generation, etc.

2.8 WORLDWIDE STANDARDS FOR HOUSEHOLD VOLTAGE AND FREQUENCY

The magnitude of the household voltage or frequency is not the same worldwide. This is mostly because of three reasons:

1. Due to the competition between the United States and Europe in the late 1800s and early 1900s, manufacturing companies in both continents have independently developed their power system equipment without coordinating their efforts.
2. Different safety concerns in Europe and the United States have led to various voltage standards.
3. Wiring and equipment costs have led nations to select the most economical voltage standards.

Table 2.1 shows the voltage and frequency standards in select countries. The voltage standard is for single-pole outlets used in most household appliances. In the United States, 120 V is used everywhere inside the house, except for heaters, dryers, and ovens where the receptacles are double-pole at 240 V. The various voltage and frequency standards worldwide have created confusion among consumers who wish to use equipment manufactured based on one standard in a country with a different standard. For example, the compressors of the refrigerators designed for 60 Hz standard can slow down by 17% when used in a 50 Hz system. Also, electrical equipment designed for 100 V standard will be damaged if it is used in 240 V systems. For small appliances, modern power electronics circuits have addressed this problem very effectively. Almost all power supplies for travel equipment (electric razors, portable computers, digital cameras, audio equipment, etc.) are designed to operate at all voltage and frequency standards.

TABLE 2.1
Standards for Voltage and Frequency in Several Nations

Country	Voltage (V)	Frequency (Hz)
Australia	230	50
Brazil	110/220	60
Canada	120	60
China	220	50
Cyprus	240	50
Egypt	220	50
Guyana	240	60
South Korea	220	60
Mexico	127	60
Japan	100	50 and 60
Oman	240	50
Russian Federation	220	50
Spain	230	50
Taiwan	110	60
United Kingdom	230	50
United States	120	60

2.8.1 VOLTAGE STANDARD

It appears that the 120 V was chosen somewhat arbitrarily in the United States. Thomas Edison came up with a high-resistance lamp filament that operated well at 120 V. Since then, the 120 V was selected in the United States. The standard for voltage worldwide varies widely from 100 V in Japan to 240 V in Cyprus. Generally, a wire is less expensive when the voltage is high; the cross section of the copper wires is smaller for higher voltages. However, from the safety point of view, lower voltage circuits are safer than higher voltage ones; 100 V is perceived to be less harmful than 240 V.

2.8.2 FREQUENCY STANDARD

Only two frequencies are used worldwide: 60 and 50 Hz. The standard frequency in North America, Central America, most of South America, and some Asian countries is 60 Hz. Almost everywhere else, the frequency is 50 Hz. In Europe, major manufacturing firms such as Siemens and AEG have established 50 Hz as a standard frequency for their power grids. Most of Asia, parts of South America, all of Africa, and the Middle East have adopted the same 50 Hz standard. In the United States, Westinghouse adopted the 60 Hz standard. Nikola Tesla actually wanted to adopt a higher frequency to reduce the size of the rotating machines, but 60 Hz was eventually selected for the following reasons:

- It is a high enough frequency to eliminate light flickers in certain types of incandescent lamps.
- It is conveniently synchronized with time.

Machines designed for 60 Hz can have less iron and smaller magnetic circuits than the ones designed for 50 Hz. In Japan, both frequencies are used: in Eastern Japan (Tokyo, Kawasaki, Sapporo, Yokohama, and Sendai), the grid frequency is 50 Hz and in Western Japan (Osaka, Kyoto, Nagoya, Hiroshima), the frequency is 60 Hz. The first generator in Japan was imported from Germany for the Kanto area during the Meiji era, and the frequency was 50 Hz. Subsequent acquisitions of power equipment were mainly from Europe and were installed in the eastern side of Japan making the frequency of the eastern grid 50 Hz. After World War II, Japan imported their power plants from the United States and installed them in the western side of the island (the first power plant was in the Kansai area). The western grid is thus operating at 60 Hz. The two frequency standards created two separate grids with the dividing line between them going from the Fuji River in Shizuoka upward to the Itoi River in Niigata. These two grids are not directly connected by an alternating current (ac) line, but are connected by direct current (dc) lines. On each end of the dc line, a power electronic system converts the ac frequency into dc.

It is interesting to know that for stand-alone systems, such as aircraft power systems, the frequency is 400 Hz. This is selected to reduce the size and weight of the rotating machines and transformers aboard the aircraft.

2.8.2.1 Frequency of Generating Plants

The frequency of the power system's voltage is directly proportional to the speed of the generators in the power plants (which is the same as the speed of the turbines). The relationship between the frequency and the speed, which is explained in detail in Chapter 12, is given in the following equation:

$$f = \frac{P}{120} n \quad (2.8)$$

where

n is the speed of the generator (rpm)

P is the number of magnetic poles of the field circuit of the generator

f is the frequency of the generator's voltage

One of the earliest ac generators was a 10-pole machine running at 200 rpm. The frequency of this generator, as explained by Equation 2.8, was $16 \frac{2}{3}$ Hz. This anomalous frequency was low enough to allow the series-wound dc motor to operate from ac supply without any modification. This was a justifiable reason because the series-wound motor was used extensively in locomotive tractions. However, this low frequency created noticeable flickers in incandescent lamps and was therefore rejected as a standard.

When the Niagara Falls power plant was built, the engineers used 12-pole generators running at 250 rpm, and the frequency was 25 Hz. The power plant was built to produce compressed air, and the low frequency was not a major concern. In the following developments, the frequency was raised to 40 Hz and then to 60 Hz to reduce the flickers.

2.8.2.2 Frequency of Power Grids

In the early days, generators operated independently without any connection between them. The typical system was composed of a single generator, feeders (transmission lines), and several loads. In such a system, the frequency can drift without any major impact on the stability of the system. In the 1940s, it became economically important to interconnect the generators by a system of transmission lines, and the power grid was born. The interconnections demanded that the frequency of the grid be fixed to a single value. If the frequencies of all generators are not exactly equal, the power system would collapse as explained in Chapter 14.

EXERCISES

- 2.1 What is the function of a power plant turbine?
- 2.2 What is the function of a power plant generator?
- 2.3 What is the function of the hydroelectric dam?
- 2.4 Why are transformers used with transmission lines?
- 2.5 A two-pole generator is to be connected to a 60 Hz power grid. Compute the speed of its turbine.
- 2.6 A two-pole generator is to be connected to a 50 Hz power grid. Compute the speed of its turbine.
- 2.7 Why are insulators used on power line towers?
- 2.8 Why are tower insulators built as disk shapes?
- 2.9 Why is the frequency of the airplane power system 400 Hz?
- 2.10 Why are there different voltage and frequency standards worldwide?
- 2.11 Why are transmission line towers higher than distribution line towers?
- 2.12 What are the various forces that an insulator must withstand?
- 2.13 Why are conductors made out of strands?
- 2.14 Why do some conductors have steel reinforcements?
- 2.15 What is corona?
- 2.16 How can corona be reduced?
- 2.17 Why do we bundle conductors?
- 2.18 Can we bundle 120 kV transmission lines?
- 2.19 What are the roles of shield wires?
- 2.20 Why are shield wires not installed on all transmission lines?
- 2.21 How is the lightning energy that strike power lines dissipated?
- 2.22 Why are series resistances not used to measure line voltage?
- 2.23 Why is the secondary of the CT shorted?
- 2.24 What is the main function of the CB?
- 2.25 What is the tap setting of the CB?
- 2.26 What is the time-dial setting of the CB?
- 2.27 What are the differences between a recloser and a CB?

- 2.28 Why are disconnect switches used in conjunction with the CBs?
- 2.29 What is the sectionalizer?
- 2.30 How is sectionalizer used in conjunction with reclosers?
- 2.31 What are the main problems associated with fault clearing?
- 2.32 Why are DSs and sectionalizers not suitable for fault clearing?
- 2.33 How to reduce the switching arc?
- 2.34 What is the function of the surge arrester?
- 2.35 Why are transformers often blown up when lightning strike reaches its terminals?
- 2.36 What are the main functions of the control center?
- 2.37 What is a mimic board?

3 Energy Resources

As shown in Figure 3.1, energy resources are often divided into three loosely defined categories:

1. Fossil fuel
2. Nuclear fuel
3. Renewable resources

Fossil fuels include oil, coal, and natural gas. Renewable energy resources include hydropower, wind, solar, hydrogen, biomass, tidal, and geothermal. All these resources can also be classified as primary and secondary resources. The primary resources are

1. Fossil fuel
2. Nuclear fuel
3. Hydropower

The secondary resources include all renewable energy minus hydropower. Over 99% of all electric energy worldwide is generated from the primary resources. The secondary resources, although increasing rapidly, have not yet achieved a level comparable to the primary resources.

In the subsequent statistics, three terminologies are used to describe electric energy: *generated energy*, *consumed energy*, and *installed capacity*. Generated energy is the amount of electrical energy produced at the power plant. This is equal to the consumed energy plus the losses in all power system equipment such as transformers and transmission lines. Installed capacity is the rated power of the power plant.

The distribution of electricity generated worldwide by primary resources is shown in Figure 3.2. Most of the electrical energy is generated by oil, coal, and natural gas. Hydroelectric energy is limited to about 6% of the world's electrical energy because of the limited water resources suitable for generating electricity. Nuclear energy is only 6% of the total electrical energy because of the public resistance to building new nuclear facilities in the past 20 years.

In the United States, about 4125 TWh of electrical energy was generated in 2010. Most of it is generated by fossil fuel as depicted in Figure 3.3. Because of its abundance, coal is by far the prevailing source of electric energy in the United States (1847 TWh). Actually, the United States has the largest coal reserve among all other countries. After coal, comes natural gas (988 TWh) and nuclear (807 TWh). Unfortunately, secondary resources produce only 427 TWh (about 10%). Some attribute this low percentage to the low cost of electricity in the United States.

Figure 3.4 shows the estimated worldwide consumption of electrical energy in 2000 and 2010. In 2010, the world's electric energy consumption was about 17,444 TWh, of which the United States consumed about 23.6% (4120 TWh). Notice the rapid increase of consumption in Asia. This is attributed mainly to the emerging economies of China and India. The rest of the world in the figure includes Eurasia, Canada, Mexico, and Africa.

The installed capacities of power plants worldwide in 2000 and 2010 are shown in Figure 3.5. The installed capacity of the world's plants in 2000 was about 3455.45 GW, and in 2010 it was about 4624.77 GW. The capacity of the United States was 811.72 GW in 2000 and 1010 GW in 2010, an increase of about 24%. In Asia and Oceania, the capacity in 2000 was 972.32 GW and about 1632.32 GW in 2010. This is an amazing almost 70% increase in a decade due to the accelerated

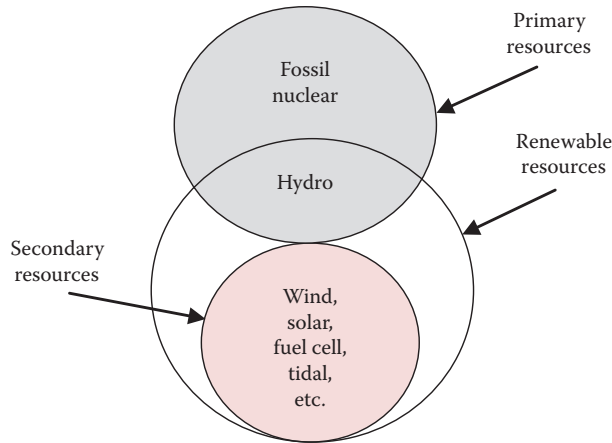


FIGURE 3.1 Energy resources.

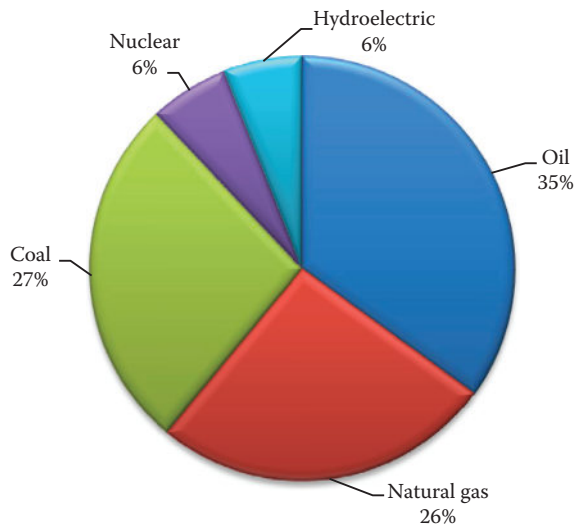


FIGURE 3.2 Primary resources used to generate electricity worldwide in 2010. (From U.S. Energy Information Administration, Washington, DC.)

installation of power plants to support the societal needs and the rapid industrial developments in the region, particularly in China and India.

Example 3.1

Compute the annual electrical energy consumption per capita worldwide in 2010.

Solution

According to the U.S. Census Bureau, the world population by the end of 2010 was about 6.89×10^9 people.

Annual electric energy consumed per capita worldwide = Total world consumption/world population = $17.444 \times 10^{12} / 6.89 \times 10^9 = 2.53$ MWh.

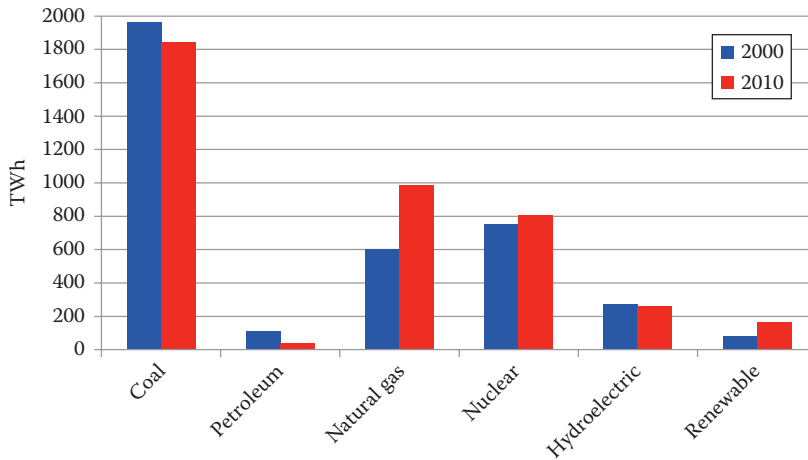


FIGURE 3.3 Primary resources used to generate electricity in the United States. (From U.S. Energy Information Administration, Washington, DC.)

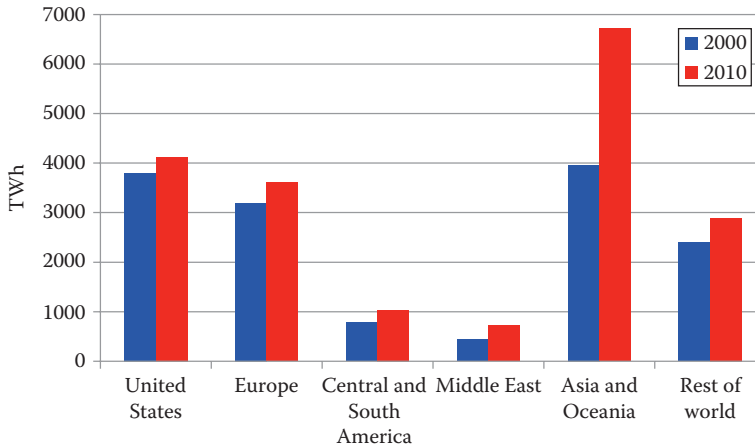


FIGURE 3.4 Consumed electricity worldwide. (From U.S. Energy Information Administration, Washington, DC.)

Example 3.2

Repeat the previous example but exclude the consumption of the United States.

Solution

The world consumption minus the consumption of the United States = $(17.444 - 4.12) \times 10^{12} = 13.324 \times 10^{12}$ kWh.

According to the U.S. Census Bureau, the U.S. population by the end of 2010 was about 310×10^6 people.

The world population minus the population of the United States = $(6.89 - 0.31) \times 10^9 = 6.58 \times 10^9$ people.

Annual electric energy consumed per capita worldwide excluding the United States = Total world consumption minus the consumption of the United States/world population minus the population of the United States = $13.324 \times 10^{12} / 6.58 \times 10^9 = 2.025$ MWh.

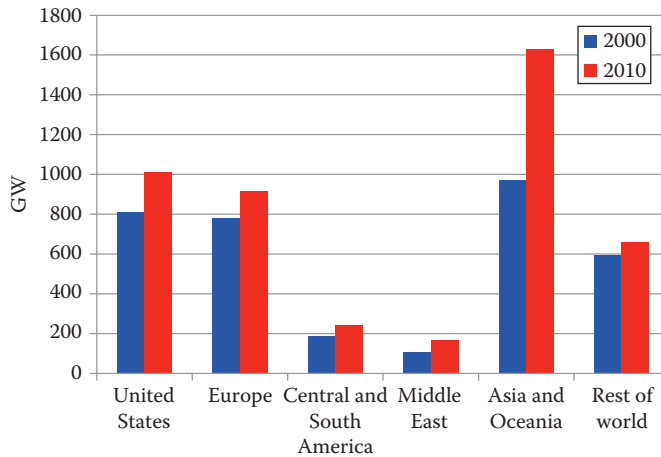


FIGURE 3.5 Installed capacity of electric power plants. (From U.S. Energy Information Administration, Washington, DC.)

Example 3.3

Compute the annual electric energy consumed per capita in the United States in 2010. Compare the result with the average of the rest of the world.

Solution

Annual electric energy consumed per capita in the United States = Total consumption in the United States / the U.S. population = $4.12 \times 10^{12} / 3.1 \times 10^8 = 13.29$ MWh.

Annual electric energy consumed per capita in the United States / annual electric energy consumed per capita worldwide excluding the United States = $13.29 / 2.025 = 6.56$ MWh.

In 2010, the average person in the United States consumed more than six times the electrical energy consumed by the average person in the rest of the world. This high consumption is not just attributed to the luxurious lifestyle in the United States, but is also due to the United States' highly industrial base. Repeat the example for France and draw a conclusion.

3.1 FOSSIL FUEL

Fossil fuels are formed from fossils (dead plants and animals) buried in the earth's crust for millions of years under pressure and heat. They are composed of high carbon and hydrogen elements such as oil, natural gas, and coal. Because the formation of fossil fuels takes millions of years, they are considered nonrenewable.

Since the start of the Industrial Revolution in Europe in the nineteenth century, the world became extremely dependent on fossil fuels for its energy needs. The bulk of fossil fuels are used in transportation, industrial processes, generating electricity, as well as for residential and commercial heating.

The use of fossil fuels to generate electricity has always been a subject of much debate. Burning fossil fuels causes widespread pollution, which includes the release of carbon dioxide and sulfur oxide into the environment and the formation of nitrogen oxide. These are harmful gases that cause health and environmental problems as discussed in Chapter 5. Moreover, the availability and price

of fossil fuels often fluctuate due to political tensions between nations. Oil production and distribution are especially vulnerable, often being interrupted during wartime or during periods of political tensions.

3.1.1 OIL

Oil is the most widely used fossil fuel worldwide. It is also called *petroleum*, which is composed of two words “petro” and “oleum.” The first is a Greek word for rock and the second is a Latin word for oil. Petroleum is extracted from fields with layers of porous rocks filled with oil. The Chinese discovered oil as early as AD 300. They used bamboo tubes to extract oil that might have been used as a medical substance. In the twelfth century, the famous traveler, Marco Polo, while in Persia near the Caspian Sea, observed a geyser gushing black substance used by the inhabitants to provide heat and light. However, it was not until the fifteenth century that oil was first commercialized in Poland and used to light streetlamps.

In the mid-eighteenth century, the first oil wells in North America were drilled in Ontario, Canada, and Pennsylvania, USA. Around 1870, John D. Rockefeller formed Standard Oil of Ohio, which eventually controlled about 90% of the U.S. refineries. In the early nineteenth century, oil was discovered in several Middle Eastern countries as well as Central and South America.

Today, oil is used mainly in the transportation and industrial sectors as seen in Figure 3.6. The generation of electrical energy uses only 6% of the total oil consumed annually. This is mainly because coal is a much cheaper option for generating electricity.

The proven oil reserve worldwide, as of the end of 2010, was about 1.341×10^{12} Barrel, mainly in the Middle East as seen in Figure 3.7. The world consumption of oil in 2010 was about 85.7×10^6 Barrel/day distributed as seen in Figure 3.8. The highest consumers of oil in 2010 were China (25.8 Barrel/day), the United States (19.18 Barrel/day), and Europe (15.32 Barrel/day). This high rate of consumption is troubling, and new fields must always be discovered before the available supply dries out.

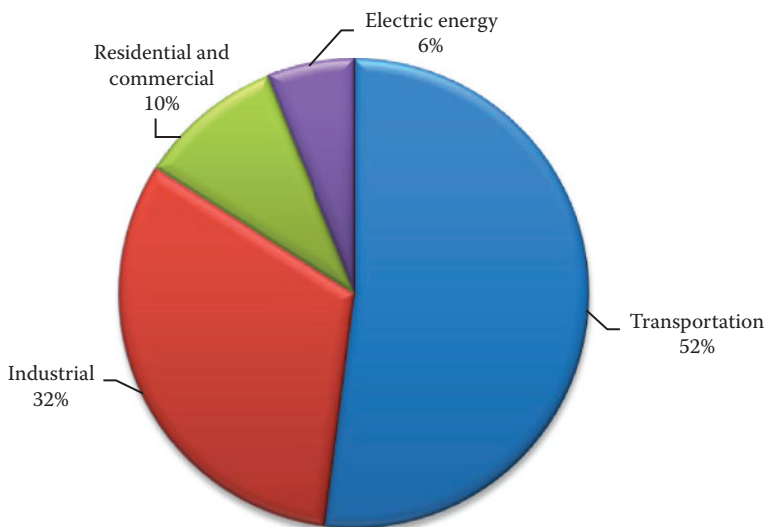


FIGURE 3.6 Consumption of oil worldwide by sectors in 2010. (From U.S. Energy Information Administration, Washington, DC.)

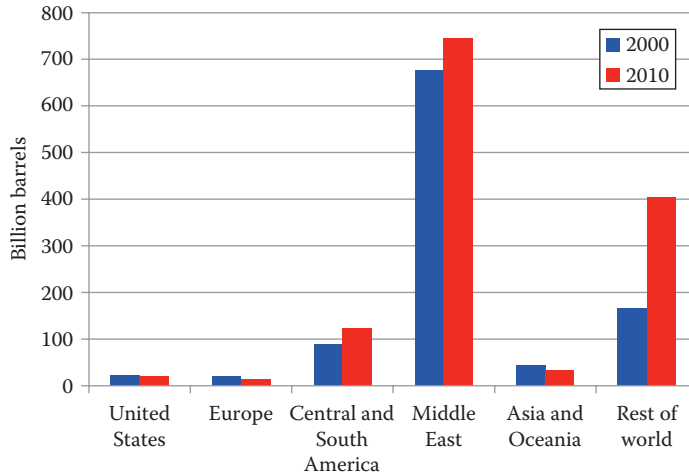


FIGURE 3.7 Oil reserves worldwide. (From U.S. Energy Information Administration, Washington, DC.)

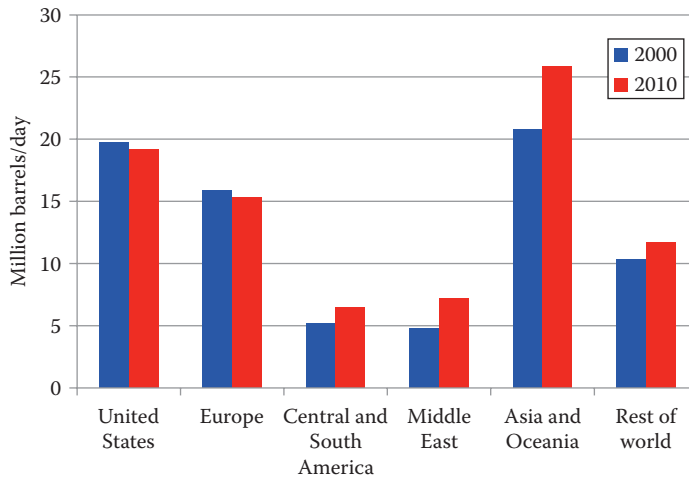


FIGURE 3.8 Oil consumption worldwide. (From U.S. Energy Information Administration, Washington, DC.)

Example 3.4

Assume no new oil field is discovered; for how long can we maintain the consumption of oil at the 2010 rate?

Solution

The world's known oil reserve is 1.341×10^{12} Barrel, and the daily world consumption is 85.7×10^6 Barrel.

Annual world consumption = $85.7 \times 10^6 \times 365 = 3.128 \times 10^{10}$ Barrel.

Hence, the world reserve will last for $1.341 \times 10^{12} / 3.128 \times 10^{10} = 42.87$ years.

This is a disturbingly short period.

3.1.2 NATURAL GAS

Although natural gas was discovered in Pennsylvania as early as 1859 by Edwin Drake, it was not utilized commercially because the process of liquefying natural gas at low temperatures was unknown before the nineteenth century. Natural gas was then considered a by-product of crude oil extraction and was often burned out in the fields. After the discovery of large reservoirs of natural gas in Wyoming in 1915, the United States developed cryogenic liquefaction methods and reliable pipeline systems for the storage and transportation of natural gas. In the 1920s, Frank Phillips (the founder of Phillips Petroleum) commercialized natural gas in the forms of propane and butane.

The distribution of the world's reserve of natural gas is shown in Figure 3.9. The data in the figure does not include the shale gas which is possible to extract with modern fracking techniques. The proven world reserve as of 2010 was about $1.78 \times 10^{14} \text{ m}^3$. The majority of this reserve is in Russia and the Middle East. The 2010 proven reserve in the United States was $7.71 \times 10^{12} \text{ m}^3$, which is about 4.3% of total world reserve.

In 2010, the world consumed about $3.27 \times 10^{12} \text{ m}^3$ of natural gas; the distribution is shown in Figure 3.10. The majority of consumed natural gas was in North America and Europe; the United States alone consumed about $6.8 \times 10^{11} \text{ m}^3$. About 32% of the natural gas production worldwide is used to generate electricity and 44% is used in the industrial sector.

Example 3.5

Assume no new natural gas field is discovered in the United States; for how long can the United States be self-sustained at the 2010 consumption rate?

Solution

The known reserve of natural gas in the United States as of 2010 was $7.71 \times 10^{12} \text{ m}^3$.

The U.S. consumption in 2010 was $6.8 \times 10^{11} \text{ m}^3$.

Hence, the reserve in the United States can sustain the 2010 consumption rate for $7.71 \times 10^{12} / 6.8 \times 10^{11} = 11.34$ years.

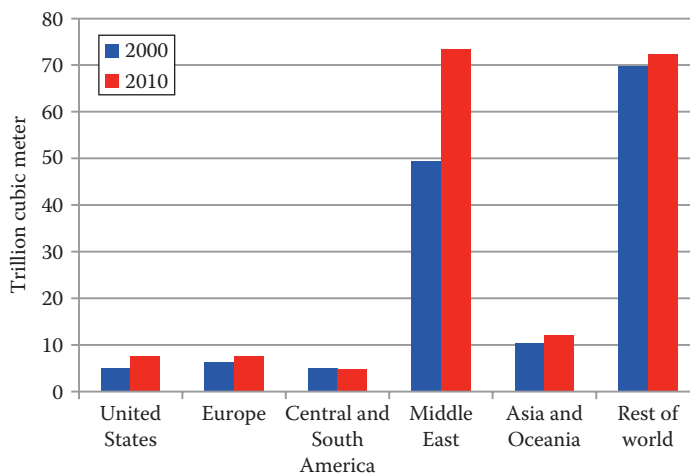


FIGURE 3.9 Known natural gas reserves. (From U.S. Energy Information Administration, Washington, DC.)

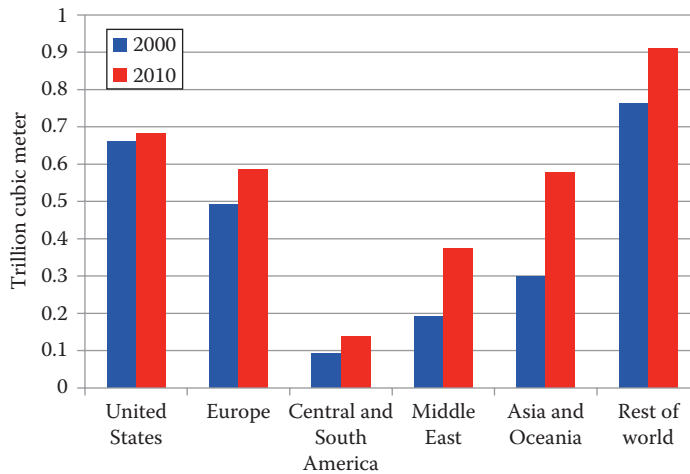


FIGURE 3.10 Consumption of natural gas worldwide. (From U.S. Energy Information Administration, Washington, DC.)

Example 3.6

Assume no new natural gas field is discovered worldwide; for how long will the natural gas last?

Solution

The known reserve of natural gas in the world as of 2010 was $1.78 \times 10^{14} \text{ m}^3$.

The world consumption in 2010 was $3.27 \times 10^{12} \text{ m}^3$.

Hence, the world reserve can sustain the 2010 consumption rate for $1.78 \times 10^{14} / 3.27 \times 10^{12} = 57.18$ years.

3.1.3 COAL

Charcoal, the black porous carbon substance produced by burning wood, is one of the earliest sources of heat and light known to man. Five thousand years ago, the ancient Egyptians used charcoal for cooking, heating, baking, and pottery as well as for liquefying metals such as gold.

Coal is another form of the carbonized vegetation formed by geological activity, heat, and pressure in the carboniferous period millions of years ago. Coal was widely used in England during the twelfth century. However, as people burned coal in closed quarters without adequate ventilation, a large number of people were poisoned from the carbon monoxide released from burning coal. Consequently, King Edward I imposed the death penalty upon anyone caught burning coal. The ban lasted for two centuries.

In the seventeenth century, English scientists discovered that coal actually burned cleaner and produced more heat (two to four times) than wood charcoal. This discovery started intense exploration of coal worldwide to provide Europe with the energy needed to power its industrial revolution. Because of coal, the Scottish inventor and mechanical engineer James Watt invented the steam engine that propelled ships, drove trains, and powered industrial machines. Coal was later used in the 1880s to generate electricity.

In the United States, the French explorers Louis Joliet and Jacques Marquette discovered coal in Illinois in 1673. This discovery was followed by many more in Kentucky, Wyoming, Pennsylvania, West Virginia, and Texas. Today, the largest sources of coal in the United States are in Wyoming and West Virginia.

The world reserve of coal as of 2010 was estimated at about 9.4×10^{11} ton distributed as shown in Figure 3.11. The U.S. reserve is 2.6×10^{11} ton (about 28% of the world reserve).

The world consumption of coal in 2010 was about 7.99×10^9 ton. The distribution of the consumption is shown in Figure 3.12. In United States, 1.05×10^9 ton of coal was consumed. Asia and Oceania are the largest consumers of coal (5.19×10^9 ton). China is the major user of coal for generating electricity. In North America and Europe, the consumption of coal is very high, but the dependency on coal for the production of electricity is reduced because of the wider use of natural gas.

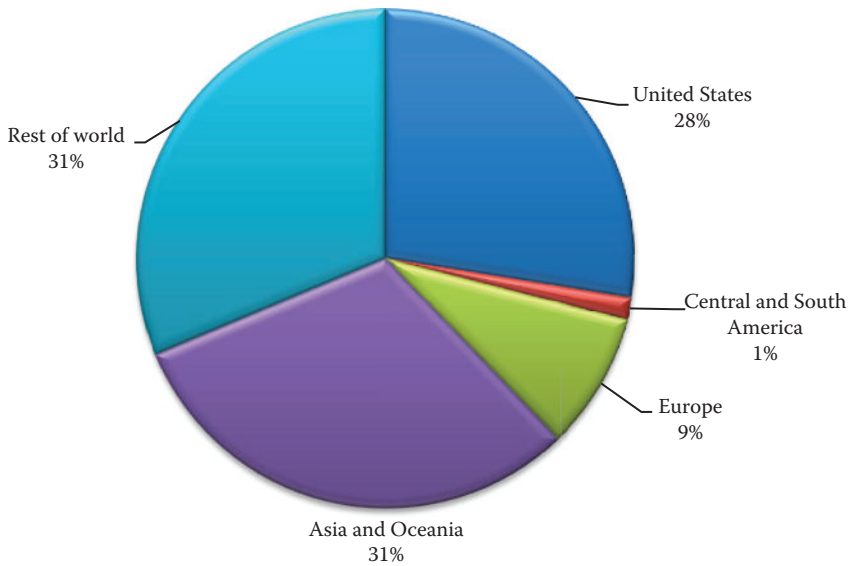


FIGURE 3.11 World's coal reserve as of 2010. (From U.S. Energy Information Administration, Washington, DC.)

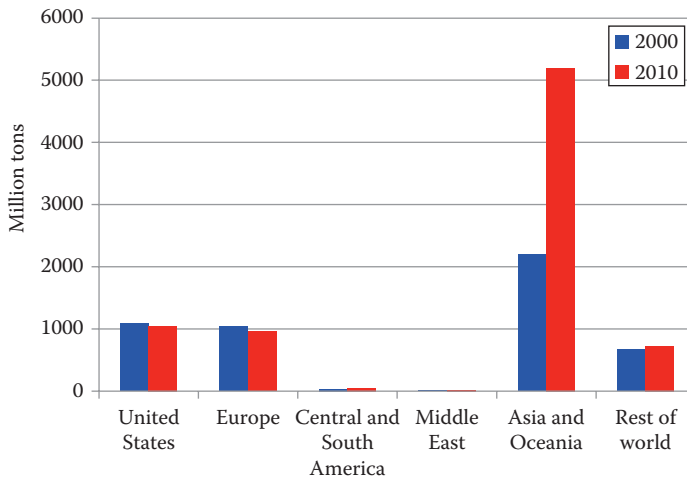


FIGURE 3.12 Consumption of coal worldwide. (From U.S. Energy Information Administration, Washington, DC.)

3.2 NUCLEAR FUEL

Nuclear fuel is heavy-nuclei material that releases energy when its atoms are forced to split and in the process some of its mass is lost. The nuclear fuel used to generate electricity is mostly uranium (U), but plutonium (Pu) is also used. Uranium is found in nature and contains several isotopes. Natural uranium is almost entirely a mixture of three isotopes, ^{234}U , ^{235}U , and ^{238}U , where the superscript numbers indicate the atomic mass of the isotopes. The concentration of these isotopes in natural uranium is 99.2% for ^{238}U and 0.7% for ^{235}U . However, only ^{235}U can fission in nuclear reactors. Since the concentration of ^{235}U in uranium ores is very low (0.7%), an enrichment process is used to increase its concentration in nuclear fuel. For nuclear power plants, ^{235}U concentration is about 3%–5%, and for nuclear weapons, it is over 90%.

The data for uranium production are not freely available for political and security reasons. However, the world's production was estimated at 41,230 ton in 2010. The largest producers of uranium are Canada (about 10,260 ton), Australia (about 7,850 ton), Niger, Namibia, Russia and the former Soviet Union states, and the United States. The U.S. production of uranium is estimated at 2030 ton annually in 2010.

Plutonium is the other nuclear fuel used to generate electricity, but it is less common than uranium. Minute amounts of plutonium can also be found naturally. So it is mainly a man-made element, which was discovered by a group of scientists from the University of Berkeley in 1941. They found that plutonium is created when ^{238}U absorbs a neutron to become ^{239}U and ultimately decays to ^{239}Pu . Plutonium is produced in breeder reactors, and it has three common isotopes: ^{238}Pu , ^{239}Pu , and ^{240}Pu . The other plutonium isotopes are created by different combinations of uranium and neutron. The isotope ^{239}Pu is used in nuclear weapons and ^{238}Pu is used in nuclear power plants. In some cases, ^{238}Pu is mixed with uranium to form a mixed-oxide fuel that increases the power plant output.

Another use of plutonium is in stand-alone power systems such as the ones installed in satellites. In addition, a minute amount of plutonium can provide long-lasting power for medical equipment such as pacemakers.

The consumption of nuclear fuel worldwide is distributed as shown in Figure 3.13. The world consumption of nuclear fuel in 2010 was about 7.03×10^8 toe (oil equivalent ton). Europe and the United States led the world in the amount of nuclear fuel used to generate electricity. The United States consumed about 2.1×10^8 ton of nuclear fuel in 2010.

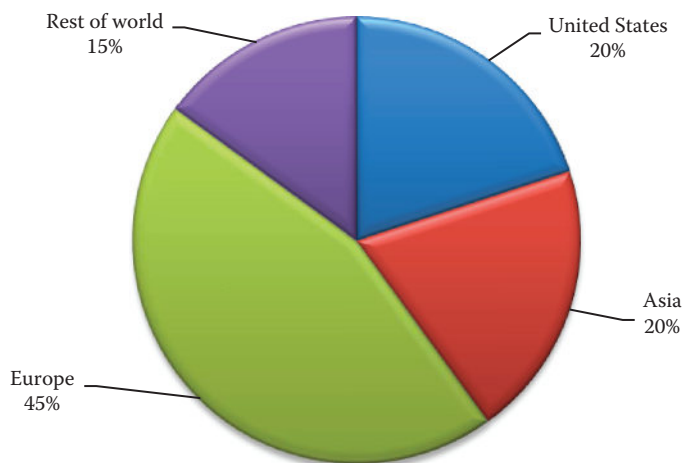


FIGURE 3.13 Consumption of nuclear fuel worldwide. (From statistical review of world energy, British Petroleum.)

EXERCISES

- 3.1 Exclude the United States and compute the generation capacity of the rest of the world. Find the world's per capita capacity.
- 3.2 Compute the generation capacity per capita in the United States. Compare the result with the world average.
- 3.3 Exclude the United States and compute the annual world consumption of electrical energy per capita. Compare the result with the U.S. consumption per capita.
- 3.4 Find the ratio of the electrical energy generation capacity to the electrical energy consumed in the United States. Identify the amount of surplus or deficit.
- 3.5 Exclude the United States and find the ratio of the electrical energy generation capacity to the electrical energy consumed worldwide. Identify the amount of surplus or deficit.
- 3.6 Assume the demand in the United States is increasing at a rate of 5% annually. For how long can the United States be self-sustained with respect to electric energy without constructing new generating plants?

4 Power Plants

The vast majority of electricity generated worldwide (about 99%) is generated from power plants using primary energy resources: hydropower, fossil fuel, and nuclear fuel. The descriptions of the power plants that use primary resources are covered in this chapter, and the methods to generate electricity from secondary resources (solar, wind, geothermal, etc.) are discussed in Chapter 6.

The geological and hydrological characteristics of the area where the power plant is to be erected determine, to a large extent, the type of the power plant. For example, fossil fuel power plants in the United States are concentrated mainly in the east and Midwest regions where coal is abundant. Similarly, hydroelectric power plants are concentrated in the northwest region where water and water storage facilities are available. Nuclear power plants, however, are distributed in all regions since their demand for natural resources is limited to the availability of cooling water.

The percentage of energy produced worldwide by primary resources is given in Chapter 3. The data in that chapter show that fossil fuels are the main source of electric energy (over 80%), and about 63% of the electric energy is produced by coal and oil-fired power plants. In the United States, coal counts for about 50% of the fuel used to generate electricity.

4.1 HYDROELECTRIC POWER PLANTS

“Hydro” is a Greek word meaning water. “Hydropower” means the power in the moving water, and hydroelectric is the process by which hydropower is converted into electricity. The hydroelectric power plant harnesses the energy of the hydrologic cycle. Water from oceans and lakes absorbs solar energy and evaporates into air forming clouds. When the clouds become heavy, rains and snows occur. The rain and melted snow travel through streams and eventually end up in oceans. The motion of water toward oceans is due to its kinetic energy (KE), which can be harnessed by the hydroelectric power plant that converts it into electrical energy. If water is stored at high elevations, it possesses potential energy (PE) proportional to that elevation. When this water is allowed to flow from a higher elevation to a lower one, the energy is converted into electrical energy by hydroelectric power plants.

The world’s first hydroelectric power plant was constructed across the Fox River in Appleton, Wisconsin, and began its operation on September 30, 1882. The plant generated only 12.5 kW, which was enough to power two paper mills and the private home of the mill’s owner. The latest and largest hydroelectric power plant, so far, is the one being built in China’s Three Gorges, which has a capacity of 22.5 GW. Some of the world’s largest hydroelectric power plants are given in Table 4.1.

4.1.1 TYPES OF HYDROELECTRIC POWER PLANTS

The common types of hydroelectric power plants are impoundment hydroelectric, diversion hydroelectric, and pumped storage hydroelectric power plants.

1. *Impoundment hydroelectric*: It is the most common type of hydroelectric power plant and is suitable for large generations. The dam in these power plants creates a reservoir at a high elevation behind the dam. A good example is the Grand Coulee Dam shown in Figure 4.1.

TABLE 4.1**World's Largest Hydroelectric Power Plants**

Name of Dam	Location	Capacity (GW)	Year of Completion
Three-Gorges	China	22.5	2010
Itaipu	Brazil/Paraguay	14	1983
Guri	Venezuela	10	1986
Tucuruí	Brazil	8.37	1984
Grand Coulee	Washington	7.0	1942
Sayano-Shushenskaya	Russia	6.4	1989
Krasnoyarsk	Russia	6	1968
Churchill Falls	Canada	5.43	1971
La Grande 2	Canada	5.33	1979
Bratsk	Russia	4.5	1961



FIGURE 4.1 The Grand Coulee dam and Franklin D. Roosevelt lake. (Image courtesy of U.S. Army Corps of Engineers, Louisville, KY.)

2. *Diversion hydroelectric*: An example of a diversion hydroelectric power plant is shown in Figure 4.2. Strong currents of rivers are utilized by low head turbines to generate electricity. This hydroelectric plant does not require a water reservoir at high elevation, so its generating capacity is less than that for the impoundment hydroelectric power plant.
3. *Pump storage hydroelectric*: A pump storage hydroelectric power plant operates as a dual-action water flow system. When the power demand is low, electricity is used to pump water from the lower water level in front of the dam to the higher water level behind the dam. This increases the PE behind the dam for later use.

Hydroelectric power plants are classified based on their size. If the plant is more than 100 MW, it is considered large. The medium size is 15–100 MW, the small size is 1–15 MW, the mini size is 100 kW–1 MW, and the micro size is 5–100 kW.



FIGURE 4.2 Fox River diversion hydroelectric power plant, Wisconsin. (Image courtesy of U.S. Army Corps of Engineers, Louisville, KY.)

4.1.2 IMPOUNDMENT HYDROELECTRIC POWER PLANTS

A typical impoundment hydroelectric power system has six key components: dam, reservoir, penstock, turbine, generator, and governor. A schematic of a hydroelectric power plant is shown in Figure 4.3.

1. **Dam:** It is a barrier that prevents water from flowing downstream, thus creating a lake behind the dam. The PE of the water behind the dam is directly proportional to the volume and height of the lake. The dam can be enormous in size; the Grand Coulee dam in

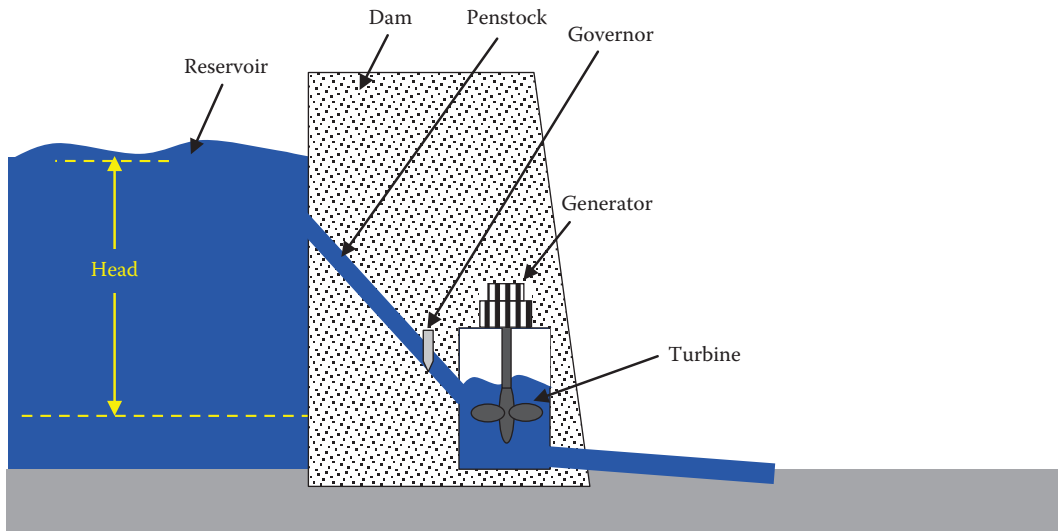


FIGURE 4.3 Simple schematic of hydroelectric power plant.

TABLE 4.2
Comparative Data on Two Large Hydroelectric Dams

	Grand Coulee Dam	Three Gorges Dam
Length of dam	1.6 km	2.34 km
Height of dam	170 m	185 m
Width at river base	150 m	115 m
Width at crest	9 m	40 m
Volume of concrete	$9.16 \times 10^6 \text{ m}^3$	$28 \times 10^6 \text{ m}^3$
Surface area of reservoir behind dam	320 km ²	72,128 km ²

Washington State, USA is 170 m in height, 1.6 km in length, and its crest is 9 m wide. Its base is 150 m wide, which makes the base about four times as large as the base of the Great Pyramid of Egypt. The volume of the concrete used to build the dam is almost $9.16 \times 10^6 \text{ m}^3$. Although massive, the Grand Coulee is not the biggest dam in the world. The Three Gorges Dam in China is the biggest dam ever built so far, followed by the Itaipu Dam in Brazil. Table 4.2 shows some structural data of the Grand Coulee and the Three Gorges dams.

2. *Reservoir*: The dam creates a lake behind its structure called a reservoir and often covers a wide area of land. The Grand Coulee dam created the Franklin D. Roosevelt artificial lake shown in Figure 4.1, which is about 250 km long, and has over 800 km of shore line. Its surface area is about 320 km², the depth of the lake ranging from 5 to 120 m.
3. *Penstock*: It is a large pipeline that channels water from the reservoir to the turbine. Figure 4.4 shows the penstock of the Grand Coulee dam during its construction. The water flow in the penstock is controlled by a valve called *governor*.

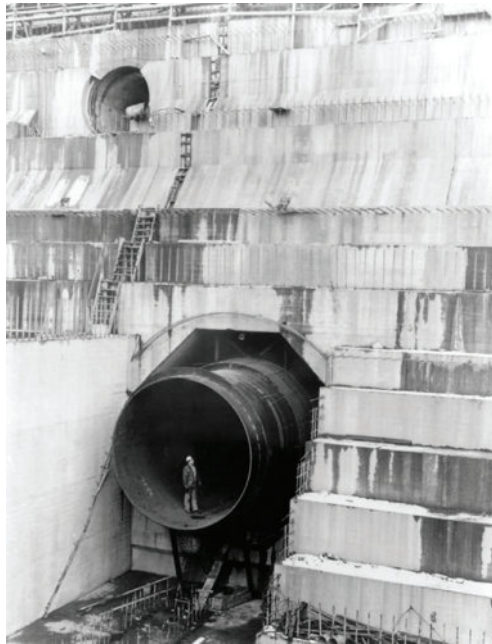


FIGURE 4.4 Penstock of Grand Coulee Dam. (Image courtesy of U.S. Bureau of Reclamation, Washington, DC.)



FIGURE 4.5 Hydroelectric turbine-generator units at the lower granite power plant, Walla Walla, Washington. (Image courtesy of U.S. Army Corps of Engineers, Louisville, KY.)

4. *Turbine*: A turbine is an advanced water wheel. The high pressure water coming from the penstocks pushes against the blades of the turbine causing the turbine shaft to rotate. The electrical generator is mounted directly on the same shaft of the turbine, thus the generator rotates at the speed of the turbine. There are mainly two types of turbines: impulse and reaction. For these two types, there are three fundamental designs used in most hydroelectric power plants: Pelton (impulse), Francis (reaction), and Kaplan (reaction). Pelton turbines are designed for high water heads (50–1300 m) and relatively low flows. The Francis turbines are suitable for low to medium heads (10–350 m). The Kaplan turbines (which are also known as propeller turbines) are suitable for low heads (less than 40 m) and high flow rates. The photo in Figure 4.5 shows several turbine-generator units in a power plant.
5. *Generator*: It is an electromechanical converter that converts the mechanical energy of the spinning turbine into electrical energy. The generators used in all power plants are of the synchronous machine type. The generator is equipped with various control mechanisms such as the excitation control and various stabilizers to maintain the voltage constant and to ensure that the generator's operation is stable.
6. *Governor*: It is the valve that regulates the flow of water in the penstock. When it is fully open the KE of the water is at its maximum. If the system is to shut down, the valve is closed fully.

The amount of the generated electric energy of the impoundment hydroelectric power plant depends on several parameters. The most important ones are as follows:

- Water head behind the dam
- Reservoir capacity
- Flow rate of the water inside the penstock
- Efficiencies of system components such as penstock, turbine, and generator

4.1.2.1 Impulse Turbine

According to Newton's first law, the force that moves an object at constant speed is equal to the net force applied on the object. The second law states that the net force is equal to the change in the object's momentum during a period of time

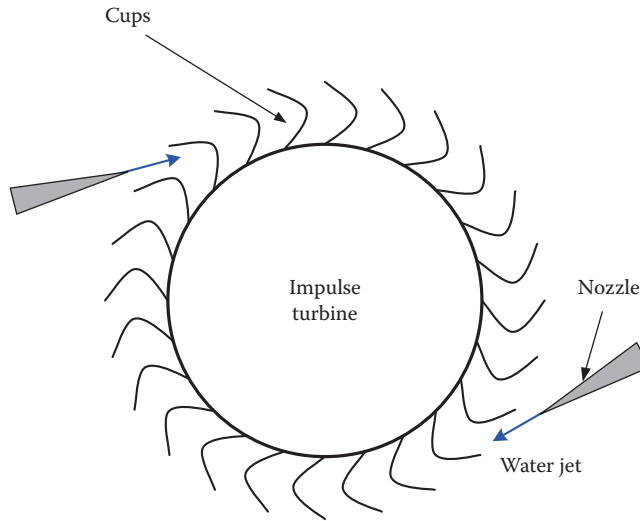


FIGURE 4.6 Impulse turbine.

$$F = \frac{\Delta M}{t} \quad (4.1)$$

where

F is the net force applied on the object (N)

M is the momentum of the object (kg m/s)

t is a time period (s)

$$M = mv \quad (4.2)$$

where

m is the mass of the object (kg)

v is the velocity of the object (m/s)

Equations 4.1 and 4.2 explain the operation of the impulse turbine. But first, let us describe the impulse turbine depicted in Figure 4.6. The turbine has buckets that look like cups mounted on a rotating wheel (known as runner). When water hits the cups, the turbine rotates according to the momentum gained by the cups. If the bucket is made out of a single cup, not all the momentum in the water jets is utilized. This is because water splashes in all directions after striking the cup. Instead, there are two cups attached together as shown in Figure 4.7. This way, when water jet hits the center area between the attached cups, the direction of the splash becomes opposite to the direction of the incident jet. When the water jet reaches the cup at speed v_i , the splash is reflected at speed v_r in the opposite direction. This simple design improves the efficiency of the system as seen in the following analyses.

In the steady-state condition, Figure 4.7, the speed of a cup (v_c) is a function of the net force applied on the cups (net momentum gained by the cups). Using the cup as our reference frame, the momentum in the water jet (M_d) that is acquired by the cup is a function of the speed of the water jet with respect to the speed of the cup this is the relative speed between v_i and v_c . Since both velocities are in the same direction, the relative speed is the subtraction of the two velocities

$$M_a = m_i (v_i - v_c) \quad (4.3)$$

where m_i is the mass of the water in the jet

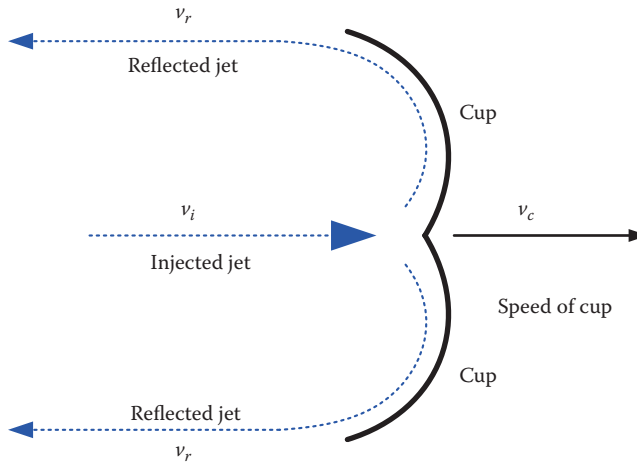


FIGURE 4.7 Water and cup velocities.

The momentum lost due to the reflected water (M_r) is also a function of the relative speed between v_r and v_c . Since the velocities are in opposite direction, the relative speed is the addition of the two

$$M_r = m_r (v_r + v_c) \tag{4.4}$$

where m_r is the mass of the reflected water, which is equal to m_i . Hence, the cup captures the net momentum which is the acquired momentum from the injected water minus the lost momentum due to the reflected waters

$$\Delta M = M_a - M_r = m_i (v_i - v_r - 2v_c) \tag{4.5}$$

It is reasonable to assume that the speed of the injected and reflected waters at the surface of the cups is equal in magnitude and opposite in direction

$$v_r = -v_i \tag{4.6}$$

Hence, Equation 4.5 can be written as

$$\Delta M = 2m_i (v_i - v_c) \tag{4.7}$$

Applying the value of the momentum in Equation 4.7 into Equation 4.1, we get the net force on the cup (F_c)

$$F_c = \frac{\Delta M}{t} = 2 \frac{m_i}{t} (v_i - v_c) \tag{4.8}$$

The power acquired by the cup (P_c) is then

$$P_c = F_c v_c \tag{4.9}$$

or

$$P_c = 2 \frac{m_i}{t} (v_i - v_c) v_c \quad (4.10)$$

From Equation 4.10, the relative speed is very important factor in optimizing the power captured by the cup. To compute the maximum possible power, we set the derivative of P_c with respect to v_c to zero.

$$\frac{\partial P_c}{\partial v_c} = 0 \quad (4.11)$$

Thus, the maximum power occurs when

$$v_i = 2v_c \quad (4.12)$$

Because the speed of the turbine (v_c) determines the frequency of the output voltage, hydroelectric turbines operate at constant speed known as synchronous speed. Therefore, v_c is always constant and we can achieve maximum power if the speed of the injected water is double the speed of the turbine.

Substituting Equation 4.12 into 4.10, we get the maximum power ($P_{c\text{-max}}$)

$$P_{c\text{-max}} = \frac{1}{2} \frac{m_i}{t} v_i^2 \quad (4.13)$$

And the maximum energy ($E_{c\text{-max}}$) is then

$$E_{c\text{-max}} = \frac{1}{2} m_i v_i^2 \quad (4.14)$$

Note that the right side of Equation 4.14 is the same as the KE of the injected water. Hence, the energy captured by the cup is equal to the KE of the water jet if the speed of the jet is double the speed of the cup.

Equations 4.10 and 4.13 are functions of the mass of water passing through the jets per unit time. A more common formula is the one that uses the flow rate of water (f) defined as the volume of injected water (vol_i) per unit time.

$$f = \frac{vol_i}{t} \quad (4.15)$$

The unit of f is m^3/s .

The mass of water is the volume multiplied by the water density (δ)

$$m_i = vol_i \delta \quad (4.16)$$

The water density δ is roughly equal to 10^3 kg/m^3 at 20°C .

The power in Equation 4.10 can then be written as

$$P_c = 2 \frac{vol_i}{t} \delta (v_i - v_c) v_c \quad (4.17)$$

Substituting Equation 4.15 into 4.17 yields

$$P_c = 2f\delta(v_i - v_c)v_c \quad (4.18)$$

Similarly, the maximum power equation is

$$P_{c-\max} = \frac{1}{2}f\delta v_i^2 \quad (4.19)$$

The flow rate in Equation 4.15 can be written as a function of water speed and cross section area of the nozzle. The volume of water leaving the nozzle of the jet is the cross section area of the nozzle (A) multiplied by the length of the water column (L).

$$vol_i = AL \quad (4.20)$$

The length of the water column is dependent on the jet velocity and time.

$$vol_i = Av_i t \quad (4.21)$$

Hence, the water flow rate is

$$f = \frac{vol_i}{t} = Av_i \quad (4.22)$$

Example 4.1

A cup receives $10 \text{ m}^3/\text{s}$ of water. The speed of the cup must be fixed at exactly 200 m/s . Compute the speed of the injected water if the power captured by the cup is 40.0 MW .

Solution

Using Equation 4.18,

$$P_c = 2f\delta(v_i - v_c)v_c$$

$$4.0 \times 10^7 = 2 \times 10 \times 10^3 (v_i - 200) \times 200$$

$$v_i = 204.0 \text{ m/s}$$

Example 4.2

The angular speed of the generator must be maintained at 180 r/min . The diameter of the runner is 10 m . Compute the maximum power captured by the cup at a flow rate of $10 \text{ m}^3/\text{s}$.

Solution

First convert the rotating speed of the generator to the linear speed for the cups

$$v_c = \omega r = \left(2\pi \frac{180}{60} \right) \times 5 = 94.25 \text{ m/s}$$

For maximum power

$$v_i = 2v_c = 2 \times 94.25 = 188.5 \text{ m/s}$$

Using Equation 4.19,

$$P_{c\text{-max}} = \frac{1}{2} f \delta v_i^2 = \frac{1}{2} \times 10 \times 10^3 \times 188.5^2 = 177.66 \text{ MW}$$

A good example of impulse turbines is the Pelton design. It was invented in 1880 by the American engineer Lester A. Pelton (1829–1908). A schematic of the turbine is shown in Figure 4.8. It consists of a volute chamber with several jets injecting high speed water into the cups. Figure 4.9 shows one of these turbines being installed. Pelton turbines are often used in high dams where water head exceeds 500 m.

4.1.2.2 Reaction Turbine

Unlike impulse turbines, the reaction turbine is completely immersed in water. Figure 4.10 shows the main component of the reaction turbine. When water enters the turbine chamber, the water flows through the blades and exists from the center pipe as shown in the figure.

According to Bernoulli's principle (conservation of energy), the energy in the water just before the blades is equal to the energy of water just after the blades plus the energy captured by the blades.

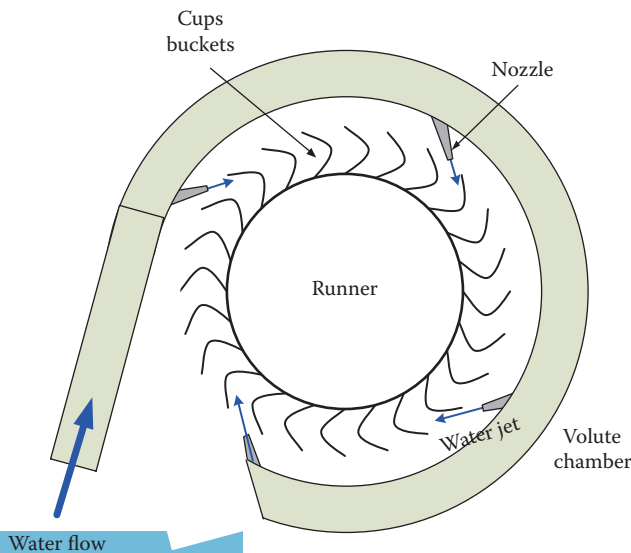


FIGURE 4.8 Pelton turbine.

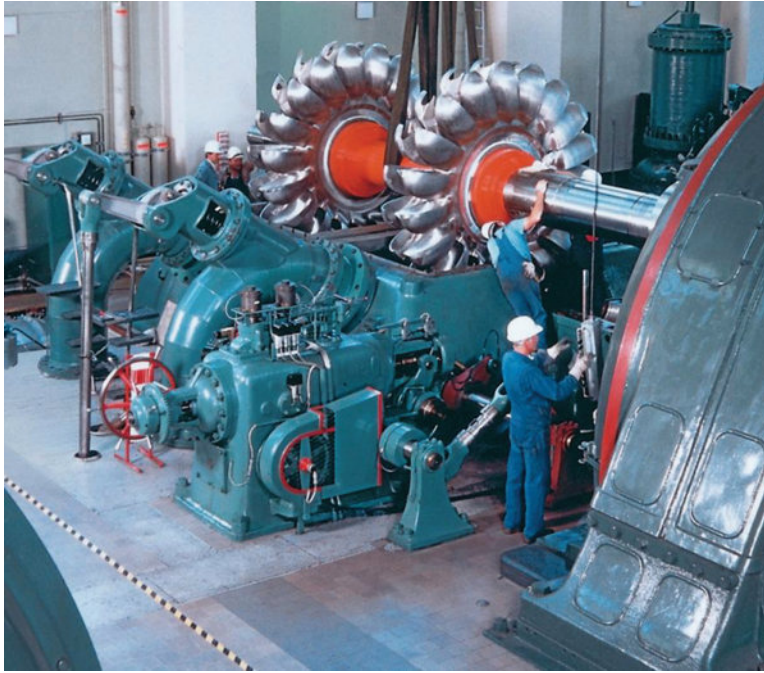


FIGURE 4.9 Pelton turbine being installed. (Courtesy of Siemens Hydro Power through Wikipedia.)

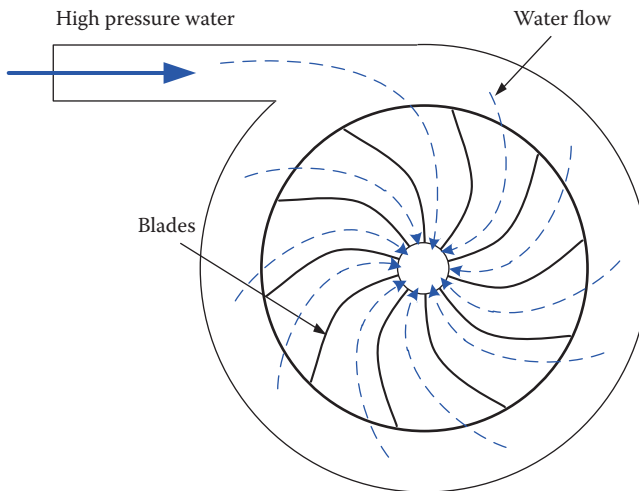


FIGURE 4.10 Reaction turbine.

Since the turbine is immersed in water, the energy components are both potential and kinetic. The general expression of the PE is

$$PE = P_r \text{ vol} \tag{4.23}$$

where

P_r is the water pressure per unit area (N/m^2)

vol is the volume of water (m^3)

Also, the general expression for the KE is

$$\text{KE} = \frac{1}{2}mv^2 \quad (4.24)$$

where

m is the water mass (kg)

v is the water velocity (m/s)

The energy of the moving water just before the blades (E_1) contains both kinetic and potential energies.

$$E_1 = P_{r1} \text{vol}_1 + \frac{1}{2}m_1v_1^2 \quad (4.25)$$

Similarly, the energy of the water just after the blades (E_2) is

$$E_2 = P_{r2} \text{vol}_2 + \frac{1}{2}m_2v_2^2 \quad (4.26)$$

Subscripts 1 and 2 indicate the water conditions just before the blades and after the blades respectively.

Hence, the energy captured by the blades is

$$E_{blade} = E_1 - E_2 \quad (4.27)$$

$$E_{blade} = \left(P_{r1} \text{vol}_1 + \frac{1}{2}m_1v_1^2 \right) - \left(P_{r2} \text{vol}_2 + \frac{1}{2}m_2v_2^2 \right) \quad (4.28)$$

Since there is no change in water volume or mass, we can rewrite Equation 4.28 as

$$E_{blade} = (P_{r1} - P_{r2})\text{vol} + \frac{1}{2}m(v_1^2 - v_2^2) \quad (4.29)$$

The first term on the right side of the Equation 4.29 is the pressure energy captured by the blades, and the second term is the KE captured by the blades. Since the turbine is fully immersed in water, the velocity of water is almost constant and slow. Thus, the pressure energy is the dominant component and we can ignore the second term.

$$E_{blade} = (P_{r1} - P_{r2})\text{vol} \quad (4.30)$$

Furthermore, the pressure of water after the blades is very small. This is because the trapped water between two adjacent blades produces little pressure. Hence, $P_{r1} \gg P_{r2}$, and Equation 4.30 can be further approximated to

$$E_{blade} = P_{r1} \text{vol} \quad (4.31)$$

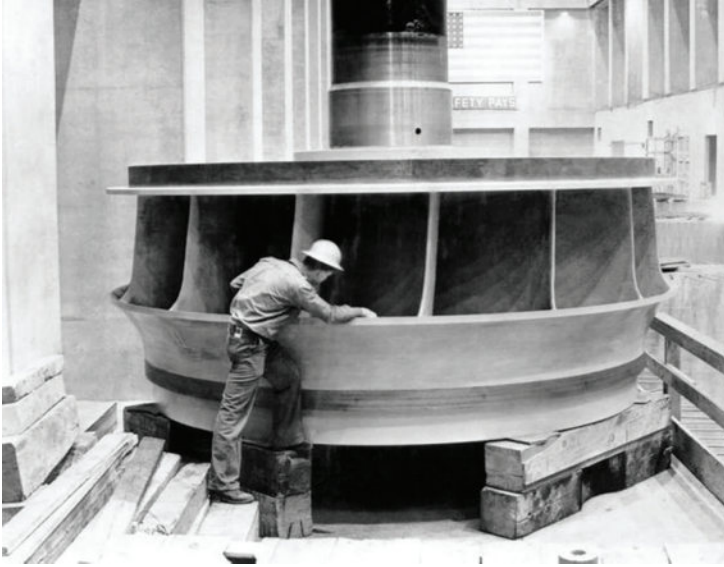


FIGURE 4.11 Francis turbine. (Images are courtesy of the U.S. Army Corps of Engineers, Louisville, KY.)

And the power captured by the blades is

$$P_{blade} = P_{r1} \frac{vol}{t} = P_{r1} f \quad (4.32)$$

where f is the flow rate of water inside the penstock.

Example of reaction turbines is the Francis and Kaplan designs. Figure 4.11 shows the Francis turbine which is suitable for water heads between 80 and 500 m. Figure 4.12 shows the Kaplan turbine (propeller turbine) which is suitable for low heads in the range of 1.5–80 m

4.1.2.3 Reservoir

The water behind the dam forms a reservoir (lake). The PE of the water in the reservoir PE_r , is a linear function of the water mass and head.

$$PE_r = MgH \quad (4.33)$$

where

M is the water mass (kg)

g is the acceleration of gravity (9.81 m/s²)

H is the water head (average elevation) behind the dam (m)

The unit of PE_r is joules (Ws). The mass of the water is a function of the water volume and water density

$$M = Vol_r \delta \quad (4.34)$$

where

Vol_r is the volume of water in the reservoir (m³)

δ is the water density in kg/m³.

At temperatures up to 20°C, δ is about 1000 kg/m³



FIGURE 4.12 Kaplan turbine. (Images are courtesy of the U.S. Army Corps of Engineers, Louisville, KY.)

Example 4.3

A hydroelectric dam forms a reservoir of 20 km^3 . The reservoir average head is 100 m. Compute the PE of the water in the reservoir.

Solution

$$PE_r = Vol_r \delta g H = 20 \times 10^9 \times 1000 \times 9.81 \times 100 = 1.962 \times 10^7 \text{ GJ}$$

This immense energy is the PE of the entire reservoir. Keep in mind that seasonal variations in rain falls or snow spills do change the volume of the reservoir; thus the PE of the reservoir is accordingly varied.

4.1.2.4 Penstock

The PE of the water exiting the penstock (PE_{p-out}) is

$$PE_{p-out} = mgh \tag{4.35}$$

where

m is the mass of water passing through the penstock (kg)

h is the effective water head at the outtake of the penstock (m). This is different from the physical head (H) as discussed later in this subsection.

The mass of water passing through the penstock is

$$m = vol \delta \quad (4.36)$$

And the flow rate is

$$f = \frac{vol}{t} \quad (4.37)$$

Hence, the PE of the water exiting the penstock is

$$PE_{p-out} = f \delta g h t \quad (4.38)$$

And the power is

$$P_{p-out} = f \delta g h \quad (4.39)$$

As given in Equation 4.32, the power at the outtake of the penstock is also the pressure at the outtake end (P_r) multiplied by the flow rate.

$$P_{p-out} = P_r f \quad (4.40)$$

Hence the relationship between the water head and water pressure is

$$h = \frac{P_r}{g \delta} = 1.02 \times 10^{-4} P_r \quad (4.41)$$

So what is the difference between the effective head (h) and the physical head (H)? The physical head is the head of water when the penstock is fully shut (closed)

$$H = 1.02 \times 10^{-4} P_{r0} \quad (4.42)$$

where P_{r0} is the water pressure when the outtake end of the penstock is closed. When the penstock gate opens, the pressure is reduced to P_r and the corresponding head (h) in Equation 4.41 is called effective head.

Example 4.4

The penstock output of Grand Coulee dam is about 800 MW when the effective water head is 87 m. The turbine is a Francis design. Compute the water flow rate inside the penstock

Solution

Using Equation 4.39, yields the flow rate

$$f = \frac{P_{p-out}}{\delta g h} = \frac{8 \times 10^8}{10^3 \times 9.81 \times 87} = 837.35 \text{ m}^3/\text{s}$$

Example 4.5

The effective water head of a hydroelectric dam is 100 m and the diameter of its penstock is 4 m. The water velocity inside the penstock is 20 m/s. Compute the power of the water exiting the penstock.

Solution

Equation 4.39 gives the output power of the penstock. Note that the flow rate is the multiplication of the cross section area by the water velocity as given in Equation 4.22.

$$P_{p-out} = f \delta gh = (A v_i) \delta gh = (\pi \times 2^2 \times 20) \times 10^3 \times 9.81 \times 100 = 246.55 \text{ MW}$$

4.1.2.5 Power Flow

The flow of power and the various losses in the hydroelectric system are depicted in Figure 4.13. The power entering the penstock (P_{p-in}) is slightly more than the power leaving penstock (P_{p-out}) due to penstock loss. The loss is due to water friction with the inside surface of the pipe. If the penstock has elbows and turns, the penstock loss increases.

The ratio between the output and input powers of the penstock is the efficiency of the penstock (η_p)

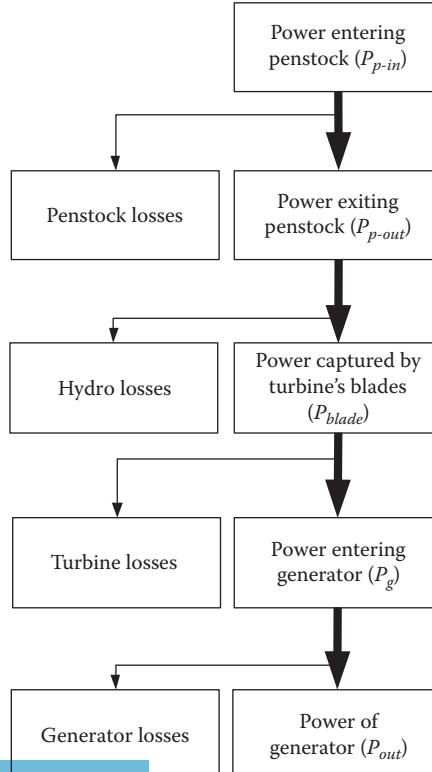


FIGURE 4.13 Power flow of hydroelectric system.

$$\eta_p = \frac{P_{p-out}}{P_{p-in}} \quad (4.43)$$

Not all the power leaving the penstock is captured by the blades of the turbine. The ratio of the power acquired by the turbine's blades (P_{blade}) to the power exiting the penstock is the hydro efficiency η_h

$$\eta_h = \frac{P_{blade}}{P_{p-out}} \quad (4.44)$$

Within the turbine, there are losses due to mechanical as well as water frictions. The turbine efficiency η_t is defined as the ratio of the power entering the generator (P_g) to the power captured by the blades of the turbine

$$\eta_t = \frac{P_g}{P_{blade}} \quad (4.45)$$

The generator has its own losses due to its winding resistance and its core. The efficiency of the generator η_g is defined as the ratio of the output power of the generator (P_{out}) to the power entering the generator.

$$\eta_g = \frac{P_{out}}{P_g} \quad (4.46)$$

Hence, the output power of the hydroelectric system is

$$P_{out} = P_{p-in} \eta_p \eta_h \eta_t \eta_g \quad (4.47)$$

Example 4.6

For the system in Example 4.5, compute the output power of the hydroelectric power plant assuming the hydro efficiency is 95%, the turbine efficiency is 90%, and the generator efficiency is 89%.

Solution

$$P_{out} = P_{p-in} \eta_p \eta_h \eta_t \eta_g = P_{p-out} \eta_h \eta_t \eta_g = 246.55 \times 0.95 \times 0.9 \times 0.89 = 187.61 \text{ MW}$$

Example 4.7

One of the Francis turbines in Grand Coulee dam has a penstock of 12 m in diameter. The flow rate of the penstock is 900 m³/s when the effective head of the water behind the dam is 100 m.

- Compute the output power of the penstock.
- Compute the speed of water at the outtake of the penstock.

Solution

- a. The output power of the penstock is

$$P_{p-out} = f\delta gh = 900 \times 10^3 \times 9.81 \times 100 = 882.9 \text{ MW}$$

- b. The flow rate is velocity time cross section area as given in Equation 4.22.

$$f = Av_i$$

$$v_i = \frac{f}{A} = \frac{900}{\pi \times 6^2} = 7.96 \text{ m/s}$$

4.2 FOSSIL FUEL POWER PLANTS

Fossil power plants (coal, oil, or natural gas) utilize the thermal cycle described by the laws of thermodynamics to convert heat energy into mechanical energy. This conversion, however, is highly inefficient as described by the second law of thermodynamics where a large amount of the heat energy must be wasted to convert the rest into mechanical energy. The conversion process is depicted in Figure 4.14. Assume that the energy source in the figure produces heat energy Q_1 at a temperature T_1 . Since heat flows only from high temperature to low temperature, a heat sink of temperature $T_2 < T_1$ is needed to facilitate the flow of heat. The second law of thermodynamics shows that the ideal efficiency η_{ideal} of a heat engine (turbine, internal combustion engine, etc.) is

$$\eta_{ideal} = \frac{T_1 - T_2}{T_1} \quad (4.48)$$

The earlier equation shows that the engine efficiency is increased when T_2 is decreased. In other words, the lower the heat sink temperature, the higher is the efficiency of the heat engine. Keep in mind that this efficiency does not include friction and other mechanical losses or heat leakages. Therefore, the real efficiency is less than η_{ideal} .

As seen in Figure 4.14, the turbine of the power plant is installed between a heat source and a heat sink (known as a cooling tower). The turbine is a thermomechanical device (heat engine) that converts heat energy into mechanical energy. It extracts some of the thermal energy in Q_1 and converts

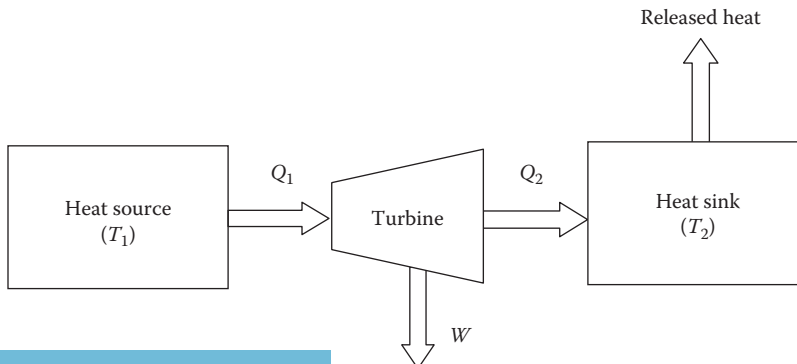


FIGURE 4.14 Second law of thermodynamics.

it into mechanical energy W . The rest is dissipated in the heat sink (cooling tower), without which no heat travels through the turbine.

The mechanical energy W is the difference between the source energy Q_1 and the energy dissipated in the heat sink Q_2 .

$$W = Q_1 - Q_2 \quad (4.49)$$

The ideal efficiency of the turbine η_{ideal} can be written in terms of heat energy as

$$\eta_{ideal} = \frac{W}{Q_1} = \frac{Q_1 - Q_2}{Q_1} \quad (4.50)$$

Note that if $T_2 = T_1$, the heat sink does not dissipate any heat energy and $Q_2 = Q_1$. In this case, no mechanical energy is produced by the turbine, and the turbine efficiency is zero.

The cooling towers can be divided into two types: dry and wet. The dry type such as the one in Figure 4.15 uses a closed loop water system where the steam generated during the extraction of Q_2 is condensed and reused. This type is suitable for areas with limited water resources. The wet type allows the steam to be vented in the air, which is suitable for areas near oceans or large lakes where water is abundant.

4.2.1 THERMAL ENERGY CONSTANT

Thermal energy constant (TEC) is defined as the amount of thermal energy produced per kg of burned fuel. The unit of TEC is called the British thermal unit (BTU); 1 BTU is equivalent to 252 cal, or 1.0548 kJ. Table 4.3 shows typical TEC values for various fossil fuels. As seen in the table, oil and natural gas produce the highest BTU among all fossil fuels.



FIGURE 4.15 Cooling tower.

TABLE 4.3
Thermal Energy Constant for
Various Fossil Fuels

Fuel Type	Thermal Energy Constant (BTU/kg)
Petroleum	45,000
Natural gas	48,000
Coal	27,000
Wood (oven dry)	19,000

Example 4.8

The cooling tower of a coal-fired power plant extracts 18,000 BTU/kg of burned coal. Compute the mechanical energy of the turbine and the overall system efficiency.

Solution

According to Table 4.3, coal has a thermal energy constant of 27,000 BTU/kg or 28.469×10^3 kJ/kg

The condenser extracts 18,000 BTU/kg or 18.979×10^3 kJ/kg

The mechanical energy of the turbine is

$$W = Q_1 - Q_2 = 28.469 - 18.979 = 9.49 \times 10^3 \text{ kJ/kg}$$

The ideal efficiency of the thermal turbine η_{ideal} is

$$\eta_{ideal} = \frac{\text{Output mechanical energy}}{\text{Input thermal energy}} = \frac{W}{Q_1} = \frac{9.49 \times 10^3}{28.469 \times 10^3} = 33.3\%$$

It is normal that the efficiency of the thermal cycle is below 50% since the heat sink dissipates (wastes) a large amount of the thermal energy to complete the thermal cycle.

4.2.2 DESCRIPTION OF THERMAL POWER PLANT

Most fossil fuel power plants have similar designs. The main differences among them are the burners, fuel feeders, and stack filters. Nevertheless, these differences are not essential for the description of the operation of any fossil fuel power plant, and therefore, we shall discuss the coal-fired type only.

As explained in Chapter 3, coal is a combustible black rock that is abundant in the Midwest and the east of the United States. Coal comes from organic matter that built up in swamps millions of years ago during the Carboniferous Period (about 30 million years ago) and became fossilized.

A typical view of the power house of a thermal power plant is shown in the photo of Figure 4.16. It consists mainly of a turbine and a generator. The turbine consists of blades mounted on a shaft. The angles and contours of the blades are designed to capture the maximum thermal energy from the steam. Figure 4.17 shows a large thermal turbine under construction.

The schematic of the main components of a coal-fired power plant is shown in Figure 4.18, and a photograph of one plant is shown in Figure 4.19. The process starts when the coal is delivered to the

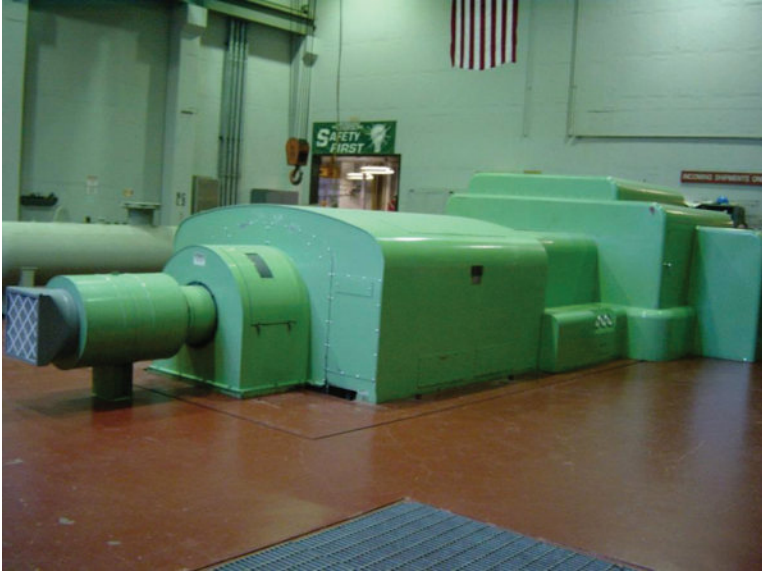


FIGURE 4.16 Inside a small-size thermal power plant.

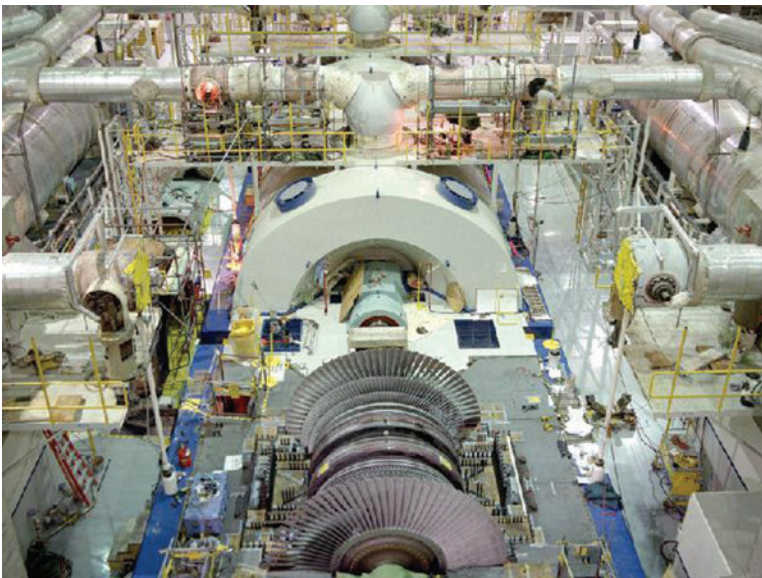


FIGURE 4.17 Thermal turbine. (Courtesy of Oregon Department of Energy, Salem, OR.)

plant by trucks and railroad trains. The coal is first crushed and delivered to the burner via conveyor belts. It is then burned to generate heat that is absorbed by water pipes inside the boiler. The water turns into high-pressure steam at high temperature. The steam leaves the boiler at a temperature higher than 500°C and enters the turbine at a velocity greater than 1600 km/h . The high speed steam hits the blades of the turbine and causes the turbine to rotate. The turbine's shaft is connected to the shaft of the generator, thus causing the generator to rotate at the same velocity and electricity is generated. Due to the presence of the cooling tower, the thermal cycle is completed as described by the second law of thermodynamics. In the cooling tower, the steam is turned into liquid and goes

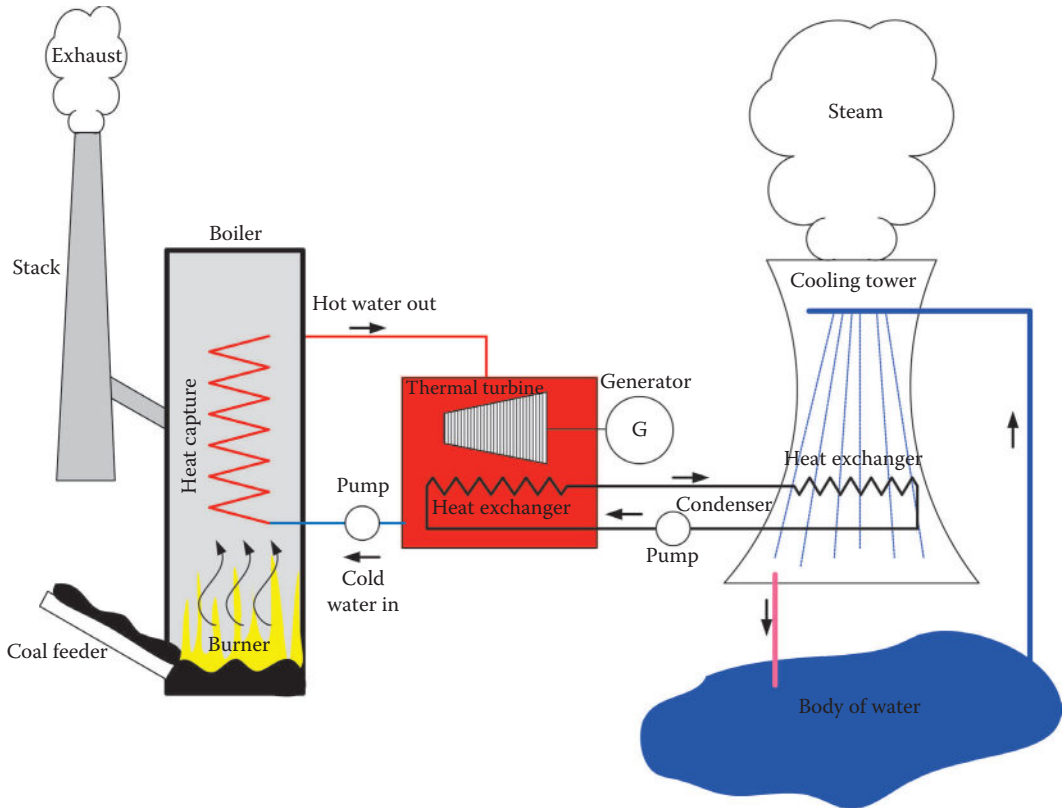


FIGURE 4.18 Main components of coal-fired power plant.



FIGURE 4.19 Weston coal-fired power plant. (Image courtesy of the U.S. Department of Energy, Washington, DC.)

back to the boiler to complete the thermal cycle. Inside the cooling tower, the condenser uses water from nearby lakes or oceans to cool down the steam inside the pipes.

Although coal-fired power plants are simple in design and easy to maintain, they are major producers of pollution as shown in Chapter 5. Carbon dioxide (CO_2), carbon monoxide (CO), sulfur dioxide (SO_2), nitrous oxide (NO_x), soot, and ashes are some of the by-products of coal combustion. In fact, coal burning by power plants and industrial sector is responsible for 30%–40% of the total CO_2 in the air. In older and unregulated plants, most of these pollutants are vented through the stack. However, with newer technologies, large amounts of the pollutants are trapped by filters or removed from the coal before it is burned. Examples of the pollution reduction measures that are taken in most coal-fired plants include the following:

- Coal is chemically treated to remove most of its sulfur before it is burned.
- Filters are used to remove the particulate (primarily fly ash) and some of the exhaust gases from the boilers. There are various types of filters; among them are the wet scrubber system and the fabric filter system. With the wet scrubber, the exhaust gas passes through liquid, which traps flying particulate and SO_2 before the gas is vented through the stacks. The fabric filter system works like a vacuum cleaner where the particulates are trapped in bags.
- SO_2 is removed by its own scrubber system.
- NO_x is reduced by upgrading the boilers to low NO_x burners.
- CO_2 removal is too expensive to implement and not all power plants use carbon dioxide scrubber system.

4.3 NUCLEAR POWER PLANTS

From the availability point of view, nuclear fuel is the most abundant source of energy. As given in Chapter 3, the common fuel for nuclear power plants is uranium; an atom of uranium produces about 10^7 times the energy produced by an atom of coal. In the United States, there are over 100 commercial nuclear power plants in operation generating about 20% of the total electric energy. Worldwide, there are about 400 power plants generating as much as 70% of the energy demand in nations such as France. However, because of public concern, few nuclear power plants have been constructed in the United States, and several are expected to be mothballed (retired) in the near future.

Nuclear power plants can generate electricity by one of two methods: fission and fusion.

1. “Fission” is the splitting of heavy nuclei elements such as uranium, plutonium, or thorium into many lighter elements. By this process, mass is converted into energy. Fission power plants have two main designs: boiling water reactor (BWR) and pressurized water reactor (PWR). About two-third of the nuclear reactors are PWRs, and almost all of the commercial nuclear power plants worldwide are fission reactors.
2. “Fusion” is a process by which two lighter elements are combined into a heavier element. The fusion technique is not yet fully developed for commercial power plants.

4.3.1 NUCLEAR FUEL

The main fuel used in nuclear power plants is uranium. The harvested uranium ore contains several other elements besides uranium. The extracted ore is crushed to a fine powder that is further processed to extract the uranium oxide from the ore. The processed material is called yellowcake or urania. The color of the yellowcake is actually brown or even black. The yellowcake contains 70%–90% uranium oxides by weight. The yellowcake is further processed chemically to produce uranium hexafluoride (UF_6). When heated, UF_6 is transformed into gaseous form. This is the material used to produce the nuclear fuel.

An atom includes subatomic particles known as protons, neutrons, and electrons. Atoms with different atomic numbers (number of protons in the nucleus) are called elements. Atoms with the same atomic number, but with a different number of neutrons are called isotopes. Different isotopes of the same element can have different masses due to the difference in the number of neutrons they possess.

Natural uranium is almost entirely a mixture of three isotopes, ^{234}U , ^{235}U , and ^{238}U ; the superscripts indicate the atomic masses of the isotopes. The concentration of these isotopes in natural uranium is 99.2% for ^{238}U and 0.7% for ^{235}U . However, only ^{235}U can fission in nuclear reactors. Since the concentration of ^{235}U in uranium ores is very low, an enrichment process is used to increase its concentration in nuclear fuel. In nuclear power plants, ^{235}U concentration is about 3%–5%, and for nuclear weapons it is over 90%.

Another way to develop a fissionable nuclear fuel is through breeder reactors. A breeder reactor uses the widely available, nonfissionable uranium isotope ^{238}U , together with small amounts of fissionable ^{235}U , to produce a fissionable isotope of plutonium, ^{239}Pu . Plutonium is a man-made element and cannot be found in nature.

4.3.2 URANIUM ENRICHMENT

There are two common methods for uranium enrichment: *gaseous diffusion* and *gas centrifuge*. The gaseous diffusion is the oldest method.

Gaseous diffusion was developed by two physicists: the German scientist Francis Simon (1893–1956) and the Hungarian scientist Nicholas Kurti (1908–1998). They devised their method at the Clarendon Laboratory of England in 1940. By their method, UF_6 is pressured through semipermeable membranes to separate the molecules of ^{235}U from ^{238}U . Many stages of this process are needed to achieve just 2% enrichment.

The gas centrifuge was actually developed in 1934 by the American physicist Jesse Wakefield Beams (1898–1977). This was one of the enrichment methods during the *Manhattan Project* time. The work, however, has stopped in 1944 because it was not ready for production to support World War II.

The Czech mechanical engineer Gernot Zippe (1917–2008) developed a device known as Zippe-centrifuge to enrich uranium using mechanical separators. The device relies on the principles of centripetal force; while rotating molecules of different masses, they are physically separated along the radius of rotation.

Figure 4.20 shows how the device works. The uranium hexafluoride (UF_6) gas enters a cylinder that rotates at a high speed. The heavier gas molecules containing ^{238}U move toward the outside of the cylinder and the lighter molecules containing ^{235}U stay closer to the center. The gas in the center which has more of ^{235}U and less of ^{238}U is enriched uranium. To reach 2%–5% enrichment, several thousands of centrifuge cycles are needed.

The enriched uranium is mixed with other compounds and is manufactured into fuel pellets as shown in Figure 4.21. Each pellet is cylindrical of about 8 mm in diameter and 10 mm in height. A pellet may contain the energy equivalent of 1000 kg of coal, 700 L of oil, or 1500 m³ of natural gas.

The pellets are loaded into zirconium alloy metal tubes known as fuel rods. Zirconium alloy is chosen because of its ability to resist radiation and thermal stresses. The fuel rods are grouped into an assembly that includes as much as 800 fuel rods as shown in Figure 4.22. In the assembly, there are also control rods that regulate the thermal energy inside the reactor. An actual fuel rod assembly is shown in Figure 4.23.

4.3.3 FISSION PROCESS

The fission process is depicted in Figure 4.24. When a nuclear power plant starts up, neutrons are let loose to strike uranium atoms at certain speed causing it to split (fission). The fission process produces the following:

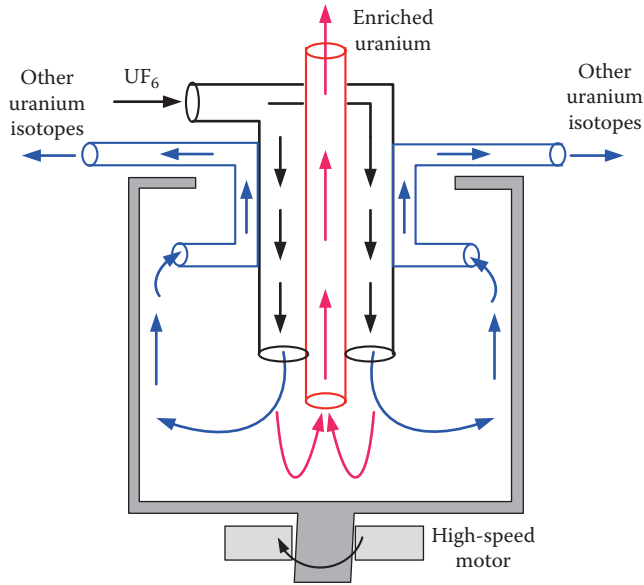


FIGURE 4.20 Gas centrifuge.

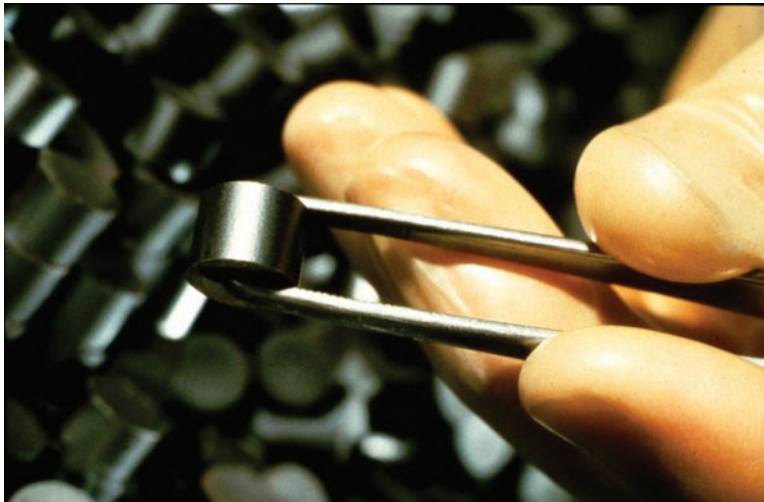


FIGURE 4.21 Fuel pellets (unirradiated [fresh] fuel pellets). (Courtesy of USA NRC, Rockville, MD.)

- *Fission fragments*: They are the leftover materials after the uranium atoms have split. They are cesium-140 and rubidium-93 which are radioactive materials.
- *Released neutrons*: After each fission action, three free neutrons are released. If they hit three other uranium atoms, they cause more fission to occur, which produces nine free neutrons and so on. This is known as a *chain reaction*. The neutrons produced by nuclear fission are fast-moving and must be slowed down to initiate further fission. The material used for this purpose is called a moderator; the common moderators are regular water (H_2O), and heavy water (D_2O) as well as graphite. Heavy water is chemically similar to regular water but the hydrogen atoms are replaced by an isotope of hydrogen called deuterium. Deuterium has one neutron more than hydrogen, which makes D_2O heavier than H_2O by about 10%.

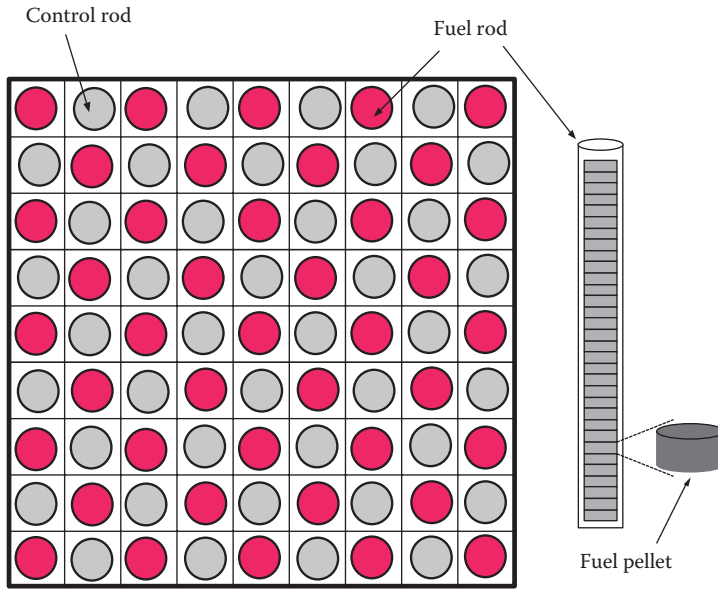


FIGURE 4.22 Fuel assembly.



FIGURE 4.23 Actual fuel rods assembly. (Courtesy of USA NRC, Rockville, MD.)

- *Energy*: The mass of the original uranium atom with the activation neutron is more than the combined masses of the fission fragments plus the released neutrons. The lost mass is converted into energy as described by Albert Einstein's formula

$$E = mc^2 \quad (4.51)$$

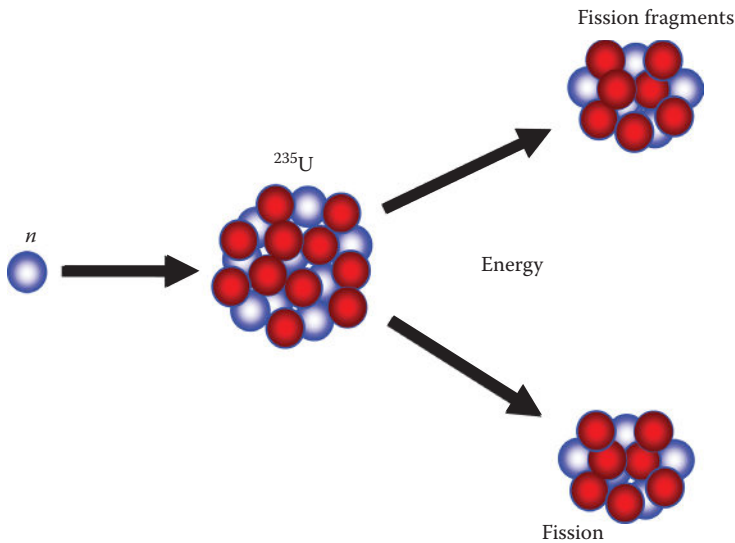


FIGURE 4.24 Fission reaction.

where

E is the released energy

m is the lost mass

C is the speed of light

Each fission event releases approximately 3.2×10^{-11} J of energy.

To put the number into perspective, 1 J of energy requires approximately 31×10^9 fission events. A 1 kg of ²³⁵U can have approximately 25.4×10^{23} fission events.

Example 4.9

A nuclear reactor produces an average of 1 GW of thermal energy annually. Compute the number of its fission events per year.

Solution

1 J requires 31×10^9 fission events.

1 W requires 31×10^9 fission events per second.

1 GW requires $10^9 (31 \times 10^9) = 31 \times 10^{18}$ fission events per second.

1 GW for 1 h requires $3600 (31 \times 10^{18}) = 11.16 \times 10^{22}$ fission events.

1 GW for 1 year requires $8760 (11.16 \times 10^{22}) = 9.7762 \times 10^{26}$ fission events.

The number of fission events in 1 year is staggering. However, in terms of nuclear fuel mass, the mass of ²³⁵U required to produce 1 GW of thermal energy for the entire year is very small, which is explained in Example 4.10.

Example 4.10

Compute the mass of ²³⁵U to produce an average of 1 GW of thermal power annually. Compare the mass of the nuclear fuel with the equivalent mass of coal.

Solution

In Example 4.9, the number of annual fission events is 9.7762×10^{26}

Since 1 kg of ^{235}U can have 25.4×10^{23} fission events, the mass of fuel needed for the reactor annually is

$$\text{Mass of } ^{235}\text{U annually} = \frac{9.7762 \times 10^{26}}{25.4 \times 10^{23}} = 385 \text{ kg}$$

About 1 kg of coal produces $27,000 \times 1.0544 = 28,469$ kW of thermal energy as given in Table 4.3.

To produce 1 GW of thermal power for 1 s, we need to burn $10^6/28,469 = 35.13$ kg of coal.

To produce 1 GW of thermal power annually, we need to burn $(60 \times 60 \times 8760) \times 35.13 = 1.107 \times 10^9$ kg of coal.

$$\frac{\text{Mass of coal}}{\text{Mass of uranium}} = 2.88 \times 10^6$$

Keep in mind that the high ratio of coal to uranium is because we assumed that the entire mass of uranium is pure ^{235}U . In a nuclear power plant the uranium is just 3%–5% enriched. Therefore, 1 kg of this enriched nuclear fuel will have much less than 25.4×10^{23} fission events. Nevertheless, the example shows that a small amount of nuclear fuel can unleash a tremendous amount of thermal energy.

4.3.4 FISSION CONTROL

The fuel assembly is placed inside the nuclear reactor as shown in Figure 4.25. The heat generated by the fission process is captured by the water inside the reactor. The water is turned into steam and used to generate electricity as discussed in the following subsections.

The fission process can be sustained indefinitely if the fuel is available and the chain reaction is maintained. To control the amount of the energy released, the chain reaction must be regulated by controlling the number of neutrons available for fission. This is done by using control rods made of material absorbent to neutrons and inserted inside the reactor between the fuel tubes as shown in Figure 4.22. The common materials used for control rods are hafnium, cadmium, or boron.

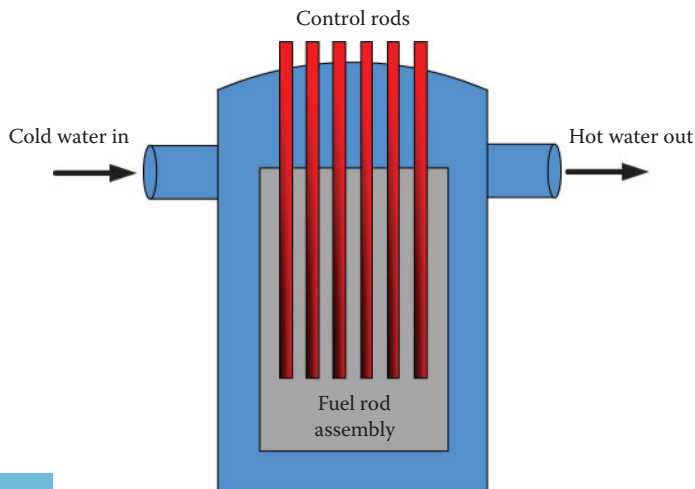


FIGURE 4.25 Reactor vessel.

The control rods can be inserted into or removed from the reactor by a motion control mechanism. When they are inserted, the rods absorb neutrons so fewer are available for fission. The reactor can be completely shut down by fully inserting the control rods into the core. In emergency situations, the rods are released and the gravity pulls them down inside the assembly to their fully inserted positions. This is called safety control rod axe man (SCRAM) process; the phrase was used for the early generation of test reactors when the rods were suspended by a rope. In an emergency, the rope was cut by an axe, and the person in charge of this process was called SCRAM.

4.3.5 BOILING WATER REACTOR

The boiling water reactor (BWR) used in commercial power plants was originally designed by the General Electric Company. The first installation was at Humboldt Bay, California in 1963. The BWR typically boils the water inside the reactor vessel itself. The operating temperature of the reactor is approximately 300°C, and its steam pressure is about $7 \times 10^5 \text{ kg/m}^2$. Current BWR reactors can generate as much as 1.4 GW with an overall efficiency of 33%.

The schematic of a BWR nuclear power plant is shown in Figure 4.26. The plant has the following key components:

- *Containment structure:* The dome structure houses the reactor and has multiple barriers of thick steel and concrete to contain the radiations inside the structure.
- *Reactor vessel:* The reactor vessel houses the fuel assembly. The vessel is filled with water, which acts as a moderator for the chain reaction and also extracts the heat energy generated

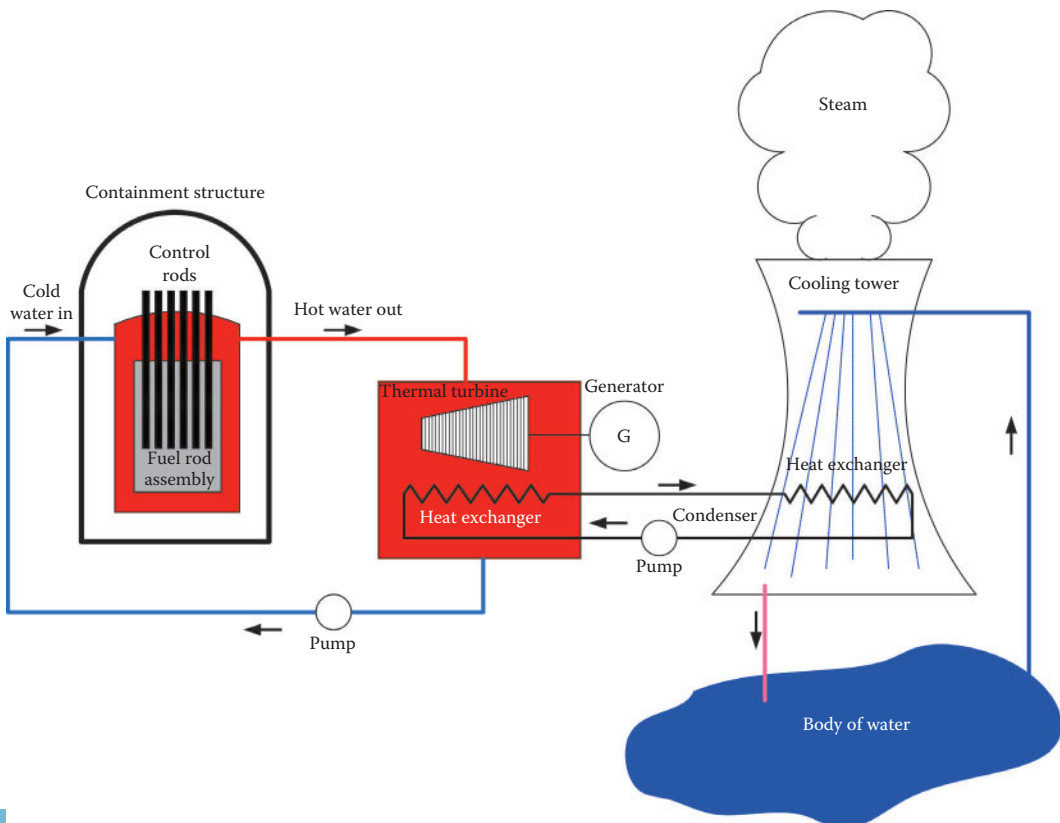


FIGURE 4.26 Main components of BWR.

by the nuclear reaction. The walls of the vessel are made of thick barriers of steel and concrete to guard against any radiation leakage or accidental meltdown.

- *Control rods:* The reactor contains the nuclear fuel assembly and the control rods. The control rods can be inserted or removed from the reactor by an actuation system to control the amount of heat generated. In case of an emergency shutdown, the rods are released and dropped to the fully inserted position to halt the chain reaction.
- *Turbine:* The energy generated by the nuclear reaction heats the water inside the reactor vessel, and steam is produced at high temperature and pressure. The steam passes through the turbine, which is a thermomechanical converter that converts the thermal energy into mechanical energy, much like the turbine of the thermal power plant.
- *Generator:* The turbine is connected to the generator via a common drive shaft. The generator is an electromechanical converter, where the mechanical energy of the turbine is converted into electrical energy.
- *Condenser:* It is the heat exchanger that extracts heat from the steam exiting the turbine. It acts as a thermal link between the turbine steam and the cooling tower.
- *Cooling tower:* The function of the cooling tower is to act as the heat sink of the thermal cycle. It uses cold water from a nearby reservoir, lake, river, or ocean. The cold water is poured over the condenser pipes to cool them down. The cooling water extracts the heat from the condenser and turns into steam, which is vented from the top of the cooling tower.

Among the advantages of the BWR are its simple design and high efficiency. However, because the fuel rods are in direct contact with the steam, the radioactive material from the nuclear reaction is carried over by the steam and eventually reaches the turbine. This radioactive steam pollutes the turbine and poses a challenge to the maintenance crew working on the turbine-generator system.

4.3.6 PRESSURIZED WATER REACTOR

A pressurized water reactor (PWR) was originally designed by Westinghouse as the power source for navy ships and submarines. The first commercial PWR plant in the United States was the Shippingport Atomic Power Station near Pittsburgh which operated from 1958 to 1982. The PWR is the most widely used type of nuclear reactor worldwide.

The PWR design is distinctly different from that of the BWR because, in PWR, a heat exchanger is placed between the water of the reactor and the steam entering the turbine. This is done to prevent the radioactive water from contaminating the turbine. This heat exchanger is called a steam generator. A schematic of a PWR power plant is shown in Figure 4.27 and a photograph of PWR power plants is shown in Figure 4.28. The water of the PWR reactor is under enough pressure to remain in liquid form even when it reaches 300°C or more; thus the system is called a PWR. Raising the temperature of the water under pressure makes it absorb more energy. The PWR has three separate heat exchange loops, or water loops, but the waters in these loops never mix. In the first loop, called primary loop, the pressurized water is pumped through the reactor to extract the thermal energy generated by the nuclear reaction and then passes through extremely strong pipes that lead to a steam-generator (heat exchanger). The water in the first loop is radioactive. The secondary loop includes the heat exchanger, the turbine, and the generator. The water in the second loop is free from any significant radioactive material. The third loop is the cooling loop that includes the turbine-generator, the condenser, and the cooling tower.

4.3.7 CANDU REACTOR

Hydrogen is one of the elements forming water. Hydrogen isotopes include *protium* and *deuterium*. Protium is the most abundant isotope as it accounts for more than 99.9% of all hydrogen isotopes. Its atom includes one proton and one electron. Deuterium, which is relatively rare element, has also

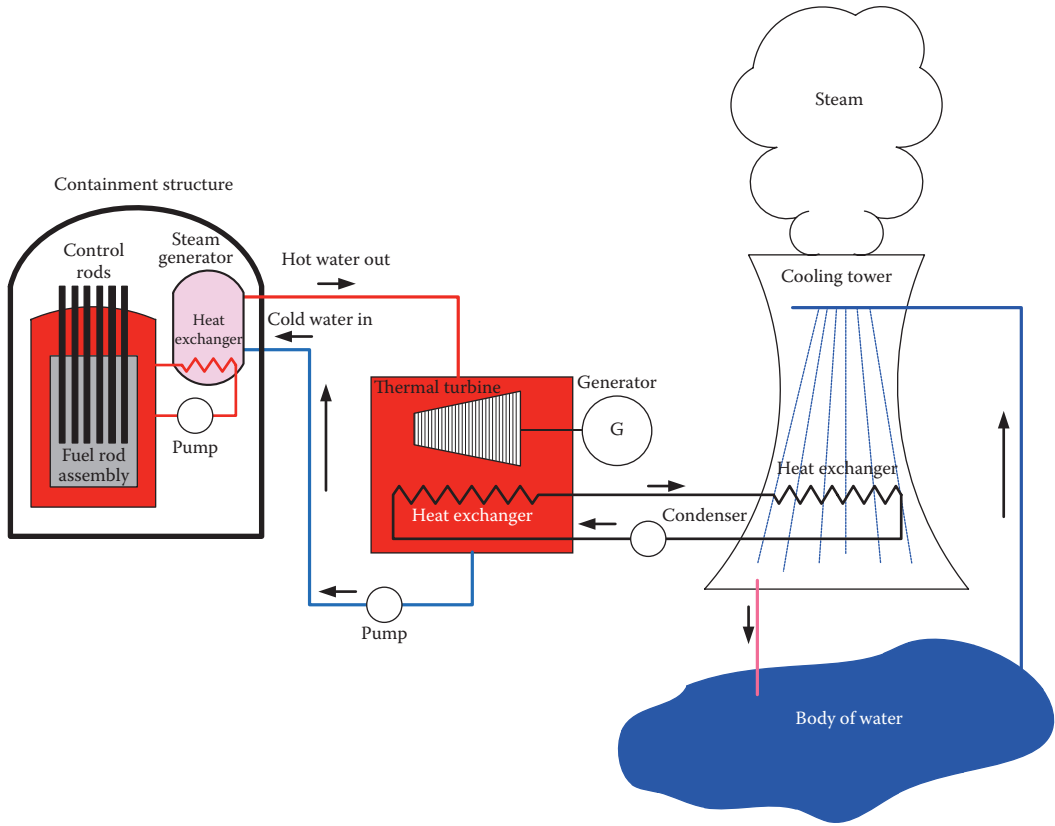


FIGURE 4.27 Pressurized water reactor.



FIGURE 4.28 PWR nuclear power plants.

one proton and one electron, but in addition has one neutron in its nucleus. It is therefore called heavy hydrogen.

Deuterium was discovered in 1931 by the American Chemist Harold Clayton Urey (1893–1981) and was awarded Nobel Prize in 1934 for his work. Later, scientists including Urey managed to produce water with highly concentrated deuterium. This water is known as heavy water (D_2O) and is used as a moderator for certain type of nuclear reactors known as CANDU (CANada Deuterium Uranium) reactors.

In regular reactors, light water (H_2O) is used. The hydrogen in light water is protium which has no neutron in its atom. When the chain reaction starts, some of the neutrons generated by the fission process are absorbed by the protium and therefore fewer neutrons are available for the chain reaction. To account for the neutrons absorption, uranium enrichment is needed.

In the CANDU reactor, the moderator is heavy water. Heavy water uses deuterium which already has neutron in its atom. Therefore the absorption of the neutrons generated by the chain reaction is substantially reduced. Hence, lower concentration of uranium can be used. It is even possible to use unenriched natural uranium directly.

4.3.8 SAFETY FEATURES IN NUCLEAR POWER PLANTS

Safety has been an important consideration from the very beginning of the nuclear era. However, in the 1940s, the developments were focused on demonstrating the potential of nuclear power as a reliable and cheap source of energy. Unfortunately, several nations sacrificed safety measures by adopting cheap and substandard designs.

The world enjoyed relatively safe nuclear power without any major accident until 1979. On March 28, 1979, a reactor at the Three Mile Island nuclear power facility near Harrisburg, Pennsylvania, suddenly overheated, releasing radioactive gases. Equipment failure and human error were the main reasons for the worst nuclear accident in the history of the United States. Although the plant engineers managed to shut down the reactor without damaging the core, public concerns regarding the safety of nuclear power plants were greatly intensified.

In April 1986, unit 4 of the Chernobyl nuclear power plant in the Ukraine was destroyed because of a combination of weak design and a series of human errors. The accident killed 31 people almost immediately and about 7 ton of uranium dioxide products escaped and began to spread across the surrounding areas.

These two accidents highlighted the need for effective safety measures to prevent future nuclear accidents. Until today, the nuclear industry is struggling to reverse the ever-growing skeptical public opinion regarding the integrity and safety of nuclear power plants. Among the reasons for public concern are the safety of the fuel assembly, the effectiveness of the control rods, and the loss of water inside the reactor. Each of these components is discussed in the following paragraphs:

Fuel rods: The fuel pellets are enriched uranium in the size of jellybeans. Most of the pellets are enriched with 3%–5% ^{235}U . The pellets are placed in tubes made of an alloy of zirconium and niobium. This alloy resists corrosion and has a low neutron absorption property. It is capable of maintaining its property even at high-temperature, high-pressure, and high-irradiation environments. The fuel assembly is often replaced every 3–5 years.

Control rods: The control rods are made of material such as boron, which absorbs neutrons. The boron, therefore, impedes the chain reaction and controls the rate of the fission reaction. The control rods are inserted between the fuel tubes or mixed with the fuel rods. During emergency conditions, the control rods would drop between the fuel rods and stop the nuclear reactions completely.

Reactor water: Reactor water removes excess heat from the reactors to prevent any meltdown. Water also slows down the neutrons and increases the probability of fission. Without water, neutrons would become too energized to initiate fission. Therefore any loss of water would slow down the fission process dramatically.

4.3.9 DISPOSAL OF NUCLEAR WASTE

The fission fragments are radioactive with a half-life of thousands of years. The spent fuel rods from a nuclear reactor are the most radioactive of all nuclear wastes. The spent fuel rods are stored in special storage facilities that prevent radiation leakages. The storage facilities are of two types: temporary and permanent. The United States lacks permanent storage facilities, and its temporary facilities store the nuclear waste for a very long time. The temporary facilities are of two types: wet storage and dry storage.

4.3.9.1 Wet Storage

When the spent fuel rods are removed from the core of the reactor, they are extremely hot and must be cooled down. The rods are, therefore, placed in a pool filled with boric acid to cool them down and to allow the boric acid to absorb some of the radiation of the fission fragments. A diluted solution of boric acid is quite safe and is commonly used as antibacterial and eye drops. The spent fuel rods are immersed in the boric acid fluid for at least 6 months before they are transported to permanent storage facilities. As an additional safety measure, control rods are placed among the spent fuel rods to inhibit any fission action of leftover U^{235} .

4.3.9.2 Dry Storage

After the spent fuel rods are cooled down in the wet storage facilities, they can be placed in temporary dry storage made of reinforced casks or buried in concrete bunkers, Figure 4.29. The casks are steel cylinders that are welded or bolted closed. Each cylinder is surrounded by an additional steel and concrete as a further measure against radiation leaks. The casks can be used for both storage and transportation.

4.3.9.3 Permanent Storage

Nuclear waste is composed of low- and high-level radiation waste. The low-level waste loses its radioactivity in a few hundred years, and is often buried in shallow sites. The high-level waste, such as the spent fuel rod, is harder to dispose because it contains fission fragments that are radioactive for thousands of years. Therefore, they are buried in deep geological permanent storage



FIGURE 4.29 Dry storage of spent fuel.

facilities. This deep site must have no or little groundwater to prevent the erosion of the containments (steel cylinders). The site must also be stable geologically, so earthquakes do not damage the containments.

EXERCISES

- 4.1 Name three types of hydroelectric power plants
- 4.2 Why are cooling towers used in thermal power plants?
- 4.3 What are the two nuclear reactions?
- 4.4 What is the enrichment process of nuclear fuel?
- 4.5 How is the chain reaction controlled in nuclear power plants?
- 4.6 What is the main difference between boiling water reactors and pressurized water reactors?
- 4.7 What is heavy water? Why is it used in nuclear power plants?
- 4.8 Write an essay on the latest technology used to dispose spent fuel rods.
- 4.9 What type of hydroelectric turbines is used in low head systems?
- 4.10 What type of hydroelectric turbines is used in high head systems?
- 4.11 What is pressure energy?
- 4.12 What is the relationship between pressure and head?
- 4.13 A hydroelectric power plant has a synchronous generator whose speed must be fixed at 180 r/min. The turbine is Francis type with 10 m runner diameter. When the flow rate at the nozzle of the penstock is $10 \text{ m}^3/\text{s}$, the generated electricity is 50 MW. If the total efficiency of the generator, turbine, and hydro is 88%, compute the velocity of the water jet.
- 4.14 The physical head of an impoundment power plant is 100 m. When the penstock is fully closed, the pressure at the outtake end is 10^6 N/m^2 . When the penstock is fully open, the pressure is reduced to $9 \times 10^5 \text{ N/m}^2$. Compute the effective head.
- 4.15 A man owns a land that includes a low head water fall and wants to build a small hydroelectric plant. The effective head of the reservoir is 20 m. He used a tube of 3 m length and 1 m diameter as a penstock. He computed the speed of the water inside the penstock by dropping a small ball at the entrance of the tube and measuring the time it took to reach the other end of the tube. The ball traveled the penstock in 2 s.
 - a. Compute the power at the outtake of the tube.
 - b. If the coefficient of performance of the turbine is 0.95, and the efficiency of the generator turbine and generator is 90%, compute the expected generation of the site.
 - c. If the cost of building the small hydroelectric system is \$10 M, compute the payback period if the cost of electricity from the neighboring utilities is \$0.2/kWh. Assume that the water flow is always constant.
 - d. Is building this small hydroelectric system a good investment?
- 4.16 A hydroelectric dam creates a reservoir of 10 km^3 . The average head of the reservoir is 100 m. Compute the PE of the reservoir.
- 4.17 A penstock is used to bring water from behind a dam into a turbine. The effective head is 20 m and the flow rate of water is $50 \text{ m}^3/\text{s}$. Compute the power of the water exiting the penstock.
- 4.18 The penstock of a hydroelectric power plant is 4 m in diameter. The water head is 60 m. Compute the water flow rate and the velocity of water inside the penstock if the power at the exit of the penstock is 10 MW.
- 4.19 A hydroelectric dam has a penstock that discharges 10^5 kg/s of water. The head of the dam is 80 m.
 - a. Compute the volume of the discharged water per second (flow rate).
 - b. Compute the power of the water entering the turbine.
 - c. Assume that hydro efficiency is 0.95, the turbine efficiency is 0.9 and the generator efficiency is 92%, estimate the generated electrical power.

- 4.20** A natural gas power plant has a condenser that extracts 28,000 Btu/kg of natural gas. Compute the mechanical energy of the turbine and the overall system efficiency.
- 4.21** An oil-fired power plant has a condenser that extracts 28,000 Btu/kg of oil. Compute the mechanical energy of the turbine and the overall system efficiency
- 4.22** Compare natural gas to oil in terms of thermal power and efficiency. Use the results of the previous two problems to verify your assessment.
- 4.23** Why are heat sinks used in thermal power plants?
- 4.24** Write an essay on the general design of oil-fired power plants.
- 4.25** What is the centrifuge?
- 4.26** What type of gas is used in the centrifuge?
- 4.27** What is the yellow cake?
- 4.28** Write an essay on the storage of nuclear waste.
- 4.29** Write an essay on the disposal of the contaminated structure of nuclear power plant.
- 4.30** Write an essay on the nuclear accident of the Three Mile Island power plant. Show the sequence of events and comment on the safety measures taken to prevent any subsequent catastrophic failure.
- 4.31** What is the CANDU reactor?
- 4.32** Write an essay on the Chernobyl nuclear accident. Show why such an accident is unlikely to happen in the United States.
- 4.33** What was the sequence of events that led to the Fukushima nuclear accident in 2011?
- 4.34** Estimate the amount of nuclear energy produced by 10 kg of ^{235}U .

5 Environmental Impact of Power Plants

Beginning from the Stone Age when fire was used for heating, humans have continually been involved in activities that have harmful effects on their health and on the environment. Unfortunately, as we become more industrially advanced, the earth's atmosphere has become more polluted, water resources further contaminated, and the earth's crust more acidic.

A good starting point in the history of pollution is the eleventh century when wood was extensively used in Europe as a major heating source. The pollution from burning wood was relatively limited, but wood became scarce and was replaced by coal at the beginning of the twelfth century. The dense smoke created by burning coal was initially viewed as just a minor discomfort. However, when coal was burned inside closed quarters with inadequate ventilation, the carbon monoxide released from the combustion suffocated a large number of people. This led King Edward I in the twelfth century to impose the death penalty upon anyone who was caught burning coal. The ban lasted for two centuries.

In the late seventeenth century, the Industrial Revolution started in Europe and spread all over the world. During this period, coal propelled the heavy industries as it was the only reliable source of energy. In the early twentieth century, oil started to replace coal, and the automobile industry flourished along with several other heavy industries such as steel and rubber. This was the period of unchecked assault on the environment with automobiles responsible for 60% of all atmospheric pollution.

Until recently, pollution was primarily an urban phenomenon in industrial countries, but now it has spread all over the world with more than 20% of the world population living in communities that do not meet the World Health Organization (WHO) air quality standards. Only recently humans have begun to comprehend the severity of the problems created by pollution. In the early 1960s, several public and scientific organizations intensified their efforts to enforce various regulations to maintain the delicate ecological balance of nature. In the United States, President Richard M. Nixon signed into law the National Environmental Policy Act on January 1, 1970. The law led to the formation of the Environmental Protection Agency (EPA), which is chartered with the protection of human health and the environment.

Because air pollution respects no national boundaries, international cooperation and treaties have been established to reduce the flow of pollution across borders. The United Nations Commission on Sustainable Development is an example of an international umbrella organization that promotes control measures leading to a cleaner and healthier environment.

In the electric energy sector, over 99% of the electric energy generated worldwide is produced by the primary resources: fossil fuels, hydropower, and nuclear energy. In 2010, the estimated worldwide consumption of electric energy from primary resources was about 17.44×10^{12} kWh. The extensive use of these primary resources is because they are readily available, produce enormous amount of energy, and are cheaper than alternative resources (solar, wind, etc.). From the viewpoint of the environment, each of these primary resources is associated with air, water, and land pollution. Although there is no pollution-free method for generating electricity (from primary or secondary resources), the primary resources are often accused of being responsible for most of the negative environmental impact. In this chapter, the various pollution problems associated with the generation of electricity are presented and discussed.

5.1 ENVIRONMENTAL CONCERNS RELATED TO FOSSIL FUEL POWER PLANTS

The earth's atmosphere is a mixture of gases and particles that surrounds the planet. Clean air is generally composed of the following mixture of gases. The ppm in the list stands for *parts per million* of the substance in air by volume, which is the number of molecules of the substance in a million molecules of air.

- Nitrogen (N₂), 78.1%
- Oxygen (O₂), 21%
- Argon (Ar), 0.9%
- Carbon dioxide (CO₂), 330 ppm
- Neon (Ne), 18 ppm
- Water vapor (H₂O)
- Small amounts of krypton (Kr), helium (He), methane (CH₄), hydrogen (H), nitrous oxide (N₂O), xenon (Xe), and ozone (O₃)

This delicate balance must be maintained for the air to be healthy for humans, animals, and vegetation. Unfortunately, the combustion of large quantities of fossil fuels could alter this balance and could introduce other polluting gases and particles in local areas. Indeed, it is alleged that fossil fuels are probably the most air-polluting energy resources, the worst among them being raw coal. A single raw-coal power plant without adequate filters can pollute an entire city of the size of New York. Although pollution from burning fossil fuels can have a direct effect on the environment, it can also combine with other gases and particles to create more potent effects. This is known as a synergistic effect among pollutants.

The question often asked is what level of pollution is considered harmful? The U.S. Environmental Protection Agency (EPA) has established the National Ambient Air Quality Standards (NAAQS) shown in Table 5.1 for six pollutants: carbon monoxide, lead, nitrogen dioxide, particulate matter, ozone, and sulfur dioxide. The table shows two types of national air quality standards: *primary* and *secondary*. The primary standards set limits to protect the health of “sensitive” population such as asthmatics, children, and the elderly. The secondary standards set limits to protect general public health as well as to guard against decreased visibility and damage to animals, crops, vegetation, and buildings.

When the level of a pollutant in an area exceeds a particular standard, the area is classified as *nonattainment* for that pollutant. In this case, the EPA imposes federal regulations on the polluters and gives deadlines by which time the area must satisfy the standard.

5.1.1 SULFUR OXIDES

Fossil fuels such as coal, oil, and diesel are not pure substances, but are often mixed with other minerals such as sulfur (S) and nitrogen (N). Mined coal, in particular, contains more than 6% sulfur. When fossil fuel is burned, the released sulfur is combined with oxygen to form sulfur oxides (sulfur dioxide [SO₂] and sulfur trioxide [SO₃]).



Sulfur dioxide (SO₂) is a corrosive, acidic, and colorless gas with a suffocating odor that can cause severe health problems. When the concentration of the gas reaches 2 ppm, the suffocating odor of the gas can be easily detected. Inhaling large amounts of SO₂ can damage the upper respiratory tract and lung tissues. This problem is more severe for the very young and the very old. In addition, asthmatic patients are more sensitive to SO₂ and their health status can deteriorate quickly. What makes SO₂ particularly dangerous is its rapid effect on people, usually within the first few minutes

TABLE 5.1
EPA's National Ambient Air Quality Standards

Pollutant	Primary Standards	Averaging Times	Secondary Standards	Additional Restrictions
Carbon monoxide	9 ppm (10 mg/m ³)	8 h	None	Not to be at or above this level more than once per year
	35 ppm (40 mg/m ³)	1 h	None	Not to be at or above this level more than once per year
Lead	1.5 µg/m ³	Quarterly	Same as primary	
Nitrogen dioxide	0.053 ppm (100 µg/m ³)	Annual	Same as primary	
Particulate matter 2.5–10 µm	50 µg/m ³	Annual	Same as primary	
	150 µg/m ³	24 h		Not to be at or above this level for more than 3 days over a 3 year period
Particulate matter <2.5 µm	15 µg/m ³	Annual	Same as primary	
	65 µg/m ³	24 h		
Ozone	0.08 ppm	8 h	Same as primary	The average of the annual fourth highest daily 8 h maximum over a 3 year period is not to be at or above this level
	0.12 ppm	1 h	Same as primary	Not to be at or above this level for more than 3 days in a 3 year period
Sulfur oxides	0.03 ppm	Annual	—	
	0.14 ppm	24 h	—	Not to be at or above this level more than once per year
	—	3 h	0.5 ppm (1300 µg/m ³)	Not to be at or above this level more than once per year

TABLE 5.2
Health Effect of SO₂

Concentration of SO ₂ (ppm)	Exposure Time	Effect
3	3 min	Increase airway resistance
0.2	4 days	Increase cardio-respiratory diseases
0.04	1 year	Increase cardiovascular diseases

of exposure. Table 5.2 summarizes various epidemiological studies linking SO₂ to respiratory and cardiovascular problems. Note that even a small value of ppm can increase the health risk.

It is hard to estimate the exact amount of sulfur dioxide released after burning fossil fuels. However, a coal-fired power plant can produce as much as 7 kg/MWh of SO₂, while a natural gas power plant emits just about 5 g/MWh. It is estimated that 20 million tons of SO₂ are released by power plants worldwide.

History has several examples of human tragedies due to excessive release of SO₂ from industrial plants other than power plants. In 1930, in Meuse Valley, Belgium, industrial pollution in the form of sulfur dioxide killed 63 people. In 1948, in Donora, Pennsylvania, sulfur dioxide emissions from industrial plants caused various respiratory illnesses in about 6000 people, and eventually caused

the death of 20 people in a few days. In 1952, London experienced the worst air pollution disaster ever reported from burning coal during a dense foggy day; about 4000 people died mainly because of sulfur dioxide. During the first Gulf War, high concentrations of sulfur dioxides were released when oil fields were set on fire. Soldiers and civilians suffered from severe cardiorespiratory ailments.

To reduce sulfur emissions, most governments have imposed various regulations (such as the NAAQS in the United States) and are closely monitoring the level of emissions released by industrial plants. Penalties are often imposed on those who exceed the government set “quota” of sulfur emissions. Since fossil fuel power plants produce almost half of all sulfur emissions worldwide, the penalties are severe for utilities with inadequate sulfur-filtering systems. These regulations have led to the decline in sulfur emissions in the United States, Canada, and many cities in Western Europe. The regulations also encourage owners of coal-fired plants to remove sulfur from coal before it is burned, or even convert their facilities to natural gas plants. However, unfortunately, sulfur emissions are still very high in a number of cities in Eastern Europe, Asia, Africa, and South America.

5.1.2 NITROGEN OXIDES

Other harmful gases produced by burning fossil fuels are the nitrogen oxides NO_x (O_x represents various levels of oxidation). Coal or natural gas power plants produce about 2 kg/MWh of NO_x .

Nitrogen oxides are toxic gases with NO_2 being a highly reactive oxidant and corrosive element. NO_2 irritates the eyes, nose, throat, and respiratory tract. Very high concentrations of NO_2 over long periods can cause respiratory infections and chronic bronchitis. In addition, NO_2 plays major roles in the formation of smog and acid rain. It absorbs sunlight, resulting in the brownish color of smog.

5.1.3 OZONE

Ozone (O_3) can be found at two different altitudes: the troposphere (up to 10 km altitude) and the stratosphere (10–50 km altitude). The stratosphere has a high concentration of ozone of about 30,000 ppm.

The *stratosphere ozone* protects the earth by absorbing the dangerous ultraviolet radiation of the sun. However, because of gases such as the chlorofluorocarbons (CFC), the ozone in the stratosphere area can be depleted. When CFC is decomposed by ultraviolet radiation, it releases chlorine atoms that react with ozone to create chlorine oxide and oxygen. By this process, one chlorine atom can destroy as many as 100,000 ozone molecules. Keep in mind that CFC is not released by power plants, but it is used as a refrigerant and can also be found in aerosol products. In 1978, CFC products were banned in the United States and more recently in most countries.

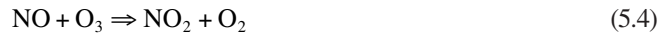
The *troposphere ozone* is formed when nitrogen dioxide (NO_2) is released by industrial plants. This pollutant, when excited by solar radiation, is converted into nitric oxide (NO) and in the process releases free oxygen atom O that can combine with oxygen molecule (O_2) to form ozone at low elevations (up to 10 km).



Nitric oxide (NO) can also be formed during lightning storms, which facilitate the reaction of nitrogen and oxygen.

Although the stratosphere ozone is beneficial, the troposphere ozone is a pollutant with harmful effects on the respiratory system and can make asthmatic patients more sensitive to SO_2 . It is also one of the main ingredients of smog that irritates lungs and causes damage to vegetation.

Fortunately, in nature, the troposphere ozone can be recycled back into nitrogen dioxide (NO_2) and oxygen molecules (O_2) when nitric oxide (NO) is available and the sun's energy is low (late afternoon or at night).



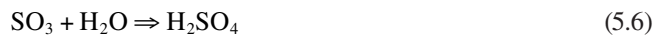
The chemical equations (5.2) through (5.4) form a delicately balanced process where ozone is formed and then destroyed. The reaction in Equation 5.4 is rapid, causing the concentration of O_3 to remain low as long as NO is available. However, when hydrocarbons are present (e.g., from automobile emissions), they react with NO to form organic radicals. These hydrocarbons then compete for the NO in air, so less of them are available to destroy the troposphere ozone. The result is an increase in the concentration of ozone at the troposphere level.

5.1.4 ACID RAIN

Sulfur and nitrogen dioxides produced by burning fossil fuels are the main ingredients of acid rain. Sulfur dioxide (SO_2) can further react with oxygen to form sulfur trioxide (SO_3).



When SO_3 reaches the clouds, it reacts with water to form sulfuric acid (H_2SO_4).



Similarly, when nitrogen dioxide (NO_2) reaches the clouds, it reacts with water and nitric acid (HNO_3) is formed.



Acid rain is the precipitation from clouds impregnated with these acids. Acid rain can be very damaging to crops, agricultural lands, and structures. When it reaches lakes, acid rain increases the acidity of water which can have severe effects on fish population. Acid rain can also damage limestone, historical buildings, and statues. Figure 5.1 shows two examples of acid rain damages. The picture on the left side shows a statue in Santiago, Spain, washed away by acid rain. The picture on the right side shows a tree that died from exposure to acid rain.

The acidity in the acid rain depends on the concentration of its hydrogen ions. Scientists have developed a scale called the *potential of Hydrogen* (pH) to quantify the degree of acidity in a solution. It is a negative logarithmic measure of hydrogen ion H^+ concentration in mols per liter of solution. The mol is a chemical unit used to measure the amount of substance that contains as many elementary entities (atoms, molecules, etc.) as there are atoms in 12 g of the isotope carbon-12 (6.023×10^{23}).

$$\text{pH} = -\log \text{H}^+ \quad (5.8)$$

Since pH is a negative logarithmic scale, a change in just one unit from pH=3 to pH=2 would indicate a 10-fold increase in the acidity. The hydrogen ion concentration in pure water is about



FIGURE 5.1 Effects of acid rain on (a) stones and (b) sensitive trees.

1.0×10^{-7} mol; hence its pH is 7. Increasing the concentration of hydrogen ions increases the acidity of the liquid; thus $\text{pH} < 7$ is considered acidic, while $\text{pH} > 7$ is considered alkaline or basic. The pH for milk is about 7, while battery acid has a pH from 0 to 1. Clean rain usually has a pH of 5.6. Rain measuring less than 5 on the pH scale is considered acid rain. The pH of the most acidic rain reported in the United States was about 4.3.

In the United States, the areas that suffer the most from acid rain are the Northeast and Midwest regions, which are known for their coal-based industries and coal-fired power plants.

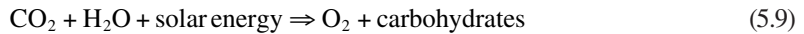
5.1.5 CARBON DIOXIDE

The temperature of the earth's surface is determined by the difference between the solar energy reaching the earth and the radiated energy from the earth back to space. Because some naturally occurring gases form thermal blankets at various altitudes, not all solar energy is radiated back to space. This phenomenon is loosely known as the *greenhouse effect*. The balance between the solar energy reaching the earth and the radiated energy is delicately maintained in nature to keep the temperature on earth at a level that can sustain life. Scientists believe that the release of *greenhouse gases* from industrial plants reduces the amount of the radiated energy and, therefore, increases the temperature on earth. This phenomenon is known as *global warming*. The greenhouse gases include carbon dioxide (CO_2), chlorofluorocarbon (CFC), methane (CH_4), nitrous oxide (N_2O), and ozone (O_3).

Global warming could lead to partial melting of glaciers and ice sheets, which can result in rising sea levels and even flooding lands that was naturally dry. Also, changes in the pattern of rain and wind can increase sea temperature. Most scientists believe that greenhouse gases have been increasing in concentration since the beginning of the industrial revolution in the seventeenth century. These scientists estimated that the global temperature on earth has increased by as much as 1°C during the last century. A counterargument made by other scientists is that while greenhouse

gases can increase the temperature, other gases such as the stratospheric ozone and sulfate cause the atmosphere to cool down. Therefore, global warming may not be as severe as some have thought. This debate is not likely to end anytime soon.

Carbon dioxide, which is one of the greenhouse gases, is a colorless, odorless, and slightly acidic gas. Nature recycles CO₂ through water, animals, and plants. Humans exhale carbon dioxide as they breathe, and plants absorb it during their photosynthesis process.



CO₂ is also absorbed in oceans. The process of generating and absorbing CO₂ is precisely sustained in nature, resulting in the right amount of CO₂ in air necessary to keep the earth's temperature at the current level. However, industrial activities that require burning of material containing carbon (coal, wood, and oil) can increase CO₂ concentration in air, thus contributing to the warming of the atmosphere.

Coal-fired power plants produce as much as 1000 kg/MWh of CO₂ and natural gas power plants produce about half this amount. But keep in mind that CO₂ is only one of the greenhouse gases with relatively limited effect since its presence in the atmosphere is for short periods. Other gases with more sinister effects include the chlorofluorocarbons (such as freon) and nitrous oxide. One molecule of CFC has the same effect as 10,000 molecules of CO₂. What makes these gases much worse than CO₂ is that they remain in the atmosphere for very long periods.

5.1.6 ASHES

Ashes are small particles (0.01–50 μm) that are suspended in air. The combustion process in fossil fuel power plants produces a large amount of ash that could stay suspended in air for days before it reaches the earth. About 7 million tons of ash is released each year by electric power plants and industrial smelters. Ash from power plants may include a variety of metals such as iron, titanium, zinc, lead, nickel, arsenic, and silicon.

Ash affects breathing, weakens the immune system, and worsens the conditions of patients with cardiovascular diseases. Smaller ash (less than 10 μm) can reach the lower respiratory tract, causing severe respiratory problems.

Most power plants install several filtering devices to eliminate or substantially reduce discharged ash. There are various types of filters; among them are the wet scrubber system and the fabric filter system. With the wet scrubber, the exhaust gas is passed through a liquid that traps flying particulates and sulfur dioxide before the gas is vented through the stacks. The fabric filter system works like a vacuum cleaner where the particulates are trapped in bags.

5.1.7 LEGIONNAIRES' DISEASE AND COOLING TOWERS

A harmful group of bacteria known as *Legionella* can live inside cooling towers as well as in hot water systems, warm freshwater ponds, and creeks. One of these bacteria causes the *Legionnaires' disease*, which is a form of infection that could lead to pneumonia.

For the cooling towers that vent their steam in air, hot water droplets carrying *Legionella* can be mixed with the steam. The droplets drift with wind and can cause infections in people several kilometers away from the cooling towers. To protect the public from these harmful bacteria, power plants install mist eliminators to prevent water droplets from escaping the cooling towers. In addition, biocides are used inside the cooling towers to prevent the growth of *Legionella*. Although these measures can be very effective in preventing the disease, not all utilities worldwide implement them.

5.2 ENVIRONMENTAL CONCERNS RELATED TO HYDROELECTRIC POWER PLANTS

Hydroelectric power is a major form of renewable energy. Although it does not emit any gas, the hydroelectric plant impacts the environment in other ways as discussed in the following:

Flooding: This is the most obvious impact of an impoundment type hydroelectric power plant. A dam is constructed to form a reservoir by flooding the upstream land. The decaying vegetations submerged by the flooding emit greenhouse gases. Flooding can also release dangerous substances embedded in rocks such as mercury, which accumulates in fish, resulting in health hazards when consumed. Socially, people can also be affected by the dam; when China constructed the Three Gorges Dam, millions of people were evicted from areas behind the dam.

Water flow: Hydroelectric dams alter the flow of water downstream, which may change the quality of water in the river as well as its flow rate.

Silt: Dams and reservoirs can trap silt that would normally be carried downstream to fertilize lands and prevent shore erosions. In addition, trapped silt behind the dam can reduce the amount of water stored in the reservoir, which can reduce the amount of generated electricity.

Oxygen depletion: In deep reservoirs, cooler water sinks to the bottom because of its higher density. This could reduce the oxygen at the bottom of the reservoir, thus altering the biota and fish population that live at the bottom of the lake.

Nitrogen: When water spills over a dam, air is trapped in the water creating turbulence. This makes the water more dissolvent to nitrogen, which could be toxic to fish.

Fish: Dams alter the downstream flow of the river, which may affect the migration of certain species of fish. Hydroelectric turbines also kill some of the fish that pass through the penstocks.

5.2.1 CASE STUDY: THE ASWAN DAM

After Egypt built the Aswan dam in the 1960s, inexpensive electricity was generated and the flow of the Nile was controlled all year around for the first time in history. However, the dam created several ecological and social problems. One of the most tragic effects of the Aswan dam was that the rising water submerged many valuable ancient monuments that are over 5000 years old. Some of these monuments, such as the temple of Abu Simbel built by Ramses II in the thirteenth century BC, were raised to higher dry lands. But the monument in its new location lost some of its miraculous engineering features such as sunlight penetration of the sanctuary on October 20 and February 20 of each year and the daily melodies played in various quarters.

One of the most important problems of the Aswan dam is the entrapment of the annual flood sediment behind the dam, creating a number of additional problems such as the following:

- Slow filling of the lake behind the dam by sediment, resulting in spilling of the water over its shores. The increase in the surface area of the lake increases the evaporation, which leads to undesired increase in humidity in the otherwise dry climate. This increased humidity negatively impacts valuable ancient monuments in the area.
- Virtual elimination of silt that used to make fertile the agricultural land downstream, thus negatively impacting farming in Egypt. Lack of sediment downstream exposes the banks of the Nile to steady erosion. Continuous recession of the shoreline of the Nile delta since the sediment that used to reach the Mediterranean shores counteracted the effects of coastal erosion.
- Mediterranean saltwater reaching upstream of the Nile, thus contaminating farmland and groundwater.
- Lack of sediment in the river allows more sunlight to penetrate the water. This increases the population of several biota and plants such as phytoplankton, which affects the fish population in the river, and makes the water more polluted; thus, more chlorine is added to the drinking water.

- Elimination of certain types of fish such as sardines and shrimps because the influx of nutrients associated with the annual silt-rich flood can no longer reach the Mediterranean Sea to feed the local biota and fish.
- Frequent weak tremors in the area, thought by some scientists to occur as a result of the sediment trapped behind the dam.

5.3 ENVIRONMENTAL CONCERNS RELATED TO NUCLEAR POWER PLANTS

The public is highly concerned about nuclear power plants. Although some of this concern is justifiable, most is based on misinformation or the erroneous association of nuclear power plants with nuclear weapons. Nuclear power plants operated safely for almost 40 years until the accident at the Three-Mile Island nuclear power plant that was followed by the Chernobyl nuclear disaster and Fukushima Daiichi accident (see Chapter 4). These three accidents intensified public pressure to set stricter safety regulations on nuclear power plants or to abandon nuclear power altogether. The debate is still ongoing and is not likely to end anytime soon. The following text discusses the concerns of the public.

5.3.1 RADIOACTIVE RELEASE DURING NORMAL OPERATION

In boiling water reactors (BWRs), the fuel rods are in direct contact with steam. Hence, some of the radioactive elements from the nuclear reaction are carried by steam and eventually reach the turbine and condenser. Although the BWR has several layers of protections that hold the radioactive steam for several half-life cycles before it is released, accidental release is still a major public concern. In pressurized water reactors (PWRs), this problem does not exist since the fuel rods are separated from the steam cycle.

The release of a small amount of radioactive gas is not necessarily a health hazard. The limit on radiation set by the Environmental Protection Agency (EPA) is 170 milliREM/year above the background radiation from all natural resources. The REM stands for the *radiation equivalent man*, which is a measure of biological damage to tissues by specific amounts of radiation. High doses of REM can cause immediate radiation sickness such as hypodermal bleeding and hair loss. Under 25 REM, no short-term effects are observed, but long-term exposure to these small amounts of REM may lead to serious health issues such as cancer and may even cause genetic abnormality in offspring.

5.3.2 LOSS OF COOLANT

One of the major public concerns is the loss of coolant inside the reactor. If the flow of water is interrupted due to breaks in pipes or pumps, fuel rods could become excessively hot and could melt down. This scenario is sensationalized in movies and is given the name *China syndrome*, where melted rods at the bottom of the reactor go through the reactor bottom into Earth and all the way to China on the other side of the globe.

The water inside the reactor is both a coolant and a moderator. The moderator slows down the neutrons to make fission possible. If the water inside the reactor is lost, the chain reaction is substantially curtailed. Nevertheless, water is still needed to cool the hot rods, thus reducing the temperature inside the reactor.

If the temperature inside the reactor reaches approximately 1200°C, the hydrogen in the water split from the oxygen. Since hydrogen is a very light element, it will be trapped at the ceiling of the reactor. If ignited, it could explode and may damage the containment structure. In this case, radioactive steam can be released in air. This is what happened in Chernobyl and Fukushima accidents.

If the temperature inside the reactor reaches about 2400°C, the uranium fuel melts down and the fuel rod becomes like melted wax. The uranium can continue to penetrate the ground and may reach and pollute water tables. At such high temperature, the pressure inside the reactor could be high enough to damage the containment structure, thus releasing radioactive steam.

5.3.3 DISPOSAL OF RADIOACTIVE WASTE

This is one of the crucial issues facing the nuclear power industry. The spent fuel contains cesium and rubidium, which are highly radioactive waste with a half-life of thousands of years. Besides being radioactive hazards, the spent fuel can stay hot for hundreds of years.

In the United States, about 2000 ton of spent fuel is produced annually from nuclear power plants, and much more is produced by several nuclear defense programs. The storage facilities of the nuclear waste must prevent the radioactive material from leaking for very long periods. One type of storage vessel used in the industry is a container composed of multiple layers of steel and concrete barriers. These containers are eventually buried in areas that are geologically stable and are surrounded by rocks to prevent any leakage from reaching the water table. Some nations store the containers on the deep ocean floor. Some scientists have proposed wild ideas such as shooting the radioactive waste into the sun or storing the radioactive material in space. This is, obviously, a highly sensitive issue for the public.

A more realistic option is to reduce or eliminate the long life radioactive waste by transmutation. Nuclear transmutation is a process by which the long life fuel waste is converted into shorter life waste that is easier to store. Transmutation occurs when radioactive waste is bombarded with charged material in accelerators.

EXERCISES

- 5.1 Name three types of major power plants.
- 5.2 How is acid rain formed?
- 5.3 What is the greenhouse effect?
- 5.4 State four drawbacks of a hydroelectric power plant.
- 5.5 What are the health effects of SO_2 ?
- 5.6 Fill in the blanks in the following sentences:
 - a. Sulfur dioxide (SO_2) emitted from power plants reacts with oxygen to form _____
 - b. When sulfur trioxide reaches the clouds, it reacts with water to form _____
 - c. When nitrogen dioxide reaches the clouds, it reacts with water and _____ is produced.
- 5.7 A coal-fired power plant produces an average of 100 MW annually; estimate the sulfur dioxide released daily and annually if no filtering system is used.
- 5.8 A natural gas power plant produces an average of 100 MW annually; estimate the sulfur dioxide released daily and annually if no filtering system is used.
- 5.9 If a 100 MW coal-fired power plant is converted into natural gas, compute the annual percentage reduction of SO_2 .
- 5.10 In 2006, the world consumed 16.28×10^{12} kWh of electricity; estimate the maximum amount of sulfur dioxide released from the coal-fired power plant worldwide.
- 5.11 Write a report on an area with severe acid rain. Discuss the pH values and their effect on the local environment.
- 5.12 How many mols of hydrogen ions are in a liquid with pH 5?
- 5.13 Choose a case study for a hydroelectric power plant. Identify the pros and cons of the plant.
- 5.14 Write a report on the impact of hydroelectric power plants on the fish population.
- 5.15 Identify a few ideas to lessen the effect of hydroelectric power plants on fish migration.
- 5.16 Identify a few ideas to increase silt in the downstream flow from hydroelectric power plants.
- 5.17 Write a report on the Three Mile Island accident. Identify the sequence of events that led to the accident. In your opinion, were the steps taken to correct the accident adequate?
- 5.18 Write a report on the Chernobyl nuclear disaster. Identify the sequence of events that led to the disaster. In your opinion, can this accident occur in the United States? Why?
- 5.19 Write a report on permanent storage of nuclear waste worldwide.

6 Renewable Energy

As seen in the previous chapters, the world relies heavily on fossil fuel (coal, oil, and natural gas) for its ever-growing appetite for energy. In the early 1950s, public concerns regarding the negative environmental impact of burning fossil fuels encouraged engineers and scientists to develop reliable alternative energy resources. The efforts were accelerated in the 1970s when oil prices soared after the Middle East war. Many countries began investing in various programs to encourage the development and testing of reliable renewable energy systems. Tax credits, investments in research and development, subsidies, and developing favorable regulations are some of the various support measures taken by governments to accelerate the development of renewable energy technologies. However, unfortunately, the development efforts are still largely dependent on the price of crude oil as well as the intensity of societal pressures.

Renewable energy is a phrase that is loosely used to describe any form of electric energy generated from resources other than fossil and nuclear fuels. Renewable energy resources include hydrokinetic, wind, solar, geothermal, biomass, and hydrogen. The sun is the source of all those renewable energies with the exception of geothermal. These resources produce much less pollution than burning fossil fuels and are constantly replenished, and thus called *renewable*.

Contrary to popular belief, renewable energy systems are not recently developed. Since the nineteenth century, scientists and engineers have worked on developing technologies to generate electricity using various forms of renewable resources. In 1842, Sir William George Armstrong invented a hydroelectric machine that produced frictional electricity. The world's first hydroelectric power plant was constructed across the Fox River in Appleton, Wisconsin in 1882. The Italian Prince, Piero Ginori Conti, invented the first geothermal power plant in 1904. The plant was located at Larderello, Italy. In 1839, the French scientist Edmond Becquerel discovered the photovoltaic effect. Charles F. Brush of the United States built the first wind turbine in 1888.

The developments in the renewable energy field during the past few years have led to more efficient and more reliable systems. Some of these systems, such as solar and fuel cells (FCs), are already used in aerospace and transportations. Today, wind energy is used to generate electricity all over the world. In this chapter, we shall discuss various renewable energy systems, but the reader should be aware that the area is growing fast, and new technologies and systems are invented or introduced every year.

6.1 SOLAR ENERGY

The sun is the primary source of energy in our solar system; the earth receives 90% of its total energy from the sun. Other natural forms of energy on earth include geothermal energy, volcanoes, and Earthquakes.

Sunrays are packed with energy. An area of 1 m^2 in space can receive as much as 1.366 kW of power from sunrays. This translates into extraterrestrial power density of about $1.366 \pm 4\% \text{ kW/m}^2$. This large amount power is weakened at the earth's surface due to several reasons, as follows:

- The various gases and water vapor in the earth's atmosphere absorb some of the solar energy.
- The distance from the sun determines the amount of the received solar energy. The distance can be measured by the projection angle of the sunrays (zenith angle); see Figure 6.1.
- The various reflections and scatterings of sunrays due to the presence of particles in air affect the amount of the received solar energy.

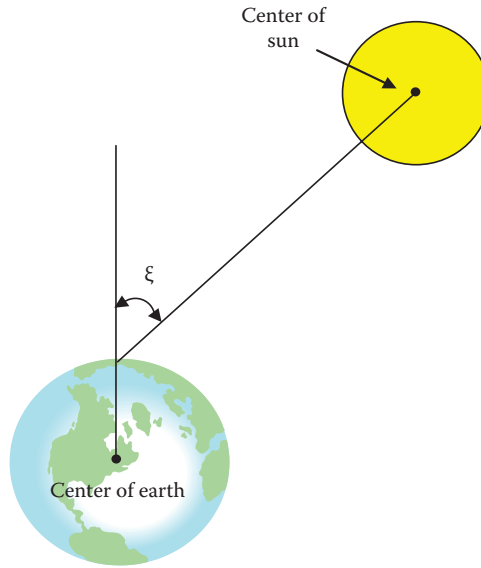


FIGURE 6.1 Zenith angle ξ .

The computation of the solar power density on the earth, also called *solar irradiance*, is complex and requires the knowledge of several hard-to-find parameters. However, approximate models can be used, such as the one developed by Atwater and Ball and given in Equation 6.1

$$\rho = \rho_o \cos \xi (\alpha_{dt} - \beta_{wa}) \alpha_p \quad (6.1)$$

where

ρ is the solar power density on the earth's surface in (kW/m²)

ρ_o is the extraterrestrial power density (the number often used is 1.353 kW/m²)

ξ is the zenith angle (angle from the outward normal on the earth's surface to the center of the sun as shown in Figure 6.1)

α_{dt} is the direct transmittance of gases except for water vapor (the fraction of radiant energy that is not absorbed by gases)

α_p is the transmittance of aerosol

β_{wa} is the water vapor absorptions of radiation

The term “aerosol” refers to the particles suspended in the earth's atmosphere such as sulfate, nitrate, ammonium, chloride, and black carbon. The sizes of these particles normally range from 10⁻³ to 10³ μm. As explained in Chapter 5, some of the aerosols such as CO₂, N₂O, and troposphere O₃ cause the atmosphere's temperature to rise; and some others such as stratospheric O₃ and sulfate cause it to cool down.

Due to the reflection, scattering, absorption, and zenith angle, the solar power at the earth's surface is a fraction of the extraterrestrial solar power. The ratio of the two solar power densities is known as the *solar efficiency* η_s .

$$\eta_s = \frac{\rho}{\rho_o} = \cos \xi (\alpha_{dt} - \beta_{wa}) \alpha_p \quad (6.2)$$

The solar efficiency varies widely from one place to another and is also a function of the season and the time of the day. It ranges between 5% and 70%. The zenith angle has a major effect on

the efficiency: for the same absorption conditions, the maximum efficiency occurs at noon in the equator when $\xi=0^\circ$.

Example 6.1

A person wants to install a solar energy system in Nevada. At a certain time in the afternoon, the zenith angle is 30° , the transmittance of all gases is 70%, the water vapor absorption is 5%, and the transmittance of aerosol is 90%. Compute the power density and the solar efficiency at that time.

Solution

By directly substituting the parameters in Equation 6.1

$$\rho = \rho_o \cos \xi (\alpha_{dt} - \beta_{wa}) \alpha_p = 1353 \times \cos(30) \times (0.7 - 0.05) \times 0.9 = 685.5 \text{ W/m}^2$$

$$\eta_s = \frac{\rho}{\rho_o} = \frac{685.5}{1353} = 0.5066 \quad \text{or} \quad 50.7\%$$

Figure 6.2 shows a map for the average solar energy in various regions of the United States in August. In the Mohave Desert and Nevada, the solar power density can be as much as 750 W/m^2 . In the Northwest region, it can be as high as 300 W/m^2 . Figure 6.3 shows the map of the annual average

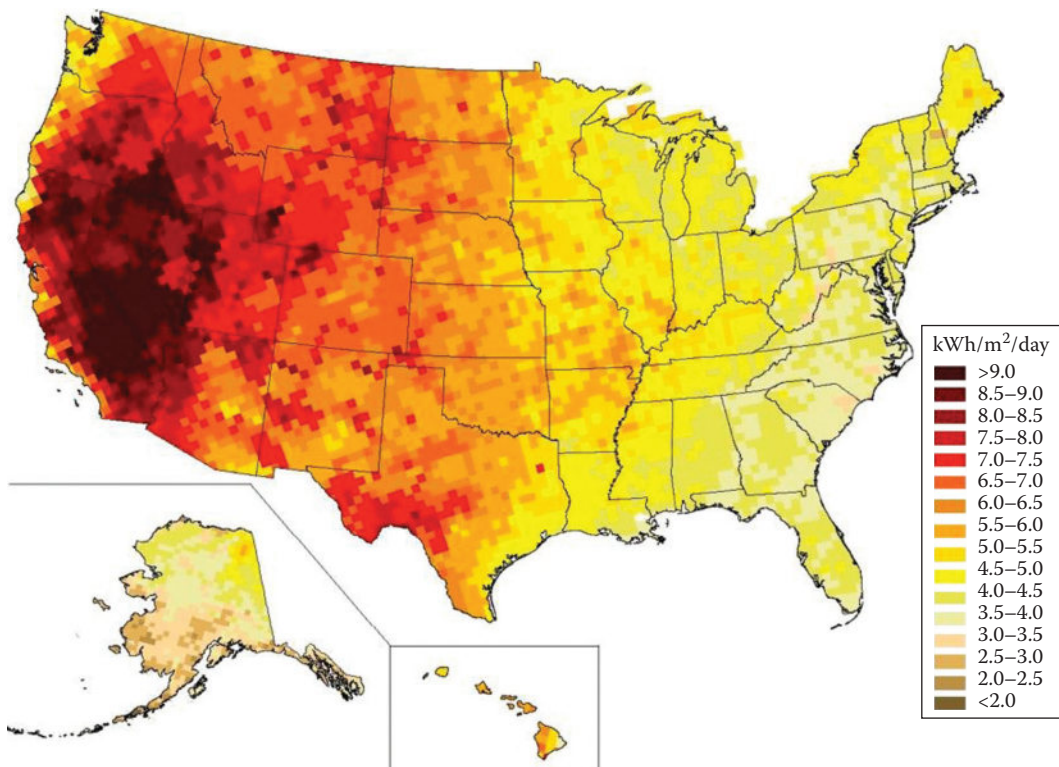


FIGURE 6.2 Average solar energy in August in the United States; resolution is 40 km. (Courtesy of the USA National Renewable Energy Laboratory.)

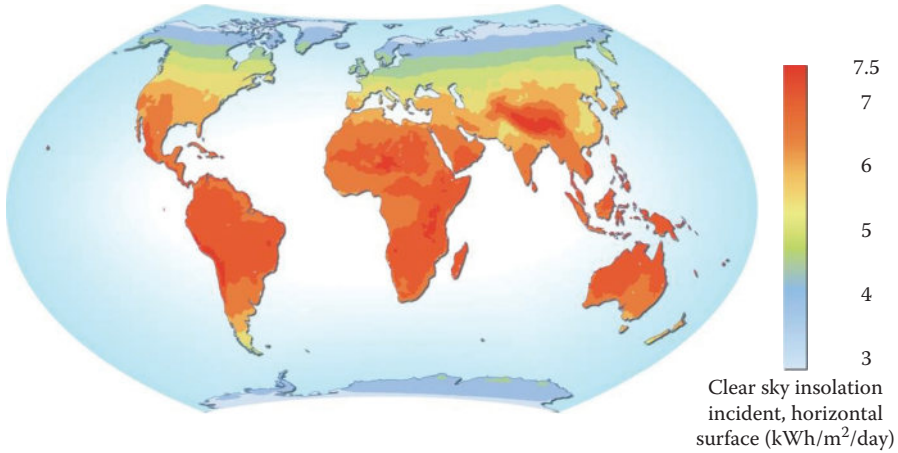


FIGURE 6.3 Average annual solar energy worldwide. (Courtesy of the National Aeronautic and Space Administration NASA.)

solar energy worldwide. The power density in central and South Africa, Argentina, Chile, Brazil, parts of China, Indonesia, and most of Australia can have a daily average of as much as 300 W/m². In these areas, the peak solar power density during the day can reach values higher than 700 W/m².

The solar power density during a typical day with stable weather can be approximated by a bell-shaped curve expressed by the normal distribution function in Equation 6.3 and Figure 6.4

$$\rho = \rho_{\max} e^{-\frac{(t-t_o)^2}{2\sigma^2}} \tag{6.3}$$

where

t is the hour of the day using the 24-h clock

ρ_{\max} is the maximum solar power density of the day at t_o (noontime in the equator)

σ is the standard deviation of the normal distribution function

The function should be used from dawn to dusk. The density ratio in Figure 6.4 is the percentage of the ratio ρ/ρ_{\max} . Note that when $t = 12 \pm \sigma$, $\rho/\rho_{\max} = 0.607$.

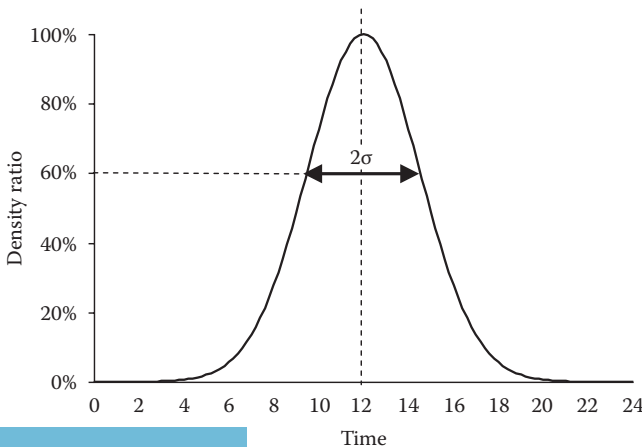


FIGURE 6.4 A typical solar distribution function (solar power density in 24 h period).

A large σ means a wider area under the distribution curve and more solar energy is acquired during the day. Near the equator, σ hardly changes with seasons. In high latitudes, σ is much smaller in winter than in summer.

Example 6.2

An area located near the equator has the following parameters:

$$\alpha_{dt} = 80\%, \quad \alpha_p = 95\%, \quad \beta_{wa} = 2\%$$

Assume that the parameters are unchanged during the day, and the standard deviation of the solar distribution function is 3.5 h. Compute the solar power density at 3:00 PM.

Solution

The first step is to compute the maximum solar power density. Since the location is near the equator, the maximum solar power density occurs around noon when the zenith angle is almost zero:

$$\rho_{max} = \rho_o \cos \xi (\alpha_{dt} - \beta_{wa}) \alpha_p = 1353 \times \cos(0) \times (0.8 - 0.02) \times 0.95 = 1.0 \text{ kW/m}^2$$

The solar power density at 3:00 PM is then

$$\rho = \rho_{max} e^{-\frac{(t-t_o)^2}{2\sigma^2}} = 1.0 \times e^{-\frac{(15-12)^2}{2 \times (3.5)^2}} = 0.694 \text{ kW/m}^2$$

The solar energy is typically harnessed by two methods: passive and active. A passive solar energy system uses the sunrays directly to heat liquid or gas that can condition air and water. An active system converts the sun's energy into electrical energy by using photovoltaic (PV) semiconductor material called a solar cell. The electricity generated by PV can be used locally, or exported to the power grid, or both.

6.1.1 PASSIVE SOLAR ENERGY SYSTEM

An example of the passive solar system is the thermosiphon hot water appliance shown in Figures 6.5 and 6.6. The system consists of a solar collector, water tank, and water tubes. The tank is located above the collector. The collector has an outer lens (or transparent glass) facing the sun, and houses a long zigzagged water tube. The lens concentrates the sunrays, thus increasing the temperature of water inside the tubes. The warm water moves naturally upward to the tank because hot water is less dense than cold water. Since the water in the upper part of the tank is warmer than the water in the lower part, the cold water at the bottom of the tank goes back to the collector. When warm water is needed inside the house, it is extracted from the top of the tank. This water is replaced by cooler water from the main water feeder of the house.

The passive solar system is simple, inexpensive, and requires little maintenance. However, it demands enough solar power density to make it viable, and it is most effective during the daytime.

On a larger scale, passive solar systems can be used to concentrate solar radiation to increase the temperature of any fluids to the level needed for industrial applications. Figure 6.7a shows one of these systems, which is known as *solar farm* or *thermosolar system*. The system can be integrated with a conventional thermal turbine to produce electricity. This system is called integrated solar combined cycle system (ISCCS). It consists of a large number of parabolic mirrors called collectors, which concentrate the solar radiation energy on a pipe system called receiver located at the focal area of the collector mirrors. The fluid of the receiver, which is often oil, is heated to about 400°C



FIGURE 6.5 Passive thermosiphon hot water solar system.

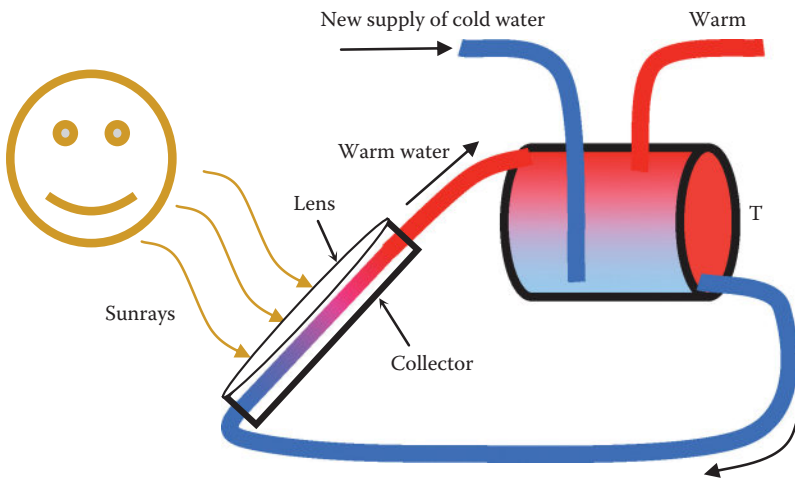


FIGURE 6.6 Thermosiphon hot water system.

and is used in a heat exchanger to produce steam that can be used to generate electricity using a thermal turbine. During the night, natural gas is used to produce the steam needed by the plant. Hence, the power generation is continuous.

Another system is shown in Figure 6.7b. The system consists of several troughs aligned to face the sun. At the focal line of the trough is a pipe carrying fluid. The troughs concentrate the solar energy at their focal line, where the pipe is located, thus heating the fluid inside the pipe. The heated fluid can be directly used as energy source or even to generate electricity.

6.1.2 ACTIVE SOLAR ENERGY SYSTEM (PHOTOVOLTAIC)

Light consists of particles called *photons*, which are the energy by-products of the nuclear reactions in the sun. Each photon is a packet of energy, but not all photons have the same amount of energy.

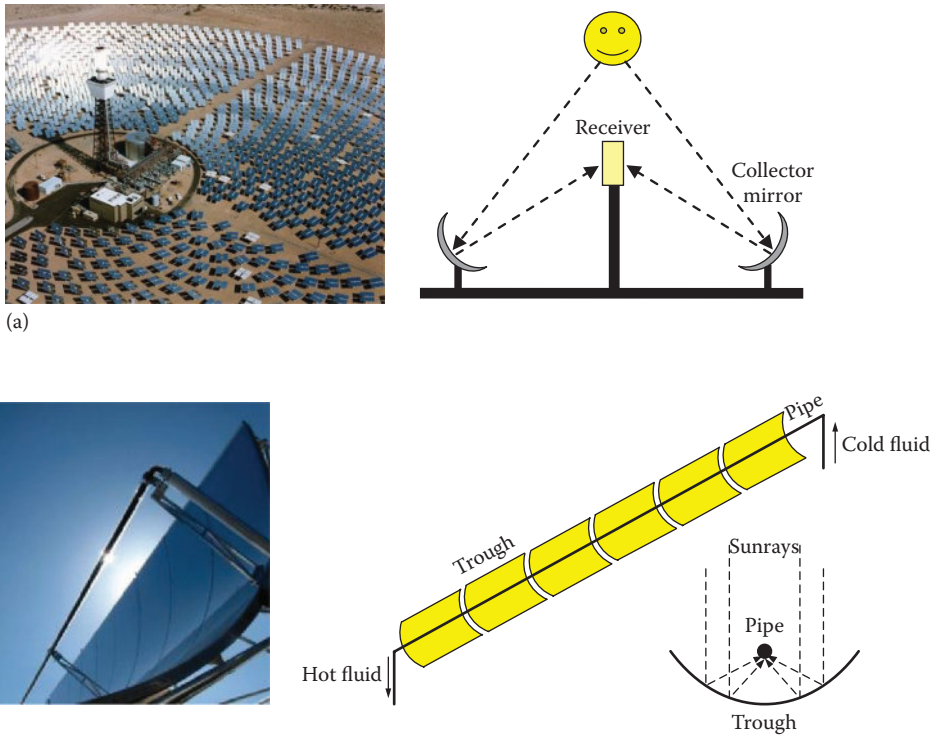


FIGURE 6.7 Solar systems: (a) integrated solar combined cycle system and (b) concentrated trough. (Images are courtesy of the US Department of Energy, Washington, DC.)

Photons with shorter wavelengths (higher frequencies) such as the gamma rays (about 10^{20} Hz) have more energy than photons with longer wavelengths such as the visible light ($4.5\text{--}7.5 \times 10^{14}$ Hz).

Converting photon energy into electricity is a photoelectric phenomenon that was discovered in 1839 by the French physicist Edmond Becquerel (1820–1891) and was further refined by the German physicist Heinrich Hertz (1857–1894) in 1887. They found that when light photons hit certain material, the electrons in the material absorb the energy of the photons. When this acquired energy is higher than the binding energy of the electrons, the electrons break away from their atoms. If the acquired energy of these electrons is harnessed, we have achieved photoelectric conversion of sunlight into electricity. The device to do this process was invented in the mid-twentieth century by the Bell Laboratories in the United States and was called *solar cell*. It was designed to collect the breakaway electrons to form electric current. Bell Laboratory used their solar cells to replace some of their dry cells (batteries) in their telephone network. The solar cell is called *photovoltaic* (PV) which is a compound word derived from two words: *photo* which is a Greek word for light, and *volt* which is a unit for measuring electric potential.

PV cells are made of semiconductor materials that include silicon (Si). A silicon atom has 14 electrons arranged in three energy levels (shells). The first two shells have 10 electrons, and the third (outer) shell has only 4 electrons, as shown in Figure 6.8. Although the atom is electrically neutral, the outer shell is only half full and there is enough space for four more electrons. Consequently, each silicon atom combines itself with four other atoms to form the silicon crystal structure shown at the right side of Figure 6.8. Now, each atom has eight electrons in its outer shell.

Since all electrons are used in atom bonding, the crystal structure of the silicon is a good insulator. To make the silicon more conductive electrically, additives (impurities) are added. Common additives are phosphorus (P) and boron (B). Phosphorus has five electrons in its outer shell while boron has only three. The process of adding these two impurities is called *doping*.

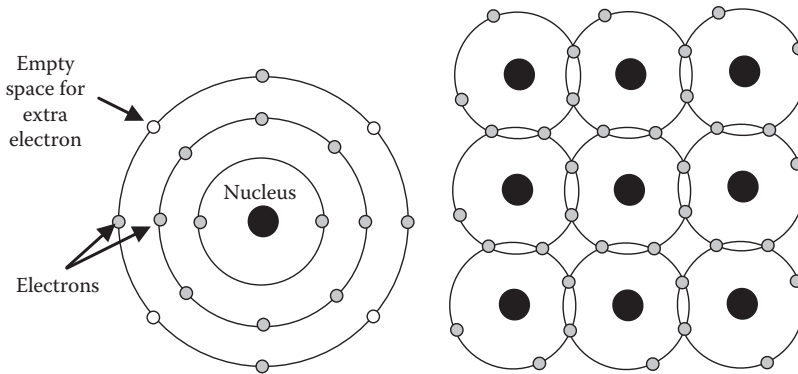


FIGURE 6.8 Silicon: atom and its crystal structures.

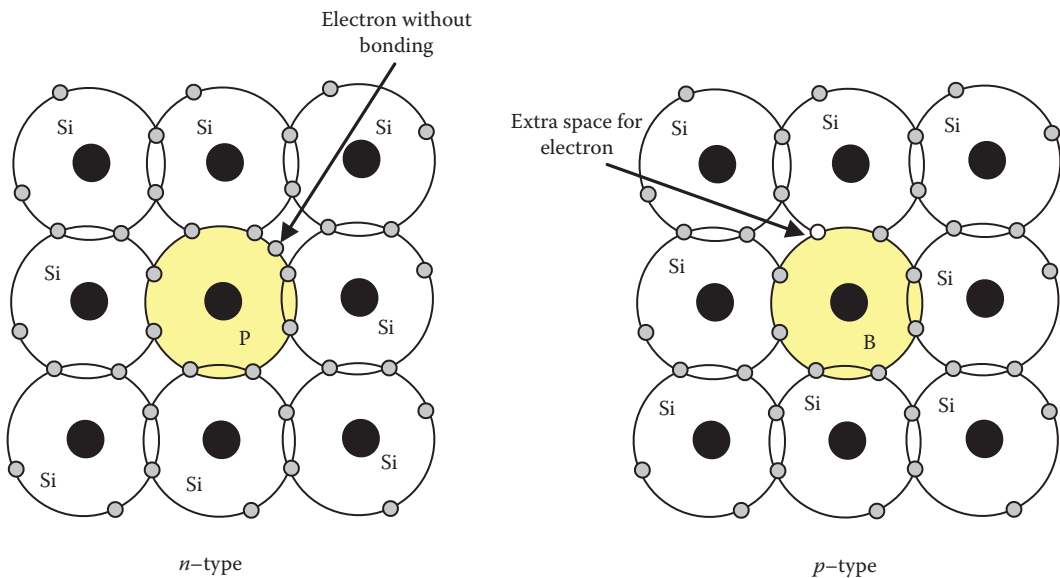


FIGURE 6.9 Silicon (Si) doped with phosphorus (P) and boron (B).

When phosphorus is added to the silicon, they bond as shown at the left side of Figure 6.9. However since phosphorous (P) has five electrons in its outer shell, one electron in the compound will not bond to any other atom. When this electron is given extra energy, it breaks free and roams inside the material looking for a positive charge (hole) to attach to it. This electron is known as *free carrier*. Because of the presence of these negatively charged free carriers, this phosphorous-silicon compound is called *n-type*. Keep in mind that this *n-type* material is still electrically neutral since the free electrons are still inside the compound.

When silicon is doped with boron as shown at the right side of Figure 6.9, the mix will have free holes since boron has only three electrons in its outer layer. This material is called *p-type*. Again, the *p-type* material is electrically neutral; the missing electrons (holes) are balanced out by the missing protons in the boron.

When the *n-type* silicon is attached to the *p-type* silicon, they turn into a device known as *diode* or *p-n junction*. When the two types are attached, free electrons in the *n-type* silicon move toward the free holes in the *p-type* silicon and vice versa. They join in the junction between the two materials, which is known as the *depletion zone*. At the equilibrium condition, the depletion

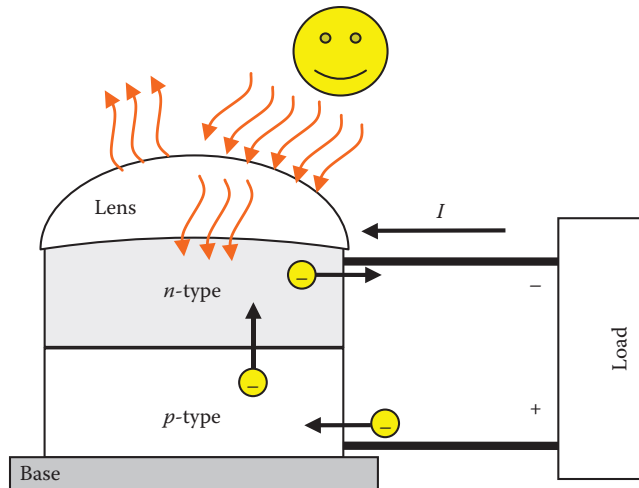


FIGURE 6.10 Concentrating PV cell.

zone creates a barrier that makes it harder for any more free electrons in the *n*-type material to move into the holes in the *p*-type. This *p-n* junction device is the main component of the PV cell.

There are two major types of PV cells: concentrating and flat-plate. The structure of the concentrating PV cell is shown in Figure 6.10. The cell consists of a convex lens mounted on top of *n*-type material. The *p*-type material is at the base of the cell. When the cell is illuminated, the electrons of the *n*-type acquire some energy from the light photons, which helps them to break free from their atoms. If we connect the two terminals of the *p-n* junction to a resistive load, the electrons move from the *n*-type material to the load and back to the *p*-type material instead of going through the barrier of the depletion zone. In this process, the energy acquired by the electrons is discharged in the load resistance. When the *p*-type material acquires electrons, it becomes negatively charged and the *n*-type material positively charged. The difference in potentials causes the electron to move back to the *n*-type material to equalize the charges. When the electron goes back to the *n*-type, it acquires new energy from the sunrays and the process is repeated. Notice that the direction of the current is opposite to the direction of the electrons; this is the convention adopted over 100 years ago.

The flat-plate PV cell, as the name implies, is rectangular and flat. This is the most common type of PV array used in commercial applications. Flat-plate cells are often mounted at fixed angles that maximize the exposure to the sun throughout the year; in the United States, it is the southern direction. In more flexible systems, the angle of the solar panel changes to track the optimal sun exposure during the day.

Because convex lenses concentrate light, concentrating PV cells require less material for the same power output than the flat-plate cells; thus they are smaller in size. However, concentrating cells operate best when the sky is clear of clouds. Diffused light through the clouds produces less power in the concentrated cell as compared to the flat-plate PV.

The construction of the solar cell requires several added components such as a cover glass, antireflective coating, and connecting grid. These components are shown in Figure 6.11. The cover glass is mounted on the top of the cell to protect it from the harsh environment (dust, scratches, bird dropping, etc.). Because silicon is a very shiny material, antireflective coating is used to reduce the reflection losses of silicon. A contact grid (mesh) is used to collect the electrons from the top of the *n*-type material. We cannot collect the electrons from the side of the junctions as this would require the electrons to travel long distances through the material, which will increase the internal losses of the PV. Of course, we cannot use solid plate instead of the mesh as it will prevent the sun's energy

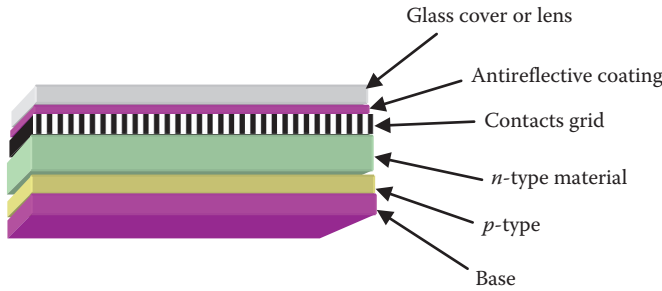


FIGURE 6.11 Main parts of PV cell.

from reaching the $p-n$ junction. The base at the bottom is made out of a solid plate if the cell is a single layer design.

Newer designs of PV cells consist of dual and triple-junction designs. These types of PV cells are made of two or three cells vertically stacked. Although more expensive, they produce more power and have higher efficiency and higher voltage than single layer PV cells.

6.1.2.1 Ideal PV Model

The $p-n$ junction diode is represented by the symbol shown in Figure 6.12. The p -type material (also known as anode) is represented by a triangle at the right side of the figure, and the n -type (cathode) is represented by the line at the top of the triangle. To obtain the current-voltage ($I-V$) characteristics of the diode, the simple circuit shown in Figure 6.13 is used. The anode of the diode is connected to a direct current (dc) adjustable voltage source and the cathode is connected to a resistive load. When the anode-to-cathode voltage (V_d) is positive (forward biased), the current flows through the diode (I_d) with little resistance. This is because the positive potential on the p -type material helps its holes to acquire enough energy to cross the barrier of the depletion zone and travel into the n -type side. When the voltage is reversed (reverse biased), almost no current flows though the diode. This is because the negative potential of the anode forces all holes to stay inside the p -type material. The ($I-V$) characteristic is shown in Figure 6.13 at the right side. When the diode is forward biased, the voltage drop across the diode is very small (about 0.6 V), and when the diode is reverse biased, the reverse saturation current of the diode (I_o) is very small.

The characteristic in Figure 6.13 can be obtained by using the diode model developed by the German physicist Walter H. Schottky (1886–1976)

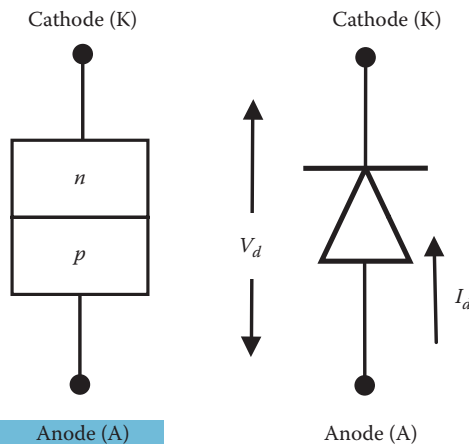


FIGURE 6.12 Representation of a $p-n$ junction diode.

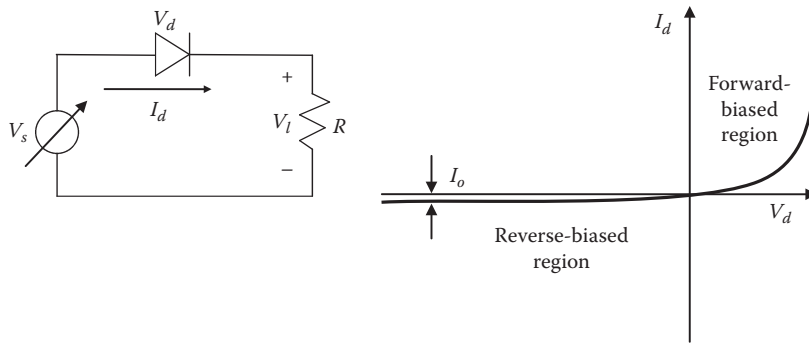


FIGURE 6.13 Characteristic of p - n junction diode.

$$I_d = I_o \left(e^{\frac{V_d}{V_T}} - 1 \right) \quad (6.4)$$

$$V_T = \frac{kT}{q}$$

where

I_o is the reverse saturation current of the diode

V_d is the voltage across the diode

V_T is thermal voltage

q is the charge of one electron which is known as the elementary charge constant ($1.602 \times 10^{-19} \text{ C}$)

T is the absolute temperature in kelvin (K); to convert from Celsius to kelvin, 273.15 is added to the Celsius value

k is the Boltzmann's constant ($1.380 \times 10^{-23} \text{ J/K}$)

Since the solar cell is just a diode without a voltage source whose electrons acquire their energy from light photons, it seems reasonable that we use the equivalent circuit in Figure 6.14. The sun in the figure represents the source of energy, and the cell is represented by a diode whose current flows from the n -junction to the p -junction then into the load, as explained earlier in Figure 6.10. However, the flow of this current creates an interesting situation; it makes the upper terminal of the load positive with respect to the lower terminal. Therefore, the diode now has a positive voltage on its anode with respect to the cathode. This is a forward-biased voltage, which causes a forward current to flow back into the diode. Now it seems that we have two currents in the circuit at the same time: the current coming out of the diode due to the acquired energy by the PV from light and the current going into the diode due to the positive polarity across the load. How can we resolve this confusion? The answer is to separate the source of energy (light) from the diode model and represent the PV's acquired energy by an electric current source whose magnitude depends on the solar power density (irradiance) as shown in Figure 6.15. The diode current is then the resultant current through the p - n junction as given in Equation 6.4. The remaining current is the load current

$$I = I_s - I_d \quad (6.5)$$

where

I_s is the solar current

I_d is the current through the diode

I is the output current of the solar cell (load current)

The solar current is a nonlinear variable that changes with light density (irradiance).

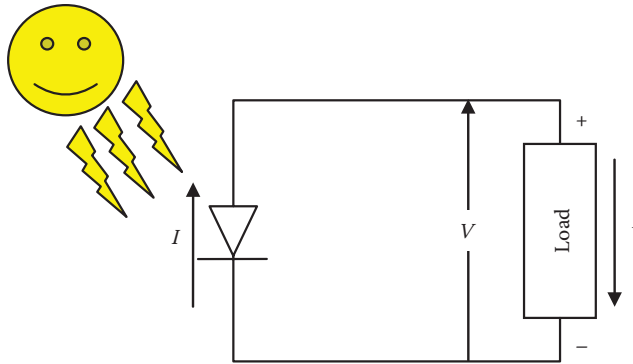


FIGURE 6.14 Representation of solar cell connected to load.

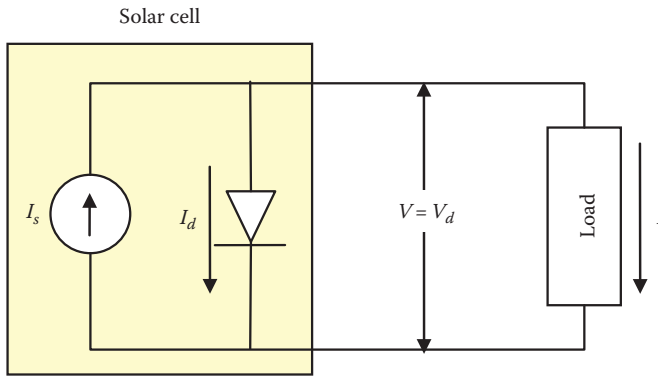


FIGURE 6.15 Modeling of ideal cell with current source.

The voltage across the load (V) is equal to the forward voltage across the diode (V_d)

$$V = V_d \tag{6.6}$$

If we assume that the solar current is independent of the load voltage, we can draw the current–voltage (I – V) characteristics as shown in Figure 6.16.

In Figure 6.16, the PV cell operates in the first quadrant Q_I only. Q_{II} and Q_{IV} are not realistic operational regions because in these quadrants, the load would be sending power to the solar cell.

The output power of the solar cell P is obtained by multiplying the output current (I) by the output voltage (V):

$$P = VI \tag{6.7}$$

Since the solar cell is essentially a p – n junction, we can compute the current (I_d) using Schottky model in Equation 6.4

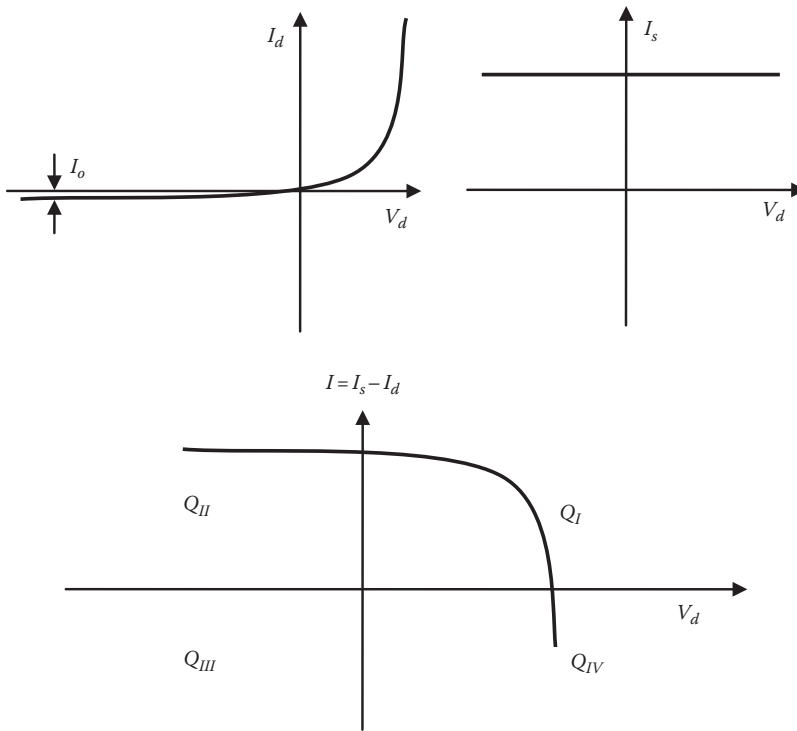


FIGURE 6.16 Current–volt characteristics of the PV cell.

$$I_d = I_o \left(e^{\frac{V_d}{V_T}} - 1 \right)$$

$$V = V_d$$

$$I = I_s - I_d$$
(6.8)

where

- I_o is the reverse saturation current
- V_d is the voltage across the diode which is the same as the voltage across the load
- V_T is the thermal voltage whose value is given in Equation 6.4

Substituting the current in Equation 6.8 into Equation 6.7 yields

$$P = VI = V_d I_s - V_d I_o \left(e^{\frac{V_d}{V_T}} - 1 \right)$$
(6.9)

Equation 6.9 represents the power–voltage characteristic P – V and Equation 6.8 represents the I – V characteristic. Both characteristics are shown in Figure 6.17. When the load current is zero, the PV voltage is at its maximum value, which is known as *open circuit voltage* (V_{oc}). When the load current increases, the voltage stays almost constant initially, then substantially reduced until it reaches zero. At zero voltage, the output current of the PV is called *short circuit current* (I_{sc}). It is the current of the PV when its terminals are shorted.

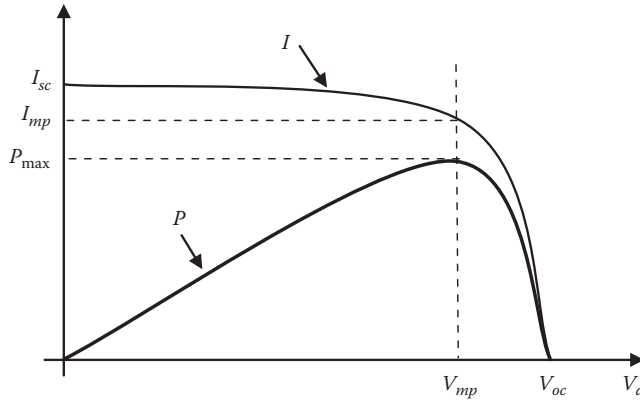


FIGURE 6.17 Current–voltage and power–voltage characteristics of PV cell.

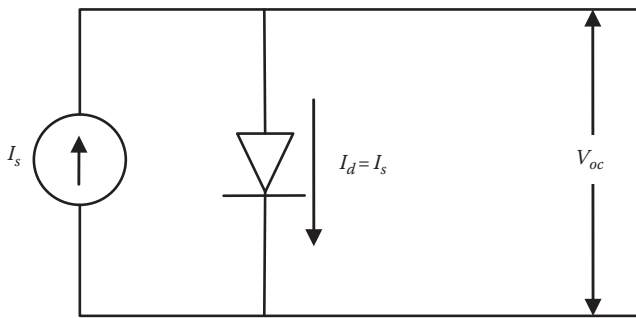


FIGURE 6.18 PV under open circuit condition.

To compute the open circuit voltage, we set the load current in Equation 6.8 to zero as shown in Figure 6.18. Hence,

$$I_d = I_s = I_o \left(e^{\frac{V_{oc}}{V_T}} - 1 \right) \tag{6.10}$$

$$V_{oc} = V_T \times \ln \left(\frac{I_s}{I_o} + 1 \right)$$

If we short-circuit the terminals of the PV cell as shown in Figure 6.19, the short circuit current of the cell (I_{sc}) is equal to the solar current (I_s). This is because the voltage across the diode is zero; hence the diode current is also zero:

$$I_{sc} = I_s \tag{6.11}$$

The P – V curve in Figure 6.17 shows that the power is zero at the short circuit and open circuit conditions. This is because either the voltage or current at any of these two points is zero. The power reaches its maximum value (P_{max}) at some point near the knee of the I – V curve. At P_{max} , the load current is I_{mp} and the load voltage is V_{mp} .

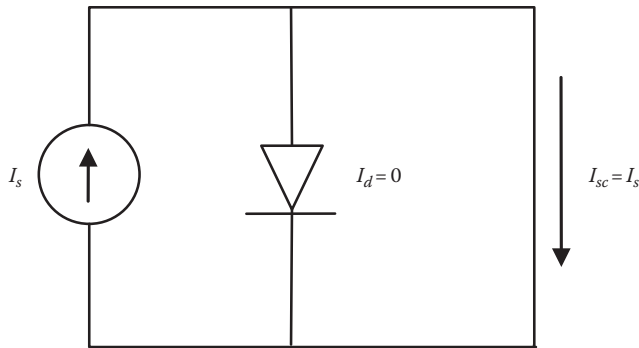


FIGURE 6.19 PV under short circuit condition.

Example 6.3

An ideal PV cell with reverse saturation current of 1 nA is operating at 30°C . The solar current at 30°C is 1 A . Compute the output voltage and output power of the PV cell when the load draws 0.5 A .

Solution

Let us first compute the thermal voltage V_T

$$V_T = \frac{kT}{q} = \frac{1.38 \times 10^{-23} \times (30 + 273.15)}{1.602 \times 10^{-19}} = 26.11 \times 10^{-3} \text{ V}$$

Use Equation 6.8 to compute the voltage

$$I = I_s - I_o \left(e^{\frac{V}{V_T}} - 1 \right)$$

$$0.5 = 1 - 10^{-9} \times \left(e^{\frac{V}{0.02611}} - 1 \right)$$

Hence, the voltage of the PV cell is

$$V = \ln \left[(1 - 0.5) \times 10^9 + 1 \right] \times V_T = 0.523 \text{ V}$$

The output power of the PV cell is

$$P = VI = 0.523 \times 0.5 = 0.2615 \text{ W}$$

Example 6.4

An ideal solar cell with reverse saturation current of 1 nA is operating at 20°C . The solar current at 20°C is 0.8 A . Compute the voltage and current of the solar cell at the maximum power point.

Solution

The output power of the PV cell is

$$P = VI$$

The voltage at maximum power can be obtained by setting the first derivative of the power equation to zero:

$$\frac{\partial P}{\partial V} = V \frac{\partial I}{\partial V} + I$$

The derivative of the current in Equation 6.8 is

$$\frac{\partial I}{\partial V} = -\frac{I_o}{V_T} e^{V/V_T}$$

Combining the two equations presented earlier yields

$$\frac{\partial P}{\partial V} = (I_s + I_o) - \left(1 + \frac{V}{V_T}\right) I_o e^{V/V_T}$$

where V_T is

$$V_T = \frac{kT}{q} = \frac{1.38 \times 10^{-23} \times (20 + 273.15)}{1.602 \times 10^{-19}} = 25.25 \times 10^{-3} \text{ V}$$

Setting the derivative of power equal to zero yields

$$\left(1 + \frac{V_{mp}}{V_T}\right) e^{V_{mp}/V_T} = \frac{I_s + I_o}{I_o}$$

$$\left(1 + \frac{V_{mp}}{25.25}\right) e^{V_{mp}/25.25} = 0.8 \times 10^9$$

This equation is nonlinear, but we can still find the value of V_{mp} graphically or by iterating the solution. While doing so, keep in mind that the slope of the power curve is sharp between the maximum power point and the open circuit point. Therefore, you should use a small step size in your iteration. Solving this equation iteratively yields the voltage at the maximum power point:

$$V_{mp} \oplus 443.894 \text{ mV}$$

Substituting the value of V_{mp} into Equation 6.8 yields I_{mp} :

$$I_{mp} = I_s - I_o \left(e^{\frac{V_{mp}}{V_T}} - 1 \right)$$

$$I_{mp} = 0.8 - 10^{-9} \left(e^{\frac{443.89}{25.25}} - 1 \right) = 756.9 \text{ mA}$$

Hence, the maximum output power of the cell is

$$P_{max} = V_{mp} \times I_{mp} = 443.89 \times 0.7569 = 335.98 \text{ mW}$$

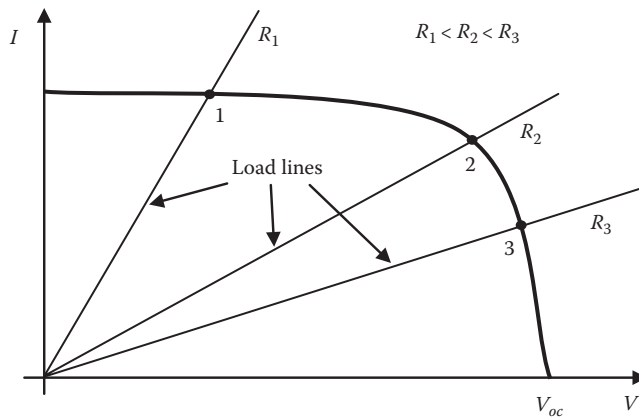


FIGURE 6.20 Operating points of the solar cell connected to a resistive load.

The operating point of the solar cell depends on the magnitude of the load resistance (R) which is the output voltage (V) divided by the load current (I). The intersection of the PV cell characteristic with the load line is the operating point of the PV cell. Consider the characteristics shown in Figure 6.20 where the straight lines are the load lines representing the resistances of the load. The slope of the load line [$\tan(I/V)$] is the inverse of the load resistance (i.e., load conductance). When the load resistance is adjusted to a value equal to R_1 , the system operates at point 1 as shown in the figure. When the load resistance increases the output voltage of the solar cell increases as well.

Example 6.5

For the solar cell in Example 6.4, compute the load resistance at the maximum output power.

Solution

The voltage and currents at the maximum output power computed in Example 6.4 are

$$V_{mp} = 443.894 \text{ mV}$$

$$I_{mp} = 0.7569 \text{ A}$$

Hence, the load resistance at the maximum power point (R_{mp}) is

$$R_{mp} = \frac{V_{mp}}{I_{mp}} = \frac{443.894}{756.9} = 0.5864 \Omega$$

Example 6.6

An ideal PV cell with a reverse saturation current of 1 nA is operating at 30°C . The solar current at 30°C is 1 A . The cell is connected to a 10Ω resistive load. Compute the output power of the cell.

Solution

Equation 6.8 shows the relationship between the diode current I_d and voltage V

$$I_d = I_o \left(e^{\frac{V}{V_T}} - 1 \right)$$

where

$$V_T = \frac{kT}{q} = \frac{1.38 \times 10^{-23} \times (30 + 273.15)}{1.602 \times 10^{-19}} = 26.1 \times 10^{-3} \text{ V}$$

The output current of the cell I is

$$I = I_s - I_d = I_s - I_o \left(e^{\frac{V}{V_T}} - 1 \right)$$

In addition, the output current is the output voltage divided by the load resistance:

$$I = \frac{V}{R}$$

Combining the two equations presented earlier yields

$$I = \frac{V}{R} = I_s - I_o \left(e^{\frac{V}{V_T}} - 1 \right)$$

or

$$V = I_s R - I_o R \left(e^{\frac{V}{V_T}} - 1 \right)$$

$$V = 10 - 10^{-8} \left(e^{\frac{V}{0.0261}} - 1 \right)$$

In this equation, the voltage is the only unknown. However, the equation is nonlinear and can be solved iteratively to compute the voltage

$$V \oplus 0.54 \text{ V}$$

Hence, the output power of the cell is

$$P = \frac{V^2}{R} = \frac{0.54^2}{10} = 29.16 \text{ mW}$$

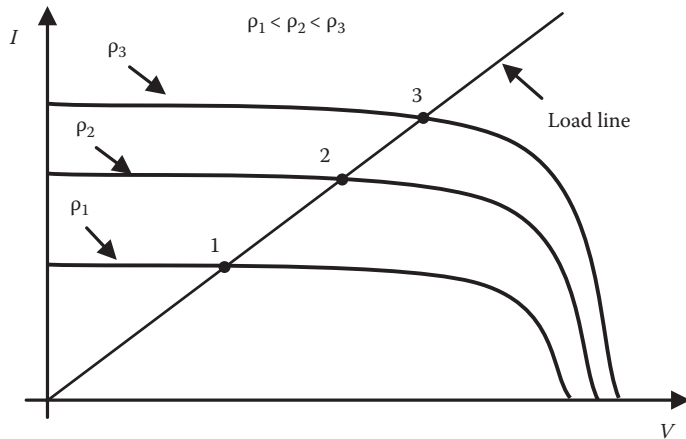


FIGURE 6.21 Effect of irradiance on the operating point.

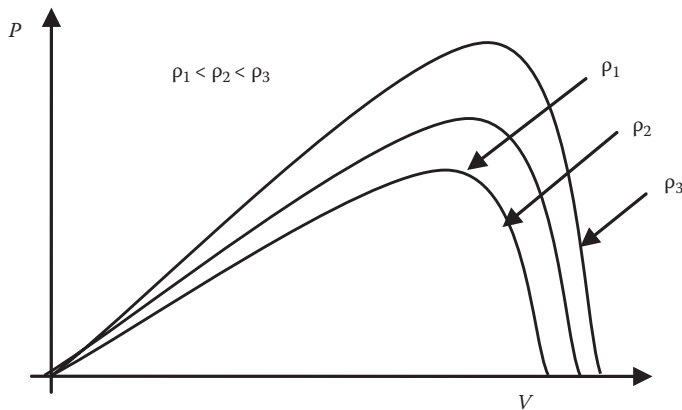


FIGURE 6.22 Effect of irradiance on PV output power.

6.1.2.2 Effect of Irradiance and Temperature on Solar Cells

There are two key variables that affect the output power of a PV cell: (1) the light power density ρ (irradiance) and (2) the temperature of the cell T .

Increasing the irradiance increases the magnitude of the solar current (I_s), and consequently increases the short circuit current and the open circuit voltage as shown in Figure 6.21. The effect of irradiance on the output power of the solar cell is shown in Figure 6.22. Notice that the operating points are all located at the intersections of the PV characteristics with the load line. Also, notice that the maximum power increases with the increase in irradiance.

As for the temperature, let us examine Equation 6.10. The thermal voltage (V_T) is linearly dependent on the temperature as given in Equation 6.4. However, the saturation current (I_o) and the solar current (I_s) are also nonlinearly dependent on the temperature. The net result is that the open circuit voltage is reduced when the temperature increases. This relationship is shown in Figure 6.23. The effect of temperature on the output power is shown in Figure 6.24. When the temperature is reduced, the output power of the solar cell increases. Therefore, a good site for a solar cell is a cool place with high enough irradiance.

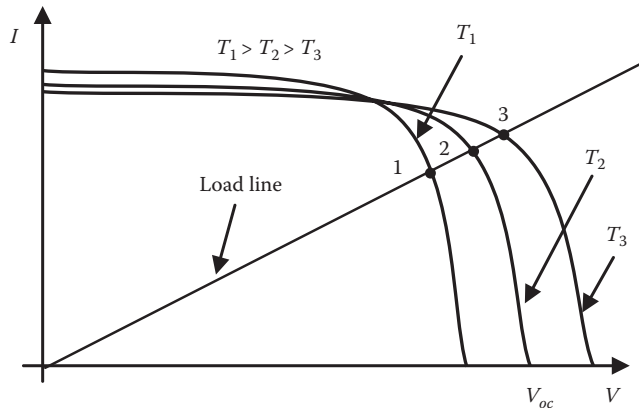


FIGURE 6.23 Effect of temperature on the operating point.

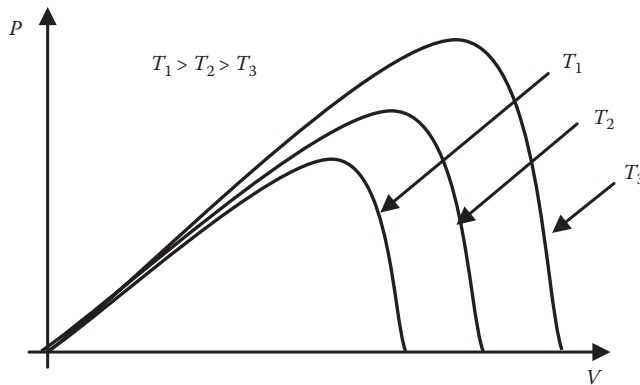


FIGURE 6.24 Effect of temperature on PV output power.

Example 6.7

An ideal solar cell with a reverse saturation current of $0.1\mu\text{A}$ is operating at 30°C . Find the short circuit current and the open circuit voltage of the cell assuming that the solar current at 30°C is 500mA .

Solution

The short circuit current is given in Equation 6.11.

$$I_{sc} = I_s = 500\text{mA}$$

The open circuit voltage V_{oc} is given in Equation 6.10

$$V_{oc} = V_T \times \ln\left(\frac{I_s}{I_o} + 1\right)$$

where

$$V_T = \frac{kT}{q} = \frac{1.38 \times 10^{-23} \times (30 + 273.15)}{1.602 \times 10^{-19}} = 26.1 \times 10^{-3} \text{ V}$$

Hence, the open circuit voltage is

$$V_{oc} = V_T \times \ln\left(\frac{I_s}{I_o} + 1\right) = 26.1 \times 10^{-3} \times \ln\left(\frac{500}{0.0001} + 1\right) = 403 \text{ mV}$$

Example 6.8

A 2 m² panel of solar cells is installed in the Nevada area discussed in Example 6.1. The overall efficiency of the PV panel is 10%:

1. Compute the electrical power of the panel.
2. Assume the panel is installed on a geosynchronous satellite. Compute its electrical power output.

Solution

1. In Example 6.1, the computed power density is 685.5 W/m². The power of sunrays on the solar panel P_s is the power density ρ multiplied by the area of the panel A :

$$P_s = \rho \times A = 685.5 \times 2 = 1.371 \text{ kW}$$

The electrical power output of the panel (P_{panel}) is the solar power input (P_s) multiplied by the efficiency of the panel (η):

$$P_{panel} = \eta P_s = 0.1 \times 1371 = 137.1 \text{ W}$$

Because of the low efficiency of this solar panel, the electric power obtained from a 2 m² panel in one of the best areas in the United States produces only 137 W. This is just enough to power two light bulbs. Higher power can be obtained if the solar panel is larger and/or the efficiency of the panel is higher.

2. If the same solar panel is mounted on a satellite, the solar power density on the panel is ρ_o . Hence,

$$P_s = \rho_o \times A = 1353 \times 2 = 2.706 \text{ kW}$$

The electrical power output of the panel is the solar power input multiplied by the panel efficiency:

$$P_{panel} = \eta P_s = 0.1 \times 2706 = 270.6 \text{ W}$$

As seen, the electric power of the same panel doubles when it is moved to the outer space.

6.1.2.3 PV Module

A single PV cell of 10 cm in diameter produces about 1 W power, which is enough to run a low-power calculator. Since the PV cell is essentially a diode, its operating voltage is about 0.6 V, which is the forward-biased voltage of a diode. To increase the power rating, several PV cells are connected in parallel and series. The parallel connection increases the overall current, and the series connection increases the overall voltage. When several PV cells are connected they form a *module* or *panel*; a



FIGURE 6.25 PV module, PV array, and PV system. (Images courtesy of the US Department of Energy, Washington, DC.)

typical module is shown in the left part of Figure 6.25. For higher power, several modules are connected together to form a PV *array* as shown in the middle part of Figure 6.25. More sophisticated PV arrays are mounted on tracking devices that follow the sun throughout the day. The tracking devices tilt the PV arrays to maximize the exposure of the cells to the sunrays, thus increasing the output power of the system. Several of these arrays form a PV *system* similar to the one shown in the right part of Figure 6.25. When a large number of these arrays produce substantial power, they are often connected to the distribution or transmission system.

Example 6.9

An ideal PV cell produces 2.5 W at 0.5 V during certain environmental conditions. Compute the output power, current, and voltage if the cells are connected in the following arrangements:

1. A panel of four parallel columns and each column has 10 series cells.
2. When several panels are connected as an array of two parallel columns and each column has four series modules.
3. When several arrays are connected as a solar system consisting of 10 parallel columns and each column has 20 series arrays.

Solution

1. The total voltage of the panel is

$$V_{\text{panel}} = 0.5 \times 10 = 5 \text{ V}$$

When the power of each cell is 2.5 W, the total power of the panel is

$$P_{\text{panel}} = P_{\text{cell}} \times (10 \times 4) = 2.5 \times 40 = 100 \text{ W}$$

The total current of the panel is

$$I_{\text{panel}} = \frac{P_{\text{panel}}}{V_{\text{panel}}} = \frac{100}{5} = 20 \text{ A}$$

2. The total voltage of the array is

$$V_{array} = V_{panel} \times (4) = 5 \times 4 = 20 \text{ V}$$

The total power of the array is

$$P_{array} = P_{panel} \times (4 \times 2) = 100 \times 8 = 800 \text{ W}$$

The total current of the array is

$$I_{array} = \frac{P_{array}}{V_{array}} = \frac{800}{20} = 40 \text{ A}$$

3. The total voltage of the system is

$$V_{system} = V_{array} \times 20 = 20 \times 20 = 400 \text{ V}$$

The total power of the system is

$$P_{system} = P_{array} \times (20 \times 10) = 800 \times 200 = 160 \text{ kW}$$

The total current of the system is

$$I_{system} = \frac{P_{system}}{V_{system}} = \frac{160,000}{400} = 400 \text{ A}$$

The model in Figure 6.15 can also be used for PV module, array, and system. To develop a model for multiple PVs, we assume that the parameters and environmental conditions are the same for every cell in the system. This assumption will simplify the modeling of the solar systems.

For the series connection, shown in Figure 6.26, the solar current is the same for any cell. The equivalent circuit in this case is shown in Figure 6.27. Because we now have the diodes in series, the

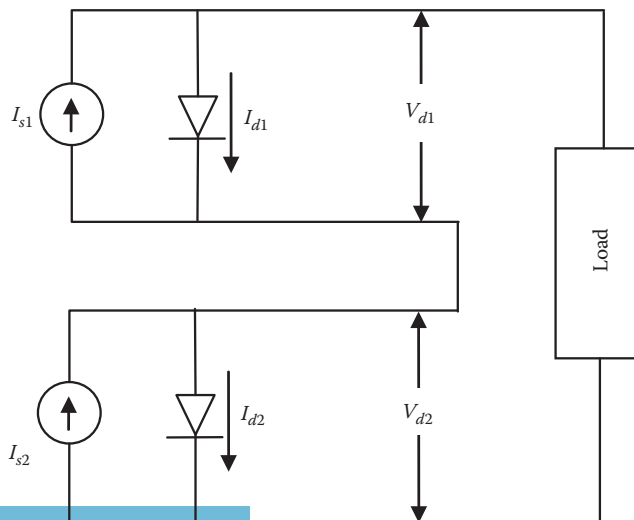


FIGURE 6.26 Solar cells in series.

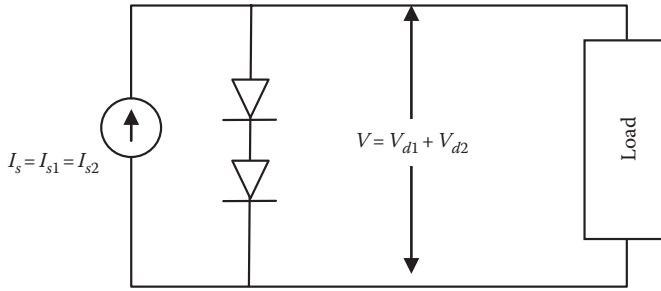


FIGURE 6.27 Equivalent circuit for solar cells in series.

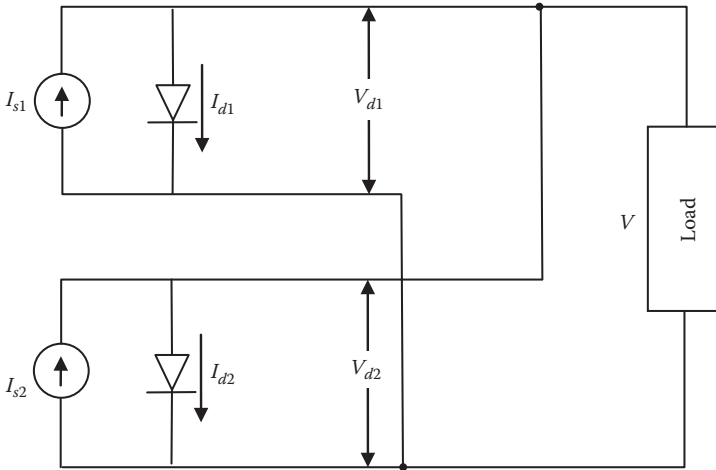


FIGURE 6.28 Solar cells in parallel.

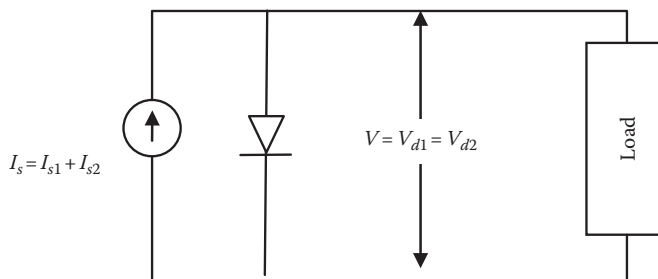


FIGURE 6.29 Equivalent circuit of solar cells in parallel.

output voltage of the module is the sum of the voltages of all cells. The output current, however, is the same as that of a single cell.

In Figure 6.28, the solar cells are connected in parallel. In this case, the voltage across the load is the same as the voltage of any one of the cells. However, the output current of the module is the sum of the output currents of all cells. The equivalent circuit of the parallel connection is shown in Figure 6.29.

Example 6.10

An ideal PV module is composed of 50 solar cells connected in series. At 20°C, the solar current of each cell is 1 A and the reverse saturation current is 10 nA. Draw the $I-V$ and $I-P$ characteristics of the module.

Solution

For each cell, the thermal voltage is

$$V_T = \frac{kT}{q} = \frac{1.38 \times 10^{-23} \times (20 + 273.15)}{1.602 \times 10^{-19}} = 25.25 \text{ mV}$$

The diode current of the cell is

$$I_d = I_o \left(e^{\frac{V}{V_T}} - 1 \right) = 10^{-8} \times \left(e^{\frac{V}{0.02525}} - 1 \right)$$

and the load current of the cell is

$$I_{cell} = I_s - I_d = 1 - 10^{-8} \times \left(e^{\frac{V_{cell}}{0.02525}} - 1 \right)$$

The power of the cell P_{cell} is

$$P_{cell} = V_{cell} I_{cell}$$

Using the two equations presented earlier, we can find the characteristics of a single cell as shown in Figure 6.30.

The voltage of the module can be obtained by multiplying the single-cell voltage by the number of series cells:

$$V_{module} = n \times V_{cell}$$

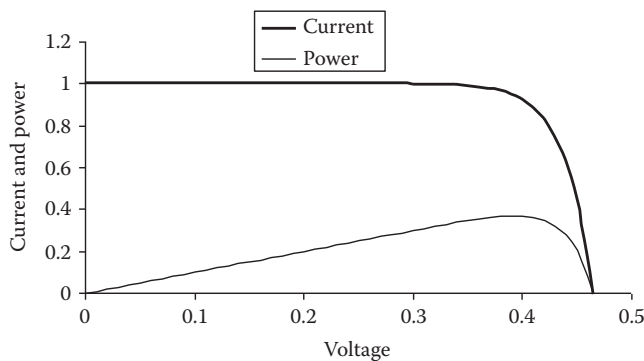


FIGURE 6.30 $I-V$ and $P-V$ characteristics of a single cell (current in A, voltage in V, and power in W).

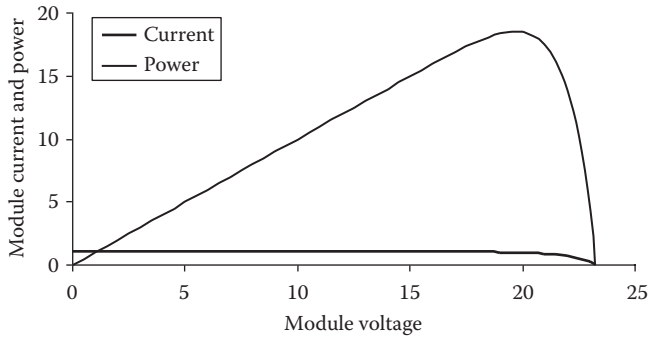


FIGURE 6.31 I - V and P - V characteristics of a single cell (current in A, voltage in V, and power in W).

Similarly, the power of the module is the power of a single cell P_{cell} multiply by the number of cells in the module:

$$P_{module} = n \times P_{cell}$$

Doing so, we can obtain the module characteristics in Figure 6.31.

6.1.2.4 Real Model of PV

Depending on the material and the structure of solar cells, the efficiency of most cells range between 2% and 20%. In recent development, multilayer solar cells have achieved efficiencies as high as 40%. The efficiency of a PV cell is dependent on many factors; the main ones are:

1. The reflection of the solar radiation at the top of the PV cell. The more the reflection, the less solar energy reaching the p - n junction.
2. Light has photons of a wide range of energy levels. Some don't have enough energy to excite the electrons and allow them to escape their atom bonding, and other photons have too much energy that is hard to capture by the electrons. These two scenarios account for as much loss as 70% of the solar energy.
3. The resistances of the collector trace at the top of the cell. This resistance is due to the relatively thin traces forming a grid at the top of the cell. Remember that we cannot cover the top with a wide metal plate to reduce the resistance as this would prevent the light from penetrating the cell. In some modern PV cells, the contacts on the top of the cell are made of somewhat transparent material to reduce their blocking of sunlight. Remember that we cannot put the contacts on the side of the cell as this would increase the internal loss of the cell as discussed earlier.
4. The resistance of the wires connecting the solar cell to the load.
5. The resistance of the semiconductor crystal.

The first two losses are called *irradiance losses* and the rest are *electrical losses*. To account for electrical losses, we can modify the model in Figure 6.15 by including the resistances of the collector traces and the external wires as well as the resistance of the crystal itself. The wires and traces can be represented by a series resistance (R_s), while the internal resistance of the crystal can be represented by a parallel resistance (R_p) as shown in Figure 6.32. The series resistance is in the range of a few milliohm and the parallel resistance is in the range of a few kilohm.

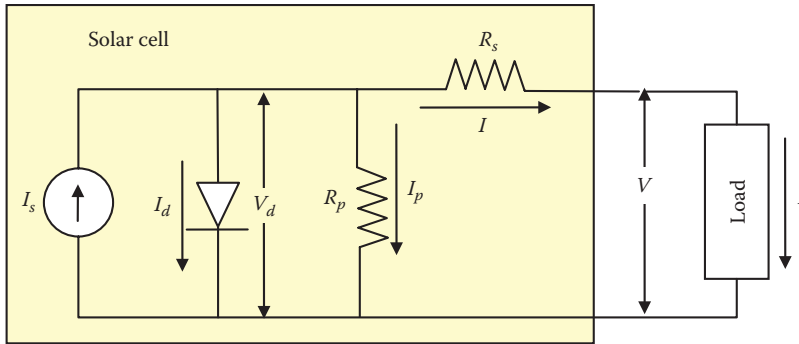


FIGURE 6.32 Model of real PV cell.

The new model requires the modification of Equation 6.8 to account for the added components. The load current should now be represented by

$$I = I_s - I_d - I_p \tag{6.12}$$

and the load voltage is

$$V = V_d - IR_s \tag{6.13}$$

To compute the efficiency of the solar cell, we need to compute the irradiance efficiency ($\eta_{irradiance}$) and the electrical efficiency (η_e)

$$\eta_{irradiance} = \frac{P_{se}}{P_s} = \frac{V_d I_s}{\rho A} \tag{6.14}$$

$$\eta_e = \frac{P_{out}}{P_{se}} = \frac{VI}{V_d I_s} \tag{6.15}$$

where

- P_{se} is solar power converted to electricity
- P_s is solar power reaching the solar cell
- P_{out} is the output power of the solar cell that is consumed by the load
- ρ is the solar power density at the surface of the cell
- A is the area of the PV cell facing the sun

The total efficiency (η) of the solar cell is then

$$\eta = \eta_{irradiance} \eta_e = \frac{P_{se}}{P_s} \frac{P_{out}}{P_{se}} = \frac{P_{out}}{P_s} = \frac{VI}{\rho A} \tag{6.16}$$

Example 6.11

A 100cm² solar cell is operating at 30°C. The output current of the cell is 1 A, the load voltage is 0.4 V, and the saturation current of the diode is 1nA. The series resistance of the cell is 10mΩ and the parallel resistance is 1kΩ. At a given time, the solar power density is 200 W/m². Compute the irradiance efficiency.

Solution

The diode current can be computed if the thermal voltage, the voltage across the diode, and the saturation current are known. The thermal voltage at 30°C is

$$V_T = \frac{kT}{q} = \frac{1.38 \times 10^{-23} \times (30 + 273.15)}{1.602 \times 10^{-19}} = 26.1 \times 10^{-3} \text{ V}$$

The voltage across the diode is

$$V_d = V + IR_s = 0.4 + 1 \times 0.01 = 0.41 \text{ V}$$

The diode current can be computed using Equation 6.8

$$I_d = I_o \left(e^{\frac{V}{V_T}} - 1 \right) = 10^{-9} \times \left(e^{\frac{0.41}{0.0261}} - 1 \right) = 6.64 \text{ mA}$$

The current in the shunt resistance is

$$I_p = \frac{V_d}{R_p} = \frac{0.41}{1000} = 0.41 \text{ mA}$$

The solar current is

$$I_s = I + I_d + I_p = 1 + 0.00664 + 0.00041 = 1.00705 \text{ A}$$

The irradiance efficiency can be calculated by Equation 6.14

$$\eta_{\text{irradiance}} = \frac{V_d I_s}{\rho A} = \frac{0.41 \times 1.00705}{200 \times 0.01} = 0.205$$

Example 6.12

For the solar cell in Example 6.11, compute the overall efficiency of the PV cell.

Solution

The electrical losses $P_{e\text{-loss}}$ of the PV cell is

$$P_{e\text{-loss}} = I^2 R_s + I_p^2 R_p = 1.0^2 \times 0.01 + (0.41 \times 10^{-3})^2 \times 1000 = 10.168 \text{ mW}$$

The electrical efficiency as given in Equation 6.15 is

$$\eta_e = \frac{P_{out}}{P_{se}} = \frac{P_{out}}{P_{out} + P_{e\text{-loss}}} = \frac{VI}{VI + P_{e\text{-loss}}} = \frac{0.4 \times 1.0}{0.4 \times 1.0 + 0.010168} = 0.975$$

As seen in these calculations, the electrical losses are relatively small compared with the irradiance losses.

The total efficiency of the cell as given in (6.16) is

$$\eta = \eta_{\text{irradiance}} \eta_e = 0.205 \times 0.975 = 0.20 \quad \text{or} \quad 20\%$$

6.1.2.5 Daily Power Profile of PV Array

The output power of a solar cell (P_{out}) can be computed by using Equation 6.16

$$P_{out} = \eta P_s = \eta \rho A \quad (6.17)$$

Hence, if we assume that the efficiency of the solar cell is approximately constant, the output power of the cell is linearly related to the solar power density. Since the solar power density over a period of 1 day is almost a bell-shaped curve as shown in Figure 6.4, the output power of the cell from dawn to dusk is also a bell-shaped curve that can be expressed by

$$P_{out} = P_{max} e^{-\frac{(t-t_o)^2}{2\sigma^2}} \quad (6.18)$$

where

P_{out} is the electric power produced by the solar cell at any time t

P_{max} is the maximum power produced during the day at t_o (noon in the equator)

The energy produced by the PV cell (E_{out}) in 1 day is the integral of Equation 6.18 from dawn to dusk:

$$E_{out} = \int_{t_{dawn}}^{t_{dusk}} P_{max} e^{-\frac{(t-t_o)^2}{2\sigma^2}} dt \approx P_{max} \sqrt{2\pi}\sigma \quad (6.19)$$

Example 6.13

The solar power density at a given site is

$$\rho = \rho_{max} e^{-\frac{(t-12)^2}{12.5}}$$

A solar panel is installed at the site and its maximum electric power measured at noon is 100 W. Compute the daily energy produced by the PV panel in 1 day.

Solution

From the equation of the solar power density, $2\sigma^2 = 12.5$

Hence,

$$\sigma = \sqrt{\frac{12.5}{2}} = 2.5$$

Using Equation 6.19, we get

$$E_{panel} = P_{max} \sqrt{2\pi} \sigma = 100 \times \sqrt{2\pi} \times 2.5 = 0.627 \text{ kWh}$$

Example 6.14

The solar power density at a given site is represented by the equation

$$\rho = 0.7e^{\frac{-(t-12)^2}{18}} \text{ kW/m}^2$$

A 4 m² solar panel is installed at the site. The maximum electric power of the panel is 320 W.

- Compute the overall efficiency of the panel.
- Compute the output power of the panel at 4:00 PM.

Solution

- Maximum solar power density from the equation given earlier is 700 W/m². Assuming the efficiency to be constant, we can compute the efficiency at the maximum operating point:

$$\eta = \frac{P_{max}}{\rho_{max} A} = \frac{320}{700 \times 4} = 11.43\%$$

- The output power of the panel at 4:00 PM can be directly computed using Equation 6.18:

$$P_{panel} = P_{max} e^{\frac{-(t-12)^2}{2\sigma^2}} = 320 \times e^{\frac{-(16-12)^2}{18}} = 131.56 \text{ W}$$

6.1.2.6 Photovoltaic System Integration

Generating a dc at low voltage is not useful for most power equipment and appliances which are designed for alternating currents at 120/240 V. Therefore, a converter is needed to change the low voltage dc waveform of the PV array to an alternating current (ac) waveform at the frequency and voltage levels required by the load equipment. The solar array and the converter are the main components of the PV system. These PV systems are quite popular for household and commercial building; some are shown in Figure 6.33.

Most PV systems have two main designs: storage and direct systems. The storage PV system is shown in Figure 6.34 and consists of four main components: solar array, charger/discharger, battery, and converter. The function of the battery is to store the excess energy of the PV system during the daytime so it can be used during the night. These batteries are deep-cycle types that can be fully discharged without being damaged. These batteries are more expensive than normal car batteries and often used in boats and recreation vehicles. The converter is used to transform the dc power of the PV array, or the battery, into ac for household or commercial use. Several of these converters are discussed in Chapter 10. The commercial converters for PV applications are in the range of 1.0–6 kW, which are adequate for most household and small commercial applications. This system is also known as a stand-alone PV system. It is most suitable for areas with no grid connection.



FIGURE 6.33 Various photovoltaic systems. (Image courtesy of the US Department of Energy, Washington, DC.)

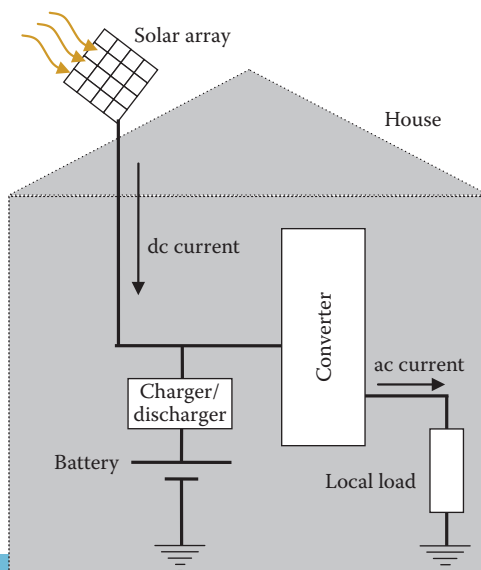


FIGURE 6.34 Storage PV system.

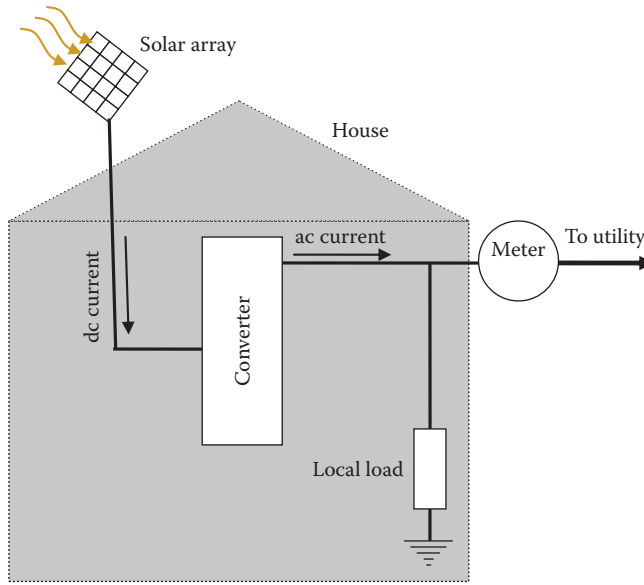


FIGURE 6.35 Direct PV system.

The use of storage batteries is the major drawback of the stand-alone PV system. This is because the batteries decrease the overall efficiency of the PV system; about 10% of the energy stored is normally lost. They also add to the total expense of the PV system, their life span is about 5 years, and they occupy considerable floor space. The leak from the batteries is very acidic and causes corrosion and damage to surrounding areas.

A simpler system that requires a direct connection to the utility grid is shown in Figure 6.35. In this system, the storage batteries and the charger are eliminated. The excess power in this solar system is sent to the power grid. The meter measures the net energy (PV power minus the consumed power of the house).

Example 6.15

A house is equipped with the solar system in Figure 6.35. The following table shows the daily load of the house (P_L), and the average output of the PV system (P_{out}). Assume that the daily pattern is repeated throughout 1 month. Compute the saving in energy cost due to the use of the PV system during the month. Assume that the cost of energy from the utility is \$0.20/kWh.

Time	Average Output of PV Array P_{out} (W)	Average House Load P_L (W)
8:00 PM–6:00 AM	0	200
6:00 AM–8:00 AM	200	800
8:00 AM–11:00 AM	300	100
11:00 AM–5:00 PM	500	100
5:00 PM–8:00 PM	200	1200

Solution

The energy consumed by the load and the energy traded with the utility are shown in the following table:

Time T	House Consumption (kWh)	Average Power Exported to Utility (W)	Energy Exported to Utility (kWh)	Average Power Imported from Utility (W)	Energy Imported from Utility (kWh)
Equations	$E_L = P_L \times T$	$P_{export} = P_{out} - P_L$	$E_{export} = P_{export} \times T$	$P_{import} = P_L - P_{out}$	$E_{import} = P_{import} \times T$
8:00 PM–6:00 AM	2.0	0	0	200	2.0
6:00 AM–8:00 AM	1.6	0	0	600	1.2
8:00 AM–11:00 AM	0.3	200	0.6	0	0
11:00 AM–5:00 PM	0.6	400	2.4	0	0
5:00 PM–8:00 PM	3.6	0	0	1000	3.0
Total daily Energy	8.1		3.00		6.2

Without the solar system, the daily cost of energy C_1 is

$$C_1 = 8.1 \times 0.2 = \$1.62$$

With the solar system, the daily cost of energy C_2 is

$$C_2 = (6.2 - 3.0) \times 0.2 = \$0.64$$

The savings in 1 month (S) is given by

$$S = (C_1 - C_2) \times 30 = \$29.4$$

Keep in mind that this saving does not reflect the cost of the PV system.

6.1.2.7 Evaluation of PV Systems

The common applications of PV cells are in consumer products such as calculators, watches, battery chargers, light controls, and flashlights. The larger PV systems are extensively used in space applications (such as satellites) where their usage has increased 1000-fold since 1970. In higher-power applications, three factors determine the applicability of the PV systems: (1) the cost and the payback period of the system, (2) the accessibility to a power grid, and (3) the individual inclination to invest in environmentally friendly technologies.

The price of electricity generated by a PV system varies widely and is based on the size of the PV system, the various design options, the installation cost, the lifetime of the system, the maintenance cost, and the solar power density at the selected site. The estimated average prices of 1 kWh of PV energy using engineering economic models over a period of 40 years are shown in Figure 6.36. From this figure, we see that the price decreases rapidly, although it is still more expensive than most utility rates; the cost of generating 1 kWh of PV electricity is more than twice the price charged by the utilities in the Northwest United States region in 2010. Nevertheless, this higher cost of PV energy production is expected to become lower as the technology improves and production increases.

In remote areas without access to power grids, the PV system is often the first choice among the available alternatives. In developing countries and remote areas, thousands of PV systems have already been installed and have improved the quality of life tremendously. These solar power systems operate clean water pumps, provide power for lighting, keep medicine refrigerated, keep equipment sterilized, operate emergency radios, and are used in many other critical applications. The larger PV systems worldwide have a total capacity of more than 70 GW in 2011; some of the large systems are shown in Figure 6.37. To put the number into perspective, the PV world capacity is equivalent to about 70 nuclear power plants.

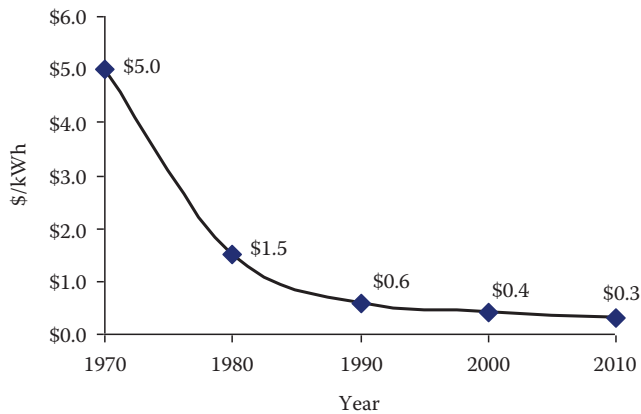


FIGURE 6.36 Price of kWh from PV systems.



FIGURE 6.37 High power PV systems. (Images are courtesy of the US Department of Energy, Washington, DC.)

The dream of solar energy proponents is to replace a large amount of the energy that is currently produced by primary resources with PV systems. This is because 1 kW generated by a PV system, instead of coal fired power plant, can reduce the annual pollution by as much as 0.25 kg of Nitrogen Oxides (NO_x), 1 kg of Sulfur Dioxide (SO_2), and 800 kg of Carbon Dioxide (CO_2).

Although solar energy is very promising, PV technology is not free from drawbacks. The following list identifies the main issues associated with PV systems:

1. Although the power generated by the PV system is pollution free, toxic chemicals are used to manufacture solar cells including arsenic and silicon compounds. Arsenic is generally an odorless and flavorless semi metallic chemical that is highly toxic and can kill humans quickly if inhaled in large amounts. Long-term exposure to small amounts of arsenic through the skin or by inhalation can lead to slow death and a variety of illnesses. Silicon, by itself, is not toxic. However, when additives are added to make the p - n junction, the compound can be extremely toxic. Since water is used in the manufacturing process, the runoff could cause the arsenic and silicon compounds to reach local streams. Furthermore, should a PV array catch fire, these chemicals can be released into the environment.
2. Solar power density can be intermittent due to weather conditions (e.g., cloud cover). It is also limited exclusively to use in daytime.

3. For high-power PV systems, the arrays spread over a large area. This makes the system difficult to accommodate in or near cities.
4. PV systems are considered by some to be visually intrusive (e.g., rooftop arrays are clearly visible to neighbors).
5. The reflections from large PV fields can alter the local weather.
6. The efficiency of the solar panel is still low, making the system more expensive and large in size.
7. Solar systems require continuous cleaning of their surfaces. Dust, shadows from falling leaves, and bird droppings can substantially reduce the efficiency of the system.

6.2 WIND ENERGY

Wind is one of the oldest forms of energy known to man; it dates back more than 5000 years to Egypt, when sailboats were used for transportation. Although no one knows exactly who built the first windmill, archaeologists discovered a Chinese vase dating back to the third millennium BC with a painting that resembles a windmill. By the second millennium BC, the Babylonians used windmills extensively for irrigation. They were constructed as a revolving doors system, similar to the vertical-axis wind machine used today. In the twelfth century, windmills were built in Europe to grind grains, pump water, and saw woods. They were also used in Holland to drain lands below the water level of the Rhine River. During this era, working in windmills was one of the most hazardous jobs in Europe. The workers were frequently injured because the windmills were constructed of a huge rotating mass with little or no control on its rotation. The grinding or hammering sounds were so loud that many workers became deaf, the grinding dust of certain material such as wood caused respiratory health problems, and the grinding stones often grind against each other causing sparks and fires.

In addition to producing mechanical power, windmills were also used to communicate with neighbors by locking the windmill sails in certain arrangement. During World War II, the Netherlanders used to set windmill sails in certain positions to alert the public of a possible attack by their enemies.

Nowadays, windmills are mostly used to generate electricity by converting the kinetic energy (KE) in wind into electrical energy. These types of windmills are often called wind turbines. The first wind turbine was built by the American inventor Charles F. Brush in 1888. It was just a 12 kW machine with an enormous structure, but it lasted for several years. Because the power grid did not reach farm lands in the United States until the second quarter of the twentieth century, farmers relied on wind turbines for their electric energy needs.

The design and operation of wind turbines have improved substantially in the last two decades. The size of wind turbines has increased from just a few kilowatt machines to up to 8 MW single unit systems. Furthermore, the reliability of wind turbines has improved substantially.

6.2.1 KINETIC ENERGY OF WIND

The role of wind turbines is to harness the kinetic energy (KE) of wind and convert it into electrical energy. The KE of an object is the energy it possesses while in motion. Starting with Newton's second law, the KE of a moving object can be expressed by

$$KE = \frac{1}{2}mw^2 \quad (6.20)$$

where

KE is the kinetic energy of the moving object (J)

m is the mass of the moving object (kg)

w is its velocity of the object in meter per second (m/s)

The unit of KE is watt second (Ws). To calculate the KE of the wind, we need to calculate the mass of air passing through a given area (A). The mass of air depends on the area, the speed of the wind, the air density (δ), and the time (t):

$$m = Aw\delta t \quad (6.21)$$

The unit of A is m^2 , the unit of w is m/s , the unit of δ is kg/m^3 , and the unit of time is second.

Substituting the mass in Equation 6.21 into Equation 6.20 yields

$$KE = \frac{1}{2} A\delta tw^3 \quad (6.22)$$

Since the energy is power multiplied by time, the wind power (P_{wind}) in watt is

$$P_{wind} = \frac{KE}{t} = \frac{1}{2} A\delta w^3 \quad (6.23)$$

Note that the KE and the power of wind are proportional to the cube of wind's speed. Hence, when wind speed increases by just 10%, the KE of wind increases by 33.1%.

From Equation 6.23, the wind power density can be written as

$$\rho = \frac{P_{wind}}{A} = \frac{1}{2} \delta w^3 \quad (6.24)$$

The air density is a function of air pressure, temperature, humidity, elevation, and gravitational acceleration. The expression commonly used to compute the air density is

$$\delta = \frac{pr}{\kappa T} e^{\left(\frac{-gh}{\kappa T}\right)} \quad (6.25)$$

where

pr is the standard atmospheric pressure at sea level (101,325 Pa or N/m^2)

T is the air temperature in degrees Kelvin ($^{\circ}\text{Kelvin} = 273.15 + ^{\circ}\text{C}$)

κ is the specific gas constant, for air $\kappa = 287 \text{ Ws}/(\text{kg Kelvin})$

g is the gravitational acceleration (9.8 m/s^2)

h is the elevation of wind above the sea level (m)

Substituting these values into Equation 6.25 yields

$$\delta = \frac{353}{T + 273} e^{\frac{-h}{29.3(T+273)}} \quad (6.26)$$

Notice that the temperature (T) in Equation 6.26 is in degree Celsius. The equation shows that when the temperature decreases, the air is denser. Also, air is less dense at high altitudes. For the same velocity, wind with higher air density (heavier air) possesses more KE .

Example 6.16

Tehachapi is a desert city in California with an elevation of about 350m and is known for its extensive wind farms. Compute the power density of wind when air temperature is 30°C and the speed of the wind is 12 m/s.

Solution

To compute the power density of the wind, you need to compute the air density

$$\delta = \frac{353}{30 + 273} e^{\frac{-350}{29.3(30+273)}} = 1.12 \text{ kg/m}^3$$

The power density by using Equation 6.24 is

$$\rho = \frac{1}{2} \delta w^3 = \frac{1}{2} 1.12 \times 12^3 = 967.7 \text{ W/m}^2$$

Compare this power density of wind with the power density of the sun computed in Example 6.1. Can you draw a conclusion?

Wind power density (ρ) in watt per square meter (W/m^2) is often used to judge the potential of a given site for wind turbine installation. Figure 6.38 shows the average wind power density in the United States at an elevation of 50 m. As you see in the map, there are areas in the western United States and Hawaii with as much wind power density as 1.5 kW/m^2 .

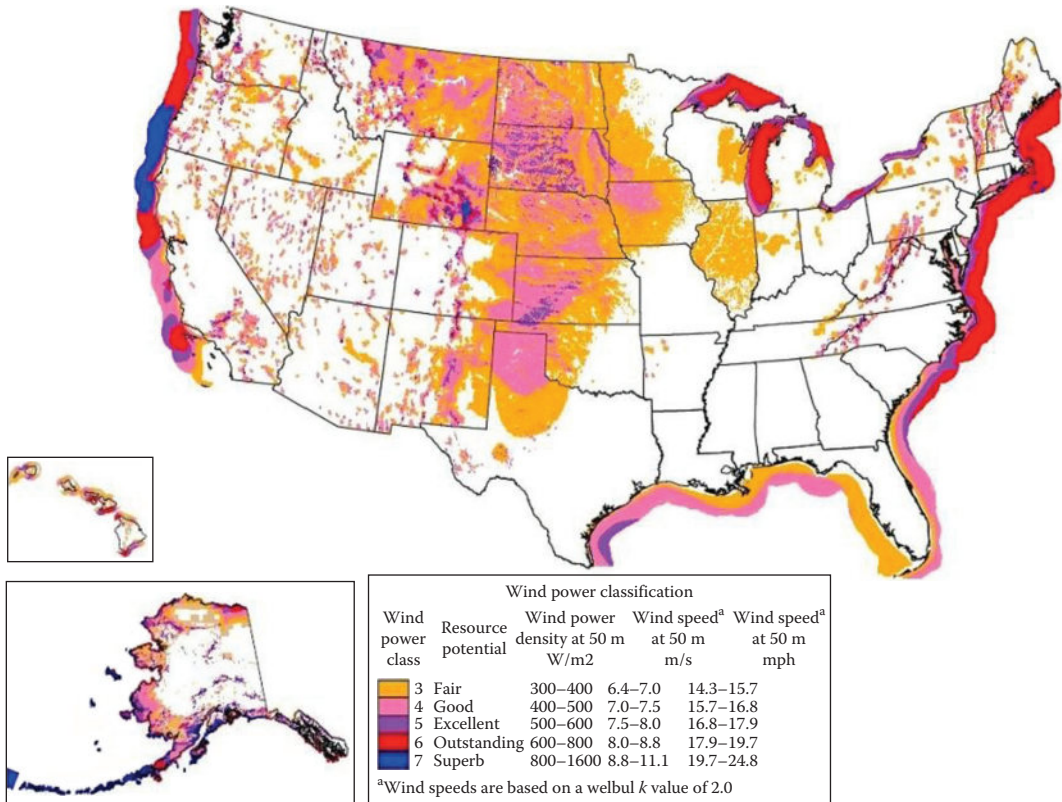


FIGURE 6.38 US average wind power density map at 50 m above sea level. (Courtesy of the USA National Renewable Energy Laboratory.)

6.2.2 WIND TURBINE

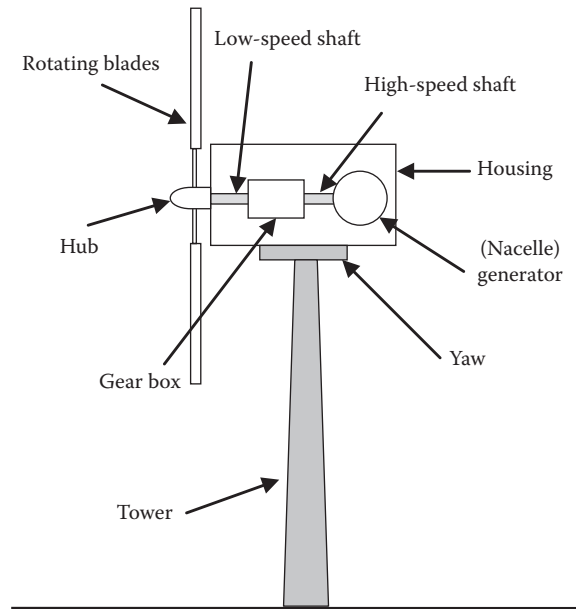
Wind turbine (WT) is a generic phrase given to the wind energy system that converts the KE in wind into electrical energy. The current size of wind turbine ranges from 50kW to up to 8MW. Wind turbines come in a variety of designs and power ratings, but the most common design is the horizontal-axis type shown in Figure 6.39. It consists of the following basic components:

- A tower that keeps the rotating blades at a sufficient height to increase the exposure of the blades to wind. Large wind turbines, in the megawatt range, have their towers as high as 250m above the base.
- Rotating blades that capture the KE of the wind. They are normally made of fiberglass-reinforced polyester or wood-epoxy material. The length of the rotating blades ranges from 5 to over 60m. Modern systems allows the blades to change their angle with respect to wind to maximize their absorption of wind's KE. Most wind turbines have three rotor blades.
- A hub that is part of the low speed shaft. The blades are mounted on to the hub and it has its own gear system and actuator to change the angle of the blade with respect to wind direction.
- A yaw mechanism that allows the housing box (nacelle) to rotate until the blades are perpendicular to the wind direction, thus increasing the exposure of the blades to wind.
- A gearbox connecting the low-speed rotating blades to the high-speed generator. It is also served as a clutch. This is because the generator operates at high speeds.
- A generator connected to the high-speed shaft of the gearbox to convert the mechanical energy of the rotating blades into electrical energy.
- A controller that integrates the wind turbine into the utility grid and regulates the generated power. It also protects the turbine against severe conditions such as grid faults and wind storms.

The nacelle and one blade of a wind-generating system are shown in Figure 6.40. These pictures were taken during the installation process of the turbine in Figure 6.39. This turbine is 1.8MW and



(a)



(b)

FIGURE 6.39 Basic components of a wind-generating system: (a) horizontal design and (b) main parts.

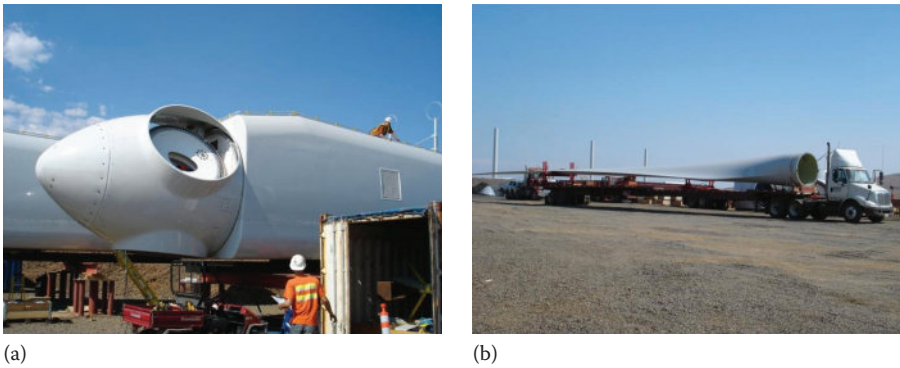


FIGURE 6.40 (a) Housing and (b) blade of a 1.8MW wind generating system.

is located in the Pacific Northwest of the United States. The enormous size of the housing can be appreciated by comparing it to the size of the worker on the top of the nacelle. Also, the length of the blade can be realized by comparing it to the size of the truck.

Example 6.17

A wind turbine at the site discussed in Example 6.16 has three rotating blades; each is 20 m in length. Compute the available power from the wind.

Solution

The wind power density computed in Example 6.16 is 967.7 W/m^2 . The area swept by the blade is circular with 40 m diameter. Hence, the available power from wind (P_{wind}) is

$$P_{wind} = A\rho = \pi r^2\rho = \pi \times 20^2 \times 967.7 = 1.216 \text{ MW}$$

where r is the length of the blade.

6.2.3 AERODYNAMIC FORCE

The blade of a wind turbine (WT) is somewhat similar to airplane's wing. The cross section of the wing (or turbine blade) is often called airfoil and its general cross section is shown in Figure 6.41. The cross section of the blade has two cambers (arcs): upper and lower. The upper camber of the wing is longer than the lower camber; this is a key design feature. The airfoil has a leading edge that faces the wind and trailing edge.

Among the key design parameters of the airfoil are the mean camber line, the center of gravity, and the cord line shown in Figure 6.42. The points on the mean camber line are the mid points

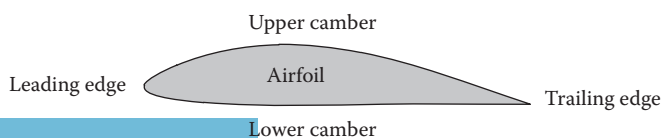


FIGURE 6.41 Airfoil.

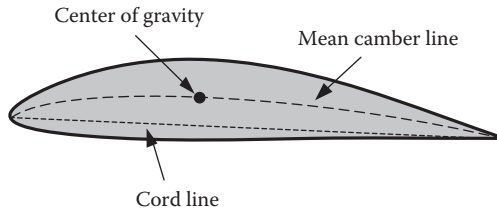


FIGURE 6.42 Mean camber line, center of gravity of airfoil, and cord line.

between the upper and lower cambers. The center of gravity is located on the mean camber line. The cord line is a straight line connecting the leading edge to the trailing edge.

When air reaches the leading edge of the airfoil, it splits into two paths as shown in Figure 6.43; one path moves air along the upper camber and the other along the lower camber. The *law of continuity* states that the air molecules separated at the leading edge meet at the trailing edge at the same time. Since the path (distance) along the upper camber is longer than that for the lower camber, the speed of air above the wing (w_1) is faster than the speed of air below the wing (w_2).

Bernoulli’s principle discovered by the mathematician Daniel Bernoulli in late 1700 states that “as the velocity of air increases, pressure decreases and vice versa.” Based on this principle, the pressure exerted on the upper camber (P_{r1}) is less than that on the lower camber (P_{r2}) as depicted in Figure 6.44. This results in a net upward pressure (P_{net}):

$$P_{net} = P_{r2} - P_{r1} \tag{6.27}$$

The net pressure (P_{net}) causes an upward force called *aerodynamic force* (F) which can be expressed as

$$F = P_{net}A \tag{6.28}$$

where

- F is the aerodynamic force created by the net pressure
- P_{net} is the net pressure exerted on the airfoil
- A is the surface area of the airfoil

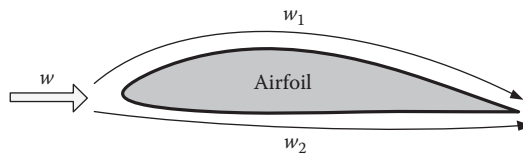


FIGURE 6.43 Flow of air around airfoil.

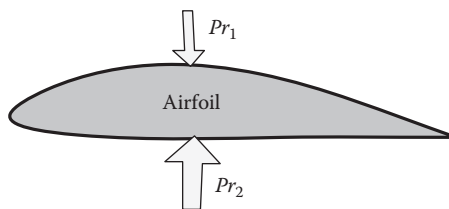


FIGURE 6.44 Bernoulli’s principle.

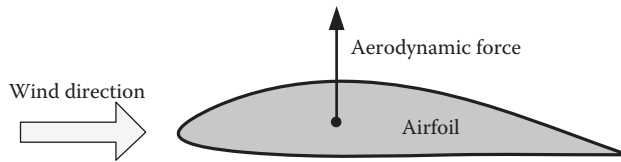


FIGURE 6.45 Aerodynamic force.

The aerodynamic force at every point on the surface of the airfoil can be aggregated into a single value at the center of gravity of the airfoil. In the case when the leading edge of the airfoil is facing the relative wind, all of the aerodynamic force is perpendicular to the flow of air, as shown in Figure 6.45. This force is what makes the wing float in air. For wind turbines, one end of each blade (wing) is mounted on a rotating hub. So the aerodynamic force creates torque causing the blade to rotate in a circular motion.

6.2.4 ANGLE-OF-ATTACK

The aerodynamic force can be controlled by the *angle-of-attack*. This is α in Figure 6.46 which is the angle between the relative wind direction (w) and the cord line. The aerodynamic force (F) at any angle-of-attack has two components; lift force (F_L) and drag force (F_D). The lift force is perpendicular to w , and the drag force is in parallel with w . For an airplane wing, the lift force is what makes the wing float in air and the drag force is a form of unwanted, but unavoidable, frictional

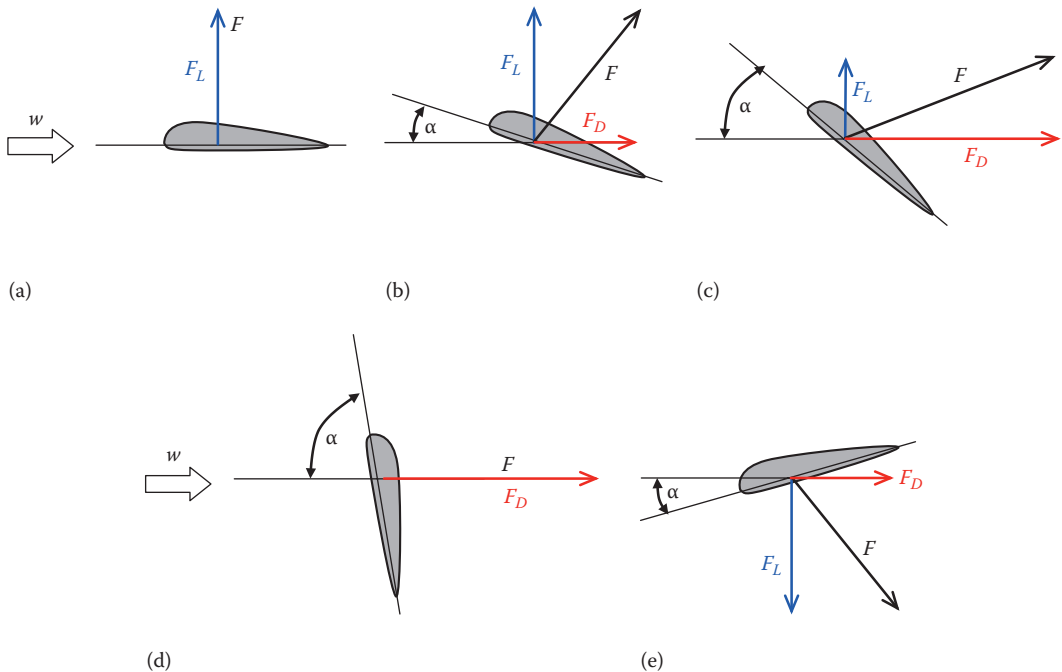


FIGURE 6.46 Aerodynamic forces and angle-of-attack: (a) horizontal position—all aerodynamic force is lift; (b) positive angle-of-attack—aerodynamic force has lift and drag; (c) increasing positive angle-of-attack, less lift, and more drag; (d) increasing positive angle-of-attack until aerodynamic force is all drag; and (e) negative angle-of-attack—lift is reversed.

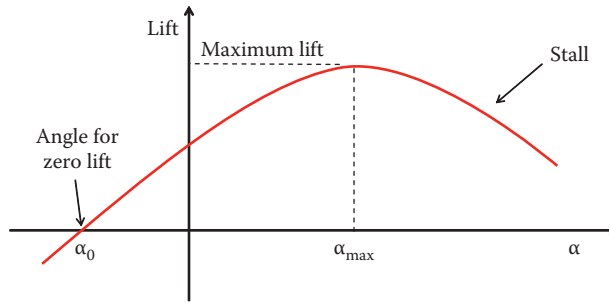


FIGURE 6.47 Lift force as a function of angle-of-attack.

loss. In Figure 6.46, the aerodynamic force is shown for several angle-of-attacks. In Figure 6.46a, the airfoil has zero angle of attack, so all the aerodynamic force is lift force. In Figure 6.46b, the airfoil is at positive α causing the aerodynamic force to have more lift and drag forces. In Figure 6.46c, the angle of attack increases causing the lift force to decrease and the drag force to increase. In Figure 6.46d, the angle increases until the lift force is vanished and the entire aerodynamic force is converted into a drag force. In Figure 6.46e the angle of attack is negative, thus reverses the direction of the lift force.

During storms, wind turbines put their blades at an angle-of-attack that results in zero lift force (called feathering the blades). This is not done by the case in Figure 6.46d because the drag force can deform or even damage the blades. Instead, the feathering is done with negative angle of attack. When you move the blades from positive, Figure 6.46b, to negative angle of attack, Figure 6.46e, the lift force goes to zero before it reverses. At zero lift force, the blades are feathered.

A typical lift force as a function of α is shown in Figure 6.47. At a negative angle α_0 , the lift is zero. This is the feathering position of wind turbines. A larger negative angle would reverse the lift. At $\alpha = 0$, the blade provides some lift. The lift increases when the angle-of-attack increases but up to α_{\max} at which the lift is maximum. Increasing α beyond α_{\max} , reduces the lift while increasing the drag. This region is known as the stall region in airplanes.

The ratio of the lift force to the entire aerodynamic force is known as the lift coefficient (C_L). Similarly, the drag coefficient (C_D) is the ratio of the drag force to the aerodynamic force:

$$C_L = \frac{F_L}{F} \quad (6.29)$$

$$C_D = \frac{F_D}{F}$$

Both C_L and C_D are functions of the shape of the blade and the angle-of-attack. To capture more energy from the wind, we need to increase C_L and reduce C_D .

Example 6.18

At a given angle-of-attack, the aerodynamic force exerted on each blade of a three-blade wind turbine is 2000 N, and the lift coefficient is 0.95. If the center of gravity of the blade is at 30 m from the hub, compute the torque generated by the three blades. If the blades rotate at 30 r/min, compute the mechanical power generated by the blades.

Solution

The torque is due to the lift force that can be computed using Equation 6.29:

$$F_L = C_L F = 0.95 \times 2000 = 1900 \text{ N}$$

The torque of one blade is

$$T = F_L d$$

where d is the distance from the hub to the center of gravity of the blade. For three-blade, the total torque is

$$T_{total} = 3F_L d = 3 \times 1900 \times 30 = 171 \text{ kNm}$$

The power generated by the blade is

$$P_{total} = T_{total} \omega_{blade} = 171 \left(2\pi \frac{n_{blade}}{60} \right) = 171 \left(2\pi \frac{30}{60} \right) = 537.2 \text{ kW}$$

6.2.5 PITCH ANGLE

From the control point of view, adjusting the angle-of-attack requires information on wind direction which is continuously changing. Instead, we can control the angle between the cord line of the blade and the vertical line representing the linear motion of the center of gravity. This angle is known as the pitch angle (β) and is shown in Figure 6.48. Note that the pitch angle is a function of the geometry of the blade and is not a function of the wind direction. The angle-of-attack (α) can still be controlled by adjusting the pitch angle of the blade. For the same relative wind speed direction, increasing the pitch angle reduces the angle-of-attack and vice versa. This is the main method used to control the output power of the turbine in modern wind energy systems.

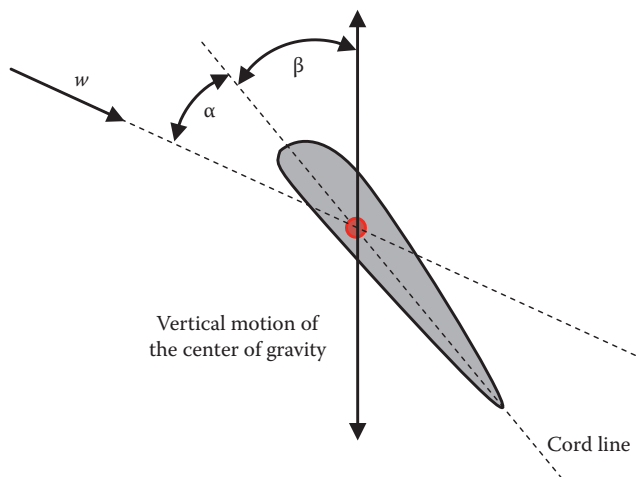


FIGURE 6.48 Relative wind speed, angle of attack and pitch angle.

Example 6.19

For a relative wind speed of $49\angle -73.31^\circ$ m/s, if the pitch angle is 5° , compute the angle of attack.

Solution

The angle of the relative wind speed is -73.31° . Using trigonometry, the angle of attack is

$$90^\circ - 73.31^\circ = \alpha + \beta$$

$$\alpha = 16.69^\circ - 5^\circ = 11.69^\circ$$

6.2.6 COEFFICIENT OF PERFORMANCE AND TURBINE EFFICIENCY

Not all wind energy is converted into electrical energy because of various losses in the system. The general power flow in wind turbines is shown in Figure 6.49. The blades of the turbine capture only part of the available wind energy reaching the sweep area of the blades. The ratio of the power captured by the blades (P_{blade}) to the available power from the wind in the sweep area of the blades (P_{wind}) is known as the *coefficient of performance* or *power coefficient* (C_p):

$$C_p = \frac{P_{blade}}{P_{wind}} \quad (6.30)$$

C_p is a major part of the overall efficiency of the system. It is the most significant energy loss in wind turbines. Even modern designs of wind turbines cannot achieve $C_p > 0.5$. Moreover, the coefficient of performance is not constant and is continuously changing based on several factors such as the pitch angle, wind speed, length of the blade, and the rotational speed of the blade as will be explained in the next section.

After the blades capture part of the wind power, some of this power is wasted in form of rotational losses (frictional and windage) in the rotating parts before entering the gearbox. The rest of the power enters the gearbox (P_{gear}), where part of it is wasted as gearbox rotational loss. The remaining power (P_g) enters the generator where some gets wasted in the form of electrical losses in the generator's windings and its core as well as the generator's own rotational losses. The remaining power (P_{out}) is the output electric power delivered to the load.

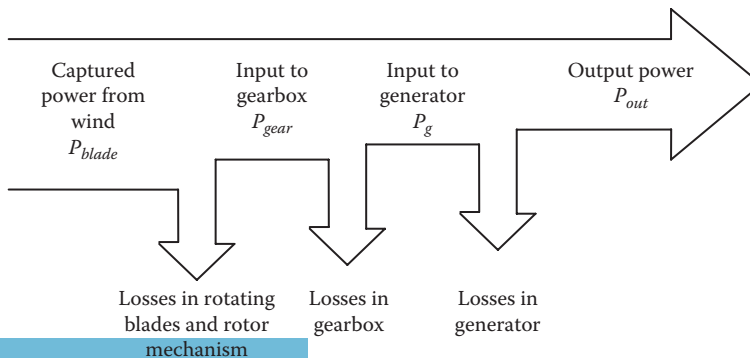


FIGURE 6.49 Power flow of a wind turbine.

Example 6.20

For the wind turbine in Example 6.17, compute the output power assuming that the coefficient of performance C_p is 0.4, the efficiency of the rotating blades and rotor mechanism (η_{blade}) is 90%, the gearbox efficiency (η_{gear}) is 95% and the generator efficiency (η_g) is 70%.

Solution

The output power of the wind turbine is the input power multiplied by the all efficiencies

$$P_{out} = \eta_{total} P_{wind} = (C_p \eta_{blade} \eta_{gear} \eta_g) P_{wind}$$

$$P_{out} = (0.4 \times 0.9 \times 0.95 \times 0.7) \times 1.216 \times 10^3 = 291.11 \text{ kW}$$

The output power is about 24% of the available wind power. Although the efficiency is low, it is still higher than the efficiency of the PV system.

6.2.7 OPERATING RANGE OF WIND TURBINE

A typical operating characteristic of a wind turbine is shown in Figure 6.50 where the output power is a function of wind speed (w). At point A, the wind speed is high enough to start generating electricity. Wind speed at this point is called *cut-in* speed or minimum speed (w_{min}). Between A and B, the turbine output is a function of the cube of w as well as the pitch angle. During this range, the pitch angle is controlled to operate the turbine near its maximum C_p to harvest as much energy from wind as possible. The power at point B represents the rated output power of the turbine (P_{rated}). If w exceeds (w_B), the machine must spill some of the wind energy to operate the turbine within its power limit. This is done by adjusting the pitch angle (angle-of-attack) to produce less lift. At point D, wind speed is the maximum allowable (w_{max}) by the structural design of the turbine. Once reached, the turbine starts feathering its blades. Wind speed at w_{max} is called cut-out speed.

6.2.8 TIP SPEED RATIO

Figure 6.51 shows a front view of the rotating blade. The linear velocity of the tip of the blade is called tip speed (v_{tip}), which is a function of the rotating speed of the blade (ω) and the length of the blade (r).

$$v_{tip} = \omega r = 2\pi \frac{n}{60} r \quad (6.31)$$

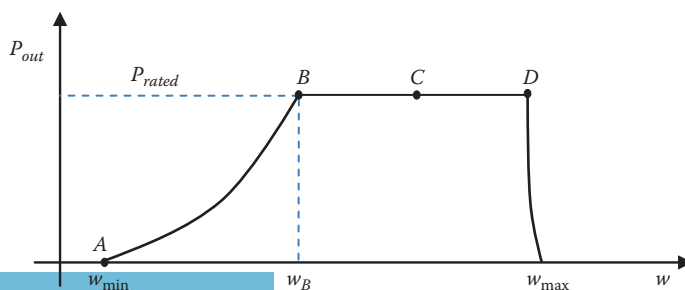


FIGURE 6.50 Output power of wind turbine.

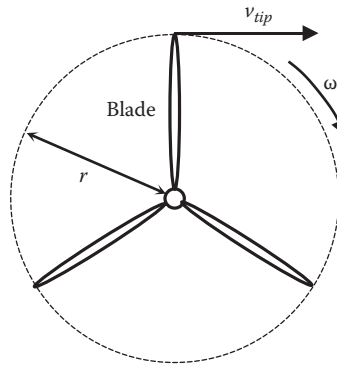


FIGURE 6.51 Tip velocity.

where

v_{tip} is the tip speed in m/s

ω is the angular speed of the blade (rad/s)

n is the number of revolutions the blade makes in one minute (rev/m or r/min)

r is the length of the blade (m)

$$n = \frac{60v_{tip}}{2\pi r} \tag{6.32}$$

The wind turbine is often designed to have its tip velocity faster than wind speed to allow the turbine to generate electricity at low wind speeds. The ratio of tip velocity (v_{tip}) to wind speed (w) is known as the *tip speed ratio (TSR)*:

$$TSR = \frac{v_{tip}}{w} \tag{6.33}$$

When a blade passes through wind, it creates a wake of air turbulence that is often damped out quickly. If the *TSR* is too small, most of the wind passes through the open areas between the rotor blades and little energy is captured by the blade. If it is too large, the next blade may arrive to the area swept by the earlier blade before the turbulence is damped out. In this case, the blade captures a smaller amount of energy because the wind is turbulent.

Based on the earlier discussions, the amount of energy captured from wind by the blade is a function of the *TSR*. Hence, the *TSR*, which is one of the most important control parameters in the operation of wind turbines, determines the coefficient of performance (C_p) of the turbine blades.

The relationship between the *TSR* and C_p is nonlinear and a typical shape is shown in Figure 6.52. The figure shows that the coefficient of performance is maximized at a specific value

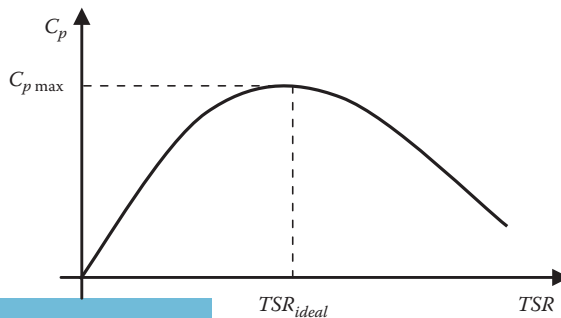


FIGURE 6.52 Coefficient of performance as a function of *TSR*.

of TSR (TSR_{ideal}). The maximum theoretical value of C_p is known as *Betz limit* which is 0.5926. No wind turbine today can reach this value.

Example 6.21

A wind turbine is designed to produce power when the speed of the generator (n_g) is at least 905 r/min, which correlates to a wind speed of 5 m/s. The turbine has a fixed tip speed ratio of 7, and a sweep diameter of 10 m. Compute the ratio of the gear system.

Solution

The tip speed

$$v_{tip} = TSR w = 7 \times 5 = 35 \text{ m/s}$$

Speed of the shaft at the low speed side of the gearbox

$$n = \frac{v_{tip}}{2\pi r} = \frac{35}{2\pi 5} \times 60 = 67 \text{ r/min}$$

Gear ratio

$$\frac{n_g}{n} = \frac{905}{67} = 13.5$$

Example 6.22

A wind turbine has its coefficient of performance represented by the equation

$$C_p = 0.4 \times \sin(TSR) + 0.03 \times \sin(3TSR - 0.2)$$

Compute the TSR that leads to maximum coefficient of performance.

Solution

To compute $C_{p \max}$, we set the derivative of the equation presented earlier to zero.

$$\frac{\partial C_p}{\partial TSR} = 0.4 \times \cos(TSR) + 0.09 \times \cos(3TSR - 0.2) = 0$$

The iterative solution of this equation leads to $TSR_{ideal} = 1.45$, at which the maximum coefficient of performance is

$$C_{p \max} = 0.4 \times \sin(1.45) + 0.03 \times \sin(4.35 - 0.2) = 0.372$$

In modern wind turbines, the value of TSR can be adjusted by changing the speed of the generator and the pitch angle of the blades. Consider the C_p curve in Figure 6.53. When wind speed results in ideal TSR , C_p is at its maximum. When wind speed increases the TSR decreases as well as the C_p .

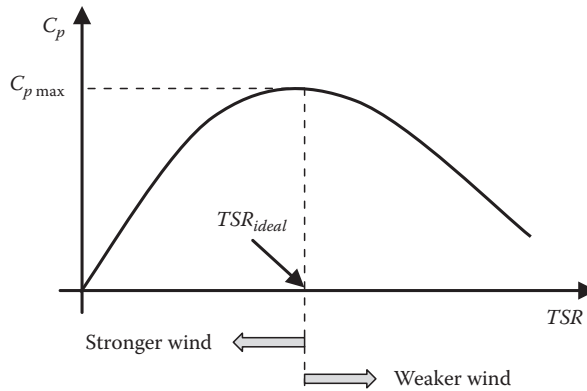


FIGURE 6.53 Tracking maximum C_p by adjusting the speed of the blade.

If we can increase the speed of the generator, which is possible with newer types of wind turbines, we can move the new TSR back to the ideal value. Similar process with reversed action can be done when the wind speed is weaker than that at the ideal TSR .

Another control action for the C_p can be made by the pitch angle (β). Figure 6.54 shows the coefficient of performance characteristics for different pitch angles. Keep in mind that decreasing the pitch angle increases the angle-of-attack.

Now consider the case in Figure 6.55. Let us assume that the wind turbine is operating at point A where the coefficient of performance is at its maximum. Now assume that wind speed is reduced

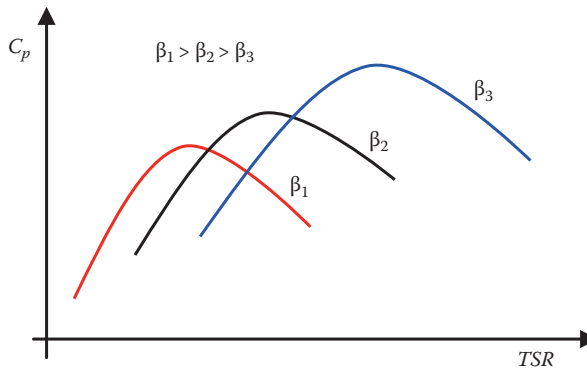


FIGURE 6.54 Coefficient of performance as a function of pitch angle.

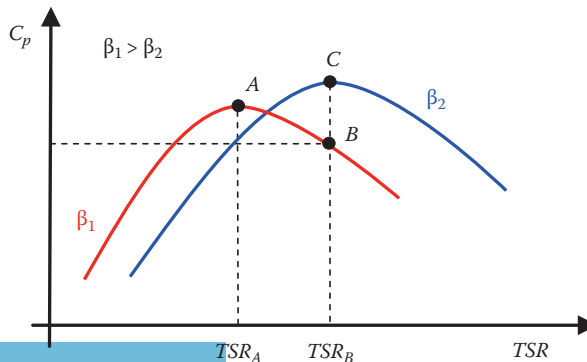


FIGURE 6.55 Tracking the maximum C_p by changing the pitch angle.

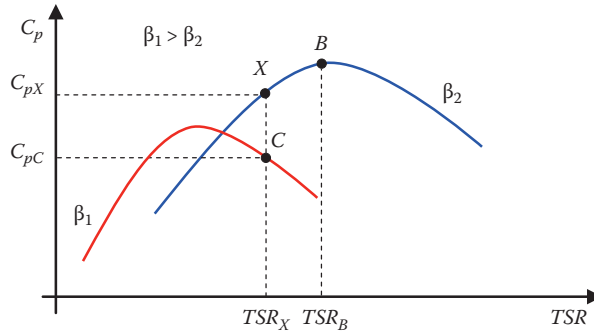


FIGURE 6.56 Spilling wind by adjusting pitch angle.

and the operating point is now at B where the TSR increased to TSR_B . At B , the coefficient of performance is reduced and less energy is captured from the wind. But, if we reduce the pitch angle to β_2 (increase the angle-of-attack), we can operate at point C where C_p is at its maximum. This is the method commonly used to track the maximum coefficient of performance.

The pitch angle control can also be used to make the wind turbine follow the operating curve in Figure 6.50. Assume that we have reached point B in Figure 6.50 when the wind speed is w_B . Assume that at this operating point, we are at the maximum C_p shown in Figure 6.56 (point B). Assume that wind speed increases which reduces the TSR from TSR_B to TSR_X . With no pitch angle control, the coefficient of performance is reduced to C_{pX} in Figure 6.56. If the blade power at point X still exceeds the rating of the turbine, we need to further reduce the coefficient of performance. This can be done by increasing the pitch angle (reducing the angle-of-attack) until the power is within the acceptable limit. This is point C in Figure 6.56, which corresponds to any operating point between B and D in Figure 6.50.

6.2.9 FEATHERING

The blades and the hub of the wind turbine experience tremendous stress due to centripetal force imposed on them by wind. The centripetal force from the spinning blade increases proportionally to the square of the rotation speed. This makes the structure sensitive to over-speeding. Therefore, when the speed of wind reaches the maximum design limit of the turbine (also known as the cut-out speed or maximum speed w_{max}), the turbine is aerodynamically stalled (known as feathering). This is done by adjusting the pitch angle to make C_p near zero, and then mechanical brakes are applied to stop the rotation of the blades. Feathering is done at point D in Figure 6.50.

6.2.10 CLASSIFICATIONS OF WIND TURBINES

Wind Turbine designs have evolved over the years, particularly in the last three decades. Nowadays, there are a number of designs and configurations that can fit sites with different wind profiles and landscapes.

Modern wind turbines are generally categorized based on the alignment of their rotation axes, their types of electrical generators, their speed of rotations, or their power electronic converters.

6.2.10.1 Alignment of Rotating Axis

The drive shaft of wind turbines can rotate horizontally or vertically. A horizontal axis wind turbine (HAWT) is shown in Figure 6.57. This is the most common type used today. Its main drive shaft, gearbox, electrical generator and the transformer are housed in the nacelle at the top of a tower. The turbine is almost always aligned to face the upwind. This way, when the blade is



FIGURE 6.57 Horizontal axis wind turbines.



FIGURE 6.58 Lifting of gearbox and brakes of HAWT. (Courtesy of Paul Anderson through Wikipedia.)

aligned with the tower, the blades are not obscured by the tower. To prevent the blades from hitting the tower at high wind conditions, the blades are placed at a distance in front of the tower and tilted up a little.

The main advantages of the HAWT are as follows:

- The tall tower allows the turbine to access strong wind.
- Every blade receives power from wind at any rotation position. This makes the HAWT a high efficiency design.

The main disadvantages of HAWT are as follows:

- It requires massive tower construction to support the heavy nacelle.
- The heavy generator, gearbox and transformer inside the nacelle have to be lifted during construction and maintenance (Figure 6.58).
- It requires an additional yaw control system to turn the blades toward wind.
- Because of their large heights, they could be visually obtrusive and can cause local opposition.

A Vertical Axis Wind Turbine (VAWT) is shown in Figure 6.59. It is known as Darrieus wind turbines and it looks like a giant upside down eggbeater. The VAWT was among the early designs of wind turbines because it is suitable for sites with shifting wind directions.



FIGURE 6.59 Vertical axis wind turbine. (Courtesy of US National Renewable Energy Lab.)

The main advantages of the VAWT are as follows:

- There is no need for a yaw mechanism to direct the blade into wind. The generator, gear-box and transformers are all located on the ground level, making the VAWT easier to install and maintain as compared with the HAWT.
- The cut-in speed of the VAWT is generally lower than that for the HAWT.

The main disadvantages of the VAWT are as follows:

- The wind speed is slower near ground. Hence, the available wind power is low.
- Large objects near ground can create turbulent flow that can produce vibration on the rotating components and causing extra stress on the turbine.
- Because of its massive inertia, they may require external power source to startup the turbine.

6.2.10.2 Types of Generators

Most wind turbines utilize asynchronous (induction) and synchronous machines. These two types of machines are covered in Chapter 12. The common generator used today in wind energy is the induction generator. There are two types of induction generators: squirrel cage and wound rotor. The squirrel cage is the cheapest and most rugged generator because its rotor is simple and the machine has no high maintenance components such as brushes or slip rings. The main drawback of the squirrel cage generator is the lack of access to its rotor circuit to implement various control actions. Because of this drawback, squirrel cage generators are used in small size turbines. The second type of induction machines is the wound rotor. The rotor of this machine is more complex than the rotor of the squirrel cage because it is made out of elaborate windings and it has brushes and slip rings mechanisms. But the wound rotor machine allows us to injection signals in the rotor to implement various control functions.

The induction generator operates at a slip so its speed is not exactly constant. The machine itself without rotor injection cannot generate electricity unless it is spun above its synchronous speed (n_s)

$$n_s = 120 \frac{f}{p} \quad (6.34)$$

where

n_s is the synchronous speed or the speed of the magnetic field inside the machine (r/min)

f is the frequency of the grid (Hz)

p is the number of poles of the machine

The slip of the machine S is defined as

$$S = \frac{n_s - n}{n_s} \quad (6.35)$$

where n is the actual speed of the rotor.

The slip of the induction generator, without rotor injection, is often small (2%–10%). The generator must have a negative slip to produce electricity. In this case, the actual speed of the rotor is higher than the speed of the magnetic field (n_s). The operation and modeling of the machine are covered in detail in Chapter 12.

The synchronous generator designs are divided into two types: electrical magnet and permanent magnet. In both types, the frequency of the power produced is directly proportional to the speed of its rotation. There is no slip in these machines. Since the rotation of the generator shaft is varying due to the variations in wind speed, the output frequency of these machines is not constant. Hence, it is common to have a converter between the generator and the grid.

The electric magnet machine allows us to access its field circuit to implement several control actions. The permanent magnet machines do not have field current control and are often made out of rare Earth magnetic material to provide a strong electric field.

6.2.10.3 Speed of Rotation

Depending on the type of generator, power electronic converters or grid interface circuits, wind turbines can be divided into constant or variable speed types. The constant speed turbine regulates its output power by adjusting the lift force, i.e., the torque on its blades. For variable speed, the power can be regulated by the torque as well as the speed of the generator.

The older systems are mostly fixed speed asynchronous generators. These turbines are simpler than the variable speeds. They generate electricity only when wind speed is high enough to spin the generator shaft above its synchronous speed. Although they are less expensive and require less maintenance than the variable speed types, they have a limited range of operation.

The variable speed turbines are more complex systems with various power electronic converters that allow the generators to produce electricity at speeds below synchronous. Thus, their range of operation is much wider than that for the fixed speed type.

6.2.11 TYPES OF WIND TURBINE

Commercially, wind turbines are currently classified into four types, with additional types expected in the future. Each type has its own standard features and operating conditions that have agreed upon by the industry. They are classified as Type 1 through 4.

6.2.11.1 Type 1 Wind Turbine

Type 1 design is the oldest and the simplest to build. The main components are shown in Figure 6.60. The system consists of a squirrel cage induction generator directly connected to the grid without power conversion. The system has a gearbox that converts the slow speed motion of the blades to fast speed, higher than the synchronous speed of the generator, to produce electricity. The system may have pitch control. The turbines at the site are connected to a bus known as a *farm connection point*. Since the output voltage of most turbines is relatively low, 120–690 V, a step-up transformer is used to increase the voltage of generated power to the voltage of the grid side. The transformer is known as *generation step-up transformer (GSU xfm)*. A large number of wind farms are located far from the utility grid. Hence, a transmission line connecting the farm to the grid is needed. This line is often called *trunk line*.

6.2.11.2 Type 2 Wind Turbine

Type 2 wind turbine design is shown in Figure 6.61. The system consists of a slip-ring (wound rotor) induction machine. The rotor of the machine is accessible and a resistance is connected to the rotor windings through a converter. The converter regulates the amount of power consumed by the resistance. This system is considered a variable slip type because the resistance changes the slip of the generator. Thus, the turbine operates at slightly variable speeds allowing the turbine to handle a wider range of wind speeds as compared with Type 1. Also, the amount of power consumed by the resistance provides some form of regulated output power feeding the grid. If less power is needed by the grid, more power is consumed in the resistance. This is similar in function to the dynamic braking of electric motors.

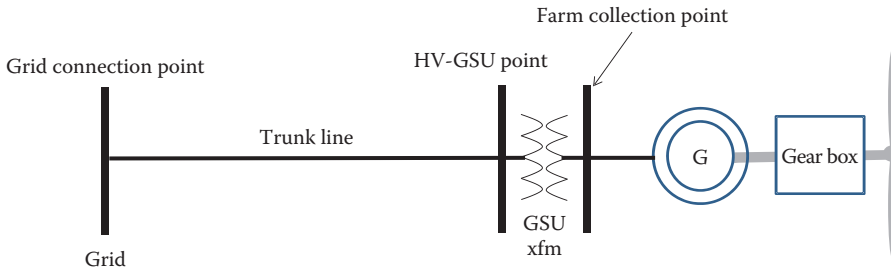


FIGURE 6.60 Type 1 wind turbine system.

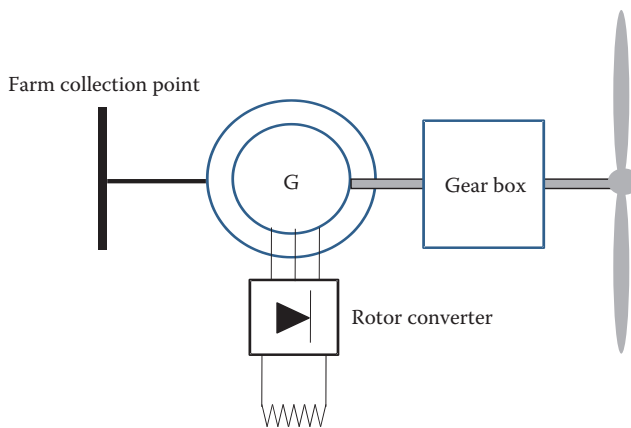


FIGURE 6.61 Type 2 wind turbine system.

6.2.11.3 Type 3 Wind Turbine

Type 3 wind turbine is the most common design today. It is known as *doubly fed induction generator* (DFIG) and its configuration is shown in Figure 6.62. The system consists of a wound rotor induction generator with two converters injecting an adjustable voltage into the rotor circuit at adjustable frequency and phase shift. Both converters operate in the forward or reversed mode (ac/dc or dc/ac). The converter that is connected to the rotor circuit is called *rotor converter*. The one connected to the grid is called *line converter*. Depending on the needed action, the power flow through the converters could be from the grid to the rotor or the other way. The converter is sized to allow as much as 1/3 of the rated power of the turbine to pass through it.

With the DFIG, the wind turbine can have flexible operation and a good level of control. Among the advantages of the DFIG are as follows:

- It can generate electricity when the speed of wind is low causing the generator to spin below its synchronous speed. This way, the generating range of the turbine is much wider than that for type 1 or 2.
- The turbine can regulate its output power and voltage.
- The system can support and stability of the grid.

The aforementioned features of the DFIG make the system similar to conventional power plants in terms of control and operation. This is one of the main reasons for the popularity of the DFIG.

6.2.11.4 Type 4 Wind Turbine

Type 4 wind turbine system is shown in Figure 6.63. In this system, the gearbox is removed. This is a major benefit as the gearbox is one of the most expensive components of the system and also fails more frequent than other key parts. The generator used in this type is often a synchronous generator with either electric or permanent magnet. In some type 4 systems, the generator can be an induction machine. In either case, the generator has a large number of poles to reduce its synchronous speed. This is important since we eliminated the gearbox. Thus, the diameter of the generator is larger than that for the other types making the nacelle wider in diameter. Figure 6.64 shows one of the world's largest Type 4 wind turbines. Note how wide the diameter of the nacelle is as compared with that for type 2 in Figure 6.39.

Since wind speed is variable, the frequency of the power output is also variable as given in Equation 6.34. This variable frequency generator cannot be connected to the fixed frequency grid.

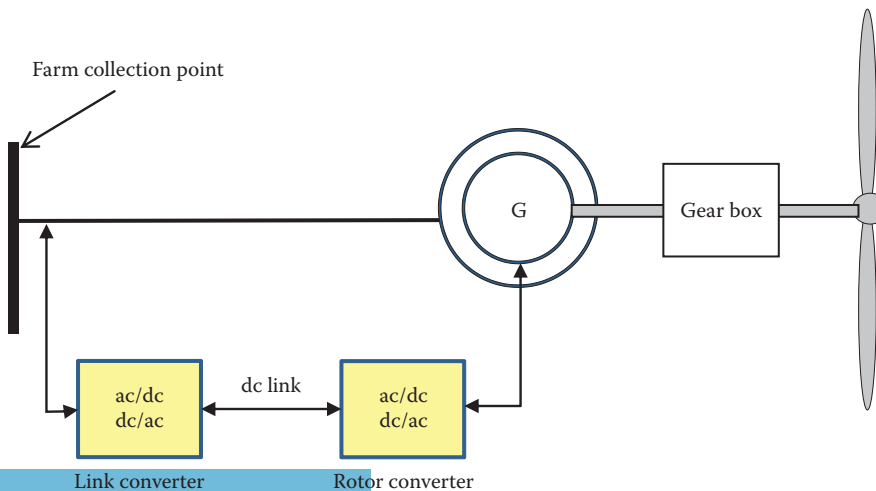


FIGURE 6.62 Type 3 wind turbine system.

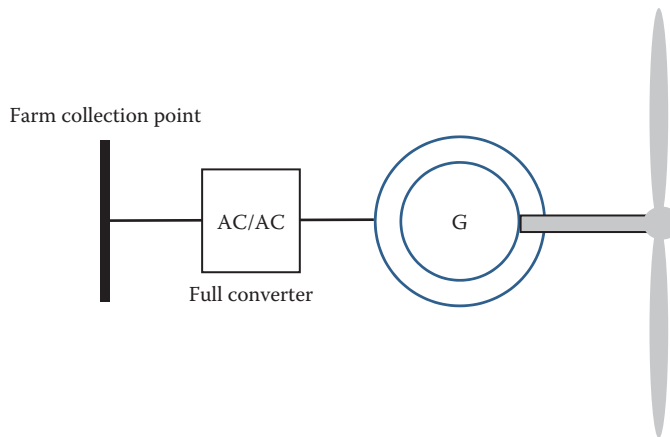


FIGURE 6.63 Type 4 wind turbine system.



FIGURE 6.64 Type 4 6 MW wind turbine made by Enercon.

To solve this problem, a converter is installed between the generator and the grid as shown in Figure 6.63. The function of the converter is to receive the variable frequency power of the generator and convert it to the fixed frequency needed by the grid. The converter of the Type 4 system is designed to handle the full power of the turbine. Thus, it is called a *full converter*.

6.2.12 WIND FARM PERFORMANCE

When a group of wind turbines is installed at one site, the site is called *wind farm*. Wind farms can have clusters of these machines as shown in Figure 6.65. Major wind farms such as the one located in Roscoe, Texas (about 800 MW capacity), have hundreds of these machines. The amount of energy generated by these farms depends on several factors, among them are:



FIGURE 6.65 Wind farm located in California. (Images are courtesy of the U.S. Department of Energy, Washington, DC.)

Wind speed and length of wind season: Wind speed determines how much power can be produced by the wind turbine. As seen in Equation 6.24, the wind power density is proportional to the cube of wind speed. Assuming all other parameters are fixed, a 10% increase in wind speed results in 33% increase in wind power.

Diameter of the rotating blades: The power captured by the blades is a function of the area they sweep as shown in Equation 6.23. The area is circular with a radius equal to the length of one blade as shown in Figure 6.51. The power is then proportional to the square of the radius. Hence, a 10% increase in the blade length will result in 21% increase in the captured power.

Efficiency of wind turbine components: As seen in Example 6.20, the low efficiency of the various components of the wind turbine reduces the output power of the system. Improvements in the design of the blades, gearbox and generator should increase the efficiency of the system.

Pitch control: With pitch control, WT can produce power at a wide range of wind speeds. However, controlling the pitch angle adds to the complexity of the system and increases the maintenance cost, so it is more suitable for large turbines.

Yaw control: Most wind turbines are equipped with a yaw mechanism to keep the blades facing into the wind when wind direction changes. Some turbines are designed to operate on downwind; these turbines do not need yaw mechanisms as the wind aligns these turbines.

Arrangement of the turbines in the farm: Layout of individual wind turbines in a wind farm is very crucial. If a wind turbine is placed in the wind shadow of other turbines, the amount of generated power can be substantially reduced. This is because the blades of the front turbines create wakes of turbulent wind, which can reach the rear turbines. When this happens, the rear turbines capture less energy from the wind because blade efficiency is reduced when wind is turbulent.

Reliability and maintenance: The cost of electricity generated by the wind farm is a function of the capital cost, land use, maintenance, and any other contractual arrangement. The early designs of wind turbines were high maintenance machines as well as cost ineffective systems. Newer designs, however, are much better with a reliability rate of around 98%.

6.2.13 EVALUATION OF WIND ENERGY

Wind power is an environmentally friendly form of generating electricity with virtually no contribution to air pollution. For this reason, wind energy industries are expanding rapidly worldwide. In 2010, the countries with the most wind power capacity are given in Table 6.1.

TABLE 6.1
Top 10 Countries with Wind Energy Capacity

Country	Wind Power Capacity (GW)
China	45
United States	40
Germany	27
Spain	21
India	13
Italy	5.7
France	5.6
United Kingdom	5.2
Canada	4
Denmark	3.7

The numbers in the table dwarf what we had in 2006. The United States went from 12 GW in 2006 to 40 GW in 2010; more than triple its size. China went from 2.6 GW in 2006 to 45 GW in 2010. The rapid rate by which wind turbines are constructed worldwide is indeed impressive. The world in 2010 had over 200 GW of wind power capacity. This is equivalent to 200 nuclear power plants.

Utilities often use the penetration factor of the wind energy systems (PF_w) to measure the size of all wind turbines in their systems. PF_w is defined as the ratio of all wind power capacity to the power generation capacity from all primary resources

$$PF_w = \frac{P_w}{P_p} \quad (6.36)$$

where

P_w is the power capacity of wind turbines in a given utility system

P_p is the power capacity from primary resources in the same utility system

In some countries, the penetration factor of wind energy is quite high. In Germany, for example, the penetration factor is above 25%. This high percentage is a great indicator for the mature and viable technology of wind energy systems.

Although it is highly popular, wind energy has some critics who often raise several issues such as (1) noise pollution, (2) aesthetics and visual pollution, and (3) bird collision. In addition, wind turbines have two main technical drawbacks: (1) voltage fluctuations and (2) wind variability.

Noise pollution: There are two potential sources of noise from a wind turbine: mechanical noise from the gearbox and generator, and aerodynamic noise from the rotor blades. Aerodynamic noise is the main component of the total noise, which is similar to the swish sound produced by a helicopter. At 400 m downwind, the turbine noise can be as high as 60 dB, which is equivalent to the noise level from a dishwasher or air conditioner. Although the noise from wind farms is far below the threshold of pain, which is 140 dB, it is a major annoyance to some people. Fortunately, newer low speed and better designs of rotor blades have reduced the aerodynamic noise dramatically.

Aesthetics: Designers of wind turbines believe their creations look pretty, but, unfortunately, not everyone agrees. Critics see wind farms as defacement of the landscape, forcing developers to install them in remote areas, including offshore as shown in Figure 6.66.



FIGURE 6.66 Two megawatt offshore wind turbine farm in Denmark. (Image courtesy of LM Glasfiber Group.)

Bird collisions: Instances of birds being hit by the moving blades have been reported. However, newer turbines are designed for low blade speeds, which reduce the severity of the problem. Off shore turbine create reef in its base, which is good. The reef attracts fish, which is also good. The fish attract birds to feed on them, which is good as well. But, the increased number of birds may cause more bird collision. Some see this as acceptable outcome as the dead birds become food for the fish!

Navigation: Off shore wind systems are not placed in the shipping lanes, so obstruction to large ships is unlikely especially when the blades reflect radar signals and can be easily detected. Most of the off-shore wind turbines are equipped with warning devices to alert ships in foul weather. However, recreational boating and small fishing vessels may stray in the area.

Ice accumulation: In areas with cold weather, ice can accumulate on the blades. When the turbine rotates, the ice can be dislodged and turned into projectiles endangering people and structures in the area. In some WT models, the blades are heated to prevent the ice for accumulating on the blades.

Sunlight flicker: Some blades reflect sunlight. When these blades rotate, the reflections of the sunlight off these blades create light flickers. This is an annoyance to some people.

Voltage fluctuations: A large number of wind turbines use induction machines as generators. These machines are very rugged and require little maintenance and control. They are also self-synchronized with the power grid without the need for additional synchronization equipment. However, because the induction machine has no field circuit, it demands a significant amount of reactive power from the utility system. When used in the generating mode, the induction machine consumes reactive power from the utility while delivering real power. In some cases, the magnitude of the reactive power imported from the utility exceeds the magnitude of the real power generated. Further, the reactive power consumed by the generator is not constant, but is dependent on the speed of its shaft. Figure 6.67 shows the relationship between the reactive power and the speed of the machine. Assume Type 1 or 2 machines which operate as generators when their rotor speeds are higher than their synchronous speeds (n_s). This is the linear region identified in the figure. Since the speed of wind changes continuously, the reactive power consumed by all induction machines in the farm also changes continuously as shown in Figure 6.68. The voltage at the wind farm is dependent on the reactive power consumed by all wind turbines in the farm; the

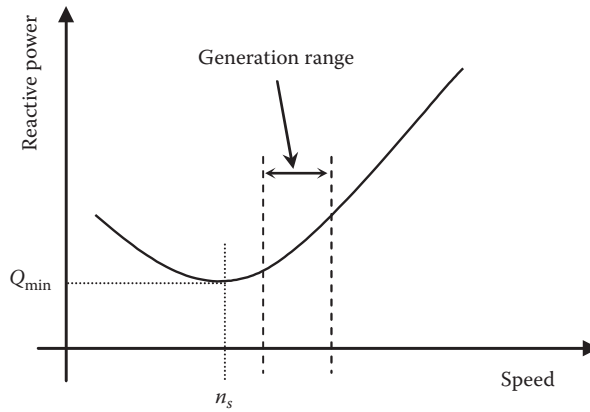


FIGURE 6.67 Reactive power of induction machine.

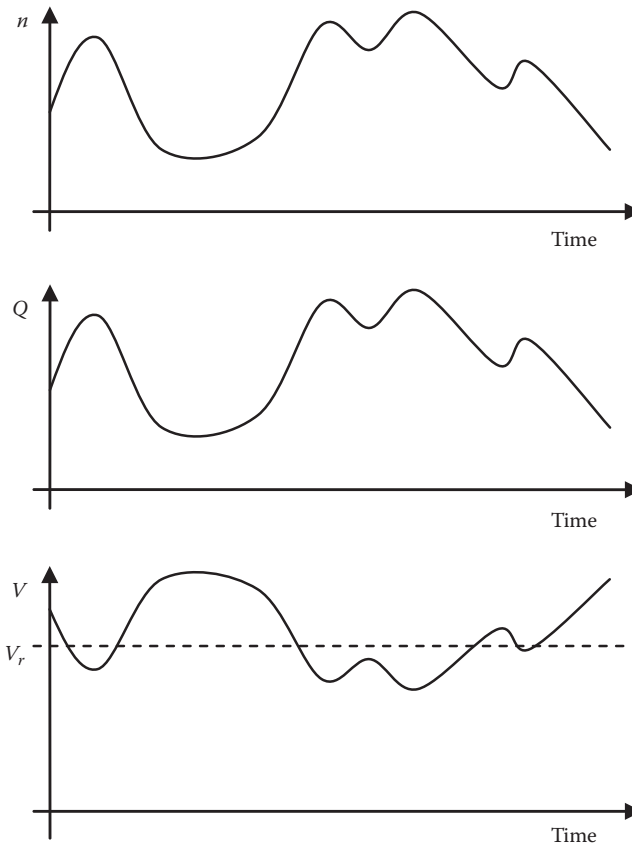


FIGURE 6.68 Wind speed, reactive power, and terminal voltage.

higher the reactive power, the lower the voltage. Thus, the voltage at the site is a mirror image of the reactive power, but at different scale as shown in Figure 6.68. V_r is the average voltage. If the voltage variation is slow, it is probably unnoticeable. However, if the variations are fast and large in magnitude, annoying voltage flickers can be produced at nearby areas. This problem can be solved by installing fast reactive power compensators or by adjusting the injected signal in the rotor of Type 3 turbines.

Wind production misalignment with demands: Most of the electric loads peak in the morning and early evening. During these times, utilities often fire their fossil fuel power plants to compensate for the extra demands. Renewable energy can play a great role during these periods by supplying the extra energy. However, because wind is not reliable, energy from wind farms is not always synchronized with the increase in demands.

Variability of wind: Wind is continuously varying and somewhat unpredictable. This makes the production of power from wind farms less reliable than conventional power plants.

6.3 HYDROKINETIC SYSTEMS

Hydrokinetic systems produce electricity by harnessing the potential and kinetic energies of a body of water. Since water density is almost 900–1000 times the density of air, a hydrokinetic system can produce much more power than wind systems with same physical size. Several studies have shown that properly designed systems placed in areas with favorable conditions in the United States can produce enough energy to power North America. A mere 0.01% of the available hydrokinetic energy in the world would be enough to power the entire world.

The hydrokinetic systems have a number of designs; the key ones are as follows:

- *Small hydroelectric system:* The system is similar to the impoundment hydroelectric power plants discussed in Chapter 4 but at a smaller scale.
- *Wave system:* The system harnesses the energy of waves near shores. The waves are caused by wind and oceanic geology.
- *Tidal system:* Created by the motion of sun and moon that cause the water level to rise and fall. The potential energy of the tide can be harnessed by dams or barrages.
- *Water stream (WS) system:* Free flowing rivers and ocean currents are loaded with kinetic energy. Some of this energy can be captured without the use of dams.

6.3.1 SMALL HYDRO SYSTEMS

Hydroelectric power is one of the oldest forms of generating electricity that dates back to 1882 when the first hydroelectric power plant was constructed across the Fox River in Appleton, Wisconsin. As seen in Chapter 4, the hydroelectric power plants are massive in size and capacity. These power plants require enormous water resources, which are available only in a very limited number of areas worldwide. However, the world has an immense number of small rivers and reservoirs that can be utilized to generate small amounts of electric energy enough to power neighborhoods and small cities. These types of power plants are called *small hydroelectric* systems.

Small hydroelectric systems are at the low end of the power ratings, up to a few megawatts. The popularity of these systems is due to their mature and proven technology, reliable operation, and their capability to produce electricity even with small head reservoirs.

6.3.1.1 Main Components of Small Hydro System

A schematic of a simple reservoir-type hydroelectric plant is shown in Figure 6.69. The system is similar to the impoundment hydroelectric system discussed in Chapter 4, but the head of the reservoir is much shorter and its capacity is much smaller. The reservoir is either a natural lake at a higher elevation than a downstream river or a lake created by a dam. The main components of the system are the reservoir, the penstock, the turbine and the generator. Because of the low head of small hydros, reaction turbines (Kaplan or Francis) are used. Impulse turbines (Pelton) are not suitable as they are designed for high heads. The reaction turbines are immersed in water so they use the pressure energy of the water.

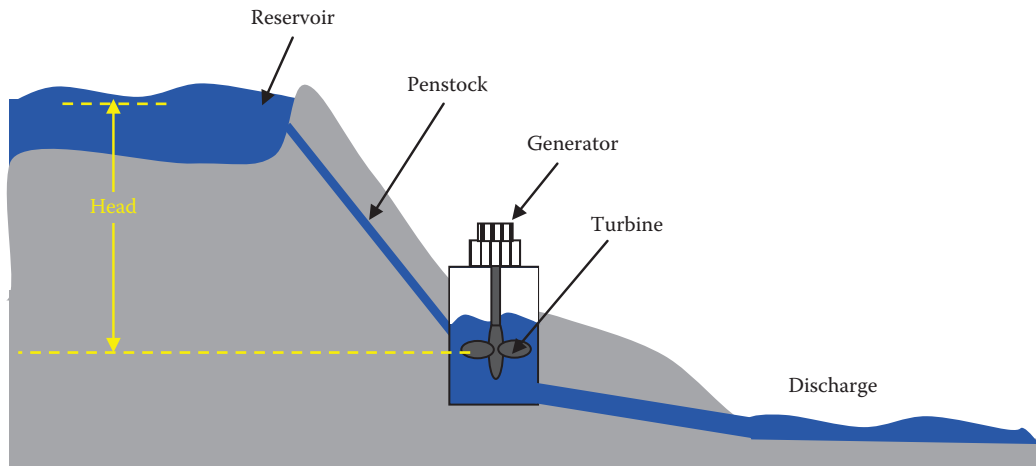


FIGURE 6.69 Small hydroelectric system with reservoir.

The potential energy of the water in the reservoir PE_r , is the weight of the water (W) in the reservoir multiplied by the elevation of the water above the turbine; known as actual or physical water head (H):

$$PE_r = WH \quad (6.37)$$

In sites where the head changes, the average value is used

$$H = \frac{1}{N} \sum_{i=1}^k n_i H_i \quad (6.38)$$

where

N is the total number of hours in 1 year

H_i is the head during n_i hours

n_i is the number of hours at which the head is H_i

The weight of the water behind the dam is equal to its mass (M) multiplied by the acceleration of gravity (g)

$$W = Mg \quad (6.39)$$

$$PE_r = MgH \quad (6.40)$$

where PE_r is the potential energy of the entire reservoir.

If we are to calculate the potential energy (PE) of the water at the end of the penstock PE_{p-out} , we use the water mass m passing through the penstock

$$PE_{p-out} = mgh \quad (6.41)$$

where

PE_{p-out} is the pressure energy at the end of penstock (J)

m is the mass of water leaving the penstock (kg)

h is the effective head at the end of the penstock (m). It is explained in the next subsection

g is the acceleration of gravity (m/s^2)

Example 6.23

Compute the potential energy in a reservoir whose annual average volume of its water is 1000 m^3 and its seasonal heads are given as follows:

- Average winter head = 15 m
- Average spring head = 25 m
- Average summer head = 20 m
- Average fall head = 25 m

Solution

To compute the annual average head, we use Equation 6.38 assuming each season is 3 month long:

$$H = \frac{1}{N} \sum_{i=1}^k n_i H_i = \frac{3}{12} (15 + 25 + 20 + 25) = 21.25 \text{ m}$$

The mass of water is its volume multiplied by its density. Assume the water density is 1000 kg/m^3

$$M = Vol \times \delta = 10^6 \text{ kg}$$

The potential energy of the reservoir can be calculated using Equation 6.40:

$$PE_r = MgH = 10^6 \times 9.81 \times 21.25 = 208.46 \text{ MW h}$$

When water moves inside a penstock, the water flow rate (f) is defined as the volume of water (vol) passing through the penstock during a time interval t :

$$f = \frac{vol}{t} \quad (6.42)$$

Hence, Equation 6.41 can be rewritten in terms of water flow as

$$PE_{p-out} = mgh = (vol \delta) gh = f \delta ght \quad (6.43)$$

where δ is the water density. The power at the end of the penstock is then

$$P_{p-out} = f \delta gh \quad (6.44)$$

6.3.1.2 Effective Head

The potential energy at the end of the penstock can be represented by water pressure measured at the end of the pipe times the volume of water passing through the pipe

$$PE_{p-out} = P_r vol \quad (6.45)$$

where

P_r is the pressure at the end of the penstock in N/m^2

vol is the volume of water passing through the pipe (m^3)

The penstock is not a lossless pipe. When water moves inside the pipe, there is water friction. This is a form of loss making the energy at the intake of the pipe higher than the energy at the outtake end. The friction losses are higher for smaller cross section pipes and for pipes with bends and elbows.

When the end of the pipe is shut by a valve (blocked), there is no water flow and the potential energy at the end of the pipe is

$$PE_{p-out0} = P_{r0} vol_0 \quad (6.46)$$

where

PE_{p-out0} is the potential energy at the output end of the penstock when water is blocked (J)

P_{r0} is the pressure at the output end of the penstock when water is blocked

vol_0 is the volume of water in penstock

At the same blocking condition, the potential energy can also be represented by

$$PE_{p-out0} = mgH \quad (6.47)$$

where H is the physical head measured at the site. It is also known as the theoretical head, gross head, or static head.

Combining Equations 6.46 and 6.47, the theoretical head can be written as

$$H = \frac{P_{r0}}{g\delta} \quad (6.48)$$

Since g and δ are constant values, the theoretical head can be related to the blocked pipe pressure at the end of the penstock by the following expression:

$$H = \frac{P_{r0}}{9.81 \times 1000} = 1.02 \times 10^{-4} P_{r0} \quad (6.49)$$

When water is allowed to flow freely (open valve), the pressure at the end of the penstock is reduced. Assume the new pressure is P_r which must correspond to new head h :

$$h = \frac{P_r}{9.81 \times 1000} = 1.02 \times 10^{-4} P_r \quad (6.50)$$

This h is known as the effective head or dynamic head. The energy produced by the hydroelectric turbine is a function of this effective head, not the static (gross) head. The relationship between the effective and the gross heads is then

$$\frac{h}{H} = \frac{P_r}{P_{r0}} \quad (6.51)$$

This is the same ratio as the penstock efficiency. The effective head is often in the range of 80%–90% of the gross head.

6.3.1.3 System Efficiency

The power flow inside the small hydroelectric system is shown in Figure 6.70. The input power entering the penstock is (P_{p-in}). Part of this power is wasted in the penstock due to water friction. The rest of the power (P_{p-out}) is at the end of the penstock. Most of P_{p-out} is captured by the turbine blades (P_{blade}). Part of P_{blade} is lost in the form of turbine rotational losses and the rest is converted into mechanical power (P_m) which is the input to the electrical generator. Part of P_m is lost due to the various losses inside the generator, and the rest is the output electric power (P_g).

The penstock efficiency (η_p) is

$$\eta_p = \frac{P_{p-out}}{P_{p-in}} \tag{6.52}$$

The ratio of the power captured by the blades (P_{blade}) to P_{p-out} is the hydro efficiency (η_h):

$$\eta_h = \frac{P_{blade}}{P_{p-out}} \tag{6.53}$$

The power captured by the blades (P_{blade}) is not all converted into the mechanical power entering the generator (P_m) due to the various rotational losses in the turbine and rotating shafts. The ratio of the two powers is known as turbine efficiency (η_t):

$$\eta_t = \frac{P_m}{P_{blade}} \tag{6.54}$$

The output electric power of the generator (P_g) is equal to its input power (P_m) minus all losses in the generator. Hence, the generator efficiency (η_g) is defined as

$$\eta_g = \frac{P_g}{P_m} \tag{6.55}$$

Using Equations 6.43 and 6.52 through 6.55, we can write the equation of the output electrical energy as a function of the flow rate and effective head

$$P_g = P_{p-out}(\eta_h \eta_t \eta_g) = f \delta g h (\eta_h \eta_t \eta_g) \tag{6.56}$$

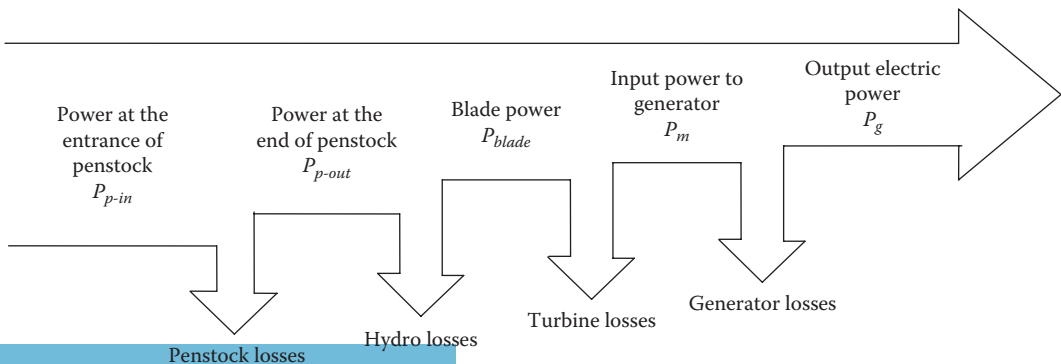


FIGURE 6.70 Power flow in small hydroelectric system.

Example 6.24

A small hydroelectric site has a reservoir with 80 m effective head. The penstock passes water at the rate of 100 kg/s. The hydro efficiency is 95%, the turbine efficiency is 85%, and the efficiency of the generator is 90%. Assume that the owner of this small hydroelectric system sells the generated energy to the local utility at \$0.15/kWh. Compute his income in 1 month.

Solution

The volumetric rate is

$$f = \frac{vol}{t} = \frac{m}{\delta t} = \frac{100}{1000} = 0.1 \text{ m}^3/\text{s}$$

Using Equation 6.56, we can compute the output electric energy for 1 month

$$E_g = f \delta g h t (\eta_h \eta_t \eta_g) = 0.1 \times 1000 \times 9.81 \times 80 \times (30 \times 24) \times (0.95 \times 0.85 \times 0.9) = 41.08 \text{ MWh}$$

The income in 1 month is

$$\text{Income} = E_g \times 0.15 = 41.08 \times 10^3 \times 0.15 = \$6162$$

6.3.1.4 Site Calculations

The amount of electric power generated by a small hydroelectric system depends on three parameters: (1) effective head h , (2) water flow rate, and (3) the efficiency of the system components. The first two are the most important parameters. To evaluate a site for small hydroelectric generation potential, we need to determine the effective head and the flow rate. The needed tools can be as simple as a pressure gage, hose, stop watch and a container of known volume.

The first step is to determine the gross head. Since the terrain where the penstock is placed on is normally inclined, curved, jagged and irregular, the measurement of the gross head could be tricky unless a highly accurate altimeter is used. Alternatively, we can use two methods: equilibrium tube or pressure gage method.

Pascal's law of equilibrium tubes can be used if the gross head is low. It requires the use of a water hose stretch along the penstock path. One end of the hose is submerged in the reservoir (end A) and the other is where the penstock ends at the proposed turbine location (end B). The water will continuously flow through end B of the hose. While standing at the turbine location, lift the downstream end B vertically until water stops flowing. The gross head is the vertical distance traveled by end B.

The pressure method uses water pressure gage and a hose of similar cross section and length to the penstock. Measure the water pressure when the valve at the end of the hose is closed, and repeat the measurement when the valve is fully open. Substitute the first pressure into Equation 6.49 to obtain the gross head, and substitute the second pressure into Equation 6.50 to obtain the effective head.

The water flow can be determined by the hose used in the pressure method. Allow the water to fill a container of known volume and record the time it takes to fill the container. The flow rate is then

$$f = \frac{vol_{container}}{t} \quad (6.57)$$

where

f is the flow rate

$vol_{container}$ is the volume of the container

t is the time it takes to fill the container

Example 6.25

The pressure at the end of a penstock is 200 kN/m^2 when the valve at the end of the penstock is fully open. If the small hydroelectric power plant produced 1 MW , compute the flow rate of the penstock. Assume the hydro, turbine, and generator efficiency combined is 80% .

Solution

Let us first calculate the effective head using Equation 6.50

$$h = 1.02 \times 10^{-4} P_r = 1.02 \times 10^{-4} \times 200 \times 10^3 = 20.4 \text{ m}$$

Use Equation 6.56 to compute the flow rate

$$f = \frac{P_g}{\delta g h (\eta_h \eta_t \eta_g)}$$

$$f = \frac{10^6}{10^3 \times 9.81 \times 20.4 (0.8)} = 6.24 \text{ m}^3/\text{s}$$

Example 6.26

At a given river, a developer wants to install 3 MW small hydro system. To do that, he needs to build a barrier (dam) to obtain the proper head and select a penstock to achieve water velocity of 20 m/s and a flow rate of $10 \text{ m}^3/\text{s}$. Estimate the height of the dam and the cross section of the penstock.

Solution

The flow rate is

$$f = \frac{\text{vol}}{t} = \frac{Avt}{t} = Av$$

where

A is the cross section area of the penstock

v is the water velocity

The diameter of the penstock is then

$$d = \sqrt{\frac{4f}{\pi v}} = \sqrt{\frac{4 \times 10}{\pi \times 20}} = 0.8 \text{ m}$$

Use Equation 6.56 to compute the effective head. Assume the value of all efficiencies is 80% :

$$h = \frac{P_g}{\delta g f (\eta_h \eta_t \eta_g)}$$

$$h = \frac{3 \times 10^6}{10^3 \times 9.81 \times 10 \times (0.8)} = 38.22 \text{ m}$$

Assume the head loss is 80%, the gross head is

$$H = \frac{h}{0.8} = 47.77 \text{ m}$$

The barrier must be more than 47.77 m high.

6.3.1.5 Evaluation of Small Hydro Systems

Small hydro systems utilize sites without enough water resources for large hydroelectric systems. Such sites are all over the globe and if fully utilized can generate enough power for local areas and small cities. However, when small hydro systems are extensively used, the environmental degradation per kW generated is likely to be similar, if not higher, than that caused by large hydropower systems. The main environmental problems with hydroelectric power plants are given in Chapter 5.

6.3.2 TIDAL AND STREAM ENERGY SYSTEM

Tides are the daily swells and sags of ocean waters relative to coastlines due to the gravitational pull of the moon and the sun. Although the moon is much smaller in mass than the sun, it exerts a larger gravitational force because of its relative proximity to earth. This force of attraction causes the oceans to rise along a perpendicular axis between the moon and earth. Because of the earth's rotation, the rise of water moves opposite to the direction of the earth's rotation creating the rhythmic rise and sag of coastal water. This tidal waves are slow in frequency (about one cycle every 12h), but contain tremendous amounts of kinetic energy, which is probably one of the major untapped energy resources of earth.

The shores of Chile, South Australia, New Zealand, Ireland, Scotland, Iceland, Canada, and South Africa have very strong tides. The Bay of Fundy in northeastern Canada has the highest tide in the world, over 16m. About 100 billion tons of water flow during one tidal cycle in that Bay.

Water Stream (WS) are due to ocean currents or fast moving rivers. Ocean current is due to several phenomena such as tide, wind speed, and the differences in temperature and salinity. River current is due to changes in elevations and depth along the river.

Strong ocean currents can be found in numerous places around the world such as in the northwest and northeast coasts of the United States and Canada, Australia, southern tip of the Korean peninsula, the western coast of Taiwan, western and northern coasts of Europe. The city of Saltstraumen in Norway claims to have the strongest tidal current in the world, about 22 knots.

Fast rivers can also be found all over the world. Among them are the Amazon in South America, Ok Tedi river in New Guinea, and the Río Atrato in northwestern Colombia.

There are two main technologies used to capture energy from tied and stream: The barrage system and the WS system. Both systems are suitable for coastal waters. But the WS system is also suitable for fast moving rivers.

There are a few major tidal and WS generating power plants in operation today. The main one is the *Le Rance River* in northern France built in 1966 and has a capacity of 240MW. Other plants are the 20MW in Nova Scotia, Canada, and the 400kW near Murmansk in Russia.

6.3.2.1 Barrage System

Tidal energy can be captured by the barrage energy system shown in Figure 6.71. The system is most suited for inlets where a channel is connecting an enclosed lagoon to the open sea. At the mouth of the channel, a dam is constructed to regulate the flow of the tidal water in either direction. A turbine is installed inside a conduit connecting the two sides of the dam. When tide is high, the water moves from the sea to the lagoon through the turbine. The turbine and its generator convert

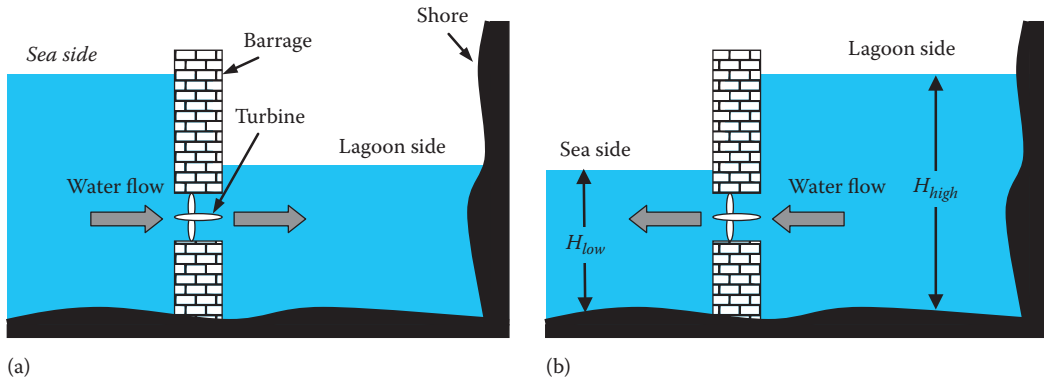


FIGURE 6.71 Barrage tidal energy system: (a) high tide and (b) low tide.

the potential energy of the water into electrical energy. When the tide is low, the stored water in the lagoon at high tides goes back to sea, and in the process electricity is generated.

Notice that the barrage technology is similar to that used in traditional impoundment hydroelectric power plants. In the impoundment hydroelectric system, we construct a dam to raise the water head thus increase the potential energy. In the barrage system, the water head is changing with tide allowing us to generate electricity during the ebb and flow of coastal tides.

The volume of water passing through the turbine is

$$Vol = A\Delta H \quad (6.58)$$

where A is the area of the base of the lagoon

ΔH is the hydraulic heads. It is the difference between the highest tide (H_{high}) and the lowest tides (H_{low}). It is also called tidal range.

$$\Delta H = H_{high} - H_{low} \quad (6.59)$$

The hydraulic head determines the amount of energy that can be captured. Since the hydraulic head is changing during the generation of electricity, we can modify Equation 6.40 to compute the energy based on the average head.

$$PE = mgH_{ave} = Vol \delta g H_{ave} \quad (6.60)$$

where

PE is the potential energy available from the barrage that is converted into electricity

m is the mass of water moving through the turbine

Vol is the volume of water passing through the turbine

g is the acceleration of gravity

H_{ave} is the average of the hydraulic head ΔH

$$H_{ave} = \frac{\Delta H}{2} \quad (6.61)$$

Hence Equation 6.60 can be rewritten as

$$PE = Vol \delta g H_{ave} = (A\Delta H) \delta g \frac{\Delta H}{2} \quad (6.62)$$

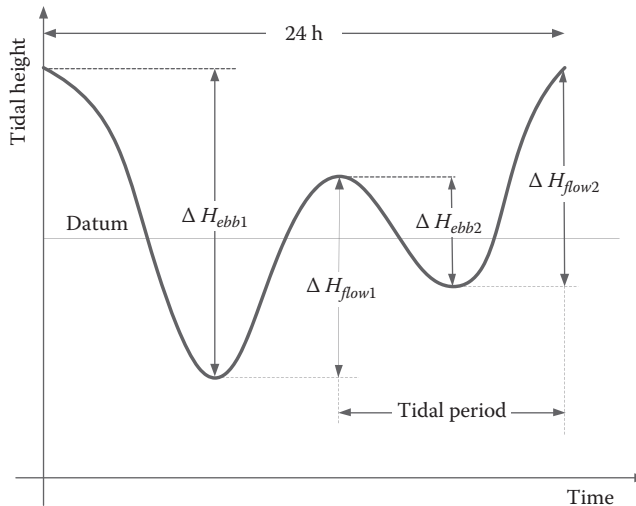


FIGURE 6.72 Semidiurnal tide.

or

$$PE = \frac{1}{2} A\delta g (\Delta H)^2 \tag{6.63}$$

In areas with semidiurnal tides, there are two tidal periods; two peaks and two lows as shown in Figure 6.72. Areas with diurnal tides have only one tidal period (one peak and one low). When water moves from the lagoon to the ocean, it is called ebbing. When water moves from ocean to lagoon, the water is flowing (or flooding).

Equation 6.63 represents the energy in single ebb or single flow. If the energy is generated during both ebbing and flowing, the total tidal hydraulic energy of the lagoon for one tidal period (PE_{period}) is

$$PE_{period} = \frac{1}{2} A\delta g (\Delta H_{ebb})^2 + \frac{1}{2} A\delta g (\Delta H_{flow})^2 = \frac{1}{2} A\delta g (\Delta H_{ebb}^2 + \Delta H_{flow}^2) \tag{6.64}$$

where

ΔH_{ebb} is the maximum hydraulic head during tidal ebbing

ΔH_{flow} is the maximum hydraulic head during tidal flow

If the site is semidiurnal, Figure 6.72, there are two tidal periods. In this case the total Hydraulic energy of the lagoon is

$$PE_{total} = \frac{1}{2} A\delta g (\Delta H_{ebb1}^2 + \Delta H_{ebb2}^2 + \Delta H_{flow1}^2 + \Delta H_{flow2}^2) \tag{6.65}$$

Because the energy is proportional to the square of the maximum hydraulic head, barrage systems are located in areas with high amplitude of tides. In North America, the maximum hydraulic head can reach more than 16m in places such as Maine, Alaska, and the Bay of Fundy on the Atlantic Ocean in Canada.

Example 6.27

A barrage tidal energy system is constructed between a lagoon and open ocean. The base of the lagoon is approximately semicircle with a diameter of 2 km. The water heads during the day are 25, 15, 22, and 12. Compute the potential energy of the barrage system. Assume the efficiencies of the various components of the turbine and generator is 80%. Compute the electric energy output and the average power generated.

Solution

The potential energy is given in Equation 6.63.

$$PE = \frac{1}{2} A \delta g (\Delta H)^2 = \frac{1}{2} \left(\frac{1}{2} \pi R^2 \right) \delta g (\Delta H)^2$$

$$PE = \frac{1}{4} (\pi \times 10^6) \times 10^3 \times 9.81 (\Delta H)^2 = 7.705 \times 10^9 (\Delta H)^2$$

For the first ebb, the potential energy is

$$PE_{ebb1} = 7.705 \times 10^9 (\Delta H_{ebb1})^2 = 7.705 \times 10^9 (25 - 15)^2 = 770.5 \text{ GJ}$$

For the first flow, the energy is

$$PE_{flow1} = 7.705 \times 10^9 (\Delta H_{ebb1})^2 = 7.705 \times 10^9 (22 - 15)^2 = 377.54 \text{ GJ}$$

For the second ebb, the energy is

$$PE_{ebb2} = 7.705 \times 10^9 (\Delta H_{ebb2})^2 = 7.705 \times 10^9 (22 - 12)^2 = 770.5 \text{ GJ}$$

For the second flow, the energy is

$$PE_{flow2} = 7.705 \times 10^9 (\Delta H_{flow2})^2 = 7.705 \times 10^9 (25 - 12)^2 = 1302.15 \text{ GJ}$$

Total energy of 1 day is

$$PE_{total} = PE_{ebb1} + PE_{flow1} + PE_{ebb2} + PE_{flow2} = 3220.69 \text{ GJ}$$

The generated energy (E_g) is

$$E_g = PE\eta = 3220.69 \times 0.8 = 2571.55 \text{ GJ} = 715.7 \text{ MWh}$$

The average power generated (P_g) is

$$P_g = \frac{E_g}{\text{time}} = \frac{715.7}{24} = 29.82 \text{ MW}$$

6.3.2.2 Water Stream Energy

The WS system converts the kinetic energy of the moving water into electrical energy much the same way as when wind turbine converts wind energy into electrical energy. The system does not require the construction of water barriers such as dams or barrages, and therefore is considered more environmentally sensitive. The WS system is also known as diversion-type small hydroelectric system. The schematic of this system is shown in Figure 6.73.

The kinetic energy of the WS passing through the sweep area of the turbine blades is

$$KE_{stream} = \frac{1}{2}mv^2 \quad (6.66)$$

where

m is the mass of water entering the sweep area of the blade

v is the velocity of water

Water mass is the volume of water (Vol) multiplied by the water density (δ)

$$m = Vol \delta \quad (6.67)$$

The volume of water entering the turbine during a time t is

$$vol = A_s vt \quad (6.68)$$

where A_s is the sweep area of the blades of the turbine in one revolution.

The KE of the stream entering the turbine (KE_{stream}) is then

$$KE_{stream} = \frac{1}{2} A_s \delta v^3 t \quad (6.69)$$

The power in the stream entering the turbine (P_{stream}) is

$$P_{stream} = \frac{1}{2} \delta A_s v^3 \quad (6.70)$$

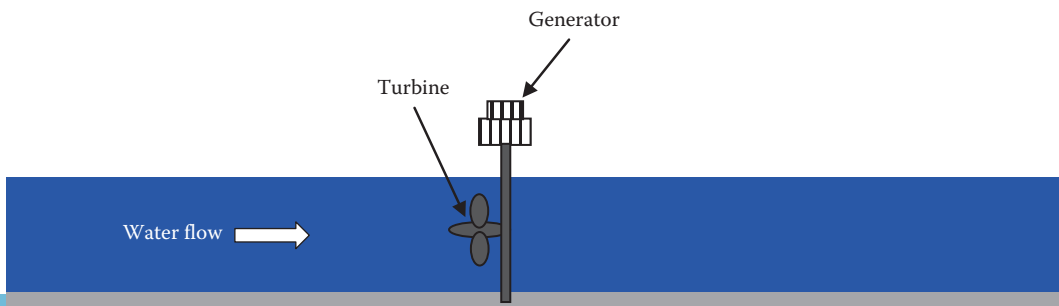


FIGURE 6.73 Diversion-type small hydroelectric system.

The blades of the turbine cannot capture all of the kinetic energy entering the turbine. The ratio of the energy captured by the blade (KE_{blade}) to the kinetic energy in the stream (KE_{stream}) is known as the *coefficient of performance* (C_p):

$$C_p = \frac{KE_{blade}}{KE_{stream}} = \frac{P_{blade}}{P_{stream}} \quad (6.71)$$

The mechanical output power of the turbine (P_m) is equal to the blade power (P_{blade}) minus the turbine losses. Hence, the efficiency of turbine (η_t) is

$$\eta_t = \frac{P_m}{P_{blade}} \quad (6.72)$$

The output electric power of the generator P_g is equal to P_m minus the losses of the generator; hence, the generator efficiency (η_g) is

$$\eta_g = \frac{P_g}{P_m} \quad (6.73)$$

Example 6.28

A WS hydroelectric system is installed in the pathway of a small river with current speed of 5 m/s. The diameter of the swept area of the turbine is 1.2 m. Assume that the coefficient of performance is 30%, the turbine efficiency is 90%, and the efficiency of the generator is 90%. Compute the output power of the plant and the energy generated in 1 year. If the price of the energy is \$0.1/kWh, compute the income from this small hydroelectric plant in 1 year.

Solution

Use Equation 6.70 to compute the stream power entering the turbine

$$P_{stream} = 500 \times A_s \times v^3 = 500 \times (\pi \times 0.6^2) \times 5^3 = 70.69 \text{ kW}$$

The output electric power is P_{stream} multiplied by the efficiencies

$$P_g = P_{stream}(C_p \eta_t \eta_g) = 70.69 \times (0.3 \times 0.9 \times 0.9) = 17.172 \text{ kW}$$

The energy generated in 1 year is

$$E_g = 17.172 \times (24 \times 365) = 150.43 \text{ MWh}$$

Income from the plant is

$$\text{Income} = 0.1 \times 150.43 = \$15,043$$

Figure 6.74a shows a WS system for ocean applications. The two blades of the turbine are immersed in water using a lifting mechanism. The blades are attached to an electrical generator mounted above the water level. Figure 6.74b shows a conceptual design of a WS farm.

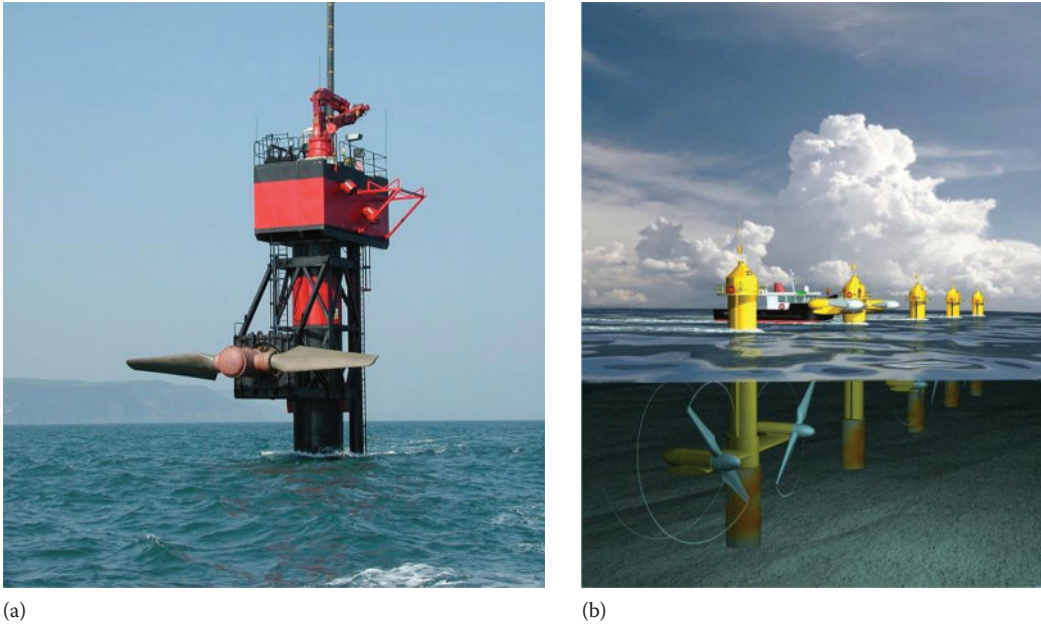


FIGURE 6.74 WS energy system: (a) turbine and (b) conceptual design of a farm. (Images courtesy of Marine Current Turbines Limited.)

Example 6.29

A WS turbine has 3 m long blades. Compute the power captured by the blades when the water current is 10 knots and the coefficient of performance of the turbine is 0.3.

Solution

Convert the nautical speed to metric

$$v = 10 \times 1.852 = 18.52 \text{ km/h}$$

$$v = 18.52 \times \frac{1000}{3600} = 5.14 \text{ m/s}$$

Use Equation 6.70 to compute the power of the stream entering the turbine:

$$P_{stream} = \frac{1}{2} A \delta v^3 = \frac{1}{2} (\pi \times 3^2) \times 1000 \times (5.14)^3 = 1.92 \text{ M}$$

The coefficient of performance C_p determines the amount of power captured by the blades:

$$P_{blade} = C_p \times P_{stream} = 0.3 \times 1.92 = 576.0 \text{ kW}$$

Example 6.30

Assume a wind turbine has the same diameter as the WS turbine in Example 6.29. Also assume that the wind speed is equivalent to the speed of the WS, and the coefficient of performance is also 0.3. Compute the power captured by the blades of the wind turbine. Also compute the ratio of the powers from WS and wind.

Solution

Assume the air density is 1.2 kg/m^3 , use Equation 6.23 to compute the wind power:

$$P_{wind} = \frac{1}{2} A \delta v^3 = \frac{1}{2} (\pi 3^2) \times 1.2 \times (5.14)^3 = 2.3 \text{ kW}$$

The coefficient of performance determines the amount of power captured by the wind turbine blades:

$$P_{blade} = C_p P_{wind} = 0.3 \times 2.3 = 0.69 \text{ kW}$$

The ratio of the steam power to the wind power is

$$\frac{P_{stream}}{P_{wind}} = \frac{576.0}{0.69} = 834.78$$

Notice that this ratio is the same as the ratio of the water density to air density. Hence, WS turbines can capture much more power as compared with the wind mill.

6.3.2.3 Evaluation of Tidal and Stream Energy

Tidal and stream energy are renewable resources with potentials to become among the major electrical power generating systems. Unlike wind and solar, the production from tidal and stream systems is predictable because water currents are known months in advance with great accuracy. This makes it easier to predict the electric power generated by a tidal and stream energy systems for a few months into the future. The predictability of power production is very important for utilities to maintain system reliability. Also, it enables owners to schedule and sell the generated power at favorable rates.

From the environmental impact point of view, the barrage system reduces coastline erosion and its anchoring systems are eventually developed into artificial reefs that improve the marine life of the area. However, barrage systems are not free from problems, including the following:

- The barrage alters the tidal flows which can potentially stimulate the growth of the red tide organism that causes sickness in shellfish.
- Water navigations for commercial shipping, fishing and recreational boating are severely limited in the area.
- Accidental spills of hydraulic fluids and other material into water can affect the aquatic life.

For WS system, some of the known environmental impacts are as follows:

- Securing the turbine to the seafloor may disturb seabed habitats during installation and operation. Turbines could inhibit large mammals from moving freely in the area. The system is often installed at 20–80 m depth. Any wildlife or fishing activities at this depth would be negatively impacted.
- Navy ships and submarines consider these systems as obstacles to their free movements and likely to impact their sonar signals.

6.3.3 WAVE ENERGY SYSTEM

Wave energy can be considered a form of solar energy. This is because different areas on earth receive different amount of solar energy in the form of heat. The uneven temperatures create wind whose speed depends on the difference in temperatures. Wind speed is the main reason for waves. The transfer of solar energy to waves is very high in three regions of the world: between 30°–60° latitude, near the equator due to the easterly surface winds (trade winds), and near the pole due to polar storms.

Scientists have estimated the annual wave energy off the coastlines in the United States to be about 2PWh. Although not all of this energy can be harnessed by today's technology, the recoverable energy can be as much as 700TWh if the right technology is developed.

An ocean wave can be described by a sinusoidal motion observed from a fixed position as depicted in Figure 6.75. The wave has crests and troughs. The distance between two crests is the wavelength (λ). The difference between the crest and the trough is the wave height (h). The distance between the crest and the average seawater level is the wave amplitude (a). Using wave theory, the period of the wave (τ) is

$$\tau = \sqrt{\frac{2\pi\lambda}{g}} \quad (6.74)$$

where g is the acceleration of gravity (9.81 m/s^2), and the unit of the period is seconds.

Also from wave theory, the power contained in a wave per one meter length of coastline (P_{wave}) is given by

$$P_{wave} = \frac{\delta g^2 a^2 \tau}{8\pi} \quad (6.75)$$

where δ is water density. If we assume that the wave amplitude is roughly half the wave height, then the wave power can be approximated to

$$P_{wave} = \frac{\delta g^2 h^2 \tau}{32\pi} \quad (6.76)$$

Since the heights of waves are continuously changing, we can use the average height (h_{ave}) of several waves in a given time period to compute the average power of the wave (P_{ave}):

$$P_{ave} = \frac{\delta g^2 h_{ave}^2 \tau}{32\pi} \quad (6.77)$$

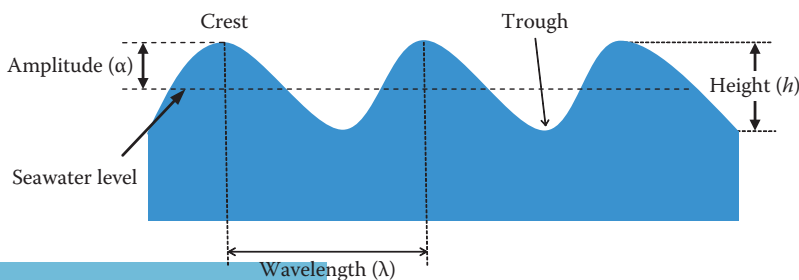


FIGURE 6.75 Wave parameters.

Example 6.31

Compute the wave power for an average wave height of 3 m and a wave period of 8 s. Also compute the wavelength.

Solution

Direct substitution in Equation 6.77 assuming the water density is 1000 kg/m^3 :

$$P_{ave} = \frac{\delta g^2 h_{ave}^2 \tau}{32\pi} = \frac{10^3 \times 9.81^2 \times 3^2 \times 8}{32\pi} = 68.92 \text{ kW/m of cost line}$$

This is a tremendous amount of power for only one meter of costal line.

Use Equation 6.74 to compute the wavelength

$$\lambda = \frac{g\tau^2}{2\pi} = \frac{9.81 \times 8^2}{2\pi} = 99.92 \text{ m}$$

The technology developed to harness wave energy can be divided into three main types: buoyant moored (BM) system, hinged contour (HC) system, and oscillating water column (OWC) system. Although we are discussing these three systems, the field is rapidly progressing and different systems are expected to become available in the future.

6.3.3.1 Buoyant Moored System

According to the theory developed by Michael Faraday, when we move a magnet inside a coil, a voltage across the coil terminals is induced. When the terminals of the coil are connected to an electric load, the voltage causes a current to flow into the load and the load receives electric energy. The source of this energy is the mechanical energy that moves the magnet. This is the fundamental theory for electrical generators as seen in Chapter 12.

The BM system uses the motion of the waves to move the magnet. One of these systems is shown in Figure 6.76. The system consists of a float, anchor, linear generator (magnet and coil) and enclosure. The function of the float is to track the motion of the waves. The enclosure is attached to the float, so it is also moving with the wave. The magnet of the linear generator is anchored to the ocean floor and can freely move through the enclosure. This way, when the wave is moving toward the crest, the enclosure moves upward with respect to the magnet. When the wave is moving toward the trough, the enclosure moves downward with respect to the magnet. Hence, the magnet is continuously moving inside the enclosure. Surrounding the magnet is a coil mounted on the enclosure. So the motion of the wave creates a relative motion between the coil and the magnet. This relative motion induces voltage (V) across the coil terminals as shown in Figure 6.76. The photo in Figure 6.77 shows one of these systems during installation.

A different design is shown in Figure 6.78 where the enclosure is anchored on the ocean floor. In this system, the enclosure is fixed and the magnet is moving. The line that ties the magnet to the float moves the magnet of the linear generator.

Another system is shown in Figure 6.79. It is known as Oyster wave energy system. It consists of a float connected to the base of the system by a hinge and a piston. The motion of waves allows the piston to pump water at high pressure to a hydroelectric power plant located on shore through a high pressure flow line. The pressurized water generates electricity in the hydroelectric plant. The Oyster wave system is designed to be used in shallow water of about 10 m in depth near shorelines.

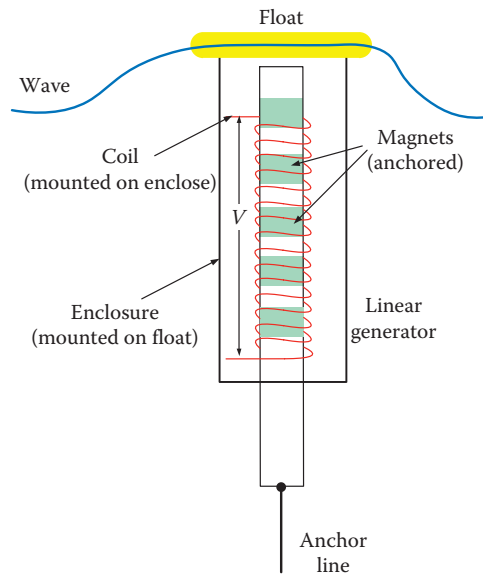


FIGURE 6.76 Buoyant moored system.

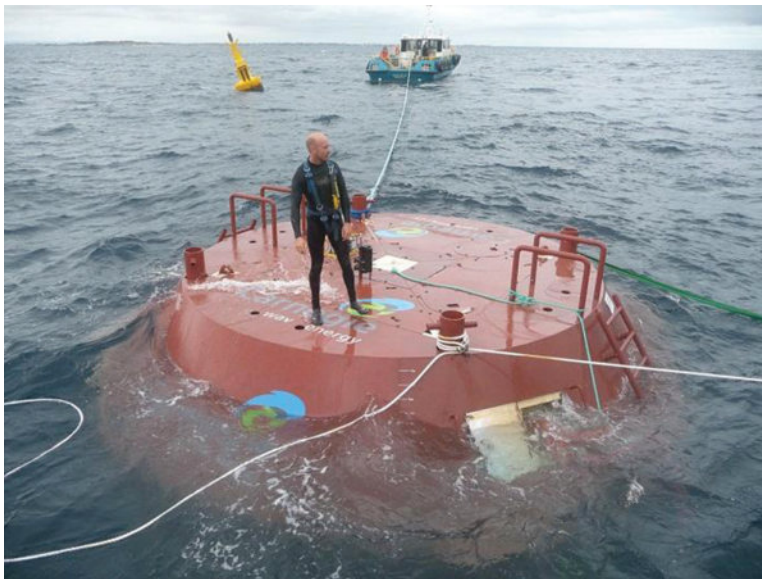


FIGURE 6.77 Buoyant actuator during the installation. (Courtesy of Carnegie Wave Energy through Wikipedia.)

6.3.3.2 Hinged Contour System

The HC system shown in Figure 6.80 consists of several floating pontoons. Each two adjacent pontoons are connected through a system of hinges and piston. The hinges are on one of the pontoons and the pistons are on the other pontoon. The system consists of several of these pontoons oriented perpendicular to the direction of waves. The differing heights of waves along the length of the system cause flexing motion at the connection of neighboring pontoons. With the motion of the wave, one of the pistons is in compression and the other is in expansion. The

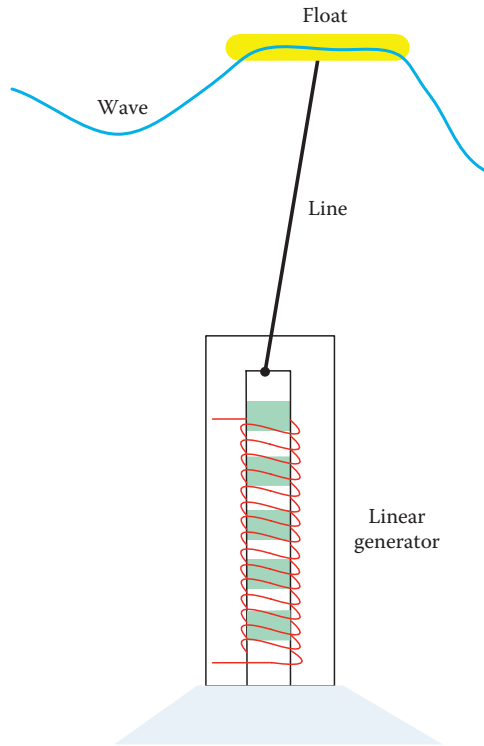


FIGURE 6.78 Buoyant moored system anchored on ocean floor.

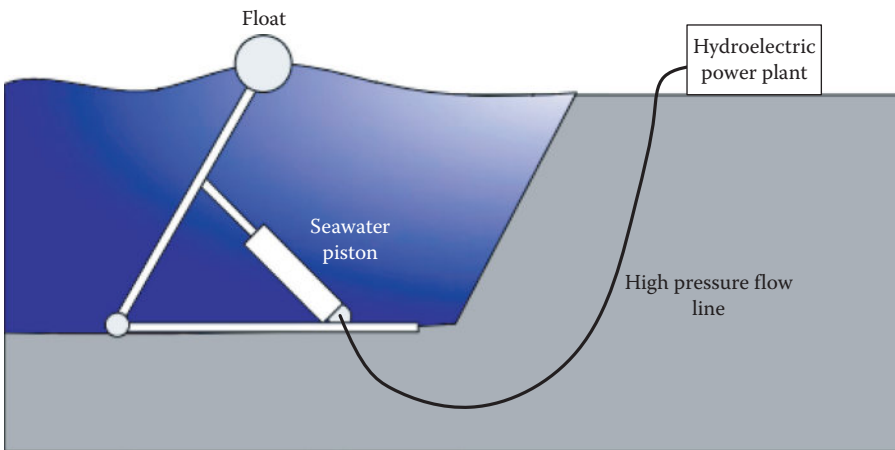


FIGURE 6.79 Oyster system.

linear motion of the pistons is translated into rotating motion through a hydraulic motor. The motor drives a generator and electricity is generated. The photos in Figures 6.81 and 6.82 show the system in operation.

6.3.3.3 Oscillating Water Column System

The OWC system is shown in Figure 6.83. It consists of a linear generator and a chamber. The chamber is anchored to the ocean floor, but allows water to enter and exit from one side at the

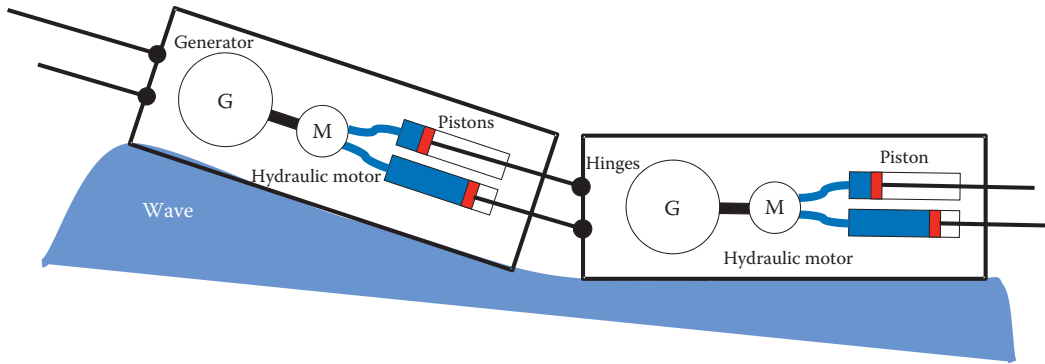


FIGURE 6.80 Main components of hinged contour system.



FIGURE 6.81 HC system. (Courtesy of Pelamis Wave Energy through Wikipedia.)



FIGURE 6.82 The front pontoon. (Courtesy of Pelamis Wave Energy through Wikipedia.)

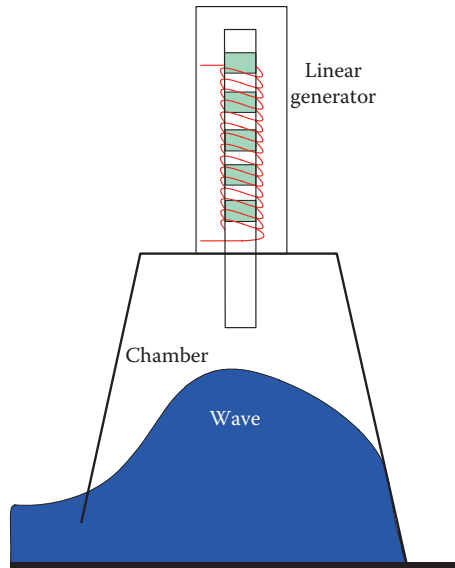


FIGURE 6.83 Oscillating column system.

bottom of the chamber. When waves enter or leave the chamber, they change the air pressure inside the chamber. The air pressure pushes the magnet when the wave is moving toward the crest and pulling it when it moves toward the trough. The system, in essence, is using a column of water as a piston to pump air. The push and pull of the magnet of the linear generator produces electricity.

6.3.3.4 Evaluation of Wave Energy

Wave characteristics are often predictable a few days in advance. This is important to the utilities and the developers. The utility needs a highly accurate forecast of power production to minimize the cost of their operation and to enhance the reliability of the grid. The developers need accurate forecast as well to sell the produced energy at favorable price instead of the spot price that is often low.

The wave energy technology is still in its infancy and more developments are needed. Among the challenges facing engineers are the high cost of the systems, their high maintenance, and their low yields. The efficiency of the current systems is still low (10%–15%). Because there are a few installations worldwide, we do not know exactly how the systems affect the environment. Nevertheless, engineers and scientists have predicated some environmental impacts such as the following:

- Noise pollution from the motion of pontoons and their hinges.
- Large wave energy farms can change the pattern of beach waves.
- Large wave energy farms can hinder commercial and recreational fishing in the areas.
- Wave farms can represent hazards to marine traffic.
- Accidental spills of hydraulic fluids and other material into water can affect the aquatic life.

6.4 GEOTHERMAL ENERGY

The cross section of the earth consists of several layers as depicted in Figure 6.84. Each one of them has its own characteristics and temperatures. The crust layer, which represents the surface of earth, is relatively shallow with thickness of about 600km. Under the crust is the mantel. It is

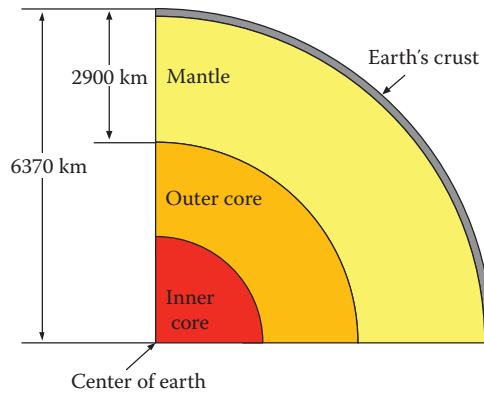


FIGURE 6.84 Cross section of Earth.

predominantly rocky shell that extends to about 2900km deep. The mantle layer is about 85% of earth's volume. This thick layer is actually moves very slowly and the crust is essentially floating on the mantle. The slow motion of the mantle is responsible for the formation of mountain ranges as well as their slow movements over very long periods. In addition, the movement of the mantle causes volcanoes and Earthquakes. Below the mantle is the outer core which is a molten rock of about 2266km thick. It is composed of iron and nickel and small amounts of sulfur and oxygen. The inner core of Earth is the hottest part and is a ball of about 1220km in radius. It is believed to consist of iron–nickel alloys.

The temperature of the outer core ranges from 4400°C to 6100°C depending on the depth. The temperature of the inner core is approximately 5500°C, which is almost the same as the temperatures on the surface of the sun. In fact, about 99% of the Earth's volume has temperatures greater than 1000°C.

Figure 6.85 shows the Earth's temperature gradient (geothermal gradient) with respect to depth. The geothermal gradient varies widely from place to place, and it is high in tectonically active regions. For most of the areas in the world, the geothermal gradient in the crust layer is between 20°C/km–30°C/km of depth.

The map in Figure 6.86 shows areas in the United States with geothermal resource potentials. It shows potential areas and sites with geothermal temperatures greater than 150°C. Note that most of the sites are located in western United States as well as Alaska.

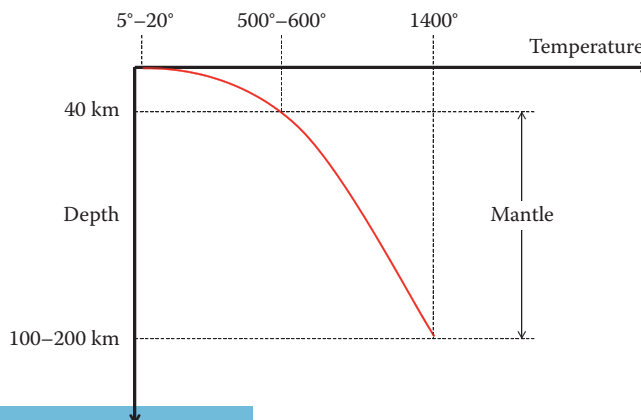


FIGURE 6.85 Geothermal gradient of Earth.

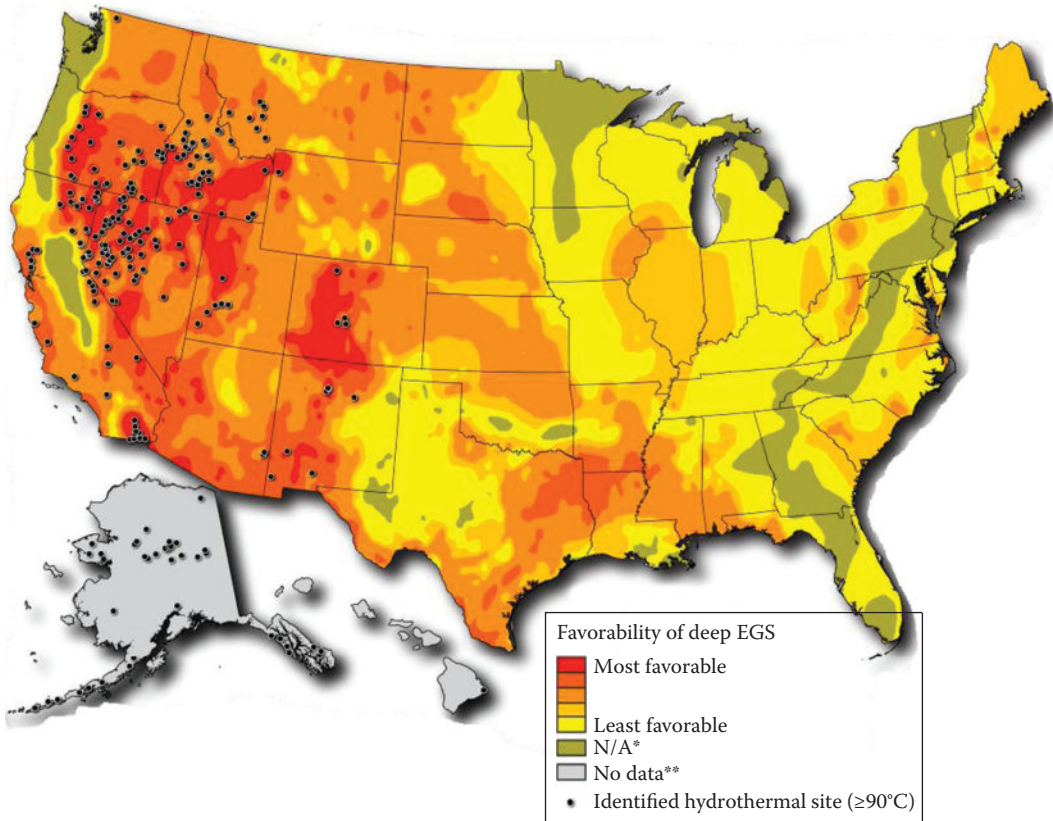


FIGURE 6.86 Geothermal map of the United States. (Courtesy of the United States National Renewable Energy Laboratory.) EGS stands for enhanced geothermal system.

Scientists have estimated that the heat energy of the core is about 10^{31} J. But, is this heat energy renewable? To answer this question, we need to know the causes of this geothermal heat. There are two main phenomena affecting the temperature of Earth: heat generating and heat dissipating phenomena.

Heat generating phenomenon: Heat is generated due to the decay of long-lived radioactive isotopes inside Earth. It is estimated to have a rate of 30 TJ/s.

Heat dissipating phenomenon: The trickling heat from the core to the crust layer. This heat naturally flows to the surface by conduction at a rate of 44.2 TJ/s. So how long would it take to deplete the heat of Earth? The answer is in the next example.

Example 6.32

How long would it take to deplete the Earth's geothermal energy?

Solution

The core loses 44.2 TJ/s and the natural decay of radioactive isotope adds 30 TJ/s
 Net geothermal losses

$$\text{Geothermal losses} = 44.2 - 30 = 14.2 \text{ TJ/s}$$

Since the heat energy of the core is about 10^{31} J, the depletion period can be approximated by

$$\text{Depletion period} = \frac{10^{31}}{14.2 \times 10^{12}} = 7.042 \times 10^{17} \text{ s} = \frac{7.042 \times 10^{17}}{3.16 \times 10^7} = 2.228 \times 10^{10} \text{ year}$$

This is 22,280 million years. Although this geothermal energy is not fully renewable, it takes an extremely long time to be depleted.

6.4.1 HEAT PUMP

At just a few meters under the Earth's surface, the soil temperature in winter is about 10°C – 20°C higher than the ambient temperature, and about 10°C – 20°C lower in the summer. At this shallow depth, heat pumps can be used to warm houses in winters and cool them down in the summers.

A typical heat pump system is shown in Figure 6.87. It consists of geo-exchanger, pump and heat distribution system. The geo-exchanger is a series of pipes buried in the ground near the building to be conditioned. The pipes are filled with water, or a mixture of water and antifreeze, to absorb the Earth's heat in the winter, or dissipate heat to the Earth in the summer. Pumps are used to circulate the water mix between the geo-exchanger and the rest of the system. In winter, the building temperature is lower than the geothermal temperature, so the geo-exchanger increases the temperature of the mixture. The pump moves the heated mixture to warm the air and water of the building. In summer, when the Earth temperature is lower than the air temperature, the process is reversed.

6.4.2 GEOTHERMAL ELECTRICITY

Enough heat can be obtained from the shallow part of the Earth crust (10–20 km depth) to generate electricity. Today's technology gives us two main systems: Geothermal reservoir and hot dry rock.

Geothermal reservoir: The system utilizes trapped hot water under pressure that would otherwise be vented through geysers or hot springs, to generate electricity by thermal turbines.

Hot dry rock: The system extracts the heat trapped in hot dry rocks.

In either system, the geothermal power plants are similar to the conventional thermal power plants in many ways, and they are operating in a similar manner.

6.4.2.1 Geothermal Reservoir

In nature, steam can be formed in various remarkable ways such as the geyser in Figure 6.88. The geyser shoots intermittent jets of heated water and steam. Steam is formed when water from rain

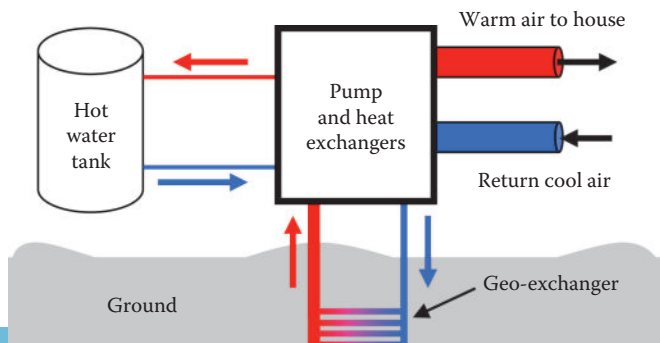


FIGURE 6.87 Heat pump system.



FIGURE 6.88 Steam generated from rain even in cold environment.

seeps into the fractured Earth's rocks for miles until it gets near the molten rocks where the water is turned into steam and pushes its way upward toward any crack on the surface of Earth.

The steam could also be trapped in geothermal reservoirs of porous rock above the magma surrounded by solid rocks. When rain or ground water comes near the molten rocks, the water absorbs the thermal energy and ascends toward a reservoir as shown in Figure 6.89. The steam in some reservoirs is at very high temperatures and can be used directly to generate electricity.

6.4.2.2 Hot Dry Rock

The vast majority of the accessible geothermal energy worldwide is stored in hot and dry rocks. Crystalline rocks, such as granite, retain a great amount of thermal energy and can be found at relatively shallow depths. So it would make engineering sense to tap this energy by injecting water into the hot rock then retrieving the steam to generate electricity. The problem, however, is that the rock is mostly solid and may not allow enough flow of water through its natural cracks and pores. The solution is shown in Figure 6.90. High-pressure cold water is pumped into the rock to fracture it. The cracks allow water to flow through the rock more efficiently. Water is then pumped into the rock and flows more freely through the cracks and open joints of the hot rock and becomes superheated. The water returns back to the surface in the form of steam.

6.4.3 GEOTHERMAL POWER PLANTS

Two geothermal power plants are shown in Figures 6.91 and 6.92. The extracted steam, which may include hot mist, is drawn from the geothermal reservoir and passes through a mist eliminator or heat exchanger. The steam going to the turbines must be free from mist as it would be very damaging to the turbine blades (runners). The dry steam enters a thermal turbine that converts the steam energy into mechanical energy much like the thermal power plant discussed in Chapter 4. This mechanical energy is converted by the generator G into electrical energy. The steam exiting the turbine is cooled down in a cooling tower where external cold water is poured in to create the heat sink needed to complete the thermal cycle. The water exiting the cooling tower is still hot and can be used to heat buildings, and then injected back into the geothermal reservoir.

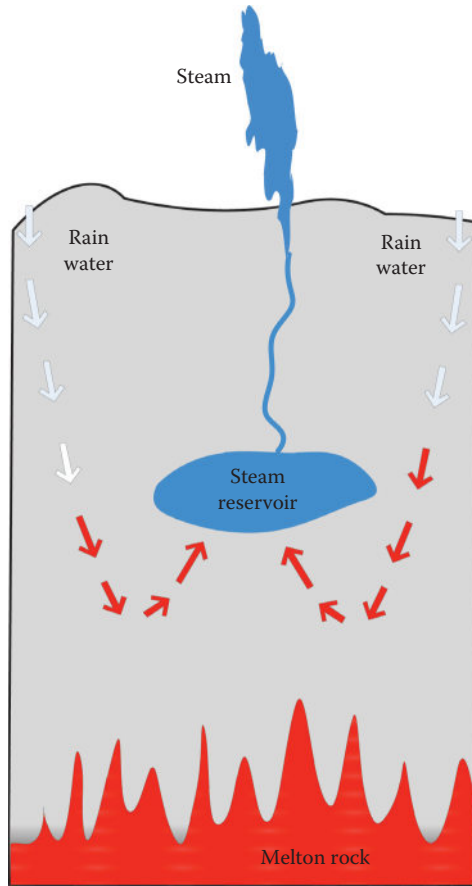


FIGURE 6.89 Geothermal reservoir.

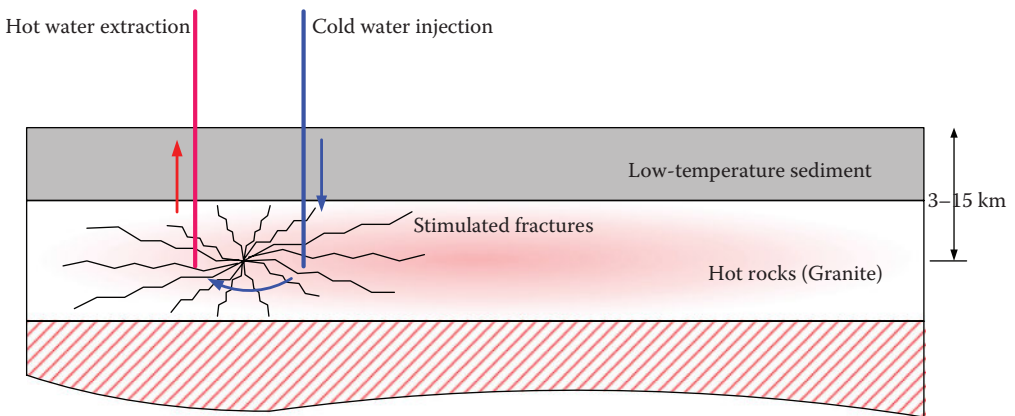


FIGURE 6.90 Hot dry rock site.

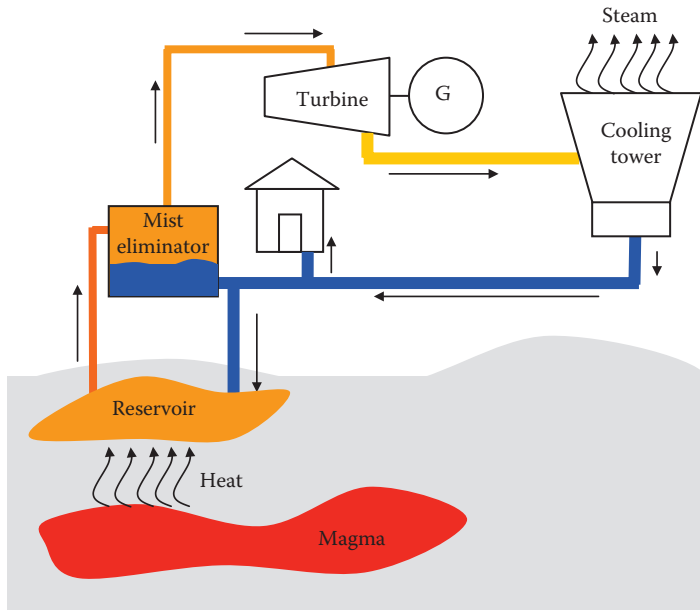


FIGURE 6.91 Reservoir type geothermal power plant.

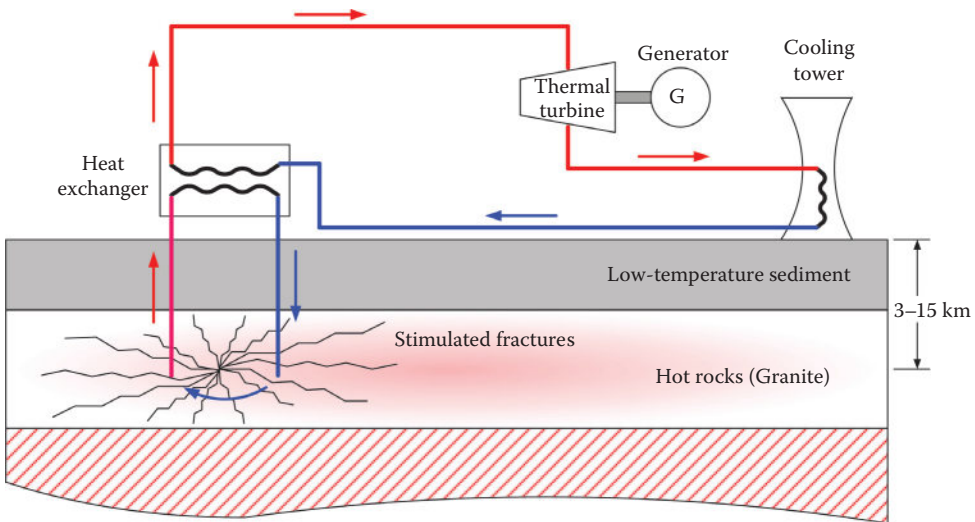


FIGURE 6.92 Hot dry rock geothermal power plant.

The steam from geothermal sites varies in temperatures and pressure which requires different power plant designs for different steam conditions. Today, we have three basic designs:

Dry steam power plants: This system is used when the steam temperature is very high (300°C) and the steam is readily available. This is the system explained in Figures 6.91 and 6.92.

Flash steam power plants: When the steam-hot water mix is above 200°C, it is drawn into an expansion tank that lowers the pressure of the mix. This causes the hot mist to rapidly vaporize (flash) into dry steam. The steam is then used to generate electricity.

Binary-cycle power plants: At moderate-temperature (below 200°C), the energy in the mix is extracted by exchanging its heat with another fluid (called binary) that has a much lower boiling point. The heat from the mix causes the secondary fluid to flash into steam, which is then used to drive the turbines.

6.4.3.1 Evaluation of Geothermal Energy

Geothermal energy in the uppermost 10 km of the Earth's crust is much more than the energy from all oil and gas resources known to us so far. The geothermal energy can be stored for thousands of years as the thermal isolation of the magma by the surrounding material cools down the magma at extremely slow rate. Hence, it is a predictable generation source.

The first experimental geothermal power plant was built in Lardarello, Italy, by Prince Gionori Conti around 1905. The first commercial power plant based on Conti's work was commissioned in 1913 at Larderello. In 1958, Wairakai's geothermal power plant was built in New Zealand, followed by Pathe's plant in Mexico in 1959, and the Geysers plant in California, in 1962. By the end of 2006, 21 countries have operational geothermal power plants with a total capacity of 8.2 GW. Iceland actually produces about 50% of its electrical energy from geothermal power plants. The geothermal power plants in the United States have a total generating capacity of 2.7 GW. The Geysers power plant in northern California, shown in Figure 6.93, is still the largest geothermal power plant with a total generation capacity of 1.7 GW. This is enough power for the San Francisco metropolitan area. Other geothermal power plants in the United States are in Nevada, Utah, and Hawaii.

Geothermal power plants can only be constructed in geothermal sites where geothermal reservoirs or hot rocks are accessible by current drilling technology. These sites are scarce worldwide. In the United States, most of the geothermal power plants are located in California and Nevada. It is expected that more installations will be added very soon. The map in Figure 6.94 shows the existing and planned installation in the United States.



FIGURE 6.93 The Geysers in northern California—the first geothermal power plant in the United States.

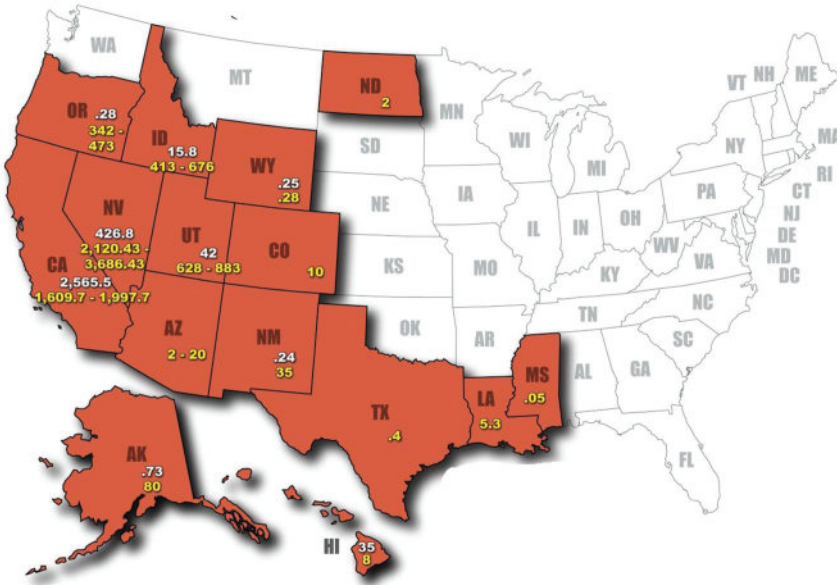


FIGURE 6.94 Geothermal power plants in the United States in 2010 (numbers in MW; white numbers for existing installations; yellow for planned installation). (Courtesy of the USA National Renewable Energy Laboratory.)

From the environmental impact point of view, geothermal power plants have several challenges, as discussed in the following:

- The geothermal fluid of the reservoir or hot rock may include other minerals and gases besides water that can be pollutant. Geothermal fields could also produce small amount of carbon dioxide.
- The geothermal fluid can produce objectionable odors due to the presence of compounds such as hydrogen sulfide.
- Fracturing rocks may cause polluted water to reach clean water resources.
- Fracturing solid rocks may cause Earth tremors.

6.5 BIOMASS ENERGY

Biomass consists of garbage, agriculture waste, or tree products. Garbage, in particular, is one of the major concerns for modern societies. In the United States, each household produces about 800 kg of garbage every year, followed by Norway (520 kg) and the Netherlands (490 kg). On the low end of the garbage production in the western world are Austria (180 kg) and Portugal (180 kg). The biomass is often collected and dumped in landfills, which are considered by many as health hazards. They produce unpleasant odors, contaminate underground water with the leachate generated when water is mixed with biomass, and they produce ethanol and methanol that increase fire hazards. In addition, housing developments are often expanded to areas closer to landfills where trucks are considered sight pollution and safety hazards.

For these reasons, it is becoming harder to build new landfills, and cities all over the United States are limiting the capacities of their landfills or eliminating them altogether. Hence, the burning of biomass to produce electricity sounds like a reasonable idea.

When biomass is burned in incinerators, the biomass volume is reduced by as much as 90%, and in the process, steam can be produced to generate electricity. One of these systems is shown

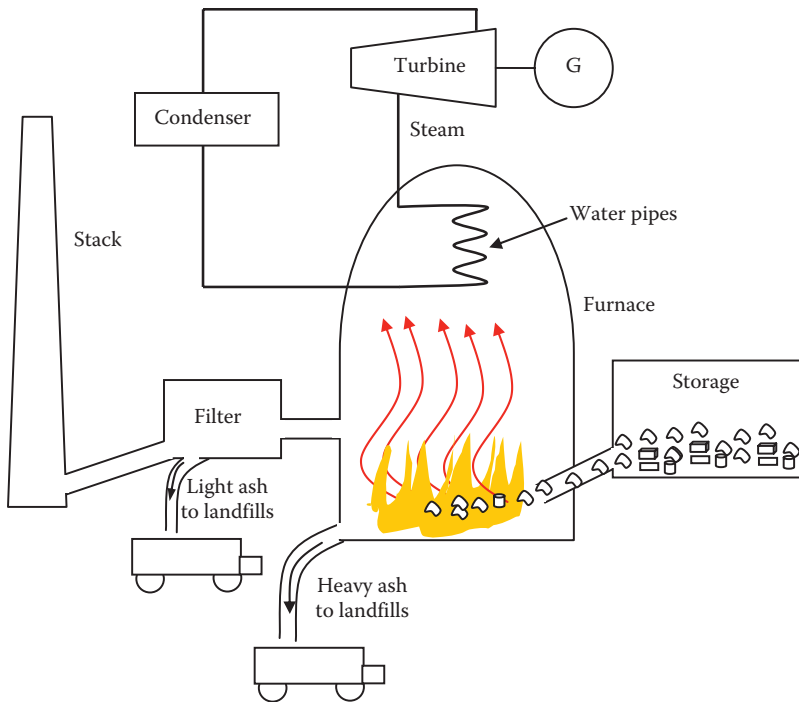


FIGURE 6.95 Biomass incineration power plant.

in Figure 6.95. The biomass material is fed to a furnace where it is burned and the heat produced is used to generate steam by heating water pipes. The steam is used to generate electricity by a turbine-generator system much like the regular thermal power plant. The steam exiting the turbine is cooled to complete the thermal cycle. The ash produced in the furnace is collected and sent to landfills. The volume of the ash is about 10% of the original volume of the biomass material. The ash generated by the combustion enters the filtering stage where more ash is extracted, collected by trucks, and sent to landfills. The process produces gases that are also filtered before they are vented through the stack.

Biomass power plants generate electricity and at the same time reduce the amount of material sent to landfills. However, biomass incineration is not free from pollution. Heavy metal and dioxins are formed during the various stages of the incinerations. Dioxin is highly carcinogenic and can cause cancer and genetic defects.

6.6 FUEL CELL

A fuel cell (FC) is an electrochemical device that uses chemical reactions to produce electricity. The FC technology was invented over a century ago, but received little attention until 1950s when NASA used it in its space programs. Sir William Grove in 1839 was the first to develop a FC device. Grove, who was an attorney by education, conducted an experiment in which he immersed parts of two platinum electrodes in sulfuric acid and sealed the remaining part of one electrode in a container of oxygen, and the other in a container of hydrogen. He noticed that a constant current flow between the electrodes and the sealed containers eventually included water and gases. This was the first known FC. In 1939, Francis Bacon built a pressurized FC from nickel electrodes, which was reliable enough to attract the attention of NASA who used his FC in its Apollo spacecraft. Since then NASA has used various designs of the FCs in several of its space vehicles including the Gemini and the space shuttles.

During the last 30 years, research and development in FC technology has exploded. New materials and technologies made FCs safer, more reliable, lighter, and more efficient than the earlier models. Today FCs are used in ground transportation, marine applications, distributed power, cogeneration, and even consumer products.

6.6.1 HYDROGEN FUEL

Most FCs utilize hydrogen and oxygen to produce electricity. Hydrogen is found in many compounds such as water and fossil fuels. Although it is the most abundant element in the universe, hydrogen is not found alone, but always combined with other elements. To separate the hydrogen from its compounds, a reformer process, such as the one shown in Figure 6.96, is often used. Inside the reformer, a fuel such as hydrocarbon (CH_2) is chemically treated to produce hydrogen. The hydrocarbon compound, which contains hydrogen and carbon atoms, can be found in fossil fuels such as natural gas and oil. The by-products of the reformer process, however, are carbon dioxide (CO_2) and carbon monoxide (CO). These undesired gases are responsible for the global warming and increased hazards to human health as discussed in Chapter 5. Since CO is more hazardous than CO_2 , the CO is further oxidized by the CO -converter. In this chemical process, water is added to the output of the reformer to convert the CO into CO_2 . Carbon dioxide is vented in air, and the hydrogen is used in the FC.

A new generation of FCs use fuels such as methane directly without the need for reformers, which are called *direct* FCs. In these systems, hydrogen is extracted directly from methane inside the FC.

In its stable gas form, hydrogen is covalent bonded, which means their electrons are shared between two hydrogen atoms as shown in Figure 6.97. The symbol of this hydrogen gas is H_2 .

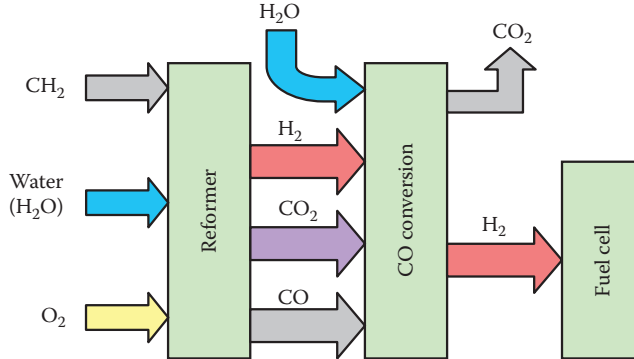


FIGURE 6.96 Generation of hydrogen.

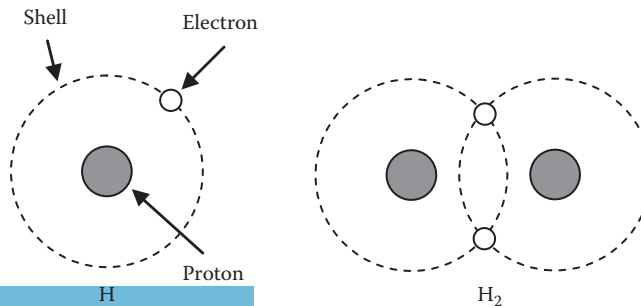


FIGURE 6.97 Hydrogen atom and hydrogen gas.

TABLE 6.2
Main Types of FCs and Their Operating Characteristics

Fuel Cell	Electrolyte	Anode Gas	Cathode Gas	Approximate Temperature (°C)	Typical Efficiency (%)
Proton exchange membrane (PEM)	Solid polymer membrane	Hydrogen	Pure or atmospheric oxygen	80	35–60
Alkaline (AFC)	Potassium hydroxide	Hydrogen	Pure oxygen	65–220	50–70
Phosphoric acid (PAFC)	Phosphorous	Hydrogen	Atmospheric oxygen	150–210	35–50
Solid oxide (SOFC)	Ceramic oxide	Hydrogen, methane	Atmospheric oxygen	600–1000	45–60
Molten carbonate (MCFC)	Alkali-carbonates	Hydrogen, methane	Atmospheric oxygen	600–650	40–55
Direct methanol (DMFC)	Solid polymer membrane	Methanol solution in water	Atmospheric oxygen	50–120	35–40

6.6.2 TYPES OF FUEL CELLS

FCs come in various configurations based on the gas used and their electrolyte. Although FCs have various designs and operating characteristics, they all work on a similar principle. Different FCs operate at diverse temperature ranges and have different start-up times. These differences make FCs useful in a wide range of applications from consumer electronics to power plants. Table 6.2 shows the main types of FCs and their electrolytes as well as their gases. The table also shows their typical efficiencies and operating temperatures. These FCs are covered in more details in the following sections.

6.6.2.1 Proton Exchange Membrane Fuel Cell

The basic components of the proton exchange membrane (PEM) FC shown in Figure 6.98 are the anode, the cathode, and the electrolyte, which is a membrane of solid polymer coated with a metal catalyst such as platinum. Figure 6.99 depicts a system consisting of several FCs in series.

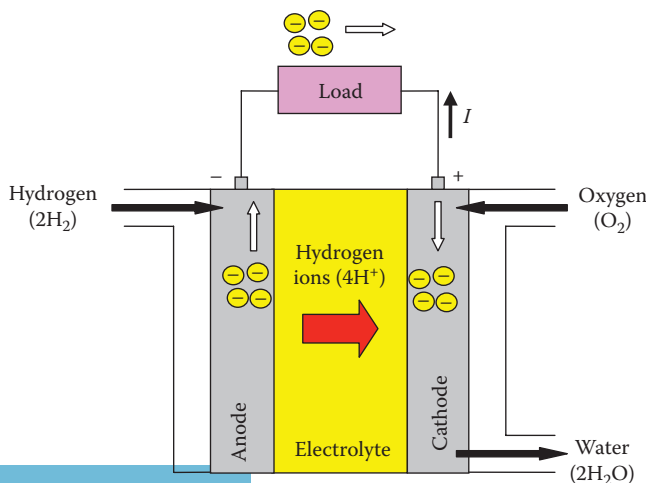


FIGURE 6.98 PEM FC.



FIGURE 6.99 PEM fuel cell.

Pressurized hydrogen enters the anode, which is a flat plate with channels built into it to disperse hydrogen gas over the surface of the catalyst. A catalyst (such as platinum) causes two hydrogen gas atoms (2H_2) to oxidize into four hydrogen ions (4H^+) and give up four electrons (4e^-). An ion is an atom or a group of atoms that lost or gained one or more electrons. The hydrogen ion is just the proton of the atom. This process is known as the *anode reaction* and can be represented by the chemical equation



The free electrons take the path of least resistance through the external load to the other electrode (cathode). Since the electric current is the flow of electrons, the load is then energized.

The hydrogen ions pass through the membrane from the anode to the cathode. When the electrons enter the cathode, they react with the oxygen from outside air plus the hydrogen ions at the cathode to form water. This is known as the *cathode reaction*:



The overall chemical reaction of the anode and cathode can be represented by Equation 6.80. The equation shows that the FC combines hydrogen and oxygen to produce water and in the process energy is released:



Keep in mind that the reformer and the CO-converter require water. Therefore, it is convenient that the FC produces water, which can be fed back to the reformer and CO-converter. Also the cathode reaction produces heat that can be used in various applications.

The PEM FC operates at relatively low temperatures, about 80°C, and its output power can be regulated fairly easy. It is relatively lightweight, has high energy density, and can start very quickly (within a few milliseconds). For these reasons, the PEM FC system, such as the one shown in Figure 6.99, is suitable for a large number of applications including transportations and distributed generation for residential loads.

The PEM FC uses platinum as a catalyst; this costly metal makes the PEM FC expensive. Furthermore, the platinum is extremely sensitive to CO and the elimination of the CO is crucial for the longevity of the FC. This adds another expense to the overall cost of the system.

6.6.2.2 Alkaline Fuel Cell

The alkaline fuel cell (AFC) is the oldest type of FCs that was developed by Francis Bacon in the last part of 1930s. Its electrolyte is liquid alkaline solution of potassium hydroxide (KOH). The AFC operates at elevated temperatures; 65°C–220°C; therefore, it is slower at starting relative to the PEM cell.

The main components of the AFC are shown in Figure 6.100. At the anode, hydrogen reacts with the hydroxyl ions OH⁻ to produce water and free electrons. The hydroxyl ions are generated at the cathode by combining oxygen, water and free electrons. Notice that part of the water produced at the anode is migrated back to the cathode.

The anode reaction of the AFC is expressed by



And the cathode reaction is



The overall cell reaction is

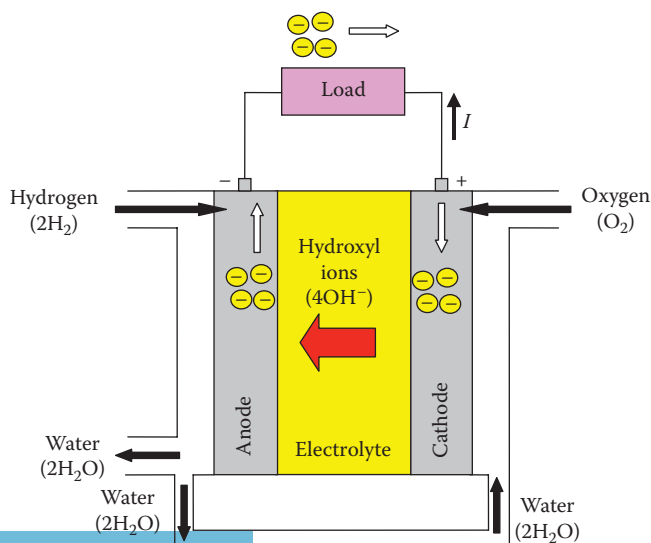


FIGURE 6.100 Alkaline FC.

The AFC is very susceptible to contamination, particularly carbon dioxide (CO_2), which reacts with the electrolyte and quickly degrades the FC performance. In addition, water and methane can also contaminate the FC. Because of its susceptibility to contaminations, the AFC must run on pure hydrogen and oxygen, which increase the cost of its operation. Therefore, the application of AFC is limited to controlled environments such as spacecrafts.

6.6.2.3 Phosphoric Acid Fuel Cell

Phosphoric acid (H_3PO_4) is the electrolyte medium for the phosphoric acid fuel cell (PAFC) shown in Figure 6.101. Its operating temperature is high, 150°C – 210°C , but is considered suitable for small and midsize generation. The PAFC is among the first generation of modern FCs, and is typically used for stationary power generation, but some are used to power large buses.

The anode reaction here is similar to that for the PEM FC. The hydrogen introduced at the anode is stripped of its electrons. The hydrogen protons (ions) migrate through the electrolyte to the cathode:



The electrons released at the anode travel through an external circuit where they give their energy to the electric load and return to the cathode. At the cathode, the hydrogen ions are combined with the four electrons and oxygen, usually from air, to produce water.



The overall cell reaction of the PAFC is



The efficiency of the PAFC is typically higher than 40%. If the steam generated by the FC heat is used in other applications such as cogeneration and air-conditioning, the efficiency of the cell can reach 80%. The electrolyte of the PAFC is not sensitive to CO_2 contamination, so it can use reformed fossil fuel. The relative simple structure, its less expensive material, and its stable electrolyte make the PAFC more popular than PEM in some applications such as in buildings, hotels, hospitals, and electric utility systems.

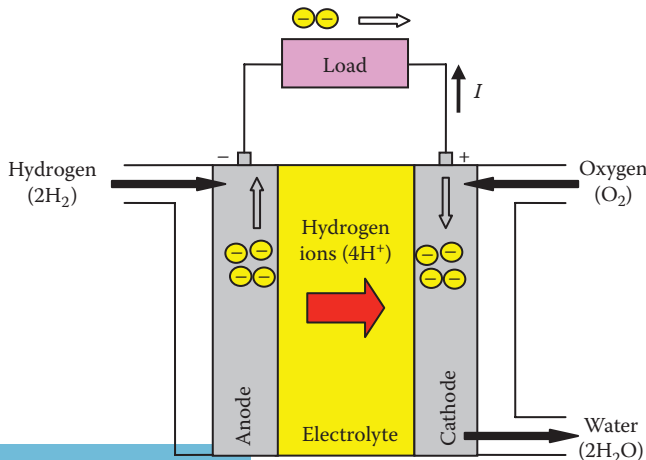


FIGURE 6.101 Phosphoric acid FC.

6.6.2.4 Solid Oxide Fuel Cell

The electrolyte of the solid oxide fuel cell (SOFC) is a hard ceramic material such as zirconium oxide. The cell shown in Figure 6.102 operates at very high temperatures (600°C–1000°C), which requires a significant time to reach its steady state. Therefore, it is slow at starting and slow at responding to changes in electricity demand. However, the high temperature makes the SOFC less sensitive to impurities in fuels such as sulfur and CO₂. For these reasons, SOFC can use fuels such as natural gas where the high temperature reforms the fuel without the need for external reformers such as the one shown in Figure 6.96. Therefore, the SOFC is suitable for large-scale stationary power generation in the MW range.

At the cathode, the oxygen molecules from air are combined with four electrons to produce the negatively charged oxygen ions O²⁻. The solid ceramic material used in the FC is conductive to these oxygen ions which migrates to the anode and combined with hydrogen to produce water. In the process, the extra four free electrons in the oxygen ions are released and passed through the electric load and then to the cathode. The anode reaction is then



And the cathode reaction is



Then, the overall cell reaction of the SOFC is



The operating efficiency of the SOFC is among the highest of the FCs, about 60%. If the steam generated by the FC is used in cogeneration or air-conditioning, the overall efficient can reach 80%.

6.6.2.5 Molten Carbonate Fuel Cell

The electrolyte for the molten carbonate fuel cell (MCFC) is a mixture of lithium carbonate and potassium carbonate, or lithium carbonate and sodium carbonate. This FC is also a high-temperature type, operating at 600°C–650°C, and is suitable for large systems in the megawatt range.

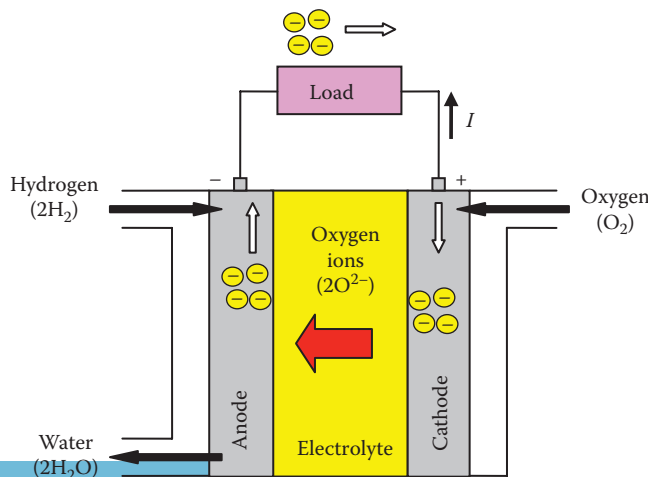


FIGURE 6.102 Solid oxide FC.

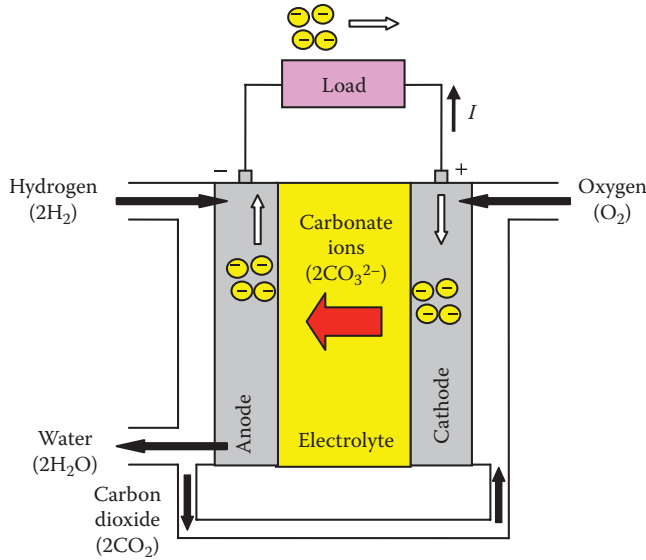
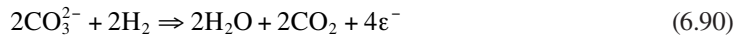


FIGURE 6.103 MCFC.

When the electrolyte of the MCFC (Figure 6.103) is heated to a temperature of around 600°C , the salt mixture melt and become conductive to carbonate ions CO_3^{2-} . These negatively charged ions flow from the cathode to the anode where they combine with hydrogen to produce water, carbon dioxide and free electrons. The anode reaction is



The carbon dioxide is routed to the cathode where the chemical reaction is



The overall cell reaction of the MCFC is



Notice that the CO_2 produced at the anode is also consumed at the cathode under ideal conditions. If the FC design can fully manage the carbon dioxide, the cell would emit no CO_2 .

The high operating temperature of the MCFC has the same advantages and disadvantages mentioned for the SOFC. One of the distinctive disadvantages of this FC is the internal corrosion that is caused by the carbonate electrolyte.

6.6.2.6 Direct Methanol Fuel Cell

The direct methanol fuel cell (DMFC) is a low temperature cell (50°C – 120°C) that can use methanol directly without the need for a reformer (Figure 6.104). For these two reasons, it is suitable for consumer electronics applications such as mobile phones, entertainment devices and portable computers as well as electric vehicles.

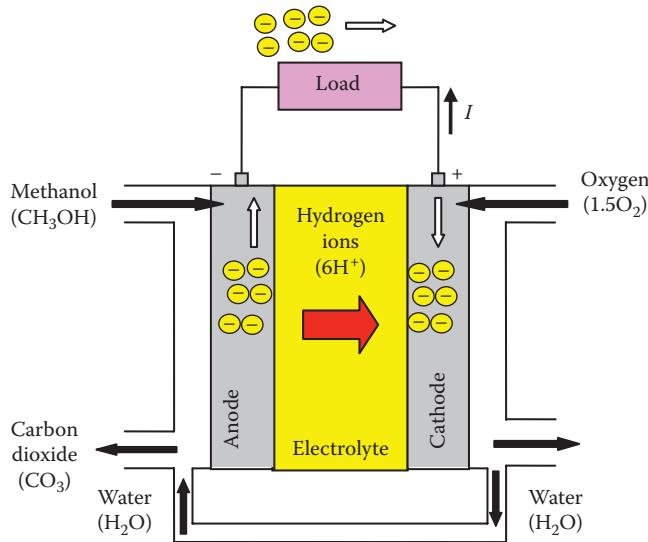
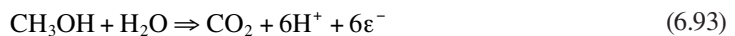


FIGURE 6.104 DMFC.

The DMFC electrolyte is a polymer, which is similar to that used in PEM FCs. At the anode, liquid methanol CH_3OH is oxidized by water producing carbon dioxide CO_2 , six hydrogen ions H^+ and six free electrons.

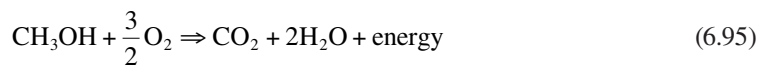
The anode reaction of the DMFC is



The free electrons travel to the external electric load where they unload their energy. The hydrogen ions pass through the electrolyte to the cathode and react with oxygen from air and the free electrons from the external circuit to form water:



The overall cell reaction of the DMFC is



Because methanol is toxic alcohol, researchers are developing FCs that use different alcohol such as ethanol $\text{C}_2\text{H}_6\text{O}$. The progress is expected to produce safer FCs with similar performance.

6.6.3 HYDROGEN ECONOMY

Hydrogen economy is a term often used to describe a complete closed-loop system that is based on extracting hydrogen and using it to produce electricity and in the process utilizing the heat of the cell in other applications. Such a system is shown in Figure 6.105. Renewable energy (wind, solar, etc.) is used to generate the electricity needed to reform fuel and produce hydrogen. It could

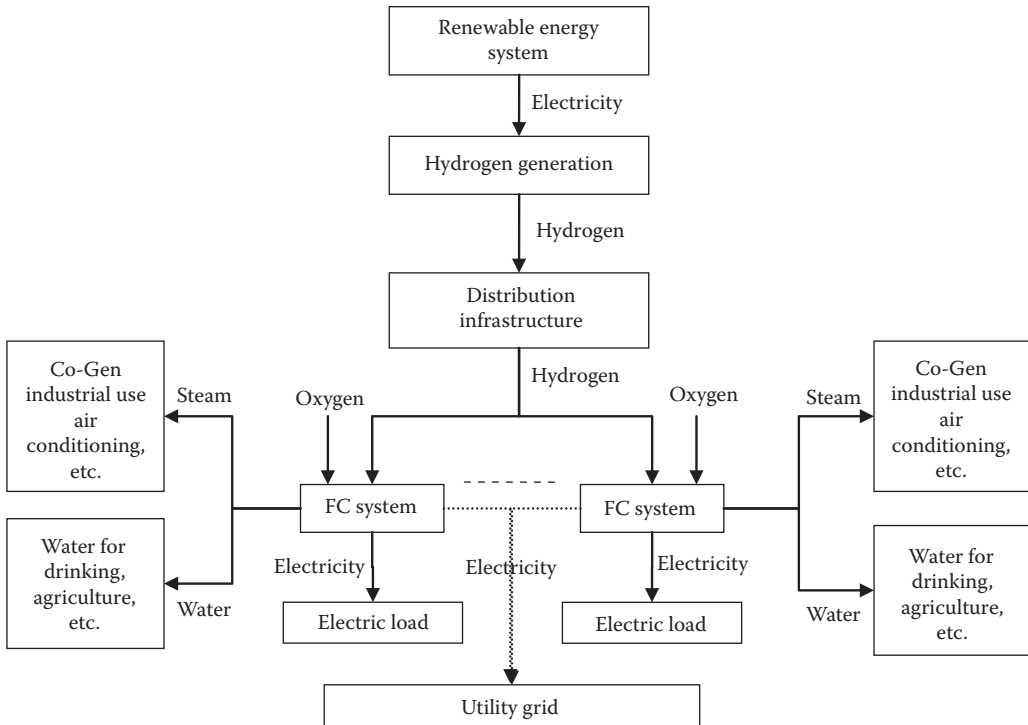


FIGURE 6.105 Hydrogen-based energy system.

also be used to extract hydrogen from water by electrolysis process. Once hydrogen is generated, it is distributed to fueling stations much like the gasoline system for automobiles. The FCs use the hydrogen to produce electricity that can be used locally, exported to utility grids, or both. If the FC is used to power automobiles, all the electrical energy is consumed by the load. If the FC is used in stationary sites with access to utility grid, then part or all of the energy can be exported to the utility.

The by-products of the FC operation are heat and water. The water can be used for drinking, agriculture, or industrial processes. The heat, in form of steam, can be used to generate electricity, air-condition buildings, and in industrial processes.

One obvious question is why we do not use the electricity generated by the renewable system directly instead of this rather elaborate process? Among the reasons are the following:

- Energy generated by renewable system depends on favorable weather conditions. During these conditions, the energy produced may not be needed by the local loads or utilities. Instead of shutting down the renewable systems, we can store the energy by the system described in Figure 6.105.
- Renewable energy systems could be located in remote areas (small islands, deserts, etc.) without access to power grid. In this case, it is better to store the electric energy in the form discussed earlier.

For stand-alone systems such as spacecraft and electric ships, PV and FCs can be incorporated into an integrated system. The solar cells power the craft during the day and at the same time generate a supply of hydrogen that is stored and used at night by the FC.

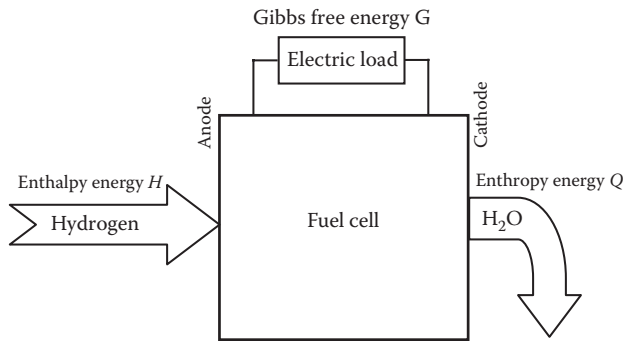


FIGURE 6.106 Gibbs free energy.

6.6.4 MODELING OF IDEAL FUEL CELLS

To understand the energy conversion of the FC, we need to analyze its thermal and electrical processes. The thermal process gives us an idea on how much energy can be produced by the FC, and the electrical process gives us the value of the produced voltage and current. The following analyses are for most types of FCs.

6.6.4.1 Thermal Process of Fuel Cells

To understand the thermal process, we need to review some key thermodynamic equations pertaining to FCs. In thermodynamics, energy is computed for a unit of substance known as *mole*. One mole of a substance contains 6.002214×10^{23} entities (molecules, ions, electrons, or particles). This constant is also known as the *Avogadro's number* $N_A = 6.002214 \times 10^{23}/\text{mol}$.

During that last part of the eighteenth century, the American physicist and chemist Josiah Willard Gibbs developed a method by which the useful energy produced by a chemical reaction can be computed. It is known as *Gibbs free energy* G , where

$$G = H - Q \quad (6.96)$$

where

H is the enthalpy of the process

Q is the entropy of the process

For the FC shown in Figure 6.106, we can view the enthalpy as the energy in the fuel (hydrogen) at the anode and the entropy as the wasted heat during the process of making water from hydrogen and oxygen at the cathode.

At 1 atmospheric pressure and 298 K, hydrogen has $H=285.83 \text{ kJ/mol}$ and $Q=48.7 \text{ kJ/mol}$. Hence, the chemical energy that is converted into electrical energy (Gibbs free energy constant) is

$$G = H - Q = 285.83 - 48.7 = 237.13 \text{ kJ/mol} \quad (6.97)$$

Example 6.33

Assume ideal conditions and compute the thermal efficiency of the FC.

Solution

The input Energy H is

$$H = 285.83 \text{ kJ/mol}$$

The energy that is converted into electricity is

$$G = H - Q = 285.83 - 48.7 = 237.13 \text{ kJ/mol}$$

The thermal efficiency η_t

$$\eta_t = \frac{\text{output energy}}{\text{input energy}} = \frac{G}{H} = \frac{237.13}{285.83} = 83\%$$

Notice that the thermal efficiency of the FC is very high relative to the thermal efficiency of power plants that cannot exceed 50%.

6.6.4.2 Electrical Process of Fuel Cells

Faraday has developed a key equation that computes the amount of electric charge q_e in a mole of electrons

$$q_e = N_A \times q \quad (6.98)$$

where

q is the charge of a single electron ($1.602 \times 10^{-19} \text{ C}$)

N_A is the Avogadro number

In FCs, two electrons are released per molecule of hydrogen gas (H_2). Thus, the number of electrons N_e released by 1 mol of H_2 is

$$N_e = 2N_A \quad (6.99)$$

The total charge of the electrons q_m released by 1 mol of hydrogen is

$$q_m = N_e \times q \quad (6.100)$$

In an electric circuit, the charge of an object is defined as the current I passing through the object during a period of time t :

$$q_m = It \quad (6.101)$$

Since the electric energy E is the power multiplied by time, we can compute the energy as follows:

$$E = VIt = Vq_m \quad (6.102)$$

where the electric energy of the FC is equal to the Gibbs free energy G given in Equation 6.96. Then, the voltage of a single FC under ideal conditions is

$$V = \frac{E}{q_m} = \frac{G}{q_m} \quad (6.103)$$

Example 6.34

Assume ideal conditions and compute the output voltage of a PEM FC.

Solution

Use Equation 6.99, we can compute the number of electrons N_e released in 1 mol of H_2 :

$$N_e = 2N_A = 1.2044 \times 10^{24}$$

The total charge released by 1 mol of hydrogen can be computed using Equation 6.100:

$$q_m = N_e \times q = 1.2044 \times 10^{24} \times 1.602 \times 10^{-19} = 1.9294 \times 10^5 \text{ C}$$

Finally, the voltage of the ideal FC can be computed using Equation 6.103:

$$V = \frac{E}{q_m} = \frac{G}{q_m} = \frac{237.13 \times 10^3}{1.9294 \times 10^5} = 1.23 \text{ V}$$

6.6.5 MODELING OF ACTUAL FUEL CELLS

From Example 6.34, the voltage of the FC under ideal conditions is about 1.23 V. However, the actual voltage is lower due to the internal losses of the cell, the sluggish reactions at the anode and cathodes, and the degradation of the FC due to the corrosion of its electrodes or the contamination of the electrolyte.

The losses of the FC can generally be divided into three categories: *activation* loss, *ohmic* loss, and *mass transport* loss. Activation loss occurs because of the way the anode and cathode reactions are carried out, especially at low currents or when the cell is activated. This is known as *electrode kinetic*, which is the way fuel and oxygen are diffused at the electrodes. Because they are not fully diffused at starting, the performance of the FC is reduced during the activation period.

Ohmic loss occurs mainly because of the resistances of the electrolyte and electrodes. This loss is small at low currents.

Mass transport loss occurs when the input reaction is less than the output reaction. This situation arises when the output current is very high and the input reaction cannot match the needed demand.

6.6.5.1 Polarization Characteristics of Fuel Cells

The polarization curve is the steady-state voltage versus current. This curve is essential in determining the best operating conditions for an FC. A typical polarization curve is shown in Figure 6.107. The thick line represents the cell voltage and the thin line represents its output power. The figure is divided into three regions: activation, ohmic, and mass transport. At no load, the voltage of the cell is close to its ideal value. When the current is slightly increased, the voltage of the cell drops rapidly due to the activation loss. Since the current is small, the ohmic loss and the mass transport loss are insignificant. In the ohmic region, the current is high enough to cause internal losses in the electrolyte and electrodes. In this region, the ohmic loss is more dominant than the activation loss or mass transport loss. The voltage in the ohmic region is fairly stable. At high currents, the mass transport loss is very dominant and the FC cannot cope with the high current demand of the load. In this case, the anode reaction is not fast enough to provide the needed output current. As a result, the voltage of the cell collapses rather rapidly. This is the region we should avoid as it causes the collapse of the FC. Keep in mind that all three losses exist at all times, but the dominant ones

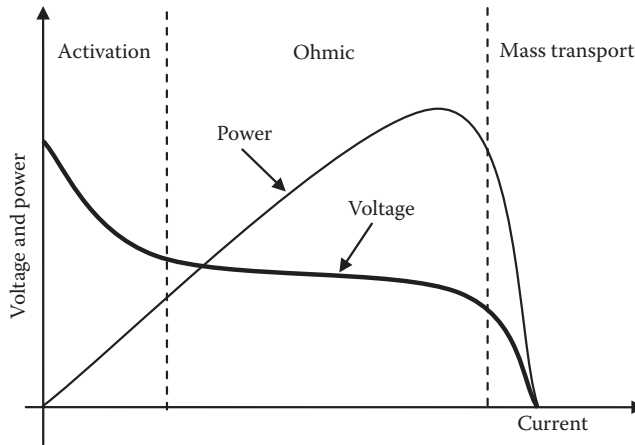


FIGURE 6.107 Polarization and power curves of FC.

depend on the operating region of the cell. The power curve in the figure shows the maximum power occurring in the ohmic region.

Example 6.35

A polarization curve of an FC can be represented by the empirical formula

$$V = 0.77 - 0.128 \times \tan(I - 1.3)$$

where

V is the voltage of the FC in volts

I is the current in amperes

Plot the polarization and power curves. Also compute the maximum power of the cell and the current at maximum power.

Solution

The plot of the polarization curve of this FC is given in Figure 6.108.

The power equation of the FC is the multiplication of voltage times current:

$$P = VI = 0.77 \times I - 0.128 \times I \times \tan(I - 1.3)$$

To compute the maximum power, we set the derivative of the power equation to zero and compute the current at maximum power:

$$\frac{\partial P}{\partial I} = 0.77 - 0.128 \times \tan(I - 1.3) - 0.128 \times I \times \sec^2(I - 1.3) = 0$$

The numerical solution of this equation yields a current of 2.145 A at which the power is maximum.

The maximum power of the cell is

$$P_{max} = 0.77 \times 2.145 - 0.128 \times 2.145 \times \tan(2.145 - 1.3) = 1.3422 \text{ W}$$

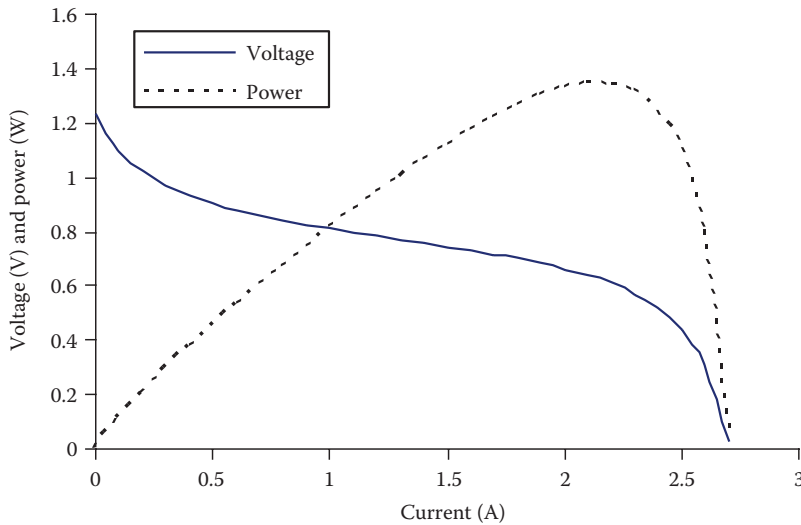


FIGURE 6.108 Polarization and power curves of FC in Example 6.35.

6.6.6 EVALUATION OF FUEL CELLS

Experts expect FCs to eventually dominate the power generation market, especially for transportation, household use and utility size generation. In automotive applications, using FCs to propel an electric motor is an ever-growing trend. The cars that are powered by FCs and use electric motors as the driving engine do not need the elaborate cooling and lubricating systems that are required by the internal combustion engines, making the car smaller, lighter, more efficient, quieter, and cheaper to maintain. Several generations of FC automobiles and buses are already roaming city streets. In addition to transportation, FCs are used as backup systems or independent source of energy. Several sensitive installations such as hospitals, satellites, and military installations are using FCs as backup systems. The efficiency of the FC alone is relatively high; the range is about 30%–80%. If the heat generated by the FC is wasted, the efficiency of the cell is at the low end of the range. When we add the efficiency of the reformer plus CO-converter, the efficiency range of the FC system drops to about 26%–40%. If the FC is used to drive an electric motor (electric car), the efficiency of the drive system is about 25%–40%. In contrast, modern internal combustion engines have efficiency around 15%–22%. High-temperature FCs produce enough heat, which can be used in industrial processes, heat buildings, and even cogeneration applications. These systems are suitable for high-power applications where portability is unnecessary. However, low temperature FCs are suitable for a wider range of applications that require small units with quick start-up time such as electric cars.

A single FC produces a dc at less than 1.5V. This is barely enough to power small consumer electronic devices. For higher voltage applications, FCs are stacked in series as shown in the photo in Figure 6.99. The dc produced by the FC system cannot be used directly to power ac devices; therefore, a converter is needed to convert the dc into ac.

One major concern about FCs is their relatively short lifetime. Their various components can suffer from pollution and corruptions. Some types of electrolyte can be contaminated by CO, CO₂ or sulfur. Carbonate electrolyte can cause internal corrosion that can rapidly degrade the cell's performance.

6.6.7 FUEL CELLS AND THE ENVIRONMENT

If we compare FCs with conventional thermal power generation, we can easily fall in love with FCs as they produce no pollution and most of them operate silently. The same assessment is true if we compare FC-powered automobiles with conventional internal combustion engine cars.

Some scientists, however, believe that the widespread use of FCs could have some negative environmental impacts due to unintended release of hydrogen in the atmosphere. This could increase the water vapor in the stratosphere zone, which could cool down the stratosphere causing more destruction to the ozone.

A more thorough analysis of the environmental impact of FCs must include the way we generate hydrogen. The processes by which hydrogen is harnessed and stored initiate most of the environmental concerns.

6.6.7.1 Generation of Hydrogen

Hydrogen is a clean gas that is completely non-toxic. Therefore, one valid question is why not just burn hydrogen in thermal power plants instead of using it in FCs? Burning hydrogen produces tremendous heat that cannot be efficiently harnessed by thermal turbines, thus reducing the system efficiency to less than 10%. But when hydrogen is used in a FC, the overall efficiency is much higher.

Because hydrogen cannot be found in nature as a free element, it must be extracted from hydrogen-rich compounds and safely stored. About 50% of world hydrogen is produced by reforming natural gas, 28% is produced by processing crude oil, 18% by processing coal, and 4% by other means.

Hydrogen reforming: This process is discussed in Section 6.6.1 and the system is shown in Figure 6.96. When a reformer alone is used, carbon monoxide and carbon dioxide are released in the atmosphere; both are polluting gases. When a reformer and CO-converter are used, only carbon dioxide is produced, which is one of the greenhouse gases.

Electrolysis of water: This process sounds very simple since water contains only hydrogen and oxygen. However the electrolysis of water is an energy intensive process that reduces the overall efficiency of the entire system to less than 10%. Furthermore, electrolysis generates indirect pollution as the electricity used in the process is probably produced by polluting power plant.

Futuristic methods: Recent research claims that hydrogen can be liberated from a solution of sodium hydride (NaH) in the presence of certain catalyst without using electric energy. Also, researchers believe that the old algae can be genetically altered to produce hydrogen instead of oxygen during their photosynthesis process. Yet another method is based on a phenomenon known in metallurgy where some metal hydrides absorb hydrogen and store it between their molecules when they are cooled. The hydride alloys release the stored hydrogen when heated. The potential of these techniques to produce hydrogen at industrial scales is remained to be seen, and the environmental impacts of the processes need to be assessed.

6.6.7.2 Safety of Hydrogen

Hydrogen is currently used in several applications such as direct combustion and rocket propulsion. However, because hydrogen is a very explosive gas, it creates tremendous anxiety among the public. Most people associate hydrogen with the well-known Hindenburg zeppelin fire that occurred in 1937. This luxury airship used hydrogen to provide the needed lift and was burned while attempting to dock at Lakehurst, New Jersey. The spectacular fire of the Hindenburg is the main factor affecting the public perception regarding the safety of hydrogen.

The hydrogen used in FC electric cars is stored in pressurized tanks. The tanks are often made from carbon fibers and aluminum cylinders mounted on the top of the car. These tanks can survive a direct force from collisions without exploding. In the worst scenario, if the hydrogen catches fire, it will escape upward leaving the people inside the car below the tank relatively safe.

An alternative option to storing hydrogen is to use natural gas, and install a reformer and CO-converter inside the car. However, the storage of pressurized natural gas has its own safety concerns. Safer systems such as the direct FCs that use methanol and perhaps ethanol are expected to be more viable options.

6.7 INTERMITTENCY OF RENEWABLE SYSTEMS

Utility engineers must balance the generated energy and consumed energy at all times. This can be depicted as two quantities in a balanced scale; all generations are on one side and all demands on the other as shown in Figure 6.109. The demands include all electric loads and system losses. If the two sides of the scale are not exactly equal at all times, grid instability could occur leading to blackouts or even total system collapse as explained in Chapter 14. Since energy consumption depends on customers' activities and needs, it is not under the control of utility engineers. Therefore, they maintain this delicate balance by continuously adjust the generation to match the needed demand. This task is done with high degree of effectiveness since the inception of the power grid.

When large amounts of renewable resources are added to the grid, they reduce the ability of utility engineers to control the system generation. This is because renewable resources such as wind and solar are intermittent and may not be available when need to balance the energy scale of the grid. Also, renewable resources could be high in times of low demand. In Denmark for example, their large amount of wind generation could exceed the demands at night. This is because wind at night is generally strong and demand at night is substantially reduced.

To operate renewable resources as conventional power plants, utility engineers need to be able to ramp up and ramp down the outputs of the renewable systems. To achieve this objective, engineers are proposing the following general techniques:

- Ramp down renewable systems by spilling energy resources when they are not needed. This is done by curtailing renewable resources. For wind energy, it is done by changing the pitch angle to reduce the amount of energy captured by the blades. For solar, by aligning the cells to captures less solar energy. Keep in mind that wasting renewable energy is not a good option, but could be necessary to maintain the stability of the grid.

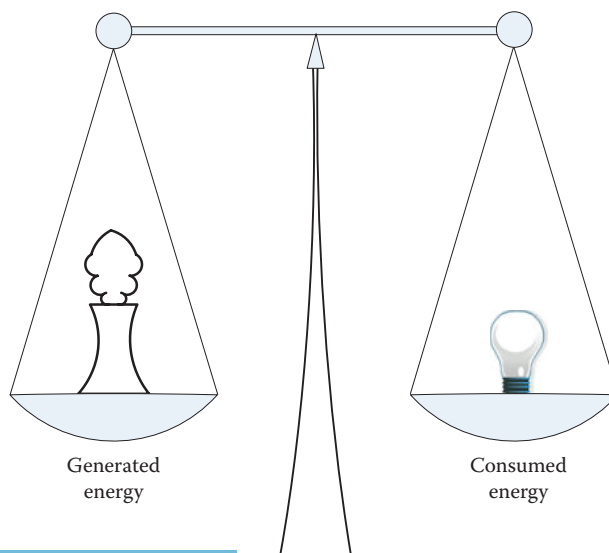


FIGURE 6.109 Balance of electric energy.

- Ramp up can be achieved by operating the renewable systems below their production level for the existing conditions. This way, there are resources available to increase the generation when needed. Again, this is a wasteful technique as the renewable plants produce less energy all the times.
- Ramp up can also be achieved by having conventional generation with fast startup time to provide the needed energy when renewable resources cannot meet their obligations. This is expensive technique and will demand a new design for generating systems that can continuously change their output while withstanding the repeated mechanical surges on its components.
- Develop effective energy storage systems that can store excess energy during times with excess generation and provide energy when resources are reduced.

6.8 ENERGY STORAGE SYSTEMS

The first energy storage system was invented by Alessandro Volta in 1800 in the form of batteries. Since then, and until a few years ago, little was done to invent different and more effective systems. Batteries are still good options, especially for low power applications without the need for fast charging.

For grid applications, there are several promising technologies. Some of them are already implemented and others are still in the prototype phases. Most systems are still expensive and certainly need more developments to increase their capacity, reduce their charging time and increase their lifetime while reducing their maintenance cycles and costs. Among the available technologies are pumped-hydro, compressed air, batteries, and flywheels.

6.8.1 PUMPED HYDRO STORAGE

The pumped hydro storage (PHS) system, shown in Figure 6.110, is one of the most effective energy storage methods. It is an impoundment hydroelectric power plant with reversed water flow. During the off-peak demand, the generator of the hydroelectric system runs as a motor, thus reversing the rotation of the turbine and the flow of water. This way, the electric energy is used to run the motor and water is collected from the river then stored in a lake at higher elevation. The lake could be natural or artificial; artificial lakes are called reservoirs. By adding more water to the lake, the potential energy of the lake is increased, thus energy is stored. During peak demand times, the system runs as a regular impoundment power plant where the stored energy in the lake is used to generate electricity.



FIGURE 6.110 PHS system. (Courtesy of the United States Army Corps of Engineers.)

Example 6.36

A PHS system is used to store electric energy from midnight to 5:00 AM. The reservoir is cylindrical with 200m radius. Just before midnight, the depth of water in the reservoir is 10 m and the water head is 100 m. If the flow rate of the turbine is $10 \text{ m}^3/\text{s}$, compute the head of water at 5:00 AM and the stored energy. Ignore penstock losses.

Solution

The volume of water in the reservoir at midnight (Vol_1) is

$$Vol_1 = \pi r^2 d_1 = \pi \times 200^2 \times 10 = 1.257 \times 10^6 \text{ m}^3$$

The additional volume of water by 5:00 AM (ΔVol) is

$$\Delta Vol = ft = 10 \times (5 \times 3,600) = 180,000 \text{ m}^3$$

The volume of water by 5:00 AM (Vol_2) is

$$Vol_2 = Vol_1 + \Delta Vol = 1.257 \times 10^6 + 1.8 \times 10^5 = 1.437 \times 10^6 \text{ m}^3$$

The extra depth of water in the reservoir by 5:00 AM (Δd) is

$$\Delta d = \frac{\Delta Vol}{\pi r^2} = \frac{180,000}{\pi \times 200^2} = 1.432 \text{ m}$$

Hence the head at 5:00 AM (h_2) is

$$h_2 = h_1 + \Delta d = 100 + 1.432 = 101.432 \text{ m}$$

The potential energy of the reservoir at midnight (PE_{r1}) is

$$PE_{r1} = Vol_1 \delta g h_1 = 1.257 \times 10^6 \times 10^3 \times 9.81 \times 100 = 1.233 \times 10^{12} \text{ J}$$

The potential energy of the reservoir at 5:00 AM (PE_{r2}) is

$$PE_{r2} = Vol_2 \delta g h_2 = 1.436 \times 10^6 \times 10^3 \times 9.81 \times 101.432 = 1.428 \times 10^{12} \text{ J}$$

Hence, the stored energy is

$$\Delta PE_r = PE_{r2} - PE_{r1} = 1.95 \times 10^{11} \text{ J} = 54.17 \text{ MWh}$$

6.8.2 COMPRESSED AIR ENERGY STORAGE

From thermodynamic theory, the energy stored in pressurized air is

$$E = P_r Vol = kT \quad (6.104)$$

where

E is the energy stored in pressurized air

P_r is the pressure of air

Vol is the volume of the pressurized air

k is the amount of substance of air multiplied by the ideal gas constant

T is the temperature of compressed air

The stored energy (ΔE) is the energy added due to compression (or subtracted due to expansion). This is expressed by

$$\Delta E = \int_{Vol_i}^{Vol_f} P_r dVol = \int_{Vol_i}^{Vol_f} \frac{kT}{Vol} dVol = kT \left(\ln \frac{Vol_f}{Vol_i} \right) \quad (6.105)$$

where subscripts i and f are for initial and final states

The compression of any gas produces heat called *heat of compression*. As the air temperature increases, it tends to resist further compression, thus limiting the amount of stored energy. So if we allow the generated heat to escape into surrounding environment, the temperature of air can be maintained constant. This is known as *isothermal process* in thermodynamics. In this case, Equation 6.104 can be written for both states as

$$P_{ri} Vol_i = P_{rf} Vol_f = kT \quad (6.106)$$

Equation 6.105 can now be rewritten as

$$\Delta E = P_{ri} Vol_i \left(\ln \frac{P_{ri}}{P_{rf}} \right) \quad (6.107)$$

Example 6.37

Energy is to be stored in 1 m³ of pressure tank. If the pressure of the tank increases to 50 times the atmospheric pressure, compute the stored energy assuming isothermal process.

Solution

The standard atmospheric pressure (1 atm) is about 10⁵ N/m² (Pa).

Using Equation 6.107,

$$\Delta E = P_{ri} Vol_i \left(\ln \frac{P_{ri}}{P_{rf}} \right) = 10^5 \times 1 \times \ln \left(\frac{1}{50} \right) = -3.91 \times 10^5 \text{ J}$$

The negative sign means the energy is acquired from the grid. Keep in mind that the electric energy used to store this amount is higher than 3.91 × 10⁵ J due to the various losses of the isothermal process.

The compressed air energy storage (CAES) system is using the isothermal process. Figure 6.111 depicts the main components of the system. When electric energy is to be stored, a motor compresses the air into an underground reservoir such as salt cavern, abandoned hard rock mine, aquifer or pressure tank. When the stored energy is needed, the compressed air is released and heated in the recuperator then fuel is added (normally natural gas) to the hot air. The mix is ignited in a gas turbine (combustion turbine) that rotates the generator.

The first CAES system was 290 MW built in 1978 in Germany. More recently, a 110 MW unit was built in McIntosh, Alabama in 1991 and a 2700 MW is built in Norton, OH

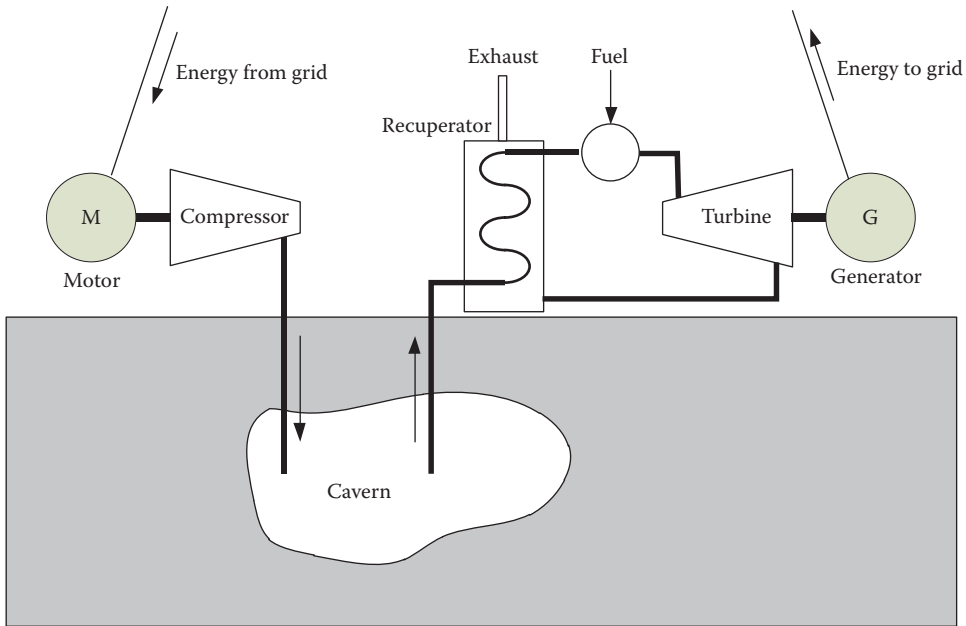


FIGURE 6.111 Main components of compressed air energy storage system.

6.8.3 BATTERIES

The development of the dream battery is taking place all over the world for essentially two main applications: electric vehicles and power grid. For batteries to be effectively used in high power applications, they must have several key features, as follows:

- *High energy densities:* Large amount of stored energy per unit volume (or weight) is very important requirement for mobile applications.
- *Slow loss of charge:* The battery need to maintain their charge for extended period of time.
- *Cost effective:* Batteries are still expensive to operate and some are expensive to maintain.
- *High charge/discharge efficiency:* Losses during the charging and discharging processes need to be minimized. Efficiencies higher than 90% is attainable.
- *Long cycle life:* Durability and long cycle life are very important as the cost of batteries are relatively expensive.
- *No memory effect:* Charging a partially charged battery should not reduce the amount of energy that can be extracted from the battery.
- *Safe to operate:* Some batteries with low charging/discharging efficiencies generate high temperatures. Other batteries need to reach high temperatures to start their functions. The high temperatures can cause overheating problems or even explosions.

Among the batteries used in high power applications are the sodium sulfur, lithium ion and the vanadium redox flow batteries. Some of these batteries are used in mobile applications and others as grid storage devices in the MWh range. One of the known large battery systems is the 60MWh in Japan.

6.8.4 FLYWHEELS

The flywheel is essentially an electric machine with three distinctive features:

- High speed machines
- Large inertia machines
- Minimum losses machine

To understand the importance of these features, let us consider the flywheel system shown in Figure 6.112. When we need to store energy, the machine operates as a motor and the energy is store in its rotating mass in the form of kinetic energy. When the energy is needed, the machine operates as a generator converting the stored kinetic energy into electrical energy. The stored kinetic energy is given by

$$E = \frac{1}{2} I \omega^2 \quad (6.108)$$

where

E is the stored kinetic energy in the rotor (J)

ω is the angular velocity of the rotor (rad/s)

I is the moment of inertia of the rotor (kg m^2)

The rotor can be considered a solid cylinder whose moment of inertia is

$$I = \frac{1}{2} m r^2 \quad (6.109)$$

where

m is the mass of the rotor (kg)

r is the radius of the rotor (m)

The stored energy is then

$$E = \frac{1}{4} m r^2 \omega^2 \quad (6.110)$$

The amount of stored energy increases if the mass of the rotor increases, the radius of the rotor increases, or the speed of rotation increases. Therefore the flywheel has a heavy mass and is rotating at very high speeds (10,000rpm or higher).

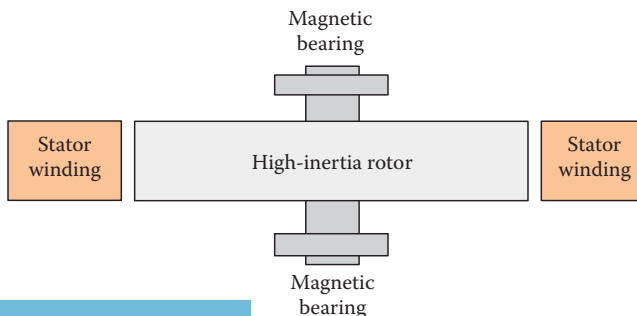


FIGURE 6.112 Main components of flywheel.

But the flywheel is an electric machine. When it is rotating, rotational losses (windage and friction) can consume the stored kinetic energy over a period of time. To reduce the windage loss, the flywheel is often placed in a vacuum container. To reduce the frictions, magnetic bearing are used to essentially float the rotor. Flywheels with magnetic bearings can achieve over 90% efficiency.

One advantage of the flywheel system is that we can estimate the stored energy with high degree of accuracy. As shown in Equation 6.110, a simple measurement of the speed gives us the exact amount of stored energy. This is because the mass and radius are constant.

One disadvantage of the flywheel system is safety. The high speed may increase the tensile strength of the rotor beyond its limit. This may shatter the rotor causing explosion. Also failure in the magnetic bearing can cause the rotor to hit the enclosure causing explosion. This is why flywheel systems are often placed inside strong containment or are buried in ground vaults.

Example 6.38

Compute the stored energy in a flywheel system rotating at 10,000r/min. The diameter of the rotor is 60 cm and its height is 20 cm. The density of the rotor material is 7 g/cm³.

Solution

First, we need to calculate the mass of the rotor:

$$m = \delta \text{ Vol} = 7 \times (\pi \times 30^2 \times 20) = 395.84 \text{ kg}$$

Using Equation 6.110, we can compute the stored energy:

$$E = \frac{1}{4} m r^2 \omega^2 = \frac{1}{4} 395.84 \times 0.3^2 \left(2\pi \frac{10,000}{60} \right)^2 = 9.77 \times 10^6 \text{ J} = 2.713 \text{ kWh}$$

EXERCISES

- 6.1 A solar panel consists of four parallel columns of PV cells. Each column has 10PV cells in series. Each cell produces 2 W at 0.5 V. Compute the voltage and current of the panel.
- 6.2 State three factors that determine the amount of power generated by wind machines.
- 6.3 What is the function of the reformer and *co*-conversion used in FC technology?
- 6.4 Compute the amount of sulfur dioxide produced when a coal fired power plant generate 50 MW of electricity.
- 6.5 A solar power density for a given area has a standard deviation of 3 h, and a maximum power of 200 W at noon. Compute the solar energy in 1 day.
- 6.6 An area located near the equator has the following parameters:

$$\alpha_{dt} = 0.82; \quad \alpha_p = 0.92; \quad \beta_{wa} = 0.06$$

The solar power density measured at 11:00 AM is 890 W/m², compute the solar power density at 4:00 PM.

- 6.7 Why do we need to dope the silicon in solar cells?
- 6.8 Which material is added to make the silicon *n*-type, and which makes the silicon *p*-type?
- 6.9 Why is the depletion zone?
- 6.10 Explain how the light energy is converted into electricity.
- 6.11 Why do we need to connect the solar cells in series?
- 6.12 Why do we need to connect the solar cells in parallel?

- 6.13** What is a solar array?
- 6.14** A solar cell with a reverse saturation current of 1 nA is operating at 35°C . The solar current at 35°C is 1.1 A . The cell is connected to a $5\ \Omega$ resistive load. Compute the output power of the cell.
- 6.15** A solar cell with a reverse saturation current of 1 nA has a solar current of 1.1 A . Compute the maximum output power of the cell per unit of thermal voltage.
- 6.16** For the solar cell in the previous problem, compute the load resistance at the maximum output power.
- 6.17** A PV module is composed of 100 ideal solar cells connected in series. At 25°C , the solar current of each cell is 1.2 A and the reverse saturation current is 10 nA . Find the module power when the module voltage is 45 V .
- 6.18** An 80 cm^2 solar cell is operating at 30°C where the output current is 1 A , the load voltage is 0.5 V and the saturation current of the diode is 1 nA . The series resistance of the cell is $10\text{ m}\Omega$ and the parallel resistance is $500\ \Omega$. At a given time, the solar power density is 300 W/m^2 . Compute the irradiance efficiency.
- 6.19** A solar cell is operating at 30°C where the output current is 1.1 A and the load voltage is 0.5 V . The series resistance of the cell is $20\text{ m}\Omega$ and the parallel resistance is $2\text{ k}\Omega$. Compute the electrical efficiency of the PV cell. Assume that the irradiance efficiency is 22% , compute the overall efficiency of the PV cell.
- 6.20** The aerodynamic force exerted on each blade of a two-blade wind turbine is 1000 N . At the given conditions, the lift coefficient is 0.9 . If the center of gravity of the blade is at 20 m from the hub, compute the following:
1. The torque generated by the two blades
 2. The blades' power at 30 r/min
- 6.21** For a relative wind speed of $20\angle -80^\circ\text{ m/s}$, compute the pitch angle if the desired angle of attack is 10° .
- 6.22** The coefficient of performance of wind turbines is often expressed by the empirical formula

$$C_p = k_1 \left(\Lambda - K_2\beta - k_3\beta^3 - k_4 \right) e^{-\Lambda k_5}$$

where

$$\Lambda = \frac{1}{TSR + k_6\beta} - \frac{k_7}{1 + \beta^3}$$

For a given turbine, the constants are

k_1	k_2	k_3	k_4	k_5	k_6	k_7
20	0.1	0.002	0.003	15	1	0.02

- a. Plot the coefficient of performance with respect to the TSR for angle of attack equal to 0° , 10° , 20° , and 30° .
 - b. Find the maximum C_p and the TSR_{ideal} for a pitch angle equal to 30° .
- 6.23** An investor wishes to install a wind farm in the Snoqualmie pass area located in Washington State, United States. The pass is about 920 m above the sea level. The average low temperature of the air is -4°C , and the average high is 18°C . Compute the power density of the wind in winter and summer assuming that the average wind speed is 15 m/s .
- 6.24** For the site in the previous problem, compute the length of the blades to capture 200 kW of wind energy during the summer.

- 6.25** A wind turbine with a gearbox ratio of 200 produces electric energy when the generator speed is at least 910 rpm. The length of each blade is 5 m. The turbine has a variable tip speed ratio (TSR). At a wind speed of 10 m/s, compute the minimum TSR of the wind turbine.
- 6.26** Generate an idea to reduce the voltage flickers associated with wind energy.
- 6.27** List the main differences between the four types of wind turbines.
- 6.28** How do you maintain the output power of wind turbine constant when wind speed varies?
- 6.29** What is feathering? How it is achieved?
- 6.30** A reservoir-type small hydroelectric system has an effective head of 10 m and a penstock of a flow rate of $1 \text{ m}^3/\text{s}$. Assume that the hydro efficiency is 85%, the turbine efficiency is 80% and the generator efficiency is 92%; compute the output electric power of the generator.
- 6.31** Assume that the penstock efficiency in the previous problem is 95%. Compute the gross head.
- 6.32** A man wants to build a reservoir-type small hydroelectric system on his property. The site can accommodate a penstock of $5 \text{ m}^3/\text{s}$ flow rate. In order for him to generate 1 MW of electricity, compute the height of the dam. Assume that the penstock efficiency is 90%, the hydro efficiency is 90%, the turbine efficiency is 90%, and the generator efficiency is 96%.
- 6.33** A person wishes to build a WS (diversion-type) small hydroelectric system on his property. To measure the speed of the water, he dropped a ping-pong ball in the river and found the ball to travel 10 m in 4 s. He also selected a turbine with a sweep diameter of 0.8 m. Assume that the coefficient of performance is 30%, the turbine efficiency is 90% and the efficiency of the generator is 96%. Compute the output power of the plant and the energy generated in 1 year. If the price of the energy sold to the neighboring utility is $\$0.06/\text{kWh}$, compute the annual income from this small hydroelectric plant.
- 6.34** A tidal mill with blade length of 2 m, compute the blade power when the tidal current is 5 knots. Assume the power coefficient of the tidal mill is 0.3.
- 6.35** A barrage tidal energy system is constructed between a lagoon and open ocean. The base area of the lagoon is 1 km^2 . The hydraulic head of the system is approximately 10 m for all ebbs and flows. Compute the average electrical power generated by the tidal system assuming the total efficiency of the system is 85%.
- 6.36** Compute the wave power hitting 10 m of a beach front. If the average height of the wave is 2 m and the wave period of 10 s.
- 6.37** What is the function of the float in a BM system?
- 6.38** Sketch a different design than given in the book of an HC system.
- 6.39** What are the main challenges facing wave energy?
- 6.40** What are the main environmental impacts of wave energy?
- 6.41** Compute the approximate core temperature after 1000 years.
- 6.42** Identify three sites using geothermal reservoir to generate electricity.
- 6.43** Identify three sites using hot rock geothermal system to generate electricity.
- 6.44** What are the benefits of using geothermal energy?
- 6.45** Why is geothermal energy a renewable resource?
- 6.46** What are the environmental effects of geothermal power plants?
- 6.47** What makes a geothermal site suitable for electric power generation?
- 6.48** What is biomass?
- 6.49** How electricity is generated from biomass power plant?
- 6.50** Is Biomass a renewable source of energy? Why?
- 6.51** What are the environmental impacts of burning biomass products?
- 6.52** What are the main advantages of direct FCs?
- 6.53** What are the main components used in FC electric vehicles? Explain the operation of the vehicle.
- 6.54** What are the different types of FCs?

- 6.55 Which FC type is suitable for high power?
 6.56 Which FC type is suitable for mobile energy?
 6.57 What are the advantages of using a FC?
 6.58 Is using hydrogen in FCs safe?
 6.59 Why not just burn hydrogen in thermal power plant instead of using it in FCs?
 6.60 A polarization curve of an FC can be represented by the empirical formula

$$V = 0.9 - 0.128 \times \tan(I - 1.2)$$

where

V is the voltage of the FC in volts

I is the current in amperes

- Plot the polarization and power curves. Also compute the voltage at the maximum power of the cell.
- 6.61 For the cell in the previous example. Compute the drop in voltage for a 10% increase in current in the activations region. Repeat the solution for the ohmic and mass transport regions.
- 6.62 Why it is important for the utility to have full control on the generation?
- 6.63 If a given utility cannot have full control on its generation, what are its options?
- 6.64 A PHS system is used to store electric energy from midnight to 5:00 AM. The reservoir is cylindrical with 200m radius. Just before midnight, the depth of water in the reservoir is 10m and the water head is 100m. To store 100MWh, compute the flow rate of the turbine. Ignore penstock losses.
- 6.65 Why batteries, in general, takes long time to charge?
- 6.66 What is the memory problem associated with some types of batteries?
- 6.67 A 1000m³ cavern is used to store 100MJ of energy, compute the cavern air pressure.
- 6.68 Why it is important to keep the temperature during air storage low?
- 6.69 A flywheel system stores 1 kJ. The diameter of the rotor is 40 cm and its height is 20 cm. The density of the rotor material is 10 g/cm³. Compute the rotation speed.
- 6.70 Can the system in the previous problem store 1 MJ of energy?
- 6.71 What are the main environmental impacts of flywheel systems?

7 Alternating Current Circuits

Nikola Tesla proposed the alternating current (ac) system as a better alternative to the direct current (dc) system. His idea was initially met with fierce resistance from Thomas Edison as explained in Chapter 1. Eventually the ac was selected for power systems worldwide essentially because of three main reasons:

1. The voltage of the ac system can be adjusted by transformers, which are relatively simple devices.
2. The voltage of the long transmission lines can increase to high levels; thus reducing the current of the line, reducing the transmission line losses, and reducing the cross section of the conductors of the transmission lines.
3. The ac systems produce rotating magnetic fields that spin electric motors. Keep in mind that electric motors represent the majority of electrical loads.

Nomenclature

In this chapter, the following nomenclatures are used:

Instantaneous current	i	Instantaneous voltage	v
Average current	I_{ave}	Average voltage	V_{ave}
Maximum (peak) current	I_{max}	Maximum (peak) voltage	V_{max}
Current magnitude in root mean square	I	Voltage magnitude in root mean square	V
Phasor current in complex form	\bar{I}	Phasor voltage in complex form	\bar{V}
Impedance in complex form	\bar{Z}	Apparent power in complex form	\bar{S}
Magnitude of impedance	Z	Magnitude of apparent power	S
Instantaneous power	p	Real power	P
Reactive power	Q		

7.1 ALTERNATING CURRENT WAVEFORM

The ideal ac circuit has its voltage and current in sinusoidal forms. A voltage waveform is shown in Figure 7.1 and can be expressed mathematically by

$$v = V_{max} \sin \omega t \quad (7.1)$$

where

v is the instantaneous voltage

V_{max} is the peak (maximum) value of the voltage

ω is the angular frequency

t is the time

The unit of ω is radian/second (rad/s) and is expressed by

$$\omega = 2\pi f \quad (7.2)$$

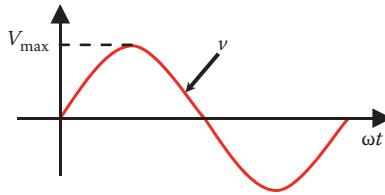


FIGURE 7.1 Sinusoidal waveform of ac voltage.

where f is the frequency of the ac waveform. In places such as North, Central, and South America, South Korea, Taiwan, The Philippines, Saudi Arabia, and Western Japan, the frequency of power supply is 60 cycle/s or 60Hz. For the rest of the world, including Eastern Japan, the supply frequency is 50Hz.

During the nineteenth century, 60Hz was chosen by Westinghouse in the United States. Meanwhile, in Germany, the giant power equipment manufacturers AEG and Siemens chose 50Hz. These companies had a virtual monopoly in Europe, and their 50Hz standard spread to the rest of Europe and most of the world.

7.2 ROOT MEAN SQUARE

The waveform in Figure 7.1 has its magnitude changing with time. For 60Hz systems, the waveform is repeated 60 times every second. Quantifying the value of this sinusoidal voltage is rather tricky. If we quantify the sinusoidal waveform by its maximum value, it would be unreliable since the peak is often skewed by the transients and harmonics that exist in power networks. Using the average value is not a good idea either, as the average value is always zero because of the symmetry of the waveform around the time axis. To address this problem, engineers developed an effective method called *root mean square* (rms) to quantify ac waveforms. The concept of this method is shown in Figure 7.2 where the rms value is computed in three steps:

Step 1: Compute the square of the waveform.

Step 2: Compute the average value of step 1.

Step 3: Compute the square root of step 2.

The idea behind step 1 (squaring the waveform) is to create another waveform that is always positive so that its average value in step 2 is nonzero. The square root in step 3 is imposed to somehow compensate for the initial squaring in step 1. Today, all ac waveforms in power circuits are quantified by their rms values.

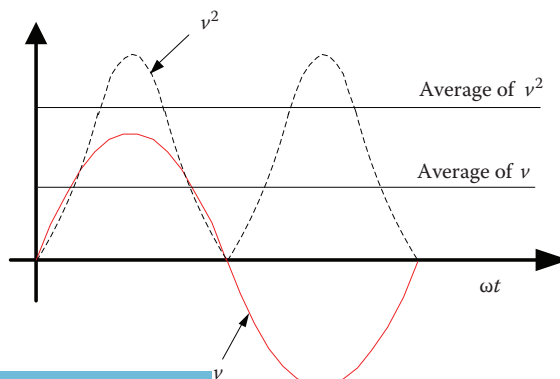


FIGURE 7.2 Concept of RMS.

The rms value can be computed by following the three steps mentioned earlier. Let us consider the waveform in Equation 7.1. The first step is to square this waveform:

$$v^2 = V_{\max}^2 \sin^2 \omega t = \frac{V_{\max}^2}{2}(1 - \cos 2\omega t) \tag{7.3}$$

The second step is to find the average value *Ave* of Equation 7.3:

$$Ave = \frac{1}{2\pi} \int_0^{2\pi} \frac{V_{\max}^2}{2}(1 - \cos 2\omega t) d\omega t = \frac{V_{\max}^2}{2} \tag{7.4}$$

The final step is to find the rms voltage *V* by computing the square root of Equation 7.4:

$$V = \sqrt{\frac{V_{\max}^2}{2}} = \frac{V_{\max}}{\sqrt{2}} \tag{7.5}$$

The rms voltage for households in North America is 120 V. For Europe and most of the Middle East, the rms voltage is 220–240 V. There are a few exceptions such as Japan where the voltage is 100 V. As mentioned in Chapter 2, it appears that 120 V was chosen somewhat arbitrarily. Actually, Thomas Edison came up with a high-resistance lamp filament that operated well at 120 V. Since then, 120 V has been used in the United States. Other nations chose higher voltage, 220–240 V, to reduce the current in the electric wires, and therefore use less expensive wires with smaller cross sections.

Example 7.1

The outlet voltage measured by an rms voltmeter is 120 V. Compute the maximum value of the voltage waveform.

Solution

$$V_{\max} = \sqrt{2} V = \sqrt{2} \times 120 = 169.7 \text{ V}$$

Notice that the voltage of all household equipment is given in rms, not the maximum value.

Example 7.2

Compute the rms voltage of the waveform in Figure 7.3.

Solution

The general equation of the rms value of *v* is

$$V = \sqrt{\frac{1}{\tau} \int_0^{\tau} v^2 dt}$$

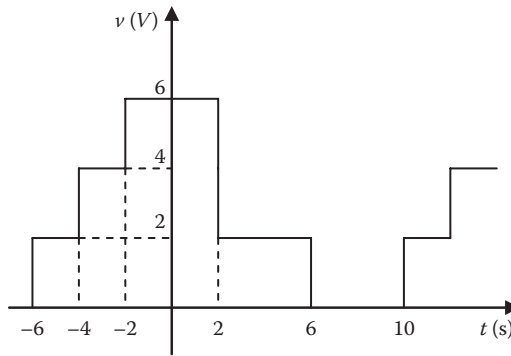


FIGURE 7.3 Discrete voltage waveform.

where τ is the period. Since the waveform in Figure 7.3 is discrete, the rms voltage can be expressed by

$$V = \sqrt{\frac{1}{\tau} \sum_k (v_k^2 t_k)}$$

$$V = \sqrt{\frac{1}{16} \sum 2^2 \times 2 + 4^2 \times 2 + 6^2 \times 4 + 2^2 \times 4} = 3.536 \text{ V}$$

7.3 PHASE SHIFT

The ideal waveforms for currents and voltages in ac circuits are sinusoidal. For a purely resistive load R , the current waveform i_R is in phase with the voltage waveform as given in Equation 7.6 and shown in Figure 7.4:

$$v = V_{\max} \sin(\omega t) = i_R R \quad (7.6)$$

$$i_R = \frac{V_{\max}}{R} \sin(\omega t)$$

If the circuit has a purely inductive load (no resistance or capacitance), the voltage–current relationship is

$$v = V_{\max} \sin(\omega t) = L \frac{di_L}{dt} \quad (7.7)$$

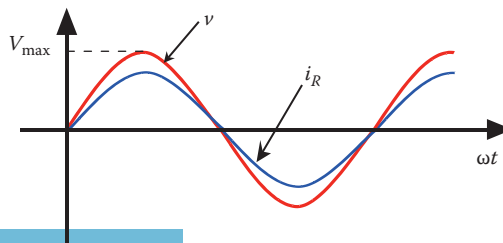


FIGURE 7.4 Voltage and current of purely resistive load.

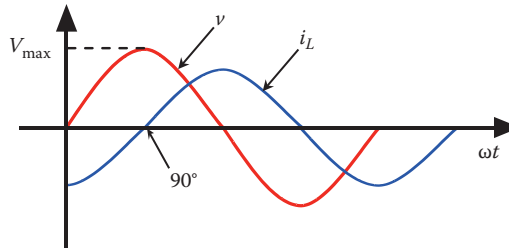


FIGURE 7.5 Voltage and current of purely inductive load.

where L is the inductance of the load. The current in this purely inductive load i_L can be obtained from Equation (7.7)

$$i_L = \frac{1}{L} \int v \, dt = \frac{V_{\max}}{L} \int \sin(\omega t) \, dt = -\frac{V_{\max}}{\omega L} \cos(\omega t) = -\frac{V_{\max}}{X_L} \cos(\omega t) \tag{7.8}$$

where $X_L = \omega L$ is the magnitude of the inductive reactance of the load. As seen in Equation 7.8, the current i_L of a purely inductive load is a negative cosine waveform which is shown in Figure 7.5. The positive peak of the current occurs 90° after the voltage reaches its own positive peak. In this case, the current is said to be *lagging* the voltage by 90° .

For a purely capacitive load, the voltage–current relationship is given by

$$v = V_{\max} \sin(\omega t) = \frac{1}{C} \int i_C \, dt \tag{7.9}$$

$$i_C = C \frac{dv}{dt}$$

where C is the load capacitance. The current i_C can be computed as

$$i_C = C \frac{d}{dt} [V_{\max} \sin(\omega t)] = \omega C V_{\max} \cos(\omega t) = \frac{V_{\max}}{X_C} \cos(\omega t) \tag{7.10}$$

where $X_C = 1/\omega C$ is the magnitude of the capacitive reactance of the load. As seen in Equation 7.10, the current of a purely capacitive load is a cosine waveform. Figure 7.6 shows the voltage across the capacitor and the current i_C . Note that the positive peak of the current waveform occurred 90° before the voltage peak. Hence, the current is said to be *leading* the voltage by 90° .

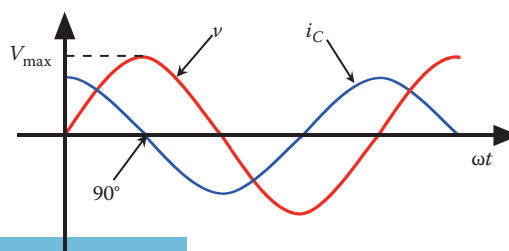


FIGURE 7.6 Voltage and current of purely capacitive load.

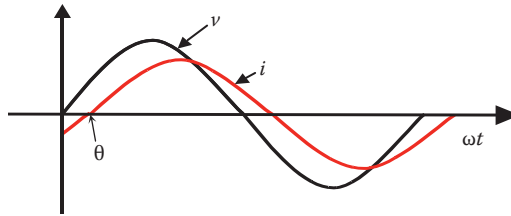


FIGURE 7.7 Lagging current.

If the load is composed of a mix of elements such as resistances, capacitances, and inductances, the phase shift angle θ of the current can be any value between -90° and $+90^\circ$. Figure 7.7 shows the current and voltage waveforms of an inductive load that is composed of a resistance and inductance. The current waveform in Figure 7.7 can be expressed mathematically by

$$i = I_{\max} \sin(\omega t - \theta) \tag{7.11}$$

7.4 CONCEPT OF PHASORS

Phasors are handy graphical representations for ac circuit analysis. They give quick information on the magnitude and phase shift of any waveform. Consider Figure 7.8; the left side of the figure shows a sinusoidal waveform without any phase shift. The waveform can be represented by the phasor on the right side of the figure. The length of the phasor is proportional to the rms value of the waveform and its phase angle with respect to the x -axis represents the phase shift of the sinusoidal waveform. Since the waveform has no phase shift, the phasor of the voltage is aligned with the x -axis.

Consider the circuit in Figure 7.9 for a purely resistive load. Since the resistance does not cause any phase shift in the current as shown in Figure 7.4, the current phasor is *in phase* with the voltage as shown on the right side of Figure 7.9.

For a purely inductive load, the current lags the voltage by 90° as given in Equation 7.8 and shown in Figure 7.5. The phasor diagram in this case is depicted on the right side of Figure 7.10. The lagging angles are always in the clockwise direction.

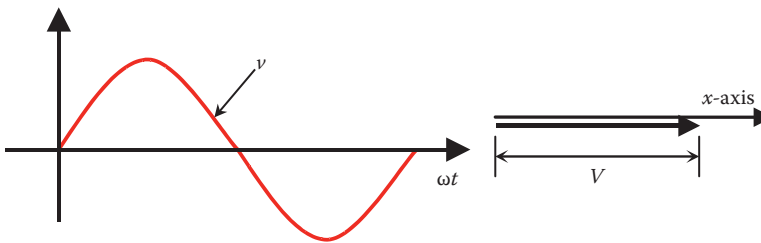


FIGURE 7.8 Phasor representation of a sinusoidal waveform.

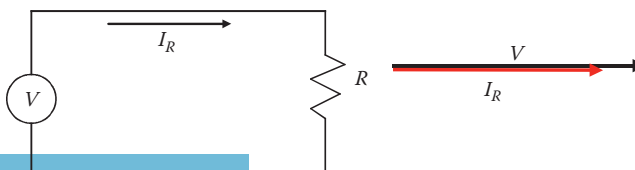


FIGURE 7.9 Phasor representation of current and voltage of purely resistive load.

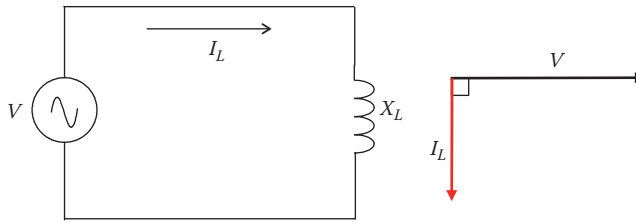


FIGURE 7.10 Phasor representation of current and voltage of purely inductive load.

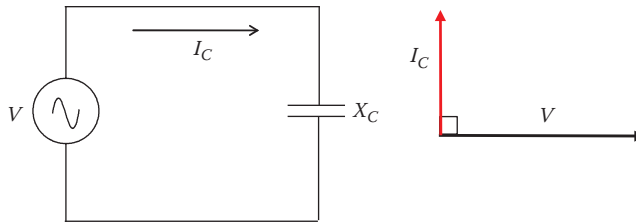


FIGURE 7.11 Phasor representation of current and voltage of purely capacitive load.

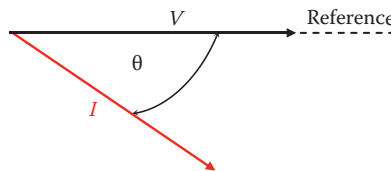


FIGURE 7.12 Phasor representation of the current and voltage in Figure 7.7.

For a purely capacitive load, the current leads the voltage by 90° as given in Equation 7.10 and shown in Figure 7.6. The phasor diagram in this case is given on the right side of Figure 7.11. The leading angles are always in the counterclockwise direction.

Now let us consider the waveforms in Figure 7.7. As seen in the figure, the current is lagging the voltage by an angle θ . These waveforms can be represented by the phasor diagram in Figure 7.12. The voltage is considered as the reference with no phase shift, so it is aligned with the x -axis. Since the current lags the voltage by θ , the phasor for the current lags the reference by θ in the clockwise direction.

7.5 COMPLEX NUMBER ANALYSIS

It is inconvenient to numerically analyze electric circuits by the graphical method of phasor diagrams. An alternative method is to use the complex number analysis, where any phasor is represented by a magnitude and an angle. For example, the voltage and current in Figures 7.7 or 7.12 can be represented by the following complex variable equations:

$$\bar{V} = V \angle 0^\circ \tag{7.12}$$

$$\bar{I} = I \angle -\theta^\circ \tag{7.13}$$

where \bar{V} is the phasor representation of the voltage. It has a bar on the top indicating that the variable is a complex number. V is the magnitude of the voltage in rms. The symbol \angle is followed by the angle of the phasor, which is zero for voltage and $-\theta$ for the lagging current.

The complex forms in Equations 7.12 and 7.13 are called *polar* forms (also known as *trigonometric* forms). The mathematics of the polar forms is very simple for multiplication and division. Let us assume that we have two complex numbers:

$$\bar{A} = A \angle \theta_1 \quad (7.14)$$

$$\bar{B} = B \angle \theta_2 \quad (7.15)$$

The multiplication and division of these two complex numbers are as follows:

$$\bar{A} \bar{B} = A \angle \theta_1 \ B \angle \theta_2 = AB \angle (\theta_1 + \theta_2) \quad (7.16)$$

$$\frac{\bar{A}}{\bar{B}} = \frac{A \angle \theta_1}{B \angle \theta_2} = \frac{A}{B} \angle (\theta_1 - \theta_2) \quad (7.17)$$

The addition and subtraction of complex numbers in polar forms are harder to implement. However, if we switch the polar form to the *rectangular* form (also known as *cartesian* form), we can perform these operations very quickly. To convert from polar to rectangular forms, consider the phasor \bar{A} in Figure 7.13. The reference in the figure represents the x -axis. The component of \bar{A} projected on the reference is $X = A \cos \theta$ and the vertical projection is $Y = A \sin \theta$. These two components can be represented by Equation 7.18.

$$\bar{A} = A \angle \theta = A [\cos \theta + j \sin \theta] = A \cos \theta + jA \sin \theta = X + jY \quad (7.18)$$

The first component along the x -axis is known as the *real* component. The second component, preceded by an operator j , is known as the *imaginary* component. Keep in mind that there is nothing imaginary about the quantity $A \sin \theta$; we simply use the label to distinguish between the directions of the real and imaginary vectors. The operator j is used to represent the counterclockwise rotation of a vector by 90° ; any quantity preceded by j is shifted in the counterclockwise direction by 90° . The basic relations of the operator j are summarized in Equation 7.19:

$$\begin{aligned} j &= 1 \angle 90^\circ \\ j^2 &= 1 \angle 180^\circ = -1 \\ j^3 &= 1 \angle 270^\circ = 1 \angle -90^\circ = -j \\ j^4 &= 1 \angle 0^\circ = 1 \\ j^5 &= 1 \angle 90^\circ = j \\ &\text{etc.} \end{aligned} \quad (7.19)$$

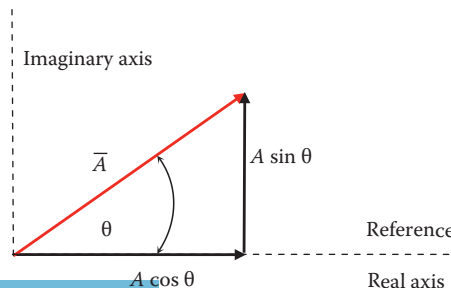


FIGURE 7.13 X and Y components of Phasor \bar{A} .

The mathematical expressions in Equation 7.19 can also be achieved by defining the operator $j = \sqrt{-1}$. By using Figure 7.13, the conversion of \bar{A} from the rectangular form to the polar form is

$$\begin{aligned}\bar{A} &= X + jY = A\angle\theta \\ A &= \sqrt{X^2 + Y^2} \\ \theta &= \tan^{-1} \frac{Y}{X}\end{aligned}\tag{7.20}$$

The addition or subtraction of complex numbers in rectangular forms is done by adding or subtracting the real and imaginary components independently

$$\begin{aligned}\bar{A} + \bar{B} &= A(\cos\theta_1 + j\sin\theta_1) + B(\cos\theta_2 + j\sin\theta_2) \\ &= (A\cos\theta_1 + B\cos\theta_2) + j(A\sin\theta_1 + B\sin\theta_2)\end{aligned}\tag{7.21}$$

$$\begin{aligned}\bar{A} - \bar{B} &= A(\cos\theta_1 + j\sin\theta_1) - B(\cos\theta_2 + j\sin\theta_2) \\ &= (A\cos\theta_1 - B\cos\theta_2) + j(A\sin\theta_1 - B\sin\theta_2)\end{aligned}\tag{7.22}$$

One of the convenient operations used in complex number analyses is the conjugate of a vector. Two complex numbers are conjugates if

- Their real components are equal and their imaginary components are equal in magnitude
- Their imaginary components have different signs

If \bar{A} is a complex vector, and \bar{A}^* is its conjugate, then

$$\begin{aligned}\bar{A} &= X + jY = \sqrt{X^2 + Y^2} \angle\theta \\ \bar{A}^* &= X - jY = \sqrt{X^2 + Y^2} \angle -\theta\end{aligned}\tag{7.23}$$

The conjugate is useful in complex operations such as inverting a phasor. Let us assume that the phasor \bar{A} is in rectangular form. To compute $1/\bar{A}$, use the following process:

$$\begin{aligned}\frac{1}{\bar{A}} &= \frac{1}{X + jY} \frac{\bar{A}^*}{\bar{A}^*} \\ \frac{1}{\bar{A}} &= \frac{1}{X + jY} \frac{X - jY}{X - jY} = \frac{X - jY}{X^2 + Y^2} \\ \frac{1}{\bar{A}} &= \frac{X}{X^2 + Y^2} - j \frac{Y}{X^2 + Y^2}\end{aligned}\tag{7.24}$$

Example 7.3

Assume $\bar{A} = 10 \angle 60^\circ$ and $\bar{B} = 5 \angle 40^\circ$, compute the following:

1. $\bar{C} = \bar{A} \bar{B}$
2. $\bar{C} = \frac{\bar{A}}{\bar{B}}$
3. $\bar{C} = \bar{A} + \bar{B}$
4. $\bar{C} = \bar{A} - \bar{B}$

Solution

1. $\bar{C} = \bar{A} \bar{B} = 10 \angle 60^\circ 5 \angle 40^\circ = (10 \times 5) \angle (60^\circ + 40^\circ) = 50 \angle 100^\circ$
2. $\bar{C} = \frac{\bar{A}}{\bar{B}} = \frac{10 \angle 60^\circ}{5 \angle 40^\circ} = \frac{10}{5} \angle (60^\circ - 40^\circ) = 2 \angle 20^\circ$
3. $\bar{C} = \bar{A} + \bar{B} = 10 \angle 60^\circ + 5 \angle 40^\circ = 10 (\cos 60^\circ + j \sin 60^\circ) + 5 (\cos 40^\circ + j \sin 40^\circ)$
 $\bar{C} = (5 + j8.66) + (3.83 + j3.21) = 8.83 + j11.87$
 $\bar{C} = \sqrt{(8.83)^2 + (11.87)^2} \angle \tan^{-1} \left(\frac{11.87}{8.83} \right) = 14.8 \angle 53.36^\circ$
4. $\bar{C} = \bar{A} - \bar{B} = 10 \angle 60^\circ - 5 \angle 40^\circ = 10 (\cos 60^\circ + j \sin 60^\circ) - 5 (\cos 40^\circ + j \sin 40^\circ)$
 $\bar{C} = (5 + j8.66) - (3.83 + j3.21) = 1.17 + j5.45$
 $\bar{C} = \sqrt{(1.17)^2 + (5.45)^2} \angle \tan^{-1} \left(\frac{5.45}{1.17} \right) = 5.57 \angle 77.88^\circ$

7.6 COMPLEX IMPEDANCE

The impedance in ac circuits can be composed of any combination of resistances, inductances and capacitances. These elements are also complex quantities and can be computed as given in Equations 7.25 through 7.27

$$\bar{R} = \frac{\bar{V}}{\bar{I}_R} = \frac{V \angle 0}{I_R \angle 0} = R \angle 0 \quad (7.25)$$

$$\bar{X}_L = \frac{\bar{V}}{\bar{I}_L} = \frac{V \angle 0}{I_L \angle -90^\circ} = \frac{V}{I_L} \angle 90^\circ = X_L \angle 90^\circ \quad (7.26)$$

$$\bar{X}_C = \frac{\bar{V}}{\bar{I}_C} = \frac{V \angle 0}{I_C \angle 90^\circ} = \frac{V}{I_C} \angle -90^\circ = X_C \angle -90^\circ \quad (7.27)$$

where the magnitudes $X_L = \omega L$ and $X_C = 1/\omega C$ as given in Equations 7.8 and 7.10.

7.6.1 SERIES IMPEDANCE

When the load is composed of different elements, the total ohmic value of the load is called *impedance*. In Figure 7.14, a resistance is connected in series with an inductive reactance. Each of these components is a complex parameter with a magnitude and phase angle as given in Equations 7.25 and 7.26. The impedance \bar{Z} of this load is

$$\bar{Z} = \bar{R} + \bar{X}_L = R\angle 0^\circ + X_L\angle 90^\circ = R + j X_L \tag{7.28}$$

The phasor diagram of the impedance is shown on the right side of Figure 7.14. Note that the impedance angle θ is positive and is equal in magnitude to the phase angle of the current in Figure 7.12.

Similarly, the capacitive load in Figure 7.15 is composed of a resistor and a capacitor connected in series. The impedance of this load can be expressed by Equation 7.29:

$$\bar{Z} = \bar{R} + \bar{X}_C = R\angle 0^\circ + X_C\angle -90^\circ = R - j X_C \tag{7.29}$$

The phasor diagram of the capacitive impedance is shown on the right side of Figure 7.15. Note that the capacitive reactance X_C lags the resistance by 90° .

Now let us assume a general case where a resistor is in series with a capacitor and an inductor. The circuit is shown in Figure 7.16. The impedance of the load can be expressed by

$$\bar{Z} = \bar{R} + \bar{X}_L + \bar{X}_C = R\angle 0^\circ + X_L\angle 90^\circ + X_C\angle -90^\circ = R + j (X_L - X_C) \tag{7.30}$$

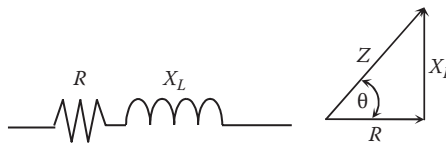


FIGURE 7.14 Series impedance of inductive load.

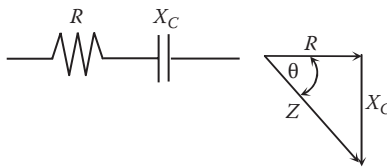


FIGURE 7.15 Series impedance of capacitive load.

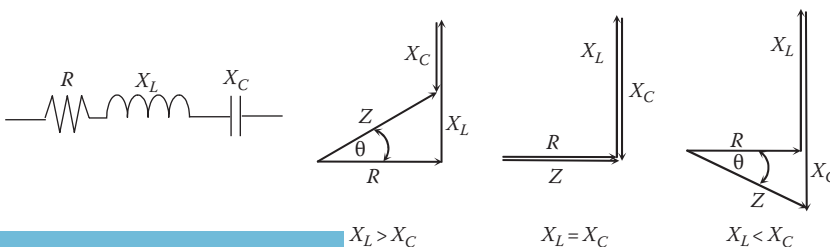


FIGURE 7.16 Series impedance of complex load.

Depending on the magnitude of the inductive reactance X_L with respect to the capacitive reactance X_C , the impedance diagram of the circuit can be any one of the three diagrams in Figure 7.16. In the first one on the left side, $X_L > X_C$ and the impedance angle is positive. Hence the circuit acts as if it contains the resistance, and an equivalent inductive reactance of a magnitude equals to $(X_L - X_C)$. When $X_L = X_C$, the impedance angle of the circuit is zero and the circuit impedance is equivalent to the resistance only. In the third case when $X_L < X_C$, the impedance angle is negative and the circuit acts as if it contains the resistance and an equivalent capacitive reactance of a magnitude equal to $(X_C - X_L)$.

Example 7.4

A load is composed of a $4\ \Omega$ resistance connected in series with a $3\ \Omega$ inductive reactance. The load is connected across a $120\ \text{V}$ source as shown in Figure 7.17. Compute the following:

1. Current of the circuit
2. Voltage across the resistance
3. Voltage across the inductive reactance

Solution

1. The current of the circuit is

$$\bar{I} = \frac{\bar{V}}{\bar{Z}}$$

where

$$\bar{Z} = R \angle 0^\circ + X_L \angle 90^\circ = R + jX_L = 4 + j3 = 5 \angle 36.87^\circ \ \Omega$$

Hence,

$$\bar{I} = 120 \angle 0^\circ / 5 \angle 36.87^\circ = 24 \angle -36.87^\circ \ \text{A}$$

2. The voltage across the resistance V_R is

$$\bar{V}_R = \bar{I} \bar{R} = (24 \angle -36.87^\circ) (4 \angle 0^\circ) = 96 \angle -36.87^\circ \ \text{V}$$

3. The voltage across the inductive reactance V_L is

$$\bar{V}_L = \bar{I} \bar{X}_L = (24 \angle -36.87^\circ) (3 \angle 90^\circ) = 72 \angle 53.13^\circ \ \text{V}$$

Keep in mind that the sum of the voltage across the resistance and across the inductive reactance yields the value of the source voltage. This, however, must be done using complex mathematics. Try it!

Also note that the impedance angle and the angle of the current are the same in magnitude, but opposite in sign, as shown in Figure 7.17.

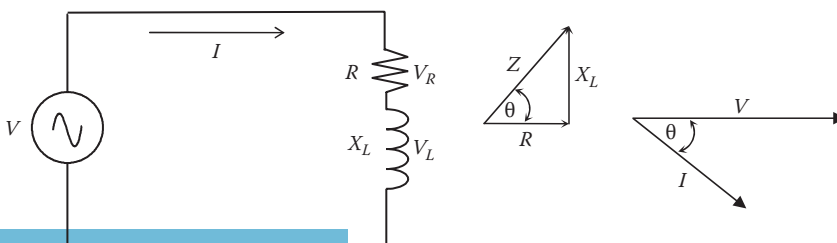


FIGURE 7.17 Circuit connection and phasor diagrams.

Example 7.5

A 120 V adjustable frequency ac source is connected in series with a resistor, an inductor, and a capacitor. At 60 Hz, the resistance is $5\ \Omega$, the inductive reactance is $3\ \Omega$, and the capacitive reactance is $4\ \Omega$:

1. Compute the load impedance at 60 Hz.
2. Compute the frequency at which the total impedance is equal to the load resistance only.

Solution

1. As given in Equation 7.30, the load impedance is

$$\bar{Z} = R + j(X_L - X_C) = 5 + j(3 - 4) = 5 - j = 5.1 \angle -11.31^\circ \Omega$$

2. First, let us compute the inductance and capacitance of the load

$$X_L = 2\pi fL$$

$$L = \frac{3}{2\pi \cdot 60} = 7.96 \text{ mH}$$

Similarly

$$X_C = \frac{1}{2\pi f_c C}$$

$$C = \frac{1}{2\pi \cdot 60} \times 4 = 663.15 \mu\text{F}$$

If $\bar{Z} = R$, then $X_L = X_C$. This can occur when the frequency of the supply voltage is changed until $X_L = X_C$. The frequency in this case is called *resonance frequency* or f_o .

$$X_L = X_C$$

$$2\pi f_o L = \frac{1}{2\pi f_o C}$$

$$f_o = \frac{1}{2\pi\sqrt{LC}} = \frac{10^3}{2\pi\sqrt{7.96 \times 0.66315}} = 69.27 \text{ Hz}$$

7.6.2 PARALLEL IMPEDANCE

In parallel connections, such as the one shown in Figure 7.18, the current of the source is divided among the parallel elements of the circuit according to the values of their impedances. The phasor

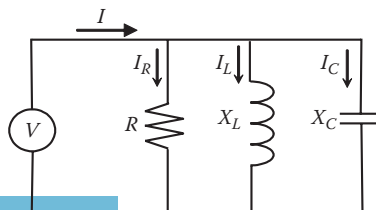


FIGURE 7.18 Parallel connection.

sum of all branch currents in a parallel circuit is equal to the current of the source. This can be represented mathematically as given in Equation 7.31.

$$\bar{I} = \bar{I}_R + \bar{I}_L + \bar{I}_C = \frac{\bar{V}}{R} + \frac{\bar{V}}{X_L} + \frac{\bar{V}}{X_C} = \bar{V} \left[\frac{1}{R} + \frac{1}{X_L} + \frac{1}{X_C} \right] = \frac{\bar{V}}{\bar{Z}} \tag{7.31}$$

Hence, the total impedance \bar{Z} is defined as

$$\frac{1}{\bar{Z}} = \frac{1}{R} + \frac{1}{X_L} + \frac{1}{X_C}$$

or

$$\bar{Y} = \bar{G} + \bar{B}_L + \bar{B}_C \tag{7.32}$$

where

$$\begin{aligned} \bar{Y} &= \frac{1}{\bar{Z}} \\ \bar{G} &= \frac{1}{R} = \frac{1}{R \angle 0^\circ} = \frac{1}{R} \angle 0^\circ \\ \bar{B}_L &= \frac{1}{X_L} = \frac{1}{X_L \angle 90^\circ} = \frac{1}{X_L} \angle -90^\circ \\ \bar{B}_C &= \frac{1}{X_C} = \frac{1}{X_C \angle -90^\circ} = \frac{1}{X_C} \angle 90^\circ \end{aligned} \tag{7.33}$$

where

G is called *conductance*, and its angle is zero

\bar{B}_L is called *inductive susceptance*

\bar{B}_C is called *capacitive susceptance*

Note that the angle of B_L is -90° as opposed to the angle of inductive reactance X_L which is $+90^\circ$. Similarly the angle of B_C is $+90^\circ$ as opposed to the angle of capacitive reactance X_C which is -90° . The sum of all conductances and susceptances is called *admittance* \bar{Y} :

$$\bar{Y} = \bar{G} + \bar{B}_L + \bar{B}_C = G + j(B_C - B_L) \tag{7.34}$$

The unit of $G, B_L, B_C,$ and Y is mho, which is the reverse spelling of the word ‘‘ohm.’’ The impedance diagram of the parallel circuit is shown in Figure 7.19. Compare these phasor diagrams with the ones shown in Figure 7.16 for series impedance.

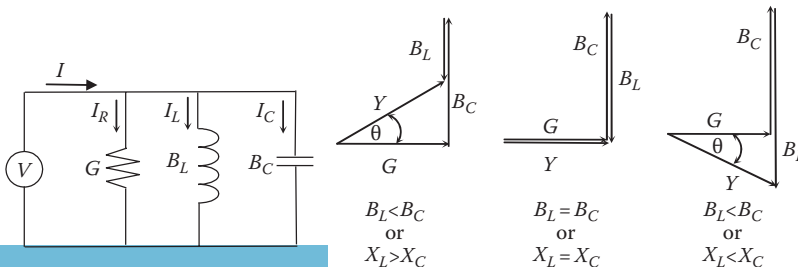


FIGURE 7.19 Parallel circuit.

Example 7.6

A 120 V adjustable frequency ac source is connected in parallel with a resistor, an inductor, and a capacitor as shown in Figure 7.18. At 60 Hz, the resistance is $5\ \Omega$, the inductive reactance is $10\ \Omega$ and the capacitive reactance is $2\ \Omega$:

1. Compute the load impedance at 60 Hz.
2. Compute the frequency at which the total impedance is equivalent to the load resistance only.

Solution

1. As given in Equation 7.34, the load admittance Y is

$$\bar{Y} = G + j(B_C + B_L) = \frac{1}{5} + \left(j\frac{1}{2} - \frac{1}{10} \right) = 0.2 + j0.4 \text{ mho}$$

The load impedance Z is

$$\bar{Z} = \frac{1}{\bar{Y}} = \frac{1}{0.2 + j0.4} = 1.0 - j2.0\ \Omega$$

2. First, let us compute the inductance and capacitance of the load $X_L = 2\pi fL$

$$L = \frac{10}{2\pi 60} = 26.5 \text{ mH}$$

Similarly

$$X_C = \frac{1}{2\pi f_C}$$

$$C = \frac{1}{2\pi 60 \times 2} = 1.326 \text{ mF}$$

If $Z = R$, then $B_L = B_C$. This can occur when the frequency of the supply voltage is changed to.

$$f_o = \frac{1}{2\pi\sqrt{LC}} = \frac{10^3}{2\pi\sqrt{26.5 \times 1.326}} = 26.83 \text{ Hz}$$

7.7 ELECTRIC POWER

The instantaneous power ρ is defined as the multiplication of the instantaneous voltage v by the instantaneous current i .

$$\rho = vi \tag{7.35}$$

Let us assume that the waveforms of the voltage and current are sinusoidal as described by Equations 7.1 and 7.7, respectively. Hence, the instantaneous power is

$$\begin{aligned} \rho &= v i = [V_{\max} \sin(\omega t)] [I_{\max} \sin(\omega t - \theta)] \\ \rho &= \frac{V_{\max} I_{\max}}{2} [\cos(\theta) - \cos(2\omega t - \theta)] \\ \rho &= \frac{V_{\max} I_{\max}}{\sqrt{2} \sqrt{2}} [\cos(\theta) - \cos(2\omega t - \theta)] \\ \rho &= VI [\cos(\theta) - \cos(2\omega t - \theta)] \end{aligned} \tag{7.36}$$

where V and I are the rms values of the sinusoidal waveforms v and i , respectively. θ is the impedance angle. Now, let us rewrite Equation 7.36 as follows:

$$\begin{aligned} \rho &= VI \cos(\theta) - VI \cos(2\omega t - \theta) \\ \rho &= P + h \end{aligned} \tag{7.37}$$

The first term P in Equation 7.37 is time invariant since V , I , and θ are all time independent. The second term h is time-varying sinusoid with a frequency equal to twice the frequency of the supply voltage and is shifted by θ . P and h are plotted in Figure 7.20.

For a purely resistive load, θ is zero.
Hence,

$$\begin{aligned} \rho &= vi = VI \cos(\theta) - VI \cos(2\omega t - \theta) \\ \rho &= VI [1 - \cos(2\omega t)] \end{aligned} \tag{7.38}$$

The power waveform for this case is shown in Figure 7.21. Note that the instantaneous power is always positive.

For a purely inductive load, the impedance angle $\theta = 90^\circ$, and its instantaneous power is given by Equation 7.39 and is shown in Figure 7.22:

$$\begin{aligned} \rho &= vi = VI [\cos(\theta) - \cos(2\omega t - \theta)] \\ \rho &= -VI \sin(2\omega t) \end{aligned} \tag{7.39}$$

Note that the average value of the instantaneous power is zero, which indicates that the inductor consumes power during the first $\frac{1}{4}$ of the voltage cycle, and then returns the power back during the second $\frac{1}{4}$ cycle. The inductor, in this case, does not consume any energy.

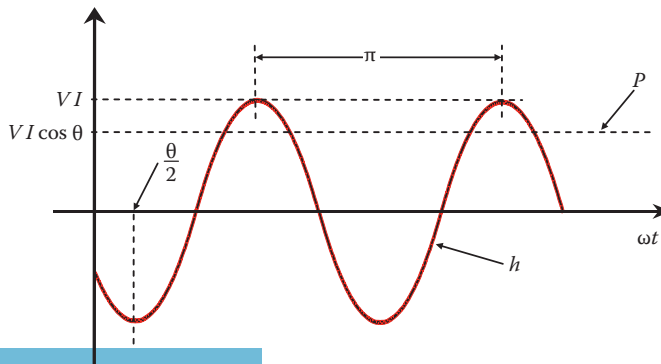


FIGURE 7.20 The two terms of the instantaneous power in Equation 7.37.

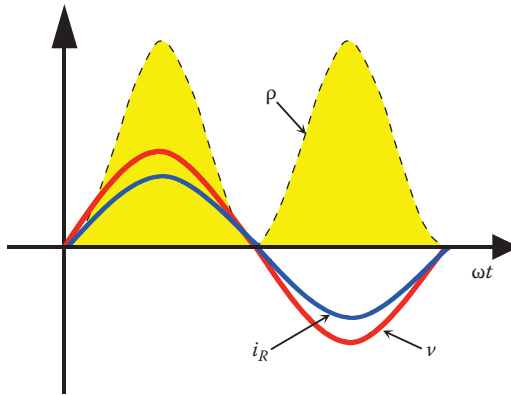


FIGURE 7.21 Instantaneous power of a purely resistive load.

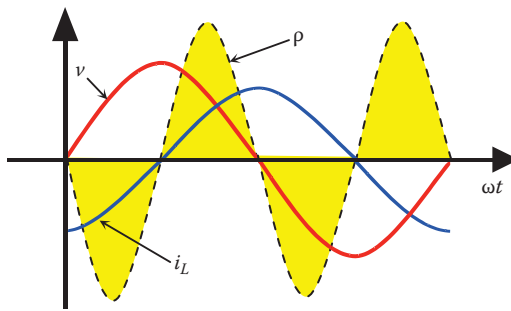


FIGURE 7.22 Instantaneous power of a purely inductive load.

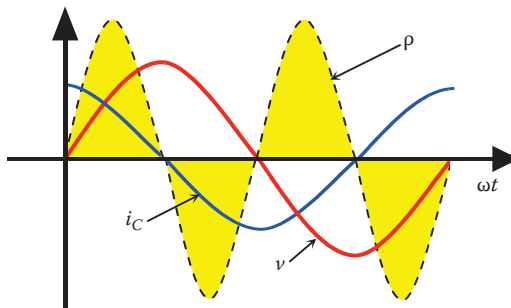


FIGURE 7.23 Instantaneous power of a purely capacitive load.

For a purely capacitive load, the impedance angle $\theta = -90^\circ$, and its instantaneous power is given by Equation 7.40 and shown in Figure 7.23.

$$\rho = vi = VI [\cos(\theta) - \cos(2\omega t - \theta)] \tag{7.40}$$

$$\rho = VI \sin(2\omega t)$$

Note that the average value of the instantaneous power for a capacitor is zero, which is similar to that for the inductance. In this case, the capacitor also exchanges energy with the source. In one cycle, the total energy consumed by the capacitor is zero.

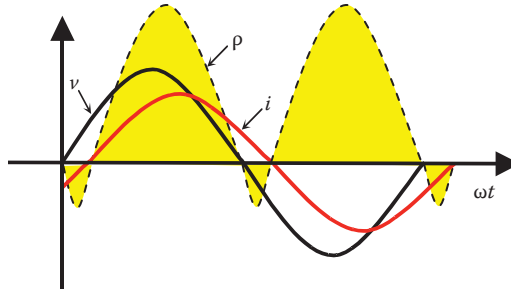


FIGURE 7.24 Instantaneous power of complex load.

For the general case of loads with any phase shift, Equation 7.37 can be used. For the case of lagging current, the waveforms are shown in Figure 7.24. Note that the average sum of the instantaneous power is nonzero.

7.7.1 REAL POWER

The power that produces energy is the average value of ρ given in Equation 7.37. Since the first term P in the equation is time invariant, its average value is the term itself. For the second term, h , its average value is zero since it is sinusoidal (i.e., symmetrical across the time axis). P is called *active power* or *real power*, and its units are Watt (W), Kilowatt (kW), Megawatt (MW), etc.:

$$P = \frac{1}{2\pi} \int_0^{2\pi} \rho \, d\omega t = \frac{1}{2\pi} \int_0^{2\pi} (P + h) \, d\omega t = \frac{VI}{2\pi} \int_0^{2\pi} [\cos \theta - \cos(2\omega t - \theta)] \, d\omega t \quad (7.41)$$

$$P = VI \cos(\theta)$$

7.7.2 REACTIVE POWER

The reactive power is the power exchanged between the source and the inductive or capacitive elements of the circuit. Recall that inductive and capacitive elements have their instantaneous powers in sinusoidal forms as shown in Figures 7.22 and 7.23. This means the power is drawn from the source and then delivered back to the source. To identify the reactive power mathematically, let us rewrite Equation 7.37 by expanding the term h :

$$\rho = VI \cos(\theta) - VI [\cos(\theta)\cos(2\omega t) + \sin(\theta)\sin(2\omega t)] \quad (7.42)$$

$$\rho = VI \cos(\theta)[1 - \cos(2\omega t)] - VI \sin(\theta)\sin(2\omega t)$$

where

$$P = VI \cos(\theta) \quad (7.43)$$

$$Q \equiv VI \sin(\theta)$$

Hence,

$$\rho = P[1 - \cos(2\omega t)] - Q \sin(2\omega t) \quad (7.44)$$

The term Q is called *imaginary power* or *reactive power*. It is time invariant and its unit is Voltampere reactive (VAr), Kilovoltampere reactive (KVAR), etc. Another method to compute the reactive power

is by using Ohm’s law. Assume that an inductive load is composed of a resistance in series with an inductive reactance. Since the magnitude of the voltage across the load is

$$V = IZ \tag{7.45}$$

and

$$\sin(\theta) = \frac{X_L}{Z}, \tag{7.46}$$

then

$$Q_L = VI \sin(\theta) = (IZ)I \frac{X_L}{Z} \tag{7.47}$$

$$Q_L = I^2 X_L$$

Similarly, for a capacitive load, it can be shown that the reactive power is

$$Q_C = I^2 X_C \tag{7.48}$$

7.7.3 COMPLEX POWER

The complex power is the phasor sum of the real and reactive powers. Let us first define complex power S as

$$\bar{S} \equiv \bar{V} \bar{I}^* \tag{7.49}$$

where \bar{I}^* is the conjugate of the current \bar{I} . If $\bar{I} = I \angle -\theta$, $\bar{I}^* = I \angle \theta$. This is the notion adapted over 100 years ago to make the reactive power of the inductor positive and that for the capacitor negative. Hence, for lagging current the complex power is

$$\bar{S} = \bar{V} \bar{I}^* = V \angle 0 \ I \angle \theta = VI \angle \theta = VI \cos(\theta) + j VI \sin(\theta) \tag{7.50}$$

Substituting the values of P and Q in Equation 7.43 into Equation 7.50 yields

$$\bar{S} = P + jQ \tag{7.51}$$

The complex power S is also known as the *apparent power*. Its units are voltampere (VA), kilovoltampere (KVA), etc. The phasor quantity \bar{S} in Equation 7.51 can be represented by the phasor diagram in Figure 7.25.

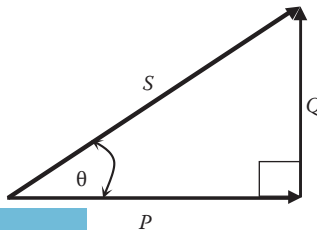


FIGURE 7.25 Phasor diagram of the complex power.

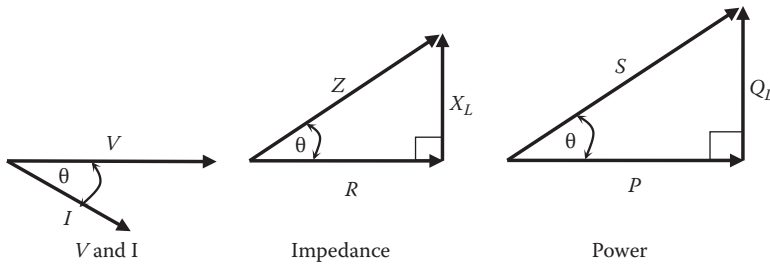


FIGURE 7.26 Phasor diagrams of inductive load.

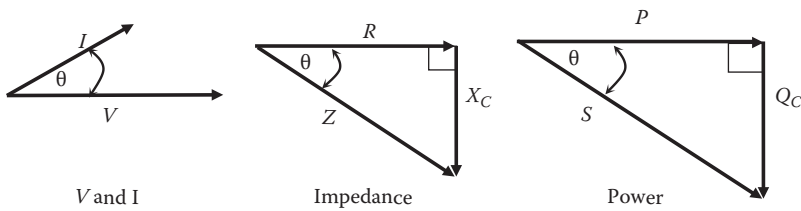


FIGURE 7.27 Phasor diagrams of capacitive load.

7.7.4 SUMMARY OF AC PHASORS

For the inductive load in Figure 7.17, the phasor diagrams of volt–current, impedance, and power are shown in Figure 7.26. In the volt–current diagram, the voltage is taken as the reference and the current lags the voltage by θ . In the impedance diagram, the resistance is always the reference and the inductive reactance leads the resistance by 90° . For the power diagram, the real power is always the reference and the inductive reactive power leads the real power by 90° .

For a capacitive load, the phasor diagrams are shown in Figure 7.27. Note that the reactive power of the capacitive load is lagging the real power by 90° , while the reactive power of the inductive load is leading.

Example 7.7

The voltage and current waveforms of an electric load are as follows:

$$v = 150 \sin(377t + 0.2) \text{ V}$$

$$i = 25 \sin(377t - 0.5) \text{ A}$$

Compute the following:

1. Frequency of the supply voltage
2. Phasor voltage
3. Phasor current
4. Real power of the load
5. Reactive power of the load

Solution

1. $\omega = 2\pi f = 377 \text{ rad/s}$

$$f = \frac{\omega}{2\pi} = \frac{377}{2\pi} = 60 \text{ Hz}$$

2. The phasor voltage is represented by the magnitude in rms and the phase angle in degrees. Note that the angles in the waveform equations are in radians:

$$\bar{V} = \frac{V_{\max}}{\sqrt{2}} \angle \theta_v = \frac{150}{\sqrt{2}} \angle \left(0.2 \frac{180}{\pi} \right) = 106.07 \angle 11.46^\circ \text{ V}$$

3. Similarly, the phasor current is

$$I = \frac{I_{\max}}{\sqrt{2}} \angle \theta_I = \frac{25}{\sqrt{2}} \angle \left(-0.5 \frac{180}{\pi} \right) = 17.68 \angle -28.65^\circ \text{ A}$$

4. The angle between the voltage and current is

$$\theta = \theta_v - \theta_I = 11.46 + 28.65 = 40.11^\circ$$

The real power of the load is

$$P = VI \cos(\theta) = 106.06 \times 17.67 \times \cos(40.11) = 1.434 \text{ kW}$$

5. The reactive power of the load is

$$Q = VI \sin(\theta) = 106.06 \times 17.67 \times \sin(40.11) = 1.208 \text{ kVAr}$$

7.7.5 POWER FACTOR

The apparent power S and the real power P are linearly related by the term $\cos(\theta)$:

$$P = VI \cos(\theta) = S \cos(\theta) \tag{7.52}$$

The ratio $P/S = \cos(\theta)$ is known as the *power factor pf*, and θ is known as the *power factor angle*. The power factor can be computed by various methods. Consider Figures 7.26 and 7.27. The *pf* in these figures is

$$pf = \cos(\theta) = \frac{P}{S} = \frac{R}{Z} \tag{7.53}$$

The power factor can be either *lagging* or *leading* depending on the angle of the current with respect to the voltage. When the current lags the voltage, the power factor is lagging. When the current leads the voltage, the power factor is leading.

7.7.6 PROBLEMS RELATED TO REACTIVE POWER

Reactive power does not produce work, and its presence in the system can create several problems. Consider the simple system in Figure 7.28 where the source is assumed to be at a distance from a

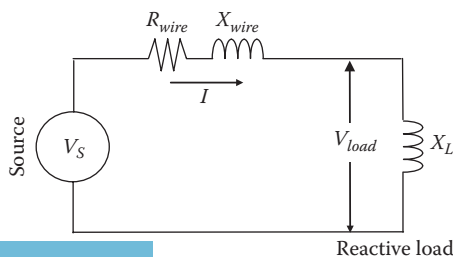


FIGURE 7.28 Currents due to inductive loads.

purely reactive load whose inductive reactance is X_L . The load is connected to the source by a cable (wire or transmission line). The wire has a resistance R_{wire} and an inductive reactance X_{wire} . The voltage of the source is V_S , and the voltage across the load is V_{load} .

The current in the wire is

$$\bar{I} = \frac{\bar{V}_S}{R_{wire} + j(X_{wire} + X_L)} \quad (7.54)$$

and the reactive power of the load is

$$Q_L = I^2 X_L \quad (7.55)$$

Keep in mind that only real power produces work and almost all utilities charge residential customers for real power only. It is highly unlikely that you pay for any reactive power that you consume in your house. Hence, the inductive load in Figure 7.28 does not generate any revenue to the utility; besides it creates several problems such as the following:

1. It increases the losses of the transmission line
2. It reduces the spare capacity of the line
3. It reduces the voltage across the load

The first problem can be understood by examining Equation 7.54. Because of the inductive load, the line current that feeds the inductive load results in real power loss in the wire P_{loss} , where

$$P_{loss} = I^2 R_{wire} \quad (7.56)$$

For the second problem, each transmission line has a capacity defined by the maximum current of the line which is determined by the wire's cross section and its material. The spare capacity is defined as the line capacity minus the actual current in the line. Because the reactive current is transmitted through the line, the spare capacity is reduced. This reduction in the spare capacity limits the ability of the utility to use the line to deliver real power to additional customers.

The third problem can be explained by considering the system in Figure 7.28, where the voltage on the load side \bar{V}_{load} can be expressed by

$$\bar{V}_{load} = \bar{I} jX_L = \bar{V}_S \frac{jX_L}{R_{wire} + j(X_{wire} + X_L)} \quad (7.57)$$

Hence, the magnitude of the load voltage V_{load} is

$$V_{load} = \frac{V_S}{\sqrt{\left(\frac{R_{wire}}{X_L}\right)^2 + \left(1 + \frac{X_{wire}}{X_L}\right)^2}} \quad (7.58)$$

Note that the load voltage decreases when the inductive reactance X_L decreases (i.e., more reactive load is added). Only when $X_L = \infty$ (i.e., no reactive load), the load voltage is equal to the source voltage.

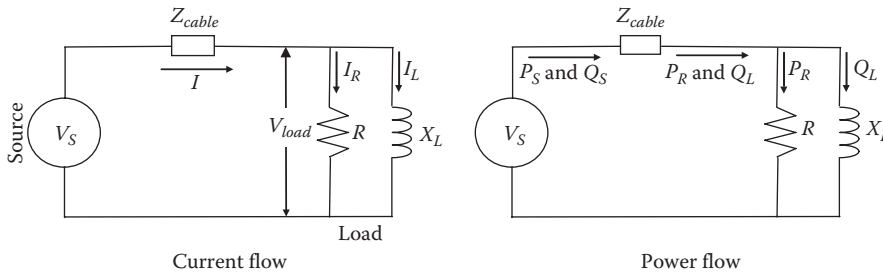


FIGURE 7.29 Current and power flow.

Example 7.8

The circuit in Figure 7.29 has a source voltage of 110 V at 60 Hz. The load, which is heavily inductive, consists of 20 Ω resistance in parallel with 10 Ω inductive reactance. The cable resistance is 1 Ω and its inductive reactance is 5 Ω. Compute the following:

1. Load impedance
2. Line current
3. Load voltage
4. Real and imaginary components of the load current
5. Real and reactive powers of the load
6. Real and reactive losses of the cable
7. Real and reactive power delivered by the source

Solution

1. The load admittance Y is

$$\bar{Y} = G - jB_L = \frac{1}{20} - j\frac{1}{10} = 0.05 - j0.1 \text{ mho}$$

The load impedance Z is

$$\bar{Z} = \frac{1}{\bar{Y}} = \frac{1}{0.05 - j0.1} = 4 + j8 \Omega$$

2. To compute the line current, we need to compute the total impedance of the circuit:

$$\bar{Z}_{total} = \bar{Z} + \bar{Z}_{cable} = (4 + j8) + (1 + j5) = 5 + j13 \Omega$$

$$\bar{I} = \frac{\bar{V}_S}{\bar{Z}_{total}} = \frac{110 \angle 0^\circ}{5 + j13} = 2.835 - j7.37 = 7.9 \angle -68.96^\circ \text{ A}$$

3. The load voltage can be computed by

$$\bar{V}_{load} = \bar{I} \bar{Z} = (7.9 \angle -68.96^\circ)(4 + j8) = 70.63 \angle -5.52^\circ \text{ V}$$

Note that the load voltage in this case is about 64% of the source voltage. This low voltage is mainly due to the voltage drop across the cable.

4. The real and imaginary components of the load current are as follows:

$$\bar{I}_R = \frac{\bar{V}_{load}}{R} = \frac{70.63\angle -5.52^\circ}{20} = 3.531\angle -5.52^\circ \text{ A}$$

$$\bar{I}_L = \frac{\bar{V}_{load}}{jX_L} = \frac{70.63\angle -5.52^\circ}{10\angle 90^\circ} = 7.06\angle -95.52^\circ \text{ A}$$

Note that the reactive current is higher than the real current. This is because X_L is smaller in magnitude than R .

5. The real and reactive power of the load are as follows:

$$P_R = I_R^2 R = (3.531)^2 \times 20 = 249.36 \text{ W}$$

$$Q_L = I_L^2 X_L = (7.06)^2 \times 10 = 498.437 \text{ VAr}$$

Note that the reactive power is higher than the real power. This is because I_L is larger in magnitude than I_R .

6. The real power loss of the cable is

$$P_{loss} = I^2 R_{cable} = 7.9^2 \times 1 = 62.41 \text{ W}$$

The reactive power loss of the cable is

$$Q_{loss} = I^2 X_{cable} = 7.9^2 \times 5 = 312.05 \text{ VAr}$$

7. The real power delivered by the source is the load's real power plus the real power loss of the line

$$P_s = P_R + P_{loss} = 249.36 + 62.41 = 311.77 \text{ W}$$

Similarly, the reactive power delivered by the source is

$$Q_s = Q_L + Q_{loss} = 498.437 + 312.05 = 810.487 \text{ VAr}$$

Example 7.9

Consider the system in Example 7.8, but assume that the load is purely resistive with no inductive elements. Compute the following:

1. Load impedance
2. Line current
3. Load voltage
4. Real and imaginary components of the load current

5. Real and reactive powers of the load
6. Real and reactive losses of the cable
7. Real and reactive power delivered by the source

Solution:

1. The load impedance Z is just the resistance only:

$$\bar{Z} = R = 20 \Omega$$

2. To compute the line current, we need to compute the total impedance of the circuit:

$$\bar{Z}_{total} = \bar{Z} + \bar{Z}_{cable} = 20 + (1.0 + j5) = 21 + j5 \Omega$$

$$\bar{I} = \frac{\bar{V}_s}{\bar{Z}_{total}} = \frac{110 \angle 0^\circ}{21 + j5} = 5.09 \angle -13.39^\circ \text{ A}$$

3. The load voltage is

$$\bar{V}_{load} = \bar{I} Z = 5.09 \angle -13.39^\circ \times 20 = 101.8 \angle -13.39^\circ \text{ V}$$

Note that the load voltage in this case is about 92% of the source voltage. This is a much higher magnitude than the case in Example 7.8.

4. The real component of the load current is the same as the line current since the imaginary current of the load is zero.

$$\bar{I}_R = \bar{I} = 5.09 \angle -13.39^\circ \text{ A}$$

5. The real power of the load is

$$P_R = I_R^2 R = 5.09^2 \times 20 = 518.16 \text{ W}$$

$$Q_L = 0 \text{ VAr}$$

6. The real power loss of the cable is

$$P_{loss} = I^2 R_{cable} = 5.09^2 \times 1 = 25.91 \text{ W}$$

The reactive power loss of the cable is

$$Q_{loss} = I^2 X_{cable} = 5.09^2 \times 5 = 129.54 \text{ VAr}$$

7. The real power delivered by the source is the load real power plus the line loss:

$$P_s = P_R + P_{loss} = 518.16 + 25.91 = 544.07 \text{ W}$$

The reactive power delivered by the source is

$$Q_s = Q_L + Q_{loss} = 0 + 129.54 = 129.54 \text{ VAr}$$

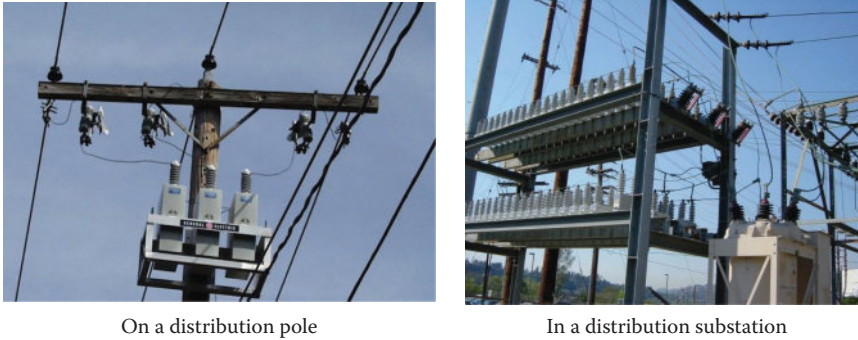


FIGURE 7.30 Capacitors for power factor correction.

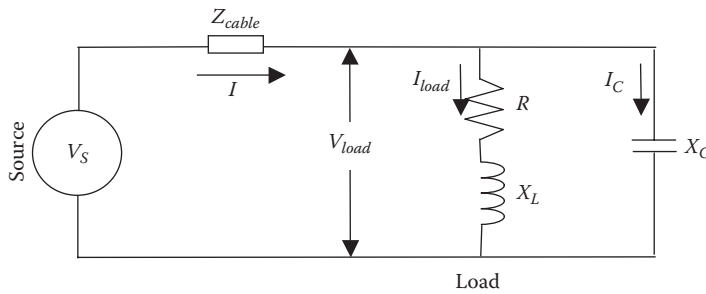


FIGURE 7.31 Power factor correction.

7.7.7 POWER FACTOR CORRECTION

As seen in the previous section, the inductive load increases cable losses, reduces the voltage across the load, and reduces the spare capacity of the transmission lines. For these reasons, most utilities install capacitors near the service areas to compensate for the reactive power consumed by the load. The photo in Figure 7.30 shows two compensation methods: the picture on the left side shows three rectangular-shaped capacitors mounted on a distribution pole close to a residential area; the picture on the right side shows a much larger compensation at a substation where a large number of capacitors are mounted on racks.

The circuit in Figure 7.31 shows a source feeding a load through a cable. Across the load, a compensation capacitor is installed. Since the reactive power of the purely inductive load is positive and that of the purely capacitive load is negative, the reactive power of the capacitor cancels the reactive power of the inductor. This process is called *power factor correction* or *reactive power compensation*. If the two reactive powers are summed up to zero, the source delivers only real power to the load. Thus, the problems associated with the reactive current on the transmission line are eliminated.

Example 7.10

The circuit in Figure 7.31 has a voltage source of 110 V, 60 Hz. The source is connected to an inductive load through a cable. The load impedance is $\bar{Z} = 3 + j4 \Omega$, the cable resistance is 1Ω , and the cable inductive reactance is 2Ω . Assume the capacitor is not connected to the circuit and compute the following:

1. Power factor of the load
2. Line current

3. Load voltage
4. Real and reactive powers of the load
5. Losses of the cable

If $6\ \Omega$ capacitive reactance is connected in parallel with the load, compute the following:

6. Power factor of the load plus the capacitor
7. Line current
8. Load voltage
9. Real and reactive powers of the load plus the capacitor

Solution

Without the capacitor

1. The power factor angle of the load is equal in magnitude to the angle of the load impedance.

$$\bar{Z} = R + jX_L = 3.0 + j4.0 = 5\angle 53.13^\circ\ \Omega$$

The power factor is

$$pf = \cos(53.13) = 0.6 \text{ lagging}$$

Note that the power factor must be identified with either *lagging* or *leading*. Lagging is when the current lags the voltage, which is the case of the inductive load.

2. To compute the line current, we need to compute the total impedance of the circuit:

$$\bar{Z}_{total} = \bar{Z} + \bar{Z}_{cable} = (3.0 + j4.0) + (1.0 + j2.0) = 4.0 + j6.0\ \Omega$$

$$\bar{I} = \frac{\bar{V}_s}{\bar{Z}_{total}} = \frac{110\angle 0^\circ}{4.0 + j6.0} = 8.461 - j12.69 = 15.254\angle -56.31^\circ\ \text{A}$$

3. The load voltage can be computed as follows:

$$\bar{V}_{load} = \bar{I} Z = (15.254\angle -56.31^\circ)(3 + j4) = 76.27\angle -3.18^\circ\ \text{V}$$

Note that the load voltage in this case is just about 69% of the source voltage.

4. The real and reactive power of the load can be computed as follows:

$$P_R = I^2 R = 15.254^2 \times 3 = 698.05\ \text{W}$$

$$Q_L = I^2 X_L = 15.254^2 \times 4 = 930.74\ \text{VAr}$$

5. The losses of the cable are as follows:

$$P_{loss} = I^2 R_{cable} = 15.254^2 \times 1 = 232.68\ \text{W}$$

$$Q_{loss} = I^2 X_{cable} = 15.254^2 \times 2 = 465.36\ \text{VAr}$$

With the capacitor

6. The load impedance Z_l is the load impedance in parallel with the capacitive reactance.

$$\bar{Y}_l = \frac{1}{\bar{Z}} + \frac{1}{\bar{X}_C} = \frac{1}{3.0 + j4.0} + \frac{1}{-j6.0} = 0.12 + j0.007 \text{ mho}$$

$$\bar{Z}_l = \frac{1}{\bar{Y}_l} = 8.32 \angle -3.18^\circ \Omega$$

The power factor is

$$pf = \cos(-3.18) = 0.9985 \text{ leading}$$

Note that the power factor is near unity.

7. Compute the total impedance of the circuit:

$$\bar{Z}_{total} = \bar{Z}_l + \bar{Z}_{cable} = 8.32 \angle -3.18^\circ + (1.0 + j2.0) = 9.307 + j1.538 \Omega$$

$$\bar{I} = \frac{\bar{V}_S}{\bar{Z}_{total}} = \frac{110 \angle 0^\circ}{9.307 + j1.538} = 11.505 - j1.901 = 11.66 \angle -9.38^\circ \text{ A}$$

Note that the line current with the capacitor installed is 11.66 A which is smaller than the line current computed in part 2 (15.254 A). This is about 23.5% reduction in the line current which increases the spare capacity of the cable.

8. The load voltage is

$$\bar{V}_{load} = \bar{I} \bar{Z}_l = 11.66 \angle -9.38^\circ (8.32 \angle -3.18^\circ) = 97.01 \angle -12.56^\circ \text{ V}$$

Note that the load voltage in this case is much higher than the case without the capacitor (in part 3).

9. Before we compute the powers, we need to compute the load current I_{load} and the capacitor current I_C :

$$\bar{I}_{load} = \frac{\bar{V}_{load}}{\bar{Z}} = \frac{97.01 \angle -12.56^\circ}{5.0 \angle 53.13^\circ} = 19.4 \angle -65.69^\circ \text{ A}$$

$$\bar{I}_C = \frac{\bar{V}_{load}}{\bar{X}_C} = \frac{97.01 \angle -12.56^\circ}{6.0 \angle -90^\circ} = 16.17 \angle 77.44^\circ \text{ A}$$

The real and reactive power of the load are

$$P_R = I_{load}^2 R = 19.4^2 \times 3 = 1.129 \text{ kW}$$

$$Q_L = I_{load}^2 X_L = 19.4^2 \times 4 = 1.505 \text{ kVAr}$$

$$Q_C = I_C^2 X_C = 16.17^2 \times 6 = 1.569 \text{ kVAr}$$

The total real power P_{total} of the load with the capacitor installed is the real power of the load alone. This is because the capacitor and the inductor consume no real power.

$$P_{total} = P_R = 1.129 \text{ kW}$$

The total reactive power Q_{total} is the phasor sum of the inductive and capacitive powers

$$\bar{Q}_{total} = \bar{Q}_L + \bar{Q}_C = j1.505 - j1.569 = -j64 \text{ VAR}$$

Note that the total reactive power on the load side without the capacitor is 930.74 VAR.

Example 7.11

The voltage source of the circuit in Figure 7.32 is 240 V, 60 Hz. The load consists of 4 Ω resistance in series with 3 Ω inductive reactance. A capacitor is installed to improve the power factor at the source side to unity. Compute the value of X_C .

Solution

We can solve this problem by several methods. One of them is to compute the reactive power of the load, then compute the value of X_C that produces capacitive reactive power equal in magnitude to the inductive power. Another method is to compute the value of X_C that would set the imaginary component of the total impedance to zero.

First method:

The current of the load is

$$\bar{I}_{load} = \frac{\bar{V}_S}{\bar{Z}} = \frac{240\angle 0^\circ}{4.0 + j3.0} = 38.4 - j28.8 = 48\angle -36.87^\circ \text{ A}$$

The reactive power of the load is

$$Q_L = I_{load}^2 X_L = (48)^2 \times 3 = 6.912 \text{ kVAR}$$

The reactive power of the capacitor must be equal (in magnitude) to the reactive power of the load:

$$Q_C = I_C^2 X_C = \frac{V_S^2}{X_C} = \frac{240^2}{X_C} = 6.912 \text{ kVAR}$$

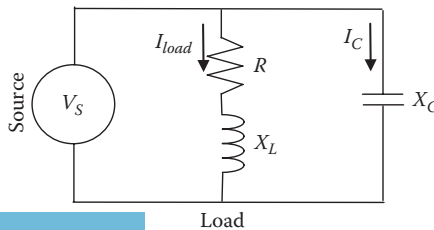


FIGURE 7.32 Compensated inductive load.

Hence,

$$X_C = \frac{240^2}{6912} = 8.33 \Omega$$

Second method:

The other method is to set the imaginary component of the total impedance equal to zero:

$$\begin{aligned} \operatorname{Im}\left(\frac{1}{Z} + \frac{1}{X_C}\right) &= 0 \\ \operatorname{Im}\left(\frac{1}{4.0 + j3.0} + \frac{1}{-jX_C}\right) &= 0 \\ 0.12 - \frac{1}{X_C} &= 0 \\ X_C &= 8.33 \Omega \end{aligned}$$

7.8 ELECTRIC ENERGY

The energy E consumed by a load is the power delivered to the load P over a period of time. The units of Energy are Watt hours (Wh), kWh, MWh, etc. For constant power during a given period τ , the energy is the shaded area under the power line in Figure 7.33.

$$E = P\tau \quad (7.59)$$

For time varying power, such as the one shown in Figure 7.34, the energy during a time period τ is the integral of the power over the period τ :

$$E = \int_0^{\tau} P dt \quad (7.60)$$

For discrete power, as in Figure 7.35, the energy is the summation of the power for each time segment:

$$E = \sum_i P_i t_i \quad (7.61)$$

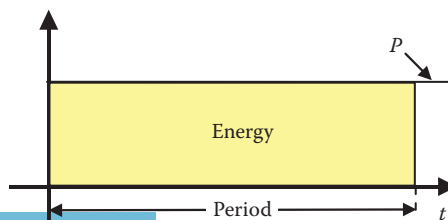


FIGURE 7.33 Energy of constant power.

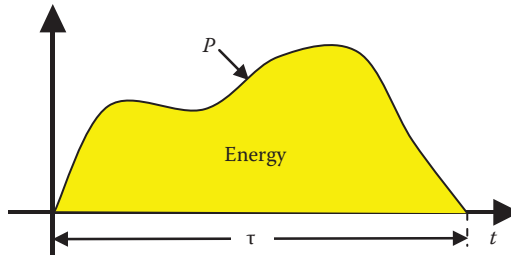


FIGURE 7.34 Energy of variable power.

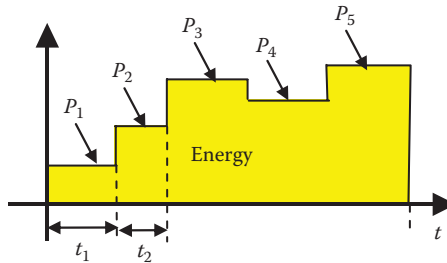


FIGURE 7.35 Energy of discrete power.

Example 7.12

An electric load is connected across a 120 V source. The load impedance is changing over a period of 24 h as follows:

Time Period	Load Impedance (Ω)	Power Factor Angle ($^\circ$)
8:00 AM–10:30 AM	10	30
11:00 AM–1:00 PM	20	0
3:00 PM–5:00 PM	15	60
5:00 PM–8:00 PM	5	45

Compute the energy consumed by the load during this 24 h period.

Solution

Time Period	Load Impedance Z (Ω)	Pf Angle θ ($^\circ$)	Load Current		Time Period (h)	Energy (Wh)
			$\frac{V_s}{Z}$ (A)	Load Power $V_s I \cos \theta$ (W)		
8:00 AM–10:30 AM	10	30	12	1247.08	2.5	3117.7
11:00 AM–1:00 PM	20	0	6	720	2	1440
3:00 PM–5:00 PM	15	60	8	480	2	960
5:00 PM–8:00 PM	5	45	24	2036.47	3	6109.41
Total Energy						11627.11

Example 7.13

A load is connected across a 120V source. The load power is represented by $P=25 + 100\sin(20t)$ kW where t is the time in hours. Compute the energy consumed by the load after 1 h and after 2 h.

Solution

$$E = \int_0^{\tau} P dt = \int_0^{\tau} (25 + 100\sin(20t)) dt = \left[25t - 100 \frac{\cos(20t)}{20} \right]_0^{\tau}$$

$$E = 25\tau - 5 \cos(20\tau) + 5$$

After 1 h, $\tau=1$

$$E = 25(1) - 5 \cos\left(20 \frac{180}{\pi}\right) + 5 = 27.96 \text{ kWh}$$

After 2 h, $\tau=2$

$$E = 25(2) - 5 \cos\left(40 \frac{180}{\pi}\right) + 5 = 58.33 \text{ kWh}$$

EXERCISES

7.1 Given the following two vectors

$$\bar{A} = 12 + j12$$

$$\bar{B} = -6 + j10,$$

Compute $\bar{A} + \bar{B}$, $\bar{A} - \bar{B}$, $\bar{A}\bar{B}$, and \bar{A}/\bar{B}

7.2 The voltage and current equations of an electric load are as follows:

$$v = V_{\max} \sin \omega t$$

$$i = I_{\max} \cos(\omega t - 30^\circ)$$

Compute the phase shift of the current.

7.3 The voltage and current of an electric load can be expressed by the following equations:

$$v = 340 \sin(628.318t + 0.5236)$$

$$i = 100 \sin(628.318t + 0.87266)$$

Calculate the following:

- The rms voltage
- The frequency of the current
- The phase shift between current and voltage in degrees

- d. The average voltage
- e. The load impedance

7.4 The current and voltage waveforms of an electric circuit are

$$i(t) = 25 \sin(377t + \pi/3) \text{A}; \quad v(t) = 169.7 \sin(377t - \pi/6) \text{V}$$

Compute the following:

- a. The rms voltage
- b. The rms current
- c. The frequency of the supply voltage
- d. The phase angle of the current with respect to voltage (indicate leading or lagging)
- e. The real power consumed by the circuit
- f. The reactive power consumed by the circuit
- g. The impedance of the circuit

7.5 An ac source is feeding a load that consists of a resistance and reactance connected in series. The voltage and current of the source are as follows:

$$v = 400 \sin(377t + 0.5236) \text{V}$$

$$i = 100 \sin(377t + 0.87266) \text{A}$$

Calculate the following:

- a. The resistance and inductive reactance of the load impedance
- b. The rms voltage across the resistance
- c. The frequency of the supply voltage
- d. Power factor at the source side, state leading or lagging
- e. The real power delivered to the load
- f. The reactive power delivered to the load

7.6 The waveform of an ac voltage can be expressed by $V = 180 \sin(300t + 3)$:

- a. Calculate the rms value of the voltage.
- b. Calculate the frequency of the supply.
- c. Calculate the phase shift in degrees.

7.7 An electric load consists of a 4Ω resistance, 6Ω inductive reactance and 8Ω capacitive reactance connected in series. The total impedance of the load is connected across a voltage source of 120 V:

- a. Compute the power factor of the load.
- b. Compute the source current.
- c. Compute the real power of the circuit.
- d. Compute the reactive power of the circuit.

7.8 A load impedance consists of 25Ω resistance in series with 38Ω inductive reactance. The load is connected across a 240 V source. Compute the real and reactive powers consumed by the load.

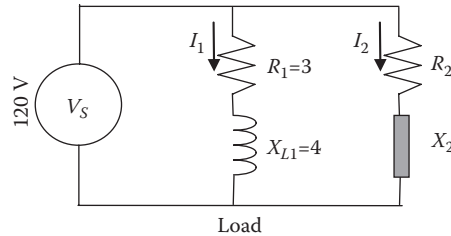
7.9 A voltage source $\bar{V} = 120 \angle 30^\circ$ is connected across a circuit consisting of $R = 3.5 \Omega$ in series with $L = 0.0833 \text{H}$. If the circuit is energized in the United States, compute the following:

- a. The load current
- b. The load power factor
- c. The real power consumed by the load
- d. The reactive power consumed by the load

7.10 A voltage source $\bar{V} = 120 \angle 30^\circ$ is connected to a circuit consisting of $R = 3.5 \Omega$ in series with $L = 0.0833 \text{H}$. If the circuit is energized in Europe, compute the following:

- a. The load current
- b. The load power factor

- c. The real power consumed by the load
 d. The reactive power consumed by the load
- 7.11** An inductive load consists of $R_1 = 3 \Omega$ in series with $X_{L1} = 4 \Omega$. The load is connected in parallel with another load of unknown impedance. The voltage source of the system is 120 V. The total real and reactive powers delivered by the source are 3 kW and 2 kVAr, respectively. Compute the impedance of the unknown load.



- 7.12** The rms voltage and current of an inductive load are 110 V and 10 A, respectively. The frequency of the voltage waveform is 60 Hz. The instantaneous power consumed by the load has no average value. Calculate the following:
- The real (active) power consumed by the load
 - The reactive power consumed by the load
 - The power factor
 - The frequency of the reactive power
- 7.13** An electric load consists of 5Ω resistance, 20Ω capacitive reactance, and 10Ω inductive reactance, all connected in parallel. A voltage source of 100 V is applied across the load. Compute the following:
- The real power of the load
 - The reactive power of the load
 - The current of the load
- 7.14** An inductive load consists of 1Ω resistance and 1.0 mH inductance connected in series. The load is connected across 120 V, 60 Hz source.
- Compute the power factor of the load.
 - A capacitor is connected in parallel with the entire load so that no reactive power is delivered by the source. Compute the value of the capacitance.
- 7.15** The power consumption of an electric load is represented by

$$P(t) = 100 \left(1 - e^{-\frac{t}{10}} \right) \text{ kW},$$

where t is the time of the day in hours.

Compute the energy consumed by the load in 24 h period.

8 Three-Phase Systems

High-power equipment such as generators, transformers, and transmission lines are built as three-phase equipment. The three-phase system has many advantages over the single-phase system; the most important ones are as follows:

1. Three-phase systems produce a rotating magnetic field inside the alternating current (ac) motors and, therefore, cause the motors to rotate without the need for extra controls. Since electric motors constitute the majority of electric energy consumed worldwide, having a rotating magnetic field is a very important advantage of three-phase systems. The theory of rotating fields is explained in Chapter 12.
2. Three-phase generators produce more power than single-phase generators of equivalent volume.
3. Three-phase transmission lines transmit three times the power of single-phase lines.
4. Three-phase systems are more reliable; when one phase is lost, the other two phases can still deliver some power to the loads.

8.1 GENERATION OF THREE-PHASE VOLTAGES

According to Faraday's law, when a conductor cuts magnetic field lines, a voltage is induced across the conductor. The synchronous generator uses this phenomenon to produce a three-phase voltage. A simple schematic of the generator is shown in Figure 8.1 and a more detailed analysis of the machine is given in Chapter 12. The generator consists of an outer frame called *stator* and a rotating magnet called *rotor*. At the inner perimeter of the stator, coils are placed inside slots. Each of the two slots separated by 180° houses a single coil ($a-a'$, $b-b'$, or $c-c'$). The coil is built by placing a wire inside a slot in one direction (e.g., a), and winding it back inside the opposite slot (a'). In Figure 8.1, we have three coils; each is separated by 120° from the other coils.

Now let us assume that the magnet is spinning clockwise inside the machine by an external prime mover. The magnetic field then cuts all coils and, therefore, induces a voltage across each of them. If each coil is connected to a load impedance, a current would flow into the load, and the generator produces electric energy that is consumed by the load. The dot inside the coil indicates a current direction toward the reader, and the cross indicates a current in the opposite direction.

The voltage across any of the three coils can be expressed by Faraday's law

$$e = nBl\omega \quad (8.1)$$

where

- e is the voltage induced across the coil
- n is the number of turns in the coil
- B is the flux density of the magnetic field
- l is the length of the slot
- ω is the angular speed of the rotor

The voltage induced on a conductor is proportional to the perpendicular component of the magnetic field with respect to the conductor. At the rotor position in Figure 8.1, coil $a-a'$ has the

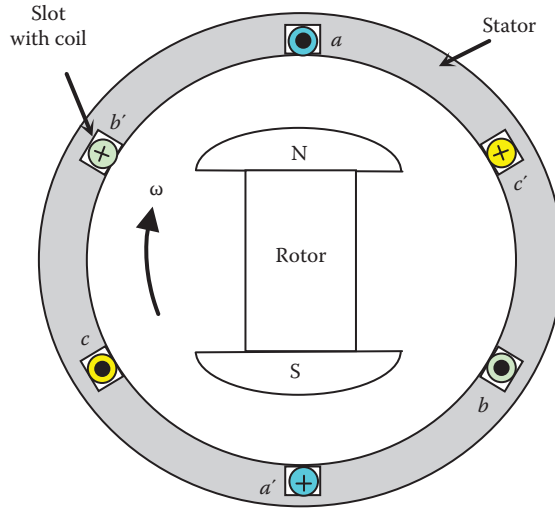


FIGURE 8.1 A three-phase generator.

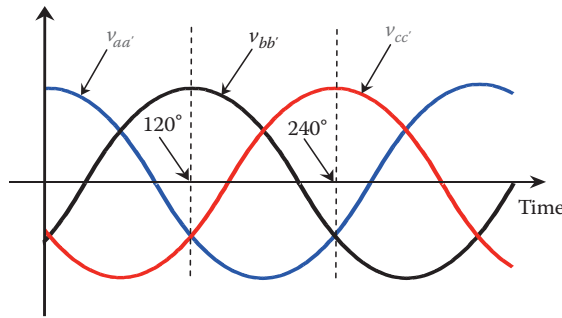


FIGURE 8.2 Waveforms of the three-phases of the generator.

maximum perpendicular field and, hence, it has the maximum induced voltage. Coil $b-b'$ will have its maximum voltage when the rotor moves clockwise by 120° , and coil $c-c'$ will have its maximum voltage when the rotor is at 240° position. If the rotation is continuous, the voltage across each coil is sinusoidal, all coils have the same magnitude of the maximum voltage, and the induced voltages are shifted by 120° from each other as shown in Figure 8.2. These characteristics form what is known as a balanced three-phase system.

To express the continuous waveforms of a balanced system mathematically, we need to select one of the waveforms as a reference and express all other waveforms in relative relations to it. Assuming that $v_{aa'}$ is our reference voltage, the waveforms in Figure 8.2 can be expressed by Equation 8.2

$$\begin{aligned}
 v_{aa'} &= V_{\max} \cos(\omega t) \\
 v_{bb'} &= V_{\max} \cos(\omega t - 120^\circ) \\
 v_{cc'} &= V_{\max} \cos(\omega t - 240^\circ) = V_{\max} \cos(\omega t + 120^\circ)
 \end{aligned}
 \tag{8.2}$$

where $v_{aa'}$, $v_{bb'}$, and $v_{cc'}$ are the instantaneous voltages of the three coils; these voltages are known as *phase voltages*. The phase in this case is the coil; so phase a is coil aa' , phase b is coil bb' , and

phase c is coil cc' . Notice that $v_{bb'}$ in Figure 8.2 lags $v_{aa'}$ by 120° , and $v_{cc'}$ leads $v_{aa'}$ by 120° . The maximum values of the phase voltages V_{\max} are equal. As given in Chapter 7, the waveforms in Equation 8.2 can be written in polar form

$$\begin{aligned} \bar{V}_{aa'} &= \frac{V_{\max}}{\sqrt{2}} \angle 0^\circ = V \angle 0^\circ \\ \bar{V}_{bb'} &= \frac{V_{\max}}{\sqrt{2}} \angle -120^\circ = V \angle -120^\circ \\ \bar{V}_{cc'} &= \frac{V_{\max}}{\sqrt{2}} \angle 120^\circ = V \angle 120^\circ \end{aligned} \tag{8.3}$$

where

- \bar{V} is the phasor voltage in complex number form
- V is the magnitude of the rms voltage

As explained in Chapter 7, the phasor diagram of $\bar{V}_{aa'}$ (the reference voltage) can be drawn as shown in Figure 8.3a. The direction of the arrow is from a' to a . The length of the arrow is equal to the rms value of $\bar{V}_{aa'}$. Similarly, the phasor diagrams of $\bar{V}_{bb'}$ and $\bar{V}_{cc'}$ are shown in Figure 8.3b and c, respectively.

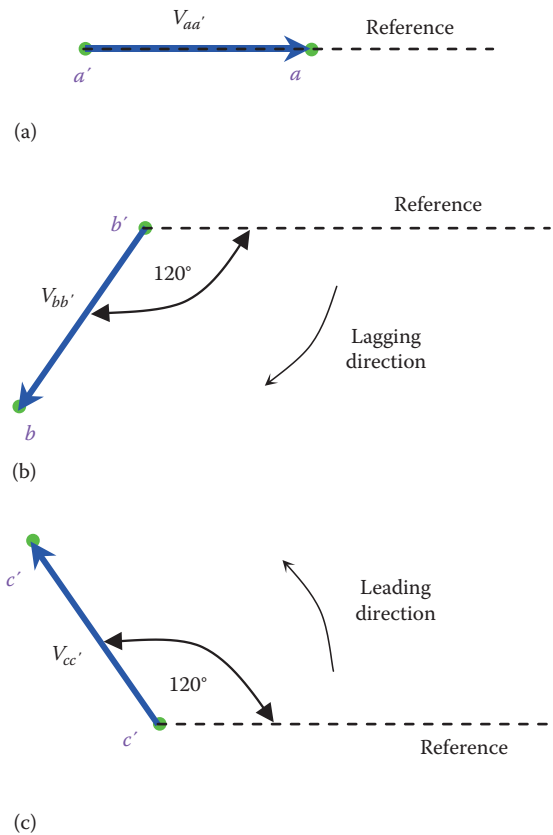


FIGURE 8.3 Phasor diagram of balanced three phases: (a) $\bar{V}_{aa'}$, (b) $\bar{V}_{bb'}$, and (c) $\bar{V}_{cc'}$.

8.2 CONNECTIONS OF THREE-PHASE CIRCUITS

The three-phase generator shown in Figure 8.1 has three independent coils and each coil represents a phase. Since each coil has two terminals, the generator has six terminals. To transmit the generated power from the power plant to the load centers, six wires seem to be needed. Since the transmission lines are often very long (hundreds of miles), the cost of the six wires is very high. To reduce the cost of the transmission system, the three coils are connected in a *wye* or *delta* configuration. The wye configuration is shown in Figure 8.4. The end of all the coils are bonded to a single point known as neutral. The other ends are connected to the three-wire (three-phase) system. In the delta configuration shown in Figure 8.5, the end of each coil is connected to the entrance of the adjacent coil. The entrance of each coil is then connected to one of the phases of the transmission line. In each of these configurations, only three wires are needed to transmit the power. These three wires are considered to be one circuit.

The generator is connected to the load via the three-wire transmission circuit as shown in Figure 8.6. This simple power circuit is divided into three distinct parts: source, load, and three-wire circuit. The three-wire circuit is called three-phase transmission line, or just transmission line. The currents in the transmission line conductors are called line currents. The voltages of the transmission line are classified by two variables: (1) line-to-neutral (line-to-ground) voltage and (2) line-to-line voltage as shown in Figures 8.4 and 8.5. The line-to-ground voltage is also called *phase voltage* or *phase-to-ground* voltage. The phase voltage is the voltage between any line and the ground (or neutral). The voltage between any two lines is the *line-to-line* voltage.

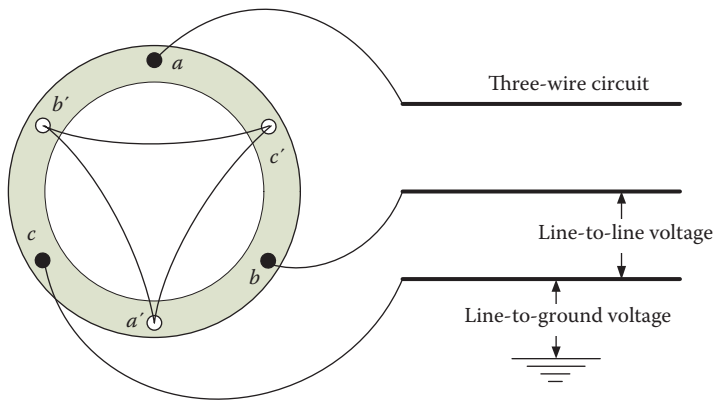


FIGURE 8.4 Wye-connected generator.

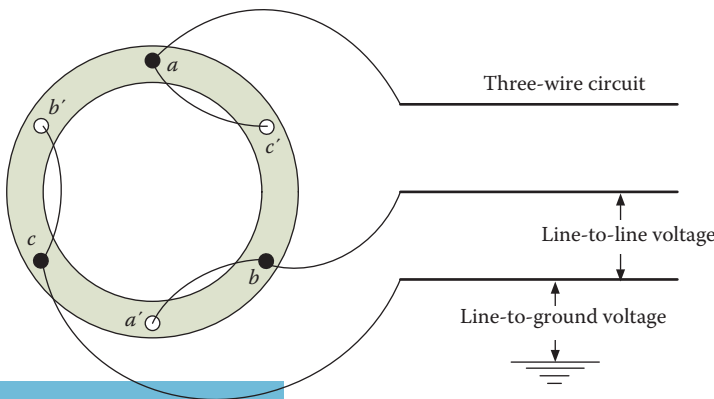


FIGURE 8.5 Delta-connected generator.

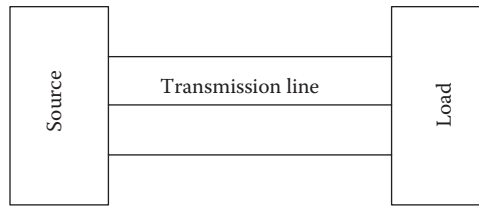


FIGURE 8.6 Circuit connection.



FIGURE 8.7 Transmission line with double circuits.

Figure 8.7 shows a photo of 500 kV transmission line that consists of two circuits. Each circuit is in three-phase configuration mounted on one side of the tower. The photo in Figure 8.8 shows a distribution pole with one circuit. The voltage level of this circuit is 15 kV. The photo also shows transformers mounted on the pole to step down the voltage from 15 kV to the household level.

8.2.1 WYE-CONNECTED BALANCED SOURCE

The wye connection is also referred to as “Y” or “Star.” For the generator in Figure 8.4, assume that the induced voltages in the three coils are represented by three voltage sources. To connect the coils in the wye configuration, terminals a' , b' , and c' of the three coils are bonded into a common point called neutral or n as shown on the left side of Figure 8.9. Since the coils are mechanically separated by 120° with respect to each other, we can also draw the three-phase wye configuration in the convenient diagram on the right side of Figure 8.9.



FIGURE 8.8 Single circuit distribution line.

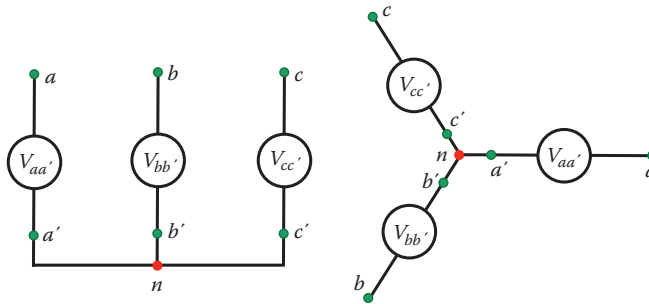


FIGURE 8.9 The connection of the three coils of the generator in wye.

The phasor diagram of the voltages of the three coils in wye configuration can be obtained by grouping the three phasors in Figure 8.3 as shown in Figure 8.10a. Since the common point is n , the phasors can be labeled \bar{V}_{an} , \bar{V}_{bn} , and \bar{V}_{cn} as shown in Figure 8.10b. Keep in mind that \bar{V}_{an} , \bar{V}_{bn} , and \bar{V}_{cn} represent the voltages of the coils.

For balanced systems, the magnitudes of the rms voltages for all phases are equal, that is,

$$V_{an} = V_{bn} = V_{cn} \tag{8.4}$$

In wye configuration, the three terminals of the generator (a , b , and c) in Figures 8.4 and 8.9 are connected to the three-wire transmission line as shown in Figure 8.11. The neutral point is often connected to the ground and no additional wire is needed. The magnitude of the phase voltage of the transmission line (V_{ph}) is equal to the voltage of any coil. Hence,

$$V_{ph} = V_{an} = V_{bn} = V_{cn} \tag{8.5}$$

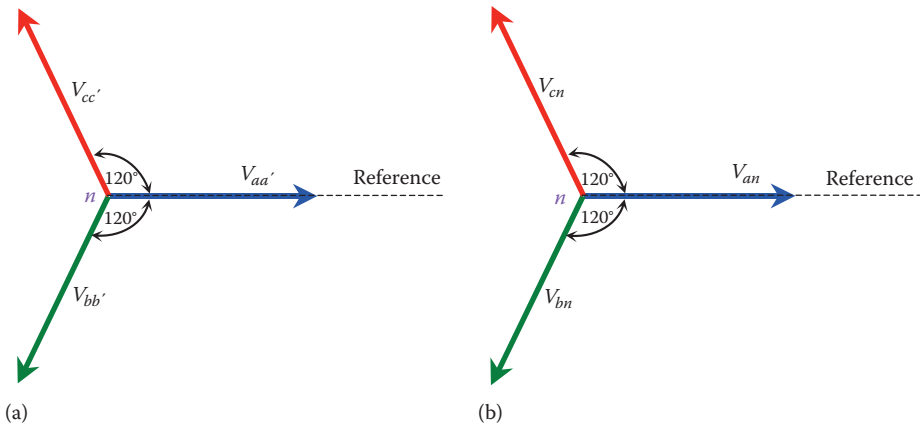


FIGURE 8.10 Phasor diagram of the three phases. (a) Terminal voltage of coil, (b) coil voltage with respect to neutral.

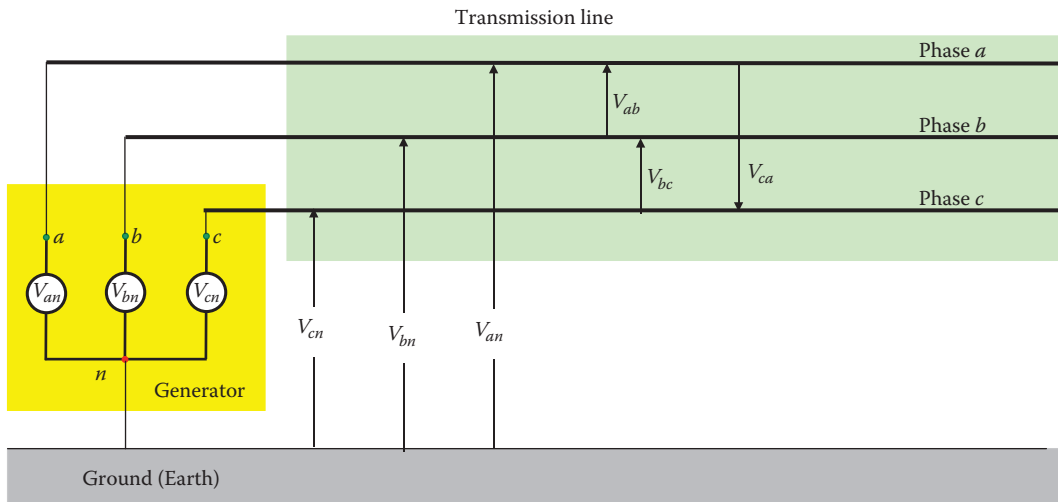


FIGURE 8.11 Three-phase wye generator connected to three-phase transmission line.

Equation 8.3 can then be rewritten as

$$\begin{aligned} \bar{V}_{an} &= V_{ph} \angle 0^\circ \\ \bar{V}_{bn} &= V_{ph} \angle -120^\circ \\ \bar{V}_{cn} &= V_{ph} \angle 120^\circ \end{aligned} \tag{8.6}$$

The line-to-line voltage of the transmission line between *a* and *b* is \bar{V}_{ab} ; it is the potential of phase *a* minus the potential of phase *b*:

$$\bar{V}_{ab} = \bar{V}_{an} - \bar{V}_{bn} \tag{8.7}$$

Substituting the values of \bar{V}_{an} and \bar{V}_{bn} of Equation 8.6 into Equation 8.7 yields

$$\bar{V}_{ab} = V_{ph} \angle 0^\circ - V_{ph} \angle -120^\circ = \sqrt{3} V_{ph} \angle 30^\circ \tag{8.8}$$

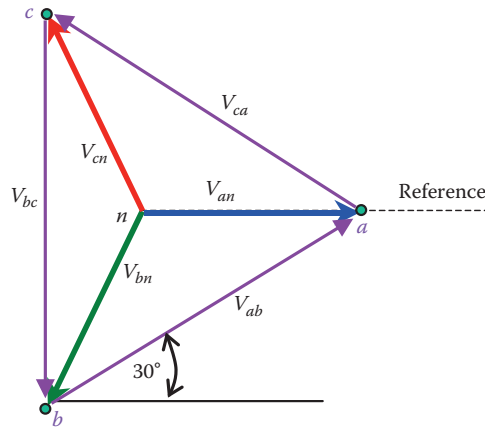


FIGURE 8.12 Phasor diagram of the phase and line-to-line voltages.

Two important observations can be made from Equation 8.8:

1. Magnitude of the line-to-line voltage of the transmission line is larger than the magnitude of its phase voltage by a factor of $\sqrt{3}$.
2. Line-to-line voltage \bar{V}_{ab} of the transmission line leads its phase voltage \bar{V}_{an} by 30° .

Similarly, the line-to-line voltages of the transmission line \bar{V}_{bc} and \bar{V}_{ca} can be computed as given in Equation 8.9:

$$\begin{aligned}\bar{V}_{bc} &= \bar{V}_{bn} - \bar{V}_{cn} = V_{ph} \angle -120^\circ - V_{ph} \angle 120^\circ = \sqrt{3} V_{ph} \angle -90^\circ \\ \bar{V}_{ca} &= \bar{V}_{cn} - \bar{V}_{an} = V_{ph} \angle 120^\circ - V_{ph} \angle 0^\circ = \sqrt{3} V_{ph} \angle 150^\circ\end{aligned}\quad (8.9)$$

Note that phasor \bar{V}_{bc} leads \bar{V}_{bn} by 30° , and phasor \bar{V}_{ca} leads \bar{V}_{cn} by 30° . The transmission line phasor diagram of all phase and line-to-line voltages is shown in Figure 8.12. Keep in mind that the direction of any phasor is determined by the subscript of the phasor, for example, the direction of \bar{V}_{ca} is from point a to point c .

From Equations 8.8 and 8.9, we can write the line-to-line voltages of the transmission line as

$$\begin{aligned}\bar{V}_{bc} &= \bar{V}_{ab} \angle -120^\circ \\ \bar{V}_{ca} &= \bar{V}_{ab} \angle 120^\circ\end{aligned}\quad (8.10)$$

Hence, the line-to-line voltages of the transmission line are also balanced; they are equal in magnitude and are shifted by 120° from each other. In generic terms, we can relate the magnitude of the line-to-line voltage V_{ll} to the phase voltage V_{ph} by

$$V_{ll} = \sqrt{3} V_{ph}\quad (8.11)$$

Example 8.1

A Y-connected balanced three-phase source has a voltage of $\bar{V}_{an} = 120 \angle 40^\circ \text{ V}$. Compute the line-to-line voltage of the transmission line.

Solution

Note that \bar{V}_{an} is not in phase with the reference. Since \bar{V}_{bc} lags \bar{V}_{an} by 120° , and \bar{V}_{cn} leads \bar{V}_{an} by 120° ,

$$\bar{V}_{bn} = \bar{V}_{an} \angle -120^\circ = (120 \angle 40^\circ) \angle -120^\circ = 120 \angle -80^\circ \text{ V}$$

$$\bar{V}_{cn} = \bar{V}_{an} \angle 120^\circ = (120 \angle 40^\circ) \angle 120^\circ = 120 \angle 160^\circ \text{ V}$$

The line-to-line voltages of the transmission line can be computed as follows:

$$\bar{V}_{bc} = \bar{V}_{bn} - \bar{V}_{cn} = (120 \angle -80^\circ) - (120 \angle 160^\circ) = 133.59 - j159.22 = 207.84 \angle -50^\circ \text{ V}$$

Note that if we use the basic relationships between the phase and line-to-line voltages given in Equations 8.8 through 8.10, we can solve this problem without the need for complex number computations. First, we know that the magnitude of the line-to-line voltage is $\sqrt{3} V_{ph}$; then

$$V_{ab} = \sqrt{3} V_{ph} = \sqrt{3} \times 120 = 207.84 \text{ V}$$

Second, we know that \bar{V}_{ab} is leading \bar{V}_{an} by 30° as given in Equation 8.8; then

$$\bar{V}_{ab} = 207.84 \angle (40^\circ + 30^\circ) = 207.84 \angle 70^\circ \text{ V}$$

From Equation 8.10, \bar{V}_{bc} lags \bar{V}_{ab} by 120°

$$\bar{V}_{bc} = \bar{V}_{ab} \angle -120^\circ = 207.84 \angle (70^\circ - 120^\circ) = 207.84 \angle -50^\circ \text{ V}$$

8.2.2 DELTA-CONNECTED BALANCED SOURCE

The delta (Δ) configuration can be made by cascading the coils of the generator as shown in Figure 8.5; terminal a' is connected to b , b' is connected to c , and c' is connected to a . The connection is also depicted on the left side of Figure 8.13. The voltage sources of the delta connection can be drawn in the convenient descriptive diagram on the right side of Figure 8.13. Since point a' is the same as b , b' is the same as c , and c' is the same as a , hence

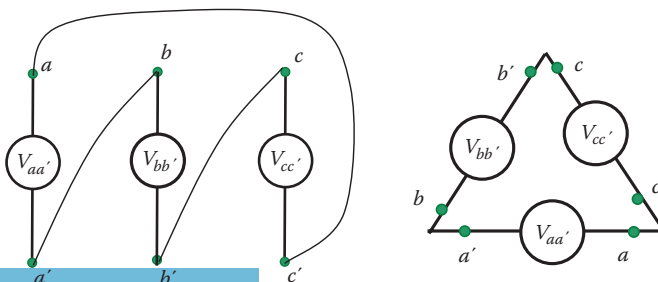


FIGURE 8.13 Delta connection.

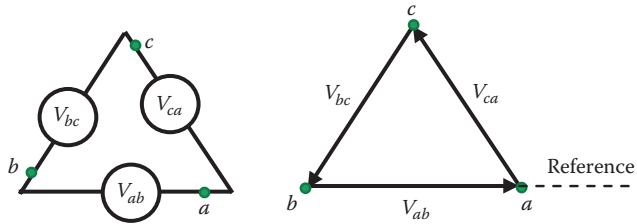


FIGURE 8.14 Delta connection and its phasor diagram.

$$\begin{aligned}
 \bar{V}_{aa'} &= \bar{V}_{ab} \\
 \bar{V}_{bb'} &= \bar{V}_{bc} \\
 \bar{V}_{cc'} &= \bar{V}_{ca}
 \end{aligned}
 \tag{8.12}$$

The wiring connection and the phasor diagram of the delta configuration are shown in Figure 8.14. In the wiring connection, a' , b' , and c' are removed as they are the same points as b , c , and a , respectively. Because the waveforms of the three phases are continuous, the reference phasor can be arbitrarily selected. The phasor diagram in Figure 8.14 has \bar{V}_{ab} as a reference.

A delta-connected generator is attached to a three-phase transmission line as shown in Figure 8.15. At the transmission line, the line-to-line voltage of the line is the same as the voltage of the coil. Hence,

$$\begin{aligned}
 \bar{V}_{ab} &= \bar{V}_{aa'} \\
 V_{bc} &= \bar{V}_{bb'} \\
 \bar{V}_{ca} &= \bar{V}_{cc'}
 \end{aligned}
 \tag{8.13}$$

8.2.3 WYE-CONNECTED BALANCED LOAD

Residential loads in the United States are normally single-phase loads at 120 and 240 V. Small loads that draw small currents such as lights, televisions, and radios are powered at 120 V. Heavier

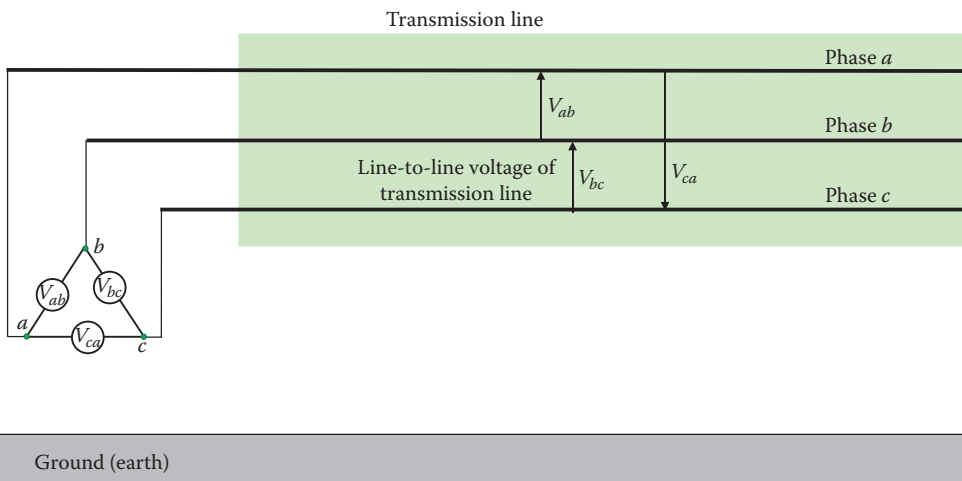


FIGURE 8.15 A three-phase generator connected to a three-phase transmission line.

loads such as furnaces, stoves, and dryers are powered at 240 V. Industrial and commercial loads are mostly three-phase loads at various line-to-line voltage levels (208 V, 480 V, 5 kV, 15 kV). As a general rule, the larger the power demand, the higher is the voltage. Although household equipment are single-phase loads, clustered residential areas are powered by three phases. Each group of houses is powered by one phase while other groups are powered by the other phases. This is done to balance the loads among the three phases. The three-phase loads are connected in various configurations with the most common ones being the wye and the delta. All residential loads and most commercial and industrial loads are connected in grounded wye to ensure that the voltage across the load is constant regardless of any fluctuation in load currents. Figure 8.16 shows a wye-connected load where Z_{an} , Z_{bn} , and Z_{cn} are called *load impedances*. For balanced systems, the load impedances are identical:

$$\bar{Z}_{an} = \bar{Z}_{bn} = \bar{Z}_{cn} = \bar{Z} \tag{8.14}$$

For residential loads, each of Z_{an} , Z_{bn} , or Z_{cn} represents a group of houses. Although the demands in any neighborhood differ from house to house due to the various energy consumption habits of the customers, three-phase loads are almost balanced over a wide residential area.

Figure 8.17 shows a wye-connected load powered by a wye-connected source. The transmission line connecting the load to the source is a four-wire system. The neutral points of the load and that of the source are connected by the fourth wire. In some cases, the neutral wire is replaced by the earth (ground). Assume that the load is balanced and the voltage \bar{V}_{an} is phase shifted from an arbitrary reference by an angle θ . The load currents can then be computed as

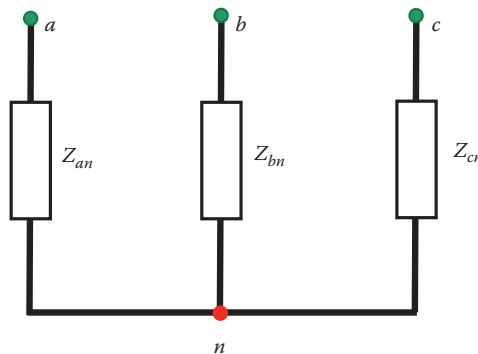


FIGURE 8.16 Three loads connected in wye.

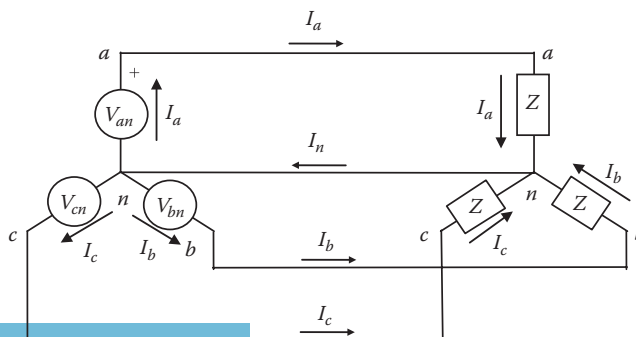


FIGURE 8.17 Loads connected in wye.

$$\begin{aligned}\bar{I}_a &= \frac{\bar{V}_{an}}{\bar{Z}_{an}} = \frac{\bar{V}_{an}}{\bar{Z}} = \frac{V_{ph}\angle\theta}{Z\angle\varphi} = \frac{V_{ph}}{Z}\angle(\theta - \varphi) \\ \bar{I}_b &= \frac{\bar{V}_{bn}}{\bar{Z}_{bn}} = \frac{\bar{V}_{bn}}{\bar{Z}} = \frac{V_{ph}\angle(\theta - 120^\circ)}{Z\angle\varphi} = \frac{V_{ph}}{Z}\angle(\theta - \varphi - 120^\circ) \\ \bar{I}_c &= \frac{\bar{V}_{cn}}{\bar{Z}_{cn}} = \frac{\bar{V}_{cn}}{\bar{Z}} = \frac{V_{ph}\angle(\theta + 120^\circ)}{Z\angle\varphi} = \frac{V_{ph}}{Z}\angle(\theta - \varphi + 120^\circ)\end{aligned}\quad (8.15)$$

Two observations can be made by examining Equation 8.15:

1. Magnitudes of \bar{I}_a , \bar{I}_b , and \bar{I}_c are equal.
2. Current \bar{I}_a leads \bar{I}_b by 120° , and \bar{I}_b leads \bar{I}_c by 120° .

The currents and voltages of the circuit are shown in Figure 8.17. The currents of the transmission line connecting the source to the load (known as *line currents*) are equal to the currents in the load impedances. The phasor diagram of the circuit is shown in Figure 8.18. Using Kirchhoff's current rule, the sum of the three line currents \bar{I}_a , \bar{I}_b , and \bar{I}_c entering the neutral node n of the load is equal to the current exiting the node \bar{I}_n . Hence,

$$\bar{I}_n = \bar{I}_a + \bar{I}_b + \bar{I}_c \quad (8.16)$$

If the load is balanced, the sum of all load currents is zero

$$\bar{I}_n = \bar{I}_a + \bar{I}_a\angle -120^\circ + \bar{I}_a\angle 120^\circ = \bar{I}_a(1 + 1\angle -120^\circ + 1\angle 120^\circ) = 0 \quad (8.17)$$

Since $\bar{I}_n = 0$, there is no need to have a wire connecting the neutral points of the Y -connected generator and the Y -connected load. Both neutrals can be connected to the local grounds.

For the three-phase system in Figure 8.17, there are three independent loops with the neutral wire as a common branch. If the system is balanced, we need to only analyze one transmission line, one generator coil, and one load impedance. The voltages and currents of the other two lines can be obtained by the relationships in Equations 8.10 and 8.15. Figure 8.19 shows a single-phase representation of a balanced three-phase system.

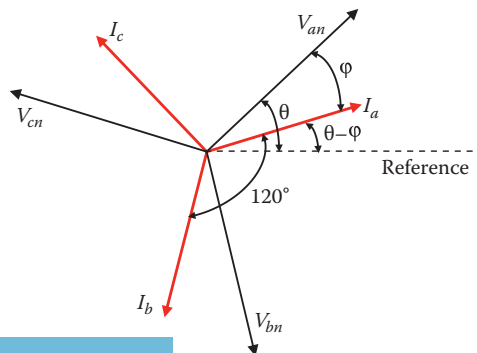


FIGURE 8.18 Phasor diagram of loads connected in wye.

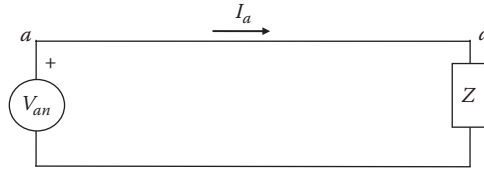


FIGURE 8.19 Single-phase representation of the circuit in Figure 8.17.

Example 8.2

The phase voltage of a balanced three-phase source is $\bar{V}_{an} = 120\angle -40^\circ \text{ V}$. The source is energizing a balanced three-phase load connected in wye. The load impedance is $\bar{Z} = 20\angle 30^\circ \Omega$. Compute the following:

1. Load currents
2. Neutral current
3. Line-to-line voltages of the transmission line

Solution

Use the single-phase representation of the balanced three-phase system shown in Figure 8.19.

1.
$$\bar{I}_a = \frac{\bar{V}_{an}}{\bar{Z}} = \frac{120\angle -40^\circ}{20\angle 30^\circ} = 6\angle -70^\circ \text{ A}$$

The currents of the other loads can be computed by the relationships of the balanced system:

$$\bar{I}_b = \bar{I}_a \angle -120^\circ = 6\angle -190^\circ \text{ A}$$

$$\bar{I}_c = \bar{I}_a \angle 120^\circ = 6\angle 50^\circ \text{ A}$$

2.
$$\bar{I}_n = \bar{I}_a + \bar{I}_b + \bar{I}_c = 6\angle -70^\circ + 6\angle -190^\circ + 6\angle 50^\circ = 0$$

3.
$$\bar{V}_{ab} = \sqrt{3} \bar{V}_{an} \angle 30^\circ = \sqrt{3} (120\angle -40^\circ) \angle 30^\circ = 207.84\angle -10^\circ \text{ V}$$

$$\bar{V}_{bc} = \bar{V}_{ab} \angle -120^\circ = (207.84\angle -10^\circ) \angle -120^\circ = 207.84\angle -130^\circ \text{ V}$$

$$\bar{V}_{ca} = \bar{V}_{ab} \angle 120^\circ = 207.84\angle 110^\circ \text{ V}$$

The main conclusions of the wye-connected load are the following:

1. For transmission line, the magnitude of the line-to-line voltage is greater than the phase voltage by a factor of $\sqrt{3}$.
2. For transmission line, the line-to-line voltage \bar{V}_{ab} leads its phase voltage \bar{V}_{an} by 30° . Similar conclusions can be made for the other two phases.
3. Line currents are equal to the corresponding currents of the loads.
4. No current flows through the neutral wire, so there is no need for a wire between the neutral points in Figure 8.17.

8.2.4 DELTA-CONNECTED BALANCED LOAD

A balanced three-phase load connected in delta is shown in Figure 8.20. The load impedance of each phase is connected between two transmission lines. Hence, the voltage across any load impedance is the line-to-line voltage of the transmission line.

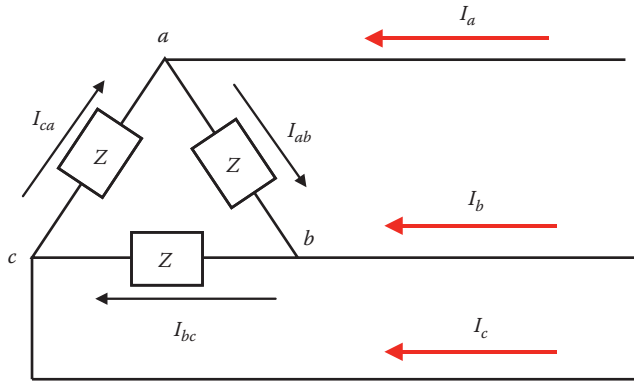


FIGURE 8.20 Three-phase load connected in delta.

At the transmission line, the currents feeding the load are \bar{I}_a , \bar{I}_b , and \bar{I}_c . The currents in the load impedances are \bar{I}_{ab} , \bar{I}_{bc} , and \bar{I}_{ca} . The relationship between the transmission line currents and the load currents can be obtained by examining Kirchhoff's nodal equations at points a , b , and c .

$$\begin{aligned}\bar{I}_{ab} &= \bar{I}_a + \bar{I}_{ca} \\ \bar{I}_{bc} &= \bar{I}_b + \bar{I}_{ab} \\ \bar{I}_{ca} &= \bar{I}_c + \bar{I}_{bc}\end{aligned}\quad (8.18)$$

The load currents can be computed by dividing the voltage across the load impedance by the load impedance. Since the voltage across the load impedance is equal to the line-to-line voltage of the transmission line, the load currents are as follows:

$$\begin{aligned}\bar{I}_{ab} &= \frac{\bar{V}_{ab}}{\bar{Z}} \\ \bar{I}_{bc} &= \frac{\bar{V}_{bc}}{\bar{Z}} \\ \bar{I}_{ca} &= \frac{\bar{V}_{ca}}{\bar{Z}}\end{aligned}\quad (8.19)$$

Since the impedances of all loads are equal and the line-to-line voltages are balanced, the load currents must also be balanced.

Example 8.3

The voltage of a three-phase, Y -connected source is $\bar{V}_{an} = 120\angle -40^\circ$ V. The source is energizing a three-phase load connected in delta. The load impedance is $\bar{Z} = 10\angle -30^\circ \Omega$. Compute the currents of the load.

Solution

The first step is to compute the voltages across all three loads, which are the same as the line-to-line voltages of the transmission line:

$$\bar{V}_{ab} = \sqrt{3} \bar{V}_{an} \angle 30^\circ = \sqrt{3} (120 \angle -40^\circ) \angle 30^\circ = 207.84 \angle -10^\circ \text{ V}$$

$$\bar{V}_{bc} = \bar{V}_{ab} \angle -120^\circ = 207.84 \angle -130^\circ \text{ V}$$

$$\bar{V}_{ca} = \bar{V}_{ab} \angle +120^\circ = 207.84 \angle 110^\circ \text{ V}$$

Now compute the load currents:

$$\bar{I}_{ab} = \frac{\bar{V}_{ab}}{\bar{Z}} = \frac{207.84 \angle -10^\circ}{10 \angle -30^\circ} = 20.784 \angle 20^\circ \text{ A}$$

$$\bar{I}_{bc} = \frac{\bar{V}_{bc}}{\bar{Z}} = \frac{207.84 \angle -130^\circ}{10 \angle -30^\circ} = 20.784 \angle -100^\circ \text{ A}$$

$$\bar{I}_{ca} = \frac{\bar{V}_{ca}}{\bar{Z}} = \frac{207.84 \angle 110^\circ}{10 \angle -30^\circ} = 20.784 \angle 140^\circ$$

Note that the load currents are equal in magnitude and are separated by 120° from one another.

As seen in Example 8.3, the load currents are balanced. Let us rewrite Equation 8.18 as follows:

$$\begin{aligned} \bar{I}_a &= \bar{I}_{ab} - \bar{I}_{ca} \\ \bar{I}_b &= \bar{I}_{bc} - \bar{I}_{ab} \\ \bar{I}_c &= \bar{I}_{ca} - \bar{I}_{bc} \end{aligned} \quad (8.20)$$

Let us assume that the load current \bar{I}_{ab} is the chosen reference. Then,

$$\begin{aligned} \bar{I}_{ab} &= I \angle 0 \\ \bar{I}_{bc} &= \bar{I}_{ab} \angle -120^\circ = I \angle -120^\circ \\ \bar{I}_{ca} &= \bar{I}_{ab} \angle 120^\circ = I \angle 120^\circ \end{aligned} \quad (8.21)$$

where I is the magnitude of the load current. Now substitute the values of the load currents in Equation 8.21 into Equation 8.20:

$$\begin{aligned} \bar{I}_a &= I \angle 0 - I \angle 120^\circ = \sqrt{3} I \angle -30^\circ = \sqrt{3} \bar{I}_{ab} \angle -30^\circ \\ \bar{I}_b &= I \angle -120^\circ - I \angle 0 = \sqrt{3} I \angle -150^\circ = \sqrt{3} \bar{I}_{bc} \angle -30^\circ \\ \bar{I}_c &= I \angle 120^\circ - I \angle -120^\circ = \sqrt{3} I \angle 90^\circ = \sqrt{3} \bar{I}_{ca} \angle -30^\circ \end{aligned} \quad (8.22)$$

As seen in Equation 8.22, the transmission line current \bar{I}_a is greater than the load current \bar{I}_{ab} by a factor of $\sqrt{3}$ and lags the load current by 30° . Similar relationships can be obtained for the other two loads.

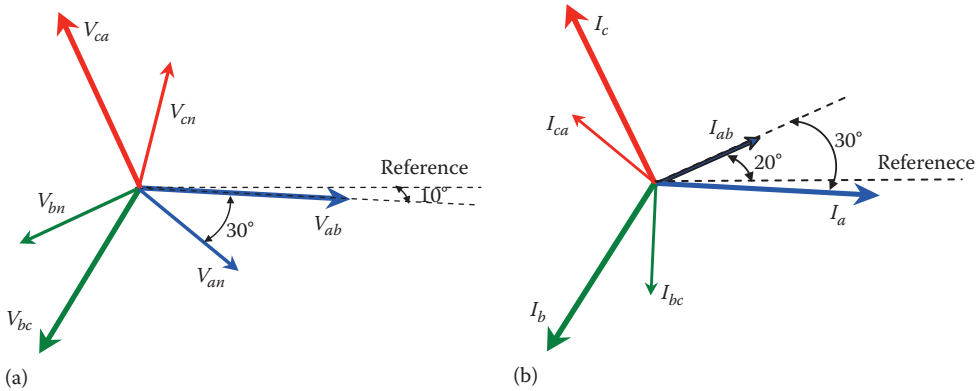


FIGURE 8.21 Phasor diagram of Example 8.4: (a) phasor diagram of voltages and (b) phasor diagram of currents.

Example 8.4

Calculate the transmission line currents in Example 8.3. Also sketch the phasor diagram showing the line-to-line voltages, load currents, and transmission line currents.

Solution

$$\bar{I}_a = \sqrt{3}\bar{I}_{ab}\angle -30^\circ = \sqrt{3}(20.784\angle 20^\circ)\angle -30^\circ = 36\angle -10^\circ \text{ A}$$

$$\bar{I}_b = \sqrt{3}\bar{I}_{bc}\angle -30^\circ = \sqrt{3}(20.784\angle -100^\circ)\angle -30^\circ = 36\angle -130^\circ \text{ A}$$

$$\bar{I}_c = \sqrt{3}\bar{I}_{ca}\angle -30^\circ = \sqrt{3}(20.784\angle 140^\circ)\angle -30^\circ = 36\angle 110^\circ \text{ A}$$

The phasor diagram is sketched in Figure 8.21.

The main conclusions of the delta-connected load are the following:

1. Voltage across the load is equal to the line-to-line voltage of the transmission line.
2. Transmission line current \bar{I}_a lags the load current \bar{I}_{ab} by 30° . Similar conclusion can be made for the other two phases.
3. Transmission line current is greater than the load current by a factor of $\sqrt{3}$.
4. Delta connection has no neutral terminal.

8.2.5 CIRCUITS WITH MIXED CONNECTIONS

The source and the load are not always connected in the same fashion; the load could be connected in delta and the source in wye, or vice versa. In either case, careful attention must be given when computing transmission line variables. Examine Example 8.5 carefully.

Example 8.5

Figure 8.22 shows a balanced delta-connected load energized by a balanced wye-connected source. The voltage of the source $\bar{V}_{an} = 120\angle 0^\circ \text{ V}$, and the transmission line current $\bar{I}_c = 10\angle 75^\circ \text{ A}$. Compute the load impedance.

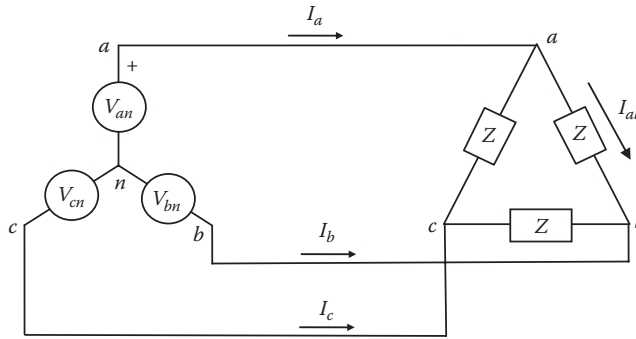


FIGURE 8.22 Circuit with wye source and delta load.

Solution

To compute the impedance, we need to compute the voltage across the load and the current of the load. The voltage across the load is the same as the line-to-line voltage of the transmission line

$$\bar{V}_{ab} = \sqrt{3} \bar{V}_{an} \angle 30^\circ = \sqrt{3} (120 \angle 0^\circ) \angle 30^\circ = 207.84 \angle 30^\circ \text{ V}$$

The current of the load can be computed by using the relationship

$$\bar{I}_a = \sqrt{3} \bar{I}_{ab} \angle -30^\circ$$

where

$$\bar{I}_a = \bar{I}_c \angle -120^\circ = (10 \angle 75^\circ) \angle -120^\circ = 10 \angle -45^\circ \text{ A}$$

Hence,

$$\bar{I}_{ab} = \frac{10 \angle -45^\circ}{\sqrt{3} \angle -30^\circ} = 5.774 \angle -15^\circ \text{ A}$$

and

$$\bar{Z} = \frac{\bar{V}_{ab}}{\bar{I}_{ab}} = \frac{207.84 \angle 30^\circ}{5.774 \angle -15^\circ} = 36 \angle 45^\circ \Omega$$

The loads in three-phase circuits can be connected in parallel even if their configurations are not the same. An example is shown in Figure 8.23 where the source is wye-connected, one of the loads is delta-connected, and the other is wye-connected. This circuit can be easily analyzed by using the superposition theorem. For example, to solve for the transmission line current \bar{I}_a , you first compute the contribution of each load to the line current independently. Then sum up the two contributions to find the line current due to both loads. Hence, the circuit in Figure 8.23 can be divided into the two subcircuits in Figures 8.24 and 8.25. In Figure 8.24, the contribution of the wye-connected load to the transmission line current is \bar{I}_{a1} . In Figure 8.25, the contribution of the

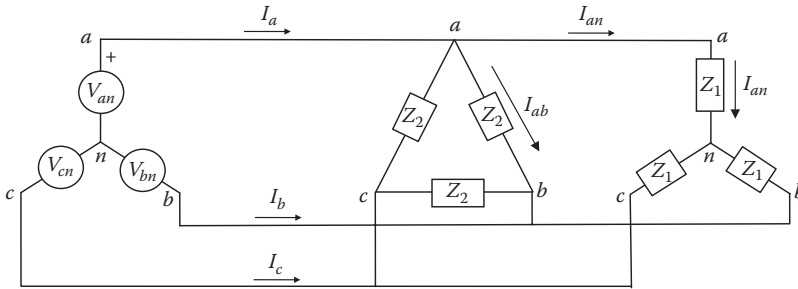


FIGURE 8.23 Circuit with wye and delta loads.

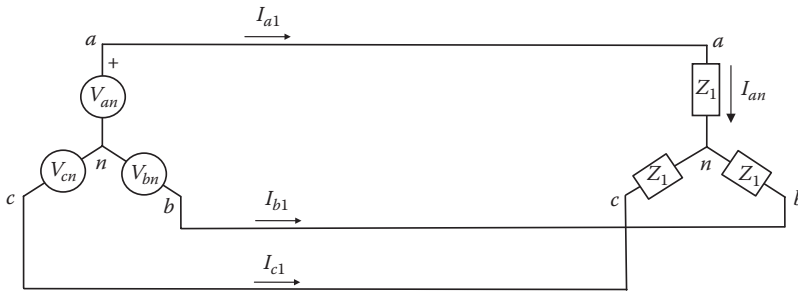


FIGURE 8.24 Contribution of the wye load.

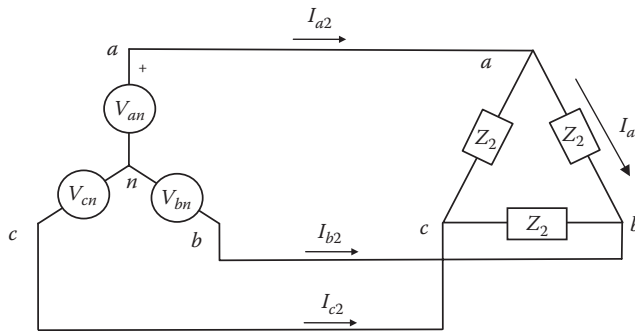


FIGURE 8.25 Contribution of the delta load.

delta-connected load to the line current is \bar{I}_{a2} . The transmission line current due to both loads is just the sum of \bar{I}_{a1} and \bar{I}_{a2} .

$$\bar{I}_a = \bar{I}_{a1} + \bar{I}_{a2} \tag{8.23}$$

Example 8.6

Assume that the source voltage in Figure 8.23 is $\bar{V}_{an} = 120\angle 0^\circ$ V, the load impedance of the wye load is $\bar{Z}_1 = 10\angle 20^\circ \Omega$, and the load impedance of the delta load is $\bar{Z}_2 = 15\angle -30^\circ \Omega$. Compute the transmission line currents at the source.

Solution

First find the contribution of the wye load to the line current \bar{I}_{a1} :

$$\bar{I}_{a1} = \bar{I}_{an} = \frac{\bar{V}_{an}}{\bar{Z}_1} = \frac{120\angle 0}{10\angle 20^\circ} = 12\angle -20^\circ \text{ A}$$

Now let us compute the contribution of the delta load \bar{I}_{a2} .

$$\bar{I}_{ab} = \frac{\bar{V}_{ab}}{\bar{Z}_2} = \frac{\sqrt{3} \bar{V}_{an}\angle 30^\circ}{15\angle -30^\circ} = \frac{\sqrt{3}(120\angle 0)\angle 30^\circ}{15\angle -30^\circ} = 13.85\angle 60^\circ \text{ A}$$

$$\bar{I}_{a2} = \sqrt{3} \bar{I}_{ab}\angle -30^\circ = \sqrt{3}(13.85\angle 60^\circ)\angle -30^\circ = 24\angle 30^\circ \text{ A}$$

The total transmission line current is

$$\bar{I}_a = \bar{I}_{a1} + \bar{I}_{a2} = 12\angle -20^\circ + 24\angle 30^\circ = 33\angle 13.84^\circ \text{ A}$$

8.2.6 WYE-DELTA TRANSFORMATION

When the source and load are both in wye or delta, the analysis of the circuit is simple. However, when the connections are different, the process is more involved as you must be attentive to the phase shifts and the changes in magnitude between the line and phase quantities. An alternative method is to find an equivalent load connection that matches that of the source. For example, if the source is wye-connected and the load is delta-connected, it would be easier to analyze the circuit if the delta load is replaced by an equivalent wye load. This is known as the wye-delta transformation.

Let us consider the delta load in Figure 8.26 where the impedance of the load is labeled \bar{Z}_Δ . Our objective is to find its equivalent wye load shown in Figure 8.27. The load impedance of the equivalent wye is \bar{Z}_Y . But how do we find the value of \bar{Z}_Y that makes the two circuits equivalent? The simplest way is to treat both circuits as an impedance box with three terminals. The two circuits are equivalent if the voltage applied between any two terminals in both circuits produces the same terminal currents. This means the impedance between any two terminals in the delta circuit is equal to the impedance between the same terminals in the wye circuit. For example, the impedance measured between terminals a and b , \bar{Z}_{ab} , must be the same for both circuits.

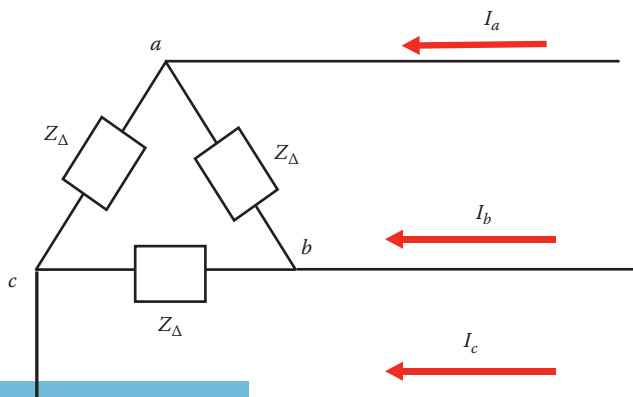


FIGURE 8.26 Delta load.

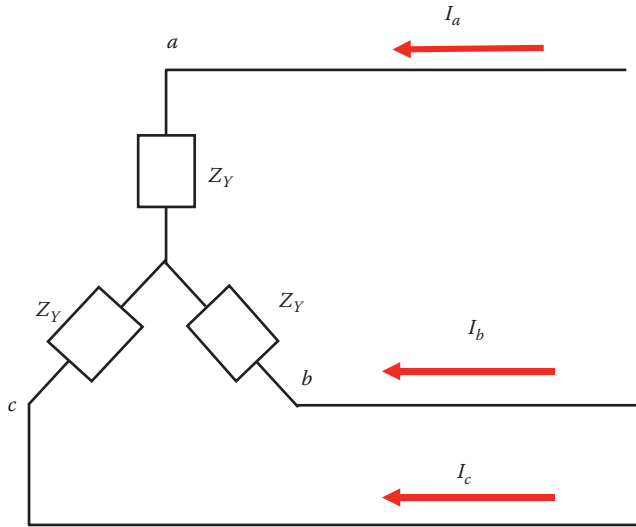


FIGURE 8.27 An equivalent wye load to the delta load in Figure 8.26.

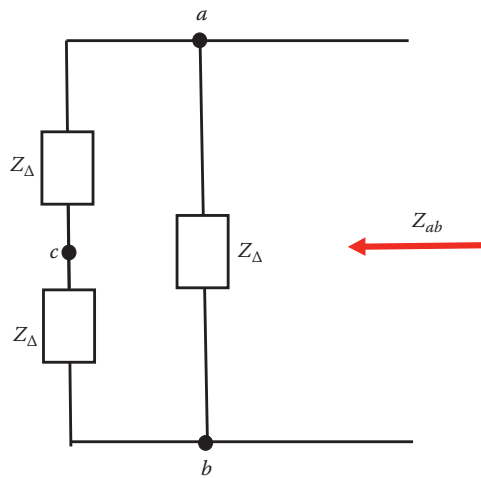


FIGURE 8.28 Terminal impedance of delta load.

\bar{Z}_{ab} of the delta-connected load can be quickly computed by rearranging the impedances in Figure 8.26 as shown in Figure 8.28. It is easy to see that the impedance measured between terminals a and b is a parallel combination of \bar{Z}_{Δ} and $2\bar{Z}_{\Delta}$ as given in Equation 8.24. Keep in mind that the third terminal c is floating (unconnected).

$$\bar{Z}_{ab} = \frac{\bar{Z}_{\Delta}(2\bar{Z}_{\Delta})}{3\bar{Z}_{\Delta}} = \frac{2}{3}\bar{Z}_{\Delta} \tag{8.24}$$

Now let us do the same with the equivalent wye load. Rearrange the wye load as shown in Figure 8.29. Since the third terminal c is floating, the impedance between terminals a and b is a series combination of two \bar{Z}_Y as given in Equation 8.25.

$$\bar{Z}_{ab} = 2\bar{Z}_Y \tag{8.25}$$

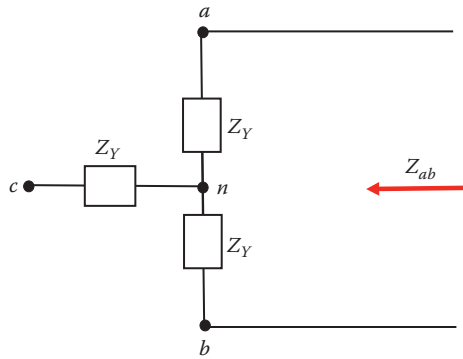


FIGURE 8.29 Terminal impedance of wye load.

To make the wye load equivalent to the original delta load, the terminal impedances of both circuits must be equal, that is, Equations 8.24 and 8.25 are equal. Hence,

$$\bar{Z}_Y = \frac{\bar{Z}_\Delta}{3} \tag{8.26}$$

The relationship in Equation 8.26 is valid for transforming either wye into delta or delta into wye.

Example 8.7

Repeat Example 8.6 by using the wye-delta transformation.

Solution

Convert the delta load in Figure 8.23 to wye.

$$\bar{Z}_Y = \frac{\bar{Z}_\Delta}{3} = \frac{\bar{Z}_2}{3} = \frac{15\angle -30^\circ}{3} = 5\angle -30^\circ \Omega$$

After the delta is converted into wye, we have two wye-connected loads in parallel as shown in Figure 8.30. These two loads can be replaced by one equivalent wye load as shown in Figure 8.31. The new value of the equivalent load impedance is

$$\bar{Z}_T = \frac{\bar{Z}_Y \bar{Z}_1}{\bar{Z}_Y + \bar{Z}_1} = \frac{(5\angle -30^\circ)(10\angle 20^\circ)}{(5\angle -30^\circ) + (10\angle 20^\circ)} = 3.6343\angle -13.84^\circ \Omega$$

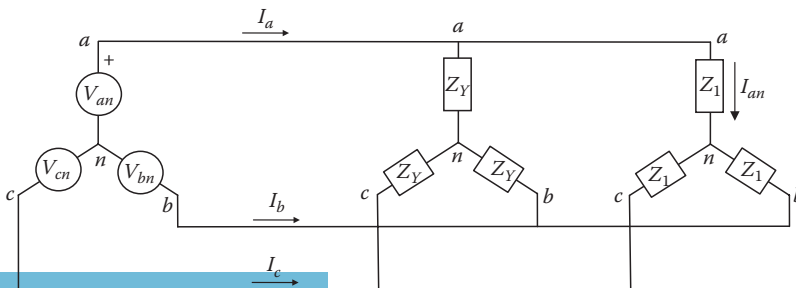


FIGURE 8.30 Equivalent circuit of the system in Figure 8.23.

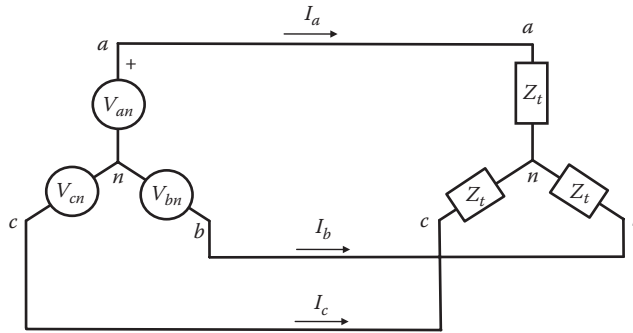


FIGURE 8.31 Equivalent wye load.

Now, the line current can be directly computed as

$$\bar{I}_a = \frac{\bar{V}_{an}}{\bar{Z}_t} = \frac{120 \angle 0}{3.6343 \angle -13.84^\circ} = 33 \angle 13.84^\circ \text{ A}$$

This process is obviously much simpler than that in Example 8.6.

8.3 POWER CALCULATIONS OF BALANCED THREE-PHASE CIRCUITS

The power in a three-phase load is the sum of the powers of each load. The voltage, current, and power of any of the three load in three-phase system are called phase quantities.

$$P_{ph} = V_{ph} I_{ph} \cos \theta \quad (8.27)$$

$$Q_{ph} = V_{ph} I_{ph} \sin \theta$$

where

P_{ph} is the real power consumed by one load (phase real power)

Q_{ph} is the reactive power consumed by one load (phase reactive power)

V_{ph} is the voltage across the load (phase voltage)

I_{ph} is the current of the load (phase current)

θ is the power factor angle (the angle between the load voltage and the load current); θ is then the impedance angle

Since the system is balanced, the three-phase power (P) is just three times the power of a single-phase:

$$P = 3 P_{ph} = 3 V_{ph} I_{ph} \cos \theta \quad (8.28)$$

A similar equation can be obtained for three-phase reactive power (Q):

$$Q = 3 Q_{ph} = 3 V_{ph} I_{ph} \sin \theta \quad (8.29)$$

8.3.1 THREE-PHASE POWER OF BALANCED WYE LOADS

When the load is connected in wye, the current in the transmission line current (I_l) is the same as the load current I_{ph} . Also, the line-to-line voltage of the transmission line (V_{ll}) is greater than the load voltage V_{ph} by a factor of $\sqrt{3}$. Hence, the power of the three-phase load is

$$P = 3 P_{ph} = 3 V_{ph} I_{ph} \cos \theta = 3 \frac{V_{ll}}{\sqrt{3}} I_l \cos \theta \quad (8.30)$$

Rewriting Equation 8.30 yields

$$P = \sqrt{3} V_{ll} I_l \cos \theta \quad (8.31)$$

Similarly, the reactive power is

$$Q = \sqrt{3} V_{ll} I_l \sin \theta \quad (8.32)$$

Keep in mind that θ is the impedance angle (angle between the load voltage and the load current).

8.3.2 THREE-PHASE POWER OF BALANCED DELTA LOADS

The voltage across the delta-connected load is the same as the line-to-line voltage of the transmission line. Also, the current in the transmission line is greater than the load current by a factor of $\sqrt{3}$. Hence,

$$P = 3 P_{ph} = 3 V_{ph} I_{ph} \cos \theta = 3 V_{ll} \frac{I_l}{\sqrt{3}} \cos \theta \quad (8.33)$$

Equation 8.33 can be rewritten as

$$P = \sqrt{3} V_{ll} I_l \cos \theta \quad (8.34)$$

Similarly, the three-phase reactive power is

$$Q = \sqrt{3} V_{ll} I_l \sin \theta \quad (8.35)$$

Note that Equations 8.31 and 8.34 are identical. Also Equations 8.32 and 8.35 are identical. Therefore, the power of a three-phase circuit can be computed by the same transmission line quantities regardless of the load connection. Keep in mind that θ is the angle between the load voltage and the load current in both cases. In other words, θ is the angle of the load impedance.

Example 8.8

A Y-connected three-phase source of $\bar{V}_{an} = 120 \angle 0^\circ$ V is powering a delta-connected load of $\bar{Z} = 15 \angle 20^\circ$. Compute the real and reactive power consumed by the load.

Solution

Compute the magnitude of the line-to-line voltage V_{ll} :

$$V_{ll} = \sqrt{3}V_{an} = 207.84 \text{ V}$$

Now compute the line current, but first calculate the magnitude of the load current I_{ab} .

$$I_{ab} = \frac{V_{ab}}{Z} = \frac{V_{ll}}{Z} = \frac{207.84}{15} = 13.85 \text{ A}$$

$$I_l = \sqrt{3}I_{ab} = \sqrt{3}13.85 = 24 \text{ A}$$

The phase angle of the load is given as 20° . Hence, the real and reactive powers are

$$P = \sqrt{3}V_{ll} I_l \cos \theta = \sqrt{3} \times 207.84 \times 24 \times \cos 20^\circ = 8.12 \text{ kW}$$

$$Q = \sqrt{3}V_{ll} I_l \sin \theta = \sqrt{3} \times 207.84 \times 24 \times \sin 20^\circ = 2.95 \text{ kVAr}$$

Example 8.9

A three-phase source of $\bar{V}_{an} = 120 \angle 0^\circ \text{ V}$ delivers 10 kW and 5 kVAr to a wye-connected load. Compute the load impedance.

Solution

Compute the power factor angle θ :

$$\theta = \tan^{-1} \left(\frac{Q}{P} \right) = \tan^{-1} \left(\frac{5}{10} \right) = 26.56^\circ$$

Compute the line-to-line voltage:

$$V_{ll} = \sqrt{3}V_{an} = 207.84 \text{ V}$$

Use the power equation to compute the line current:

$$P = \sqrt{3}V_{ll} I_l \cos \theta$$

$$10,000 = \sqrt{3} \times 207.84 \times I_l \times \cos 26.56^\circ$$

$$I_l = 31.05 \text{ A}$$

The line current is the same as the load current in wye connection. Now compute the magnitude of the load impedance:

$$Z = \frac{V_{ph}}{I_{ph}} = \frac{120}{31.05} = 3.86 \Omega$$

The complex value of the load impedance is

$$\bar{Z} = Z(\cos \theta + j \sin \theta) = 3.86(\cos 26.56 + j \sin 26.56) = 3.45 + j1.73 \Omega$$

EXERCISES

- 8.1** A Y-connected balanced three-phase source is feeding a balanced three-phase load. The voltage and current of the source coil are

$$v(t) = 340 \sin(377t + 0.5236) \text{ V}$$

$$i(t) = 100 \sin(377t + 0.87266) \text{ A}$$

Calculate the following:

- The rms phase voltage.
 - The rms line-to-line voltage.
 - The rms current in the source.
 - The rms current in the transmission line.
 - The frequency of the supply.
 - The power factor at the source side, state leading or lagging.
 - The three-phase real power delivered to the load.
 - The three-phase reactive power delivered to the load.
 - If the load is connected in delta configuration, calculate the load impedance.
- 8.2** The current and voltage of a Y-connected load are $\bar{V}_{ca} = 480 \angle -60^\circ \text{ V}$, $\bar{I}_b = 20 \angle 120^\circ \text{ A}$.
- Compute \bar{V}_{an} .
 - Compute \bar{I}_a .
 - Compute the power factor angle.
 - Compute the real power of the load.
- 8.3** A three-phase, 480 V system is connected to a balanced three-phase load. The transmission line current I_a is 10 A and is in phase with the line-to-line voltage V_{bc} . Calculate the impedance of the load for the following cases:
- If the load is wye-connected
 - If the load is delta-connected
- 8.4** The waveforms of the line-to-line voltage and line current of a three-phase transmission line connected to a delta-load are

$$v_{ll} = V_{\max} \sin \omega t$$

$$i_l = I_{\max} \sin(\omega t - 50^\circ)$$

Calculate the power factor angle.

- 8.5** A balanced wye-connected load of $(4 + j3) \Omega$ is connected across a three-phase source of 173 V (line-to-line).
- Find the transmission line current.
 - Find the power factor, the complex power, the real power, and the reactive power of the load.
 - With V_{ab} as the reference, sketch the phasor diagram that shows all voltages and currents.

- 8.6** Two three-phase wye-connected loads are in parallel across a three-phase supply. The first load draws a current of 20 A at 0.9 power factor leading, and the second load draws a current of 30 A at 0.8 power factor lagging. Calculate the following:
- The transmission line current
 - The power factor of the load
 - The real power supplied by the source if the line-to-line voltage of the transmission line is 400 V
- 8.7** The line-to-line voltage of a three-phase transmission line is $\bar{V}_{bc} = 340\angle 20^\circ\text{V}$.
- Calculate the phase voltage \bar{V}_{an} .
 - If a wye load impedance of $Z = 10\angle 60^\circ\ \Omega$ is connected to the transmission line, calculate the transmission line current \bar{I}_b .
 - Calculate the current in the neutral line \bar{I}_n .
- 8.8** A three-phase motor is rated at 5.0 hp. What is the power of the motor per phase in kW?
- 8.9** The following are the voltage and current measured for a Y-connected load.

$$\bar{V}_{ab} = 200\angle 50^\circ, \quad \bar{I}_c = 10\angle 140^\circ$$

- Calculate the power factor angle.
 - Calculate the real power consumed by the load.
- 8.10** A delta-connected source is energizing two parallel loads. One of the loads is connected in delta and the other in wye. The line-to-line voltage of the transmission line is 208 V. The delta load has impedance $\bar{Z}_\Delta = 10\angle -25^\circ\ \Omega$. The wye load has impedance $\bar{Z}_Y = 5\angle 40^\circ\ \Omega$. Compute the current in transmission line a .
- 8.11** A three-phase Y-connected source is energizing a delta-connected load. The phase voltage of the transmission line is $\bar{V}_{bn} = 120\angle 0^\circ\text{V}$, and the load impedance is $\bar{Z} = 9\angle 30^\circ\ \Omega$. Compute \bar{I}_a and the power consumed by the delta load.

9 Electric Safety

Electricity is one of the best forms of energy known to man; it is clean, readily available, quiet, and highly reliable. Equipment powered by electricity is pollution free and is more compact than those powered by other energy forms such as gas or oil. Because of the overwhelming advantages of electricity, it has become widely available by just the flip of a switch.

Electricity is completely safe if used properly. However, when the electric equipment is partially damaged or improperly used, hazardous conditions can develop. For example, loose-fitting plugs can overheat and lead to fire, water intrusion inside a plugged in appliance can lead to electrical shock, and cracks or damage in electrical insulations can lead to fires and electrical shocks.

Since the early days of the electrical revolution, electricity has been recognized as hazardous to humans and animals. Today, even with safe products on the market, more than 1000 people are killed each year in the United States alone due to electric shocks and several thousands more are injured. The popular myth that only high voltages are dangerous to humans makes some of us unfortunately careless when we use regular household equipment. Indeed, most of the electric shocks occur at the low household voltage level. The potential hazards of electricity make the manufacturers of electric equipment very sensitive to the safety of their products. Several regulations and standards are developed to address every electric safety issue known to man so far. In the United States, the Occupational Safety and Health Administration (OSHA) enforces the basic safety standards. On a more global level, the Institute of Electrical and Electronics Engineers (IEEE) sets several standards for various electric safety issues that are normally adopted by OSHA and other similar agencies all over the world.

9.1 ELECTRIC SHOCK

Electric shocks occur when people become part of electrical circuits and accordingly electrical currents flow through their bodies. The electric current can cause a wide range of harmful effects on humans and animals, ranging from minor sensations to death. The current flowing inside a body can overheat the cells, leading to internal and external burns. The most sensitive organs to this effect are the lungs, brain, and heart. The degree of injuries depends on several factors such as the magnitude of the current, the duration of the shock, the pathway of the current, and its frequency. These factors are discussed in more detail in this chapter. Generally, electric shocks are divided into two categories: *secondary shocks* and *primary shocks*. The secondary shock is due to low currents that may cause pain without physical harm. The primary shock, however, is due to higher currents that produce physical harm or death. Most of us probably experience the secondary shock when we use some types of appliance or equipment. Sometimes, when we lightly touch a charged object, we may experience tingling effects due to the small current passing through our fingers. If we grip that object, the current is spread out over wider contact area and we may not feel anything. The incredible question is how to find out the safe limit of electrical current; it is hard to find volunteers for primary shock experiments! Early researchers, however, carried out their secondary shock studies on human volunteers and the primary shock experiments on animals with similar weight and general biological characteristics as humans. It was also reported that some bizarre research on primary shocks was done on inmates condemned to death. Among the highly respected researchers in this area was Charles Dalziel from the University of California, Berkeley. Dalziel conducted extensive lab tests during the mid-twentieth century. In one of his papers published in 1972, Dalziel summarizes the results of his various lab tests, which until today are used as the *de facto* standard. In his study, he had several men and a few women volunteers. Figure 9.1 shows a photo of one of Dalziel's



FIGURE 9.1 A volunteer during secondary electric shock test. (From Charles F. Dalziel, Electric shock hazard, IEEE spectrum, 1972, Courtesy of IEEE.)

tests published in his 1972 paper. The caption of the figure states that “Muscular reaction at the let-go current value is increasingly severe and painful, as shown by the subject during laboratory tests.” Today, many people find this type of test incredible!

9.1.1 CURRENT LIMITS OF ELECTRIC SHOCKS

The results of Dalziel’s work as well as those of other researchers are summarized in Tables 9.1 and 9.2. Table 9.1 shows the levels of direct current (dc) and alternating current (ac) that produce various types of secondary shocks on men and women. Although secondary shock can be painful, it is not life threatening. As in Table 9.1, the following conclusions regarding secondary shocks can be made:

TABLE 9.1
Effects of AC and DC Secondary Shock Current

Reaction	Current (mA)			
	dc		ac	
	Men	Women	Men	Women
No sensation on hand	1.0	0.6	0.4	0.3
Tingling (threshold of perception)	5.2	3.5	1.1	0.7
Shock: Uncomfortable, muscular control not lost	9.0	6.0	1.8	1.2
Painful shock, muscular control is not lost	62.0	41.0	9.0	6.0

Source: IEEE Standard 524a, 1993.

TABLE 9.2
Threshold Limit of AC Primary Shock Current

Threshold	Current in mA			
	0.5% of Population		50% of Population	
	Men	Women	Men	Women
Let-go: Worker cannot release wire	9	6	16	10.5
Respiratory tetanus			23	15
Ventricular fibrillation	100	67		

Source: IEEE Standard 1048, 1990.

- Women are more sensitive to electrical current than men.
- It takes less of ac current than dc to produce the same effect on people.
- It takes as little as 1.2 mA for women and 1.8 mA for men to produce uncomfortable effects. For currents less than 6 mA in women and 9 mA in men, the person, while in pain, can still control his or her muscles.

The more critical statistics are the ones related to primary shock shown in Table 9.2. In this table, the population is divided into sensitive and average sets. The sensitive population, about 0.5% of the total population, is harmed at lower currents than the rest of the population. The average population forms 50% of the total population. The table shows three key effects for the primary shocks: *let go*, *respiratory tetanus*, and *ventricular fibrillation*.

For 50% of the male population, when a person grips an energized conductor and the current passing through his muscles is about 16 mA, the person may not be able to control his muscles and thus may not release the gripped conductor. In this case, the current passes through the person's body for as long as the circuit is energized. This is known as the let-go current level.

A current above the let-go threshold passing through the chest can cause involuntary contraction of the muscles, which will arrest breathing as long as the current continues to flow. This is known as *respiratory tetanus*. If the current passing through the chest disturbs the heart's own electrical stimulation, the heart experiences an uncontrolled vibration and may even cease to beat. This is known as *ventricular fibrillation*.

9.1.2 FACTORS DETERMINING THE SEVERITY OF ELECTRIC SHOCKS

The harmful effects of electric shocks depend mainly on seven factors:

1. Voltage level of the gripped or touched equipment
2. Amount of current passing through the person's body
3. Resistance of the person's body
4. Pathway of the current inside the body
5. Duration of the shock
6. Frequency of the source
7. Ground resistance

9.1.2.1 Effect of Voltage

Most electric shocks occur at 100–400 V because it is readily available to everyone, it is high enough to produce significant current in the body, and can cause muscles to contract tightly to the

energized object. A higher voltage, in kilovolts range, is even more lethal because it causes high currents to pass through the person, but the access to this voltage is normally limited to professionals such as linemen. The general public rarely comes in contact with high-voltage wires, unless a wire is downed, a person climbs a high object and touches the wire, etc. Therefore, the number of deaths from high voltage is much less than that from low voltage.

When a person touches a high-voltage wire, fierce involuntary muscle contractions may throw the person away from the hazard. However, it may cause the person to fall from the high elevation of the power line to the ground.

9.1.2.2 Effect of Current

Contrary to popular belief, it is the current, not voltage, that causes death. However, the current is a function of the voltage and the impedance of the body as described by Ohm's law. Electric currents can interfere with the normal operation of the heart and lungs causing the heart to beat out of step and the lungs to function irregularly. Moreover, electric currents passing through tissues produce thermal heat, which is a form of energy that is proportional to the square of the current. This thermal energy E can permanently damage tissues and organs in the body

$$E = I^2 R t \quad (9.1)$$

where

I is the current in the body

R is the body resistance

t is the time duration of the current

9.1.2.3 Effect of Body Resistance

The higher the body resistance, the lower is the current flowing through the person. The body resistance is highly nonlinear and is a function of several factors such as the hydration condition of the body, skin condition, and fat concentration. Palm resistance, for example, can range from 100Ω to $1\text{ M}\Omega$ depending on the skin condition of the person. Dry skin tends to have higher resistance, and sweat tends to lower the resistance. Nerves, arteries, and muscles are low in resistance, while bones, fat, and tendons are relatively high in resistance. The IEEE established the ranges for body resistances shown in Table 9.3. These numbers can be used to roughly estimate the current through the body. However, the variability in human body resistance could make the results inaccurate for people with body resistances outside the specified range.

Because of the wide range of human resistances, it is hard to analyze the electric safety for a specific individual. Instead, the community has decided to use common values for body

TABLE 9.3
Body Resistance in Ohms

Resistance	Hand-to-Hand		Hand-to-Feet
	Dry Condition	Wet Condition	Wet Condition
Maximum	13,500	1,260	1,950
Minimum	1,500	610	820
Average	4,838	865	1221

Source: IEEE Standard 1048, 1990.

TABLE 9.4
Suggested Values for Body Resistance

Body Part	Resistance (Ω)
Each hand plus arm	500
Each leg	500
Torso	100

resistances. These values are shown in Table 9.4. A 1000Ω between two hands or two feet is a good number to use.

9.1.2.4 Effect of Current Pathway

A current passing through the skin is not as harmful as a current passing through vital organs. Fatal currents often pass through the heart, lungs, and brain. A mere $10\mu\text{A}$ passing directly through the heart can cause cardiac arrest. At lower currents, the heart muscles could beat out of step, resulting in insufficient blood being pumped throughout the body. A current in the spinal cord may also alter the respiratory control mechanism.

9.1.2.5 Effect of Shock Duration

The longer the duration of the shock the higher is the likelihood of death. This is because sensitive organs such as the heart and lungs will eventually stop functioning and the increased thermal heat inside the body can permanently damage muscles. Keep in mind that when the current is above the let-go threshold, the person is incapable of releasing his or her grip on the wire and the shock duration is therefore long.

Charles Dalziel carried out research on the time–current relationship for primary shocks. He, and other researchers, obtained his results by experimenting on animals of weights and organ sizes similar to humans. Although inconclusive, the data of these experiments are the best available information to date. Based on these studies, Dalziel developed the following empirical current duration formula for ventricular fibrillation (VF)

$$I = \frac{K}{\sqrt{t}} \quad (9.2)$$

where

I is the current in mA that induces VF

t is the time duration of the current in seconds

K is a constant that depends on the weight of the test subject: for people weighing less than 70 kg (154 lb), $K=116$; and for people weighing more than 70 kg, $K=157$

Figure 9.2 is a graph of Dalziel's formula. As seen in the figure, it takes a very short time to induce ventricular fibrillation. For instance, if the current is about 80 mA, it takes about 4 s to kill a person over 70 kg, while a person weighing less than 70 kg may survive for just 2 s. In either case, the survival duration is very short for such a small current.

9.1.2.6 Effect of Frequency

The frequency that impacts humans can be divided into two categories:

- Non-ionizing frequency (0–100 PHz), which includes power line frequency, radio, microwave, and infrared frequencies.
- Ionizing frequency (>100 PHz), which includes x-rays and gamma-rays.

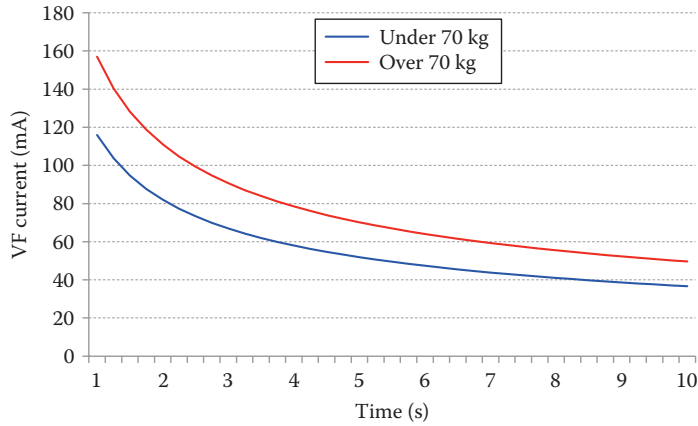


FIGURE 9.2 Ventricular fibrillation current as a function of shock duration.

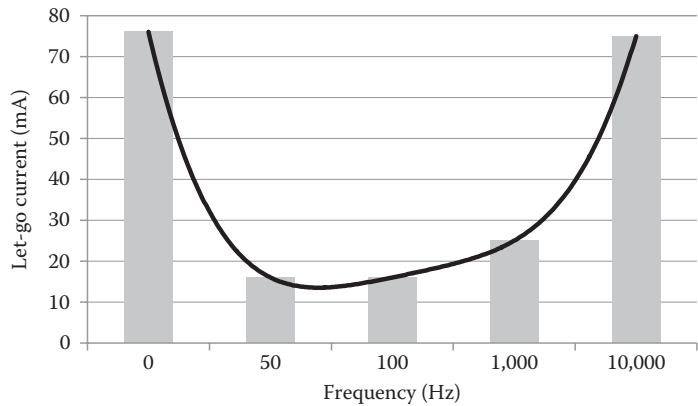


FIGURE 9.3 Let-go current as a function of frequency for men.

From the electric safety point of view, we are focusing on the low end of the non-ionizing frequencies (up to 10kHz). In this range, research indicates that the let-go level is almost a parabolic function with respect to the frequency as shown in Figure 9.3. Unfortunately, at 50–60Hz, humans are very vulnerable to electric shock. At the DC level or the high frequency range (3–10kHz), our tolerance is relatively high.

Table 9.5 shows additional data for the 10kHz shocks. The table includes the dc and ac data given in Tables 9.1 and 9.2. Notice that while the perception threshold for men is 1.1 mA at 60Hz, it is 12 mA at 10kHz (more than 10 times). The let-go threshold for men at 60Hz is 16 mA while it is 75 mA at 10kHz (almost six times). This is why in some rare cases a human may survive a lightning strike.

9.1.2.7 Effect of Ground Resistance

If a person touching an energized conductor is standing on insulated material, the current through his body is insignificant. However, if he is standing on the ground with bare feet, a current will pass through his body on its way to ground. The magnitude of this current depends on the resistances in the system as well as the resistance of his body and the ground resistance under his feet.

TABLE 9.5
Effect of Frequency on Electric Shocks

Effect	Current (mA)					
	Direct Current		Alternating Current			
	0 Hz		60 Hz		10 kHz	
	Men	Women	Men	Women	Men	Women
Slight sensation on hand	1.0	0.6	0.4	0.3	7	5
Perception threshold, median	5.2	3.5	1.1	0.7	12	8
Shock: not painful and no loss of muscular control	9	6	1.8	1.2	17	11
Painful shock: muscular control is not lost	62	41	9	6	55	37
Painful shock: let-go threshold, median	76	51	16	10.5	75	50
Painful and severe shock: breathing difficult, muscular control lost	90	60	23	15	94	63

Example 9.1

A person touching 120 V conductor while standing with bare feet on dry sand. The ground resistance (R_g) under his feet is 20 k Ω . Estimate the current through his body. Repeat the calculation if the soil is wet organic with a ground resistance of 30 Ω .

Solution

Using Ohm's law, the current passing through the person in the case of sand soil is

$$I_{man} = \frac{V}{R_{man} + R_g} = \frac{120}{1,000 + 20,000} = 5.71 \text{ mA}$$

The current passing through the person in the case of wet-organic soil is

$$I_{man} = \frac{V}{R_{man} + R_g} = \frac{120}{1000 + 30} = 116.5 \text{ mA}$$

Note that the person will survive the shock in the first case and will likely die in the second case.

Example 9.2

A child climbs a tree to retrieve his kite that is tangled on a utility line. The voltage of the line with respect to ground is 120 V. The resistance of the wire from the source to the location of the kite is 0.2 Ω . The tree has a resistance of 500 Ω . The ground resistance of the tree is 30 Ω . Assume that the child's resistance is 1000 Ω . If the child touches the power line with his hand, estimate the current through his body. Also, estimate the time it takes to induce ventricular fibrillation.

Solution

If you trace the path of the current starting from the source, you can obtain the electrical circuit shown in Figure 9.4. The current passing through the child starts at the source passes through the line to the child, then to the tree, and finally to the ground. The current in this case is

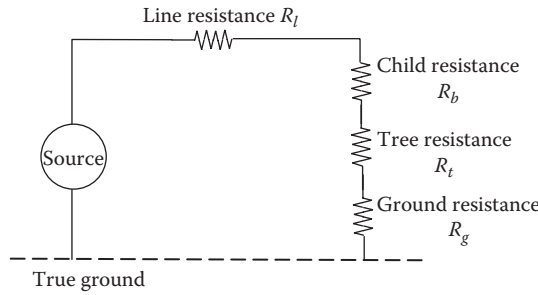


FIGURE 9.4 Model representation of the accident.

$$I_{child} = \frac{V}{R_l + R_{child} + R_t + R_g} = \frac{120}{0.2 + 1000 + 500 + 30} = 78.42 \text{ mA}$$

According to Dalziel’s formula, the child will survive only for

$$t = \left(\frac{K}{I} \right)^2 = \left(\frac{116}{78.42} \right)^2 = 2.19 \text{ s}$$

Note that we used $K=116$, as the child is assumed to weigh less than 70kg. Also notice that the wire resistance has very little effect on the current since it is much smaller than the other resistances. One important resistance is the ground resistance. It varies widely and can have a major effect on the value of the current.

9.2 GROUND RESISTANCE

The center of earth is the only absolute zero potential point; any other location inside earth has a nonzero potential. Hence, objects on the surface of earth such as water pipes, building foundations, and steel structures have nonzero potentials. Figure 9.5 shows a simple schematic of earth with an object at the earth’s surface. The object, which is in contact with the soil, has a potential higher than zero. Hence, the potential difference V between the object and the center of earth can be represented by Ohm’s law $V=IR$, where I is the current flowing from the object to the center of earth, and R is the resistance between the object and the center of earth. This resistance R is called the *ground resistance* of the object.

The ground resistance of an object is nonlinear and is dependent of several factors such as the shape of the object, the type of ground soil, and the dampness of the soil. An exact computation of the ground resistance of an object is a very tedious task that requires the knowledge of highly varying parameters that are hard to measure under all possible conditions. Nevertheless, a simplified computation of the ground resistance of an object can be made with a reasonable degree of accuracy.

9.2.1 GROUND RESISTANCE OF OBJECTS

Assume the simple case in Figure 9.6 of a hemisphere buried in soil. Assume that the soil is homogeneous with a resistivity ρ . If the hemisphere is connected to a conductor that carries a current I , the current enters the hemisphere then disperses uniformly through earth. The current density at the surface of the hemisphere J is the current leaving the hemisphere divided by the surface area of the hemisphere.

$$J = \frac{I}{2\pi r^2} \tag{9.3}$$

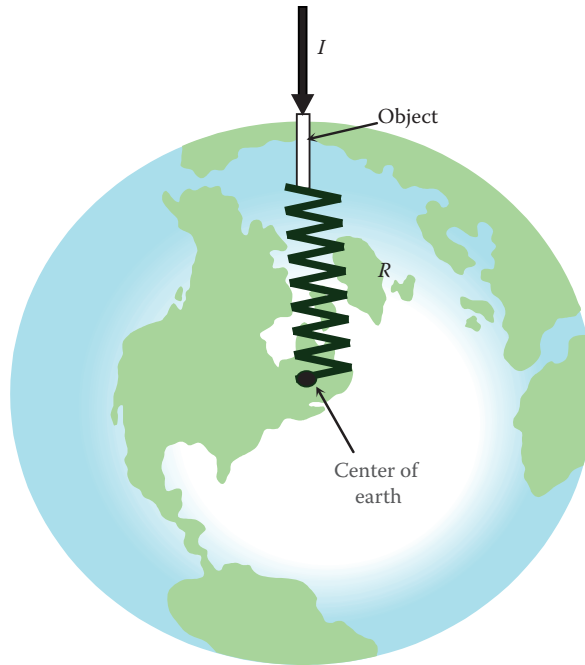


FIGURE 9.5 Ground resistance.

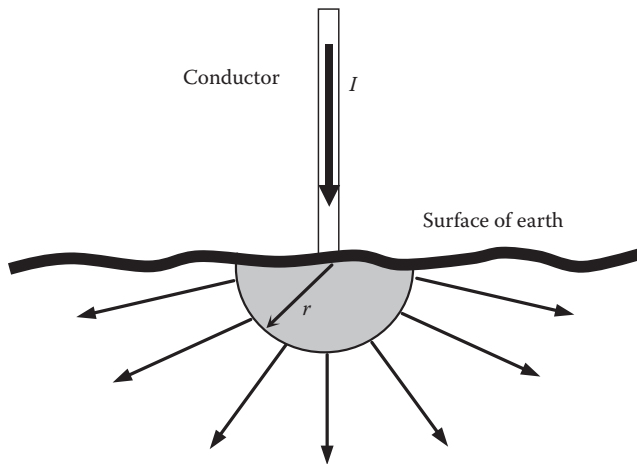


FIGURE 9.6 Current dispersion of a hemisphere.

Assuming the soil to be homogeneous, the current density at any point x from the center of the hemisphere and outside the hemisphere, can be computed as

$$J(x) = \frac{I}{2\pi x^2}; \quad x \geq r \tag{9.4}$$

Ohm's law states that electric field intensity (E) is equal to the current density multiplied by the resistivity of the medium. Hence, $E(x)$ at any distance x outside the hemisphere is

$$E(x) = \rho J(x); \quad x \geq r \tag{9.5}$$

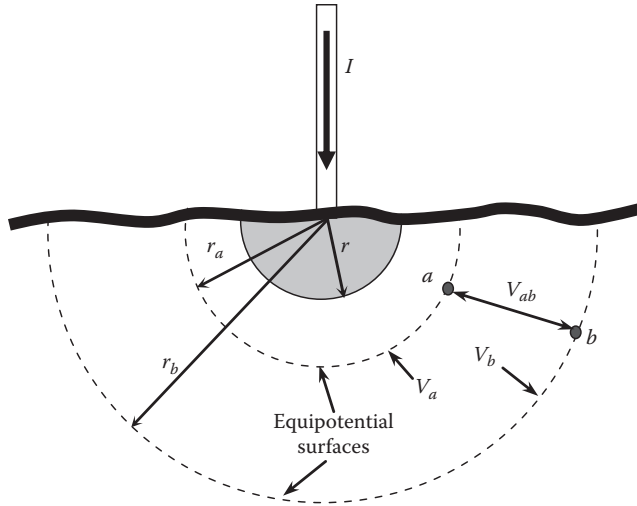


FIGURE 9.7 Equipotential surface.

For homogeneous soil, the potentials of all points located at the same distance from the center of the hemisphere are equal. The surface of these points is known as the *equipotential surface* shown in Figure 9.7. The potential difference between any two points (such as *a* and *b*) inside earth can be computed by integrating the electric field intensity between these two points. Hence, V_{ab} in the figure is the potential difference between the two equipotential surfaces where *a* and *b* are located. This voltage can be computed as

$$V_{ab} = \int_{x=a}^{x=b} E(x) dx = \int_{x=a}^{x=b} \rho J(x) dx = \frac{\rho I}{2\pi} \left[\frac{1}{r_a} - \frac{1}{r_b} \right] \tag{9.6}$$

where r_a and r_b are the distances of points *a* and *b* from the center of the hemisphere respectively. Hence the resistance between *a* and *b* is

$$R_{ab} = \frac{V_{ab}}{I} = \frac{\rho}{2\pi} \left[\frac{1}{r_a} - \frac{1}{r_b} \right] \tag{9.7}$$

The ground resistance of the hemisphere R_g is the resistance between the surface of the hemisphere and the center of earth. This can be computed using Equation 9.7 by setting r_a equal to the radius of the hemisphere, and r_b to ∞

$$R_g = \frac{\rho}{2\pi r} \tag{9.8}$$

The ground resistance can also be computed for other shapes; however, the process is more involved. Table 9.6 shows the ground resistance of some common objects.

Table 9.7 shows the resistivity of various soil compositions. Note that the value of the resistivity is substantially reduced if the soil is wet or organic.

TABLE 9.6
Ground Resistance of Common Objects

Object	Ground Resistance	Parameters
Rod	$\frac{\rho}{2\pi l} \ln\left(\frac{2l+r}{r}\right)$	l is the length of the rod r is the radius of the rod
Circular plate (disk) at the surface	$\frac{\rho}{4r}$	r is the radius of the disk
Buried wire	$\frac{\rho}{2\pi l} \left(\ln\left(\frac{l}{r}\right) + \ln\left(\frac{l}{2d}\right) \right)$	l is the length of the wire r is the radius of the wire d is the depth at which the wire is buried

TABLE 9.7
Soil Resistivity

	Soil Composition			
	Wet Organic	Moist	Dry	Bedrock
Resistivity ρ (Ω -m)	10	100	1,000	10,000

Example 9.3

A hemisphere 2 m in diameter is buried in wet-organic soil. Compute the ground resistance of the hemisphere. Also compute the ground resistance at 2, 10, and 100 m away from the hemisphere.

Solution

$$R_g = \frac{\rho}{2\pi r} = \frac{10}{2\pi 1} = 1.6 \Omega$$

The resistance between two points can be computed by using Equation 9.7

$$R_{ab} = \frac{\rho}{2\pi} \left[\frac{1}{r_a} - \frac{1}{r_b} \right]$$

At 2 m

$$R_{ab-2} = \frac{10}{2\pi} \left[\frac{1}{1} - \frac{1}{2} \right] = 0.8 \Omega$$

At 10 m

$$R_{ab-10} = \frac{10}{2\pi} \left[\frac{1}{1} - \frac{1}{10} \right] = 1.4 \Omega$$

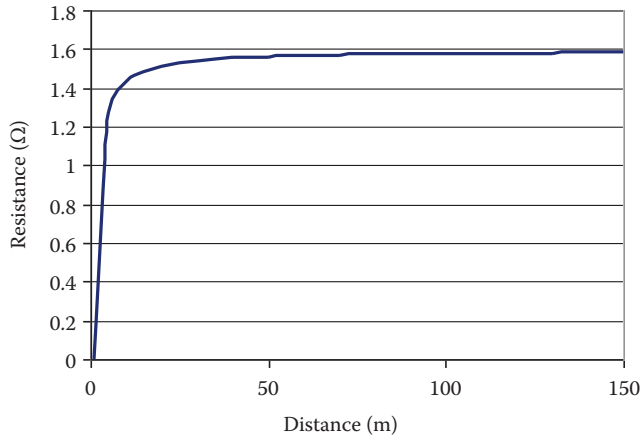


FIGURE 9.8 Ground resistance between the hemisphere and points at various distances.

At 100m

$$R_{ab-100} = \frac{10}{2\pi} \left[\frac{1}{1} - \frac{1}{100} \right] = 1.6 \Omega$$

Figure 9.8 shows the ground resistance between the hemisphere and points at various distances. Notice that the change in ground resistance is insignificant when the distance from the hemisphere increases beyond 10m. Therefore, the ground resistance of an object is practically a function of the immediate distance, rather than the distance to the center of earth.

9.2.2 MEASURING GROUND RESISTANCE OF OBJECTS

The ground resistance can be measured using a technique known as the fall-of-potential method. The method, which is also known as the three-point test, is explained in Figure 9.9. The setup consists of the object whose ground resistance is to be determined, a current electrode, and a potential probe. The electrode is a small copper rod that is driven into the soil. A voltage source is connected between the object and the current electrode. A voltmeter is connected between the object and the potential probe. The potential probe moves along the line between the object and the current electrode. At each position, the current of the electrode and the voltage of the probe are recorded and plotted as shown at the bottom of Figure 9.9. When the potential probe touches the object under test, the measured voltage is zero, and when it touches the current electrode, the voltage is equal to the source voltage. The magnitude of the measured voltage is a nonlinear function with respect to distance x . However, the voltage is often unchanged for a wide range of x as shown in the flat region in the figure. At the middle of this region, V_f is recorded at the distance x_f . The ratio V_f/I can be used as the ground resistance of the object.

9.2.3 GROUND RESISTANCE OF PEOPLE

A person standing on the ground has a ground resistance under his/her feet as shown in Figure 9.10. Each foot has a ground resistance R_f between the bottom of the foot and the center of earth. The trick is how to model the bottom of a shoe. An approximation is often made by using a circular plate that has the same area as the footprint of an average person. Using the ground resistance equation of the circular plate given in Table 9.6, the ground resistance of a single foot R_f is

$$R_f = \frac{\rho}{4r} \quad (9.9)$$

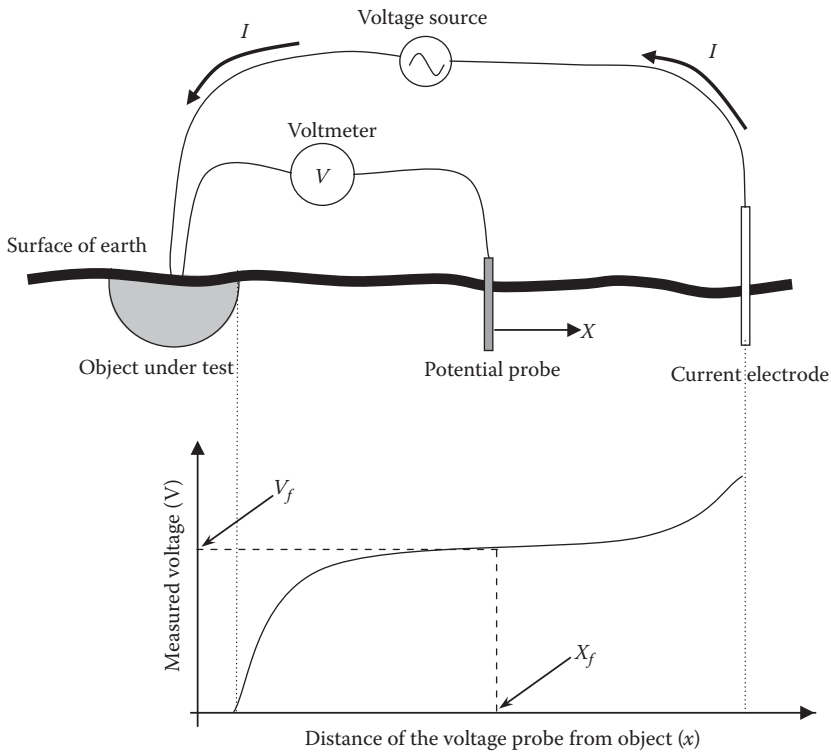


FIGURE 9.9 Fall-of-potential method to measure ground resistance.

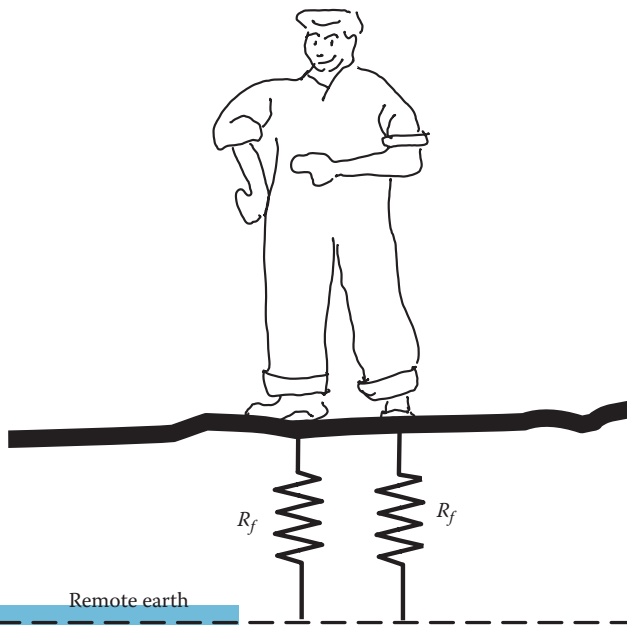


FIGURE 9.10 Feet resistance.

The area of the circular plate is

$$A = \pi r^2 \quad (9.10)$$

The approximate area for an average footprint is about 0.02 m^2 . Hence, the ground resistance of the person in Equation 9.9 is

$$R_f = \frac{\rho}{4 \sqrt{\frac{A}{\pi}}} = \frac{\rho}{4 \sqrt{\frac{0.02}{\pi}}} \approx 3\rho \quad (9.11)$$

The total ground resistances of a walking person and standing person are different. If you assume that the standing person has his feet close enough to each other, then the total ground resistance R_g is the parallel combination of two R_f :

$$R_g = \frac{R_f \times R_f}{R_f + R_f} = 0.5 R_f \approx 1.5\rho \quad (9.12)$$

9.3 TOUCH AND STEP POTENTIALS

The direct hazard of electricity is due to an energized object touching a person. However, there are indirect hazards that are less obvious but equally dangerous, such as that due to excessive touch and step potentials. The touch potential could be present if a person touches a metallic structure that attains a charge. If the person is standing on the ground, he may have a potential difference between his hand and feet. This voltage could be hazardous.

When a person is walking adjacent to an object that discharges current into the ground, the person could have a potential difference between his two feet. This voltage could also be hazardous.

9.3.1 TOUCH POTENTIAL

To explain the hazards of touch potentials, let us consider the tower of the power line shown in Figure 9.11. The tower is built out of steel trusses with several cross arms. On the cross arms, insulators are mounted whereas on their other sides, high-voltage wires are attached. In areas known for their lightning activities, ground wires (also known as static wires or overhead ground wire, OHGW) are installed on the top of the tower to protect the energized lines from being hit by lightning bolts that could damage the insulators and render the power line inoperable. The ground wires are often bonded to the tower structure which is grounded through a local ground under the tower footage.

Although made of steel and grounded locally, the tower structure is not always at zero potential because the structure could carry current due to a number of reasons such as the following:

Ground wire discharge: Because of the presence of the energized lines in the vicinity of a ground wire, a voltage is induced on the ground wire. The ground wire discharges its acquired energy through all adjacent grounds including the tower ground. This may result in currents passing through the structure hardware to the local ground underneath the tower.

Insulator leakage: In humid environments, especially close to seas, the surface of an insulator could become contaminated with dirt and salty moisture. This mix can provide a path for the current from the energized line to the tower structure as shown in Figure 9.12. This is known as *insulator leakage*. This could even lead to a *flashover* on the surface of the insulator.

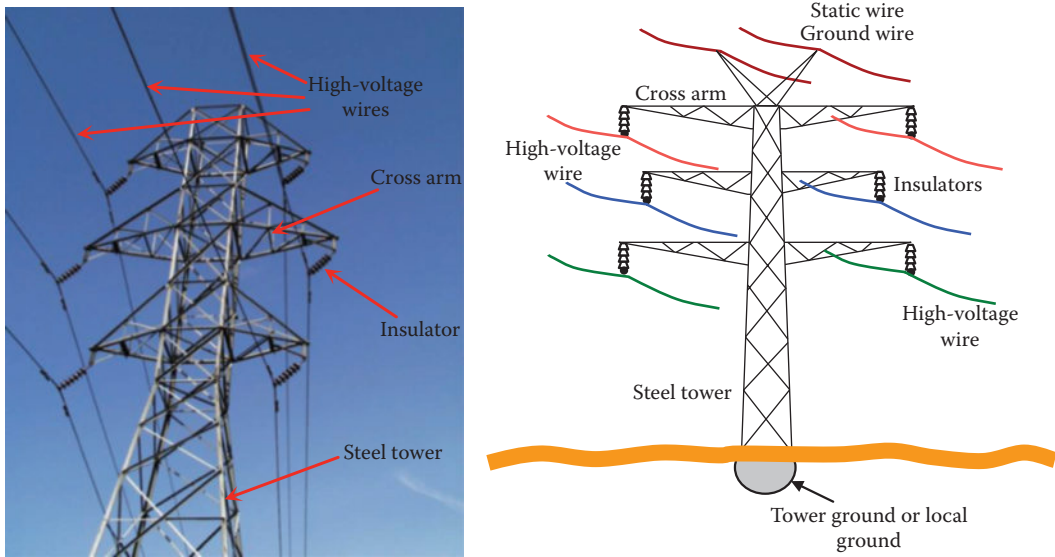


FIGURE 9.11 Main components of a steel power line.

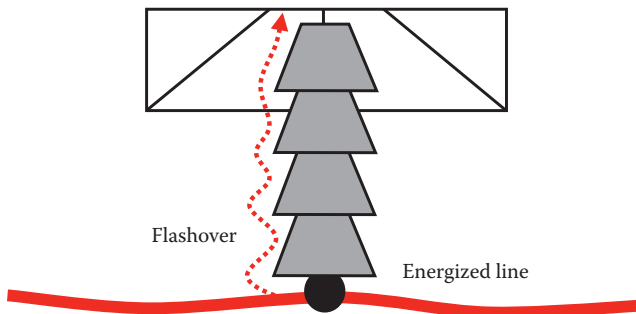


FIGURE 9.12 Insulation leakage or flashover due to conductive depositions on the insulator.

Accident: While linemen are working on power lines, accidents could happen when an energized conductor comes in contact with the structure of the tower.

Now assume that a person is touching the steel tower while standing on ground as shown in Figure 9.13. If the structure carries a current I , most of the current passes through the structure and goes to the ground of the tower I_{tg} , and the rest of the current goes through the man touching the tower I_{man} . Keep in mind that the ground resistance of the man is $0.5 R_f$ as given in Equation 9.12.

Figure 9.14 shows a circuit diagram representing the case in Figure 9.13. Let us assume that we need to compute the current going through the man. This can be done using the current divider equation:

$$I_{man} = I \frac{R_g}{R_g + R_{man} + 0.5 R_f} \tag{9.13}$$

The potential of the structure is known as the *ground potential rise (GPR)*. It is the voltage that the grounded object attains with respect to remote earth (center of earth).

$$GPR = I_{tg} R_g \tag{9.14}$$

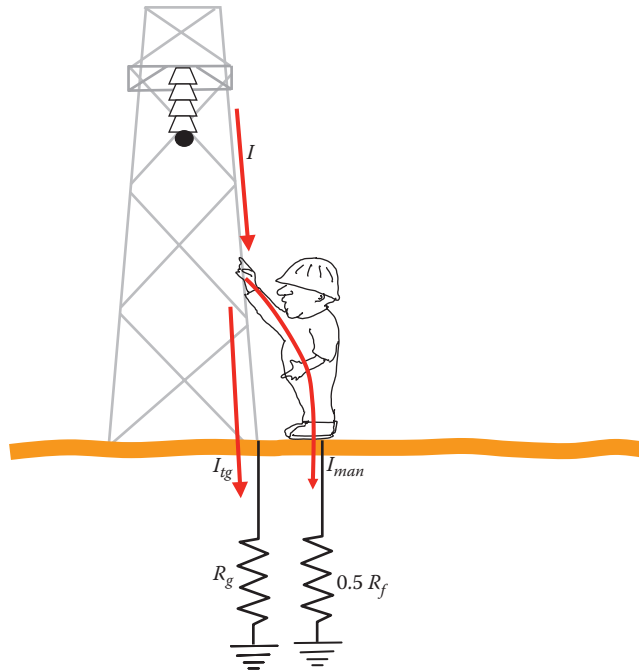


FIGURE 9.13 Touch potential.

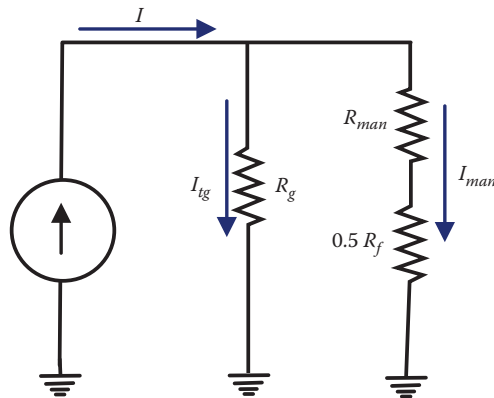


FIGURE 9.14 Circuit diagram of Figure 9.13.

Example 9.4

A power line insulator has partially failed and 10 A passes through the tower structure to the ground. Assume that the tower ground is a hemisphere with a radius of 0.5 m, and the soil surrounding the hemisphere is moist.

1. Compute the voltage of the tower.
2. Assume that a man with body resistance of $1.0 \text{ k}\Omega$ touches the tower while standing on ground. Compute the current passing through the man.
3. Use Dalziel's formula and compute the man's survival time.

Solution

1. Table 9.7 gives the resistivity of moist soil. The ground resistance of the hemisphere R_g is

$$R_g = \frac{\rho}{2\pi r} = \frac{100}{2\pi \times 0.5} = 32 \Omega$$

The voltage of the tower is the GPR of the tower:

$$V = I R_g = 10 \times 32 = 320 \text{ V}$$

2. To compute the current through the man, first compute R_f :

$$R_f = 3\rho = 300 \Omega$$

The current through the man is given in Equation 9.13:

$$I_{man} = I \frac{R_g}{R_g + R_{man} + 0.5 R_f} = 10 \frac{32}{32 + 1000 + 150} = 270.72 \text{ mA}$$

3. According to Dalziel's formula, the man can survive for

$$t = \left(\frac{K}{I_{man}} \right)^2 = \left(\frac{157}{270.72} \right)^2 = 336.32 \text{ ms}$$

Example 9.5

Repeat Example 9.4 assuming that a grounding rod is used instead of the hemisphere. Assume that the rod is 4 cm in diameter and is driven 1 m into ground.

Solution

1. The ground resistance of the rod R_g is

$$R_g = \frac{\rho}{2\pi l} \ln \left(\frac{2l + r}{r} \right) = \frac{100}{2\pi \times 1} \ln \left(\frac{2 + 0.02}{0.02} \right) = 73.45 \Omega$$

The voltage of the tower is the GPR of the tower

$$V = I R_g = 10 \times 73.45 = 734.5 \text{ V}$$

Notice that the GPR of a ground rod is much higher than the GPR of a hemisphere.

2.
$$I_{man} = I \frac{R_g}{R_g + R_{man} + 0.5 R_f} = 10 \frac{73.45}{73.45 + 1000 + 150} = 600.35 \text{ mA}$$

3. According to Dalziel's formula, the man can survive for

$$t = \left(\frac{K}{I_{man}} \right)^2 = \left(\frac{157}{600.35} \right)^2 = 68.4 \text{ ms}$$

If the ground rod is driven 1 m into the soil, it provides less protection than the hemisphere. Repeat the problem by assuming that the ground rod is driven 2 m into the soil. Can you develop a conclusion?

9.3.2 STEP POTENTIAL

A person walking adjacent to a structure that passes large current into ground could be vulnerable to electric shocks. This is particularly hazardous in substations, near power line towers that carry high currents, or during lightning storms. Figure 9.15 shows a person walking near a structure that discharges current into ground. The ground current may cause a high enough potential difference between the person's feet resulting in current through his legs and abdomen. This current can be computed using Thevenin's theorem where Thevenin's voltage V_{th} is the open circuit voltage between point a and b as shown in Figure 9.16. This is the same voltage V_{ab} in Equation 9.6 for the case of hemisphere grounding object. r_a is the distance from the center of the hemisphere to the person's rear foot assuming the grounding hemisphere is behind the walking person. r_b is the distance from the center of the hemisphere to his front foot. Thevenin's resistance R_{th} is the open circuit resistance between point a and b (excluding the person) as shown in Figure 9.16.

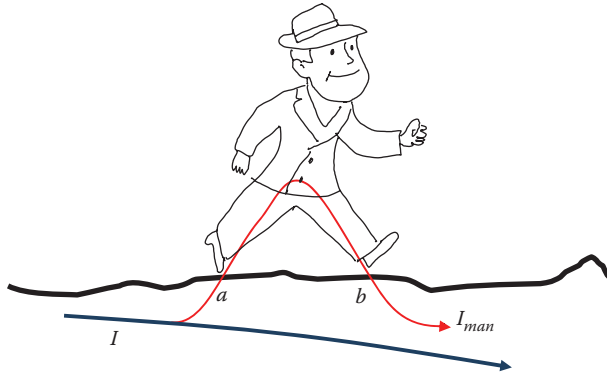


FIGURE 9.15 Current through a person due to step potential.

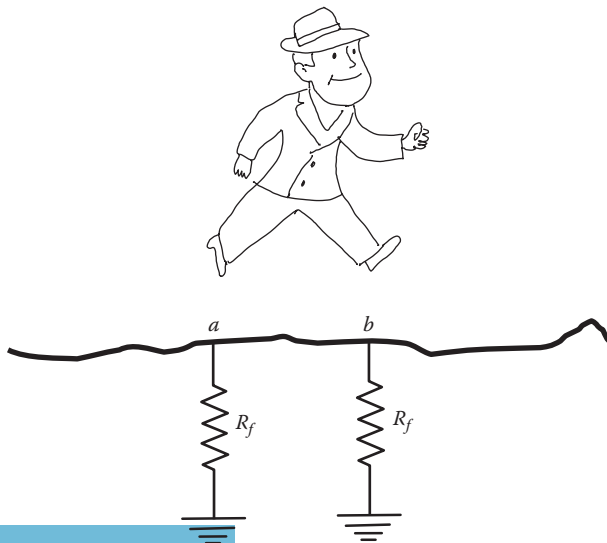


FIGURE 9.16 Thevenin's impedance.

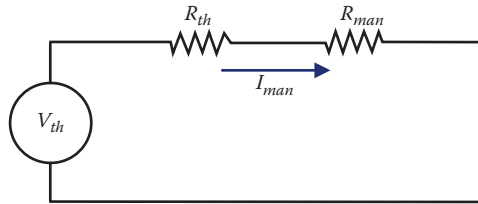


FIGURE 9.17 Equivalent circuit for the step potential.

$$R_{th} = 2R_f \quad (9.15)$$

Figure 9.17 shows the equivalent circuit for the step potential calculations. The body resistance of the person is the resistance of his legs and abdomen. The current through the man can be computed using Thevenin's theorem as given in Equation 9.16:

$$I_{man} = \frac{V_{th}}{R_{th} + R_{man}} = \frac{V_{th}}{2R_f + R_{man}} \quad (9.16)$$

Example 9.6

A short circuit current of 1000 A passes through hemisphere grounding object. A person is walking 5 m away from the center of the hemisphere. Assume that the leg-to-leg body resistance of the person is 1 k Ω , and the soil surrounding the hemisphere is moist. Compute the current through the person and his step potential.

Solution

For moist soil, $\rho = 100 \Omega\cdot\text{m}$. Assume that the step of the person is about 0.6 m. Thevenin's voltage can be computed using Equation 9.6.

$$V_{th} = \frac{I\rho}{2\pi} \left[\frac{1}{r_a} - \frac{1}{r_b} \right] = \frac{1000 \times 100}{2\pi} \left[\frac{1}{5} - \frac{1}{5.6} \right] = 341 \text{ V}$$

$$R_f = 3\rho = 300 \Omega$$

The current through the man can be computed by Equation 9.16

$$I_{man} = \frac{V_{th}}{2R_f + R_{man}} = \frac{341}{600 + 1000} = 213.13 \text{ mA}$$

The step voltage is the voltage between the person's feet:

$$V_{step} = I_{man} \times R_{man} = 213.13 \times 1000 = 213.13 \text{ V}$$

Example 9.7

Repeat Example 9.6 assuming that a grounding rod is used instead of the hemisphere. Assume the rod is inserted 1 m into ground.

Solution

Using the rod equation in Table 9.6, we can obtain Thevenin's voltage:

$$V_{th} = \frac{I\rho}{2\pi l} \left[\ln\left(\frac{2l+r_a}{r_a}\right) - \ln\left(\frac{2l+r_b}{r_b}\right) \right] = \frac{1000 \times 100}{2\pi} \left[\ln\left(\frac{2+5}{5}\right) - \ln\left(\frac{2+5.6}{5.6}\right) \right] = 495 \text{ V}$$

Notice that the voltage on the ground is higher for the ground rod than for the hemisphere.

The current through the man is given in Equation 9.16

$$I_{man} = \frac{V_{th}}{2R_f + R_{man}} = \frac{495}{600 + 1000} = 308.75 \text{ mA}$$

Notice that the ground rod provides less protection than the ground hemisphere.

The step potential of the man is

$$V_{step} = I_{man} \times R_{man} = 308.75 \times 1000 = 308.75 \text{ V}$$

As seen in Examples 9.6 and 9.7, the current through the person is very high. This current may not seem fatal since it does not pass through the heart, lungs, or brain. However, it could be painful enough to cause the person to lose balance and fall on the ground. Then a lethal current could flow through his vital organs.

Example 9.8

During a weather storm, an atmospheric discharge hits a lightning pole. The pole is grounded through a hemisphere and the maximum lightning current through the pole is 20 kA.

1. A person is playing golf 30 m away from the center of the hemisphere. The distance between his feet is 0.3 m, and his leg-to-leg resistance is 1 k Ω . Assume that the soil surrounding the hemisphere is moist. Compute the current through the person and his step potential.
2. Another person is 3 m away from the center of the hemisphere. The distance between his feet is also 0.3 m, and his leg-to-leg resistance is 1 k Ω as well. Compute the current through the person and his step potential.

Solution

For moist soil, $\rho = 100 \Omega\text{-m}$.

(1) Thevenin's voltage can be computed using Equation 9.6:

$$V_{th} = \frac{I\rho}{2\pi} \left[\frac{1}{r_a} - \frac{1}{r_b} \right] = \frac{20,000 \times 100}{2\pi} \left[\frac{1}{30} - \frac{1}{30.3} \right] = 105 \text{ V}$$

$$R_f = 3\rho = 300 \Omega$$

The current through the man can be computed by Equation 9.16:

$$I_{man} = \frac{V_{th}}{2R_f + R_{man}} = \frac{105}{600 + 1000} = 65.63 \text{ mA}$$

The step voltage is the voltage between the person's feet:

$$V_{step} = I_{man} \times R_{man} = 65.63 \times 1000 = 65.63 \text{ V}$$

(2) For the person 3 m away:

$$V_{th} = \frac{I\rho}{2\pi} \left[\frac{1}{r_a} - \frac{1}{r_b} \right] = \frac{20,000 \times 100}{2\pi} \left[\frac{1}{3} - \frac{1}{3.3} \right] = 9.646 \text{ kV}$$

The current through the man can be computed by Equation 9.16:

$$I_{man} = \frac{V_{th}}{2R_f + R_{man}} = \frac{9646}{600 + 1000} = 6.03 \text{ A}$$

$$V_{step} = I_{man} \times R_{man} = 6.03 \times 1000 = 6.03 \text{ kV}$$

The step voltage for the second person is extremely high and it is unlikely that the person can maintain his balance. If he falls on the ground, a lethal current could pass through his vital organs.

9.4 ELECTRIC SAFETY AT HOME

A typical dwelling in the United States is served by one phase of a three-phase 15kV-class distribution feeder as shown in Figure 9.18. The dwelling is fed by three wires from the service transformer (xfm), two hot wires at 120 V each and one neutral wire. The 120 V, which is between a hot wire and the neutral, serves all outlets except the ones for heavy loads such as water heaters and dryers. For these heavy loads, they are powered by 240 V, which is the voltage between the two hot wires. The neutral line, which carries the return electric current, is grounded at the transformer pole and may also be grounded at other poles. The neutral line (also known as the primary neutral), is directly connected to the neutral wire at the customer's site (secondary neutral).

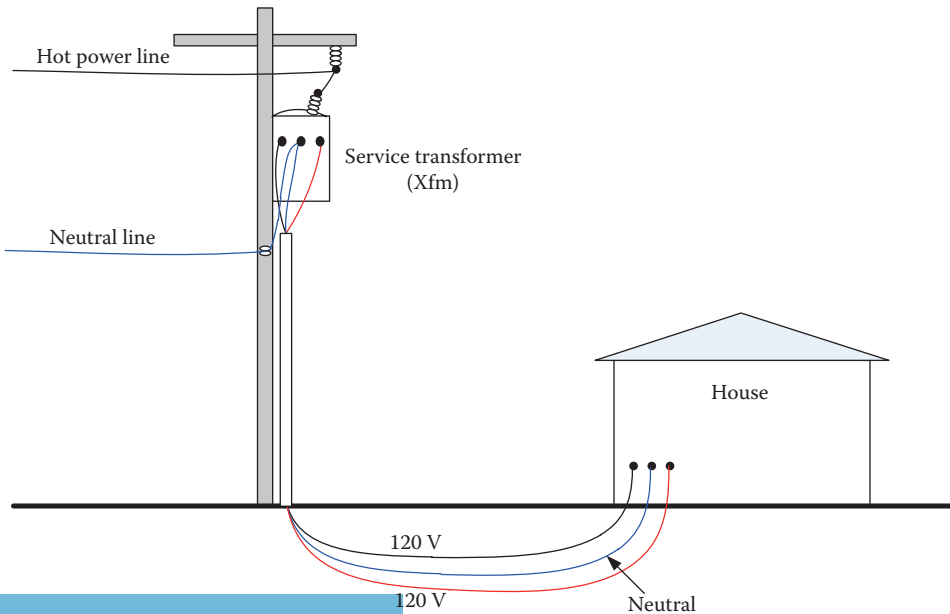


FIGURE 9.18 Dwelling service.

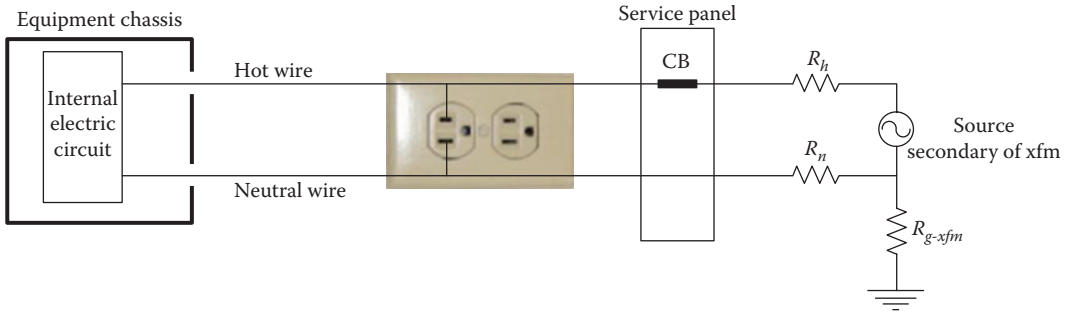


FIGURE 9.19 A basic connection of electrical equipment.

9.4.1 NEUTRAL VERSUS GROUND

You probably noticed that in addition to the hot and neutral wires, you have a ground wire inside your house or apartment. Actually, one of the most confusing issues in electric safety is the difference between the neutral wire and the ground wire. What makes it even more confusing is that the neutral wire is also grounded. So why do we have both of them? To answer this question, let us examine the generic representation of the electric equipment shown in Figure 9.19. The equipment consists of an internal electric circuit housed inside a chassis. The equipment is powered from the secondary of the service transformer (xfm) through two wires: hot, whose resistance is R_h , and neutral, with resistance R_n . The transformer's neutral is grounded through R_{g-xfm} . At the entrance of the customer's dwelling, a service panel is installed to branch the power to the various loads. Each branch (circuit) is served through a dedicated circuit breaker (CB) designed to isolate (disconnect) the branch in case of any fault in the circuit. In the United States, the panel circuit breakers serving the 120 V loads are often rated at 10, 15, and 20 A. For heavier loads served by 240 V, the breakers are often rated at 30 and 40 A.

The electric circuit of the house equipment is normally isolated from the chassis. If the chassis is metallic (conductive), faults inside the electric circuit or insulation failures could elevate the voltage of the chassis. This is a hazardous situation. Take, for example, the case in Figure 9.20. Assume that the hot wire comes in contact with the chassis of the equipment due to insulation failure. If a person standing on grounded object touches the conductive enclosure, the person completes an electrical circuit and the fault current passes through his body. What makes this problem more severe is that the current through the person could be deadly, but still below the clearing level of the circuit breaker of the affected branch as shown in the next example.

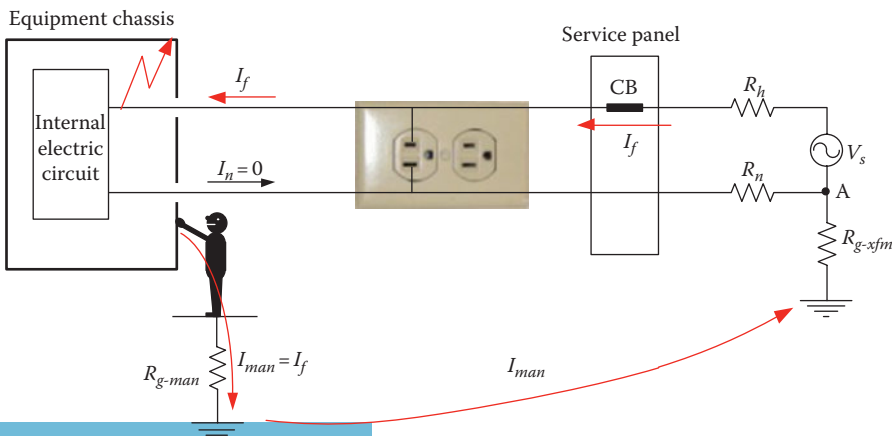


FIGURE 9.20 A person touching a floating chassis of faulty equipment.

Example 9.9

For the case in Figure 9.20, assume that the circuit breaker is rated 20 A, the source voltage is 120 V, $R_n = R_h = 0.5 \Omega$, $R_{g-man} = 500 \Omega$, $R_{man} = 1000 \Omega$, and $R_{g-xfm} = 20 \Omega$. Compute the current through the person touching the chassis.

Solution

The current through the person is the fault current:

$$I_{man} = I_f = \frac{V_s}{R_h + R_{man} + R_{g-man} + R_{g-xfm}} = \frac{120}{0.5 + 1000 + 500 + 20} = 78.92 \text{ mA}$$

This level of current is high enough to cause ventricular fibrillation. Additionally, the current through the person will not be interrupted by the circuit breaker.

As seen in the last example, the person is left without protection. To improve the safety of the circuit, let us consider the following solutions:

1. Grounding the chassis
2. Bonding the chassis to the neutral wire
3. Grounding the chassis and bonding the ground wire to the secondary neutral

9.4.1.1 Grounding Chassis

Let us connect the metallic enclosure to the local ground at the service panel as shown in Figure 9.21. The conductor that connects the chassis to the local ground is called *Equipment Grounding Conductor* (EGC). The local ground can be established by a ground rod outside the dwelling, a wire connected to a well-grounded metal water pipe, or both. In this system, when fault occurs, the fault current is branched into two paths as shown in Figure 9.21: one through the EGC wire (I_{EGC}) and the other through the person (I_{man}).

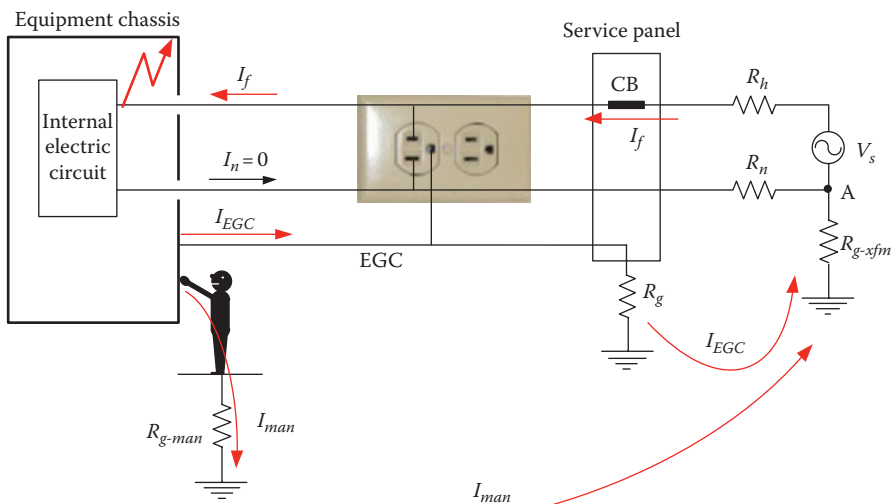


FIGURE 9.21 A person touching a chassis with EGC during fault.

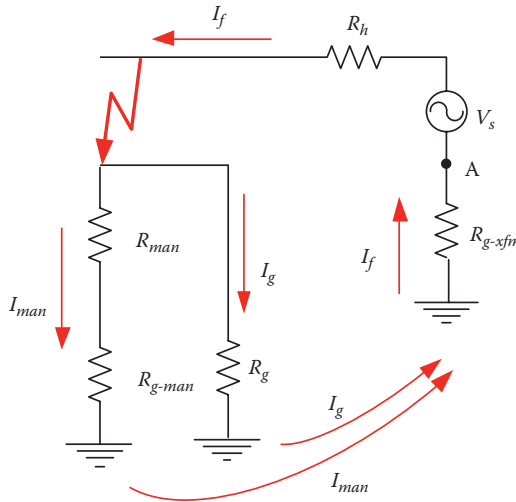


FIGURE 9.22 Equivalent circuit for the system in Figure 9.21.

Example 9.10

For the case in Figure 9.21, assume that the circuit breaker is rated 20 A, the source voltage is 120 V. The system parameters are $R_n=R_h=0.5\ \Omega$, $R_{g-man}=500\ \Omega$, $R_{man}=1000\ \Omega$, $R_g=10\ \Omega$, and $R_{g-xfm}=20\ \Omega$. Compute the fault current and the current through the person touching the chassis.

Solution

The equivalent circuit of the system in Figure 9.21 is shown in Figure 9.22

Since R_g is in parallel with the person plus his ground resistance, the equivalent resistance of this combination is

$$R_{eq} = \frac{R_g (R_{man} + R_{g-man})}{R_g + (R_{man} + R_{g-man})} = \frac{10 \times (1000 + 500)}{10 + 1000 + 500} = 9.93\ \Omega$$

The fault current is then

$$I_f = \frac{V_s}{R_h + R_{eq} + R_{g-xfm}} = \frac{120}{0.5 + 9.93 + 20} = 3.94\ \text{A}$$

This fault current is still below the clearing limit of household circuit breakers and will not be cleared. The current through the person is

$$I_{man} = I_f \frac{R_g}{R_g + (R_{man} + R_{g-man})} = 3.94 \frac{10}{10 + (1000 + 500)} = 26.1\ \text{mA}$$

Because of grounding the chassis, the current through the person is reduced as compared with that in Example 9.9. However, it is still hazardous.

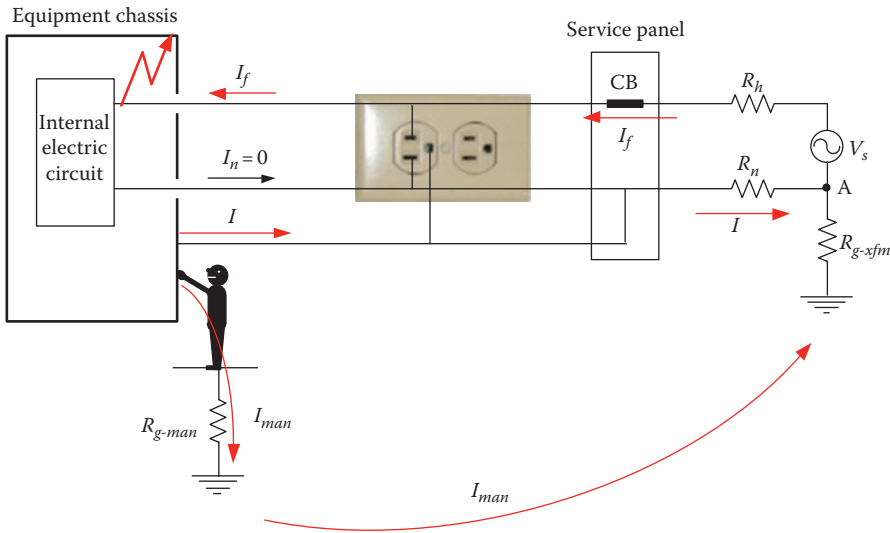


FIGURE 9.23 A person touching a chassis bonded to system neutral.

Based on the previous example, we can conclude that grounding the chassis alone is not protecting the person during faults. This is because of two major problems:

1. Current through the person is still hazardous.
2. Fault current is below the activation level of the circuit breaker.

The low value of the fault current is due to the high resistance path through the local ground resistance R_g and the ground resistance at the transformer R_{g-xfm} . Intuitively, we need to have a low resistance path for the fault current to activate the circuit breaker. This is our next system.

9.4.1.2 Bonding Chassis to Neutral

The main objective of any protection technique is to have the fault current as large as possible to open the circuit breaker and isolate the faulty branch. To do this, it is important to have a low resistance path for the fault current. The system in Figure 9.23 satisfies this objective. In this system, the chassis is bonded to the neutral wire at the service panel. This should be the best way to clear faults as seen in the next example.

Example 9.11

In the case in Figure 9.23, assume that the circuit breaker is rated at 20 A and the source voltage is 120 V. The system parameters are $R_n = R_h = 0.5 \Omega$, $R_{g-man} = 500 \Omega$, $R_{man} = 1000 \Omega$, $R_g = 10 \Omega$, and $R_{g-xfm} = 20 \Omega$. Compute the fault current.

Solution

The equivalent circuit for the case in Figure 9.23 is shown in Figure 9.24.

Notice that R_n is in parallel with $R_{g-man} + R_{man} + R_{g-xfm}$. The equivalent resistance of this combination R_{eq} is

$$R_{eq} = \frac{R_n (R_{man} + R_{g-man} + R_{g-xfm})}{R_n + (R_{man} + R_{g-man} + R_{g-xfm})} = \frac{0.5 \times (1000 + 500 + 20)}{0.5 + 1000 + 500 + 20} \approx 0.5 \Omega$$

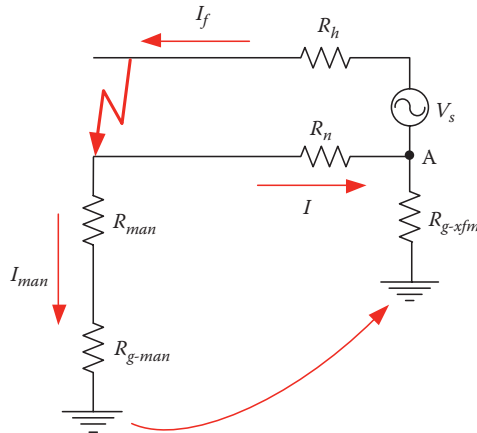


FIGURE 9.24 Equivalent circuit for Figure 9.23.

The fault current is then

$$I_f = \frac{V_s}{R_h + R_{eq}} = \frac{120}{0.5 + 0.5} = 120 \text{ A}$$

This current is very high and will certainly activate the circuit breaker. Thus, the person is isolated from the hazard.

Although the system in Figure 9.23 is very good at clearing faults, it has a weakness. Bonding the chassis to the neutral may cause elevated voltage on the chassis during normal operation, especially for heavily loaded branch and long feeders (high resistance). Consider the system in Figure 9.25 where the equipment is assumed to be drawing heavy current that is still below the circuit breaker

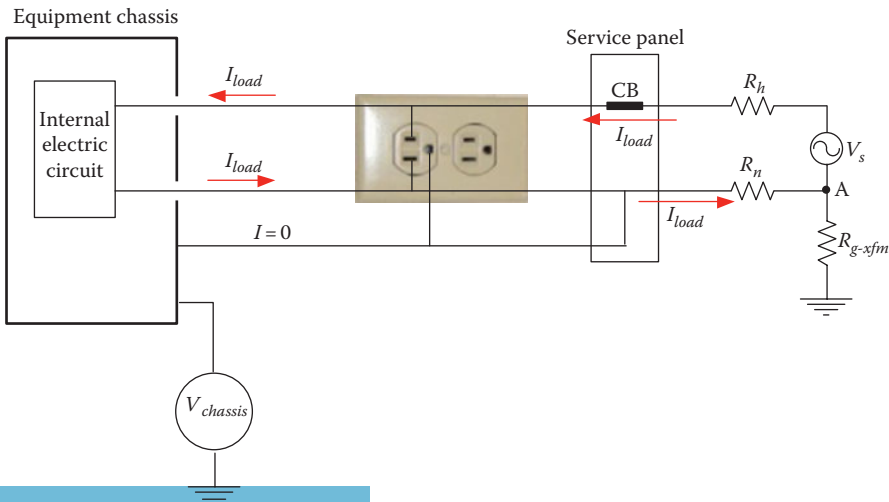


FIGURE 9.25 Chassis voltage of heavily loaded equipment.

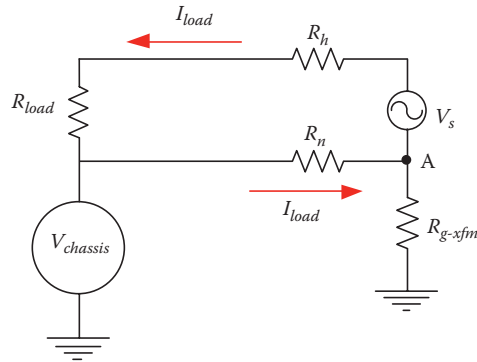


FIGURE 9.26 Equivalent circuit for Figure 9.25.

clearing limit. If we measure the chassis voltage $V_{chassis}$ using a voltmeter between the chassis and ground, the voltage could be elevated as seen in the next example.

Example 9.12

In the case in Figure 9.25, assume that the circuit breaker is rated at 20 A and the source voltage is 120 V. The system parameters are $R_n = R_h = 0.5 \Omega$, $R_{g-man} = 500 \Omega$, $R_{man} = 1000 \Omega$, $R_g = 10 \Omega$, and $R_{g-xfm} = 20 \Omega$. Compute the voltage of the chassis during normal operation when the load resistance of the equipment is 6Ω .

Solution

The equivalent circuit for the case in Figure 9.25 is shown in Figure 9.26.

Since there is no current through R_{g-xfm} , point A is at the ground potential level. Then, the voltage on the chassis is the voltage drop across R_n . Let us compute the load current

$$I_{load} = \frac{V_s}{R_n + R_h + R_{load}} = \frac{120}{0.5 + 0.5 + 6} = 17.14 \text{ A}$$

The current is within the operating range of the 20 A circuit breaker.

The voltage across the chassis is

$$V_{chassis} = I_{load} R_n = 17.14 \times 0.5 = 8.57 \text{ V}$$

This level of voltage on a chassis is considered high.

9.4.1.3 Grounding Chassis and Bonding Ground to Neutral

To address the problem associated with the elevated chassis voltage during normal operation and to ensure that the fault current is high enough to trip the circuit breaker, electrical engineers have combined the systems in Figures 9.21 and 9.23. This is shown in Figure 9.27 where the EGC is grounded locally and is also bonded to the neutral conductor. This is the system adapted in the United States and most of the world. The system ensures that the circuit breaker trips when internal fault occurs and also reduces the voltage on any equipment chassis during normal operation. These two advantages are examined in the following two examples.

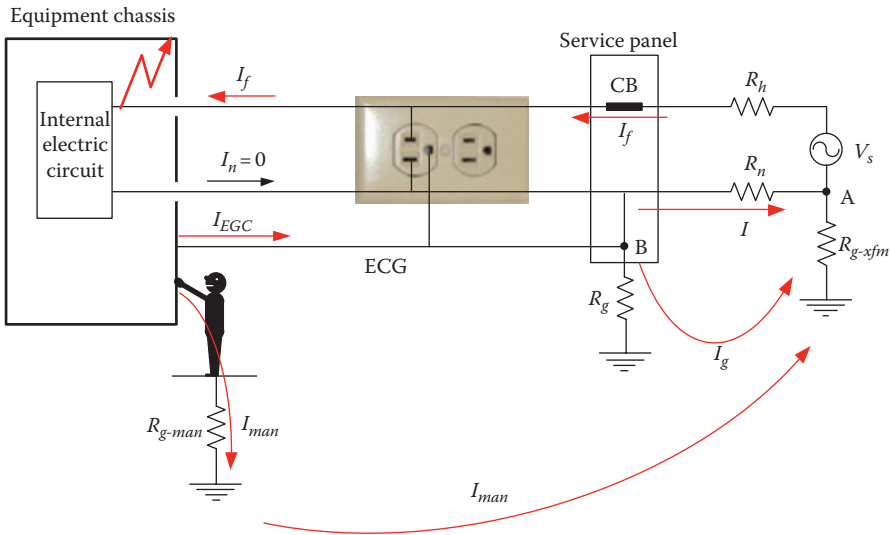


FIGURE 9.27 Modern wiring system.

Example 9.13

For the case in Figure 9.27, assume that the circuit breaker is rated at 20 A and the source voltage is 120 V. The system parameters are $R_n = R_h = 0.5 \Omega$, $R_{g-man} = 500 \Omega$, $R_{man} = 1000 \Omega$, $R_g = 10 \Omega$, and $R_{g-xfm} = 20 \Omega$. Compute the fault current.

Solution

The equivalent circuit of the system in Figure 9.27 is shown in Figure 9.28
 R_g is in parallel with the person plus his ground resistance.

$$R_{eq1} = \frac{R_g (R_{man} + R_{g-man})}{R_g + (R_{man} + R_{g-man})} = \frac{10 \times (1000 + 500)}{10 + 1000 + 500} = 9.93 \Omega$$

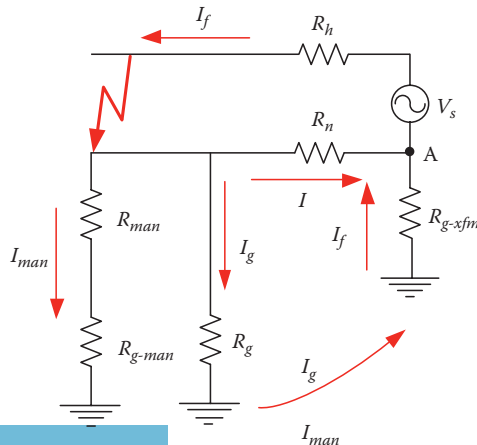


FIGURE 9.28 Equivalent circuit for the system in Figure 9.27.

R_{eq1} is in series with R_{g-xfm} .

$$R_{eq2} = R_{g-xfm} + R_{eq1} = 20 + 9.93 = 29.93 \Omega$$

The equivalent resistance representing R_n in parallel with R_{eq2} is

$$R_{eq} = \frac{R_n R_{eq2}}{R_n + R_{eq2}} = \frac{0.5 \times 29.93}{0.5 + 29.93} = 0.492 \Omega$$

The fault current is then

$$I_f = \frac{V_s}{R_h + R_{eq}} = \frac{120}{0.5 + 0.492} = 120.97 \text{ A}$$

This fault current is very high and the circuit breaker will clear the fault.

Example 9.14

In the case in Figure 9.29, assume that the circuit breaker is rated at 20 A and the source voltage is 120 V. The system parameters are $R_n = R_h = 0.5 \Omega$, $R_{g-man} = 500 \Omega$, $R_{man} = 1000 \Omega$, $R_g = 10 \Omega$, and $R_{g-xfm} = 20 \Omega$. Compute the voltage of the chassis during normal operation when the load resistance is 6Ω .

Solution

The equivalent circuit for the case in Figure 9.29 is shown in Figure 9.30.

The voltage of the chassis is the voltage drop across R_g . But first, let us compute the equivalent resistance of R_n , R_g , and R_{g-xfm} :

$$R_{eq} = \frac{R_n (R_g + R_{g-xfm})}{R_n + R_g + R_{g-xfm}} = \frac{0.5 \times (10 + 20)}{0.5 + 10 + 20} = 0.492 \Omega$$

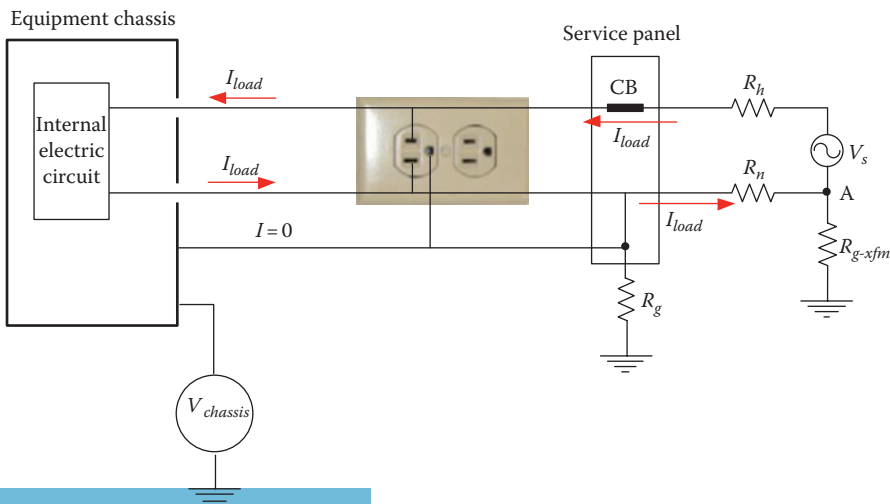


FIGURE 9.29 Chassis voltage of heavily loaded equipment with local ground.

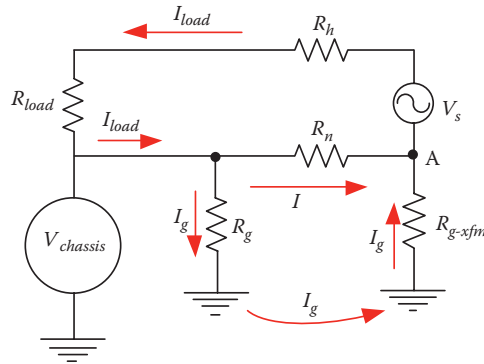


FIGURE 9.30 Equivalent circuit for Figure 9.29.

The load current is

$$I_{load} = \frac{V_s}{R_{eq} + R_h + R_{load}} = \frac{120}{0.492 + 0.5 + 6} = 17.16 \text{ A}$$

The current is within the normal value for the 20 A circuit breaker.

The current through R_g is

$$I_g = I_{load} \frac{R_n}{R_n + R_g + R_{g-xfm}} = 17.16 \frac{0.5}{0.5 + 10 + 20} = 0.281 \text{ A}$$

The voltage across the chassis is

$$V_{chassis} = I_g R_g = 0.281 \times 10 = 2.81 \text{ V}$$

This level of voltage is one third of that computed in Example 9.12. Keep in mind that the voltage of the chassis will never be at zero potential. Our objective is to make it as small as possible.

9.4.2 DWELLING DISTRIBUTION CIRCUITS

In the United States and most of the world, the wires coming from the service transformer enter the dwelling through a utility meter then into a distribution panel as shown in Figure 9.31. There are two functions to this panel: (1) distribute the power to the various loads inside the dwelling and (2) protect the individual circuits from internal fault by tripping the corresponding circuit breaker.

The dwelling is fed by three wires from the service transformer, two at 120 V and one is neutral. The neutral wire, which is grounded at the transformer pole, is also grounded at the entrance of the dwelling to provide the local ground required by the National Electric Code (NEC) as discussed earlier. The local ground is achieved by using copper or alloy rod inserted into the ground, by bonding the neutral to metal pipes, bonding the neutral to steel reinforcement bars, or any combination of these. The NEC requires that this local ground be 5 ft (1.524 m) or less from the point of entry (distribution panel). A separate EGC wire (green or uninsulated wire) is used to bring all conductive enclosures inside the dwelling to the local ground level.

To ensure that the users cannot connect the equipment in a wrong way (hot wire goes to the chassis, for example), the outlets (receptacles or sockets) and plugs are carefully designed. Worldwide, there are several types of outlets and plugs depending on the standard adapted by the various countries.

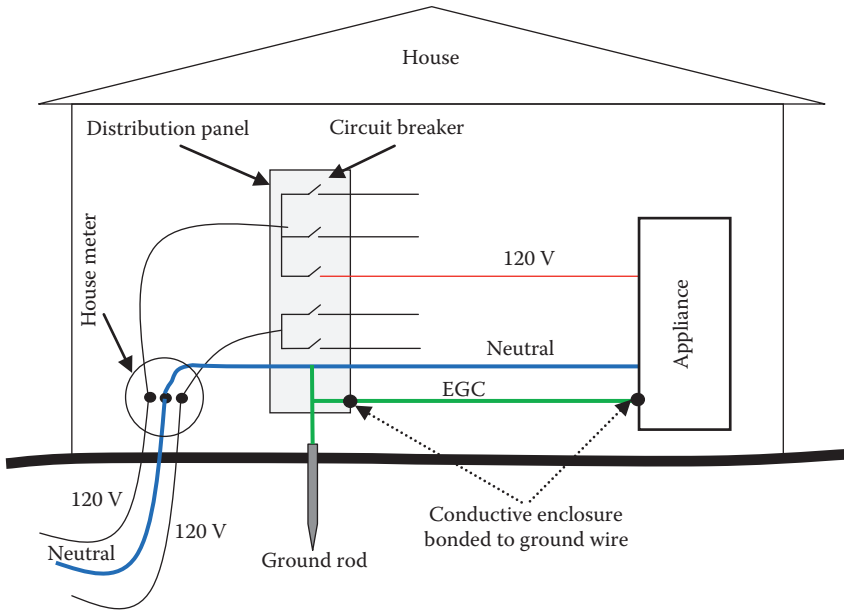


FIGURE 9.31 Electric circuit distribution inside a dwelling.

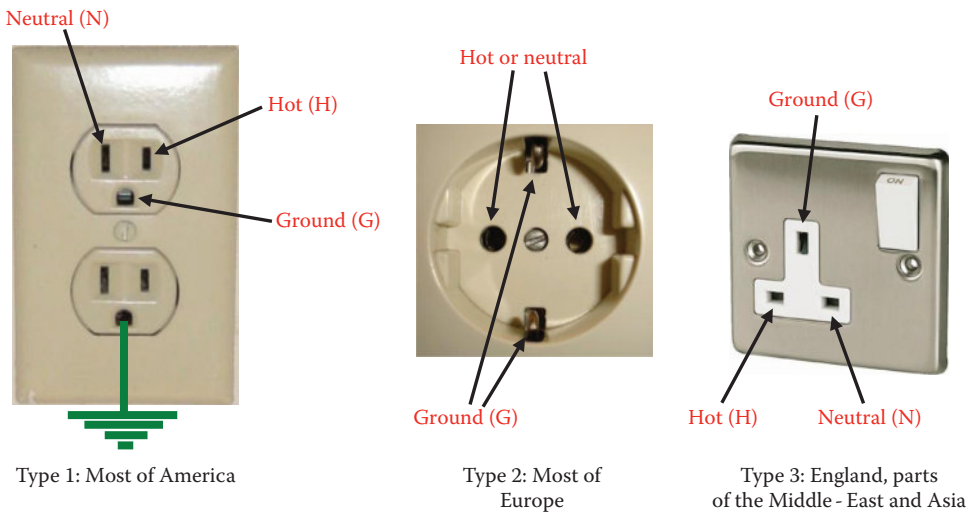


FIGURE 9.32 Three types of household outlets.

The world has 13 different types of receptacles, but most of them are exclusively used by a few countries. The most common power outlets are shown in Figure 9.32. Each of the outlets in the figure has the three terminals discussed earlier: hot, neutral, and ground (EGC). The wires are color coded. In the United States, hot is black or red, neutral is white, and ground is either green or uninsulated. In North America, the hot and neutral terminals accept plugs with flat prongs and the ground terminal accepts a rounded prong. The opening of the neutral terminal is often wider than that for the hot terminal. This is known as polarized socket. This polarization is very important as some equipment use two-prong plugs and their chassis are used as common neutral for their electrical circuits. Therefore the chassis must not be connected to the hot wire of the system. The narrow terminal of the hot wire in the socket guarantees that the neutral of the plug cannot be inserted into the hot terminal.



FIGURE 9.33 Common household plugs in North America. (a) Type 1: unpolarized, (b) Type 1: polarized, and (c) Type 1: three prongs.

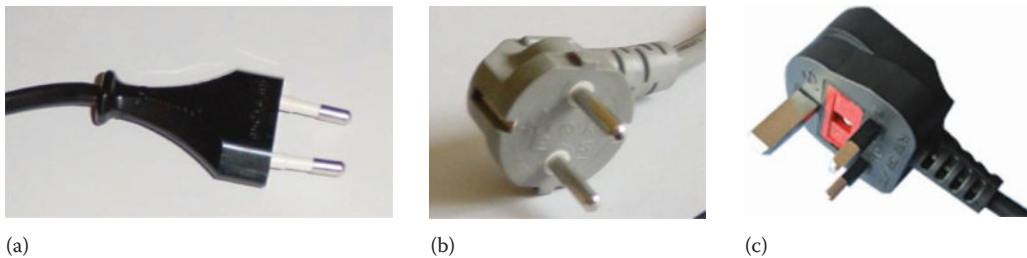


FIGURE 9.34 Common international household plugs. (a) Type 2: unpolarized, (b) Type 2: three prongs, and (c) Type 3: three prongs.

For Type 2 socket, there are two ground terminals; one at the top of the socket and the other at the bottom. The hot and neutral terminals are round shaped. In the British system, Type 3, all terminals are flat.

Household plugs also come in various shapes such as the ones in Figure 9.33 for Type 1 socket and in Figure 9.34 for Type 2 and 3 receptacles. In Figure 9.33a, the plug is unpolarized with two equal-width prongs; therefore either prong can be connected to the neutral terminal of the outlet. This is used with equipment that has chassis made of insulated material. In Figure 9.33b, the plug has two prongs as well, but it is polarized where the neutral prong is wider than the hot prong. This way, the neutral side of the plug can only fit the neutral side of the outlet. Figure 9.33c, shows the three-prong plug where two of the prongs are flat and the third is rounded. The ground prong (EGC) is longer than the other two. In this configuration, when the plug is inserted into the outlet, the ground terminal is connected to the chassis before the circuit is energized. Also, in this configuration, the neutral and hot terminals cannot be interchanged.

The international plug versions are shown in Figure 9.34. In Figure 9.34a, the prongs are rounded and unpolarized which is suitable for insulated chassis. In Figure 9.34b, the ground terminals are embedded on both sides of the plug. This way, when the plug is inserted into the socket either straight or upside down, the ground connection is established. Notice that Type 2 socket is deep. This way when the plug is inserted into the socket, the ground connection is established first before any of the neutral or hot prongs are inserted into the socket. In Figure 9.34c, the ground prong is longer than the other two to ensure that the ground terminal of the plug is connected before its other two terminals. In some Type 3 receptacles, the neutral and hot terminals are closed until the ground terminal of the plug is inserted first.

9.4.3 GROUND FAULT CIRCUIT INTERRUPTER

One of the most common electric shock scenarios is when electric equipment is mixed with water. Tap water is conductive, and its intrusion allows the circuit components to be electrically connected to the chassis.

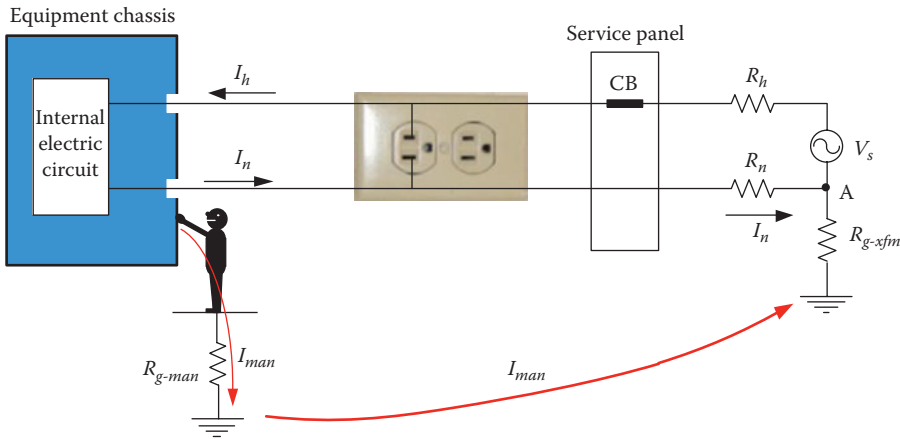


FIGURE 9.35 Water inside a device can create hazardous condition.

Equipment with insulated chassis, such as hair dryer, often has two-prong plug. Because the chassis is insulated, the EGC is often not used. If water gets into the hair dryer, the high voltage wires and the circuit components may come in contact with the dryer’s chassis. If a person touches the wet dryer while part of his/her body is in contact with a grounded surface, such as faucets, the person could be electrocuted as depicted in Figure 9.35. The fundamental question is why does not the dwelling breaker interrupt the circuit? After all, the breakers are installed to disconnect faulty circuits. Remember Example 9.9 when the current through the person is deadly, but still below the breaker clearing limit. For this reason, a *ground fault circuit interrupter* (GFCI) is used in wet areas such as kitchens, bathrooms, gardens.

The GFCI receptacle is similar in shape to the regular outlet as shown in Figure 9.36, but has two buttons and a built-in circuit interrupter. The circuit interrupter of the GFCI is shown in Figure 9.37. It consists of a core, activation circuit and a relay switch. The hot and neutral wires go through the ring of the core. The core has winding wrapped around it. If the current in the hot wire I_h is exactly equal to the neutral current I_n , the total magnetic field (MF) produced by both wires is zero. Hence, no voltage is induced across the winding. When a ground current (I_g) is present, I_h is higher than



FIGURE 9.36 GFCI outlet.

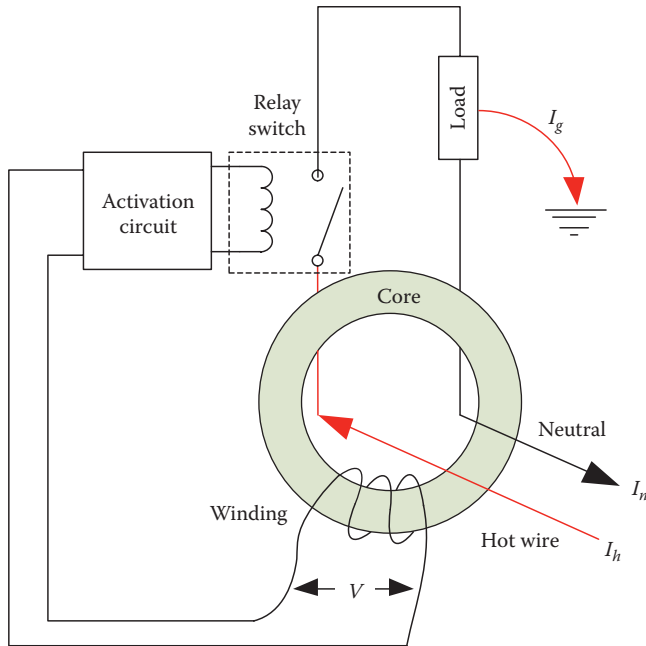


FIGURE 9.37 GFCI circuit.

I_n and the total MF is nonzero. Hence, a voltage V is induced across the winding of the core. This voltage through the activation circuit energizes a relay that disconnects the hot wire. The GFCI has two buttons: one is used to test the circuit for functionality and the other is used to reset the circuit after interrupting a fault.

9.4.4 NEUTRAL INTEGRITY

The integrity of the neutral wire is a major safety requirement. Deteriorated or severed neutral wire can affect the safety in the dwelling as well as in the neighborhood connected to the same power circuit. A single transformer can serve more than one dwelling as shown in Figure 9.38. The figure shows a system with two loads (houses) powered by the same hot and neutral wires. In each house, the EGC is bonded to the neutral wire and is also connected to local grounds (R_{g1} and R_{g2}). The resistance of the neutral wire between the first and second house is R_{n1} , and between the second house and the transformer is R_{n2} . Under normal operation, the current flow is shown in the figure.

Let us assume that the neutral wire between the two houses is broken, and let us even assume that the equipment in the second house is not energized as shown in Figure 9.39. In this case, the current in the first load I_1 returns back to the source via several ground paths as shown in the figure. The current I_1 leaving the first house and going to ground makes the potential of the EGC of the first house positive with respect to ground. When I_{g2} enters the second house through its ground resistance R_{g2} , the potential of the EGC of the second house is negative with respect to ground.

$$V_{EGC1} = V_{chassis1} = I_1 R_{g1}$$

$$V_{EGC2} = V_{chassis2} = -I_{g2} R_{g2} \tag{9.17}$$

If a person in either house is standing on grounded object while touching the chassis, the person will form an additional path for I_1 . Let us assume that the person is in the second house. Because the

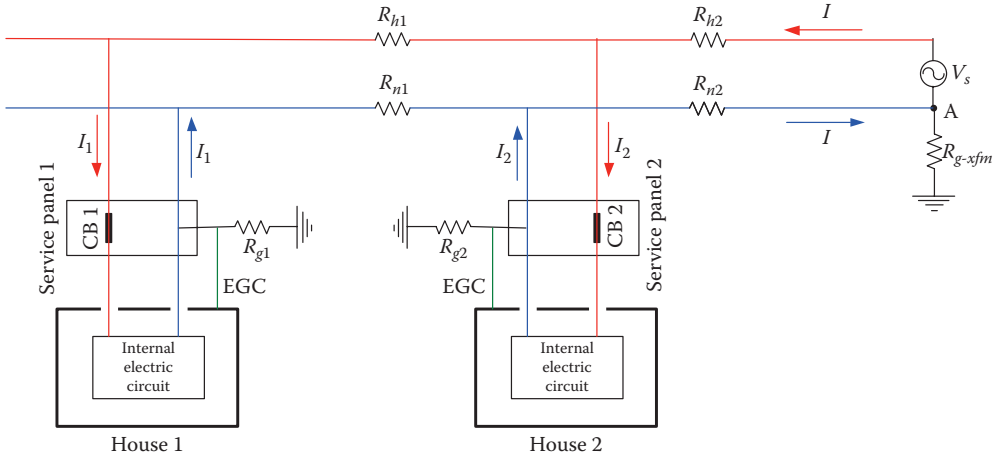


FIGURE 9.38 More than one house served by the same transformer.

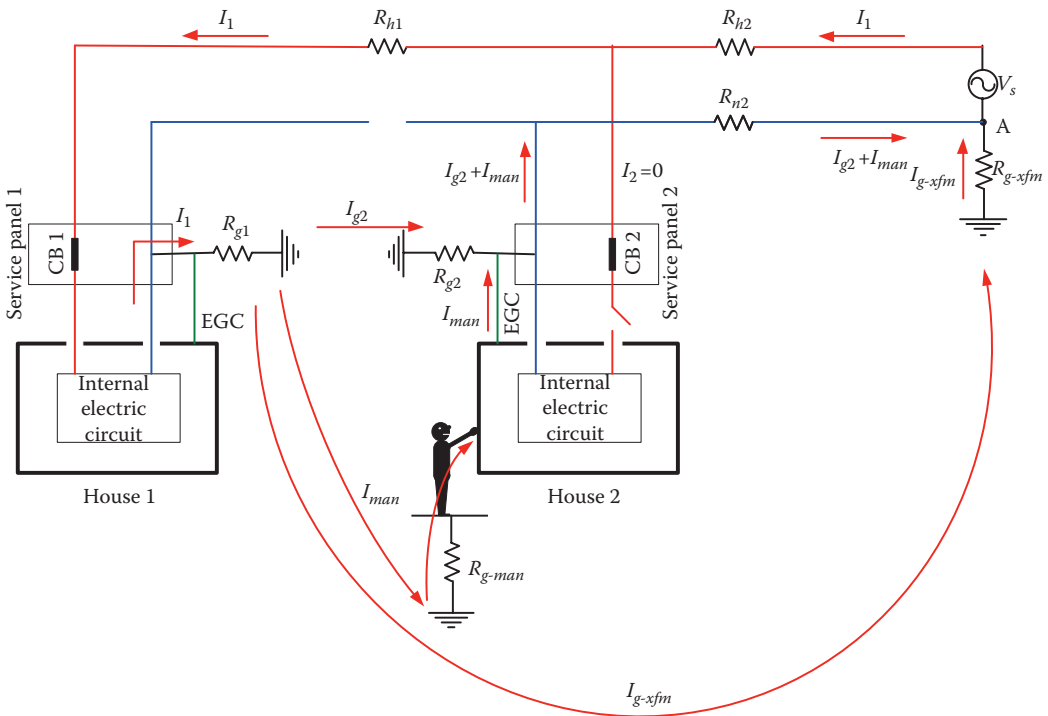


FIGURE 9.39 Hazard due to broken neutral wire.

potential of the chassis is negative with respect to ground, a current will flow from the ground to the person, then to the chassis and back to the source via the neutral wire of the second house as shown in Figure 9.39. This current could be lethal.

Example 9.15

For the system in Figure 9.39, assume that the neutral wire between the two loads is broken. The system parameters are $R_{man} = 1000\ \Omega$, $R_{g-man} = 500\ \Omega$, $R_{g-xfm} = 20\ \Omega$, $R_{g1} = R_{g2} = 10\ \Omega$ and

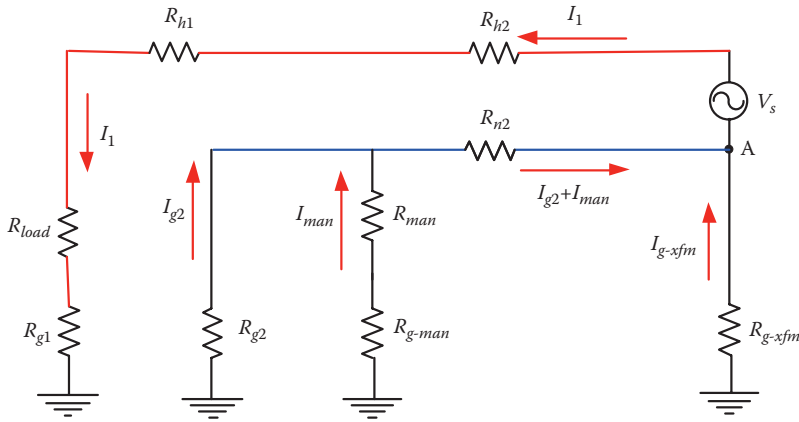


FIGURE 9.40 Equivalent circuit of system in Figure 9.39.

$R_{n2} = R_{h1} = R_{h2} = 0.5 \Omega$. Assume that the total load of the house 1 is 5Ω . Compute the voltage of the chassis in both houses. Also compute the current through a person touching the chassis of the equipment in the second house.

Solution

The equivalent circuit of the system in Figure 9.39 is shown in Figure 9.40. To compute the load current, we need to compute the equivalent resistance of the second house plus the neutral and transformer resistances.

$$R_{eq1} = \frac{R_{g2} (R_{man} + R_{g-man})}{R_{g2} + R_{man} + R_{g-man}} = \frac{10 \times (1000 + 500)}{10 + 1000 + 500} = 9.93 \Omega$$

$$R_{eq} = \frac{R_{g-xfm} (R_{eq1} + R_{n2})}{R_{g-xfm} + R_{eq1} + R_{n2}} = \frac{20 \times (9.93 + 0.5)}{20 + 9.93 + 0.5} = 6.855 \Omega$$

The current in house 1 is

$$I_1 = \frac{V_s}{R_{h1} + R_{h2} + R_{load} + R_{g1} + R_{eq}} = \frac{120}{0.5 + 0.5 + 5 + 10 + 6.855} = 5.25 \text{ A}$$

Notice that the current is within the normal operation level and the circuit breaker will not trip.

The potential of chassis 1 is the voltage drop across R_{g1} :

$$V_{chassis1} = I_1 R_{g1} = 5.25 \times 10 = 52.5 \text{ V}$$

This voltage is very high and could be lethal.

The current through the person in the second house can be computed as

$$I_{g2} + I_{man} = I_1 \frac{R_{g-xfm}}{R_{g-xfm} + R_{eq1} + R_{n2}} = 5.25 \frac{20}{20 + 9.93 + 0.5} = 3.45 \text{ A}$$

The current through the man is then

$$I_{man} = 3.45 \frac{R_{g2}}{R_{g2} + R_{man} + R_{g-man}} = 3.45 \frac{10}{10 + 1000 + 500} = 22.85 \text{ mA}$$

This is a lethal current even though the second house is not energized.

The voltage across the *chassis* in the second house is

$$V_{chassis2} = -I_{g2} R_{g2} = -(3.45 - 0.02285) \times 10 = -34.27 \text{ V}$$

Notice that although the second house is de-energized, the voltage on its appliance is 34.27 V due to the broken neutral wire.

The previous example shows that electrical safety depends on the entire network connected through the transformer instead of only the configuration of a single circuit. Notice that the loss of the hot wire will just disconnect the circuit, but the loss of neutral wire can cause hazardous conditions.

9.4.5 WORLD'S RESIDENTIAL GROUNDING PRACTICES

When it comes to the wiring practice worldwide, there is a great deal of confusion about the roles of the neutral and ground wires. Often, you find no ground wires in some countries while others just bond the chassis to the neutral. The system with the worst safety configuration is the one shown in Figure 9.41. The system does not have ground wire and has no protection against internal faults.

For the system in Figure 9.42, the chassis is bonded to the neutral wire. In this case, the utility provides only two wires; hot and neutral. The system protects against internal faults, but the chassis could have elevated voltage during heavy loading conditions as discussed in Example 9.12.

The system in Figure 9.43 is the one adapted in the United States and several other countries. It is still two-wire system, but because of the local grounding and the bonding of the EGC to the neutral wire, the system protects against internal faults and during heavy loading conditions. This is especially true if the local ground resistance is low.

The system in Figure 9.44 has three separate wires coming from the utility: hot, neutral, and ground (EGC). The neutral and ground wires are separated, so the potential on the chassis during heavy loading condition does not exist. Moreover, the path resistance of internal fault is very

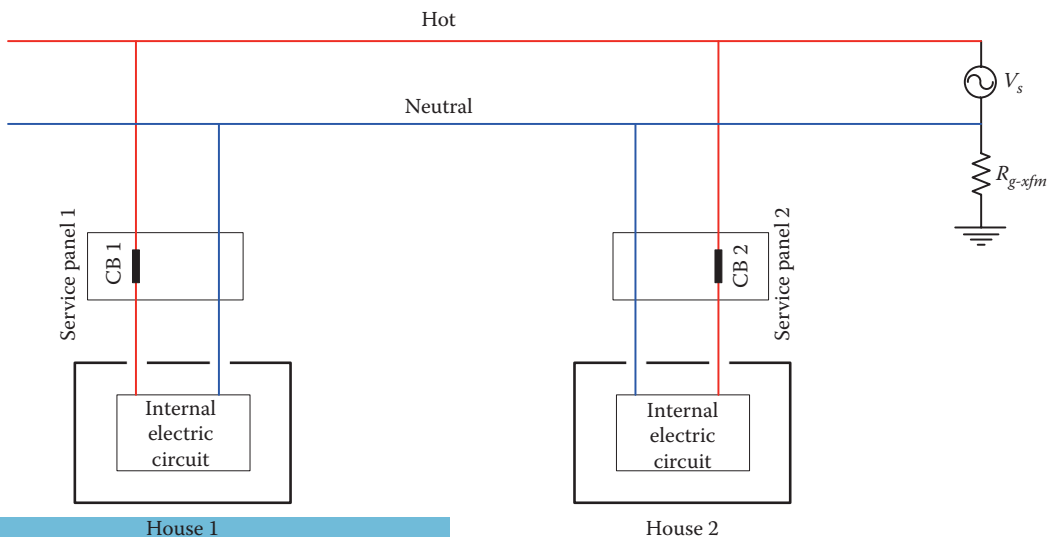


FIGURE 9.41 System without ground wire.

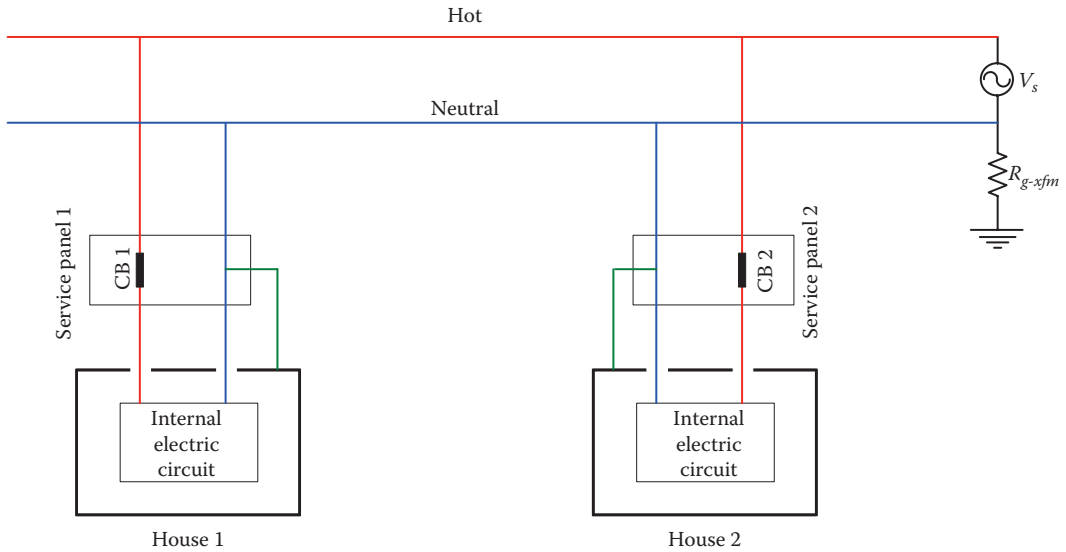


FIGURE 9.42 System without bonded neutral to chassis.

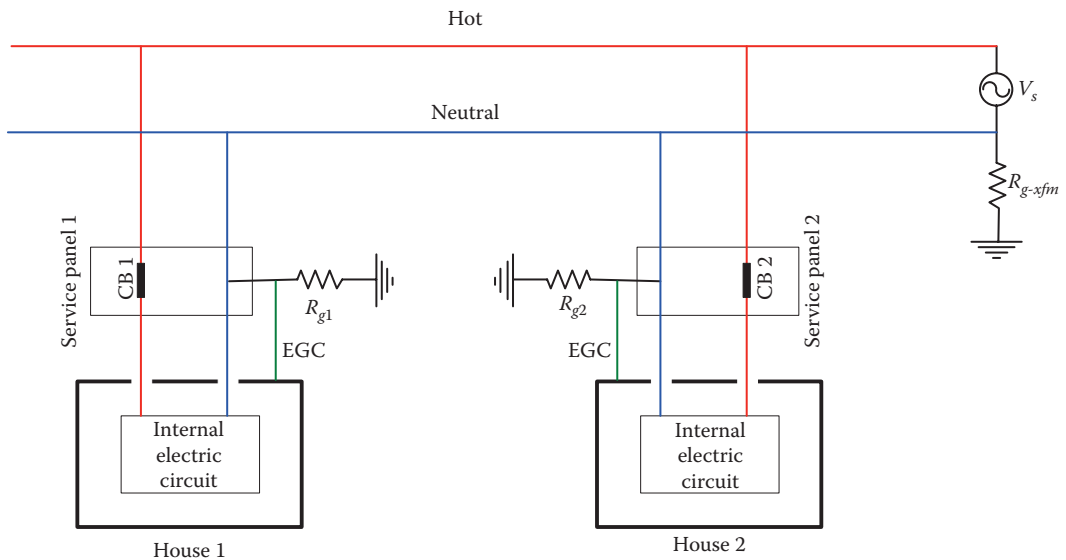


FIGURE 9.43 System with bonded and grounded neutral.

low, making the fault current high and simple to clear by circuit breakers. This system is the safest design. However, it required additional conductor to be delivered from the service transformer to all houses. This is an extra expense that some utility see unnecessary.

9.5 LOW FREQUENCY MAGNETIC FIELD AND ITS HEALTH EFFECTS

The health effect of low-frequency magnetic field (MF) is a controversial issue that creates strong emotion on all fronts. The interest in the subject started in the Soviet Union in the 1960s after health problems were observed in personnel working in electric switchyards. These health problems were thought to be associated with MF exposure. The study created widespread scientific interest in the

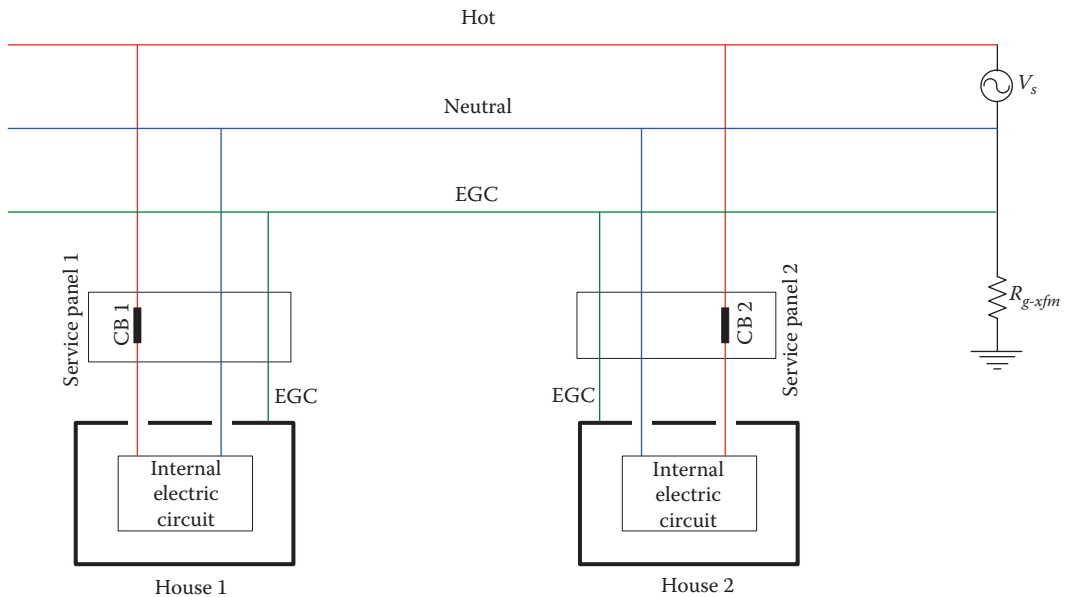


FIGURE 9.44 System with separated ground wire.

subject among epidemiologist scientists. One of the famous studies was made in Denver, Colorado, in 1979 where epidemiologists suggested that children who had died from cancer were two to three times more likely to have lived in homes near high-current power lines than children in the general population. A large number of additional epidemiological studies followed, but the results were highly inconsistent and contradictory. The outcomes of these studies frustrate the public and spread anxiety and speculation than resolve their concern.

In the opinion of a large segment of the scientific community, most of these epidemiological studies were flat out flawed due to the small samples they used and the single statistical association technique they assumed. In some studies, the samples did not exceed 100 people. In most of the studies, no other factor that may affect public health besides the MF was considered. For example, power lines are often located near heavily traveled highways where the pollution from cars and trucks contributes to health conditions. Also, work environments often present many other exposures that could negatively affect the health, such as toxic chemicals.

9.5.1 LOW-FREQUENCY MAGNETIC FIELDS

Each electrically powered device is surrounded by an electromagnetic field (EMF). An EMF is composed of electric field (EF) due to voltage and MF due to current. The interest in the potential health effects focused mainly on the MF. Besides the MF created by electric currents, MF occurs in nature where the earth's MF density B ranges between 300 and 600 mG (milligauss). The lower number is for South America and South Africa, and the higher number is for areas near the earth's magnetic poles such as northern Canada. Solar flare and cosmic radiation also produce MFs.

In most homes, the MF density B in the center of a room averages to less than 1 mG. Homes close to power lines tend to have higher MF density than average. Home appliances emit MF that is dependent on their operating voltage and power. Figure 9.45 shows typical values of B for some popular home appliances. The figure shows the values of B measured at various distances from the appliances. Notice that the MF is substantially reduced when we move away from the appliance.

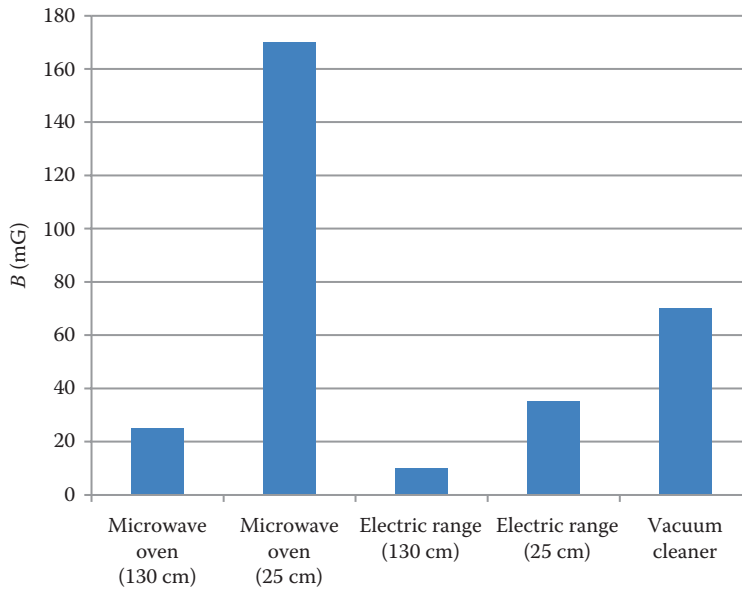


FIGURE 9.45 MF density of home appliances.

For power lines, the MF density varies widely depending on the amount of current passing through their conductors. However, a typical value for 500kV fully loaded line is about 100mG under the line and about 5 mG when we move just 70m away from the energized conductor.

9.5.2 BIOLOGICAL EFFECTS OF MAGNETIC FIELD

Scientists have tried to pinpoint whether the low-frequency MF affects people, animals, or vegetation. Several cell level laboratory studies have indicated that MF exposure may cause some temporary biological effects such as changes in hormone levels. The studies have shown that currents induced in humans due to low-frequency MF are weaker than the natural electrical signals that control the brain and heart. These low-frequency currents pass mostly between the cells and do not penetrate the cell membranes.

The World Health Organization (WHO) has coordinated several extensive studies on the EMF and its effects on public health and the environment. In their information sheet published in February 2005, several areas were addressed: biological effects on humans and animals, vegetation, and aquatic life. The following are direct quotes from the report.

... ..

Animals

Most studies of EMF effects in animals have been conducted to investigate possible adverse health effects in humans. These are usually performed on standard laboratory animals used in toxicological studies, e.g. rats and mice, but some studies have also included other species such as short-living flies for the investigation of genotoxic effects. The subject of this information sheet, however, is whether EMF can have harmful impacts on species of wild and domestic animals. Under consideration are:

Species, in particular certain fish, reptiles, mammals and migratory birds, which rely on the natural (geomagnetic) static magnetic field as one of a number of parameters believed to be used for orientation and navigational cues Farm animals (e.g. swine, sheep or cattle) grazing under power lines (50/60Hz) or in the vicinity of broadcasting antennas Flying fauna, such as birds and insects, which may pass through the main beam of high power radio-frequency antennas and radar beams or through high intensity ELF fields near power lines. Studies performed to date have found little evidence of EMF effects on fauna

at levels below ICNIRP's guideline levels. In particular, there were no adverse effects found on cattle grazing below power lines. However, it is known that flight performance of insects can be impaired in electric fields above 1 kV/m, but significant effects have only been shown for bees when electrically conductive hives are placed directly under power lines. Un-insulated un-earthed conductors placed in an electric field can become charged and cause injury or disrupt the activity of animals, birds and insects.

Vegetation

Field studies of 50–60 Hz exposure to plants and crops have shown no effects at the levels normally found in the environment, nor even at field levels directly under power lines up to 765 kV. However, the variability of parameters associated with environmental conditions that affect plant growth (e.g. soil, weather) would likely preclude observation of any possible low-level effects of electric field exposure. Damage to trees is well known to occur at electric field strengths far above ICNIRP's levels due to corona discharge at the tips of the leaves. Such field levels are found only close to the conductors of very high voltage power lines.

Aquatic Life

Although all organisms are exposed to the geomagnetic field, marine animals are also exposed to natural electric fields caused by sea currents moving through the geomagnetic field. Electrosensitive fish, such as sharks and rays in oceans and catfish in fresh water, can orient themselves in response to very low electric fields by means of electroreceptive organs. Some investigators have suggested that human-made EMF from undersea power cables could interfere with the prey sensing or navigational abilities of these animals in the immediate vicinity of the sea cables. However, none of the studies performed to date to assess the impact of undersea cables on migratory fish (e.g. salmon and eel) and all the relatively immobile fauna inhabiting the sea floor (e.g. molluscs), have found any substantial behavioural or biological impact.

CONCLUSION

The limited number of published studies addressing the risk of EMF to terrestrial and aquatic ecosystems show little or no evidence of a significant environmental impact, except for some effects near very strong sources. From current information the exposure limits in the ICNIRP guidelines for protection of human health are also protective of the environment."

9.5.3 STANDARDS FOR MAGNETIC FIELD

It is rare to find an enforceable standard for MF exposure at low frequency (50 or 60 Hz). However, IEEE has established the maximum permissible exposure (MPE) levels for controlled (workers) and uncontrolled (unwilling individual) environments. Table 9.8 shows the highlights of this IEEE standard. The table shows that MPE is substantially reduced when the frequency of the MF increases. This is mainly because high-frequency currents penetrate the body's cells, causing internal heat. This is why we use microwaves to cook our food!

There is no U.S. federal standard limiting occupational or residential exposure to 60 Hz MF. However, some states have set guidelines. For example, Florida limits B at the edge of the right-of-way (ROW) to 250 mG and New York limits it to 200 mG.

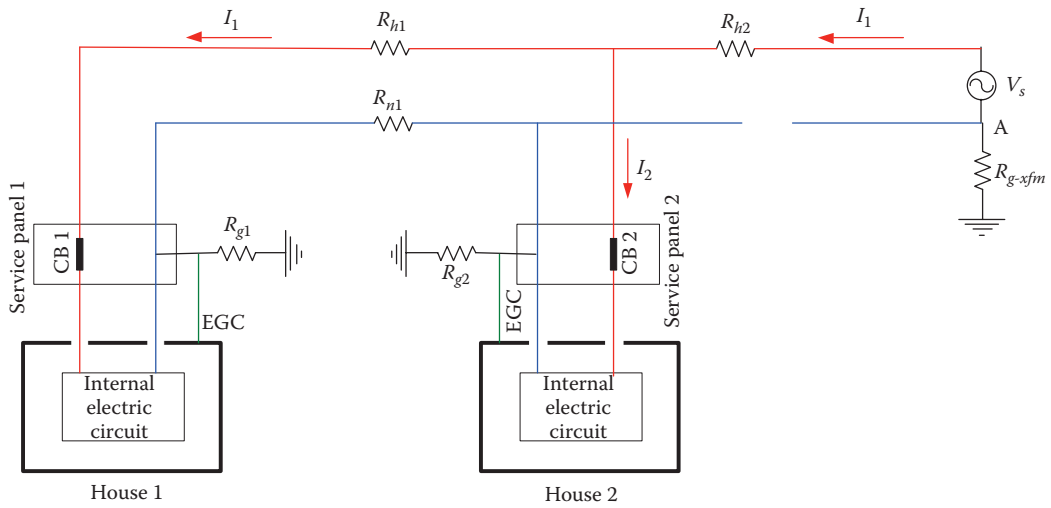
TABLE 9.8
Maximum B Exposure

Frequency	Maximum Exposure for General Public
DC	1.0 kG
30–100	2.0 G
15,000–300,000	10.0 mG

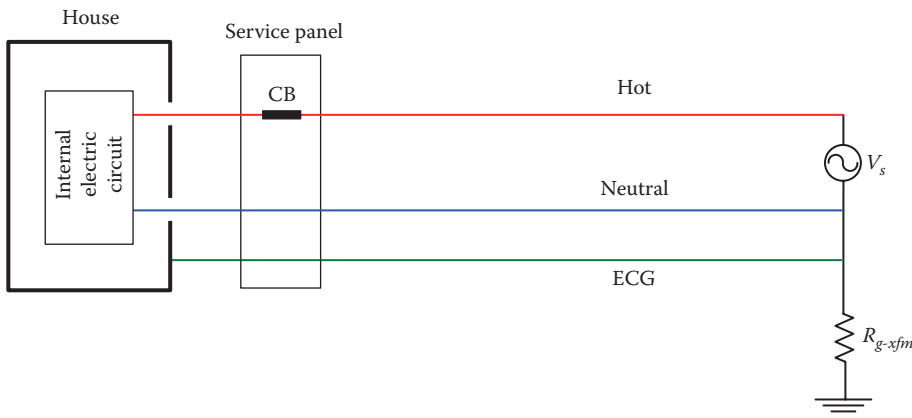
Source: IEEE Standard C95.1, 1991.

EXERCISES

- 9.1** A person is standing on a wet organic soil; compute his or her ground resistance.
- 9.2** Compute the resistance of a 10 m wide stretch of soil that is 2 m away from the edge of a grounded hemisphere. The radius of the hemisphere is 0.5 m. Assume that the soil is dry.
- 9.3** A person is working on a steel structure while standing on the ground. An accident occurred where 5 A pass through the structure to the ground. The structure is grounded by a metal rod 6 cm in diameter. The rod is dug 2 m into the ground. The surrounding soil is dry. Assume that the resistance of the man's body is $2000\ \Omega$. Compute the current through the man.
- 9.4** Compute the survival time of the man in the previous problem by using Dalziel's formula. Assume that the weight of the man is 80 kg.
- 9.5** Repeat Problems 3 and 4 for wet organic soil.
- 9.6** During a weather storm, an atmospheric discharge hits a lightning pole. The pole is grounded through a hemisphere. The maximum value of the lightning current through the pole is 10 kA. The soil of the area is moist. A man who is walking 20 m away from the center of the hemisphere experiences an excessive step potential. The man's body resistance is $1500\ \Omega$. Assume that the step of the person is about 0.6 m. Compute the current through his legs and his step potential.
- 9.7** During a weather storm, an atmospheric discharge hits a lightning pole that is grounded through a hemisphere. The maximum value of the lightning current through the rod is 20 kA. The soil of the area is moist. A man is playing golf 50 m away from the center of the hemisphere. At the moment of the lightning strike, the distance between his two feet is 0.4 m. Compute the current through the person assuming that the resistance between his legs is $1500\ \Omega$.
- 9.8** Repeat the previous problem and assume the person is 5 m away from the center of the hemisphere. What is the effect of the proximity of the man to the grounding hemisphere?
- 9.9** A power line insulator partially fails and 10 A pass through the structure to the tower's ground. The tower's ground is a hemisphere with a radius of 0.5 m. The soil resistivity is $100\ \Omega\text{m}$. Assume that a man touches the tower while standing on the ground. Compute the current going through the man, assuming his body resistance is $1000\ \Omega$.
- 9.10** An electric circuit is powered by unpolarized 120 V, 60 Hz outlet. The circuit is inside ungrounded chassis. A 100 nF capacitance exists between the circuit and the chassis. If a man touches the chassis, compute the current through his body. Assume that the body resistance of the man plus his ground resistance is $1000\ \Omega$.
- 9.11** An industrial electric circuit is powered by a two-prong polarized outlet through a feeder. The resistance of the neutral wire is $1.0\ \Omega$. The ground resistance at the service transformer is $20\ \Omega$. The chassis of the circuit is metallic and is connected to the neutral terminal of the outlet. A current of 200 A is drawn from the outlet through the hot wire. If a person with $2\ \text{k}\Omega$ resistance (including ground resistance) touches the chassis, compute the current through his body. Also state the type of hazard the person is exposed to.
- 9.12** State six factors that determine the severity of the electric shock when a person comes in contact with an energized conductor.
- 9.13** Compute the survival time of a heavy man receiving an electric shock of 100 mA.
- 9.14** Consider the system where the neutral and ground wires are bonded at the customer's side. Assume that the neutral wire from the utility has a resistance of $2\ \Omega$; the neutral wire is grounded at the source side where the ground resistance is $15\ \Omega$. The chassis of the equipment at the load side is grounded through a ground rod whose resistance is $30\ \Omega$. Assume the equipment draws a current of 15 A; compute the voltage on the chassis.
- 9.15** For the system in the following figure, assume the neutral wire is broken at the utility side. The currents drawn by the first house is 2 A and that for the second house is 4 A. The system has $R_g = 20\ \Omega$, $R_{g1} = R_{g2} = 30\ \Omega$, and $R_{n1} = R_{n2} = 1\ \Omega$. Also compute the ground potential rise at the utility side due to the two load currents.



- 9.16 What is the main problem associated with bonding the chassis of an equipment to the system neutral?
- 9.17 Why do we need to bond the local ground to the system neutral?
- 9.18 What is the advantage of having a separate EGC delivered by the utility?
- 9.19 Can we remove the voltage on the chassis in the U.S. system?
- 9.20 Can we depend on the ground path to trigger the circuit breakers? Why?
- 9.21 For the system in Figure 9.27, the circuit breaker is rated at 20 A and the source voltage is 120 V. The system parameters are $R_n=R_h=0.5\ \Omega$, $R_{g-man}=500\ \Omega$, $R_{man}=1000\ \Omega$, $R_g=10\ \Omega$, and $R_{g-xfm}=20\ \Omega$. Assume that the circuit breaker failed and did not clear the fault; compute the current through the person.
- 9.22 For the system in the figure, what is the voltage on the chassis during heaving loading condition? Why?



- 9.23 Write a technical report on the grounding practice of residential loads in any of the following countries: England, Japan, India, Australia, or South Africa.
- 9.24 Why it is important to separate the ground wire from the neutral wire in residential wiring?
- 9.25 What are the advantages and disadvantages of using water pipes as ground path?
- 9.26 Can we use the natural gas pipes as ground path for current? Why?

10 Power Electronics

The electric power grid must operate at fairly constant voltage and fixed frequency to ensure that all generators are synchronized and that the entire system is stable. If any generator produces voltage or frequency different from the rest of the system, blackouts can occur as discussed in Chapter 14. Because of this limitation, all electrical devices and equipment were designed to operate at the voltage and frequency of the utility's feeders. Accordingly, they were limited in performance, heavy in weight, and inefficient in operation. With the development of power electronic devices and circuits, the newer apparatuses and equipment have electronic converters that allow users to change the voltage and frequency applied to the equipment to achieve better performance and higher efficiencies. The new washing machine, for example, allows the user to change the speed and torque of the washing cycles by adjusting the voltage and frequency of its electric motor, thus optimizing the washing process. Another example is the air conditioning systems; the older ones were inefficient because of their switch-in and switch-out operation, whereas the newer ones operate continuously at variable speeds to maximize their efficiencies and to maintain the environment to the users' settings with minimum deviations. Devices that could not have existed before due to the restrictions on the voltage and frequency are now widely available. This includes microwave ovens whose power electronic circuits operate their magnetrons at very high frequencies (usually above 2 GHz). Other examples include household items such as light dimmers, chargers of electronic devices and computers, variable speed power tools, dishwashers, dryers, heat pumps, and electric stoves.

Besides household usage, power electronics provide the industry with effective methods to save energy and improve performance. The following are some examples:

- Electric load that demands different waveforms from that provided by the utility can still be energized from the utility supply through a proper converter. For example, the motors used in all printers, scanners, and hard disks cannot operate at the utility voltage or frequency, but can still be energized from the utility through power electronic converters.
- Power electronic circuits can increase the efficiency of the system for a wide range of operating conditions. Equipment operating by power electronic devices is more reliable and lasts longer.
- Equipment designed to operate by a power electronic converter is lighter in weight and smaller in volume than the ones designed to operate at the utility's fixed voltage and frequency.
- Performance of the electric load can be greatly enhanced, and the load can perform functions that are difficult to implement without power electronics. For example, the smooth speed control and braking of the electric vehicles cannot be achieved without the use of power electronic circuits.
- Performance of electrical equipment can be easily and effectively controlled by power electronic converters.

The history of power electronics started with the vacuum tube invented in 1904 by the British scientist John Fleming. Fleming's vacuum tube is quite revolutionary because it allows the electric current to flow in one direction only, thus acting as a diode. Later developments created tubes that amplified signals and changed the shape of electric waveforms. After the end of World War II, Bill Shockley, John Bardeen, and Walter Brattain invented the first transistor in 1947. Their invention opened the door wide to the use of solid-state devices in almost all electrical equipment manufactured today.

The research team named their device *transistor* because it is essentially a trans-resistance, that is, a variable resistance. In 1956, these scientists received the Nobel Prize for their marvelous transistor.

Since the invention of the transistor, scientists have worked diligently to invent other semiconductor devices with broader characteristics and higher power ratings. The early transistors were rated at a small fraction of an ampere and at very low voltages. Nowadays, a single solid-state device can be built to withstand about 5kV and can carry thousands of amperes.

10.1 POWER ELECTRONIC DEVICES

Power electronic devices can be divided into two categories: single component and hybrid component. The single component is composed of one solid-state device, and the hybrid component is a combination of several single components manufactured as a single block. The single devices for power applications are loosely divided into three types: (1) two-layer devices such as the diodes, (2) three-layer devices such as the transistors, and (3) four-layer devices such as the thyristors. The hybrid components include a wide range of devices such as the insulated gate bipolar transistor (IGBT), the static induction transistor (SIT), and the Darlington transistor (DT).

Solid-state devices are the main building components of any converter. Their function is mainly to mimic the mechanical switches by connecting and disconnecting electric loads, but at very high speeds. The characteristics of the ideal mechanical switch are shown in Figure 10.1. When the mechanical switch is open (off), the current through the switch is zero and the voltage across its terminals is equal to the source voltage. When the switch is closed (on), its terminal voltage is zero and its current is determined by the load impedance. A major part of the ongoing research and development in power electronic devices is devoted to improving the characteristics of the solid-state devices to make them as close to the mechanical switch as possible.

10.1.1 SOLID-STATE DIODES

The diode, which is the simplest power electronic device, allows the current to flow only in one direction. It is built of two types of semiconductor material, *p*-type and *n*-type, placed in contact with each other as shown on the left side of Figure 10.2. The symbol for the diode is shown in the middle of the figure. The *p*-junction is the *anode* of the device and the *n*-junction is the *cathode*. The current of the diode flows only from the anode to the cathode when the anode-to-cathode voltage V_{AK} is positive (forward biased), as shown on the right side of the figure. When the voltage V_{AK} is reversed (reverse biased), almost no current flows through the diode. However, if this reverse-biased

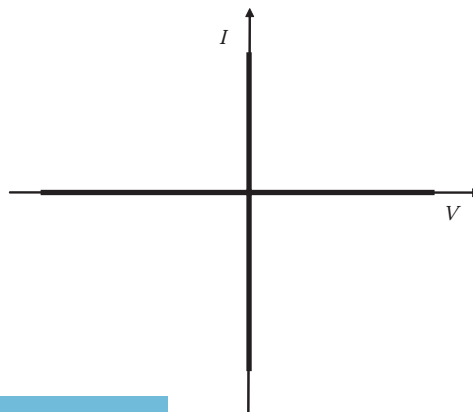


FIGURE 10.1 Current–voltage characteristics of a mechanical switch.

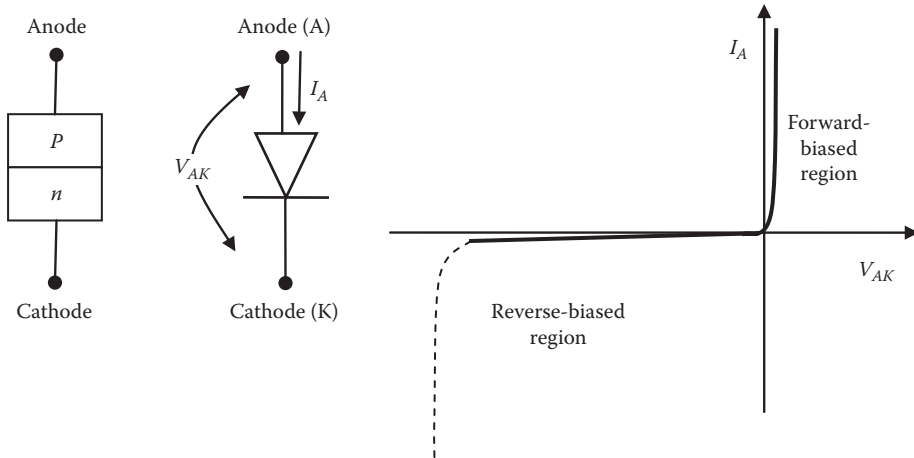


FIGURE 10.2 Solid-state diode.



FIGURE 10.3 Different rating diodes.

voltage is increased to an excessive value beyond the device rating, the diode is destroyed by the current avalanche, shown by the dashed section of the characteristics. When the diode is forward biased, the voltage drop across the diode V_{AK} is very small (about 0.7 V), and the diode in this case resembles a closed mechanical switch. When the diode is reverse biased (the thick portion of the line), the diode's current is very small and the diode resembles an open mechanical switch.

Figure 10.3 shows a picture of several diodes ranging from 6 V to 5 kV. Current ratings can be in the thousands of kA. For higher voltage applications, several single-component diodes are often connected in series to achieve a voltage level as high as 1 MV.

10.1.2 TRANSISTORS

In power electronic applications, transistors are mainly used as high-frequency electronic controlled switches. Two main types of transistors are commonly used: the bipolar junction transistor (BJT) and the field effect transistor (FET).

10.1.2.1 Bipolar Junction Transistor

The BJT consists of three layers of semiconductor material in *n-p-n* or *p-n-p* arrangements; the *n-p-n* shown on the left side of Figure 10.4 is more common in power electronic applications. The middle layer of the transistor is thin compared to the other two layers. The three layers of the transistor are called *collector* (C), *base* (B), and *emitter* (E). The bipolar transistor can be viewed as a pair of solid-state diodes joined back-to-back. But because the middle layer is fairly thin, the transistor behaves differently from just two back-to-back diodes. If we apply a positive voltage between the collector and emitter V_{CE} , the top back-to-back diode is reverse biased. If we apply a small positive voltage between the base and emitter V_{BE} , the base–emitter junction is forward biased, and a current flows between the base and emitter as if the junction is a forward-biased diode. In this case, electrons move from the emitter to the base. Once the electrons reach the base layer, they are quickly attracted to the collector layer because its voltage is positive. Hence, a current I_C flows through the collector terminal. This collector current is a function of the voltage we apply between the base and the emitter V_{BE} . Figure 10.5 shows bipolar power transistors of various sizes. The rating of the largest one in the photo is 100 A. The basic equations of the BJT are

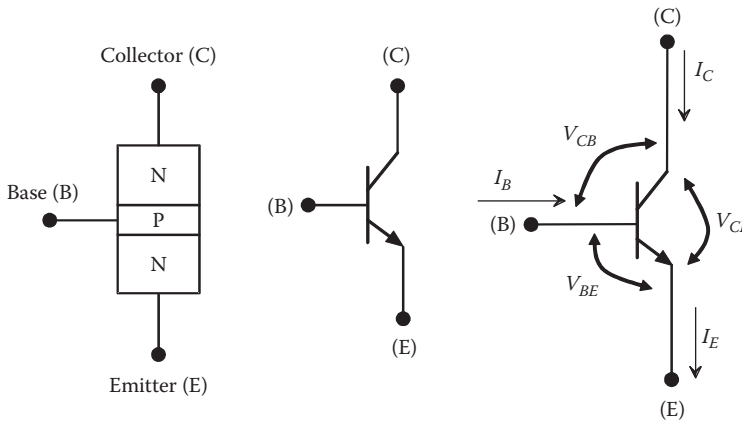


FIGURE 10.4 Bipolar junction transistor.

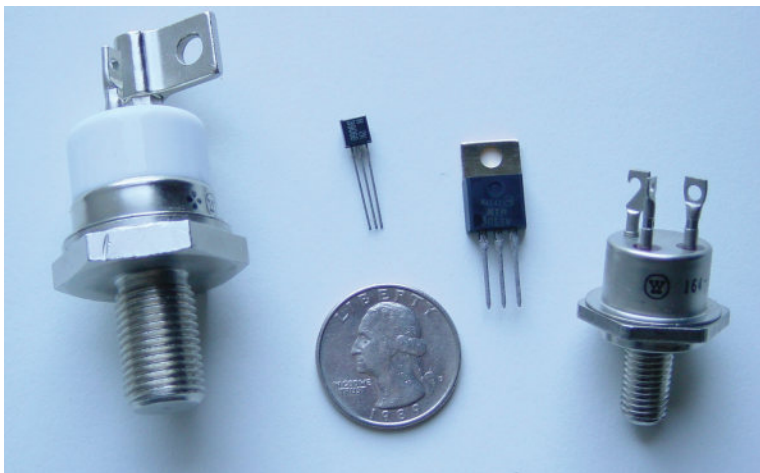


FIGURE 10.5 Various size transistors.

$$I_C = \beta I_B \quad (10.1)$$

$$I_E = I_B + I_C \quad (10.2)$$

$$V_{CE} = V_{CB} + V_{BE} \quad (10.3)$$

where

β is the current gain (the ratio of collector to base currents)

I_B is the base current

I_E is the emitter current

I_C is the collector current

V_{CE} is the collector–emitter voltage

V_{CB} is the collector–base voltage

V_{BE} is the base–emitter voltage

The characteristics of the transistor are shown in Figure 10.6. The base characteristic (I_B versus V_{BE}) is very similar to the characteristic of a diode in the forward bias mode. In the forward direction, the base–emitter voltage V_{BE} is below 0.7 V. The collector characteristic is I_C versus V_{CE} for various values of base currents I_B . This characteristic can be divided into three regions: *linear*, *cutoff*, and *saturation*. In the linear region, the transistor operates as an amplifier, where β is almost constant and in the order of a few hundreds. Hence, any base current is amplified a few hundred times in the collector circuit. This is the operating region of most audio and video amplifiers.

The cutoff region is the area of the characteristic where the base current is zero. In this case, the collector current is negligibly small regardless of the value of the collector–emitter voltage. In the saturation region, the collector–emitter voltage is very small compared to the transistor ratings, and the collector current is determined by the load. β in the saturation region is often less than 30. When a transistor is used to emulate a mechanical switch, it operates in the cutoff and saturation regions. Power transistors cannot operate in the linear region for long periods because V_{CE} in the linear region is high and the current of power electronic circuits is often high. Therefore, the power

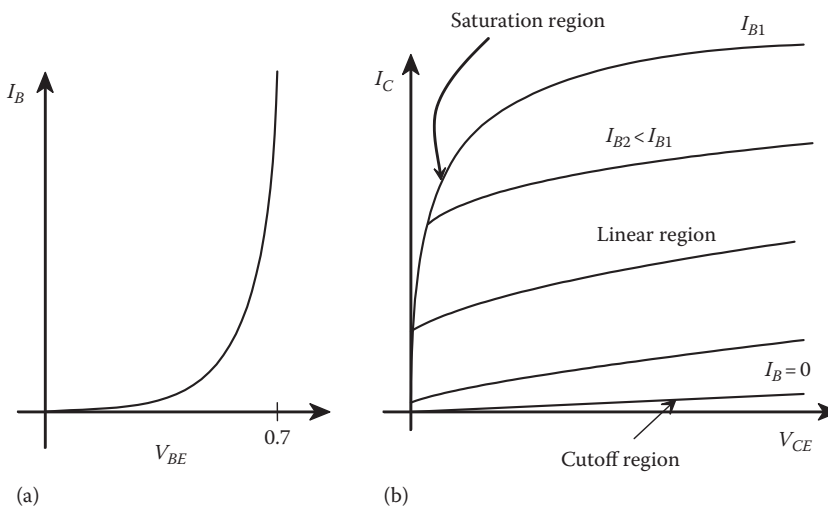


FIGURE 10.6 Characteristics of BJT: (a) base characteristics and (b) collector characteristics.

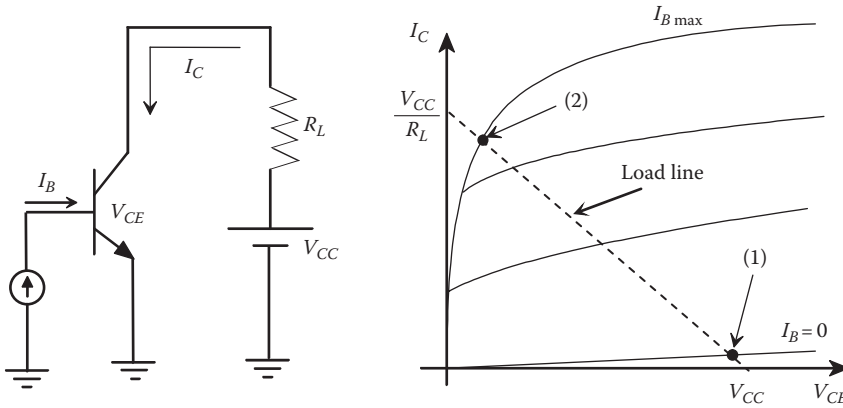


FIGURE 10.7 Switching of a transistor.

loss of the power transistor ($V_{CE}I_C$) is excessive and eventually will damage the transistor due to the excessive thermal heat.

The circuit in Figure 10.7 explains how the transistor operates as a switch. The transistor is connected to an external circuit consisting of a direct current (dc) source V_{CC} (which is the source of energy), and a load resistance R_L . The base circuit of the transistor is connected to a separate current source to produce the base current I_B . The loop equation of the collector circuit is

$$V_{CC} = V_{CE} + R_L I_C \quad (10.4)$$

The collector equation, which is also known as the *load line equation*, shows a linear relationship between I_C and V_{CE} . The equation has a negative slope and intersects the x -axis at V_{CC} , and the y -axis at V_{CC}/R_L . If the base current is zero, the operating point of the circuit is in the cutoff region at point 1. The collector current in this case is very small and the collector–emitter voltage of the transistor is almost equal to the source voltage V_{CC} . Hence, the operation of the transistor in the cutoff region resembles an open mechanical switch. If the base current is set to its maximum value, the transistor is in the saturation region at point 2. At this operating point, the voltage drop across the collector–emitter is very small and the collector (or load) current is almost equal to V_{CC}/R_L . The transistor in this case is equivalent to a closed mechanical switch.

The bipolar transistor emulates a normally open mechanical switch; it is always open unless a control current (base current) is injected into the base. The transistor will remain closed as long as the base current exists. To open the transistor, the base current must be removed from the base circuit.

The BJT has several advantages; the best among them are its high switching speeds and high reliability. However, the BJT has two main drawbacks:

1. When the transistor is closed in the saturation region, V_{CE} is about 0.1 V, which is very low for high-voltage circuits. However, if the transistor carries high currents while closed, the losses could be excessive, leading to high internal heat. This heat must be dissipated as quickly as it is generated to prevent the transistor from being damaged.
2. BJT is a current-controlled device; the transistor is closed and maintained in the closed position only if its maximum base current is present. Since β is small in the saturation region, the base current is a large percentage of the collector current. This high base current causes high losses in the base circuit. Furthermore, the driving circuit that generates this base current must be capable of producing high currents for as long as the transistor is closed. Such a circuit is large in size and complex to build.

Example 10.1

A BJT has a current gain of 10 in the saturation region. When the transistor is closed, the collector current is 100 A, compute the following:

1. Minimum base current to keep the transistor closed
2. Losses of the transistor

Solution

$$1. \quad I_B = \frac{I_C}{\beta} = \frac{100}{10} = 10 \text{ A}$$

Notice that the base current is very high and may require an elaborate driving circuit.

2. The losses inside the transistor are mainly in the base–emitter loops and the collector–emitter loop. The base–emitter loss is

$$P_{BE} = I_B \times V_{BE}$$

Since the base–emitter junction is just a diode in the forward bias, we can assume that V_{BE} is about 0.7 V.

$$P_{BE} = I_B \times V_{BE} = 10 \times 0.7 = 7 \text{ W}$$

The collector–emitter loss is

$$P_{CE} = I_C \times V_{CE}$$

Assume that V_{CE} is about 0.1 V when the transistor is fully closed:

$$P_{CE} = I_C \times V_{CE} = 100 \times 0.1 = 10 \text{ W}$$

Total losses = 17 W.

Example 10.2

In the saturation region, the BJT circuit shown in Figure 10.7 has a current gain of 20 and $V_{CE} = 0.5 \text{ V}$. The source voltage is 100 V and the load resistance is 5Ω .

1. Calculate the minimum base current that maintains the transistor closed.
2. Calculate the losses in the collector–emitter loop.
3. Assume that the base current is reduced to half the value computed in part 1, and the transistor is pulled out of the saturation region and moved into the linear region where the current gain is 30; compute the losses in the collector–emitter circuit.

Solution

1. First compute the collector current by using Equation 10.4

$$I_C = \frac{V_{CC} - V_{CE}}{R_L} = \frac{100 - 0.5}{5} = 19.9 \text{ A}$$

Hence, the minimum base current is

$$I_B = \frac{I_C}{\beta} = \frac{19.9}{20} = 0.995 \text{ A}$$

2. $P_{CE} = I_C \times V_{CE} = 19.9 \times 0.5 = 9.95 \text{ W}$

3. When the base current is reduced, V_{CE} increases as shown by the load line in Figure 10.7. But first, let us compute the new collector current in the linear region.

$$I_C = \beta I_B = 30 \times \frac{0.995}{2} = 14.925 \text{ A}$$

$$V_{CE} = V_{CC} - R_L I_C = 100 - 5 \times 14.925 = 25.375 \text{ V}$$

The new loss is

$$P_{CE} = I_C \times V_{CE} = 14.925 \times 25.375 = 378.72 \text{ W}$$

Notice that the loss in the collector–emitter loop is much higher when the transistor is outside the saturation region. This is why the power transistor must always be in the saturation region when closed.

10.1.2.2 Metal Oxide Semiconductor Field Effect Transistor

The metal oxide semiconductor field effect transistor (MOSFET), unlike the BJT, is a voltage-controlled device. This is a great advantage over the BJT as the MOSFET is a more efficient device that requires a simpler driving circuit. The MOSFET is widely used in digital circuits as well as high-power electronic circuits.

The MOSFET is based on the main principle that operates all field effect transistors (FETs). The field effect theory states that the current near the surface of a semiconductor material can be altered by imposing an electric field on the surface. Since the electric field is produced by voltage, the current of the FET is, therefore, controlled by a voltage signal. This is different from the BJT whose collector current is controlled by the current in the base circuit. The MOSFET is structured as a three-layer semiconductor material where the middle layer is subjected to an external electric field that controls the flow of current between the top and the bottom layers. The strength of the electric field depends on the applied voltage (not current). The three terminals of the MOSFET in Figure 10.8 are the *drain* (D), the *source* (S), and the *gate* (G). The control signal V_{GS} is applied between the gate and the source, and the load current is the drain current I_D . There are two main

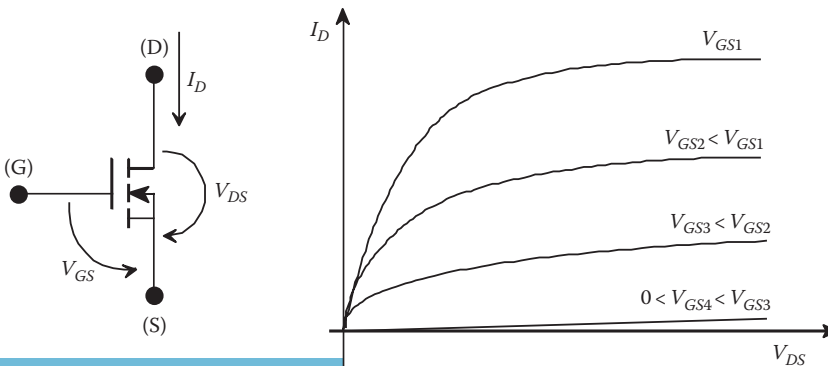


FIGURE 10.8 Enhanced-mode MOSFET.

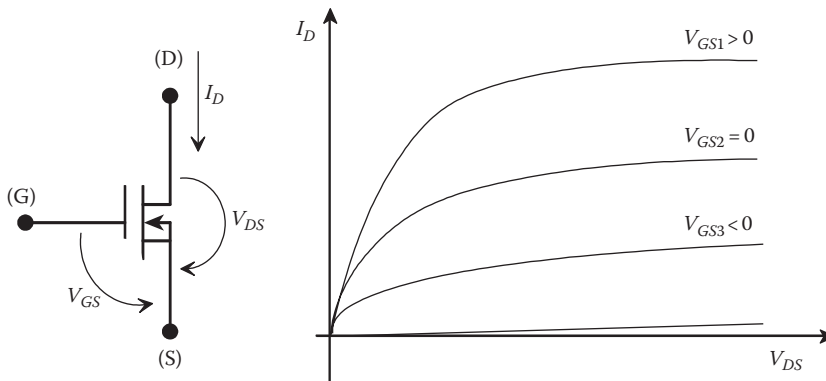


FIGURE 10.9 Enhanced- and depletion-mode MOSFET.

types of MOSFETs, the enhanced mode and the enhanced-depletion mode. The characteristic of the enhanced mode is shown in Figure 10.8 where V_{GS} is always positive. The enhanced-depletion-mode MOSFET has its V_{GS} either positive or negative as shown in Figure 10.9.

The power MOSFET has several advantages; among them are the following:

- MOSFET behaves as a voltage-controlled resistance; the value of the gate voltage determines the on-resistance of the MOSFET (V_{DS}/I_D). When fully closed, the on-resistance is just a few milliohms.
- Its input resistance is high since the gate current is almost zero. Because of its low on-resistance and the lack of current in the gate loop, the losses of the MOSFET are lower than that of the BJT.
- MOSFET can be connected in parallel for heavier loads. This is not possible with the BJT.

The main disadvantage of the MOSFET is its high gate-source capacitance. This is due to the difference in charges between the gate and the source, and the high input resistance of the gate. Therefore, the switching frequency of the MOSFET is limited by this input capacitance. High switching frequency may result in excessive capacitive current in the gate circuit.

10.1.3 THYRISTORS

The thyristors family includes several devices such as the silicon controlled rectifier (SCR), the bidirectional switch (Triac), and the gate turn-off (GTO) SCR. These devices are widely used in high-power applications as they can handle thousands of amperes and can be cascaded to withstand hundreds of kilovolts. The photo in Figure 10.10 shows various high-current SCRs with the large one rated at 300 A. The thyristors family also has several devices in the low-power range such as the silicon diode for alternating current (SIDAC), the silicon unilateral switch (SUS), and the bilateral diode (Diac).

10.1.3.1 Silicon-Controlled Rectifier

The SCR is built of four layers of semiconductor material as shown in Figure 10.11. The device has three terminals: *anode* (A), *cathode* (K), and *gate* (G). When the anode-to-cathode voltage V_{AK} is negative, the SCR is reverse biased and a small leakage of current flows from the cathode to the anode; the device in this case is open. If the reverse-biased voltage reaches the *reverse breakdown* limit V_{RB} of the device, the SCR is destroyed. When the anode-to-cathode voltage is positive, the SCR is forward biased. If no current pulse is applied at the gate, no current flows in the anode loop as long as V_{AK} is less than the *breakover* voltage V_{BO} of the SCR. In this case, the SCR is open.



FIGURE 10.10 High-power SCRs.

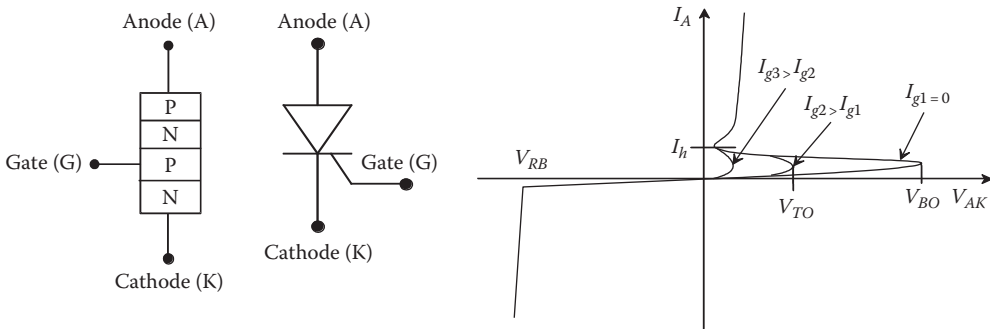


FIGURE 10.11 SCR structure, symbol, and characteristics.

However, if a gate current pulse I_G is applied when $V_{AK} < V_{BO}$, the SCR is closed. The voltage at which the SCR is closed is called *turn-on voltage* V_{TO} . The higher the gate current, the lower is the turn-on voltage. If we desire to close the SCR when the turn-on voltage is near zero, the gate pulse must be the maximum allowed by the SCR’s specification. If the gate signal is removed after the SCR is closed, the SCR remains latched closed unless the anode current falls below the holding value I_h . At or below the holding current, the SCR is opened.

The SCR is highly popular in heavy-power applications due to several reasons; among them are the following:

- SCRs are much cheaper than BJT and MOSFETs. SCR is triggered by a single pulse, instead of the continuous current needed by the BJT. Thus, the input losses are much less than that for the BJT.
- In ac circuits, the SCR can be self-commutated (opened) without the need for external commutation circuit. This is because the ac current naturally goes through zero values twice in one cycle.
- SCR can be built with much larger current and voltage ratings than the BJT or MOSFET.

10.1.3.2 Silicon Diode for Alternating Current

The SIDAC is a silicon bilateral-voltage-triggered switch used mainly in low-power control circuits. As seen in the characteristics of the SIDAC in Figure 10.12, when the anode-to-cathode voltage exceeds the breakover voltage of the SIDAC, the device switches on (closes) and the anode current flows in the circuit. The conduction is continuous until the current drops below the minimum holding current of the device. The turn-on voltage of the SIDAC is a fixed value and cannot be controlled.

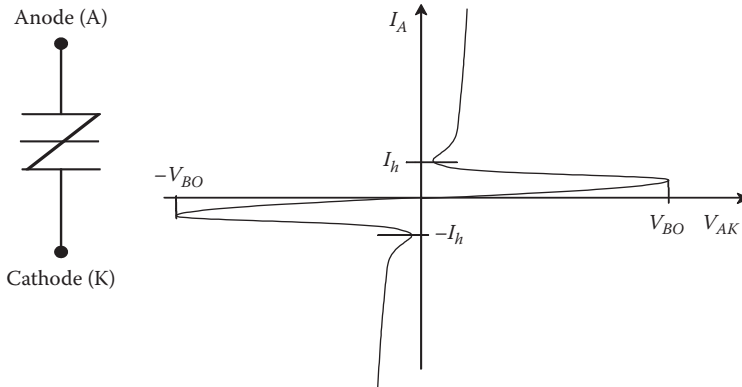


FIGURE 10.12 Characteristics of the SIDAC.

10.1.4 HYBRID POWER ELECTRONIC DEVICES

There are various hybrid devices composed of several components such as BJT and MOSFET, SCR and FET, and cascaded BJTs. Hybrid structures offer desirable features such as higher switching speeds, higher currents, higher current gains, or higher efficiencies. The hybrid device research is fast growing and newer designs are continuously developed. Here, two of the common ones are discussed.

10.1.4.1 Darlington Transistor

One of the main problems with the BJT is its low current gain in the saturation region, which demands a high base current. This problem is solved by cascading two bipolar transistors in the configuration shown in Figure 10.13. The collector current of Q_1 is $\beta_1 I_{B1}$, and its emitter current is

$$I_{E1} = I_{B1} + I_{C1} = (1 + \beta_1) I_{B1} \tag{10.5}$$

This emitter current is also equal to the base current of transistor Q_2 , and the emitter current of Q_2 is

$$I_{E2} = (1 + \beta_2) I_{B2} = (1 + \beta_2) (1 + \beta_1) I_{B1} \tag{10.6}$$

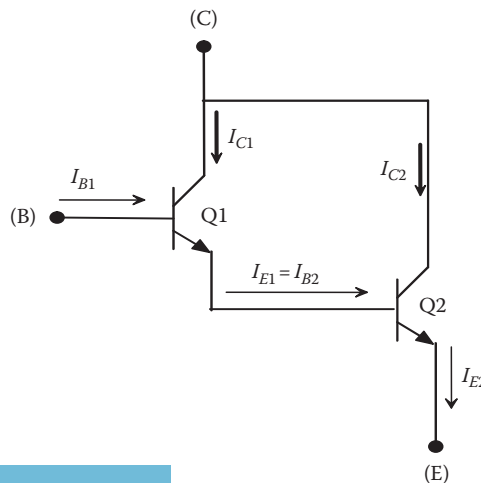


FIGURE 10.13 Darlington transistor.

Hence, the ratio of the emitter current of Q_2 (which is the load current) and the base current of Q_1 (which is the control current) is

$$\frac{I_{E2}}{I_{B1}} = (1 + \beta_1)(1 + \beta_2) \quad (10.7)$$

Example 10.3

A BJT has $\beta=9$ in the saturation region. When the transistor is closed, the emitter current is 100 A. Compute the following:

1. Base current to keep the transistor closed.
2. If two of these transistors are connected in Darlington configuration, compute the new base current that produces the same value of emitter current.

Solution

$$1. \quad I_B = \frac{I_E}{1 + \beta} = \frac{100}{10} = 10 \text{ A}$$

2. With Darlington connection

$$I_B = \frac{I_{E2}}{(1 + \beta_1)(1 + \beta_2)} = \frac{100}{10 \times 10} = 1 \text{ A}$$

Notice that the base current of this darlington transistor (DT) is 10% of the base current of the single BJT.

10.1.4.2 Insulated Gate Bipolar Transistor

BJTs are very reliable devices that can operate at high switching frequencies. However, they are low current gain switching devices that demand high base currents to keep the devices latched in the closed position. This requires triggering circuits that are bulky, expensive, and low in efficiency. The MOSFETs, on the other hand, are voltage-controlled devices and their triggering circuits are much simpler and less expensive. For these reasons, power electronic engineers have merged these two devices into the configuration shown in Figure 10.14 to produce a high-current voltage-triggered device. This device is called insulated gate bipolar transistor (IGBT). The symbol and the characteristics of the IGBT are shown in Figure 10.15.

10.2 SOLID-STATE SWITCHING CIRCUITS

Solid-state switching circuits have various configurations and are often called converters. There are four types of converters as shown in Figure 10.16. The ac/dc converter converts any ac waveform into a dc waveform with adjustable voltage. The dc/dc converter converts a dc waveform into adjustable dc voltage. The dc/ac converter converts a dc waveform into ac with adjustable voltage and frequency. The ac/ac converter converts the fixed voltage, fixed frequency waveform into waveforms with adjustable voltage and frequency.

10.2.1 AC/DC CONVERTERS

These are very common converters used to drive dc equipment from ac sources such as power supplies and chargers. There are three main types of ac/dc converters: fixed voltage, variable voltage,

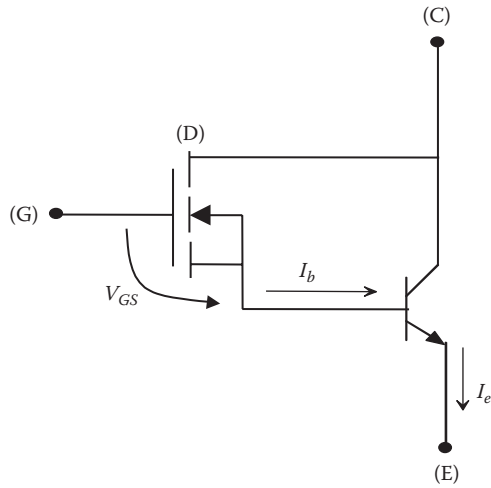


FIGURE 10.14 MOSFET and bipolar circuit.

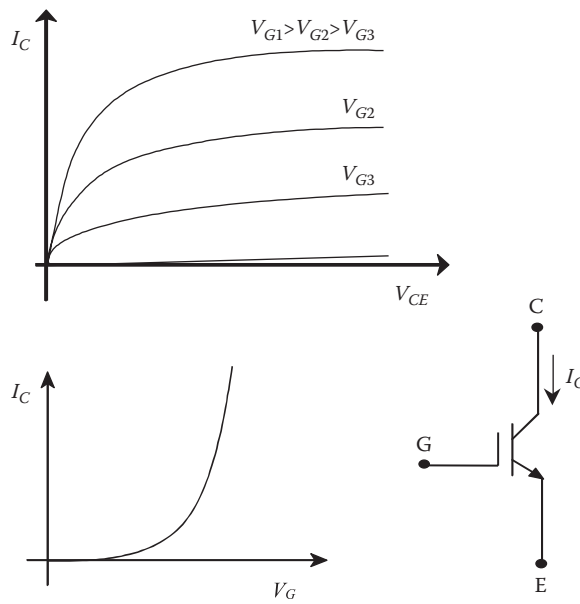


FIGURE 10.15 Characteristics of IGBT.

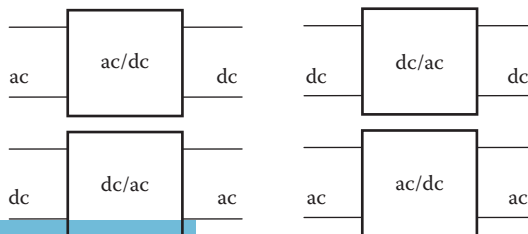


FIGURE 10.16 Four types of converters.

and fixed current. The fixed voltage circuits produce constant voltage across the load and the circuit is known as a rectifier circuit. For variable voltage across the load, a switching device such as the BJT, MOSFET, or SCR is used to regulate the flow of current in the external circuit, thus controlling the voltage across the circuit. The fixed current circuit is used in applications such as battery chargers and constant torque of electromechanical devices.

10.2.1.1 Rectifier Circuits

The simplest form of an ac/dc converter is the half-wave diode rectifier circuit shown in Figure 10.17. The circuit consists of an ac source of potential v_s , a load resistance R , and a diode connected between the source and the load. Because of the diode, the current flows only in one direction when the voltage source is in the positive half of its cycle; the diode is then forward biased. Hence, the terminal voltage of the load v_t is only present when the current flows in the circuit as shown in Figure 10.18.

A full-wave rectifier circuit is shown in Figure 10.19. Because the diodes are connected in the bridge configuration as shown in the figure, the current of the load flows in the same direction whether the source voltage is in the positive or negative half of its ac cycle. In the positive half cycle, point A has higher potential than point B . Hence, diodes D_1 and D_2 are forward biased and the current flows as shown by the solid arrows. During the negative half, point B has higher potential than point A . Hence, D_3 and D_4 are forward biased and the current flows as shown by the dashed arrows. In either half of the ac cycle, the current in the load is unidirectional, hence, it is dc. The waveforms of the circuit are shown in Figure 10.20.

Let us assume that the source voltage is sinusoidal, expressed by the equation

$$v_s = V_{\max} \sin(\omega t) \quad (10.8)$$

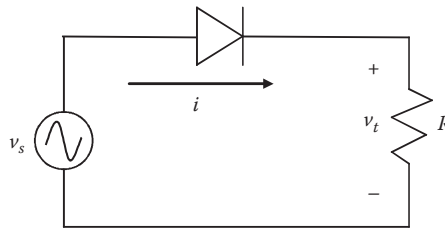


FIGURE 10.17 Half-wave rectifier circuit.

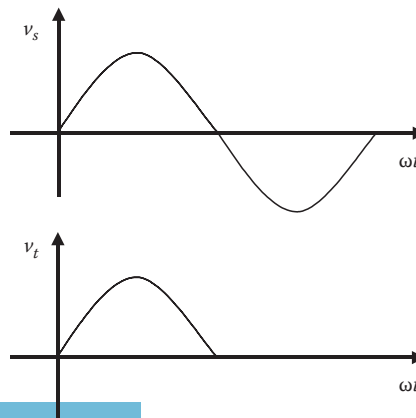


FIGURE 10.18 Waveforms of half-wave rectifier circuit.

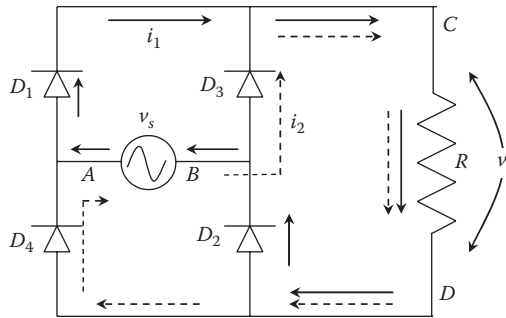


FIGURE 10.19 Full-wave rectifier circuit.

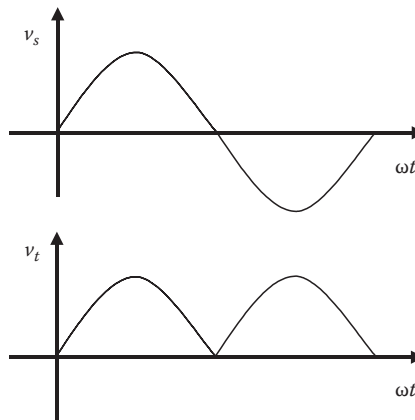


FIGURE 10.20 Waveforms of full-wave rectifier circuit.

The dc voltage across the load can be expressed by the average value of v_t . For the half-wave rectifier circuit in Figure 10.17, the average voltage across the load is

$$V_{ave-hw} = \frac{1}{2\pi} \int_0^{2\pi} v_t \, d\omega t = \frac{1}{2\pi} \int_0^{\pi} v_s \, d\omega t = \frac{1}{2\pi} \int_0^{\pi} V_{max} \sin(\omega t) \, d\omega t = \frac{V_{max}}{\pi} \tag{10.9}$$

For the full-wave rectifier circuit in Figure 10.19, the average voltage is

$$V_{ave-fw} = \frac{1}{2\pi} \int_0^{2\pi} v_t \, d\omega t = \frac{1}{\pi} \int_0^{\pi} v_s \, d\omega t = \frac{1}{\pi} \int_0^{\pi} V_{max} \sin(\omega t) \, d\omega t = \frac{2V_{max}}{\pi} \tag{10.10}$$

Notice that the average voltage across the load for a full-wave circuit is double that for a half-wave circuit. The current and voltage are often expressed by their root-mean-square (rms) values. As given in Chapter 7, the rms voltage is defined as

$$V_{rms} = \sqrt{\frac{1}{2\pi} \int_0^{2\pi} [v(t)]^2 \, d\omega t} \tag{10.11}$$

Hence, the rms voltage across the load for the half-wave rectifier circuit is

$$V_{rms-hw} = \sqrt{\frac{1}{2\pi} \int_0^{2\pi} v_t^2 d\omega t} = \sqrt{\frac{1}{2\pi} \int_0^{\pi} (V_{max} \sin \omega t)^2 d\omega t} \quad (10.12)$$

$$V_{rms-hw} = \sqrt{\frac{V_{max}^2}{4\pi} \int_0^{\pi} (1 - \cos 2\omega t) d\omega t} = \frac{V_{max}}{2}$$

For full-wave rectifier circuit, the rms voltage across the load is

$$V_{rms-fw} = \sqrt{\frac{1}{2\pi} \int_0^{2\pi} v_t^2 d\omega t} = \sqrt{\frac{1}{\pi} \int_0^{\pi} (V_{max} \sin \omega t)^2 d\omega t} \quad (10.13)$$

$$V_{rms-fw} = \sqrt{\frac{V_{max}^2}{2\pi} \int_0^{\pi} (1 - \cos 2\omega t) d\omega t} = \frac{V_{max}}{\sqrt{2}}$$

Notice that the rms voltage across the load for the full-wave rectifier circuit is the same as the rms for the source voltage. The rms current of the load in either circuit can be computed as

$$I_{rms} = \frac{V_{rms}}{R} \quad (10.14)$$

The electric power consumed by the resistive load is

$$P = \frac{V_{rms}^2}{R} = I_{rms}^2 R \quad (10.15)$$

Hence, for half- and full-wave rectifier circuits, the load powers are

$$P_{hw} = \frac{V_{rms-hw}^2}{R} = \frac{V_{max}^2}{4R}$$

$$P_{fw} = \frac{V_{rms-fw}^2}{R} = \frac{V_{max}^2}{2R} \quad (10.16)$$

Example 10.4

A full-wave rectifier circuit converts a 120 V (rms) source into dc. The load of the circuit is a 10 Ω resistance. Compute the following:

1. Average voltage across the load
2. Average voltage of the source
3. rms voltage of the load
4. rms current of the load
5. Power consumed by the load

Solution

$$1. \quad V_{ave-fw} = \frac{2V_{max}}{\pi} = \frac{2(\sqrt{2}120)}{\pi} = 108 \text{ V.}$$

2. The average voltage of the source is zero because the source waveform is symmetrical across the time axis.

$$3. \quad V_{rms-fw} = \frac{V_{max}}{\sqrt{2}} = 120 \text{ V.}$$

$$4. \quad I_{rms-fw} = \frac{V_{rms-fw}}{R} = \frac{120}{10} = 12 \text{ A.}$$

$$5. \quad P_{fw} = \frac{V_{rms-fw}^2}{R} = 1.44 \text{ kW.}$$

10.2.1.2 Voltage-Controlled Circuits

The simple half-wave SCR converter in Figure 10.21 allows us to control the voltage across the load. The circuit consists of an ac source of potential v_s , a load resistance R , and an SCR connected between the source and the load. The triggering circuit of the SCR is not shown in the figure.

The waveforms of the circuit are shown in Figure 10.22. When the SCR is open, the current of the circuit is zero and the load voltage is also zero. When the SCR is triggered at $\omega t = \alpha$, the SCR is closed and the voltage across the load resistance is equal to the source voltage. Since the source is a sinusoidal waveform, the current of the circuit is zero at π . Hence, the SCR is opened at π (the SCR opens when the current is below its holding value, which is very small). The period during which the current flows in the circuit is called the conduction period γ . Hence,

$$\gamma = \pi - \alpha \quad (10.17)$$

The full-wave SCR circuit is shown in Figure 10.23. It consists of two SCRs and two diodes in bridge configuration. The waveforms of the circuit are shown in Figure 10.24. The current flow in the full-wave SCR circuit is similar to that explained for the full-wave rectifier circuit except that the current starts flowing after the triggering pulse is applied on S_1 at α during the positive half of the ac cycle, and on S_2 at $\alpha + 180^\circ$ during the negative half of the cycle.

The average voltage across the load for the half-wave SCR circuit is

$$V_{ave-hw} = \frac{1}{2\pi} \int_0^{2\pi} v_t \, d\omega t = \frac{1}{2\pi} \int_\alpha^\pi v_s \, d\omega t = \frac{1}{2\pi} \int_\alpha^\pi V_{max} \sin(\omega t) \, d\omega t \quad (10.18)$$

$$V_{ave-hw} = \frac{V_{max}}{2\pi} (1 + \cos \alpha)$$

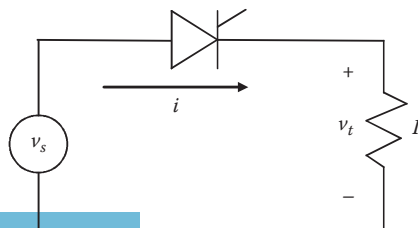


FIGURE 10.21 Half-wave SCR circuit.

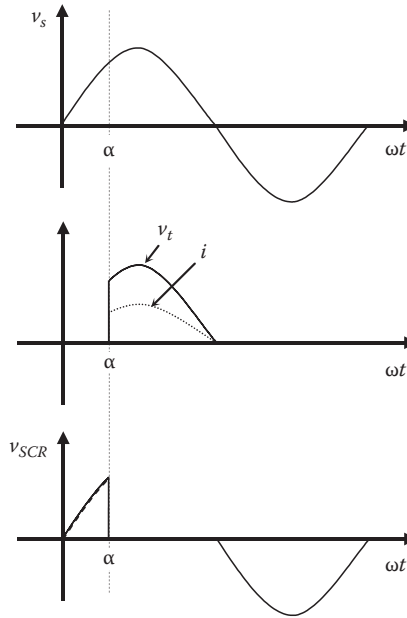


FIGURE 10.22 Waveforms of half-wave SCR circuit.

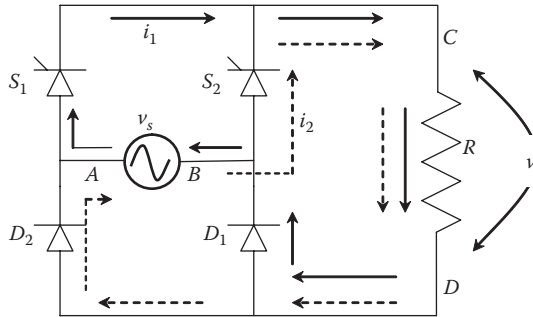


FIGURE 10.23 Full-wave SCR circuit.

For the full-wave SCR circuit, the average voltage across the load resistance is

$$V_{ave-fw} = \frac{1}{2\pi} \int_0^{2\pi} v_t d\omega t = \frac{1}{\pi} \int_{\alpha}^{\pi} v_s d\omega t = \frac{1}{\pi} \int_{\alpha}^{\pi} V_{max} \sin(\omega t) d\omega t$$

$$V_{ave-fw} = \frac{V_{max}}{\pi} (1 + \cos \alpha)$$
(10.19)

The rms voltage across the load for the half-wave SCR circuit can be computed as

$$V_{rms-hw} = \sqrt{\frac{1}{2\pi} \int_0^{2\pi} v_t^2 d\omega t} = \sqrt{\frac{1}{2\pi} \int_{\alpha}^{\pi} (V_{max} \sin \omega t)^2 d\omega t}$$

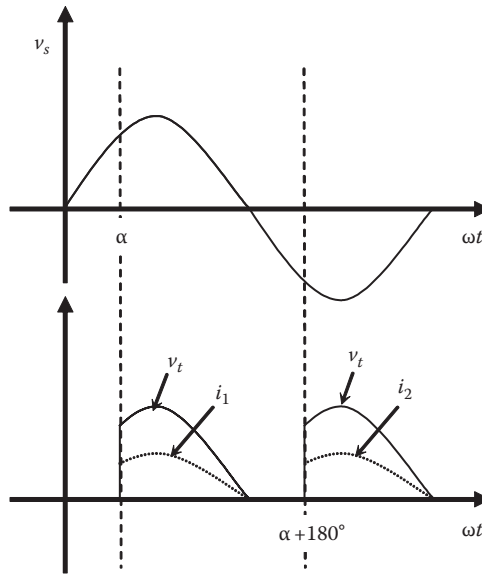


FIGURE 10.24 Waveforms of full-wave SCR circuit.

$$V_{rms-hw} = \sqrt{\frac{V_{max}^2}{4\pi} \int_{\alpha}^{\pi} (1 - \cos 2\omega t) d\omega t} = \frac{V_{max}}{2} \sqrt{\left(1 - \frac{\alpha}{\pi} + \frac{\sin 2\alpha}{2\pi}\right)} \tag{10.20}$$

A similar process can be used to compute the rms voltage across the load for the full-wave SCR circuit

$$V_{rms-fw} = \sqrt{\frac{1}{2\pi} \int_0^{2\pi} v_t^2 d\omega t} = \sqrt{\frac{1}{\pi} \int_{\alpha}^{\pi} (V_{max} \sin \omega t)^2 d\omega t} \tag{10.21}$$

$$V_{rms-fw} = \frac{V_{max}}{\sqrt{2}} \sqrt{\left(1 - \frac{\alpha}{\pi} + \frac{\sin 2\alpha}{2\pi}\right)}$$

The rms voltage across the load for the full-wave SCR circuit is shown in Figure 10.25. As you can see, the load voltage is controlled from zero to $V_{max}/\sqrt{2}$ by adjusting the triggering angle.

The power across the load can be computed as

$$P = \frac{V_{rms}^2}{R} = I_{rms}^2 R$$

$$P_{hw} = \frac{V_{max}^2}{8\pi R} (2(\pi - \alpha) + \sin 2\alpha)$$

$$P_{fw} = \frac{V_{max}^2}{4\pi R} (2(\pi - \alpha) + \sin 2\alpha) \tag{10.22}$$

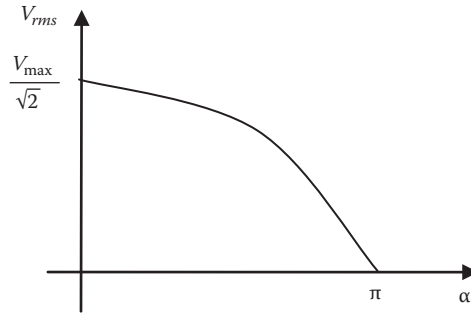


FIGURE 10.25 Root-mean-square voltage of the load for the full-wave SCR circuit.

Example 10.5

A full-wave SCR converter circuit is used to regulate power across a $10\ \Omega$ resistance. The voltage source is 120 V (rms). What is the triggering angle when the power across the load is 1 kW? Compute the average and rms currents of the load.

Solution

The power expression in Equation 10.22 is nonlinear with respect to the triggering angle α .

$$P_{fw} = \frac{V_{\max}^2}{4\pi R} [2(\pi - \alpha) + \sin(2\alpha)] = \frac{(\sqrt{2} \times 120)^2}{4\pi \times 10} [2(\pi - \alpha) + \sin(2\alpha)] = 1000$$

$$2\alpha - \sin(2\alpha) = 1.92$$

The solution of the aforementioned nonlinear equation is iterative

$$\alpha = 71.9^\circ$$

To compute the average current of the load, we need to compute the average voltage across the load as given by Equation 10.19:

$$V_{ave-fw} = \frac{V_{\max}}{\pi} (1 + \cos \alpha) = \frac{\sqrt{2} \times 120}{\pi} (1 + \cos 71.9^\circ) = 70.8\ \text{V}$$

$$I_{ave-fw} = \frac{V_{ave-fw}}{R} = 7.08\ \text{A}$$

For the rms current, we can compute the rms voltage first and then divide the voltage by the resistance of the load. Another simple method is to use the power formula in Equation 10.15.

$$I_{rms} = \sqrt{\frac{P_{fw}}{R}} = 10\ \text{A}$$

10.2.1.3 Constant-Current Circuits

Constant-current circuits are used mainly to charge batteries as well as to drive electric motors in constant torque applications. The current must be controlled during the charging process of the

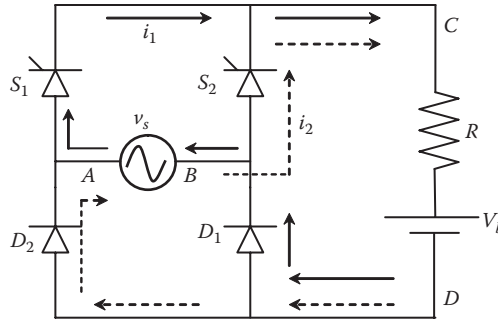


FIGURE 10.26 Full-wave charger circuit.

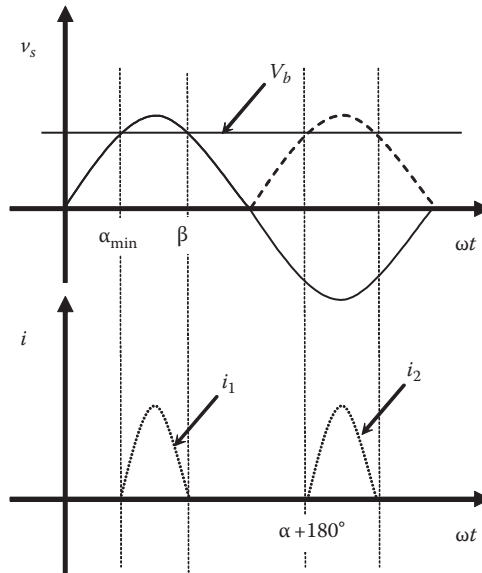


FIGURE 10.27 Waveforms of the full-wave charger circuit.

battery to prevent the battery from being damaged by excessive charging currents. The simplest charging circuit is the full-wave shown in Figure 10.26. The load of this circuit is the battery and the resistance R represents the internal resistance of the battery.

The range of the triggering angle of the charger circuit is less than the range for the full-wave SCR circuit in Figure 10.23. This is because the minimum triggering angle and the conduction period depend on the voltage of the battery. Examine the circuit in Figure 10.26 and its waveforms in Figure 10.27. During the first half of the ac cycle, S_1 can only close when the source voltage is higher than the battery voltage (when $\beta > \alpha \geq \alpha_{\min}$), where α_{\min} is the angle at which the source voltage is equal to the battery voltage. If the triggering angle of the SCRs $\alpha < \alpha_{\min}$, the voltage across S_1 or D_1 is negative and the SCRs cannot close. At α_{\min} ,

$$V_b = V_{\max} \sin \alpha_{\min} \tag{10.23}$$

The current to the battery will flow as long as $V_b < v_s$. Hence, the current is commutated at β , where

$$\beta = 180^\circ - \alpha_{\min} \tag{10.24}$$

During the charging process, the voltage of the battery changes, so the triggering angle must change accordingly to maintain the current constant. When the voltage of the battery is low, the triggering angle increases, so that the current is reduced to the level safe for charging the battery. When the voltage of the battery increases, the current in the battery is reduced so that the triggering angle is reduced to compensate for the current reduction.

Example 10.6

A 120 V full-wave battery charger is designed to provide 0.1 A of charging current. A battery set with $1\ \Omega$ internal resistance is connected across the charger. At the beginning of the charging process, the voltage of the battery is 45 V. After 3 h of charging, the voltage of the battery is 50 V. Compute the triggering angle of the converter at these two times. Also compute the conduction periods.

Solution

The instantaneous charging current can be expressed as

$$i = \frac{v_s - V_b}{R}$$

Hence, the average charging current is

$$I_{ave} = \frac{1}{2\pi} \int_0^{2\pi} i d\omega t = \frac{1}{\pi} \int_0^{\pi} i d\omega t$$

$$I_{ave} = \frac{1}{R\pi} \int_{\alpha}^{\beta} (V_{max} \sin \omega t - V_b) d\omega t = \frac{1}{R\pi} [V_{max} (\cos \alpha - \cos \beta) - V_b (\beta - \alpha)]$$

At the beginning of the charging process

We can compute β by using Equations 10.23 and 10.24.

$$\beta = 180^\circ - \alpha_{min} = 180^\circ - \sin^{-1} \left(\frac{V_b}{V_{max}} \right) = 180^\circ - \sin^{-1} \left(\frac{45}{\sqrt{2} * 120} \right) = 164.62^\circ$$

Hence,

$$I_{ave} = \frac{1}{R\pi} [V_{max} (\cos \alpha - \cos \beta) - V_b (\beta - \alpha)]$$

$$0.1 = \frac{1}{\pi} \left[\sqrt{2} \times 120 (\cos \alpha - \cos 164.62) - 45 \left(164.62 \frac{\pi}{180} - \alpha \right) \right]$$

$$\alpha \approx 161^\circ$$

The conduction period γ is

$$\gamma = \beta - \alpha = 164.62 - 161 = 3.62^\circ$$

After 3 h

$$\beta = 180^\circ - \alpha_{min} = 180^\circ - \sin^{-1} \left(\frac{V_b}{V_{max}} \right) = 180^\circ - \sin^{-1} \left(\frac{50}{\sqrt{2} \times 120} \right) = 162.86^\circ$$

Hence,

$$I_{ave} = \frac{1}{R\pi} [V_{max} (\cos \alpha - \cos \beta) - V_b (\beta - \alpha)]$$

$$0.1 = \frac{1}{\pi} \left[\sqrt{2} \times 120 (\cos \alpha - \cos 62.86) - 50 \left(162.86 \frac{\pi}{180} - \alpha \right) \right]$$

$$\alpha \approx 159.2^\circ$$

The conduction period γ is

$$\gamma = \beta - \alpha = 162.86 - 159.2 = 3.66^\circ$$

10.2.1.4 Three-Phase Circuits

Heavy loads are powered by three-phase systems in either half-wave or full-wave configuration. A half-wave, three-phase circuit is shown in Figure 10.28. In each phase, a single diode is used. The anode of each diode is connected to one phase, and the cathodes of all diodes are connected to one side of the load. The other side of the load is connected to the neutral point of the three-phase system.

The waveforms of the circuit are shown in Figure 10.29. When v_{an} is greater than the other two voltages (v_{bn} and v_{cn}), the SCR of phase a can be triggered (the anode is positive with respect to cathode). Hence, the triggering angle must be greater than 30° . After it is triggered, the current flows through the circuit starting from the triggering angle α_a and until π where the current goes to zero. The voltage across the load in this period is the same as v_{an} . Similarly, when v_{bn} is greater than the

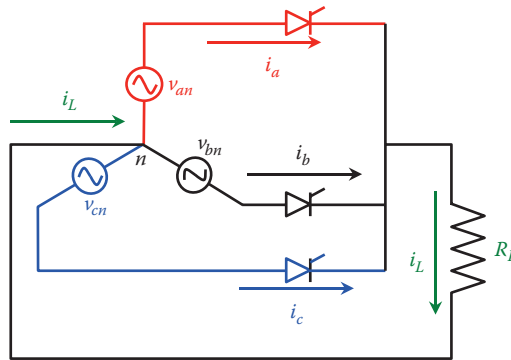


FIGURE 10.28 Three-phase half-wave ac/dc switching circuit.

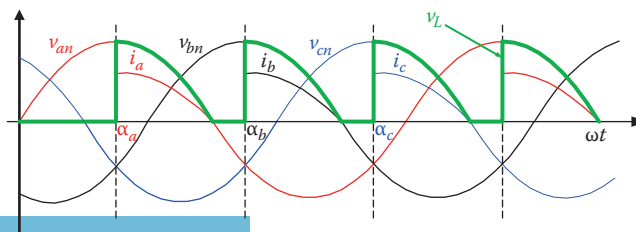


FIGURE 10.29 Waveforms of the circuit in Figure 10.28.

other two voltages, the SCR of phase b can be triggered and the voltage across the load is the same as v_{bn} during the period from α_b to $\pi + 120^\circ$. When v_{cn} is greater than the other two voltages, the SCR of phase c can be triggered and the voltage across the load is the same as v_{cn} during the period from α_c to $\pi + 240^\circ$.

Since the waveform of the load voltage in one 360° period consists of three equal segments, we can compute the average voltage across the load using one segment and then multiply the value by three:

$$V_{ave} = 3 \left[\frac{1}{2\pi} \int_{\alpha_a}^{\pi} v_{an} d\omega t \right] = \frac{3}{2\pi} \int_{\alpha_a}^{\pi} V_{\max} \sin(\omega t) d\omega t = \frac{3V_{\max}}{2\pi} [1 + \cos \alpha_a] \quad (10.25)$$

Similarly, the rms voltage across the load can be obtained by

$$V_{rms} = \sqrt{\frac{3}{2\pi} \int_{\alpha_a}^{\pi} (V_{\max} \sin \omega t)^2 d\omega t} \quad (10.26)$$

$$V_{rms} = \frac{\sqrt{3}}{2} V_{\max} \sqrt{\left[1 - \frac{\alpha_a}{\pi} + \frac{\sin(2\alpha_a)}{2\pi} \right]}$$

Keep in mind that α_a is measured from the zero crossing of v_{an} . It must be between 30° and 150° . This is the range at which v_{an} is larger than all other voltages:

$$30^\circ \geq \alpha_a \leq 150^\circ \quad (10.27)$$

Example 10.7

For the circuit in Figure 10.28, assume that the SCRs are replaced by diodes. If the line-to-line voltage of the circuit is 415.7 V and the load resistance is $10\ \Omega$, compute the average voltage across the load and the rms current of the load.

Solution

For the three-phase, half-wave diode circuit, the current starts flowing in phase a at 30° . This is when the voltage of phase a starts to become higher than all other voltages. The commutation angle β is $\pi - 30^\circ$ when the voltage of phase a falls below the phase voltage of phase b . In this case, the diode is commutated. The waveforms of the diode circuit are shown in Figure 10.30.

Using Equation 10.25, we can compute the average voltage across the load:

$$V_{ave} = 3 \left[\frac{1}{2\pi} \int_{\alpha_a}^{\beta_a} v_{an} d\omega t \right] = \frac{3}{2\pi} \int_{30^\circ}^{150^\circ} V_{\max} \sin(\omega t) d\omega t = \frac{3\sqrt{3}V_{\max}}{2\pi}$$

$$V_{ave} = \frac{3\sqrt{3} \left(\sqrt{2} \frac{415.7}{\sqrt{3}} \right)}{2\pi} = 280.7\text{ V}$$

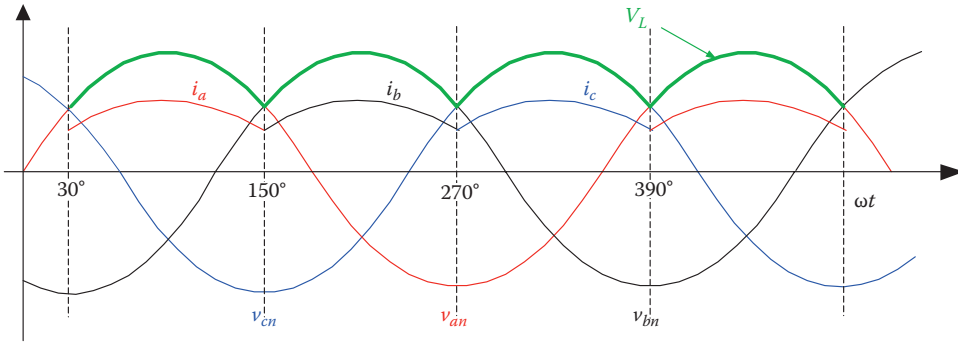


FIGURE 10.30 Three-phase half -wave ac/dc diode waveforms.

To compute the rms current, we need to compute the rms voltage using Equation 10.26, but modify the equation for the new conduction period:

$$V_{rms} = \sqrt{\frac{3}{2\pi} \int_{30^\circ}^{150^\circ} (V_{max} \sin \omega t)^2 d\omega t} = \frac{\sqrt{3}}{2} V_{max} \left[\sqrt{1 + \frac{\sqrt{3}}{2\pi}} \right]$$

$$V_{rms} = \frac{\sqrt{3}}{2} \left(\sqrt{2} \frac{415.7}{\sqrt{3}} \right) \left[\sqrt{1 + \frac{\sqrt{3}}{2\pi}} \right] = 332 \text{ V}$$

The rms current is

$$I_{rms} = \frac{V_{rms}}{R_L} = \frac{332}{10} = 33.2 \text{ A}$$

In heavier load applications, a full-wave, three-phase circuit similar to the one in Figure 10.31 can be used. The circuit consists of three switching legs, each has two SCRs. The center point of each leg is connected to the terminal of one of the phases of the source. The load is connected

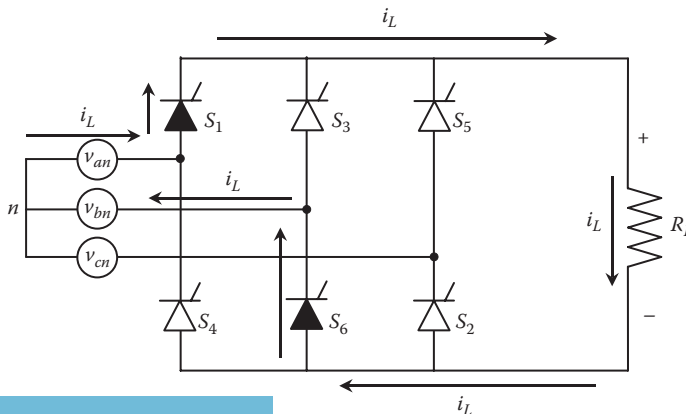


FIGURE 10.31 Three-phase full-wave ac/dc switching circuit operating between points 1 and 2.

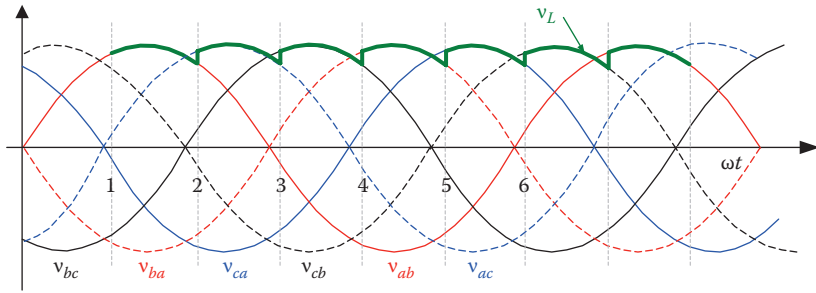


FIGURE 10.32 Three-phase full-wave ac/dc switching circuit waveforms.

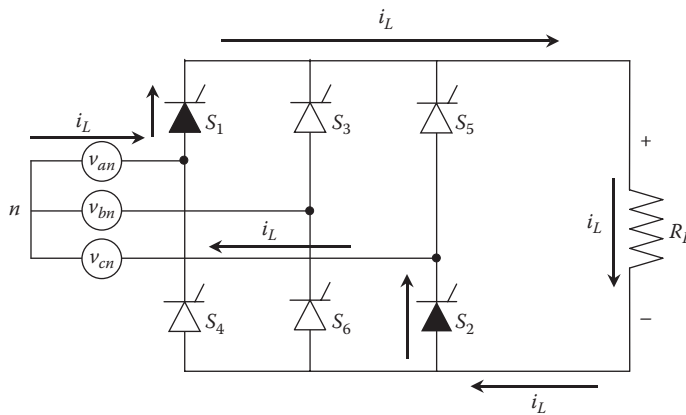


FIGURE 10.33 Three-phase full-wave ac/dc switching circuit operating between points 2 and 3.

between the cathodes of the upper SCRs and the anodes of the lower SCRs. The waveforms of the line-to-line voltages v_{ab} , v_{bc} , and v_{ca} are shown in Figure 10.32. The figure shows three other waveforms, v_{ba} , v_{cb} , and v_{ac} . Consider the period from point 1 to point 2. The voltage v_{ab} during this switching event is higher than all other voltages in the circuit (v_{bc} , v_{ca} , v_{ba} , v_{cb} , and v_{ac}). Hence, if we close S_1 and S_6 during this period, the current flows in the circuit as shown in Figure 10.31 and the load voltage is equal to v_{ab} .

Now consider the period from point 2 to point 3. The voltage v_{ac} during this period is higher than all other voltages in the circuit. Hence, if we close S_1 and S_2 during this period, the current flows in the circuit as shown in Figure 10.33. The load voltage during this switching period is equal to v_{ac} . When the process is repeated for all other intervals, the load voltage traces the top parts of the line-to-line waveforms.

During any switching event, the load voltage is equal to the corresponding line-to-line voltage. Since we have six switching events in one cycle, the conduction period of each event is 60° . Hence, the average voltage of the circuit is

$$V_{ave} = 6 \left(\frac{1}{2\pi} \int_{\alpha_{ab}}^{\alpha_{ab}+60^\circ} v_{ab} d\omega t \right) \tag{10.28}$$

Keep in mind that α_{ab} is measured from the zero crossing of the line-to-line voltage v_{ab} . Hence, the average voltage can be written as

$$V_{ave} = 6 \left[\frac{1}{2\pi} \int_{\alpha_{ab}}^{\alpha_{ab}+60^\circ} v_{an} d\omega t \right] = \frac{3}{\pi} \int_{\alpha_{ab}}^{\alpha_{ab}+60^\circ} \sqrt{3} V_{max} \sin(\omega t) d\omega t = \frac{3\sqrt{3}V_{max}}{\pi} \sin(\alpha_{ab} + 30) \quad (10.29)$$

where V_{max} is the maximum value of the phase voltage (not line-to-line voltage). The rms voltage across the load is

$$V_{rms} = \sqrt{\frac{6}{2\pi} \int_{\alpha_{ab}}^{\alpha_{ab}+60^\circ} (\sqrt{3}V_{max} \sin \omega t)^2 d\omega t} = \frac{3}{\sqrt{2}} V_{max} \sqrt{\left(\frac{1}{3} - \frac{\sqrt{3}}{2\pi} \cos(2\alpha_{ab} + 60) \right)} \quad (10.30)$$

Keep in mind that α_{ab} must be between 60° and 120° . This is the range at which v_{ab} is larger than all other voltages:

$$60^\circ \geq \alpha_{ab} \leq 120^\circ \quad (10.31)$$

Example 10.8

For the circuit in Figure 10.31, assume that the SCRs are replaced with diodes. If the line-to-line voltage of the circuit is 415.7 V and the load resistance is 10Ω , compute the average voltage across the load and the rms current of the load.

Solution

For the diode circuit, the conduction period is 60° and α_{ab} is also 60° . Using Equation 10.29, we can compute the average voltage across the load:

$$V_{ave} = \frac{3\sqrt{3}V_{max}}{\pi} \sin(\alpha_{ab} + 30) = \frac{3\sqrt{3} \left(\sqrt{2} \frac{415.7}{\sqrt{3}} \right)}{\pi} \sin(60 + 30) = 561.39 \text{ V}$$

To compute the rms current, use Equation 10.30:

$$V_{rms} = \frac{3}{\sqrt{2}} V_{max} \sqrt{\left(\frac{1}{3} - \frac{\sqrt{3}}{2\pi} \cos(2\alpha_{ab} + 60) \right)}$$

$$V_{rms} = \frac{3}{\sqrt{2}} \left(\sqrt{2} \frac{415.7}{\sqrt{3}} \right) \sqrt{\left(\frac{1}{3} - \frac{\sqrt{3}}{2\pi} \cos(120 + 60) \right)} = 561.88 \text{ V}$$

Note that the rms voltage is almost the same as the average voltage. Can you tell why?

The rms current is

$$I_{rms} = \frac{V_{rms}}{R_L} = \frac{561.88}{10} = 56.188 \text{ A}$$

10.2.2 DC/DC CONVERTERS

The dc/dc converters are normally designed to provide adjustable dc voltage waveforms at the output. There are three basic types of dc/dc converters:

1. *Buck converter*: This is a step-down converter where the output voltage is less than the input voltage.
2. *Boost converter*: This is a step-up converter where the output voltage is higher than the input voltage.
3. *Buck–boost converter*: This is a step-down/step-up converter where the output voltage can be made either lower or higher than the input voltage.

10.2.2.1 Buck Converter

Figure 10.34 shows a simple buck converter (also known as chopper). The circuit has a transistor as a switching device and the load is connected between the source and the collector of the transistor. The top waveform in the figure is for the base current of the transistor where the transistor is closed throughout the time segment t_{on} of the period τ of one cycle. Only when the transistor is closed is the voltage across the load V_t equal to the source voltage V_s ; otherwise, $V_t=0$. The current in the circuit flows only when the transistor is closed.

The average voltage across the load V_{ave} is

$$V_{ave} = \frac{1}{\tau} \int_0^{t_{on}} V_s dt = \left(\frac{t_{on}}{\tau} \right) V_s = K V_s \tag{10.32}$$

where $K=t_{on}/\tau$ is called the *duty ratio*. The maximum value of K is 1 when $t_{on}=\tau$. In this case, the transistor is always closed and the average load voltage is equal to the source voltage. For any other value of K (when $t_{on}<\tau$), the average load voltage is less than the source voltage. The output voltage of the converter can then be controlled by fixing the period τ and adjusting the on-time t_{on} .

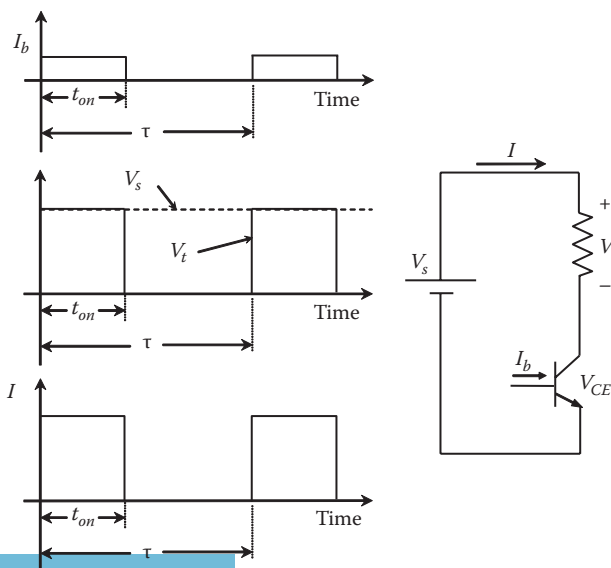


FIGURE 10.34 Simple chopper circuit.

Example 10.9

The switching frequency of a chopper is 10 KHz, and the source voltage is 40 V. For an average load voltage of 20 V and a load resistance of 10 Ω , compute the following:

1. Duty ratio
2. On-time and switching period
3. Average voltage across the transistor
4. Average current of the load
5. rms voltage across the load
6. Load power

Solution

1. As given in Equation 10.32, the duty ratio is

$$K = \frac{V_{ave}}{V_s} = \frac{20}{40} = 0.5$$

2. Before we compute the on-time, we need to compute the period:

$$\tau = \frac{1}{f} = \frac{1}{10} = 0.1 \text{ ms}$$

$$t_{on} = K\tau = 0.5 \times 0.1 = 0.05 \text{ ms}$$

3. The average voltage across the transistor V_{ave-tr} is

$$V_{ave-tr} = V_s - V_{ave} = 40 - 20 = 20 \text{ V}$$

4. The average load current is

$$I_{ave} = \frac{V_{ave}}{R} = \frac{20}{10} = 2 \text{ A}$$

5. The rms voltage of the load can be computed using the standard formula for the rms quantity

$$V = \sqrt{\frac{1}{\tau} \int_0^{t_{on}} V_s^2 dt} = \sqrt{\frac{V_s^2}{\tau} t_{on}} = V_s \sqrt{\frac{t_{on}}{\tau}} = 28.28 \text{ V}$$

6.
$$P = \frac{V^2}{R} = \frac{28.28^2}{10} = 80 \text{ W}$$

10.2.2.2 Boost Converter

A boost converter can increase the dc voltage across the load to values higher than the source voltage. A simple circuit for the boost converter is shown on the top part of Figure 10.35. The load of this circuit is the resistance R . The transistor is closed for a time interval t_{on} and is open during t_{off} . When the transistor is closed, the current i_{on} flows and the energy is stored in the

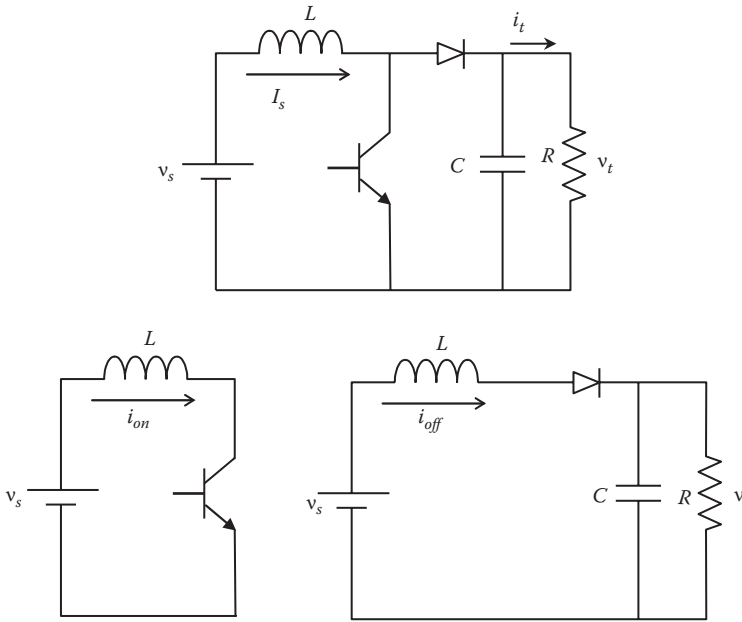


FIGURE 10.35 A simple boost converter.

inductor as depicted in the lower left side of the figure. In this process, the voltage across the inductor v_L is

$$v_L = L \frac{di_{on}}{dt} \approx L \frac{\Delta i_{on}}{t_{on}} \tag{10.33}$$

where Δi_{on} is the change in the current during the period t_{on} . Since the voltage across the inductor is equal to the source voltage when the transistor is closed, Equation 10.33 can be rewritten as

$$V_s = L \frac{\Delta i_{on}}{t_{on}} \tag{10.34}$$

When the transistor is opened, the stored energy in the inductor is transferred to the load via the diode. The inductor current in this case is i_{off} as depicted in the circuit on the lower right side of Figure 10.35. If we ignore the current through the capacitor, the voltage loop can be written as

$$v_t = V_s - v_L = V_s + L \frac{\Delta i_{off}}{t_{off}} \tag{10.35}$$

Because the inductor is producing energy during t_{off} , and because the current through the inductor does not change its direction, the voltage polarity across the inductance is reversed. This is the reason for the positive sign in front of L in Equation 10.35. At steady state when $\Delta i_{on} = \Delta i_{off}$ as shown in the current waveforms in Figure 10.36, Equation 10.35 can be rewritten as

$$v_t = V_s + L \frac{\Delta i_{off}}{t_{off}} = V_s \left(1 + \frac{t_{on}}{t_{off}} \right) \tag{10.36}$$

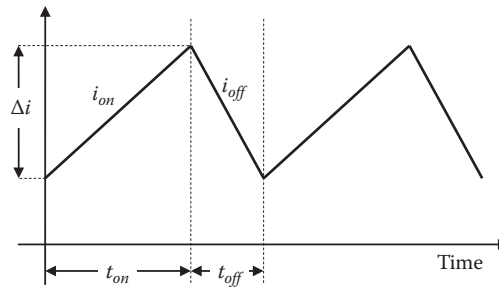


FIGURE 10.36 Waveform of boost converter.

This equation shows that the voltage across the load can be adjusted by adjusting t_{on} and t_{off} . Furthermore, the load voltage is always higher than the source voltage when $t_{on}/t_{off} > 0$.

The capacitor in the circuit is used as a filter to reduce the voltage ripples across the load, and the diode is used to block the capacitor from discharging through the transistor when it is closed. If the capacitance is large enough, v_t can be assumed ripple free. Hence, we can rewrite Equation 10.36 as

$$V_t = V_s + L \frac{\Delta i_{off}}{t_{off}} = V_s \left(1 + \frac{t_{on}}{t_{off}} \right) \quad (10.37)$$

where V_t is the average voltage across the load. If we assume that the average currents and the average voltages are much larger than their ripples, the rms and the average values can be considered equal. Hence, we can compute the input and output powers by using the average values

$$\begin{aligned} P_{in} &= V_s I_s \\ P_{out} &= V_t I_t \end{aligned} \quad (10.38)$$

where

P_{in} is the input power to the converter

P_{out} is the output power consumed by the load

I_s and I_t are the average currents of the source and load, respectively

If we further assume that the components of the circuit are ideal, the input power to the converter is equal to the output power. Hence,

$$V_t I_t = V_s I_s \quad (10.39)$$

Example 10.10

A boost converter is used to step up 20 V source to 50 V on the load. The switching frequency of the transistor is 5 kHz, and the load resistance is 10 Ω. Compute the following:

1. Value of the inductance that would limit the current ripple at the source side to 100 mA
2. Average current of the load
3. Power delivered by the source
4. Average current of the source

Solution

1. We can use Equation 10.34 to compute the inductance. But first, we need to compute t_{on} using Equation 10.37:

$$V_t = V_s \left(1 + \frac{t_{on}}{t_{off}} \right)$$

$$50 = 20 \left(1 + \frac{t_{on}}{t_{off}} \right)$$

$$t_{on} = 1.5 \times t_{off}$$

Since the switching frequency is 5 kHz,

$$t_{on} + t_{off} = \frac{1}{5} = 0.2 \text{ ms}$$

then

$$t_{on} = 1.5 \times t_{off} = 1.5 \times (0.2 - t_{on})$$

$$t_{on} = 0.12 \text{ ms}$$

To compute the value of the inductance, we can use Equation 10.34:

$$V_s = L \frac{\Delta i_{on}}{t_{on}}$$

$$20 = L \frac{100}{0.12}$$

$$L = 24 \text{ mH}$$

$$2. \quad I_t = \frac{V_t}{R} = \frac{50}{10} = 5 \text{ A}$$

3. The power delivered by the source is the same power consumed by the load, assuming that the system components are all ideal:

$$P = V_t \times I_t = 50 \times 5 = 250 \text{ W}$$

4. The average current of the source can be computed using Equation 10.39:

$$I_s = \frac{P}{V_s} = \frac{250}{20} = 12.5 \text{ A}$$

10.2.2.3 Buck–Boost Converter

The buck–boost converter has the same components as the boost converter but is structured differently as shown on the top part of Figure 10.37. When the transistor is closed, as shown in the bottom left side of Figure 10.37, the current i_{on} flows through the inductor, and energy is acquired by the inductor. When the transistor is opened, the inductor delivers its stored energy to the load as shown

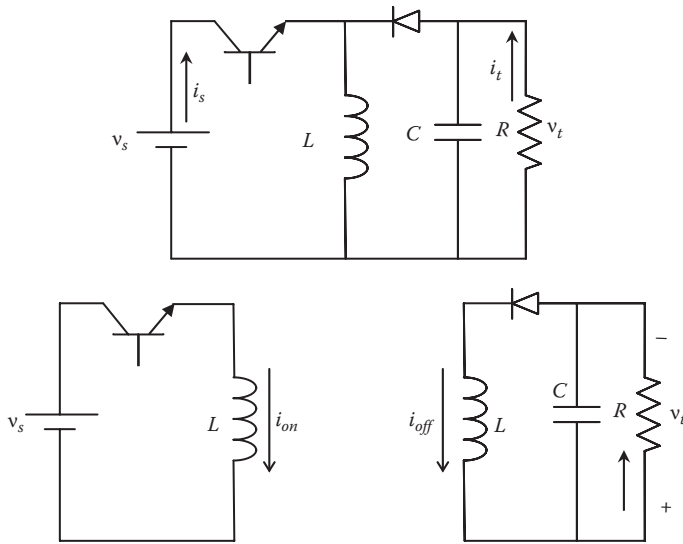


FIGURE 10.37 A simple buck–boost converter.

on the bottom right side of Figure 10.37. The inductor current in this period is i_{off} . The capacitor is used as a filter to minimize the voltage ripples across the load, and the diode is used to prevent the load from being energized when the transistor is closed. The capacitor current can be assumed very small compared with the load current.

When the transistor is closed, the voltage across the inductor is

$$v_L = L \frac{di_{on}}{dt} \approx L \frac{\Delta i_{on}}{t_{on}} \tag{10.40}$$

Note that when the transistor is closed, the voltage across the inductor is equal to the source voltage. Hence,

$$V_s = L \frac{\Delta i_{on}}{t_{on}} \tag{10.41}$$

When the transistor is open, the voltage across the inductor reverses because the inductor becomes a source of energy and the voltage across the inductor is

$$v_L = -L \frac{\Delta i_{off}}{t_{off}} \tag{10.42}$$

The voltage across the load when the transistor is open is equal to the inductor voltage. Hence,

$$v_t = -L \frac{\Delta i_{off}}{t_{off}} \tag{10.43}$$

Assume that the capacitor is large enough so that the voltage v_t is equal to the average voltage across the load V_t . At steady state, when $\Delta i_{on} = \Delta i_{off}$, Equations 10.41 and 10.43 can be combined as

$$V_t = -V_s \frac{t_{on}}{t_{off}} \tag{10.44}$$

As seen in Equation 10.44, the average value of the load voltage can be controlled by adjusting the ratio t_{on}/t_{off} . If the on-time is zero, the load voltage is zero. If $0 < t_{on} \leq t_{off}$, the load voltage is lower than the source voltage. If $t_{on} = t_{off}$, the load voltage is equal to the source voltage. If $t_{on} > t_{off}$, the load voltage is higher than the source voltage. Keep in mind that Equation 10.44 is not valid when $t_{off} = 0$; that is, the transistor never opens. The system in this case is unstable as the current i_{on} will reach very high values because the inductor acts as a short circuit when continuous dc flows through it.

If we assume that the circuit's components are ideal, the input power to the converter is equal to the output power. Hence,

$$P_m = P_{out} = V_t I_t = V_s I_s \quad (10.45)$$

Example 10.11

A buck–boost converter with an input voltage of 20 V is used to regulate the voltage across a $10\ \Omega$ load. The switching frequency of the transistor is 5 kHz. Compute the following:

1. On-time of the transistor to maintain the output voltage at 10 V
2. Output power
3. On-time of the transistor to maintain the output voltage at 40 V
4. Output power

Solution

1. The period can be computed from the switching frequency f

$$\tau = \frac{1}{f} = \frac{1}{5} = 0.2\ \text{ms}$$

Use Equation 10.44 to compute the time ratio. We only need to use the magnitudes of the voltages

$$\frac{t_{on}}{t_{off}} = \frac{V_t}{V_s} = \frac{10}{20} = 0.5$$

Hence,

$$t_{on} = 0.0667\ \text{ms}$$

2. The output power

$$P = \frac{V_t^2}{R} = 10\ \text{W}$$

3.
$$\frac{t_{on}}{t_{off}} = \frac{V_t}{V_s} = \frac{40}{20} = 2$$

Hence,

$$t_{on} = 0.1333\ \text{ms}$$

4. The output power

$$P = \frac{V_l^2}{R} = \frac{40^2}{10} = 160 \text{ W}$$

As you have seen, the inductor plays a major role in dc/dc converters. It acts as a temporary storage device that transfers the energy from the source to the load. This inductor can be built using a toroid as explained in Appendix D.

10.2.3 DC/AC CONVERTERS

The dc/ac converter is also known as an *inverter*. The inverter is used in applications such as uninterruptible power supplies, variable speed drives, and dc transmission lines. It is also common to use this converter to convert the 12 V dc waveform of automobiles into household alternating voltage to power small equipment such as personal computers and televisions.

There are two types of dc/ac converters: single phase and multiphase. The first is used in low-to-medium power applications and the second is used with heavy industrial loads.

10.2.3.1 Single-Phase DC/AC Converter

Figure 10.38 shows a simple dc/ac converter in H-bridge configuration. It consists of a dc source, four transistors, and a load. The desired frequency of the output waveform determines the switching period of the transistors. During the first half of the period, Q_1 and Q_2 are closed, and during the

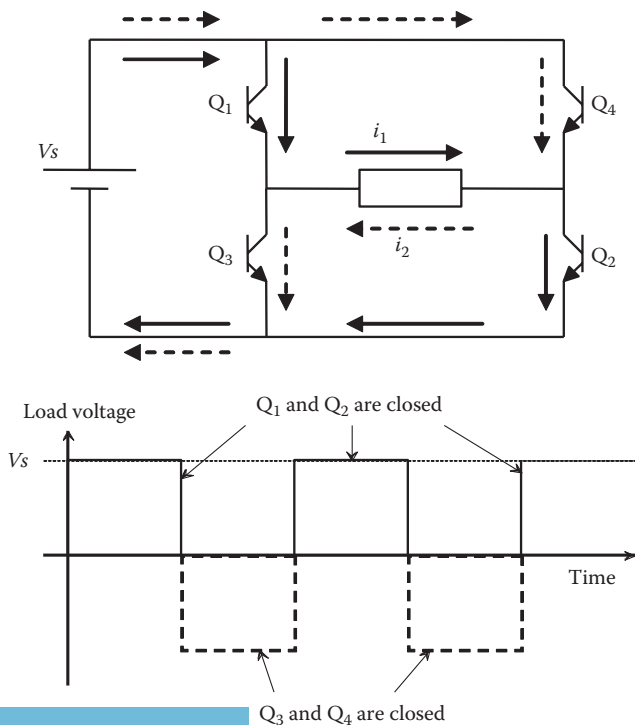


FIGURE 10.38 Single-phase dc/ac converter.

second half, Q_3 and Q_4 are closed. The voltage waveform of the circuit is also shown in the figure. During the first half of the period, the current i_1 (in solid arrows) flows through the load. Similarly, during the second half, the current i_2 (in dashed arrows) flows through the load in the opposite direction to i_1 . Thus, the load current is alternating. Notice that the waveform in Figure 10.38 is not sinusoidal, but still considered an ac waveform.

Example 10.12

The source voltage of a single-phase dc/ac converter is 100 V. The switching frequency of the transistors is 1 kHz. Compute the following:

1. rms voltage across the load
2. Average voltage across the load

Solution

1. As given in Chapter 7, the rms voltage of an arbitrary waveform v is

$$V = \sqrt{\frac{1}{\tau} \int_0^{\tau} v^2 dt}$$

where $\tau = 1/f = 1 \text{ ms}$

$$V = \sqrt{\frac{1}{\tau} \int_0^{\tau} v^2 dt} = \sqrt{\frac{2}{\tau} \int_0^{\tau/2} V_s^2 dt}$$

where V_s is the source voltage

$$V = \sqrt{\frac{2}{\tau} 10^4 \int_0^{\tau/2} dt} = \sqrt{\frac{2}{\tau} 10^4 \frac{\tau}{2}} = 100 \text{ V}$$

The rms voltage across the load is equal to the dc voltage of the source. This is because the ac waveform is rectangular and symmetrical.

2. The average voltage across the load is zero since the waveform is symmetrical around the time axis.

10.2.3.2 Three-Phase DC/AC Converter

Three-phase waveforms can be obtained using the dc/ac converter shown in Figure 10.39. The converter is composed of six transistors, a dc source, and a three-phase load. This circuit is also known as *six-pulse converter*. The transistors are arranged in three legs, each leg has two transistors, and the midpoint of each leg is connected to one of the terminals of the three-phase load. The switching sequence of the transistors is shown at the top part of Figure 10.40. The cycle is divided into six intervals, so that each interval is 60° . Each transistor is closed for three consecutive intervals (180°) and opened for the following three consecutive intervals. The switching of the transistors is based on their ascending numbers. For example, transistor Q_1 is closed first and then Q_2 after one time interval, Q_3 after additional time interval, and so on. During any time interval, one transistor per

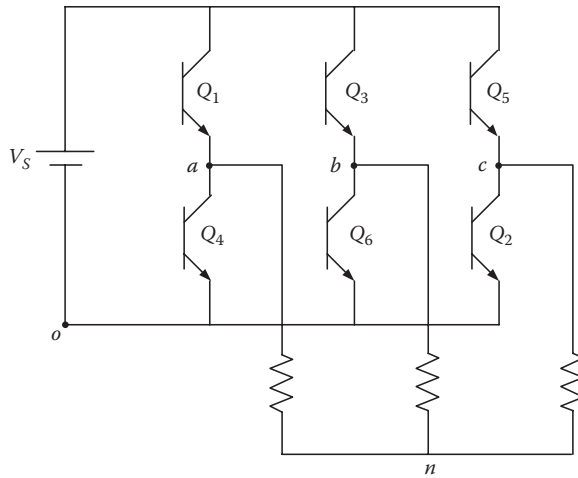


FIGURE 10.39 Three-phase dc/ac inverter.

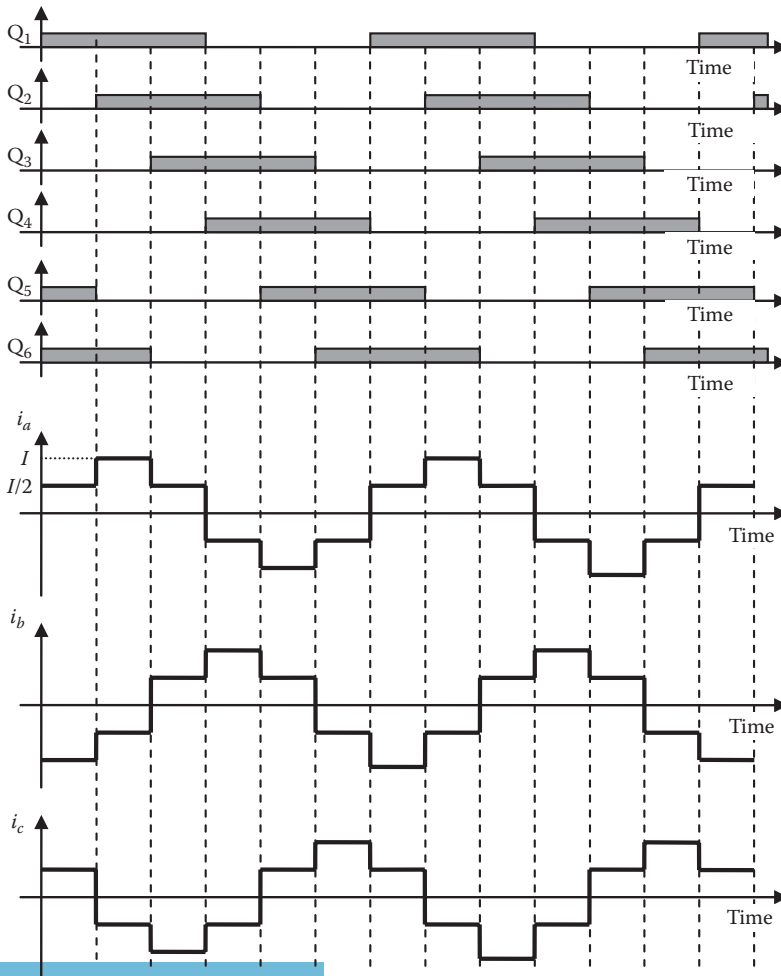


FIGURE 10.40 Timing of transistors and the phase currents.

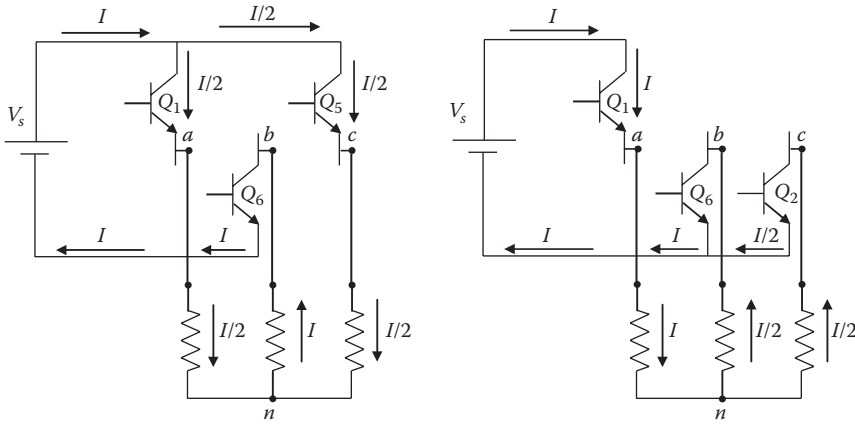


FIGURE 10.41 Active transistors and current flow during the first two intervals.

leg is closed. No two transistors on the same leg are closed at the same time as this creates a short circuit across the supply.

Now let us study the effect of the switching pattern during the first time interval when transistors Q_1 , Q_5 , and Q_6 are closed. This interval is depicted on the left side of Figure 10.41, which shows only the transistors that are closed. During this interval, the current from the source I is divided into two equal components; one passes through Q_1 and the other through Q_5 . At the neutral point n , the two currents are summed up and returned to the source through Q_6 . The load currents during this interval are

$$i_a = i_c = \frac{I}{2}$$

$$i_b = -I$$
(10.46)

These load currents during the first interval are shown at the lower part of Figure 10.40. Now let us study the second interval when Q_1 , Q_2 , and Q_6 are closed. The flow of the current during this interval is shown on the right side of Figure 10.41. The current from the source passes through Q_1 and at the neutral point branches into two equal components; one goes through Q_2 and the other through Q_6 . The load currents during this interval are

$$i_a = I$$

$$i_b = i_c = -\frac{I}{2}$$
(10.47)

If you follow the same procedure for the other intervals, you will get the current waveforms in Figure 10.40. Note the following:

- Current waveforms are symmetrical around the time axis. All phase currents have the same maximum value.
- i_b lags i_a by two time intervals, that is, 120° .
- i_c lags i_b by two time intervals, that is, 120° .

Hence, the output currents of the converter are balanced three-phase waveforms.

The frequency of the load current is dependent on the interval time of one segment t_i . Since the cycle is composed of six segments, the frequency of the ac waveform is

$$f = \frac{1}{6t_i} \quad (10.48)$$

To change the frequency of the ac waveform, the time of the interval must change.

Example 10.13

A three-phase dc/ac converter is used to power a three-phase, Y-connected, resistive load of 10Ω (per phase). The dc voltage is 300 V. Compute the following:

1. Time interval, if the desired frequency of the ac waveform is 200 Hz
2. Current of the dc source
3. rms current of the load
4. rms voltage across each phase of the load

Solution

1. Use Equation 10.48 to compute the interval

$$t_i = \frac{1}{6f} = \frac{1}{6 \times 200} = 833 \mu\text{s}$$

2. During any given interval, the load has two of its phases in parallel, and the combination is in series with the third phase. In the circuit on the left side of Figure 10.41, the load resistances of phases a and c are in parallel, and this combination is in series with the resistance of phase b . Similar combinations are true during all other time intervals. Hence,

$$R_{total} = 10 + \frac{10 \times 10}{10 + 10} = 15 \Omega$$

Then the source current is

$$I = \frac{V_s}{R_{total}} = \frac{300}{15} = 20 \text{ A}$$

3. The rms current of phase a is

$$I_a = \sqrt{\frac{1}{6t_i} \int_0^{6t_i} i_a^2 dt}$$

If you examine the waveform of i_a for one period, you will discover that the magnitude of the current is equal to I during two time intervals, and is equal to $I/2$ during four intervals. Hence, the rms current of phase a can be written as

$$I_a = \sqrt{\frac{1}{6t_i} \left(\int_0^{2t_i} I^2 dt + \int_0^{4t_i} \left(\frac{I}{2}\right)^2 dt \right)} = \sqrt{\frac{I^2}{6t_i} (3t_i)} = \frac{I}{\sqrt{2}} = 14.14 \text{ A}$$

This rms current is the same as that computed for the purely sinusoidal waveform where I is the maximum current of the instantaneous waveform.

4. The rms phase voltage of the load is

$$V_{an} = I_a R = 14.14 \times 10 = 141.1 \text{ V}$$

10.2.3.3 Pulse Width Modulation

Pulse width modulation (PWM) technique is used in dc/ac converter to control three variables:

- Magnitude of output voltage
- Frequency of output voltage
- Phase sequence of output voltages

The PWM circuit generates four low-voltage signals: one high-frequency carrier and three control signals (one for each phase). The carrier is fixed voltage and frequency. The voltage and frequency of the control signals are adjustable. The PWM circuit determines the switching status of the transistors in Figure 10.39. The top part of Figure 10.42 shows the carrier ($v_{carrier}$) and the control signal of phase a ($v_{a-control}$) and for phase b ($v_{b-control}$). The control signals are shifted from each other by the 120° of the balanced three-phase system. The switching of the transistors in Figure 10.39 at any leg is determined by the relative magnitude of the control signal of the corresponding phase and the carrier signal. For example, the switching of transistors Q_1 and Q_4 in leg a is determined by Δv_a , where

$$\Delta v_a = v_{a-control} - v_{carrier} \quad (10.49)$$

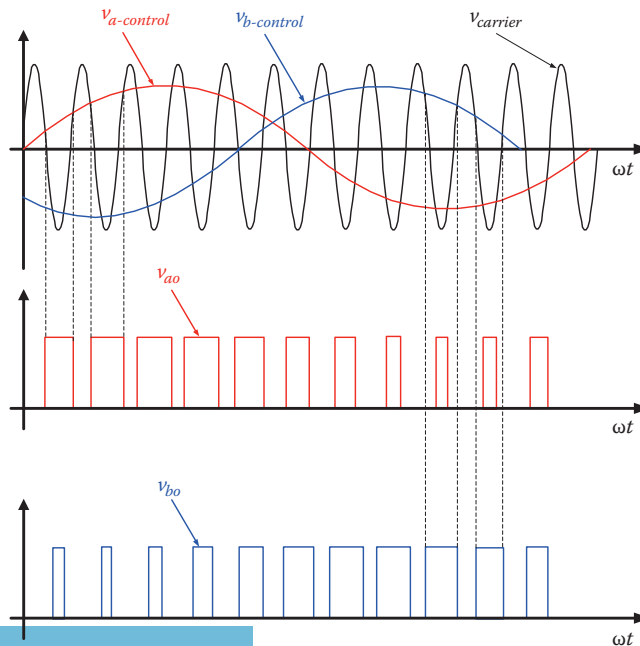


FIGURE 10.42 PWM signals and voltage waveforms.

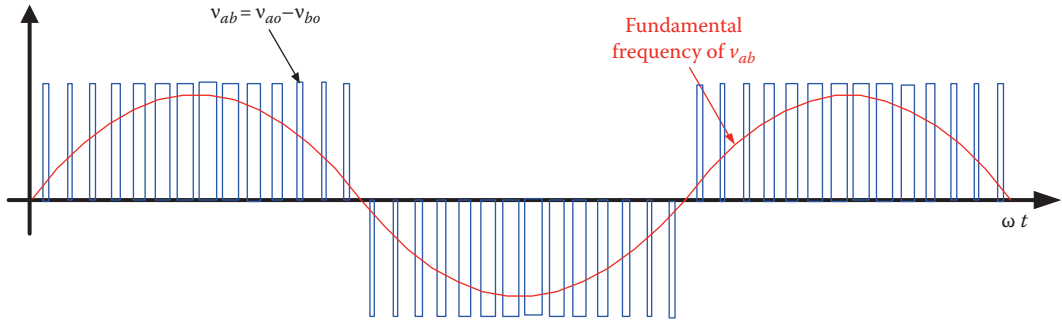


FIGURE 10.43 Line-to-line voltage.

The switching logic of Q_1 and Q_4 is as follows:

$$\text{IF } \Delta v_a > 0, Q_1 \text{ is closed and } Q_4 \text{ is opened}$$

$$\text{IF } \Delta v_a < 0, Q_4 \text{ is closed and } Q_1 \text{ is opened} \tag{10.50}$$

The logic is repeated for the other two legs based on their correspondent values of Δv_b and Δv_c . The middle part of Figure 10.42 shows the voltage v_{ao} between terminal a and o (the negative side of the dc source in Figure 10.39). The bottom part shows v_{bo} . Note that the maximum value of either v_{ao} , v_{bo} , or v_{co} is constant and equal to the source voltage (V_s). Also, notice that the duration of any switching period varies. This is what the “width modulation” term describes. The line-to-line voltage v_{ab} is

$$v_{ab} = v_{ao} - v_{bo} \tag{10.51}$$

The voltage v_{ab} is shown in Figure 10.43. The voltage can be represented by a Fourier series as

$$v_{ab} = m_a \frac{V_s}{2} \sin(2\pi f_s t) + \text{higher harmonics} \tag{10.52}$$

where

- V_s is the source voltage on the dc side
- f_s is the frequency of the control signal
- m_a is amplitude modulation defined by

$$m_a = \frac{V_{control}}{V_{carrier}} \tag{10.53}$$

where

- $V_{control}$ is the rms of the control signal
- $V_{carrier}$ is the rms of the carrier signal

If we ignore the higher harmonics in Equation 10.53, we get

$$v_{ab} \approx m_a \frac{V_s}{2} \sin(2\pi f_s t) \tag{10.54}$$

With PWM, we can control the voltage, frequency, and phase sequence as follows:

- Voltage control is implemented by adjusting the voltage of the control signal. Hence, m_a is adjusted in Equation 10.54.
- Frequency control is implemented by adjusting the frequency of the control signal f_s .
- Phase sequence can be changed from abc to acb by swapping the signals of any two legs.

This powerful PWM technique is widely used in dc/ac applications such as adjustable speed drives, wind turbines, power supplies, and actuation. Newer PWM circuits are specifically designed to switch the transistors in specific pattern to reduce the harmonic content.

10.2.4 AC/AC CONVERTERS

A simple ac/ac converter is shown in Figure 10.44 and the waveforms of the circuit are shown in Figure 10.45. The circuit consists of two SCRs connected in parallel in the back-to-back configuration. When the voltage of the source is in the positive half of its ac cycle and the top SCR is

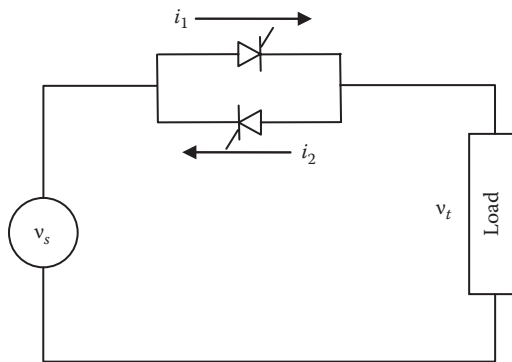


FIGURE 10.44 AC/AC converter.

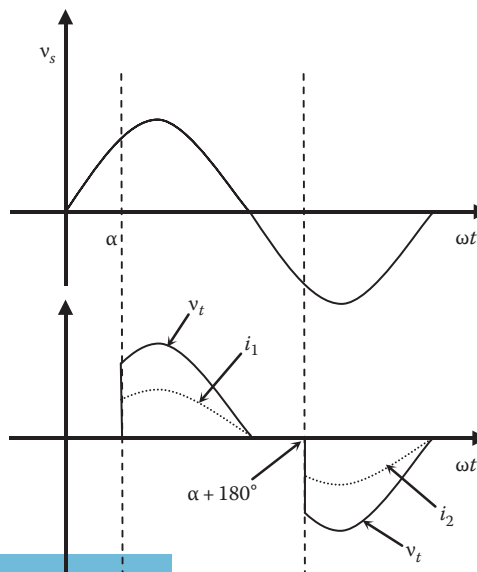


FIGURE 10.45 Waveform of ac/ac converter in Figure 10.44.

triggered, the SCR closes and the current i_1 flows through the load. When the source voltage is at its negative half of the cycle, the bottom SCR is triggered and the load current is i_2 , which is opposite to the direction of i_1 .

If the top SCR is triggered at α , and the bottom SCR is triggered at $\alpha + 180^\circ$, the waveform of the load voltage or the load current is symmetrical around the time axis. Therefore, the average voltage or average current of the load is zero.

The rms voltage and current of the load are exactly the same as those discussed for the full-wave ac/dc circuits:

$$V_{rms} = \sqrt{\frac{1}{2\pi} \int_0^{2\pi} v_r^2 d\omega t} = \sqrt{\frac{1}{\pi} \int_\alpha^\pi (V_{max} \sin \omega t)^2 d\omega t}$$

$$V_{rms} = \frac{V_{max}}{\sqrt{2}} \sqrt{\left(1 - \frac{\alpha}{\pi} + \frac{\sin 2\alpha}{2\pi}\right)} \tag{10.55}$$

The power across the load can be computed as

$$P = \frac{V_{rms}^2}{R} = I_{rms}^2 R$$

$$P = \frac{V_{max}^2}{4\pi R} (2(\pi - \alpha) + \sin 2\alpha) \tag{10.56}$$

A more elaborate form of ac/ac converter that allows for the adjustment of the output frequency, in addition to the output voltage, is the one shown in Figure 10.46. The system consists of two ac/dc converters connected back-to-back as shown in the figure. In the first converter, the input ac waveform is converted into dc through the first ac/dc converter. The dc is then converted back to ac waveform through the dc/ac converter. The connection between the two converters is called dc link.

This type of converter is commonly used as an uninterruptible power supply (UPS). A UPS system is shown in Figure 10.47. The system is similar to that shown in Figure 10.46, but a rechargeable

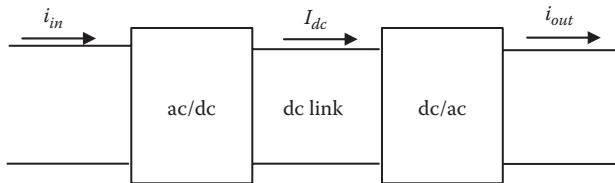


FIGURE 10.46 AC/AC converter with dc link.

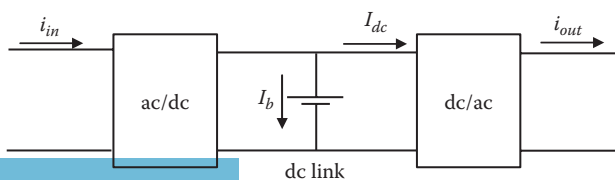


FIGURE 10.47 Normal operation of UPS system.

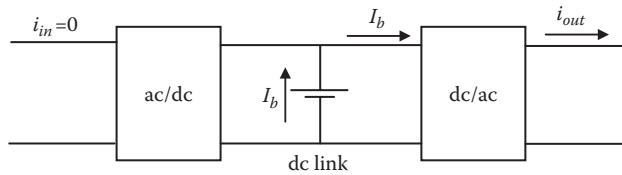
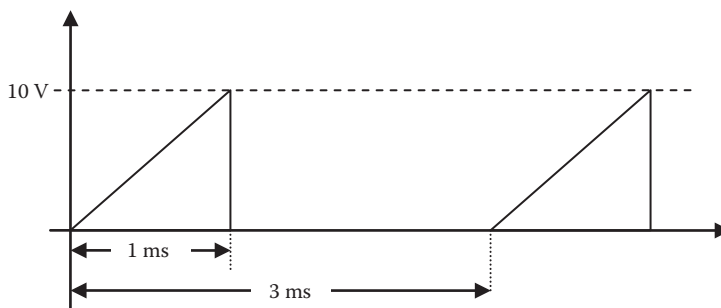


FIGURE 10.48 UPS operation during power outage.

battery is added in the dc link. In normal operations, the input ac current i_{in} is converted into dc, where part of the current I_b charges the battery and the other part I_{dc} is converted into the ac i_{out} . If the input power is lost due to an outage, the energy stored in the battery is used to feed the load through the dc/ac converter as shown in Figure 10.48. Hence, the load power is not interrupted. This system can provide temporary power until the battery is fully discharged.

EXERCISES

- 10.1** A bipolar transistor is connected to a resistive load as shown in Figure 10.7. The source voltage $V_{CC}=40\text{ V}$ and $R_L=10\ \Omega$. In the saturation region, the collector-emitter voltage $V_{CE}=0.1\text{ V}$ and $\beta=5$. While the transistor is in the saturation region, calculate the following:
- Load current
 - Load power
 - Losses in the collector circuit
 - Losses in the base circuit
 - Efficiency of the circuit
- 10.2** For the transistor in the previous problem, compute the load power and the efficiency of the circuit when the transistor is in the cutoff region. Assume that the collector current is 10 mA in the cutoff region.
- 10.3** A BJT operating in the saturation region has a base current of 10 A and a collector current of 50 A. Compute the following:
- Current gain of the transistor in the saturation region
 - Losses of the transistor
- 10.4** Compute the rms voltage of the following waveform



- 10.5** A half-wave rectifier circuit converts a 120 V (rms) into dc. The load of the circuit is $5\ \Omega$ resistance. Compute the following:
- Average voltage across the load
 - Average voltage of the source

- c. rms voltage of the load
 - d. rms current of the load
 - e. Power consumed by the load
- 10.6** A half-wave SCR converter circuit is used to regulate the power across a $10\ \Omega$ resistance. When the triggering angle is 30° , the power consumed by the load is 500 W. Compute the rms voltage of the source, and the average and rms currents of the load.
- 10.7** An ac/dc half-wave SCR circuit is used to energize a resistive load. At a triggering angle of 30° , the average voltage across the load is 45 V.
- a. Compute the source voltage in rms.
 - b. If a full-wave circuit is used, while the triggering angle is maintained at 30° , compute the average voltage across the load.
- 10.8** A full-wave SCR converter circuit is used to regulate the power across a $10\ \Omega$ resistance. The voltage source is 120 V (rms). At a triggering angle of 72° , compute the power across the load and the rms currents of the load.
- 10.9** A 120 V full-wave SCR battery charger is designed to provide 1.0 A of charging current. The battery has $1\ \Omega$ internal resistance. At the beginning of the charging process, the voltage of the battery set is 60 V. Compute the triggering angle of the converter.
- 10.10** A full-wave, ac/dc converter is connected to a resistive load of $5\ \Omega$. The voltage of the ac source is 120 V (rms). If the triggering angle of the converter is 90° , compute the rms voltage across the load and the power consumed by the load.
- 10.11** A boost converter has a source voltage $v_s = 20\ \text{V}$ and a load resistance $R = 10\ \Omega$. If the duty ratio of the transistor is 50%, compute the voltage across the load and the power consumed by the load.
- 10.12** A boost converter is used to step up 25 V into 40 V. The switching frequency of the transistor is 1 kHz, and the load resistance is $100\ \Omega$. Compute the following:
- a. The current ripple when the inductor is 30 mH
 - b. The average current of the load
 - c. The power delivered by the source
- 10.13** A buck–boost converter has an input voltage of 30 V. The switching frequency of its transistor is 5 kHz, and its duty ratio is 25%. Compute the average voltage across the load.
- 10.14** A buck–boost converter with an input voltage of 40 V is used to regulate the load voltage from 10 to 80 V. The on-time of the transistor is always fixed at 0.1 ms and the switching frequency is adjusted to regulate the load voltage. Compute the range of the switching frequency.
- 10.15** A three-phase dc/ac converter is used to power a three-phase, Y-connected, resistive load of $50\ \Omega$ (per phase). The dc voltage is 150 V. Compute the following:
- a. The frequency of the ac waveform if the time interval is $100\ \mu\text{s}$
 - b. The current of the dc source
 - c. The rms current of the load
 - d. The rms of the line-to-line voltage across the load
- 10.16** A full-wave ac/dc SCR converter circuit is used to power a resistive load of $10\ \Omega$. The ac voltage is 120 V (rms), and the triggering angle of the SCR is adjusted to 60° . Calculate the following:
- a. The conduction period
 - b. The average voltage across the load
 - c. The average voltage across the SCRs
 - d. The rms voltage across the load
 - e. The average current
 - f. The load power

- 10.17** A dc/dc converter consists of a 100 V dc source in series with $10\ \Omega$ load resistance and a bipolar transistor. For each cycle, the transistor is turned on for $200\ \mu\text{s}$ and turned off for $800\ \mu\text{s}$. Calculate the following:
- The switching frequency of the converter
 - The average voltage across the load
 - The average load current
 - The rms voltage across the load
 - The rms current of the load
 - The rms power consumed by the load
- 10.18** A dc/dc buck converter has an input voltage of 100 V and a duty ratio of 0.2. Compute the following:
- The load voltage
 - The switching frequency of the converter if the on-time is 0.1 ms
- 10.19** The load of the full-wave SCR circuit in Figure 10.23 consumes 130 W. The rms voltage across the load is 80 V, and its average voltage is 50 V.
- Compute the average voltage across any SCR.
 - The triggering circuit of one SCR failed and that SCR is not conducting anymore. If the triggering angle of the rest of the SCRs is unchanged, compute the average voltage of the load and the load power.
- 10.20** A resistive load of $5\ \Omega$ is connected to an ac source of 120 V (rms) through a back-to-back SCR circuit (two parallel SCRs, with the anode of each one connected to the cathode of the other). The triggering angle of the forward SCR (the one that conducts at the positive half of the cycle) is 30° . The triggering angle of the other SCR is $(180^\circ + 30^\circ)$. Calculate the following:
- Average voltage across the load
 - Power consumed by the load

11 Transformers

The Italian scientist Antonio Pacinotti, who invented the transformer in 1860, granted the power industry with one of its most important devices, without which the power grid would not exist. The transformer is used to step up (increase) or step down (decrease) the voltage. This capability allows us to transmit and distribute massive amounts of power in today's extensive power grid. Because power is the product of current and voltage, a large power at a low voltage leads to a high current. Since the current determines the cross section of the transmission line wires, large currents require unrealistic large cross section wires. These impractical wires are heavy and expensive to manufacture and require enormous towers with short spans to carry them. The transformer provides us with the solution; it allows us to increase the voltage of the transmission lines so that the current is reduced. Thus, the cross section of the wire is reasonably small and the cost of the transmission line is dramatically reduced.

Figure 11.1 shows a schematic of a power system with its main transformers. The system has four types of transformers: transmission, distribution, service, and circuit transformers.

1. *Transmission transformers* Figure 11.2a: These transformers are connected to both ends of the transmission line. At the generating power plants, the transformer steps up the voltage of the generators to very high levels (220 kV–1 MV) so that the current can be reduced substantially. At the other end of the transmission line, the transformer steps down the voltage to a lower level suitable for distribution to load centers. Since the transmission transformers carry the bulk power of the system, they are very large in size. The internal losses of the transformer, which are due to the high currents in the windings and core losses, can cause excessive heat inside the container of the transformer. Therefore, the transformer is immersed in cooling medium such as oil and the container is equipped with a system of pipes and fans to extract heat from the cooling medium much like the radiators in automobiles. The medium also increases the dielectric strength of the windings so that the transformer can withstand higher voltages.
2. *Distribution transformers* Figure 11.2b: These transformers are installed in distribution substations near the load centers. They are designed to reduce the output voltage of the transmission transformers to a lower level of 5–220 kV as shown in Figure 11.1.
3. *Service transformers* Figure 11.2c: These transformers are located near customers' loads. They are designed to lower the distribution voltage to the household level (120/240 V in the United States). They are normally mounted on power poles, placed inside vaults, or installed inside large buildings.
4. *Circuit transformers* Figure 11.2d: These are small transformers extensively used in power supplies and electronic circuits where the household voltage is stepped down to the circuit voltage level of a few volts. Other applications of the circuit transformers include impedance matching, filters, and electrical isolation.

11.1 THEORY OF OPERATION

The basic components of a transformer are shown in Figure 11.3. The transformer consists of at least two windings wrapped around a laminated iron alloy core. These windings are electrically isolated from the core by a varnished insulation material capable of withstanding the voltage of the windings. The core provides a low reluctance path for the magnetic flux. An alternating current (ac) voltage

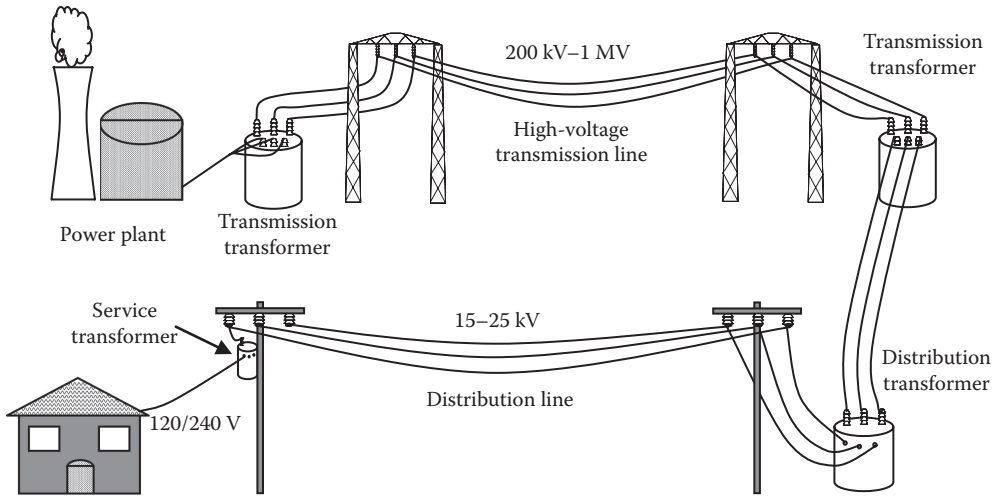


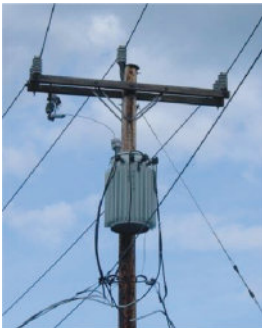
FIGURE 11.1 Various transformers in power system.



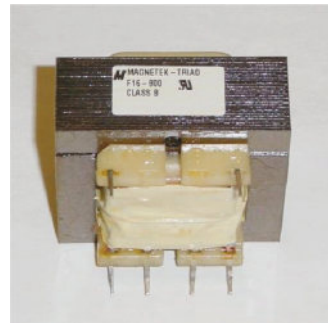
(a)



(b)



(c)



(d)

FIGURE 11.2 Various types of transformers: (a) transmission transformer, (b) distribution transformer, (c) service transformer, and (d) circuit transformer.

source is connected across one of the windings and the current of the winding produces flux that passes through the core and links the second winding. Since the current is alternating, the flux in the core changes its direction 120 times per second for the 60 Hz system. This change in flux induces a voltage on the second winding.

The rapid change in the flux induces a voltage in the core itself, thus creating currents that move within the core in circular paths. This current, which is called *eddy current*, creates heat in

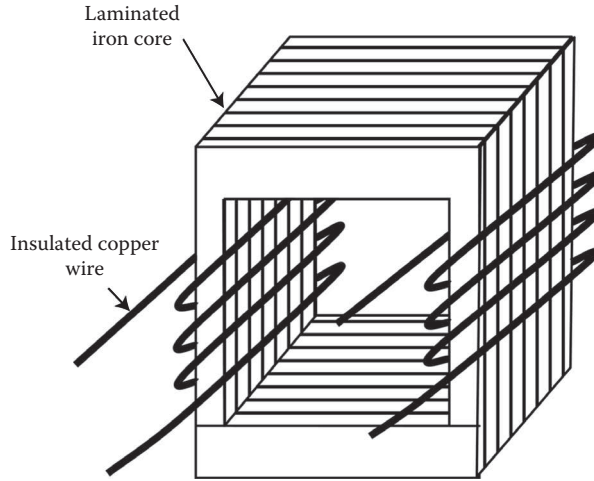


FIGURE 11.3 Main components of a transformer.

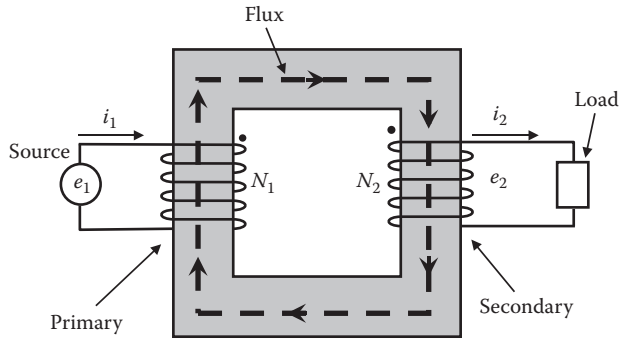


FIGURE 11.4 Flux linkage of the transformer.

the core and results in wasted energy. To reduce eddy current, the electrical resistance of the core must increase. This is done by laminating the core as shown in Figure 11.3. Each laminated plate is insulated by oxidized material or varnish. The cross section of a laminated sheet is much smaller than the total cross section of the core, thus the circular eddy current is substantially reduced.

Assume that an ac voltage source is connected across one of the windings, and a load is connected across the other winding as shown in Figure 11.4. The winding connected to the source is called *primary winding*, and the winding connected to the load is called *secondary winding*. The number of turns of the primary winding is N_1 and that for the secondary winding is N_2 . The analysis of this transformer is given in the following sections.

11.1.1 VOLTAGE RATIO

According to Faraday’s law, the instantaneous voltage e_1 across the primary winding produces a flux ϕ , where

$$e_1 = +N_1 \frac{d\phi}{dt} \tag{11.1}$$

$$\phi = \frac{1}{N_1} \int e_1 dt$$

Assume that the core captures all the flux produced by e_1 , and the flux links the secondary winding. According to Faraday's law, the flux induces voltage e_2 across the secondary winding, where

$$e_2 = -N_2 \frac{d\varphi}{dt} \quad (11.2)$$

The positive sign in Equation 11.1 indicates that e_1 induces the flux, and the negative sign in Equation 11.2 indicates that the flux induces e_2 .

The dot at one end of each winding indicates that the potentials at the dotted terminals are in phase; that is e_1 and e_2 are in phase. Moreover, the current i_1 flowing into the dotted terminal of the primary winding is in phase with the current i_2 leaving the dotted terminal of the secondary windings.

If we are interested in the magnitudes of e_1 and e_2 , Equations 11.1 and 11.2 can be rewritten as

$$\frac{e_1}{N_1} = \frac{e_2}{N_2} = \frac{d\varphi}{dt} \quad (11.3)$$

Equation 11.3 shows that the *voltage per turn* is the same for the primary or secondary winding. This is a key equation for the transformer and is only true if no flux escapes the core into air.

In root mean square (rms) quantities, we can rewrite Equation 11.3 as

$$V_T = \frac{E_1}{N_1} = \frac{E_2}{N_2} \quad (11.4)$$

where

V_T is the voltage per turn

E is the rms value of e

Equation 11.4 can also be rewritten as

$$\frac{E_1}{E_2} = \frac{N_1}{N_2} \quad (11.5)$$

Equation 11.5 shows that the voltage ratio of the transformer is equal to the turns ratio. If $N_2 < N_1$, the secondary voltage E_2 is less than the primary voltage E_1 , and the transformer is called a *step-down* transformer. When $N_2 > N_1$, the secondary voltage E_2 is higher than the primary voltage E_1 , and the transformer is called a *step-up* transformer.

Example 11.1

A transformer has 4000 turns in the primary winding and 100 turns in the secondary winding. If 120 V is applied to the primary winding, compute the voltage across the secondary winding.

Solution

The voltage ratio of the transformer is

$$\frac{E_1}{E_2} = \frac{N_1}{N_2}$$

Hence,

$$E_2 = E_1 \frac{N_2}{N_1} = 120 \frac{100}{4000} = 3 \text{ V}$$

Example 11.2

Compute the voltage per turn for the transformer in Example 11.1.

Solution

The voltage per turn is

$$V_T = \frac{E_1}{N_1} = \frac{E_2}{N_2} = \frac{120}{4000} = 30 \text{ mV/turn}$$

11.1.2 CURRENT RATIO

If we assume that the transformer is ideal without losses, the input power to the transformer is equal to the output power consumed by the load. In complex number form, the apparent power of the primary winding S_1 is equal to the apparent power of the secondary winding S_2 :

$$\begin{aligned}\bar{S}_1 &= \bar{S}_2 \\ \bar{S}_1 &= \bar{E}_1 \bar{I}_1^* \\ \bar{S}_2 &= \bar{E}_2 \bar{I}_2^*\end{aligned}\tag{11.6}$$

\bar{I}^* is the conjugate of the current \bar{I} . Based on Equations 11.4 and 11.6, we can write the current relationship as

$$\frac{I_1}{I_2} = \frac{E_2}{E_1} = \frac{N_2}{N_1}\tag{11.7}$$

Notice that the current ratio is the inverse of the voltage ratio. Hence, the winding with higher voltage carries lower current. Equation 11.7 can be rearranged as

$$\mathfrak{F} = I_1 N_1 = I_2 N_2\tag{11.8}$$

\mathfrak{F} is known as the *magnetomotive force* of the primary or secondary winding. It is the current of the winding multiplied by its number of turns and its unit is ampere turn (At). Equation 11.8 is another key relationship for the transformer; the ampere turns (or magnetomotive force) of the primary and secondary windings are equal. If you open a transformer, you will find two sets of windings: one has a larger number of turns made of a small cross section wire, and the other has a smaller number of turns made of a thicker wire. The number of turns is determined by the voltage/turn ratio of the transformer, and the cross section of the wire is determined by the amount of current passing through the windings. Can you tell which winding has the higher voltage and which one has the higher current?

11.1.3 REFLECTED LOAD IMPEDANCE

Assume that the load impedance in Figure 11.4 is Z_{load} , where

$$Z_{load} = \frac{E_2}{I_2}\tag{11.9}$$

This load impedance when seen from the primary winding is Z'_{load} , where

$$Z'_{load} = \frac{E_1}{I_1} \quad (11.10)$$

Hence,

$$\begin{aligned} \frac{Z'_{load}}{Z_{load}} &= \frac{E_1 I_2}{E_2 I_1} = \left(\frac{N_1}{N_2} \right)^2 \\ Z'_{load} &= Z_{load} \left(\frac{N_1}{N_2} \right)^2 \end{aligned} \quad (11.11)$$

Z'_{load} is known as the *reflected impedance* of the load, or the *load impedance referred to the primary winding*.

Example 11.3

If the load of a transformer in Example 11.1 is 3 VA, compute the reflected impedance of the load as seen from the primary winding.

Solution

The magnitude of the load current is

$$I_2 = \frac{S}{E_2} = \frac{3}{3} = 1 \text{ A}$$

The magnitude of the load impedance is

$$Z_{load} = \frac{E_2}{I_2} = \frac{3}{1} = 3 \Omega$$

The magnitude of the reflected impedance of the load is

$$Z'_{load} = Z_{load} \left(\frac{N_1}{N_2} \right)^2 = 3 \left(\frac{4000}{100} \right)^2 = 4.8 \text{ k}\Omega$$

Example 11.4

A transformer with turns ratio $N_1/N_2 = 2$ is connected to a load impedance of $3 + j4 \Omega$. Compute the reflected impedance of the load.

Solution

$$\bar{Z}'_{load} = \bar{Z}_{load} \left(\frac{N_1}{N_2} \right)^2 = (3 + j4)4 = 12 + j16 \Omega$$

11.1.4 TRANSFORMER RATINGS

The transformer has electrical and mechanical ratings. The electrical ratings include voltages, currents, and powers. The mechanical ratings include thermal limits, container dimensions, weight, volume, etc. The rated voltages and currents are the values at which the transformer can operate continuously without any damage to its components. Exceeding these values can cause instant or gradual damage to the transformer. Excessive voltage can cause the insulation of the windings to fail very rapidly leading to internal short circuits. Excessive current causes heat buildup inside the transformer causing eventual meltdown of the insulation varnish of the winding leading to short circuits. Two important electrical ratings are of particular importance to the analysis of the transformer and are always included in the nameplate data: the voltage ratio and the apparent power. For example, the nameplate data may read “10kVA, 8kV/240V.” With this data, you can extract the following information:

1. Rated apparent power of the transformer is 10kVA
2. Voltage ratio is

$$\frac{E_1}{E_2} = \frac{8000}{240} = 33.33.$$

Keep in mind that the voltage ratio is the same as the turns ratio N_1/N_2 . However, we cannot assume that $N_1 = 8000$ turns or $N_2 = 240$ turns, but we can assume that the ratio

$$N_1/N_2 = 33.33$$

3. Rated current of the primary winding is

$$I_1 = \frac{S}{E_1} = \frac{10,000}{8,000} = 1.25 \text{ A}$$

4. Rated current of the secondary winding is

$$I_2 = \frac{S}{E_2} = \frac{10,000}{240} = 41.67 \text{ A}$$

5. At full load, meaning the current and voltage are at their rated values, the magnitude of the load impedance is

$$Z_{load} = \frac{E_2}{I_2} = \frac{240}{41.67} = 5.76 \Omega$$

6. Magnitude of the reflected impedance of the load is

$$Z'_{load} = Z_{load} \left(\frac{N_1}{N_2} \right)^2 = 5.76 (33.33)^2 = 6.4 \text{ k}\Omega$$

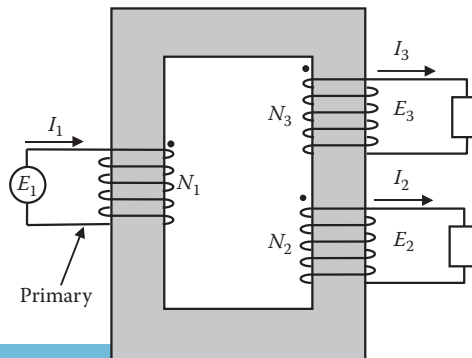


FIGURE 11.5 Transformer with multiple-secondary windings.

11.2 MULTI-WINDING TRANSFORMER

The transformer can have multiple secondary windings to provide different voltage levels to different loads. An example of a transformer with two secondary windings is shown in Figure 11.5. The numbers of turns of the two secondary windings are N_2 and N_3 , respectively.

Since the voltage per turn V_T for the transformer is constant, hence

$$V_T = \frac{E_1}{N_1} = \frac{E_2}{N_2} = \frac{E_3}{N_3} \quad (11.12)$$

The computations of the current ratios require more attention. If we use the superposition theorem, and assume that the load of winding N_3 is removed, then the current of the primary winding I_{12} due to I_2 alone can be computed by using the magnetomotive force in Equation 11.8

$$I_{12}N_1 = I_2N_2 \quad (11.13)$$

Now let us assume that the load of winding N_2 is removed, and that of N_3 is connected. The primary current I_{13} due to I_3 is

$$I_{13}N_1 = I_3N_3 \quad (11.14)$$

Hence, the total primary current I_1 is the phasor sum of I_{12} and I_{13} :

$$\bar{I}_1 = \bar{I}_{12} + \bar{I}_{13} = \bar{I}_2 \frac{N_2}{N_1} + \bar{I}_3 \frac{N_3}{N_1} \quad (11.15)$$

$$\bar{I}_1 N_1 = \bar{I}_2 N_2 + \bar{I}_3 N_3$$

Equation 11.15 shows that the magnetomotive force of the primary winding is equal to the sum of the magnetomotive forces of all secondary windings. Hence, the currents are shared between the windings based on their respective number of turns.

For this multi-winding transformer, the source of power is connected to the primary winding and the loads are connected to the secondary windings. Hence, the sum of the apparent powers of all loads in the secondary windings is equal to the apparent power delivered by the source in the primary winding.

$$\begin{aligned} \bar{S}_1 &= \bar{S}_2 + \bar{S}_3 \\ \bar{E}_1 \bar{I}_1^* &= \bar{E}_2 \bar{I}_2^* + \bar{E}_3 \bar{I}_3^* \end{aligned} \quad (11.16)$$

Example 11.5

The transformer shown in Figure 11.6 consists of one primary winding and two secondary windings. The numbers of turns of the windings are $N_1=4000$; $N_2=1000$; $N_3=500$. A voltage source of 120 V is applied across the primary winding, and purely resistive loads are connected across the secondary windings. A wattmeter placed in the primary circuit measures 300 W. Another wattmeter placed in the secondary winding N_2 measures 90 W. Compute the following:

1. Voltages of the secondary windings
2. Current in N_3
3. Power of the load connected across N_3

Solution

1. Compute the voltage per turn as given in Equation 11.4:

$$V_T = \frac{E_1}{N_1} = \frac{120}{4000} = 30 \text{ mV/turn}$$

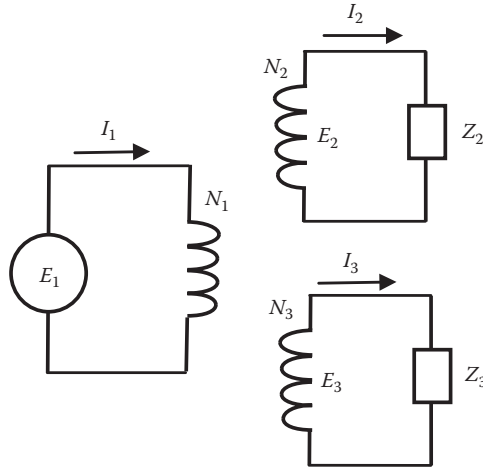


FIGURE 11.6 Three F_1 winding transformer.

Now, we can compute the voltages of the secondary windings:

$$E_2 = V_T N_2 = 30 \times 1000 = 30 \text{ V}$$

$$E_3 = V_T N_3 = 30 \times 500 = 15 \text{ V}$$

2. Before we compute the currents of the secondary winding N_3 , we need to compute I_1 and I_2 . Since the loads are purely resistive, the power factor everywhere is unity:

$$I_1 = \frac{P_1}{E_1 \cos \theta_1} = \frac{300}{120} = 2.5 \text{ A}$$

$$I_2 = \frac{P_2}{E_2 \cos \theta_2} = \frac{90}{30} = 3 \text{ A}$$

Since all loads are resistive, we do not need to include the phase angles in Equation 11.15:

$$I_1 N_1 = I_2 N_2 + I_3 N_3$$

$$2.5 \times 4000 = 1000 \times 3 + 500 I_3$$

$$I_3 = 14 \text{ A}$$

We can arrive at the same result by using Equation 11.16:

$$\bar{S}_1 = \bar{S}_2 + \bar{S}_3$$

Since the loads are resistive, the angles of all currents are zero:

$$\bar{E}_1 \bar{I}_1^* = \bar{E}_2 \bar{I}_2^* + \bar{E}_3 \bar{I}_3^*$$

$$E_1 I_1 = E_2 I_2 + E_3 I_3$$

$$120 \times 2.5 = 30 \times 3 + 15 I_3$$

$$I_3 = 14 \text{ A}$$

$$\begin{aligned}
 3. \quad & P_1 = P_2 + P_3 \\
 & 300 = 90 + P_3 \\
 & P_3 = 210 \text{ W}
 \end{aligned}$$

Example 11.6

For the transformer in Example 11.5, assume that the load impedances connected across the secondary windings are $\bar{Z}_2 = 3 + j4 \Omega$ and $\bar{Z}_3 = 5 + j0 \Omega$

A voltage source of 120 V is applied across the primary winding. Compute the following:

1. Currents in all windings
2. Real and reactive powers in the primary windings

Solution

1. Assume that the voltage of the primary winding is the reference voltage, thus all voltages have zero phase angles. Hence, the currents in the secondary windings are

$$\bar{I}_2 = \frac{\bar{E}_2}{\bar{Z}_2} = \frac{30 \angle 0^\circ}{3 + j4} = 6 \angle -53.1^\circ \text{ A}$$

$$\bar{I}_3 = \frac{\bar{E}_3}{\bar{Z}_3} = \frac{15 \angle 0^\circ}{5 + j0} = 3 \angle 0^\circ \text{ A}$$

Using Equation 11.15

$$\begin{aligned}
 \bar{I}_1 N_1 &= \bar{I}_2 N_2 + \bar{I}_3 N_3 \\
 \bar{I}_1 4000 &= (6 \angle -53.1^\circ) \times 1000 + 3 \times 500 \\
 \bar{I}_1 &= 1.276 - j1.2 = 1.75 \angle -43.26^\circ \text{ A}
 \end{aligned}$$

2. The complex power of the primary winding is

$$\bar{S}_1 = \bar{E}_1 \bar{I}_1^* = (120 \angle 0^\circ)(1.75 \angle 43.26^\circ) = 153 + j144 \text{ VA}$$

Hence,

$$P_1 = 153 \text{ W}$$

$$Q_1 = 144 \text{ VAR}$$

11.3 AUTOTRANSFORMER

An autotransformer has its primary and secondary windings connected in series as shown in Figure 11.7. The primary terminal X_2 is connected to the secondary terminal Y_1 , and the source voltage

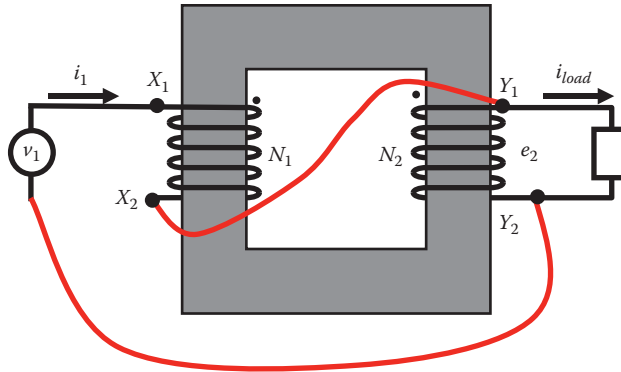


FIGURE 11.7 Connecting a regular transformer as autotransformer.

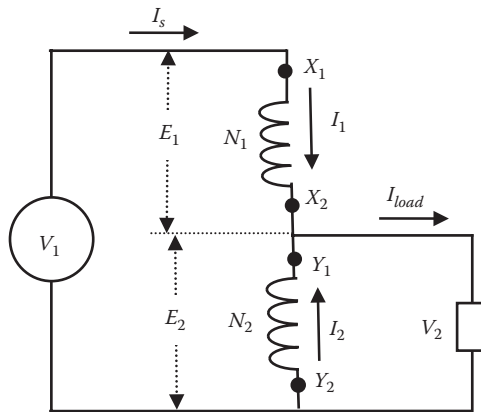


FIGURE 11.8 Wiring connection of the autotransformer in Figure 11.7.

V_1 is connected between X_1 and Y_2 . The load is connected between Y_1 and Y_2 . This way, almost any transformer can be connected as an autotransformer. The wiring diagram of an autotransformer is shown in Figure 11.8. Let us assume that the rated voltage of the primary winding is E_1 , and that for the secondary winding is E_2 . Also assume that the rated current of the primary winding is I_1 and that for the secondary winding is I_2 .

As stated in Equation 11.4, the volt per turn ratio V_T is constant for any winding. Hence,

$$V_T = \frac{E_1}{N_1} = \frac{E_2}{N_2} = \frac{V_1}{(N_1 + N_2)} = \frac{V_2}{N_2} \tag{11.17}$$

The voltage ratio (input voltage versus output voltage) is

$$\frac{V_1}{V_2} = \frac{N_1 + N_2}{N_2} \tag{11.18}$$

Using the magnetomotive force relationship in Equation 11.8, we can write the current equation as

$$\mathfrak{F} = N_1 I_1 = N_2 I_2 \tag{11.19}$$

As shown in Figure 11.8, the load and source currents are

$$I_{load} = I_1 + I_2 \quad (11.20)$$

$$I_s = I_1$$

Hence, the current ratio of the autotransformer (output current versus input current) is

$$\frac{I_{load}}{I_s} = \frac{I_1 + I_2}{I_1} = \left(1 + \frac{I_2}{I_1}\right) \quad (11.21)$$

Substituting Equation 11.19 into (11.21) yields

$$\frac{I_{load}}{I_s} = 1 + \frac{I_2}{I_1} = 1 + \frac{N_1}{N_2} = \frac{N_1 + N_2}{N_2} \quad (11.22)$$

The apparent power can be computed for the input or output circuits of the autotransformer.

$$\bar{S} = \bar{V}_1 \bar{I}_s^* = (\bar{E}_1 + \bar{E}_2) \bar{I}_1^* = \bar{E}_1 \bar{I}_1^* + \bar{E}_2 \bar{I}_1^* \quad (11.23)$$

Note that $E_1 I_1$ is the apparent power of the regular transformer as given in Equation 11.6. Hence, the autotransformer can handle more power than the regular transformer without exceeding the rated voltage or the rated current of any winding.

Example 11.7

A 1 kVA transformer has a voltage ratio of 120/240 V. It is desired to change the voltage ratio of the transformer to 360/240 V by connecting it as an autotransformer. Compute the new power rating of the autotransformer.

Solution

If you assume that the voltage of winding $X_1 - X_2$ is 120 V in Figure 11.7 and $Y_1 - Y_2$ is 240 V, the voltage ratio is

$$\frac{V_1}{V_2} = \frac{E_1 + E_2}{E_2} = \frac{120 + 240}{240} = \frac{360}{240}$$

As a regular transformer, the rated currents of the windings are

$$I_1 = \frac{S}{E_1} = \frac{1000}{120} = 8.33 \text{ A}$$

$$I_2 = \frac{S}{E_2} = \frac{1000}{240} = 4.167 \text{ A}$$

The power of the autotransformer is

$$S = E_1 I_1 + E_2 I_1 = 1000 + 240 \times 8.33 = 3.0 \text{ kVA}$$

This new power rating of the autotransformer is three times the power rating of the regular transformer.

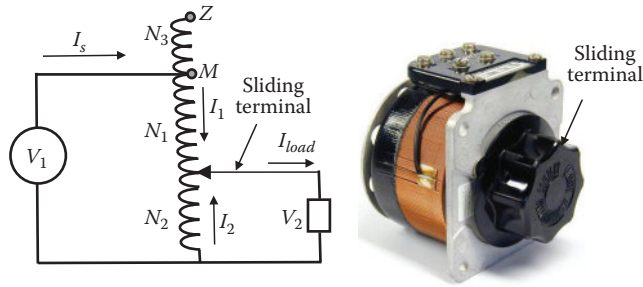


FIGURE 11.9 Autotransformer with adjustable voltage.

The autotransformer can be built to provide adjustable output voltage. This type of autotransformer, shown in Figure 11.9, consists of one winding where the primary voltage is applied across a part of the winding. The number of turns of the secondary winding can be changed by sliding one of the secondary terminals over the winding. This requires a mechanism by which the winding and the sliding terminal are always connected electrically. In the position shown in the figure, the secondary winding is N_2 . Hence, the secondary voltage is

$$V_2 = V_1 \frac{N_2}{N_1 + N_2} = V_T N_2 \tag{11.24}$$

In Equation 11.24, $V_2 < V_1$. When the slider is moved to position M , the voltage across the load is

$$V_2 = V_1 \frac{N_1 + N_2}{N_1 + N_2} = V_T (N_1 + N_2) \tag{11.25}$$

Hence, $V_2 = V_1$. To make $V_2 > V_1$, we move the slider to point Z , where

$$V_2 = V_1 \frac{N_1 + N_2 + N_3}{N_1 + N_2} = V_T (N_1 + N_2 + N_3) \tag{11.26}$$

This autotransformer, which is also known as *variac*, can adjust the load voltage from zero to greater than the supply voltage. The variac is very useful in laboratories and test setups where the load voltage is easily adjusted to any desired value. It can also be used in speed control and startup for electric motors.

11.4 THREE-PHASE TRANSFORMER

The three-phase transformers can be constructed of a three-legged core as shown in Figure 11.10. The primary and secondary windings of each phase are placed on the same leg of the core. The primary windings are labeled $a a'$, $b b'$, and $c c'$. The secondary windings are labeled $A A'$, $B B'$, and $C C'$. N_1 is the number of turns of any primary winding, and N_2 is the number of turns of any secondary winding. A more convenient schematic representation of the three-phase windings is shown in Figure 11.11.

11.4.1 THREE-PHASE TRANSFORMER RATINGS

The ratings of three-phase transformers are given in three-phase quantities. The nameplate data can read, for example, “60 kVA, 8 kV(Δ)/416 V(Y).” This nameplate data can provide us with the following information:

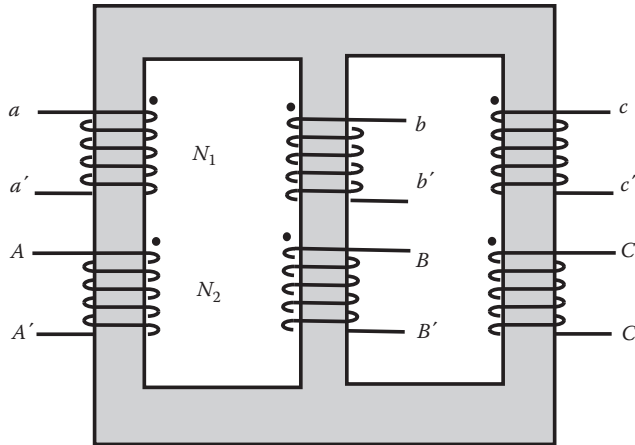


FIGURE 11.10 Configuration for three-phase transformer.

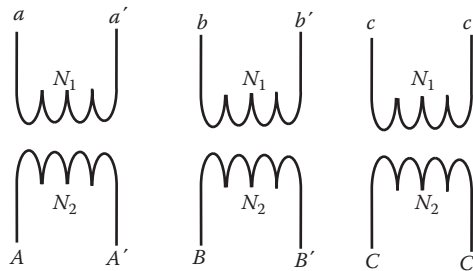


FIGURE 11.11 Schematic of three-phase transformer.

1. The rated apparent power of the three phases is 60 kVA.
2. The rated apparent power of each phase is $60/3 = 20$ kVA.
3. The primary windings are connected in delta.
 - a. The rated line-to-line voltage of the primary circuit is 8 kV.
 - b. The voltage across any primary winding is 8 kV.
4. The secondary windings are connected in Y.
 - a. The rated line-to-line voltage of the secondary circuit is 416 V.
 - b. The voltage across any secondary winding is $416/\sqrt{3} = 240$ V.
5. The line-to-line voltage ratio of the transformer is $8000/416 = 19.23$.
6. The voltage per turn is constant in any winding of the transformer. Hence,

$$V_T = \frac{V_{\text{phase of primary}}}{N_1} = \frac{V_{\text{phase of secondary}}}{N_2}$$
 The turns ratio is the ratio of the *phase* voltages.

11.4.1.1 Wye–Wye Transformer

A three-phase transformer connected in wye–wye (Y–Y) is shown in Figure 11.12. The top figure shows the wiring of the transformer where terminals a' , b' , and c' of the primary windings are connected to a common point called neutral n . The secondary windings are similarly connected. A more convenient schematic is the one at the bottom of Figure 11.12.

The turns ratio of the transformer is N_1/N_2 , while the line-to-line voltage ratio of the transformer is V_{ab}/V_{AB} . These two ratios are equal only if the connections of the primary and secondary windings are the same, that is, both windings are connected in wye (Y) or delta. The best way to compute the turns ratio is to use the voltage per turn V_T ,

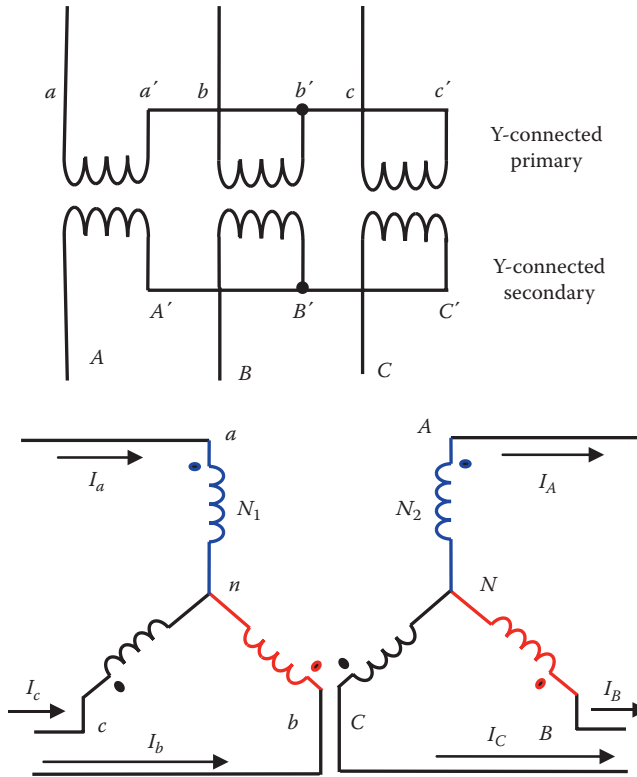


FIGURE 11.12 Y-Y transformer.

$$V_T = \frac{V_{an}}{N_1} = \frac{V_{AN}}{N_2} \tag{11.27}$$

$$\frac{N_1}{N_2} = \frac{V_{an}}{V_{AN}} = \frac{\sqrt{3}V_{an}}{\sqrt{3}V_{AN}} = \frac{V_{ab}}{V_{AB}}$$

The current ratio is the inverse of the turns ratio. We can arrive at this conclusion by using the magnetomotive force equation where any winding current multiplied by its number of turns is constant for any winding.

$$\begin{aligned} \mathfrak{F} &= I_a N_1 = I_A N_2 \\ \frac{N_1}{N_2} &= \frac{I_A}{I_a} \end{aligned} \tag{11.28}$$

Example 11.8

A 12 kVA transformer has a voltage ratio of 13.8 kV(Y)/416 V(Y). Compute the following:

1. Ratio of the phase voltages
2. Turns ratio
3. Rated current of the primary and secondary winding

Solution

1. The transformer is connected in Y–Y configuration. Consider Figure 11.12, the phase voltage ratio is V_{an}/V_{AN} . Hence,

$$\frac{V_{an}}{V_{AN}} = \frac{\frac{V_{ab}}{\sqrt{3}}}{\frac{V_{AB}}{\sqrt{3}}} = \frac{V_{ab}}{V_{AB}} = \frac{13,800}{416} = 33.17$$

Note that the line-to-line voltage ratio is the same as the phase voltage ratio. This is true only if both the primary and secondary windings have the same connection.

2. The turns ratio is N_1/N_2 , which is the same as the phase voltage ratio V_{an}/V_{AN}

$$\frac{N_1}{N_2} = \frac{V_{an}}{V_{AN}} = 33.17$$

3. The current of the primary winding is

$$I_a = \frac{S}{\sqrt{3}V_{ab}} = \frac{12}{\sqrt{3} \times 13.8} = 0.502 \text{ A}$$

The current of the secondary winding is

$$I_A = \frac{S}{\sqrt{3}V_{AB}} = \frac{12,000}{\sqrt{3} \times 416} = 16.65 \text{ A}$$

11.4.1.2 Delta–Delta Transformer

The Δ – Δ connection of a three-phase transformer is shown in Figure 11.13. Each phase in the delta configuration is connected between two lines of the three-phase circuit. Hence, the voltage of any winding is equal to the line-to-line voltage of the circuit. Keep in mind that the currents in the transformer windings are phase currents, and the currents in the circuit feeding the transformers are the line currents.

The current inside the windings follows the same rule discussed in Section 11.1.1. That is, the current inside the primary winding is flowing from the dotted terminal and that for the secondary winding is flowing into the dotted terminal.

The turns ratio of the transformer is N_1/N_2 . The voltage ratio of the transformer is the ratio of the voltages V_{ab}/V_{AB} , which are the same as the ratio of the line-to-line voltages in the delta configuration. Keep in mind that the voltage per turn is constant in any winding. Hence,

$$V_T = \frac{V_{ab}}{N_1} = \frac{V_{AB}}{N_2} \tag{11.29}$$

$$\frac{N_1}{N_2} = \frac{V_{ab}}{V_{AB}}$$

Using the magnetomotive force equation, we can compute the current ratio

$$\mathfrak{F} = I_{ab}N_1 = I_{AB}N_2 \tag{11.30}$$

$$\frac{N_1}{N_2} = \frac{I_{AB}}{I_{ab}}$$

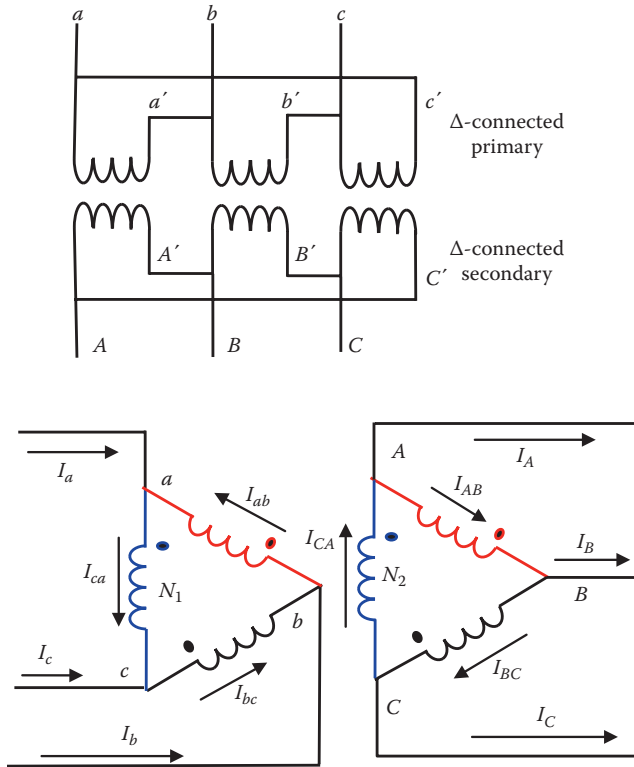


FIGURE 11.13 Transformer connected in Δ - Δ .

Example 11.9

A 15 kVA transformer has a voltage ratio of 25 kV(Δ)/5 kV(Δ). Compute the following:

1. Turns ratio
2. Line current in the primary circuit
3. Currents of the primary and secondary windings

Solution

1. The transformer is connected in Δ - Δ . As shown in Figure 11.13, the turns ratio is the ratio of the winding voltages which are equal to the line-to-line voltages.

$$\frac{N_1}{N_2} = \frac{V_{ab}}{V_{AB}} = \frac{25}{5} = 5$$

2. The line current of the source is

$$I_a = \frac{S}{\sqrt{3}V_{ab}} = \frac{15}{\sqrt{3} \times 25} = 0.346 \text{ A}$$

3. The current of the primary winding is

$$I_{ab} = \frac{I_a}{\sqrt{3}} = \frac{0.346}{\sqrt{3}} = 0.2 \text{ A}$$

The current of the secondary winding is

$$\mathfrak{S} = I_{ab}N_1 = I_{AB}N_2$$

$$I_{AB} = \frac{N_1}{N_2} I_{ab} = 5 \times 0.2 = 1 \text{ A}$$

11.4.1.3 Wye–Delta Transformer

The Y– Δ transformer has one set of windings (primary or secondary) connected in wye and the other windings connected in delta as shown in Figure 11.14. The analysis of the wye–delta transformer requires some attention when computing the various ratios. In Figure 11.14, the voltage across N_1 is the phase voltage of the primary circuit V_{an} , and the voltage across N_2 is the line-to-line voltage of the secondary circuit V_{AB} . Since the voltage per turn is constant in any winding, we can write the turns ratio as

$$V_T = \frac{V_{an}}{N_1} = \frac{V_{AB}}{N_2} \tag{11.31}$$

$$\frac{N_1}{N_2} = \frac{V_{an}}{V_{AB}}$$

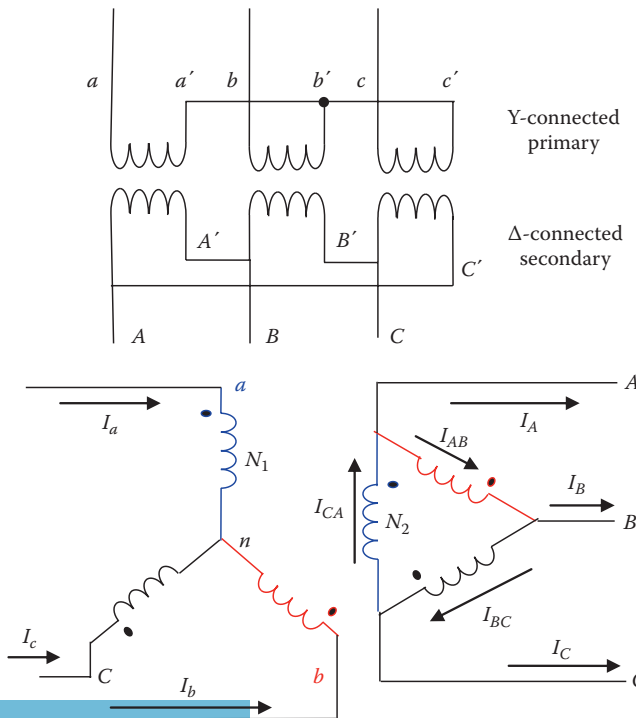


FIGURE 11.14 Y- Δ transformer.

Similarly, the current through N_1 is the line current of the primary circuit I_a , and the current through N_2 is the phase current of the secondary winding I_{AB} . Hence, we can compute the current ratio using the ampere-turn equation.

$$\begin{aligned}\mathfrak{S} &= I_a N_1 = I_{AB} N_2 \\ \frac{N_1}{N_2} &= \frac{I_{AB}}{I_a}\end{aligned}\tag{11.32}$$

Example 11.10

A 25 kVA transformer has a voltage ratio of 20 kV(Y)/10 kV(Δ). Compute the following:

1. Winding voltages
2. Turns ratio
3. Line currents in the primary and secondary circuits
4. Phase currents of the transformer

Solution

1. The primary windings of the transformer are connected in wye. Hence, the voltage across the winding is

$$V_{an} = \frac{V_{ab}}{\sqrt{3}} = \frac{20}{\sqrt{3}} = 11.55 \text{ kV}$$

The secondary windings are connected in delta. Hence, the winding voltage is equal to the line-to-line voltage

$$V_{AB} = 10 \text{ kV}$$

2. The turns ratio is the ratio of the voltages of the windings

$$\frac{N_1}{N_2} = \frac{11.55}{10} = 1.155$$

3. The line current in the primary circuit is

$$I_a = \frac{S}{\sqrt{3}V_{ab}} = \frac{25}{\sqrt{3} \times 20} = 0.7217 \text{ A}$$

The line current in the secondary circuit is

$$I_A = \frac{S}{\sqrt{3}V_{AB}} = \frac{25}{\sqrt{3} \times 10} = 1.4434 \text{ A}$$

4. Since the primary windings are connected in wye, the phase current of the primary winding is the same as the line current of the primary circuit. The secondary windings are connected in delta, hence the phase current of the secondary winding is

$$I_{AB} = \frac{I_A}{\sqrt{3}} = \frac{1.4434}{\sqrt{3}} = 0.8333 \text{ A}$$

11.4.2 TRANSFORMER BANK

A transformer bank is two or three single-phase transformers connected as a three-phase transformer. These transformer banks are often used in distribution systems. Consider the cases in Figure 11.15. Figure 11.15a shows a power pole with one single-phase transformer. The load served by this transformer is small enough and one transformer is adequate. If more loads are added to the circuit, an additional single-phase transformer is installed as shown in Figure 11.15b. Further increase in loads may demand a third single-phase transformer as shown in Figure 11.15c.

The three single-phase transformers can be connected in several configurations. One of these is the Δ -Y connection shown in Figure 11.16. The analysis of the transformer bank is the same as that for the three-phase transformers.



FIGURE 11.15 Transformer banks: (a) single-phase transformer, (b) two transformer bank, and (c) three transformer bank.

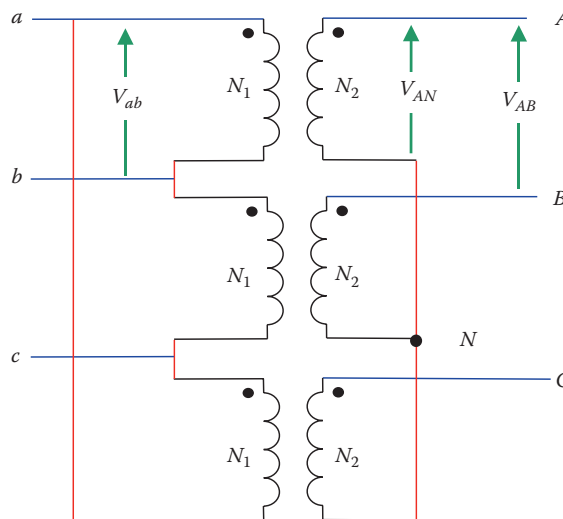


FIGURE 11.16 Δ -Y connection of a transformer bank.

Example 11.11

To provide electric power to a residential area, three single-phase transformers are connected in the Δ -Y configuration shown in Figure 11.16. Each single phase transformer is rated at 10 kVA, 15 kV/240 V. Compute the ratings of the transformer bank and the turns ratio.

Solution

The ratings of the transformer bank are the same as the ratings of the three-phase transformer; that is the power rating is for the three phases and the voltage ratings are for the line-to-line voltage. The power rating of the transformer bank is

$$S = 3 \times 10 = 30 \text{ kVA}$$

The primary windings are connected in delta. Therefore, the voltage across N_1 is the same as the line-to-line voltage. Hence

$$V_{ab} = 15 \text{ kV}$$

The secondary windings are connected in wye. The voltage across N_2 is the phase voltage. The line-to-line voltage of the secondary is

$$V_{AB} = \sqrt{3}V_{AN} = \sqrt{3} \times 240 = 415.7 \text{ V}$$

The ratings of the transformer bank are 30 kVA, 15 kV(Δ)/415.7 V(Y)

The turns ratio of the transformer bank is the ratio of its winding voltages

$$\frac{N_1}{N_2} = \frac{V_{ab}}{V_{AN}} = \frac{15000}{240} = 62.5$$

11.5 ACTUAL TRANSFORMER

The transformers we discussed so far are ideal without any internal losses. Actual transformers have parasitic parameters such as the resistances and inductances of the windings and core. The resistance and inductance of the windings can be modeled as shown in Figure 11.17. The dashed box shows the ideal transformer we discussed so far. R_1 and X_1 are the resistance and inductive reactance of the

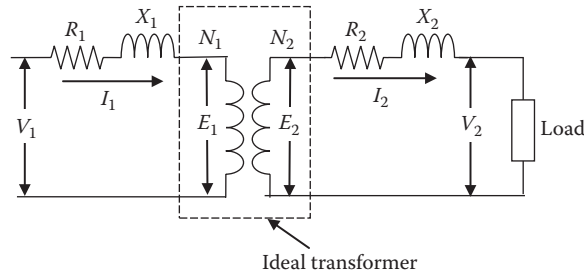


FIGURE 11.17 Winding impedance of the transformer.

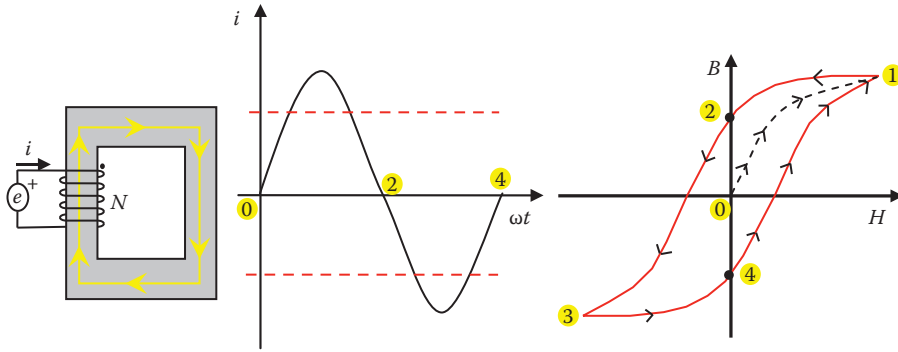


FIGURE 11.18 *B*–*H* relationship and core hysteresis.

primary winding, respectively. R_2 and X_2 are the resistance and inductive reactance of the secondary winding, respectively. The input voltage of the transformer is V_1 and the load voltage is V_2 . V_1 and V_2 are known as *terminal voltages*. One major difference between the ideal transformer and actual transformer is that the turns ratio of the actual transformer is not equal to the ratio of its terminal voltages. Let us explain this by looking at the volt per turn V_T of the actual transformer, which is

$$V_T = \frac{E_1}{N_1} = \frac{E_2}{N_2} \tag{11.33}$$

Due to the presence of the resistances and inductive reactances, E_1 and V_1 are not equal, and neither are E_2 and V_2 . Then,

$$\frac{N_1}{N_2} = \frac{E_1}{E_2} \neq \frac{V_1}{V_2} \tag{11.34}$$

Modeling the core of the transformer is a more involved process because of the nonlinear behavior of the flux in the core. Consider the case shown on the left side of Figure 11.18 where a coil is wrapped around a core. Let us assume that the current of the coil is sinusoidal as shown in the middle figure. This current produces a sinusoidal flux ϕ in the core that has a flux density B , where

$$B = \frac{\phi}{A} \tag{11.35}$$

A is the cross sectional area of the core. The relationship between the flux density and the magnetic field intensity H in the core is

$$B = \mu_o \mu_r H \tag{11.36}$$

where $\mu_o = 4\pi \times 10^{-7}$ H/m. It is a constant value known as the absolute permeability. μ_r is the relative permeability; its magnitude depends on the material of the core. For air $\mu_r = 1$, and for iron $\mu_r \approx 5000$.

The relationship between the flux density B and the flux intensity H is nonlinear as shown on the right side of Figure 11.18. The curve is known as the hysteresis loop. Let us assume that the core has never been used before. If the current in the winding starts from zero (point 0), the flux starts to flow in the core as shown by the dashed line in the hysteresis loop. Unlike air, the core cannot carry unlimited amounts of flux. When the current exceeds a certain limit (e.g., above or below the dashed lines in the middle figure), no appreciable increase occurs in the flux, and the core is said to be *saturated*.

This is shown in the area around point 1 in the figure. When the current starts to fall, the flux starts to decrease. At point 2, the current is zero, but the flux density is nonzero. This is known as *residual flux*. The core at this point acts as a magnet. When the current is further reduced, the flux is also reduced to zero, and then reverses its direction. After reaching point 3, if the current increases, the flux increases along the rightmost path of the hysteresis loop. This hysteresis loop is repeated in every ac cycle.

To model the hysteresis loop, we can use an approximate process with linear elements: resistance and inductance. Using Faraday’s law, we can write the expression for the flux as

$$e = \frac{d\phi}{dt} \tag{11.37}$$

Hence, the flux density is

$$B = \frac{\Phi}{A} \sim \int e dt \tag{11.38}$$

Equation 11.38 shows that the flux density is directly proportional to the integral of the voltage across the winding. Keep in mind that the magnetic field intensity is directly proportional to the current. Hence, the B versus H characteristics in Figure 11.18 can be approximated by $\int e dt$ versus i relationship. This relationship can be obtained by the two circuits in Figures 11.19 and 11.20. In Figure 11.19, the resistive circuit on the left side is connected across a sinusoidal voltage source

$$e = E_{\max} \sin \omega t \tag{11.39}$$

The voltage integral and currents of this circuit are

$$\int e dt = -\frac{E_{\max}}{\omega} \cos \omega t \tag{11.40}$$

$$i_R = \frac{e}{R} = \frac{E_{\max}}{R} \sin \omega t \tag{11.41}$$

Note that $\int e dt$ and i_R are phase-shifted by 90° . The relationship of $\int e dt$ versus i_R is shown on the right side of Figure 11.19. Because of the phase shift, the relationship has an elliptical shape with

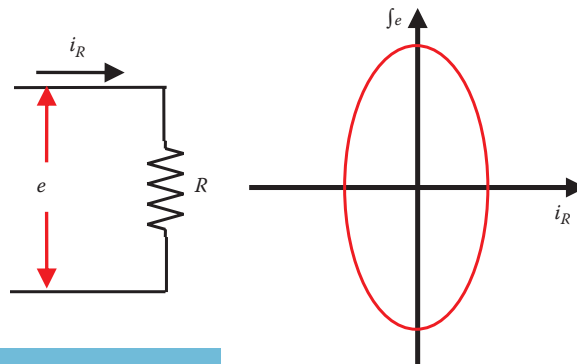


FIGURE 11.19 Voltage integral versus current of resistive element.

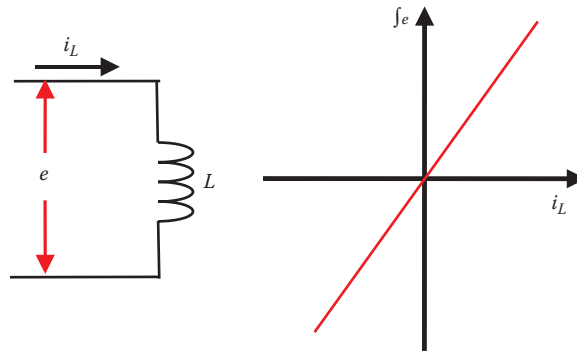


FIGURE 11.20 Voltage integral versus current of inductive element.

two radii that are functions of the resistance and the angular frequency. For the inductive element in Figure 11.20, $\int e dt$ and i_L are computed as follows:

$$\int e dt = -\frac{E_{\max}}{\omega} \cos \omega t \tag{11.42}$$

$$e = L \frac{di_L}{dt} \tag{11.43}$$

$$i_L = \frac{1}{L} \int e dt = -\frac{E_{\max}}{\omega L} \cos \omega t$$

where L is the inductance. $\int e dt$ and i_L are in phase, forming a straight line relationship as shown in Figure 11.20.

Now let us add the two elements in parallel as shown in Figure 11.21. The total current in this case is

$$i = i_R + i_L \tag{11.44}$$

Combining the two characteristics in Figures 11.19 and 11.20 gives the elliptically bent shape shown at the lower right side of Figure 11.21. This shape is similar enough to the hysteresis loop in Figure 11.18, and is used as an approximate representation of the core. The parameters of the core model are often computed from the primary side of the transformer. Hence, the core is often included in the primary circuit as shown in Figure 11.22. I_o is known as the *excitation current* representing the magnetic field intensity of the hysteresis loop. R_o and X_o are the equivalent core resistance and core inductive reactance of the hysteresis model, respectively.

11.5.1 ANALYSIS OF ACTUAL TRANSFORMER

The transformer model in Figure 11.22 can be used to compute the relationships between all currents and voltages. For example, the primary current I_1 of the transformer is

$$\bar{I}_1 = \bar{I}_o + \bar{I}'_2 \tag{11.45}$$

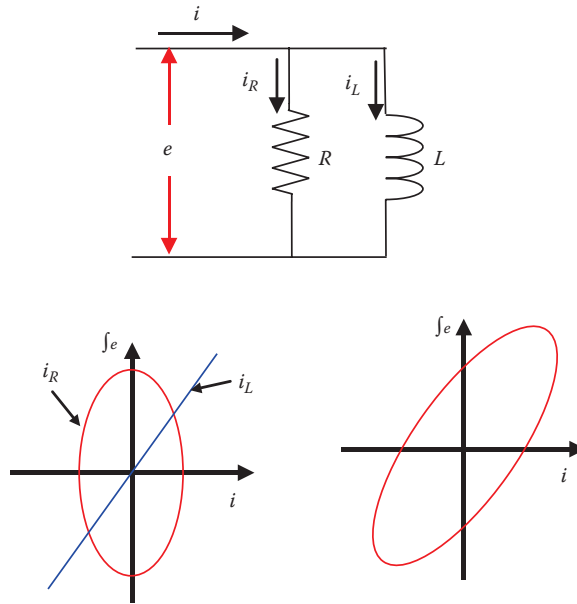


FIGURE 11.21 Approximate representation of hysteresis.

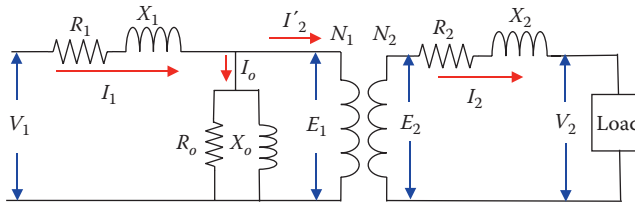


FIGURE 11.22 Equivalent circuit of a transformer.

The current I'_2 is equal to the load current as seen from the primary side. This is also known as the reflected load current. The relationship between I_2 and I'_2 is the turns ratio of the transformer as given by the equation of the magnetomotive force.

$$\begin{aligned} \mathfrak{S} &= I'_2 N_1 = I_2 N_2 \\ \frac{I'_2}{I_2} &= \frac{N_2}{N_1} \end{aligned} \tag{11.46}$$

The voltage equations of the primary and secondary circuits are

$$\bar{V}_1 = \bar{E}_1 + \bar{I}_1 (R_1 + jX_1) \tag{11.47}$$

$$\bar{E}_2 = \bar{V}_2 + \bar{I}_2 (R_2 + jX_2) \tag{11.48}$$

We can rewrite Equation 11.47 by substituting Equation 11.48 into Equation 11.47.

$$\begin{aligned} \bar{V}_1 &= \bar{E}_2 \frac{N_1}{N_2} + \bar{I}_1 (R_1 + jX_1) \\ \bar{V}_1 &= \left[\bar{V}_2 + \bar{I}_2 (R_2 + jX_2) \right] \frac{N_1}{N_2} + \bar{I}_1 (R_1 + jX_1) \\ \bar{V}_1 &= \left[\bar{V}_2 + \bar{I}_2' \frac{N_1}{N_2} (R_2 + jX_2) \right] \frac{N_1}{N_2} + \bar{I}_1 (R_1 + jX_1) \\ \bar{V}_1 &= \left[\bar{V}_2 \frac{N_1}{N_2} + \bar{I}_2' \left(\frac{N_1}{N_2} \right)^2 (R_2 + jX_2) \right] + \bar{I}_1 (R_1 + jX_1) \end{aligned} \tag{11.49}$$

The following variables and parameters can be defined as

$$\begin{aligned} \bar{V}_2' &= \bar{V}_2 \frac{N_1}{N_2} \\ R_2' &= R_2 \left(\frac{N_1}{N_2} \right)^2 \\ X_2' &= X_2 \left(\frac{N_1}{N_2} \right)^2 \end{aligned} \tag{11.50}$$

where

V_2' is known as the *reflected voltage* of the secondary terminal voltage (or *secondary voltage referred to primary*)

R_2' is the *reflected resistance of the secondary winding* (or *secondary winding resistance referred to the primary*)

X_2' is the *reflected inductive reactance of the secondary winding* (or *secondary winding inductive reactance referred to the primary*)

Substituting Equation 11.50 into Equation 11.49 yields

$$\bar{V}_1 = \bar{V}_2' + \bar{I}_2' (R_2' + jX_2') + \bar{I}_1 (R_1 + jX_1) \tag{11.51}$$

The transformer model representing Equation 11.51 is shown in Figure 11.23. This circuit is easier to use than the one shown in Figure 11.22. Further approximation of the transformer model can

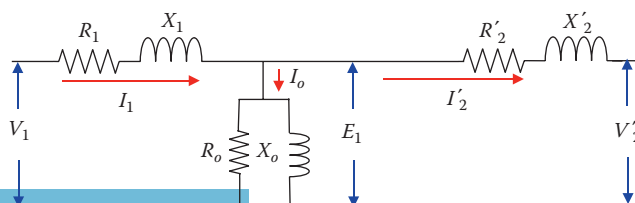


FIGURE 11.23 Modified equivalent circuit of the transformer.

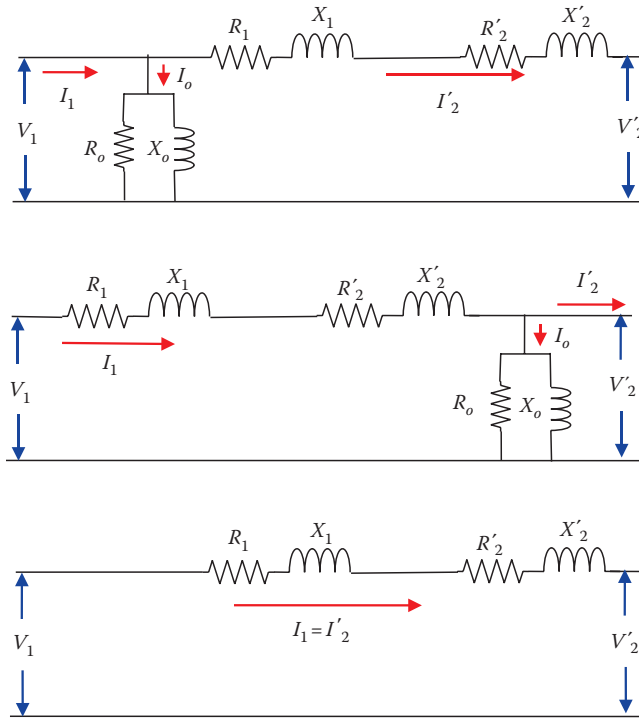


FIGURE 11.24 Acceptable equivalent circuits for the transformer.

be made since the excitation current I_o is often less than 5% of the rated primary current. In this case, moving the core branch anywhere in the model, or even eliminating it altogether, as shown in Figure 11.24 should not introduce significant errors.

Example 11.12

A single-phase transformer has the following parameters:

$$\frac{N_1}{N_2} = 10; \quad R_{eq} = R_1 + R'_2 = 1\Omega; \quad X_{eq} = X_1 + X'_2 = 10\Omega; \quad R_o = 1000\Omega; \quad X_o = 5000\Omega$$

The rated voltage of the primary winding is 1000 V. A $0.5\angle 30^\circ \Omega$ load is connected across the secondary terminals. Compute the load voltage.

Solution

Let us use the equivalent circuit in Figure 11.25. The magnitude of the load impedance referred to the primary side is

$$Z'_L = Z_L \left(\frac{N_1}{N_2} \right)^2 = 50 \Omega$$

The current I_2^E is

$$\bar{I}_2^E = \frac{\bar{V}_1}{(R_{eq} + jX_{eq}) + Z'_L} = \frac{1000\angle 0^\circ}{(1 + j10) + 50\angle 30^\circ} = 17.7\angle -38.31^\circ \text{ A}$$

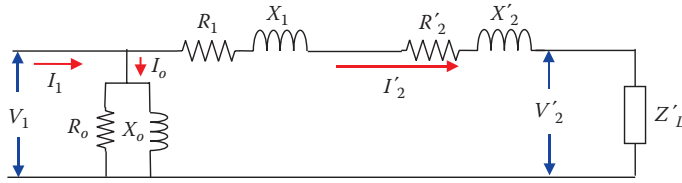


FIGURE 11.25 Equivalent circuit of the transformer with load.

The load voltage referred to the primary side V'_2 is

$$\bar{V}'_2 = \bar{I}'_2 Z'_L = (17.7 \angle -38.31^\circ)(50 \angle 30^\circ) = 885 \angle -8.31^\circ \text{ V}$$

Use Equation 11.50 to compute the actual voltage across the load

$$V_2 = V'_2 \frac{N_2}{N_1} = 885 \frac{1}{10} = 88.5 \text{ V}$$

11.5.2 TRANSFORMER EFFICIENCY

The efficiency η of any equipment is defined by

$$\eta = \frac{\text{Output power}}{\text{Input power}} = \frac{\text{Output energy}}{\text{Input energy}} = \frac{\text{Output power}}{\text{Output power} + \text{losses}} = \frac{\text{Input power} - \text{losses}}{\text{Input power}} \quad (11.52)$$

The losses of the transformer are due to R_1 , R_2 , and R_o . The losses in R_1 and R_2 are the winding losses, and are named *copper losses* P_{cu} (the windings are made of copper material). The loss in R_o is known as *iron loss* P_{iron} (the core is made of iron). Using Figure 11.22, the losses can be computed as

$$P_{cu} = I_1^2 R_1 + I_2^2 R_2 \quad (11.53)$$

$$P_{iron} = \frac{E_1^2}{R_o} \quad (11.54)$$

These losses can also be computed using the approximate equivalent circuits in Figure 11.24. A good approximation for the losses is given as follows:

$$P_{cu} \approx I_1^2 (R_1 + R_2) \approx (I'_2)^2 (R_1 + R'_2) \quad (11.55)$$

$$P_{iron} \approx \frac{V_1^2}{R_o} \approx \frac{(V'_2)^2}{R_o} \quad (11.56)$$

Using Equation 11.52, the efficiency of the transformer can be computed as

$$\eta = \frac{P_{out}}{P_{input}} = \frac{V'_2 I'_2 \cos \theta_2}{V'_2 I'_2 \cos \theta_2 + P_{cu} + P_{iron}} = \frac{V_1 I_1 \cos \theta_1 - P_{cu} - P_{iron}}{V_1 I_1 \cos \theta_1} \quad (11.57)$$

Where

θ_1 is the phase angle of I_1 with respect to input voltage

θ_2 is the phase angle of I_2 with respect to load voltage, which is also the angle of the load impedance

Example 11.13

Compute the efficiency of the transformer in Example 11.12.

Solution

$$P_{cu} = (I_2')^2 R_{eq} = 17.7^2 \times 1 = 313.29 \text{ W}$$

$$P_{iron} = \frac{V_1^2}{R_o} = \frac{1000^2}{1000} = 1 \text{ kW}$$

The output power is

$$P_{out} = V_2' I_2' \cos \theta_2 = 885 \times 17.7 \times \cos 30 = 13.57 \text{ kW}$$

The efficiency of the transformer is

$$\eta = \frac{P_{out}}{P_{input}} = \frac{V_2' I_2' \cos \theta_2}{V_2' I_2' \cos \theta_2 + P_{cu} + P_{iron}} = \frac{13570}{13570 + 313.29 + 1000} = 91.2\%$$

11.5.3 VOLTAGE REGULATION

The voltage regulation VR of the transformer is defined as

$$VR = \frac{|V_{no\ load}| - |V_{full\ load}|}{|V_{full\ load}|} \quad (11.58)$$

where

$|V_{no\ load}|$ is the magnitude of the open circuit voltage measured at the load terminals

$|V_{full\ load}|$ is the magnitude of the voltage at the load terminals when the rated current is delivered to the load

The VR represents the change in the load voltage from no load to full load. It indicates the voltage reduction due to the various parameters of the transformer.

Consider the equivalent circuit in Figure 11.25. At no load (open circuit), $I_2' = 0$. Hence, the voltage measured at the load terminals is

$$V_{no\ load} = V_1 \quad (11.59)$$

At full load,

$$V_{full\ load} = V_2' \quad (11.60)$$

Hence, the voltage regulation of the transformer is

$$VR = \frac{V_1 - V_2'}{V_2'} \quad (11.61)$$

Example 11.14

Compute the voltage regulation of the transformer in Example 11.12. Assume that the secondary winding of the transformer carries the full load current when $0.5\angle 30^\circ \Omega$ is connected across the secondary terminals.

Solution

$$VR = \frac{V_1 - V_2'}{V_2'} = \frac{1000 - 885}{885} = 13\%$$

EXERCISES

- 11.1** A single-phase transformer has a turns ratio of 10,000/5,000. A direct current voltage of 30 V is applied to the primary winding, compute the voltage of the secondary winding.
- 11.2** A single-phase transformer is rated at 2 kVA, 240/120 V. The transformer is fully loaded by an inductive load of 0.8 power factor lagging. Compute the following:
- Real power delivered to the load
 - Load current
- 11.3** A single-phase transformer is rated at 10 KVA, 220/110 V.
- Compute the rated current of each winding.
 - If a 2Ω load resistance is connected across the 110 V winding, what are the currents in the high-voltage and low-voltage windings?
 - What is the equivalent load resistance referred to the 220 V side?
- 11.4** Three single-phase transformers are connected in wye/delta configuration. Each single-phase transformer has an identical number of turns in the primary and secondary windings. If a line-to-line voltage of 480 V is applied on the wye windings, compute the line-to-line voltage on the delta windings.
- 11.5** Three single-phase transformers, each is rated at 10 kVA, 400/300 V are connected as wye-delta configuration. Compute the following:
- Rated power of the transformer bank
 - Line-to-line voltage ratio of the transformer bank
- 11.6** A single-phase transformer has a voltage regulation of 5%. The input voltage of the transformer is 120 V, and the turns ratio N_1/N_2 is 2. Compute the voltage across the load V_2 .
- 11.7** Three single-phase transformers are connected as a transformer bank rated at 18 MVA, 13.8 kV(Δ)/120 kV(Y). One side of the transformer bank is connected to a 120 kV transmission line, and the other side is connected to a three-phase load of 12 MVA at 0.8 lagging power factor. Compute the following:
- Turns ratio of the transformer bank
 - Line current at the 120 kV side

- 11.8** A single-phase 10kVA, 2300/230 V two-winding transformer is connected as an autotransformer to step up the voltage from 2300 to 2530 V.
- Draw the schematic diagram of the autotransformer showing the winding connections and all voltages and currents at full-load.
 - Find the kVA rating of the autotransformer. Do not allow the currents of windings to exceed their rated values.
- 11.9** A single phase, 240/120 V transformer has the following parameters:

$$R_1 = 1 \Omega; \quad R_2 = 0.5 \Omega; \quad X_1 = 6 \Omega; \quad X_2 = 2 \Omega$$

$$R_o = 500 \Omega; \quad X_o = 1.5 \text{ k}\Omega$$

- A load of 10Ω at 0.8 power factor lagging is connected across the low-voltage terminals of the transformer. The voltage measured across the load side is 110 V. Compute the following:
- Load voltage referred to the primary side
 - Currents of the primary and secondary winding
 - Source voltage
 - Voltage regulation
 - Load power
 - Efficiency of the transformer
- 11.10** Three identical single-phase transformers each rated at 100kVA, 7kV/3.5kV are connected as a three-phase transformer bank. The high-voltage side of the transformer is connected in delta and the low-voltage side is connected in wye. A 200kVA, wye-connected load is attached across the secondary winding. Compute the following:
- Ratio of the line-to-line voltages
 - Line current on both sides of the transformer
- 11.11** The transformer shown in Figure 11.6 consists of one primary winding and two secondary windings. The numbers of turns of the windings are: $N_1 = 10,000$; $N_2 = 5,000$, and $N_3 = 1,000$. A voltage source of 120 V is applied to the primary winding. The load of winding N_2 consumes 600 W and 300 VAR inductive power. The load of winding N_3 consumes 24 W and 36 VAR capacitive power. Compute the following:
- Voltages of the secondary windings
 - Currents of all windings
- 11.12** A single-phase transformer has three windings. The primary winding N_1 carries a current of $I_1 = 10 \text{ A}$. One of the secondary windings has 3000 turns and carries 2 A, and the other secondary winding has 6000 turns and carries 1 A. All currents are in phase. Compute the number of turns in the primary winding.
- 11.13** Three single-phase transformers are used to form a three-phase transformer bank rated 13.8 kV(Δ)/120 kV(Y). One side of the transformer bank is connected to a 120 kV transmission line, and the other side is connected to a three-phase load of 12 MVA at 0.8 power factor lagging. Determine the turns ratio of each transformer and the line current at the 120 kV side.

12 Electric Machines

Most electric machines are dual-action electromechanical converters. The machines that convert electrical energy into mechanical are called *motors*, and the machines that convert mechanical energy into electrical are called *generators*. Electric motors are probably the most used power devices anywhere. You can find them in almost every equipment with mechanical movements from children's toys to spacecrafts. They play incredible roles in our daily life by performing numerous vital tasks in various applications. Refrigerators, washers, dryers, stoves, air conditioners, hair dryers, computers, printers, clocks, electric toothbrushes, electric shavers, and fans are some of the household devices that use motors. In the industrial and commercial sectors, motors are used in numerous applications such as transportation vehicles, elevators, forklifts, blowers, robots, actuators, electric and hybrid cars, machine tooling, paper mills, cooking machines, medical tools, assembly lines, and conveyor belts. The computer hard disk, for example, has at least two motors and the computer printer has at least four motors. National Aeronautics and Space Administration (NASA)'s Mars exploration rover built by the Jet Propulsion Laboratory (JPL) has about 200 motors; most are used for actuation, sensing, sampling, and control. Many of them are for one-time use only during the cruising phase and the *entry, descent, and landing* (EDL) phase. In total, about 65% of the electrical energy in the United States is consumed by electric motors, and over 99% of the energy produced by utilities worldwide is produced by electrical generators. In stand-alone systems such as aircrafts, ships and automobiles, the generators are the main source of electric power for these mobile systems. Electrical machines come in various sizes and power levels. Their weights range from micrograms for motors installed inside silicon chips to the 7700 ton for the generator built by the consortium from Hewitt, Siemens, and General Electric for China's Yangtze River Three Gorges Hydraulic Power plant. The power capacity of the machines is also of a wide range, from microwatts to more than 2 GW.

12.1 ROTATING MAGNETIC FIELD

A multiphase alternating current (ac) source produces a rotating magnetic field inside ac motors, which causes the shaft of the motor to spin. Before we explain how an ac machine rotates, we need to understand the concept of rotating magnetic fields. Consider the conceptual diagram of the stator of a three-phase machine shown in Figure 12.1. The figure shows three windings mounted symmetrically inside a hollow metal tube called stator, which are shifted by 120° from each other. Each winding goes along the length of the stator on one side and then returns from the other side. If we apply a three-phase balanced voltage across the terminals of the windings, the currents of the windings create balanced three-phase magnetic fields inside the tube as shown in Figure 12.2.

Figure 12.3 shows a more convenient representation of the stator windings. The circles embedded inside the stator represent the windings of the motor; $a-a'$ represent the winding of phase a , $b-b'$ represent the winding of phase b , and $c-c'$ represent the winding of phase c . The crosses and dots inside the circles represent current entering and leaving the windings, respectively.

Because of the mechanical arrangement of the stator windings, the flux of each phase, according to the right hand rule, travels along the axis shown in Figure 12.3. This flux is inside the tube; thus it is called *airgap flux*.

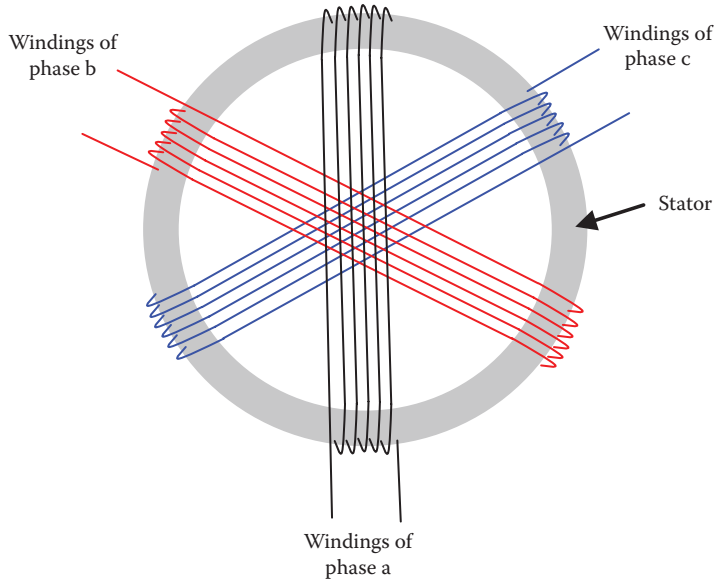


FIGURE 12.1 Three-phase windings mounted on a stator.

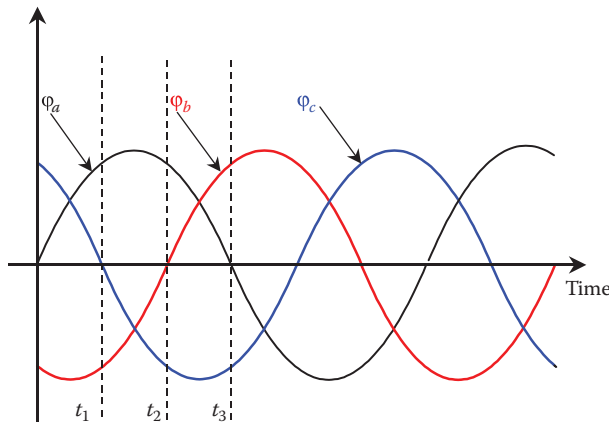


FIGURE 12.2 Airgap flux of the three phases.

Now, let us consider any three consecutive time instances (e.g., t_1 , t_2 , and t_3 shown in Figure 12.2). At t_1 , the angle is 60° , and the magnitude of the flux of each phase is

$$\begin{aligned} \varphi_a &= -\varphi_b = \frac{\sqrt{3}}{2} \varphi_{\max} \\ \varphi_c &= 0 \end{aligned} \tag{12.1}$$

The fluxes at t_1 are mapped along their corresponding axes on the left side in Figure 12.4. Note the direction of the current in each winding as it determines the direction of its flux according to the right hand rule. The total airgap flux is the phasor sum of all fluxes present in the airgap. Hence, at t_1 ,

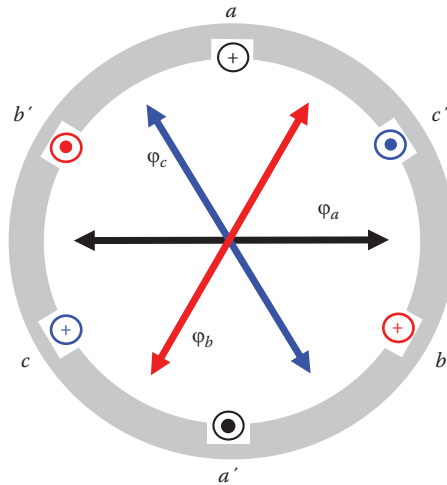


FIGURE 12.3 Loci of airgap fluxes.

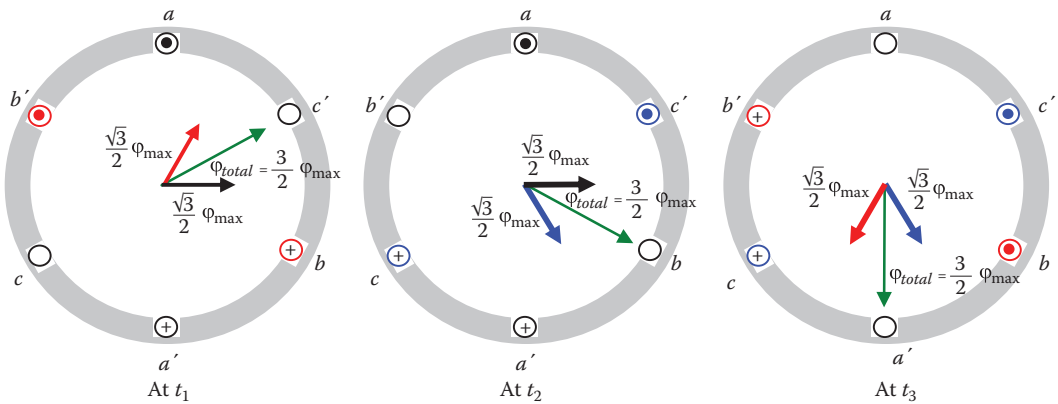


FIGURE 12.4 Rotating airgap flux.

$$\bar{\Phi}_{total}(t_1) = \bar{\Phi}_a(t_1) + \bar{\Phi}_b(t_1) + \bar{\Phi}_c(t_1) = \frac{\sqrt{3}}{2} \Phi_{max} \angle 0^\circ + \frac{\sqrt{3}}{2} \Phi_{max} \angle 60^\circ + 0 \tag{12.2}$$

$$\bar{\Phi}_{total}(t_1) = \frac{3}{2} \Phi_{max} \angle 30^\circ$$

Similarly, at t_2 , the angle is 120° , and the magnitudes of the fluxes of the three phases are

$$\Phi_a = -\Phi_c = \frac{\sqrt{3}}{2} \Phi_{max} \tag{12.3}$$

$$\Phi_b = 0$$

These fluxes are shown in the middle of Figure 12.4, where the total airgap flux at t_2 is

$$\begin{aligned}\bar{\varphi}_{total}(t_2) &= \bar{\varphi}_a(t_2) + \bar{\varphi}_b(t_2) + \bar{\varphi}_c(t_2) = \frac{\sqrt{3}}{2} \varphi_{max} \angle 0^\circ + 0 + \frac{\sqrt{3}}{2} \varphi_{max} \angle -60^\circ \\ \bar{\varphi}_{total}(t_2) &= \frac{3}{2} \varphi_{max} \angle -30^\circ\end{aligned}\quad (12.4)$$

Finally, at t_3 , the angle of the waveform is 180° , and the magnitudes of the fluxes of the three phases are

$$\begin{aligned}\varphi_a &= 0 \\ \varphi_b &= -\varphi_c = \frac{\sqrt{3}}{2} \varphi_{max}\end{aligned}\quad (12.5)$$

These fluxes are shown at the right side of Figure 12.4. In this case, the total airgap flux at t_3 is

$$\begin{aligned}\bar{\varphi}_{total}(t_3) &= \bar{\varphi}_a(t_3) + \bar{\varphi}_b(t_3) + \bar{\varphi}_c(t_3) = 0 + \frac{\sqrt{3}}{2} \varphi_{max} \angle -120^\circ + \frac{\sqrt{3}}{2} \varphi_{max} \angle -60^\circ \\ \bar{\varphi}_{total}(t_3) &= \frac{3}{2} \varphi_{max} \angle -90^\circ\end{aligned}\quad (12.6)$$

By examining Equations 12.2, 12.4, and 12.6, we can conclude the following:

- Magnitude of the total flux in the airgap is constant and equal to $1.5 \varphi_{max}$.
- Angle of the total airgap flux changes with time. The flux in the aforementioned case is rotating in the clockwise direction. This rotating flux is one of the main reasons for the development of three-phase systems.
- Total flux in the airgap completes one revolution in every ac cycle. Hence, the mechanical speed of the total flux in the airgap n_s is one revolution per ac cycle.

$$n_s = f \text{ rev/s} \quad (12.7)$$

where f is the frequency of the ac supply (Hz). The mechanical speed is often measured in revolution per minute (rpm). Hence,

$$n_s = 60f \text{ rpm} \quad (12.8)$$

The speed n_s is known as *synchronous speed* because its value is determined by the frequency of the supply voltage; that is, the speed is synchronized with the supply frequency.

The machine in Figure 12.3 is considered two-pole because every phase has one winding that creates one north pole and one south pole. If each phase is composed of two windings (i.e., $a_1-a'_1$ and $a_2-a'_2$) arranged symmetrically along the inner circumference of the stator as shown in Figure 12.5, the machine is considered to have four poles. In this arrangement, the mechanical angle between the phases is 60° instead of the 120° for the two-pole machine. If you repeat the analyses in Equations 12.1 through 12.6, you will find that the flux moves 180° (mechanical angle) for each complete ac cycle. Hence, we can write a general expression for the mechanical speed of the airgap flux as

$$n_s = \frac{60f}{pp} = 120 \frac{f}{p} \text{ rpm} \quad (12.9)$$

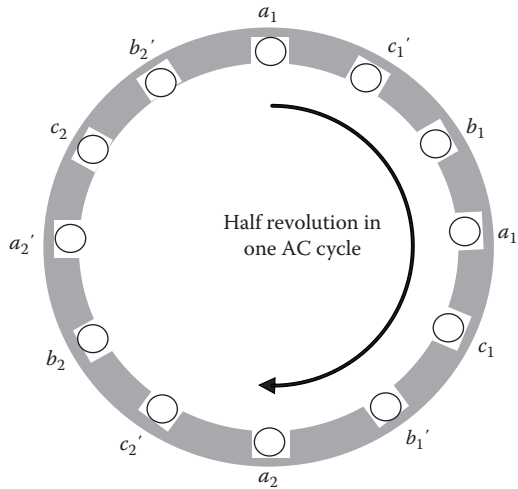


FIGURE 12.5 Four-pole arrangement.

where

pp is the number of pole pairs

p is the number of poles ($p = 2 pp$)

Example 12.1

Compute the synchronous speed for 2, 4, 6, 8, and 10-pole machines operating at 50 and 60 Hz.

Solution

With the direct substitution in Equation 12.9, you can get the following tabulated data:

Number of Poles	Synchronous Speed (rpm)	
	50 Hz	60 Hz
2	3000	3600
4	1500	1800
6	1000	1200
8	750	900
10	600	720

Note that the synchronous speed for the 50Hz system is slower than that for the 60Hz systems.

12.2 ROTATING INDUCTION MOTOR

About 65% of the electric energy in the United States is consumed by electric motors. In the industrial sector alone, about 75% of the total energy is consumed by motors. Some of the unfamiliar uses of electric motors are shown in Figure 12.6.

Over 90% of the energy consumed by electric motors is consumed by induction motors. This is because they are rugged, reliable, easy to maintain, and relatively inexpensive. The induction motor is composed of one stator and one rotor; a small induction motor is shown in Figure 12.7. The stator



MARS rover (courtesy of NASA)



Underwater unmanned robot



Electric propulsion ferry



Hybrid electric vehicle



City transportation



City electric bus



Maglev train
(courtesy of transrapid int.)



Electric train

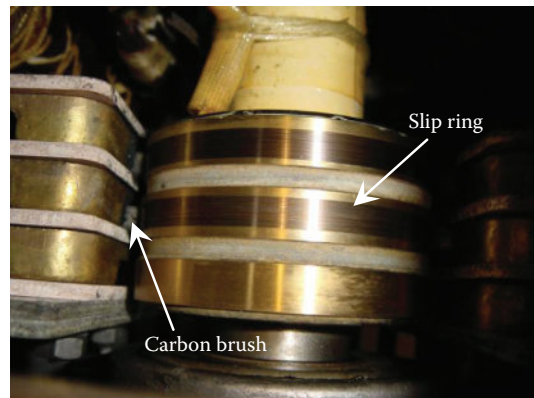


Monorail

FIGURE 12.6 Induction machines are the prime movers of these vehicles.



Stator



Slip ring rotor

FIGURE 12.7 Main parts of induction machine.

has three-phase windings, which are excited by a three-phase supply. The rotor, as the name implies, is the rotating part of the motor. It is mounted inside the stator and is supported by two ball bearings; one on each end of the rotor. The mechanical load of the motor is attached to the shaft of the rotor. The rotor circuit consists of windings that are shorted either permanently as part of the rotor structure, or externally through a system of slip rings and brushes. The rotor with an external short,

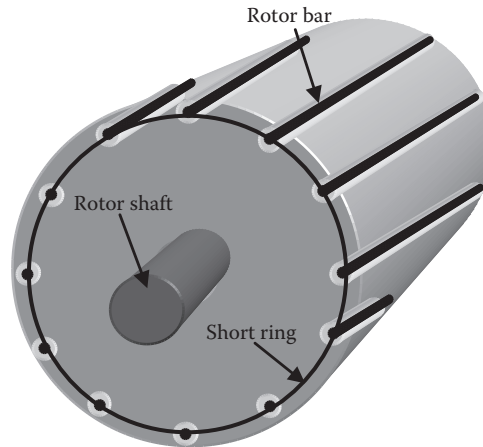


FIGURE 12.8 Squirrel cage rotor.

called a *slip ring* rotor, has three rings mounted on the rotor shaft inside the motor structure as shown in Figure 12.7. These slip rings are electrically isolated from one another, but each is connected to one terminal of the three-phase windings of the rotor; most rotor windings are connected in wye. Carbon brushes mounted on the stator structure are placed to continuously touch the rotating slip rings, thus achieving connectivity between the rotor windings and any external device. The rotor circuit with an internal short, called *squirrel cage* rotor, consists of slanted wire bars shorted on both ends of the rotor as shown in Figure 12.8.

12.2.1 ROTATION OF INDUCTION MOTOR

The rotation of the induction motor can be explained using Faraday's law and Lorentz equation. When a conductor carries a current in a uniform magnetic field, the electromechanical relationships can be represented by the following:

$$e = Bl\Delta v \quad (12.10)$$

$$force = Bli$$

where

e is the induced voltage across the conductor

B is the flux density

l is the length of the conductor

Δv is the relative speed between the conductor and the field

i is the current of the conductor

$force$ is the mechanical force exerted on the conductor

If we generalize Equation 12.10 for rotating fields, we can rewrite them in the following forms:

$$e = f(\varphi, \Delta n) \quad (12.11)$$

$$T = f(\varphi, i) \quad (12.12)$$

where

$f(\cdot)$ is functional relationship

T is the torque of the conductors

Δn is the difference in angular speed between the conductor and the flux in the airgap

To understand the mechanism by which the rotor is spinning, let us assume that the rotor is at stand-still. When a three-phase voltage is applied across the stator windings, a rotating flux at synchronous speed n_s is produced in the airgap. The speed difference Δn is the difference between the rotor speed n and the speed of the airgap flux n_s :

$$\Delta n = n_s - n \quad (12.13)$$

Since the rotor is stationary, Δn is equal to the synchronous speed n_s . Hence, the rotating field induces a voltage e in the rotor windings as given in Equation 12.11. Since the rotor windings are shorted, the induced voltage causes a current i to flow in the rotor windings, producing the Lorentz torque T in Equation 12.12. This torque spins the rotor. As you may conclude from Equations 12.11 and 12.12, the induction motor cannot spin at the synchronous speed. This is because Δn in this case is zero, resulting in no induced voltage across the rotor windings; so no current is flowing in the windings and therefore no torque is developed to spin the motor. So what is the steady-state speed of the induction motor? The answer depends on the load torque. The third law of motion developed by Isaac Newton in 1686 states that “whenever one body exerts a force on another, the second exerts a force on the first that is equal in magnitude, opposite in direction and has the same line of action.” For the induction motor, this theory means that the motor develops a torque equal in magnitude and opposite in direction to the load torque. Hence, the steady-state operation is achieved when the motor, on a continuous basis, provides the torque needed by the load. Assuming that the flux is unchanged, this developed torque needs certain magnitude of rotor current i as shown in Equation 12.12. The magnitude of this rotor current requires a certain value of induced voltage e in the rotor windings that is equal to the rotor current i multiplied by the rotor impedance. This voltage in turn requires a certain speed difference Δn as given in Equation 12.11. Hence, the steady-state speed of the rotor must always be slightly less than the synchronous speed to maintain the balance between the load torque and the motor’s developed torque. Δn is larger for heavy load torques and smaller for light load torques.

The per unit value of the speed difference is known as slip S :

$$S = \frac{\Delta n}{n_s} = \frac{n_s - n}{n_s} \quad (12.14)$$

If we use the angular speed ω instead of n , the slip of the motor is

$$S = \frac{\Delta \omega}{\omega_s} = \frac{\omega_s - \omega}{\omega_s} \quad (12.15)$$

Keep in mind that the unit of n is revolution per minute (rpm) and that for ω is radian per second (rad/s). Hence,

$$\omega = \frac{2\pi}{60} n \quad (12.16)$$

The slip at starting, when the rotor speed is zero, is equal to one. At no load when the motor speed is very close to the synchronous speed, the slip is close to zero. During a normal steady-state operation, the slip is small and often less than 0.1.

Example 12.2

A two-pole, 60Hz induction motor operates at a slip of 0.02. Compute its rotor speed.

Solution

First, let us compute the synchronous speed

$$n_s = 120 \frac{f}{p} = 120 \frac{60}{2} = 3600 \text{ rpm}$$

Use Equation 12.14 to compute the speed of the rotor

$$S = \frac{n_s - n}{n_s}; n = n_s (1 - S) = 3600(1 - 0.02) = 3528 \text{ rpm}$$

Example 12.3

The steady-state speed of a 60Hz induction motor is 1150 rpm. Compute the number of poles of the induction motor, and the slip.

Solution

As stated earlier, during the steady-state operation, the speed of the motor is just below the synchronous speed. Using the table in Example 12.1, you will find that the synchronous speed just above 1150 is 1200. Hence the motor is a six-pole machine.

$$S = \frac{n_s - n}{n_s} = \frac{1200 - 1150}{1200} = 0.0417 \quad \text{or} \quad 4.17\%$$

12.2.2 EQUIVALENT CIRCUIT OF INDUCTION MOTOR

Since the induction motor is considered a balanced three-phase device, a single-phase equivalent circuit is adequate to model the machine. The stator of the machine consists of a set of copper windings mounted on an iron core. This is almost the same as the primary circuit of the transformer. The stator winding can be represented by a resistance R_1 and inductive reactance X_1 . Since the stator copper windings are imbedded in the stator's iron core, the core can be represented by a parallel combination of a core resistance R_c and a core inductive reactance X_c . By using these parameters, it can be observed that the model for the stator circuit shown in Figure 12.9 is very similar to the model for the primary circuit of the transformer. The sum of the currents in R_c and X_c is called *magnetizing* (or core) *current* I_c . E_1 in the figure is equal to the source voltage V minus the drop across the copper impedance.

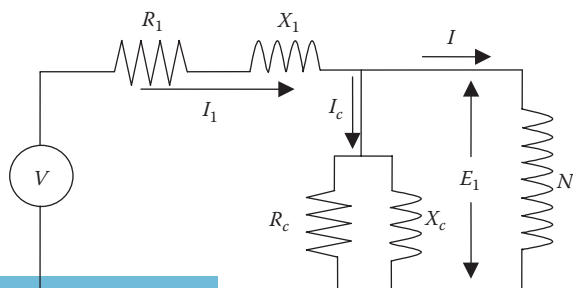


FIGURE 12.9 Equivalent circuit of the stator.

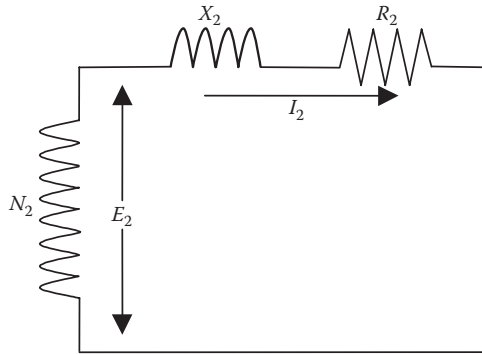


FIGURE 12.10 Equivalent circuit of the rotor at standstill.

$$\bar{E}_1 = \bar{V} - \bar{I}_1(R_1 + jX_1) \tag{12.17}$$

The equivalent circuit of the rotor is also similar to the equivalent circuit for the secondary circuit of the transformer, but only at standstill (where $n=0$) and when the secondary winding is shorted (because the rotor windings are shorted). The rotor can be represented by its winding resistance R_2 and inductive reactance X_2 as shown in Figure 12.10. E_2 is the induced voltage across the rotor winding at standstill. If you assume that the number of turns of the stator winding is N_1 and that for the rotor winding is N_2 , then

$$\frac{E_2}{E_1} = \frac{N_2}{N_1} \tag{12.18}$$

The inductive reactance X_2 of the rotor winding is

$$X_2 = 2\pi f L_2 \tag{12.19}$$

where

- f is the frequency of the supply voltage
- L_2 is the inductance of the rotor winding

When the rotor spins, two variables change: (1) induced voltage across the rotor winding and (2) frequency of the rotor current (or rotor voltage). As shown in Equation 12.11, the induced voltage across the rotor winding is proportional to the speed difference Δn . Hence, the induced voltage E_2 is at standstill when $n=0$:

$$E_2 \sim \Delta n = n_s \tag{12.20}$$

At any other speed, the induced voltage across the rotor winding E_r is

$$E_r \sim \Delta n = n_s - n \tag{12.21}$$

Dividing Equations 12.21 by (12.20), we get the relationship between the induced voltage of the rotor at any speed and the induced voltage at standstill:

$$\frac{E_r}{E_2} = \frac{n_s - n}{n_s} = s \tag{12.22}$$

Hence, the voltage across the rotor winding at any speed E_r is equal to the rotor voltage at standstill E_2 multiplied by the slip S . In other words, the induced voltage across the rotor windings is always equal to

$$E_r = SE_2 = \frac{N_2}{N_1} SE_1 \tag{12.23}$$

The frequency of the rotor current is directly proportional to the rate at which the magnetic field cuts the rotor winding. At standstill, the airgap flux cuts the rotor windings at a rate proportional to the synchronous speed n_s . Hence, the frequency of the rotor current at standstill is f_s and is proportional to the synchronous speed. This makes f_s equal to the frequency of the stator voltage f . If the rotor is spinning at a speed n , the flux cuts the rotor windings at a rate proportional to Δn . Hence, the frequency of the rotor current at any speed f_r is proportional to Δn :

$$\begin{aligned} f &= f_s \sim n_s \\ f_r &\sim \Delta n \end{aligned} \tag{12.24}$$

Hence, the frequency of the rotor current at any speed is

$$\begin{aligned} \frac{f_r}{f} &= \frac{\Delta n}{n_s} = S \\ f_r &= S f_s = S f \end{aligned} \tag{12.25}$$

The equivalent circuit of the rotor at any speed is shown in Figure 12.11. Because the rotor voltage and rotor frequency are changing with speed, it is hard to use the equivalent circuit in Figure 12.11. Hence, we need to modify the circuit to make it easier to analyze at any speed. The inductive reactance of the rotor X_r is different from X_2 in Equation 12.19 because the rotor frequency at any speed is f_r . Hence,

$$X_r = 2\pi f_r L_2 \tag{12.26}$$

Substituting the value of f_r in Equation 12.25 into Equation 12.26 yields

$$X_r = 2\pi f_r L_2 = 2\pi(S f)L_2 \tag{12.27}$$

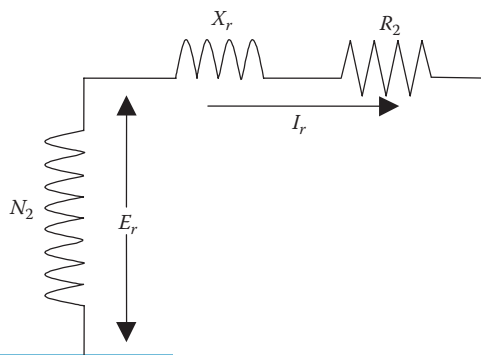


FIGURE 12.11 Equivalent circuit of the rotor at any speed.

Using the value of X_2 in Equation 12.19 yields

$$X_r = 2\pi(Sf)L_2 = S X_2 \tag{12.28}$$

The rotor current I_r for the circuit in Figure 12.11 is

$$\bar{I}_r = \frac{\bar{E}_r}{R_2 + j X_r} = \frac{S \bar{E}_2}{R_2 + j S X_2} = \frac{\bar{E}_2}{\frac{R_2}{S} + j X_2} \tag{12.29}$$

Using Equation 12.29, the equivalent circuit of the rotor can be modified as shown in Figure 12.12. Now we can add the stator circuit to complete the model for the motor as shown in Figure 12.13. This circuit can further be modified as shown in Figure 12.14 by referring the rotor circuit to the

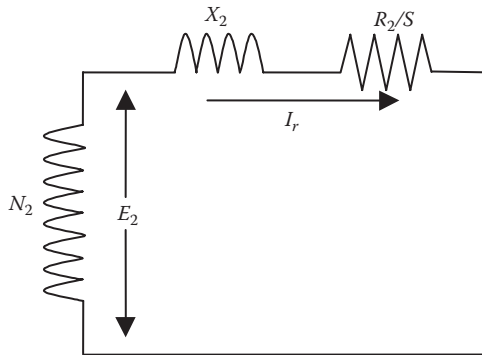


FIGURE 12.12 Modified equivalent circuit of the rotor at any speed.

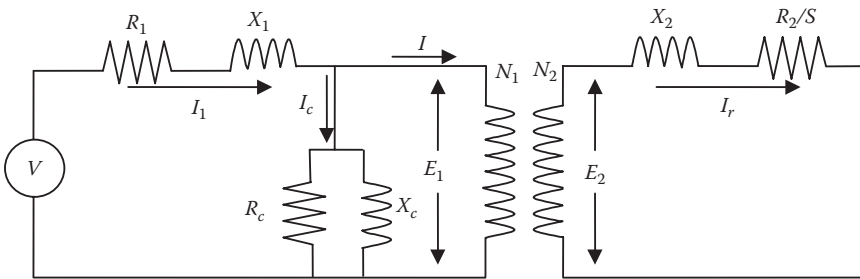


FIGURE 12.13 Equivalent circuit for induction motor.

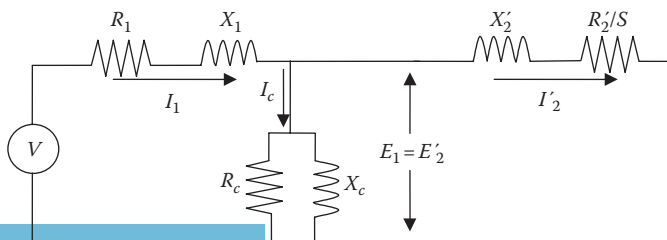


FIGURE 12.14 Equivalent circuit for induction motor referred to the stator.

stator using the turns ratio. This is the same process used to refer the secondary circuit of the transformer to the primary side. Thus, the resistance R_2' and inductive reactance X_2' of the rotor winding referred to the stator circuit are computed as follows:

$$R_2' = R_2 \left(\frac{N_1}{N_2} \right)^2 \quad (12.30)$$

$$X_2' = X_2 \left(\frac{N_1}{N_2} \right)^2 \quad (12.31)$$

where N_1 and N_2 are the number of turns of the stator and rotor windings, respectively. Also, the rotor current referred to the stator circuit I_2' can be computed as

$$I_2' = I_r \left(\frac{N_2}{N_1} \right) \quad (12.32)$$

The resistance R_2'/S has two components; one of them is the resistance of the rotor winding R_2'

$$\frac{R_2'}{S} = R_2' + \frac{R_2'}{S} (1 - S) = R_2' + R_d \quad (12.33)$$

where

$$R_d = \frac{R_2'}{S} (1 - S) \quad (12.34)$$

The resistance R_d is an electrical representation of the mechanical load of the motor. The power consumed by this resistance is the developed mechanical power of the motor. R_d is known as *load resistance* or *developed power resistance*. The parsing of R_2'/S leads to the equivalent circuit in Figure 12.15a. We can further modify the equivalent circuit by assuming that the core current I_c is much smaller than I_1 . Hence, $I_1 \approx I_2'$ and we can thus assume that the impedances of the stator and rotor windings are in series as shown in Figure 12.15b.

R_{eq} and X_{eq} in Figure 12.15c are defined as

$$R_{eq} = R_1 + R_2' \quad (12.35)$$

$$X_{eq} = X_1 + X_2'$$

12.2.3 POWER ANALYSIS

Figure 12.16 shows the power flow of the induction motor. The motor receives input power P_{in} from the electric source, where

$$P_{in} = 3V I_1 \cos \theta_1 \quad (12.36)$$

where

P_{in} is the input power of the motor from the three-phase source

V is the phase voltage of the source

I_1 is the phase current of the stator

θ_1 is the phase angle of the current (the angle between the phase voltage and phase current)

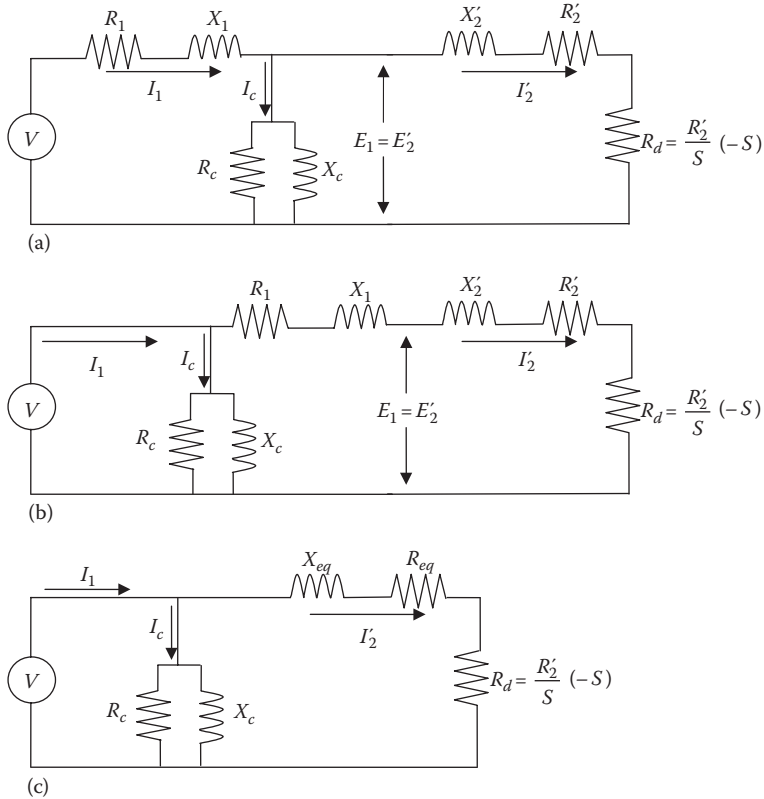


FIGURE 12.15 More equivalent circuits for the induction motor (a) detailed, (b) approximate, (c) approximate and lumped parameters.

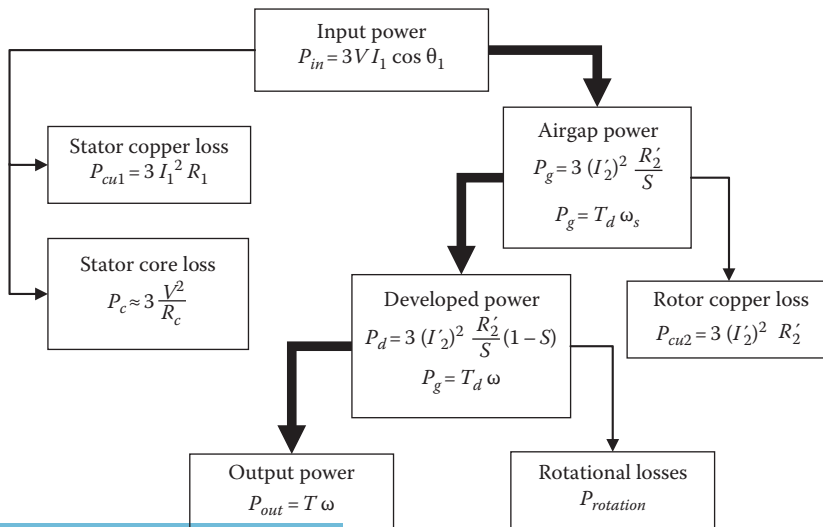


FIGURE 12.16 Powers flow of induction motor.

Part of the input power is wasted in the stator circuit in the form of copper loss inside the windings P_{cu1} and core loss P_c . These losses can be computed using the equivalent circuit in Figure 12.15a:

$$P_{cu1} = 3 I_1^2 R_1$$

$$P_c \oplus 3 \frac{V^2}{R_c} \quad (12.37)$$

The rest of the power is transmitted to the rotor by the airgap flux; thus it is called *airgap power* P_g , which is consumed in R_2'/S :

$$P_g = 3(I_2')^2 \frac{R_2'}{S} \quad (12.38)$$

The airgap power is also a form of mechanical power since it involves the mechanical rotation of the airgap flux. Therefore, P_g can also be written in the mechanical form

$$P_g = T_d \omega_s \quad (12.39)$$

where

T_d is the developed torque of the airgap flux

ω_s is the synchronous speed of the flux

When the airgap power enters the rotor circuit, part of it is wasted in the copper winding of the rotor P_{cu2} :

$$P_{cu2} = 3(I_2')^2 R_2' \quad (12.40)$$

The rest of the power is the *developed power* P_d consumed by R_d

$$P_d = 3(I_2')^2 R_d = 3(I_2')^2 \frac{R_2'}{S} (1 - S) \quad (12.41)$$

This developed power can be represented in the mechanical form

$$P_d = T_d \omega \quad (12.42)$$

where ω is the speed of the rotor (not the synchronous speed). The developed power P_d is not completely converted to useful power (shaft power) as part of it is wasted in the form of rotational losses such as friction and windage. The output power of the motor is equal to the output torque on the motor shaft T (not the developed torque) multiplied by the rotor speed.

$$P_{out} = T \omega \quad (12.43)$$

Note that the relationships between the airgap power, developed power, and rotor copper loss are

$$P_{cu2} = S P_g$$

$$P_d = (1 - S) P_g \quad (12.44)$$

Example 12.4

A 60Hz, three-phase, Y -connected induction motor produces 100hp at 1150rpm. The friction and windage losses of the motor are 1.2kW, the stator copper and core losses are 2.1kW. Compute the input power and the efficiency of the motor.

Solution

The mechanical unit for the output power is horsepower (hp) which can be converted into kilowatt by the conversion factor given in the Appendix.

$$P_{out} = 100 \times 746 = 74.6 \text{ kW}$$

To compute the input power, we can use the power diagram in Figure 12.16. We can work the problem from the output toward the input. First, calculate the developed power

$$P_d = P_{out} + P_{rotation} = 74.6 + 1.2 = 75.8 \text{ kW}$$

To compute the airgap power, we need to know the rotor copper loss which is not explicitly provided. Another alternative is to compute the slip and use the relationship in Equation 12.44 to compute the airgap power. To calculate the slip, we need the synchronous speed and the actual speed of the motor. The actual speed is given, but not the synchronous speed. However, from the principle of operation, the speed of the induction motor is just below the synchronous speed. Using the table in Example 12.1, we can find that the number of poles of this machine is six, and its synchronous speed is 1200rpm. Hence,

$$S = \frac{n_s - n}{n_s} = \frac{1200 - 1150}{1200} = 0.0417$$

Using Equation 12.44, we can compute the airgap power

$$P_g = \frac{P_d}{1 - S} = \frac{75.8}{0.9583} = 79.1 \text{ kW}$$

Now use the diagram in Figure 12.16 to compute the input power

$$P_{in} = P_g + P_{cu1} + P_c = 79.1 + 2.1 = 81.2 \text{ kW}$$

The motor efficiency η is

$$\eta = \frac{P_{out}}{P_{in}} = \frac{74.6}{81.2} = 91.88\%$$

12.2.4 SPEED–TORQUE RELATIONSHIP

By using the mechanical expression for the developed power in Figure 12.16, we can compute the developed torque of the induction motor:

$$T_d = \frac{P_d}{\omega} = \frac{3(I_2')^2 R_2'(1 - S)}{S\omega} \quad (12.45)$$

From the equivalent circuit in Figure 12.15c, the rotor current is

$$I_2' = \frac{V}{\sqrt{\left(R_1 + \frac{R_2'}{S}\right)^2 + X_{eq}^2}} \tag{12.46}$$

Substituting Equation 12.46 into (12.45) leads to

$$T_d = \frac{3V^2 R_2' (1 - S)}{S\omega \left[\left(R_1 + \frac{R_2'}{S}\right)^2 + X_{eq}^2 \right]} \tag{12.47}$$

From Equation 12.15, the speed of the motor ω can be written in terms of the synchronous speed and slip

$$\omega = \omega_s (1 - S) \tag{12.48}$$

Substituting Equation 12.48 into (12.47), we can obtain Equation 12.49 for the developed torque:

$$T_d = \frac{3 V^2 R_2'}{S \omega_s \left[\left(R_1 + \frac{R_2'}{S}\right)^2 + X_{eq}^2 \right]} \tag{12.49}$$

Keep in mind that V is the phase voltage, and the torque is developed by all three phases. Equation 12.49 gives torque as a function of the slip, which can be modified to represent the torque as a function of speed:

$$T_d = \frac{3V^2 R_2'}{(\omega_s - \omega) \left[\left(R_1 + \frac{\omega_s R_2'}{(\omega_s - \omega)}\right)^2 + X_{eq}^2 \right]} \tag{12.50}$$

The speed–torque or slip–torque characteristic of the induction motor based on Equations 12.49 and 12.50 is shown in Figure 12.17. The characteristic is nonlinear and has several key operating

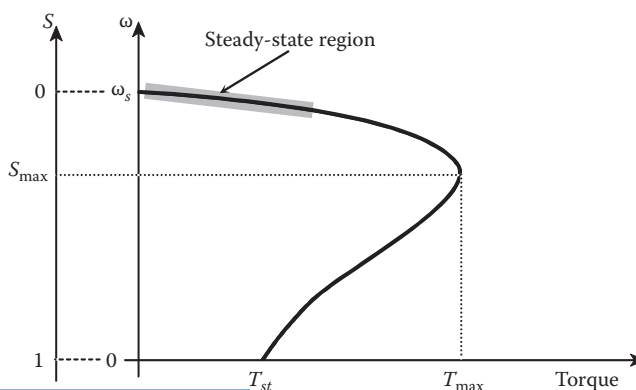


FIGURE 12.17 Speed–torque characteristic of induction motor.

points. When the motor starts (at zero speed), the motor develops a starting torque T_{st} that spins the motor. When the motor accelerates while starting, the developed torque increases until it reaches its maximum value T_{max} at the slip S_{max} . The speed of the motor continues to increase until it reaches the steady-state operating region (the shaded area) where the speed of the motor is constant and the developed torque of the motor is equal to the load torque.

Example 12.5

A 480 V, 60 Hz, three-phase, four-pole induction motor has the following parameters:

$$R_1 = 0.3 \Omega; R_2' = 0.2 \Omega; X_{eq} = 2.0 \Omega$$

At full load, the motor speed is 1760 rpm. Calculate the following:

1. Slip of the motor
2. Developed torque of the motor at full load
3. Developed power in horsepower
4. Rotor current as seen from the stator winding
5. Copper losses of the motor

Solution

1. The synchronous speed of the motor can be computed by using Equation 12.9:

$$n_s = 120 \frac{f}{p} = 120 \frac{60}{4} = 1800 \text{ rpm}$$

$$\omega_s = \frac{2\pi}{60} n_s = \frac{2\pi}{60} 1800 = 188.5 \text{ rad/s}$$

Using Equation 12.15, we can compute the slip of the motor:

$$S = \frac{n_s - n}{n_s} = \frac{1800 - 1760}{1800} = 0.0222$$

2. Equation 12.49 or Equation 12.50 can be used to compute the load torque:

$$T_d = \frac{3V^2 R_2'}{S \omega_s \left[\left(R_1 + \frac{R_2'}{S} \right)^2 + X_{eq}^2 \right]} = \frac{3 \left(\frac{480}{\sqrt{3}} \right)^2 0.2}{0.0222 \times 188.5 \left[\left(0.3 + \frac{0.2}{0.0222} \right)^2 + 4 \right]} = 121.56 \text{ Nm}$$

3. The angular speed of the motor is

$$\omega = \frac{2\pi}{60} n = \frac{2\pi}{60} 1760 = 184.3 \text{ rad/s}$$

The developed power of the motor is

$$P_d = T_d \omega = 121.56 \times 184.3 = 22.4 \text{ kW}$$

The developed power in hp unit is

$$P_d = 22.4 \times 1.34 = 30 \text{ hp}$$

4. The rotor current can be computed using Equation 12.46:

$$I_2' = \frac{V}{\sqrt{\left(R_1 + \frac{R_2'}{S}\right)^2 + X_{eq}^2}} = \frac{\frac{480}{\sqrt{3}}}{\sqrt{\left(0.3 + \frac{0.2}{0.0222}\right)^2 + 4}} = 29.1 \text{ A}$$

5. The copper losses of the motor are in the stator and rotor windings, that is,

$$P_{cu} = P_{cu1} + P_{cu2} = 3(I_2')^2 R_{eq} = 3 \times (29.1)^2 (0.3 + 0.2) = 1.27 \text{ kW}$$

12.2.5 STARTING TORQUE AND STARTING CURRENT

At starting, the speed of the motor is zero and $S=1$. Substituting these values either in Equation 12.49 or 12.50 yields the starting torque T_{st} :

$$T_{st} = \frac{3V^2 R_2'}{\omega_s \left[(R_1 + R_2')^2 + X_{eq}^2 \right]} = \frac{3V^2 R_2'}{\omega_s Z_{eq}^2} \quad (12.51)$$

where

$$Z_{eq} = \sqrt{(R_1 + R_2')^2 + X_{eq}^2} = \sqrt{R_{eq}^2 + X_{eq}^2} \quad (12.52)$$

The starting current of the motor I_{st} can be computed using Equation 12.46 when $S=1$:

$$I_{st}' = \frac{V}{\sqrt{(R_1 + R_2')^2 + X_{eq}^2}} = \frac{V}{Z_{eq}} \quad (12.53)$$

Example 12.6

For the motor in Example 12.5, compute the following:

- Starting torque
- Starting current
- Ratio of the starting torque to the full load torque
- Ratio of the starting current to the full load current

Solution

a. The starting torque can be computed using Equation 12.51:

$$T_{st} = \frac{3V^2 R_2'}{\omega_s Z_{eq}^2} = \frac{480^2 \times 0.2}{188.5(0.5^2 + 4)} = 57.52 \text{ Nm}$$

b. Using Equation 12.53, we can compute the starting current:

$$I'_{st} = \frac{V}{Z_{eq}} = \frac{\frac{480}{\sqrt{3}}}{\sqrt{0.5^2 + 4}} = 134.42 \text{ A}$$

c. The full load torque computed in Example 12.5 is 121.46 Nm. The ratio of the starting torque to the full load torque is

$$\frac{T_{st}}{T_d} = \frac{57.52}{121.56} = 0.473$$

As seen, the starting torque is less than half the full load torque. Heavily loaded induction motors may not start with low starting torques. In the following sections, we shall discuss some techniques to increase the starting torque.

d. The full load current computed in Example 12.5 is 29.1 A. The ratio of the starting current to the full load current is

$$\frac{I_{st}}{I_2} = \frac{134.42}{29.1} = 4.61$$

The starting current of this motor is more than four times the rated current. This excessive current could damage the motor. In the next sections, we shall discuss methods by which the starting current can be reduced.

12.2.6 MAXIMUM TORQUE

The maximum torque of the induction motor can be computed by setting the derivative of the torque equation with respect to the slip to zero. The slip that satisfies Equation 12.54 is the slip at the maximum torque S_{\max} :

$$\frac{dT_d}{dS} = 0; \quad S \Rightarrow S_{\max} \quad (12.54)$$

$$(R_1^2 + X_{eq}^2)S_{\max}^2 - (R_2')^2 = 0$$

Hence,

$$S_{\max} = \frac{R_2'}{\sqrt{R_1^2 + X_{eq}^2}} \quad (12.55)$$

Substituting the value of S_{\max} into Equation 12.49 leads to the maximum torque of the motor:

$$T_{\max} = \frac{3V^2}{2\omega_s \left(R_1 + \sqrt{R_1^2 + X_{eq}^2} \right)} \quad (12.56)$$

Example 12.7

For the motor in Example 12.5, compute the following:

- Slip at maximum torque
- Speed at maximum torque
- Maximum torque
- Ratio of the maximum torque to the full load torque
- Current at the maximum torque

Solution

$$a. \quad S_{\max} = \frac{R_2'}{\sqrt{R_1^2 + X_{eq}^2}} = \frac{0.2}{\sqrt{0.3^2 + 4}} = 0.0989$$

- b. Using Equation 12.48, we can compute the speed at maximum torque:

$$n = n_s(1 - S_{\max}) = 1800(1 - 0.0989) = 1621.98 \text{ rpm}$$

- c. Using Equation 12.56, we can compute the maximum torque:

$$T_{\max} = \frac{3V^2}{2\omega_s \left[R_1 + \sqrt{R_1^2 + X_{eq}^2} \right]} = \frac{480^2}{2 \times 188.5 \left[0.3 + \sqrt{0.3^2 + 4} \right]} = 263.16 \text{ Nm}$$

- d. The full load torque computed in Example 12.5 is 121.46 Nm. The ratio of the maximum torque to the full load torque is

$$\frac{T_{\max}}{T_d} = \frac{263.16}{121.56} = 2.165$$

The maximum torque is larger than the full load torque.

- e. The rotor current at S_{\max} can be computed using Equation 12.46:

$$I_2' = \frac{V}{\sqrt{\left(R_1 + \frac{R_2'}{S_{\max}} \right)^2 + X_{eq}^2}} = \frac{\frac{480}{\sqrt{3}}}{\sqrt{\left(0.3 + \frac{0.2}{0.0989} \right)^2 + 4}} = 90.42 \text{ A}$$

The current at the maximum torque is smaller than the starting current, but is larger than the full load current.

12.2.7 STARTING METHODS

The induction motor has two problems during starting: the starting current is large and the starting torque is small. The large starting current can damage the rotor windings due to the excessive thermal heat inside the windings. The small starting torque may not be enough to start the motor under heavy loading conditions. As shown in Equation 12.53, the starting current can be reduced if we reduce the terminal voltage of the motor or increase its equivalent impedance Z_{eq} . These two methods are explored in the following sections.

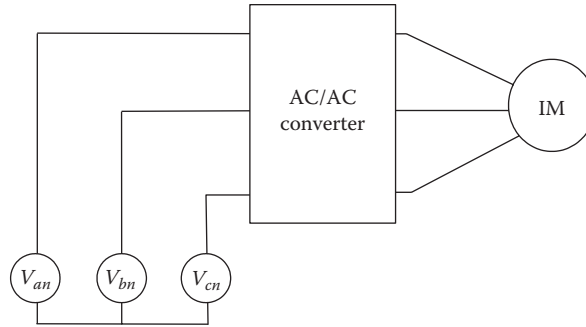


FIGURE 12.18 Voltage control of induction motor.

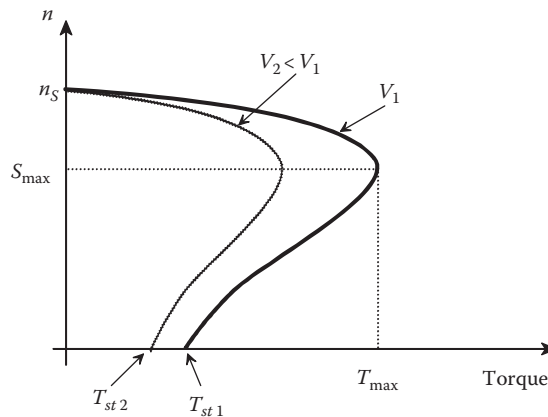


FIGURE 12.19 Speed–torque characteristics at different voltage levels.

12.2.7.1 Voltage Reduction

If an ac/ac converter is used to drive the induction motor as shown in Figure 12.18, the voltage across the motor at starting can be reduced, thus reducing the starting current. However, the reduction of the stator voltage can also reduce the starting torque and the maximum torque as shown in Figure 12.19 and explained by Equations 12.51 and 12.56; a 20% reduction in the stator voltage reduces the starting torque and the maximum torque by 36% each.

Example 12.8

For the motor in Example 12.5, compute the following:

- Terminal voltage that limit the starting current to twice the full load current
- Reduction in the starting torque
- Reduction in the maximum torque

Solution

- The full load current computed in Example 12.5 is 29.1 A. Hence, the starting current is limited to 58.2 A

$$I'_{st} = \frac{V_{st}}{Z_{eq}} = \frac{V_{st}}{\sqrt{0.5^2 + 4}} = 58.26 \text{ A}$$

where V_{st} is the reduced phase voltage at starting.

$$V_{st} = 120.11 \text{ V}$$

The line-to-line voltage at starting is $\sqrt{3} \times 120.11 = 208.05 \text{ V}$, which is about 43% of the rated voltage.

b. The starting torque can be computed using Equation 12.51:

$$T_{st} = \frac{3 V_{st}^2 R_2'}{\omega_s Z_{eq}^2} = \frac{208.05^2 \times 0.2}{188.5 (0.5^2 + 4)} = 10.81 \text{ Nm}$$

This starting torque is about 19% of the starting torque computed in Example 12.6 for the full voltage. Hence, the reduction in the starting torque is about 81%

c. Using Equation 12.56, we can compute the maximum torque for the new voltage:

$$T_{\max} = \frac{3 V_{st}^2}{2\omega_s [R_1 + \sqrt{R_1^2 + X_{eq}^2}]} = \frac{208.05^2}{2 \times 188.5 [0.3 + \sqrt{0.2^2 + 4}]} = 49.44 \text{ Nm}$$

This maximum torque is also about 19% of the maximum torque computed in Example 12.7 for the full voltage. The reduction is about 81%.

12.2.7.2 Insertion of Resistance

As seen in Example 12.8, the voltage reduction at starting reduces the starting current, which is desirable. However, the method leads to undesirable reduction in the starting torque. Therefore, the motor may produce less torque at starting than that needed by the load. To address this problem, we should use other methods that can increase the starting torque while reducing the starting current. One of these methods is based on increasing the rotor resistance. For the squirrel cage rotor, the windings can be designed from material that exhibits skin effects at the frequency of the source voltage, thus increasing its resistance at starting only. When the rotor speed is close to the full load speed, the rotor frequency is very low, thus no skin effect is present. For the slip ring motor, the rotor windings are accessible from the stator through the slip-ring mechanism shown in Figure 12.7. Thus an external resistance can be added to the rotor circuit at starting as shown in Figure 12.20. In either type of motors, when the rotor resistance increases, the starting current decreases as shown in Equation 12.53. But how do the starting and maximum torques change? Upon the first examination

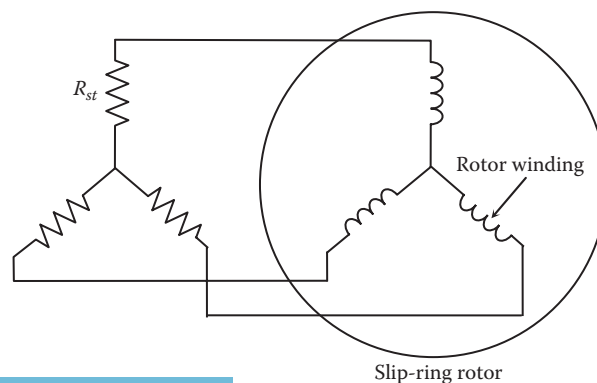


FIGURE 12.20 Starting of induction motor by inserting a resistance in the rotor circuit.

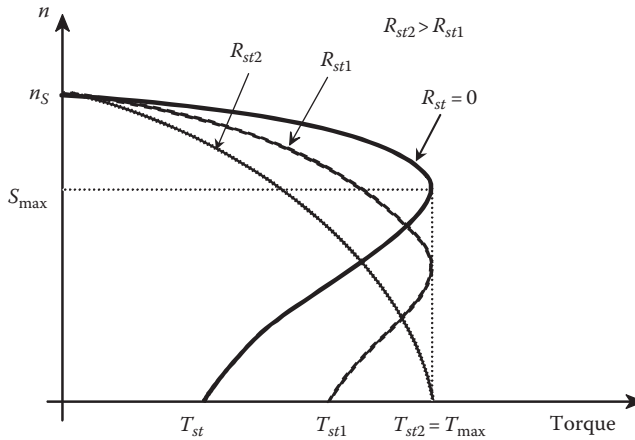


FIGURE 12.21 Speed–torque characteristics when a resistance is added to the rotor circuit.

of Equation 12.51, it is hard to tell whether the increase in the rotor resistance would increase the starting torque. However, because most machines have their $R_{eq}^2 \ll X_{eq}^2$, we can approximate the starting torque equation as

$$T_{st} = \frac{3V^2 R_2'}{\omega_s [(R_1 + R_2')^2 + X_{eq}^2]} \approx \frac{3V^2 R_2'}{\omega_s X_{eq}^2} \tag{12.57}$$

Now, it is obvious that the increase in the rotor resistance would result in an increase in the starting torque. This is another desirable feature. The maximum torque, as shown in Equation 12.56, is unaffected by the increase in the rotor resistance. However, the slip at maximum torque S_{max} in Equation 12.55 increases when the rotor resistance is increased. This means that the maximum torque occurs at lower speeds. In fact, if enough resistance is added to the rotor circuit so that $S_{max} = 1$, the starting torque is equal to the maximum torque of the motor as shown in Figure 12.21.

Example 12.9

For the motor in Example 12.5, compute the following:

- a. Resistance that should be added to the rotor circuit to achieve the maximum torque at starting
- b. Starting current

Solution

- a. To compute the value of the inserted resistance in the rotor circuit to achieve the maximum torque at starting, we set the maximum slip in Equation 12.55 to 1.

$$S_{max} = \frac{R_2' + R_{st}'}{\sqrt{R_1^2 + X_{eq}^2}} = 1$$

Hence,

$$R_{st}' = \sqrt{R_1^2 + X_{eq}^2} - R_2' = \sqrt{0.3^2 + 4} - 0.2 = 1.822 \Omega$$

This is the starting resistance referred to the stator circuit. The actual rotor resistance can be computed if we know the turns ratio of the motor windings.

- b. The starting current in Equation 12.53 can be modified to include the starting resistance in the rotor circuit

$$I'_{st} = \frac{V}{\sqrt{(R_1 + (R'_2 + R'_{st}))^2 + X_{eq}^2}} = \frac{\frac{480}{\sqrt{3}}}{\sqrt{(0.3 + (0.2 + 1.822))^2 + 4}} = 90.42 \text{ A}$$

Comparing this starting current to that computed in Example 12.6, you will find that the starting current is decreased because of the insertion of the starting resistance.

12.3 LINEAR INDUCTION MOTOR

The *linear induction motors* (LIMs) are very effective drive mechanisms for transportation and actuation systems. High-power LIMs are used in rapid transportations, baggage handling systems, conveyors, crane drives, theme park rides, and flexible manufacturing systems. Low-power ones are used in robotics, gate controls, guided trajectories (e.g., aluminum can propulsion), and stage and curtain movements. NASA envisions the use of such motors in launching spacecrafts in the future. LIMs come in two general designs: *wheeled linear induction motor* (WLIM) and *magnetically levitated linear induction motor* (Maglev). The Maglev technology, which was developed in 1934 by Hermann Kemper, is becoming popular for high-speed transportation. Some of the LIM applications are shown in Figure 12.22.



Roller coaster



Maglev launcher
(courtesy of NASA Marshall Space Flight Center)



Maglev rapid transportation
(images are courtesy of Transrapid International)

FIGURE 12.22 Example of linear induction motors applications.

12.3.1 WHEELED LINEAR INDUCTION MOTOR

The LIM is similar to the rotating induction motor except that the LIM has a flat structure instead of the cylindrical structure of the rotating motor. Consider the rotating induction motor on the left side of Figure 12.23. If you imagine that we can cut the motor along the dashed line and flatten the machine, we will get the wheeled linear motor (WLIM) on the right side of the figure, which can now be used to propel a train. In this case, the rotor is the track of the train, and the stator is the train's engine. The stator of the LIM is called *primary circuit*, and the rotor is called *secondary circuit*. In rotating motors, the separation between the rotor and stator is maintained by the ball bearings of the rotor's shaft. In WLIMs, the separation is maintained by the wheels of the train.

For the rotating induction motors on the left side of Figure 12.24, when the stator is anchored and the rotor is allowed to rotate freely, the speed of the rotor is in the same direction as the speed of the magnetic field. However, if you hold the rotor stationary and allow the stator to spin, the stator rotates in the direction opposite to the synchronous speed of the field as shown on the right side of Figure 12.24. Similarly, for the LIM, the primary circuit moves opposite to the synchronous speed of the field.

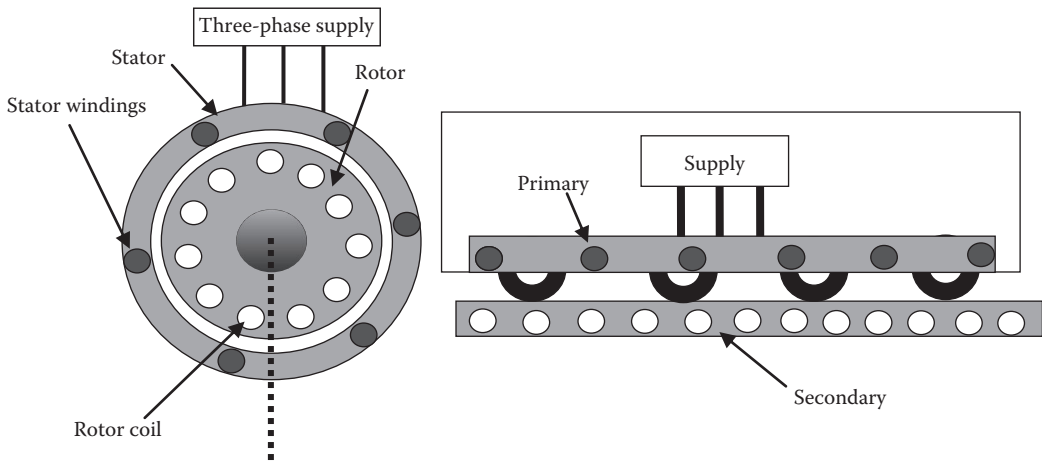


FIGURE 12.23 Wheeled linear induction motor.

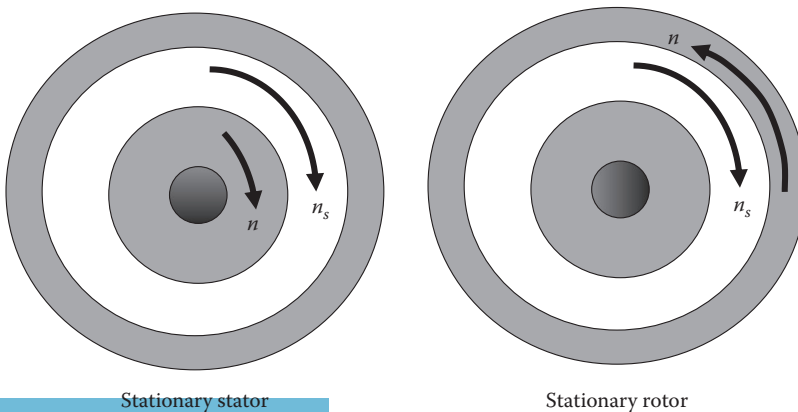


FIGURE 12.24 Relative speed of rotating induction motor.

The synchronous speed of the rotating field of the rotating induction motor is given in Equation 12.9. The linear synchronous speed v_s of this rotating field at any point located along the inner surface of the stator is

$$v_s = \omega_s r = \left(\frac{2\pi}{60} n_s \right) r = \left(\frac{2\pi}{60} \frac{120f}{p} \right) r = 2 \left(\frac{2\pi r}{p} \right) f = 2\tau_p f \tag{12.58}$$

where

- r is the inner radius of the stator (m), Figure 12.25
- n_s is the synchronous speed of the field in rpm
- ω_s is the synchronous speed of the field in rad/s
- τ_p is the pole pitch

The pole pitch is the circumference of the inner circle of the stator divided by the number of poles. This is the separation between $a-a'$, $b-b'$, or $c-c'$ as shown in Figure 12.25.

Let us consider the train that is powered by the WLIM in Figure 12.26. The primary windings are mounted under the floor of the train's compartment which is called *bogie*. The secondary windings are

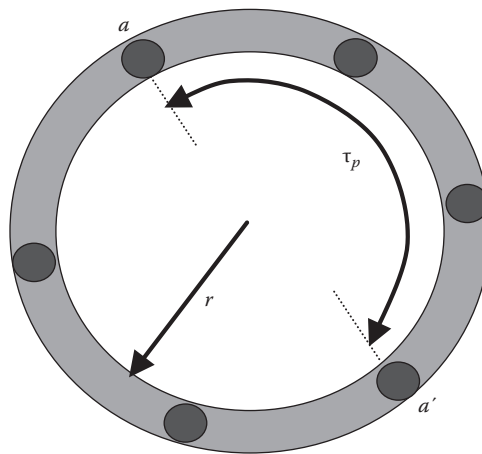


FIGURE 12.25 Pole pitch of motor.

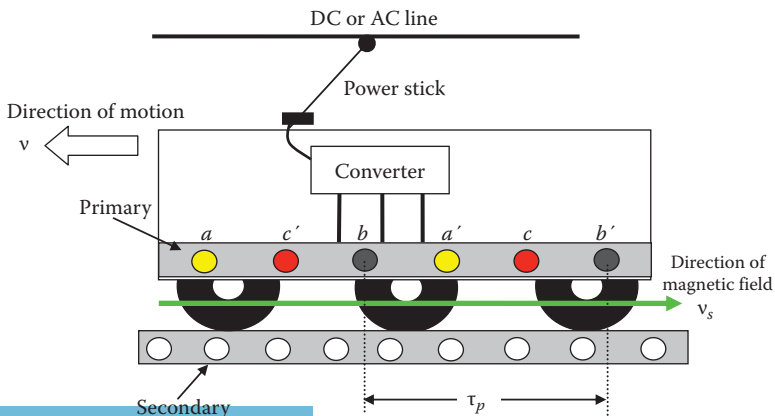


FIGURE 12.26 Motion of linear induction motor.

consist of metal alloy bars embedded along the track's guideway and are perpendicular to the track. They are called *reaction plates*. The length of the secondary circuit is the length of the track itself. The train is energized through a power line alongside the track or above it. The power line can either be direct current (dc) or alternating current (ac). The train taps its energy from the power line through brushes that are always in contact with the line. A converter is mounted on the vehicle to convert the waveform of the power line into balanced multiphase waveforms with variable voltage and frequency.

The three-phase current of the LIM produces a magnetic field traveling in the direction shown in Figure 12.26. The speed of this magnetic field is given in Equation 12.58. The train itself moves opposite to the direction of the magnetic field as explained earlier. The pole pitch of the LIM is the distance between the opposite poles of any winding; that is the distance between a and a' .

The equivalent circuit of the LIM is basically the same as that for the rotating induction motor in Figure 12.15. One key difference is that the resistance of the secondary winding of the LIM is made larger than the rotor resistance of the rotating motor. This way, the motor develops a large torque at starting.

In linear motion analysis, force is used instead of torque. The developed force of the LIM F_d is also known as *thrust* of the motor. It can be computed from the developed torque in Equation 12.49, but modified for a linear motion where angular velocities are replaced by linear speeds

$$P_d = \frac{3V^2 R_2' v}{S v_s \left[\left(R_1 + \frac{R_2'}{S} \right)^2 + X_{eq}^2 \right]} \quad (12.59)$$

where

v is the actual speed of the train

v_s is the synchronous speed of the magnetic field

The slip S is defined as

$$S = \frac{v_s - v}{v_s} \quad (12.60)$$

In linear motion, the developed power in the mechanical form is the force multiplied by the speed:

$$P_d = F_d v \quad (12.61)$$

Substituting Equation 12.61 into (12.59), we can compute the thrust of the LIM:

$$F_d = \frac{P_d}{v} = \frac{3V^2 R_2'}{S v_s \left[\left(R_1 + \frac{R_2'}{S} \right)^2 + X_{eq}^2 \right]} \quad (12.62)$$

The speed–thrust characteristic of the LIM is shown in Figure 12.27. The developed thrust must compensate for three main components: the friction between the wheels and the track, the drag force, and the acceleration/deceleration force. For steady-state speed, the third component is zero.

The friction force $F_{friction}$ is a function of the normal force F_{normal} on the track

$$F_{friction} = \mu F_{normal} \quad (12.63)$$

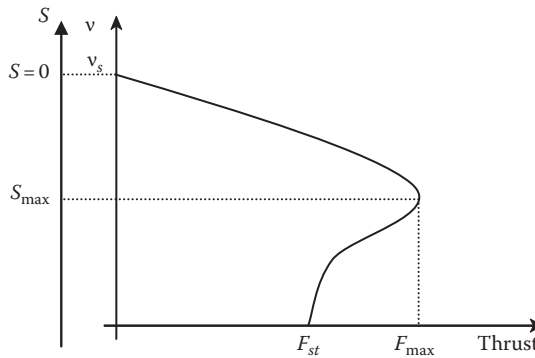


FIGURE 12.27 Speed–thrust of LIM.

where μ is the coefficient of friction between the wheels and the track. For a leveled track, the normal force is the weight of the vehicle

$$F_{normal} = mg \tag{12.64}$$

where

- m is the mass of the moving vehicle
- g is the acceleration of gravity (9.81 m/s^2)

For an inclined track, the normal force is the component of the weight that is perpendicular to the track

$$F_{normal} = mg \cos \theta \tag{12.65}$$

where θ is the inclination angle of the track. Example 12.12 deals with an inclined track.

The air drag force, which slows down the moving vehicle, is due to many factors such as the frontal area of the vehicle, the shape of the vehicle, the velocity of the vehicle, and the air density. The air drag force F_{air} can be computed by

$$F_{air} = 0.5 \delta v^2 A C_d \tag{12.66}$$

where

- δ is the air density (about 1 kg/m^3)
- v is the velocity of the vehicle (m/s)
- A is the frontal area of the vehicle that is perpendicular to the air flow (m^2)
- C_d is the coefficient of drag that depends on the shape of the frontal area of the vehicle

C_d can be about 1 for train, 0.4 for roller coaster, and 0.5 for a typical passenger car.

Example 12.10

A train with wheeled LIM is traveling at 100 km/h . The frontal area of the train is 20 m^2 and the coefficient of its drag is 0.8. The friction coefficient between the wheels of the train and the track is 0.05, and the weight of the train is $100,000 \text{ kg}$. Compute the thrust of the motor at steady-state. Also compute the developed power of the motor in horsepower.

Solution

At steady-state, the induction motor produces enough thrust to compensate for the friction force plus the drag force. The frictional force is computed based on the normal force of the vehicle and the coefficient of friction μ .

$$F_{normal} = mg = 105 \times 9.81 = 981 \text{ kN}$$

$$F_{friction} = \mu F_{normal} = 0.05 \times 981 = 49 \text{ kN}$$

The drag force can be computed using Equation 12.66:

$$F_{air} = 0.5 \delta v^2 A C_d = 0.5 \times 1 \times \left(100 \times \frac{1000}{3600}\right)^2 \times 20 \times 0.8 = 6.174 \text{ kN}$$

The developed force is the sum of the frictional force and the drag force:

$$F_d = F_{friction} + F_{air} = 49 + 6.174 = 55.174 \text{ kN}$$

The developed power of the LIM is

$$P_d = F_d v = 55.174 \times 27.78 = 1532.7 \text{ kW}$$

$$P_d = 1532.7 \times 1.34 = 2054 \text{ hp}$$

Example 12.11

A vehicle with WLIM has a mass of 4000 kg. The friction coefficient between the wheels of the vehicle and the track is 0.05. The pole pitch of the vehicle is 3 m. At steady-state, the slip of the motor is 0.1 when the frequency of the primary windings is 10 Hz. Assume that the drag force at steady-state is 5000 N. Compute the developed power of the motor.

Solution

At steady-state, there is no acceleration, so the induction motor produces enough thrust to compensate for the friction force plus the drag force:

$$F_{normal} = mg = 4000 \times 9.81 = 39.28 \text{ kN}$$

$$F_{friction} = \mu F_{normal} = 0.05 \times 39.28 = 1.96 \text{ kN}$$

To compute the developed power, we need the speed of the vehicle. The synchronous speed of the magnetic field is

$$v_s = 2\tau_p f = 2 \times 3 \times 10 = 60 \text{ m/s}$$

Hence, the speed of the vehicle is

$$v = v_s(1 - S) = 60(1 - 0.1) = 54 \text{ m/s}$$

The developed power is

$$P_d = F_d v = (F_{friction} + F_{air})v = (1.96 + 5000) \times 54 = 375.84 \text{ kW}$$

The equations for the maximum developed force (maximum thrust) and the slip at maximum force for the LIM are the same as Equations 12.56 and 12.55 for the rotating motor:

$$S_{\max} = \frac{R_2'}{\sqrt{R_1^2 + X_{eq}^2}} \quad (12.67)$$

$$F_{\max} = \frac{3V^2}{2 v_s \left(R_1 + \sqrt{R_1^2 + X_{eq}^2} \right)} \quad (12.68)$$

For the LIM, the rotor resistance is higher than that for the rotating motor. Hence, S_{\max} for the linear motor is large and occurs near the starting region. This way, the linear motor develops enough thrust at starting to speed up the train even at heavy loading conditions. Therefore, a reasonable approximation is to assume that the speed–thrust characteristic of the motor is linear between the operating slip S and S_{\max} ; that is,

$$S = \frac{F_d}{F_{\max}} S_{\max} \quad (12.69)$$

Example 12.12

A theme ride vehicle is moving uphill at a constant speed. The slope of the hill is 10° . The mass of the vehicle plus the riders is 2000 kg. The vehicle is powered by a WLIM. The pole pitch of the motor is 0.5 m. The friction coefficient of the surface is 0.01. The primary circuit resistance R_1 is 0.5Ω , and the secondary resistance referred to the primary circuit R_2' is 1.0Ω . The equivalent inductance of the primary and secondary circuits is 0.01 H. The line-to-line voltage of the primary windings of the motor is 480 V, and its frequency is 15 Hz. Assume the drag force is 500 N. Compute the speed of the vehicle.

Solution

The system can be described by Figure 12.28. The weight of the vehicle is resolved into two components, one normal to the road surface F_{normal} and the other F_g parallel to the road surface, pulling the vehicle down due to gravity. F_{normal} produces the frictional force $F_{friction}$.

$$F_d = F_g + F_{friction} + F_{air}$$

$$F_{normal} = m g \cos \theta = 2000 \times 9.81 \times \cos 10 = 1.93 \times 10^4 \text{ N}$$

$$F_{friction} = \mu F_{normal} = 0.01 \times 1.93 \times 10^4 = 193 \text{ N}$$

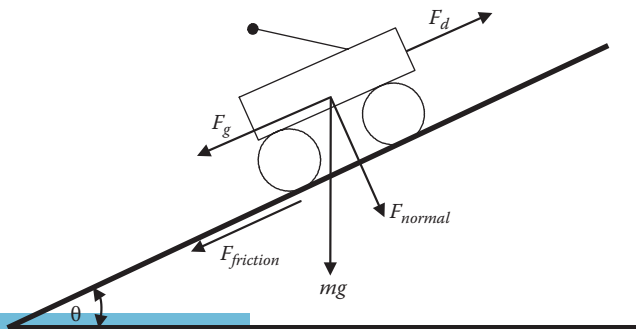


FIGURE 12.28 Force vectors of vehicle moving uphill.

$$F_g = m g \sin \theta = 2000 \times 9.81 \times \sin 10 = 3.403 \times 10^3 \text{ N}$$

$$F_d = F_g + F_{friction} + F_{air} = 4.097 \text{ kN}$$

The synchronous speed of the motor is

$$v_s = 2 \tau_p f = 2 \times 0.5 \times 15 = 15 \text{ m/s}$$

The motor speed can be computed using the relationship in Equation 12.69. But first, let us compute the maximum force and the slip at maximum force:

$$S_{\max} = \frac{R_2'}{\sqrt{R_1^2 + X_{eq}^2}} = \frac{1.0}{\sqrt{0.5^2 + (2\pi \times 15 \times 0.01)^2}} = 0.9373$$

$$F_{\max} = \frac{3V^2}{2v_s \left[R_1 + \sqrt{R_1^2 + X_{eq}^2} \right]} = \frac{480^2}{2 \times 15 \left[0.5 + \sqrt{0.5^2 + (2\pi \times 15 \times 0.01)^2} \right]} = 4.901 \text{ kN}$$

Now, we have the information needed to compute the slip of the motor:

$$S = \frac{F_d}{F_{\max}} S_{\max} = \frac{4.097}{4.901} 0.9373 = 0.784$$

Hence, the speed of the vehicle is

$$v = v_s(1 - S) = 15(1 - 0.784) = 3.24 \text{ m/s or } 11.66 \text{ km/h}$$

12.3.2 MAGNETICALLY LEVITATED INDUCTION MOTOR

One of the main limitations of the WLIM is the friction between the wheels and the track. Besides the extra power consumption, the friction limits the maximum speed of the vehicle as well as its maximum acceleration and deceleration.

The magnetically levitated induction motor (Maglev) allows the vehicle to magnetically levitate with virtually no friction between the bogie of the vehicle (undercarriage) and the track. The technology is based on having magnetic poles on the track that are similar to the magnetic poles on the bogie of the vehicle (both are North or South). These poles repel each other and the bogie then levitates. Hence, a Maglev train can achieve very high speeds and very smooth rides because the vehicle essentially flies. In addition, the Maglev trains can climb steep hills that regular trains cannot reach. With the current technology, a Maglev train can speed up to 600 km/h, which is much faster than any other ground transportation system. The travel time of a medium trip (1000 km) on a Maglev train is essentially equal to the travel time of the airplane when you include the check-in time at the airport as well as the taxing time of the airplane. There are two types of Maglev systems: *levitation* and *propulsion*. In both systems, magnetic force is developed along the track to repel the bogie of the vehicle. This is done in various ways; one of them is to install magnetic coils along the track as shown in Figure 12.29. These coils are excited by a separate source when the vehicle approaches them, thus keeping the vehicle levitated along the track. This system, however, is suitable for short tracks as the excitation of long tracks is expensive and difficult to implement. Another alternative is to induce voltage in the coils of the track by the vehicle itself. When the vehicle moves over a coil in the track, the electric magnets installed in the bogie are switched on to induce a voltage on the coil of the track. If the track coil is wound in the direction that creates poles with similar polarity to the magnetic poles at the bottom of the bogie's magnets, a repulsive force is created that levitates the vehicle.

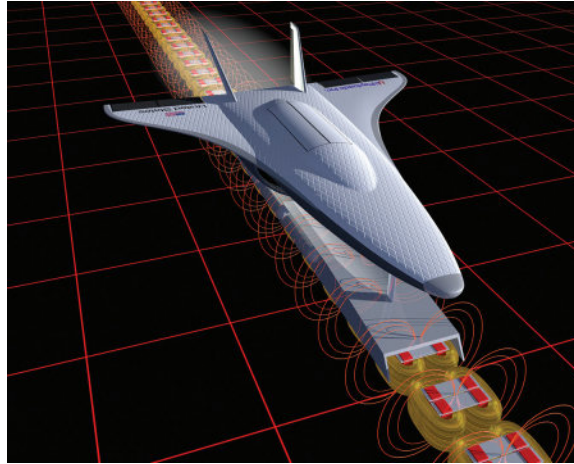


FIGURE 12.29 Concept of Maglev for space launcher. (Courtesy of NASA Marshall Space Flight Center, Huntsville, AL.)

For the propulsion Maglev, the magnetic force of the track coils propels the vehicle along the track in addition to lifting the bogie. To understand this, assume that you have two magnets on top of each other with their similar poles facing each other. The top magnet will levitate due to the magnetic lifting force. Now, fix the bottom magnet to a table and keep the top magnet at constant vertical distance but free to move horizontally. In this case, a repulsion force will move the top magnet horizontally. Hence, we have achieved levitation and propulsion at the same time. The Maglev propulsion is created by switching the magnets of the bogie as they leave track coils.

Besides ground transportation, the U.S. Sandia National Laboratories developed the Maglev technology for high-power, high thrust military applications. The Maglev is also developed for satellite launchers where the spacecraft accelerates to 1000 km/h at the end of the track, causing it to take off like an airplane. While airborne, the spacecraft uses conventional rocket engines to reach its orbit.

12.4 INDUCTION GENERATOR

Induction generator is widely used in wind energy and other renewable energy systems. This is because the machine is simple and less expensive than other types. It is easier to synchronize with the grid than synchronous generators.

The model for the induction generator is the same as the one for the induction motor in Figure 12.15. Keep in mind that the developed resistance R_d represents the conversion from electrical to mechanical powers and vice versa. In motor operation, the machine rotates below the synchronous speed. Hence, the slip is positive and the developed resistance is positive as well. When the resistance is positive, it consumes electric power. In this case, R_d acquires electric power from the grid and converts it into mechanical power. When the shaft of the machine is forced to rotate above its synchronous speed by external mechanical system (such as wind turbine), the slip of the machine is negative. Hence, R_d is also negative. Negative resistance produces electric power. Hence, R_d acquires mechanical power from the turbine blades and delivers electrical power to the grid. This is a generator operation.

If we expand the speed–torque characteristic of the induction machine based on Equation 12.49 to include the negative slip, we get the characteristics in Figure 12.30. When the speed of the machine n is below its synchronous speed n_s , the machine operates in the first quadrant; this is the motor operation. When the speed of the machine is above the synchronous speed (negative slip), the machine operates in the second quadrant where the torque is reversed while the speed is still in the same direction of rotation. Since the power is torque multiplied by angular speed, the power in the first quadrant is positive (motor operation) and that for the second quadrant is negative (generator operation).

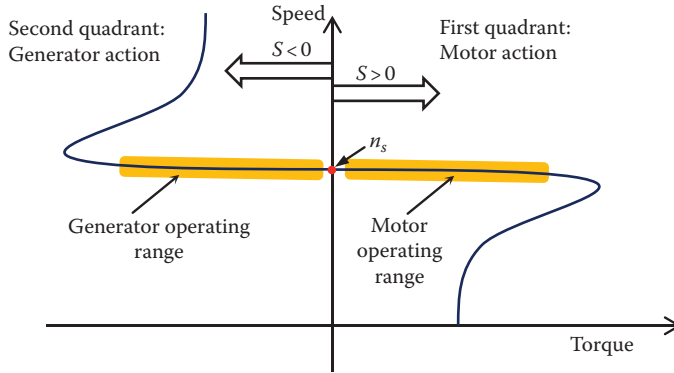


FIGURE 12.30 Speed–torque characteristics of induction machine.

The range of the operating speed in the first or second quadrant is very limited as shown in Figure 12.30. A large change in torque does not cause the machine to change its speed by much. This is why the induction machine is considered almost fixed speed machine.

When the machine operates in the second quadrant, the developed power is negative when we use the generic model in Figure 12.15. Alternatively, we can use the generator model in Figure 12.31 where we reverse the flow in the windings to represent the generator mode, and replace the developed resistance by a power source whose voltage is V_d . To maintain the polarity of the voltage across the developed resistance unchanged, the developed voltage V_d is then

$$V_d = -I_2' \frac{R_2'}{S} (1 - S) \tag{12.70}$$

In the generator model, we do not have to worry about the sign of power if we consider the flow of power is always from V_d to V . This makes all powers positive. The power flow of the induction generator is shown in Figure 12.32. The input power is mechanical P_m . Part of this power is lost due to rotational losses and the rest is the developed power P_d .

$$P_d = 3V_d I_2' = -3(I_2')^2 \frac{R_2'}{S} (1 - S) \tag{12.71}$$

where V_d and I_2' are phase quantities.

The developed resistance has two components, one of them is the actual resistance of the rotor winding R_2' :

$$R_d = \frac{R_2'}{S} (1 - S) = \frac{R_2'}{S} - R_2' \tag{12.72}$$

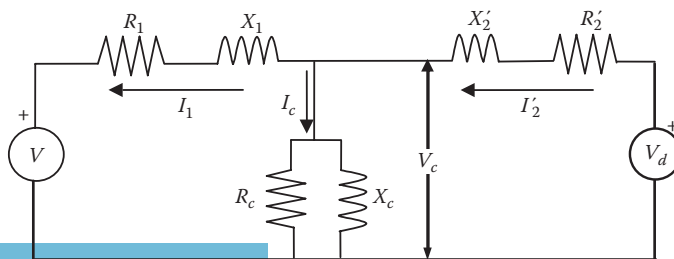


FIGURE 12.31 Induction machine model.

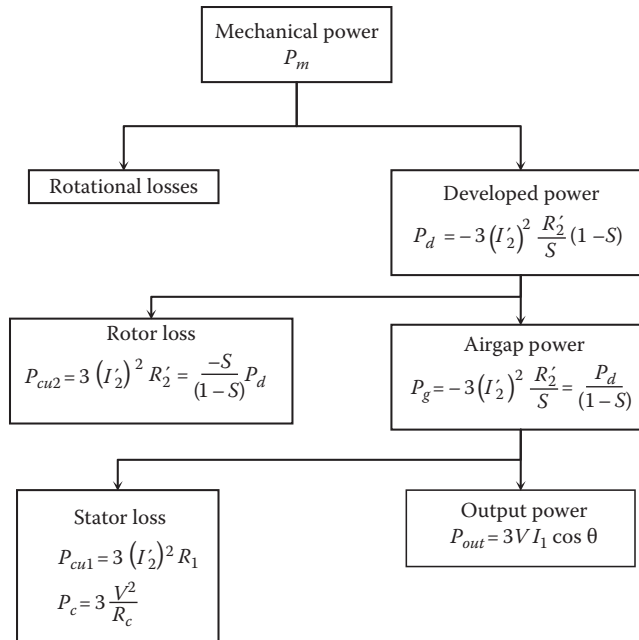


FIGURE 12.32 Power flow of induction generator.

The loss in the rotor resistance P_{cu2} represents the loss of the rotor windings. This is known as *copper loss* of the rotor (the windings are made of copper material). For three-phase machine, P_{cu2} is

$$P_{cu2} = 3(I_2')^2 R_2' \tag{12.73}$$

The power that travels through the airgap to the stator is the developed power minus the rotor copper losses. This is known as *airgap power* P_g :

$$P_g = P_d - P_{cu2} = -3(I_2')^2 \frac{R_2'}{S} \tag{12.74}$$

After the airgap power enters the stator, part of the power is lost in the stator and the rest is delivered to the grid. The stator losses include loss in the stator windings P_{cu1} and loss in the iron core P_c :

$$P_{cu1} = 3(I_1')^2 R_1$$

$$P_c = 3 \frac{V_c^2}{R_c} \tag{12.75}$$

The output power of the generator is

$$P_{out} = 3V I_1 \cos \theta \tag{12.76}$$

where θ is the power factor angle at the terminals of the generator.

If we consider a wind turbine system, the mechanical power of the generator P_m is the power captured by the blades of the turbine P_{blade} . The turbine has two efficiencies: mechanical efficiency

η_m and electrical efficiency η_e . The mechanical efficiency gives the share of the blade power that is converted into developed power. The rest of the power is rotational losses, friction, windage, etc.:

$$\eta_m = \frac{P_d}{P_{blade}} \quad (12.77)$$

The electrical efficiency provides the amount of developed power that is delivered to the grid. The rest are electrical losses in the machine windings and core:

$$\eta_e = \frac{P_{out}}{P_d} \quad (12.78)$$

The total wind turbine efficiency η_t gives the amount of blade power that is delivered to the grid:

$$\eta_t = \frac{P_{out}}{P_{blade}} = \eta_m \eta_e \quad (12.79)$$

The total system efficiency η_{total} provides the amount of wind power P_w that is delivered to the grid

$$\eta_{total} = \frac{P_{out}}{P_w} = C_p \eta_m \eta_e \quad (12.80)$$

where C_p is the coefficient of performance of the turbine discussed in Chapter 6.

Example 12.13

A six-pole, 60Hz three-phase induction generator is receiving 1000hp on its shaft and is rotating at 1260rpm. The electrical efficiency of the generator is 95%. Ignore the rotational losses and compute the following:

- Slip of the generator
- Power delivered to the stator
- Output electric power of the generator
- Rotor copper loss
- Stator losses

Solution

- To compute the slip, we first need to compute the synchronous speed of the machine. The synchronous speed is given in Equation 12.9

$$n_s = 120 \frac{f}{p} = 120 \frac{60}{6} = 1200 \text{ rpm}$$

The slip is given in Equation 12.9

$$S = \frac{n_s - n}{n_s} = \frac{1200 - 1260}{1200} = -0.05$$

- The airgap power of the generator P_g is computed using the developed power:

$$P_d = 1000 \times 0.746 = 746 \text{ kW}$$

$$P_g = \frac{P_d}{(1 - S)} = \frac{746}{(1 + 0.05)} = 710.48 \text{ kW}$$

c. The output power of the generator using Equation 12.78 is

$$P_{out} = P_d \eta_e = 710.48 \times 0.95 = 674.96 \text{ kW}$$

d. Rotor copper loss is

$$P_{cu2} = P_d - P_g = P_d \frac{-S}{1-S} = 746 \frac{0.05}{1.05} = 35.52 \text{ kW}$$

e. Stator loss is

$$P_{loss1} = P_{cu1} + P_c = P_g - P_{out} = 710.46 - 674.96 = 35.5 \text{ kW}$$

Example 12.14

A wind turbine with ten-pole, 60 Hz three-phase, Y-connected induction generator is delivering 1 MW to the grid at 0.8 pf lagging. The terminal voltage of the generator is 690 V. The parameters of the machine are

$$R_1 = R'_2 = 0.02 \Omega; \quad X_{eq} = 0.1 \Omega$$

Ignore the core of the machine and the rotational losses. Compute the following:

- Stator current
- Airgap power
- Speed of the generator
- Developed voltage
- Developed power
- Efficiency of the generator

Solution

a. We can compute the stator current using the output power in Equation 12.76:

$$P_{out} = 3V I_1 \cos \theta$$

where V is the voltage of the grid

$$I_1 = \frac{10^6}{\sqrt{3} \times 690 \times 0.8} = 1045.92 \text{ A}$$

b. The airgap power is the output power plus the stator losses. Since we ignored the core, the airgap power is

$$P_g = P_{out} + 3I_1^2 R_1 = 10^6 + 3 \times 1045.92^2 \times 0.02 = 1.0656 \text{ MW}$$

c. To compute the speed of the generator, we need to compute the slip using Equation 12.74:

$$S = -3(I'_2)^2 \frac{R'_2}{P_g} = -3 \times 1045.92^2 \times \frac{0.02}{1.0656 \times 10^6} = -0.0616$$

The synchronous speed of the generator is

$$n_s = 120 \frac{f}{p} = 120 \frac{60}{10} = 720 \text{ rpm}$$

The speed of the generator is

$$n = n_s(1 - S) = 720 \times (1 + 0.0616) = 764.35 \text{ rpm}$$

d. The developed voltage is

$$\bar{V}_d = \bar{V} + \bar{I}_1(R_{eq} + jX_{eq})$$

where

$$\bar{I}_1 = 1045.92 \angle -\cos^{-1}(0.8) \text{ A}$$

Take the source voltage as a reference phasor. The phase quantity of the developed voltage is then

$$\bar{V}_d = \frac{690}{\sqrt{3}} \angle 0^\circ + 1045.92 \angle -36.87^\circ \times (0.04 + j0.1) = 498.05 \angle 6.75^\circ \text{ V}$$

e. The developed power is

$$P_d = 3V_d I_2' \cos \theta$$

Since we ignored the core, $I_2' = I_1$ and θ is the angle between the phase voltage V_d and the current I_1 :

$$\theta = 36.87^\circ + 6.75^\circ = 43.62^\circ$$

$$P_d = 3 \times 498.05 \times 1045.92 \cos(43.62^\circ) = 1.131 \text{ MW}$$

You can also compute the developed power by adding the losses to the output power.

f. The generator efficiency is

$$\eta = \frac{P_{out}}{P_{input}}$$

Since we ignored the rotational losses, the generator efficiency is

$$\eta = \frac{P_{out}}{P_d} = \frac{1.0}{1.131} = 88.4\%$$

12.5 SYNCHRONOUS GENERATOR

The synchronous generator is the most used machine for generating electricity. All power plants use synchronous generators to convert the mechanical power of the turbine into electrical power. Synchronous generators can have enormous capacity; a single generator can be built to produce over 2 GW of electric power. The large ones are used in nuclear power plants and major hydro plants such as China's Yangtze River Three Gorges Hydraulic Power Plant.

Figure 12.33 shows the stator of one of the synchronous generators in the Grand Coulee hydroelectric power plant on the Columbia River in Washington State. To put the size into perspective, the photograph on the right side shows part of the stator during the construction of the generator. The area in this photo is almost the same as the boxed area in the left side photo. Figure 12.34 shows the rotor of the same synchronous generator.

The main components of the synchronous generator are shown in Figure 12.35. The stator of the synchronous machine is similar to the stator of the induction motor; it consists of three-phase

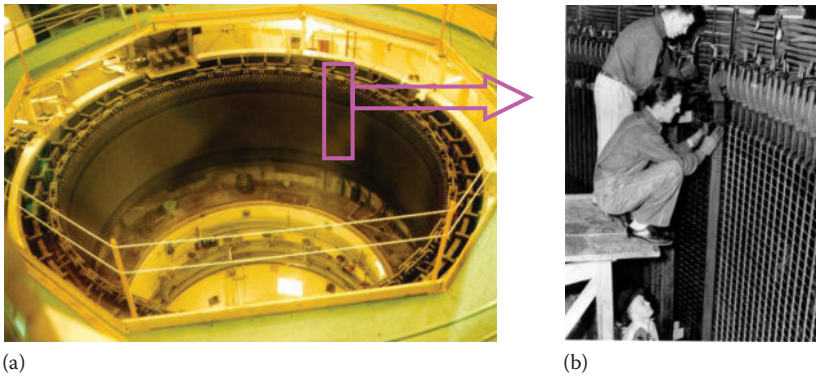


FIGURE 12.33 Stator of a synchronous generator in Grand Coulee Dam. (Courtesy of the U.S. Bureau of Reclamation, Washington, DC.)

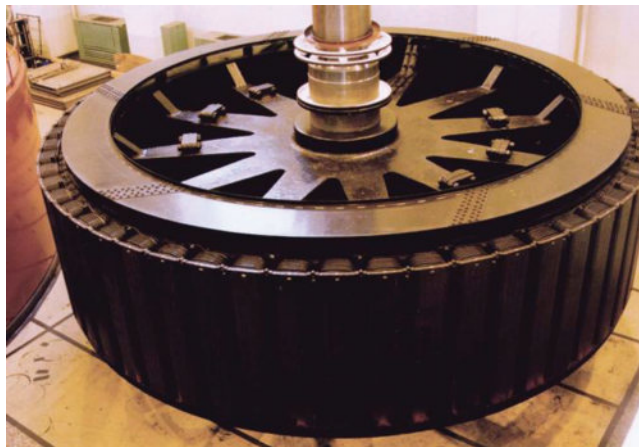


FIGURE 12.34 Rotor of a synchronous generator in Grand Coulee Dam. (Courtesy of the U.S. Bureau of Reclamation, Washington, DC.)

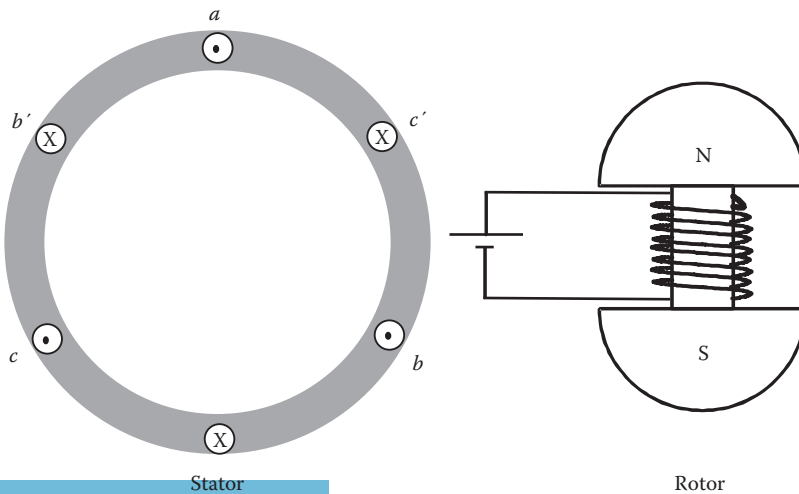


FIGURE 12.35 Basic components of synchronous generator.

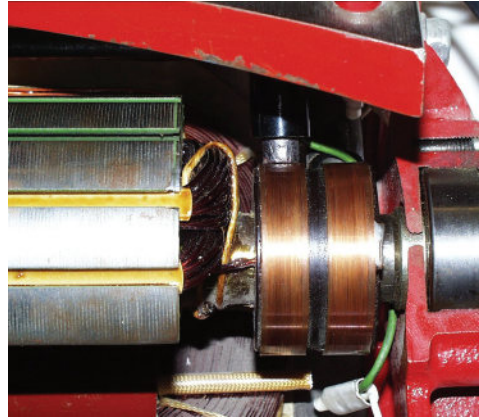


FIGURE 12.36 Slip-ring arrangement.

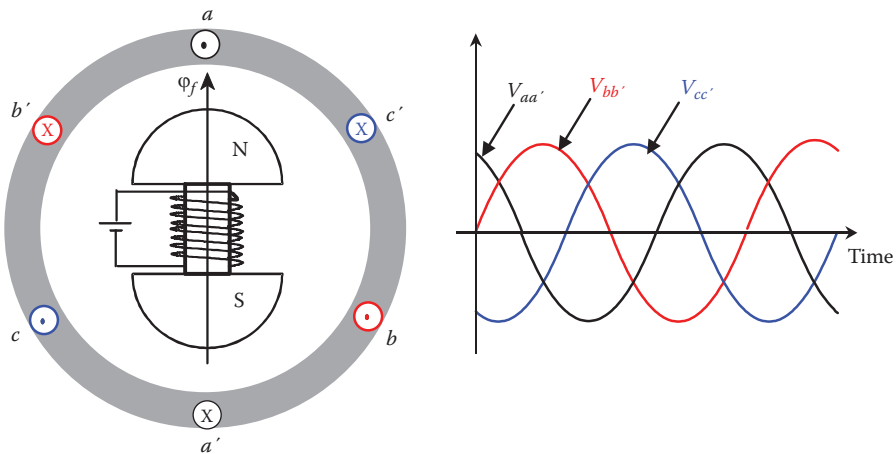


FIGURE 12.37 Three-phase voltage waveforms due to the clockwise rotation of the rotor magnet.

windings mounted symmetrically inside the stator core. The stator windings are also known as *armature windings*. The winding of the rotor of the synchronous machine is excited by an external dc source through a slip ring system similar to the one shown in Figure 12.36. The rotor winding, which is also known as *field winding* or *excitation winding*, produces a stationary flux with respect to the rotor; that is, the rotor is an electric magnet. The rotor is assembled inside the stator as shown on the left side of Figure 12.37. Two sets of ball bearings are used on both ends of the rotor to allow the rotor to spin freely inside the stator. The rotor of the synchronous generator is connected to a prime mover such as a hydro or thermal turbine. When the turbine spins the rotor of the synchronous generator, the magnetic field cuts the stator windings, thus inducing sinusoidal voltages across the stator windings. Since the three stator windings are equally spaced from each other, the induced voltages across the phase windings are shifted by 120° from each other as shown on the right side of Figure 12.37. The frequency of the induced voltage is dependent on the speed of the rotor. The relationship between the speed of the magnetic field and the frequency of the induced voltage is given in Equation 12.9. Hence, to maintain the frequency of the induced voltage at 60Hz, the rotor speed must be n_s , where

$$n_s = 120 \frac{f}{p} = \frac{7200}{p} \tag{12.81}$$

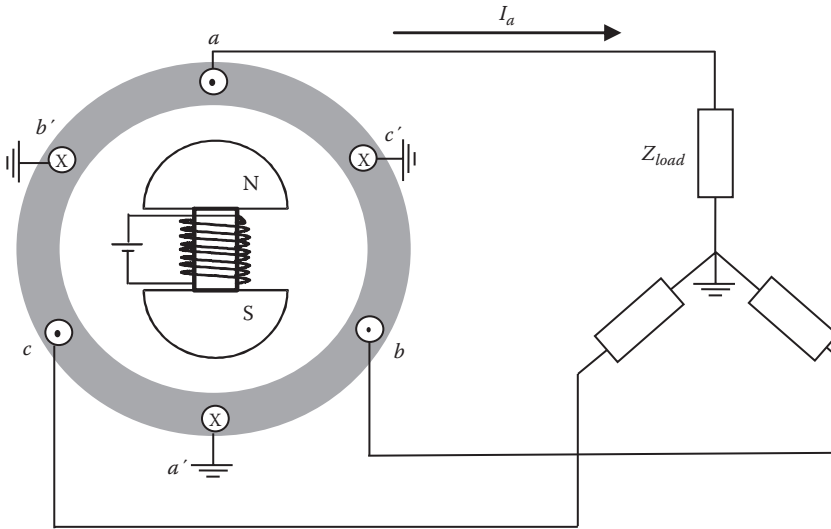


FIGURE 12.38 Loaded synchronous generator.

Any slight variation in this synchronous speed will result in a frequency variation for the induced voltage. This can cause a stability problem if the machine is connected to a fixed frequency power grid as discussed in Chapter 14. Therefore, the speed of the turbine must be delicately controlled so that the rotor is always spinning at the synchronous speed.

When the field circuit of the synchronous generator is excited and the rotor is spinning, a balanced three-phase voltage is induced in the stator windings. If an external three-phase load is connected across the stator windings as shown in Figure 12.38, three-phase currents will flow into the load. The current of the load is known as *armature current*. If the load is balanced, the armature currents are balanced and a single-phase representation is all we need to model the generator.

The airgap of the synchronous generator has two fields as shown in Figure 12.39:

1. Excitation field ϕ_f which is stationary with respect to the rotor. When a turbine spins the rotor at the synchronous speed, ϕ_f rotates with respect to the stator at the synchronous speed.
2. Stator flux ϕ_s due to the three-phase armature currents. This flux, which is only present when the generator is loaded, rotates at the synchronous speed inside the airgap similar to the rotating field inside the induction motor. Hence, the net magnetic field in the airgap ϕ_g is the phasor sum of both fields:

$$\bar{\phi}_g = \bar{\phi}_f + \bar{\phi}_s \tag{12.82}$$

The equivalent circuit of the synchronous generator can be developed by using the schematic of the single-phase representation of the generator in Figure 12.40. The figure shows the rotor circuit excited by a dc source V_f , which produces an excitation current I_f . The excitation current produces the field ϕ_f . The armature current I_a produces the rotating field ϕ_s , which is known as *armature reaction*.

Assume first that the armature is unloaded, that is, $I_a = 0$ and $\phi_s = 0$. In this case, the induced voltage across the armature winding e_f is a function of ϕ_f only

$$e_f = N \frac{d\phi_f}{dt} \tag{12.83}$$

where

N is the number of turns in the armature winding

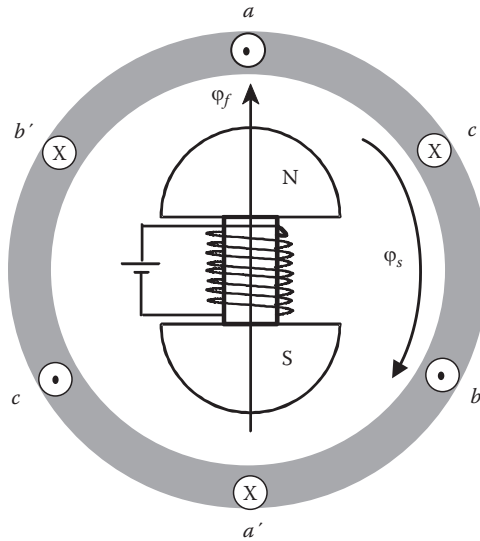


FIGURE 12.39 Total airgap flux inside synchronous generator.

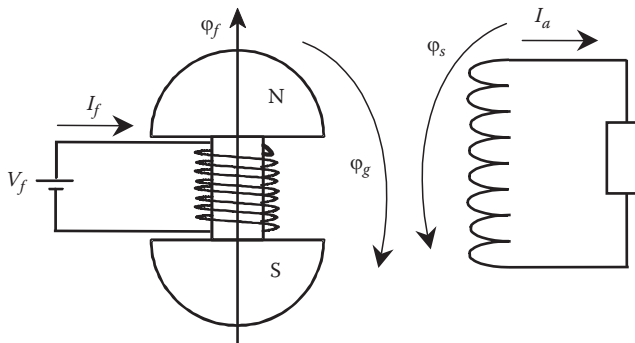


FIGURE 12.40 Representation of synchronous generator.

e_f is directly proportional to the excitation current I_f . The rms value of e_f is E_f which is known as *equivalent excitation voltage*.

Now assume that an electric load is connected across the armature windings. In this case, the induced voltage across the winding e_g is a function of the total airgap flux ϕ_g :

$$e_g = N \frac{d\phi_g}{dt} \tag{12.84}$$

The rms component of e_g is E_g . This induced voltage is not equal to the voltage across the load V_t because of the reactance X and resistance R of the armature winding. Hence,

$$\bar{E}_g = \bar{V}_t + \bar{I}_a(R + jX) \tag{12.85}$$

where

V_t is the phase value of the terminal voltage across the load

I_a is the armature current.

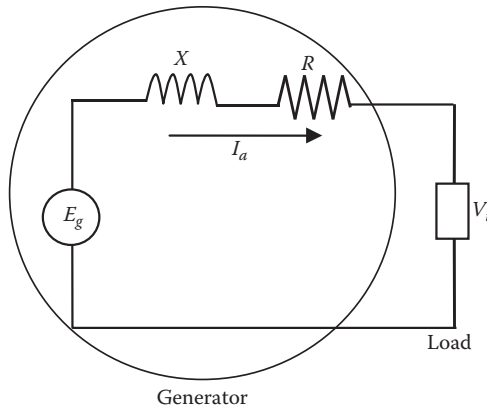


FIGURE 12.41 Equivalent circuit of synchronous generator.

The equivalent circuit represented by Equation 12.85 is shown in Figure 12.41. Note that the magnitude of E_g is a function of φ_f and φ_s . Hence, E_g changes its value with any change in the load current. Therefore, it is difficult to analyze the synchronous generator at all loading conditions by the aforementioned model. However, we can modify the equivalent circuit by representing E_g in terms of E_f which is independent of the load current. This can be done by representing the instantaneous voltage e_g in Equation 12.84 as

$$\bar{e}_g = N \frac{d\bar{\varphi}_g}{dt} = N \frac{d\bar{\varphi}_f}{dt} + N \frac{d\bar{\varphi}_s}{dt} \tag{12.86}$$

The magnitude of the term $N \frac{d\bar{\varphi}_f}{dt}$ is equal to e_f which is the *induced voltage* across the stator winding due to flux φ_f . The magnitude of the second term $N \frac{d\bar{\varphi}_s}{dt}$ is the voltage across the stator windings due to the armature currents that produce the flux φ_s . Hence, the second term represents a *voltage drop* across the stator windings. Since Faraday’s law gives a positive sign for the induced voltage and a negative sign for the drop voltage, Equation 12.86 can be rewritten as

$$\bar{e}_g = N \frac{d\bar{\varphi}_f}{dt} + N \frac{d\bar{\varphi}_s}{dt} = \bar{e}_f - \bar{e}_s \tag{12.87}$$

where e_s is the voltage drop across the armature winding due to the armature current. The magnitude of e_s is then

$$e_s = N \frac{d\varphi_s}{dt} = L_a \frac{di_a}{dt} \tag{12.88}$$

where

- i_a is the instantaneous current of the armature winding (the current that produces φ_s)
- L_a is the equivalent inductance

Based on Equation 12.88, we can conclude that e_s is a voltage drop across an inductor L_a . In terms of rms, Equation 12.86 can be rewritten as

$$\bar{E}_g = \bar{E}_f - \bar{E}_s = \bar{E}_f - \bar{I}_a \bar{X}_a \tag{12.89}$$

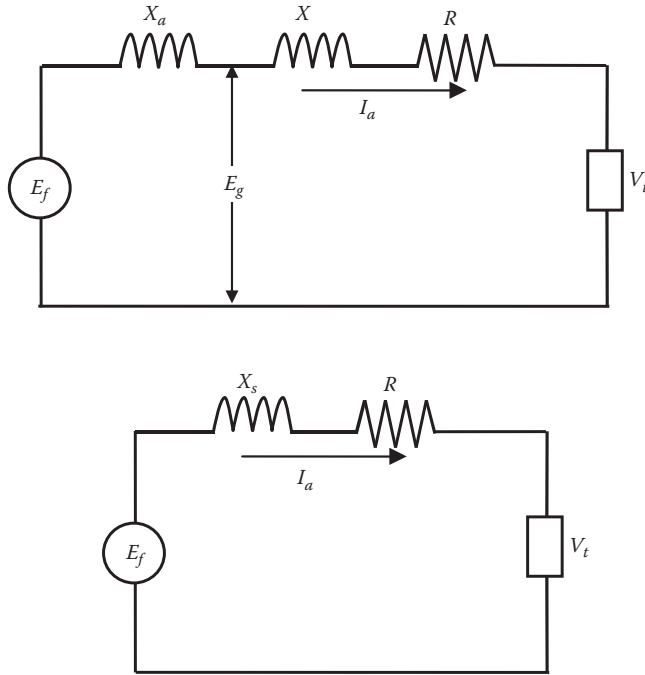


FIGURE 12.42 Equivalent circuit of synchronous generator.

where $X_a = \omega L_a$. Using Equation 12.89, we can modify the equivalent circuit in Figure 12.41 as shown in Figure 12.42. X_s in Figure 12.42 is known as *synchronous reactance* and is equal to $X + X_a$.

The model for the synchronous generator can be further simplified by ignoring the resistance of the armature windings. This is justified for large machines with windings made of large cross-section wires. In this case, the synchronous generator model can be represented by

$$\bar{E}_f = \bar{V}_t + \bar{I}_a \bar{X}_s \tag{12.90}$$

The phasor diagram of Equation 12.90 is shown in Figure 12.43. Note that E_f leads V_t .

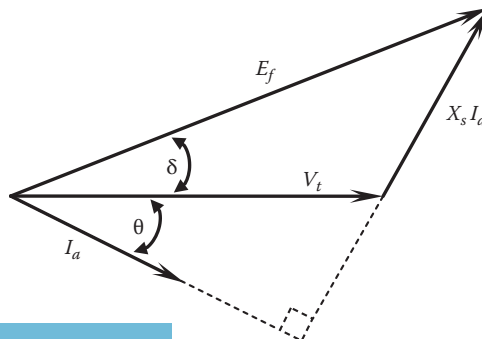


FIGURE 12.43 A phasor diagram of synchronous generator.

Example 12.15

A 60 Hz, four-pole synchronous generator of a thermal power plant has a synchronous reactance of $5\ \Omega$. The stator windings are connected in wye, and the line-to-line voltage is 15 kV. The line current of the generator is 1 kA at 0.9 power factor lagging. Compute the following:

- Equivalent field voltage E_f
- Real power delivered to the power grid
- Reactive power delivered to the power grid

Solution

- a. The equivalent field voltage can be computed by Equation (12.90), assuming the reference to be the terminal voltage:

$$\bar{E}_f = \bar{V}_t + \bar{I}_a \bar{X}_s = \frac{15}{\sqrt{3}} \angle 0^\circ + (1 \angle -\cos^{-1} 0.9) \times 5 \angle 90^\circ = 11.74 \angle 22.54^\circ \text{ kV}$$

- b. $P = \sqrt{3} V_{t-ll} I_a \cos \theta = \sqrt{3} \times 15 \times 1 \times 0.9 = 23.38 \text{ MW}$

where V_{t-ll} is the line-to-line voltage

- c. $Q = \sqrt{3} V_{t-ll} I_a \sin \theta = \sqrt{3} \times 15 \times 1 \times \sin(\cos^{-1} 0.9) = 11.32 \text{ MVAr}$

12.5.1 SYNCHRONOUS GENERATOR CONNECTED TO INFINITE BUS

The infinite bus, by definition, is a large power grid consisting of a number of large generators. The voltage and frequency of the infinite bus are constant and cannot be changed regardless of any action made by any one generator. The infinite bus can absorb or deliver any amount of active or reactive powers without any change in its voltage or frequency.

When a synchronous generator is connected to an infinite bus as shown in Figure 12.44, the voltage and frequency at the infinite bus are constant and cannot be changed due to any change in the excitation current I_f or the speed of the generator. This is much like having two objects tied together. If the mass of one object is much larger than the mass of the other, any attempted movement by the small object may not affect the large object. The infinite bus in this scenario is the large object and the synchronous generator is the small one.

When the generator is connected directly to an infinite bus, the terminal voltage of the machine V_t in Figure 12.42 is equal to the infinite bus voltage V_o . Since V_o is constant, V_t is also constant. Keep in mind that E_f is a function of the field current I_f . Hence, E_f is controlled by the operator of the generator. The phasor diagram of the synchronous machine connected to an infinite bus is shown in Figure 12.45. Note that the only difference between this phasor diagram and the one in Figure 12.43 is that the terminal voltage of the generator is equal to the infinite bus voltage.

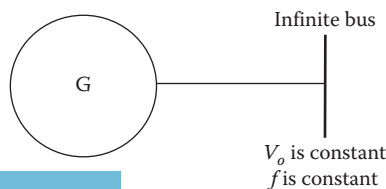


FIGURE 12.44 Synchronous generator connected to an infinite bus.

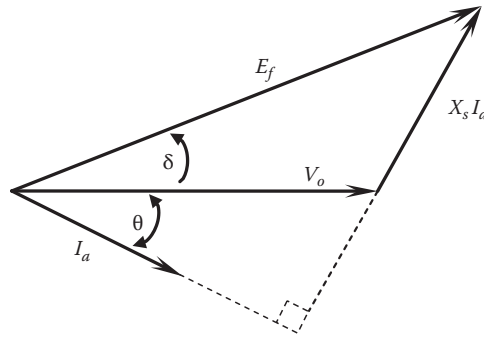


FIGURE 12.45 Phasor diagram of synchronous generator connected to infinite bus.

12.5.1.1 Power of Synchronous Generator

The apparent power (complex power) delivered to the infinite bus by the synchronous generator is

$$\bar{S} = 3\bar{V}_o\bar{I}_a^* = P + jQ \quad (12.91)$$

where \bar{I}_a^* is the conjugate of the current. This is the norm used by the forefathers of power system to make the reactive power of an inductor positive and that for the capacitor negative. Equation 12.91 can be rewritten in the form

$$\bar{S}^* = 3\bar{V}_o^*\bar{I}_a = P - jQ \quad (12.92)$$

where

$$\bar{I}_a = \frac{\bar{E}_f - \bar{V}_o}{\bar{X}_s} = \frac{E_f(\cos \delta + j \sin \delta) - V_o}{jX_s} \quad (12.93)$$

where δ is the angle between the infinite bus voltage and the equivalent field voltage E_f . δ is known as *power angle*.

In Equation 12.93, V_o and E_f are phase quantities. Substituting Equation 12.93 into Equation 12.92, yields

$$\bar{S}^* = 3 \frac{E_f V_o}{X_s} \sin \delta - j3 \frac{V_o}{X_s} (E_f \cos \delta - V_o) = P - jQ \quad (12.94)$$

The real power delivered to the infinite bus is

$$P = 3 \frac{E_f V_o}{X_s} \sin \delta \quad (12.95)$$

And the reactive power delivered to the infinite bus is

$$Q = 3 \frac{V_o}{X_s} (E_f \cos \delta - V_o) \quad (12.96)$$

Equation 12.95 is called *power-angle equation*; it relates the output power of the generator to the power angle δ as well as other parameters and variables. Equation 12.97 shows that the maximum

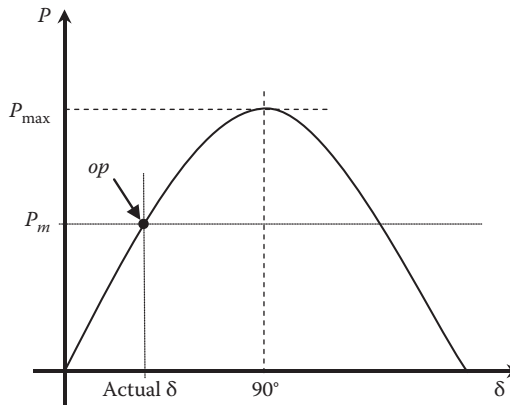


FIGURE 12.46 Real power as a function of the power angle.

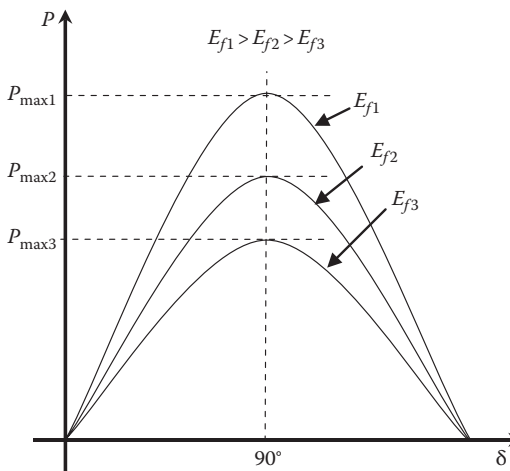


FIGURE 12.47 Pullover power due to changes in excitation current.

power that can be generated by the machine P_{\max} , which is known as *pullover power*, occurs when $\delta = 90^\circ$:

$$P_{\max} = \frac{3V_o E_f}{X_s} \tag{12.97}$$

Figure 12.46 shows the power-angle curve representing Equation 12.95. Let us assume that the internal losses of the generator are insignificant. In this case, the input mechanical power P_m to the generator is equal to the electrical power P delivered to the infinite bus. The mechanical power P_m is controlled by the operator at the power plant. Hence, the point at which the mechanical power equals the electrical power is the operating point *op* of the generator. The power angle at this point is the actual angle between the infinite bus voltage V_o and the equivalent field voltage E_f .

As seen in Equation 12.97, the maximum power P_{\max} of the system increases when E_f increases. However, the power delivered to the infinite bus will not increase unless the input mechanical power to the generator increases. Therefore, increasing P_{\max} increases the capacity of the generator to deliver more power. Changing E_f is done by changing the excitation current I_f , which is continuously controlled at the power plant. Figure 12.47 shows various values of pullover powers due to different E_f .

Example 12.16

A synchronous generator is connected directly to an infinite bus. The voltage of the infinite bus is 23 kV. The excitation of the generator is adjusted until the equivalent field voltage E_f is 25 kV. The synchronous reactance of the machine is 2Ω .

- If the output mechanical power of the turbine is 100 MW, compute the power angle.
- Compute the pullover power.
- If the excitation of the generator is decreased by 10%, compute the power angle and the pullover power.

Solution

- The electric power of the generator is equal to the mechanical power of the turbine. By direct substitution in Equation 12.95, we can compute the power angle. Keep in mind that all voltages in the equation are phase quantities and all powers are for the three phases. Also, synchronous generators are almost always connected in wye:

$$P = \frac{3V_o E_f}{X_s} \sin \delta$$

$$100 = \frac{3 \frac{23}{\sqrt{3}} \frac{25}{\sqrt{3}}}{2} \sin \delta$$

$$\delta = 20.35^\circ$$

- The pullover power can be computed using Equation 12.97:

$$P_{\max} = \frac{3V_o E_f}{X_s} = \frac{23 \times 25}{2} = 287.5 \text{ MW}$$

- Assume a linear relationship between the excitation current and the equivalent field voltage. When the excitation decreases by 10%, the equivalent field voltage decreases by 10% as well:

$$P = \frac{3V_o E_f}{X_s} \sin \delta$$

$$100 = \frac{23 \times (0.9 \times 25)}{2} \sin \delta$$

$$\delta = 22.74^\circ$$

$$P_{\max} = \frac{3V_o E_f}{X_s} = \frac{23 \times (0.9 \times 25)}{2} = 258.75 \text{ MW}$$

The reactive power delivered by the synchronous generator to the infinite bus Q is computed in Equation 12.96. The equation shows that the reactive power delivered to the infinite bus is dependent on the magnitude of E_f . The reactive power can be positive, negative, or zero depending on the level of excitation of the synchronous generator.

- Overexcited generator:* this is when the excitation is adjusted so that $E_f \cos \delta > V_o$. The reactive power in this case is positive, meaning the generator is consuming reactive power. The phasor diagram in this case is shown in Figure 12.45. Note that the current lags the voltage of the infinite bus.

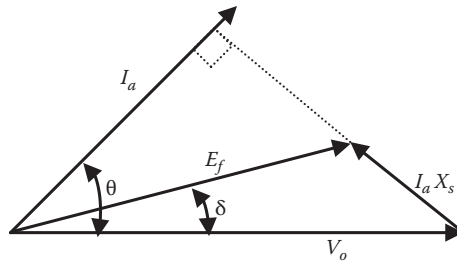


FIGURE 12.48 Underexcited synchronous machine.

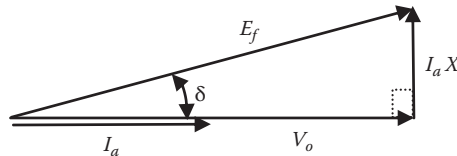


FIGURE 12.49 Synchronous machine with exact excitation.

2. *Underexcited generator*: if the excitation is adjusted so that $E_f \cos \delta < V_o$, the reactive power is negative; that is, the generator is producing reactive power. The phasor diagram in this case is shown in Figure 12.48 where the current is leading the infinite bus voltage.
3. *Exactly excited generator*: if the excitation is adjusted so that $E_f \cos \delta = V_o$, there is no reactive power at the terminals of the generator. The phasor diagram is shown in Figure 12.49. The current in this case is in phase with the infinite bus voltage.

Example 12.17

For the synchronous machine in Example 12.16, compute the equivalent excitation voltage E_f required to deliver 100 MW of real power and no reactive power to the infinite bus.

Solution

The terminal voltage of the machine is unchanged since it is connected to an infinite bus. However, we cannot assume that the power angle is equal to that computed in Example 12.16 because the equivalent excitation voltage must change to modify the reactive power. As seen in Figure 12.47, the change in the excitation alone leads to a change in the power angle. Our problem has two unknowns: the equivalent excitation voltage and the power angle. To solve these two unknowns, we need two equations, namely, the real and reactive power equations:

$$P = \frac{3V_o E_f}{X_s} \sin \delta$$

$$100 = \frac{3 \frac{23}{\sqrt{3}} E_f}{2} \sin \delta$$

$$E_f \sin \delta = 5.02 \text{ kV}$$

For zero reactive power at the generator terminals, the generator must be exactly excited. Hence,

$$E_f \cos \delta = V_o = \frac{23}{\sqrt{3}} = 13.28 \text{ kV}$$

Hence,

$$\frac{E_f \sin \delta}{E_f \cos \delta} = \tan \delta = \frac{5.02}{13.28} = 0.38$$

$$\delta = 20.7^\circ$$

Now, we can solve for the phase value of the equivalent excitation voltage:

$$E_f = \frac{5.02}{\sin \delta} = 14.2 \text{ kV}$$

The line-to-line equivalent excitation voltage is $14.2\sqrt{3} = 24.59 \text{ kV}$.

12.5.2 SYNCHRONOUS GENERATOR CONNECTED TO INFINITE BUS THROUGH A TRANSMISSION LINE

Most power plants are located in remote areas where the energy resources are available or easily transportable, and the possible pollution from the power plants is kept away from population centers. The energy generated by these power plants must then be transmitted to the load centers (cities, factories, etc.) by a system of transmission lines. Figure 12.50 shows a one line diagram of a simple system where the generator is connected to an infinite bus through a transmission line. The terminal voltage of the generator is V_t and the voltage at the infinite bus is V_o . The transmission line is a high voltage wire that has a resistance and an inductive reactance X_l . However, the resistance is often much smaller than the inductive reactance and is normally ignored.

The equivalent circuit of the system is shown in Figure 12.51. The power angle δ in this case is defined as the angle between the infinite bus voltage V_o and the equivalent field voltage E_f . The basic equations of the system are

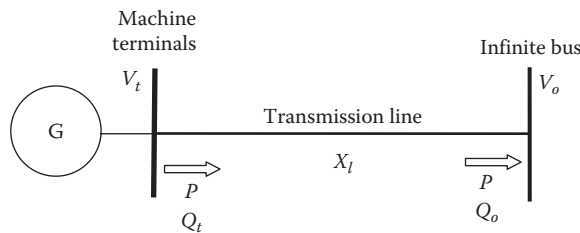


FIGURE 12.50 A synchronous generator connected to infinite bus through a transmission line.

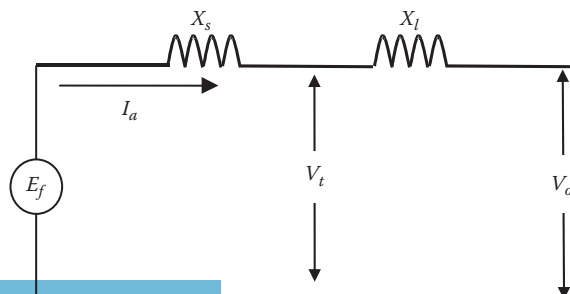


FIGURE 12.51 Equivalent circuit of the system in Figure 12.50.

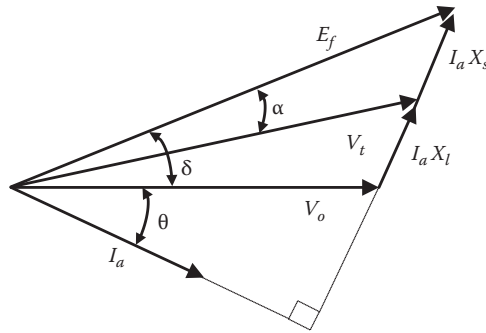


FIGURE 12.52 Phasor diagram of Equation 12.98.

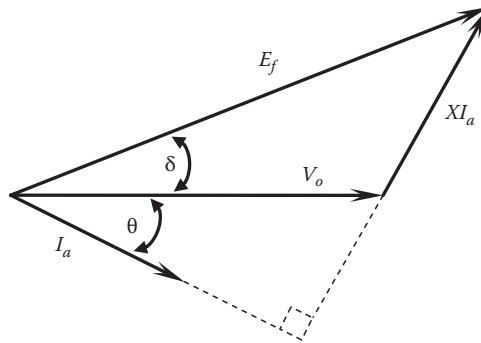


FIGURE 12.53 Simplified phasor diagram of Equation 12.98.

$$\begin{aligned} \bar{E}_f &= \bar{V}_t + \bar{I}_a \bar{X}_s \\ \bar{V}_t &= \bar{V}_o + \bar{I}_a \bar{X}_l \\ \bar{E}_f &= \bar{V}_o + \bar{I}_a \bar{X}_l + \bar{I}_a \bar{X}_s \end{aligned} \tag{12.98}$$

These equations can be interpreted by the phasor diagram in Figure 12.52, where the current is assumed to be lagging the infinite bus voltage. Equation 12.98 can also be simplified as

$$\bar{E}_f = \bar{V}_o + \bar{I}_a (\bar{X}_s + \bar{X}_l) = \bar{V}_o + \bar{I}_a \bar{X} \tag{12.99}$$

where $\bar{X} = \bar{X}_s + \bar{X}_l$. The simplified phasor diagram is shown in Figure 12.53.

The power equations for the case of transmission line between the generator and infinite bus are the same as Equations 12.95 and 12.96, respectively. The only difference is that X_s is replaced by X . Hence, the equation for the real power is

$$P = \frac{3V_o E_f}{X} \sin \delta \tag{12.100}$$

Similarly, the reactive power delivered to infinite bus Q_o is

$$Q_o = \frac{3V_o}{X} (E_f \cos \delta - V_o) \tag{12.101}$$

The reactive power at the generator's terminal Q_t is

$$Q_t = \frac{3V_t}{X_s} (E_f \cos \alpha - V_t) \quad (12.102)$$

Where α is the angle between the terminal voltage of the generator and E_f as shown in Figure 12.52.

Example 12.18

A synchronous generator is connected to an infinite bus through a transmission line. The infinite bus voltage is 23 kV, the inductive reactance of the transmission line is 1Ω , and the synchronous reactance of the machine is 2Ω . When the excitation of the generator is adjusted so that the line-to-line equivalent field voltage is 28 kV, the generator delivers 100 MW of real power to the infinite bus. Compute the following:

- Terminal voltage of the machine
- Reactive power at the infinite bus
- Reactive power consumed by the transmission line
- Reactive power at the terminals of the generator

Solution

- The terminal voltage of the generator can be computed if we know the current in the transmission line. The current is a function of the angle between the infinite bus voltage and the equivalent field voltage. From the power equation, we can compute the angle δ :

$$P = \frac{3V_o E_f}{X} \sin \delta$$

$$100 = \frac{23 \times 28}{(2+1)} \sin \delta$$

$$\delta = 27.76^\circ$$

The current in the transmission line can be computed using the model in Figure 12.51:

$$\bar{I}_a = \frac{\bar{E}_f - \bar{V}_o}{\bar{X}} = \frac{\frac{28}{\sqrt{3}} \angle 27.76^\circ - \frac{23}{\sqrt{3}} \angle 0^\circ}{3 \angle 90^\circ} = 2.53 \angle -7.75^\circ \text{ kA}$$

$$\bar{V}_t = \bar{V}_o + \bar{I}_a \bar{X}_t = \frac{23}{\sqrt{3}} \angle 0^\circ + (2.53 \angle -7.75^\circ) 1 \angle 90^\circ = 13.85 \angle 10.44^\circ \text{ kV}$$

The line-to-line terminal voltage is $\sqrt{3} \times 13.85 = 24 \text{ kV}$.

$$b. \quad Q_o = \frac{3V_o}{X} (E_f \cos \delta - V_o) = \frac{\sqrt{3} \times 23}{3} \left(\frac{28}{\sqrt{3}} \cos(27.76^\circ) - \frac{23}{\sqrt{3}} \right) = 13.62 \text{ MVar}$$

- The reactive power consumed by the transmission line is

$$Q_t = 3I_a^2 X_t = 3 \times 2.53^2 \times 1 = 19.25 \text{ MVar}$$

- d. The reactive power at the terminals of the generator can be computed by two methods. The first is to sum the reactive powers at the infinite bus and the reactive power consumed by the transmission line:

$$Q_t = Q_o + Q_l = 32.87 \text{ MVAr}$$

The other method is to use Equation 12.102. But first, we need to calculate the angle α using the phasor diagram in Figure 12.52:

$$\alpha = \delta - \angle \bar{V}_t = 27.76^\circ - 10.44^\circ = 17.32^\circ$$

$$Q_t = \frac{3V_t}{X_s} (E_f \cos \alpha - V_t) = \frac{3 \times 13.85}{2} \left(\frac{28}{\sqrt{3}} \cos 17.32^\circ - 13.85 \right) = 32.87 \text{ MVAr}$$

Example 12.19

A synchronous generator of a power plant is connected to an infinite bus through a transmission line. The infinite bus voltage is 23 kV, the inductive reactance of the transmission line is 1Ω , and the synchronous reactance of the machine is 2Ω . The reactive power measured at the machine's terminals is zero, and the machine delivers 1 kA to the infinite bus. Compute the following:

- Equivalent field voltage
- Real power delivered to the infinite bus
- Real power at the terminals of the machine

Solution

- a. Since there is no reactive power at the terminals of the generator, the current I_a is in phase with the terminal voltage V_t . Using the equivalent circuit in Figure 12.51, the phasor diagram can be constructed as shown in Figure 12.54.

The equivalent field voltage can be computed using Equation 12.98:

$$\bar{E}_f = \bar{V}_t + \bar{I}_a \bar{X}_s$$

$$\bar{V}_t = \bar{V}_o + \bar{I}_a \bar{X}_l$$

Since I_a is in phase with V_t , the voltage drop $I_a X_l$ is leading V_t by 90° . Hence we can use the Pythagorean theorem to compute the terminal voltage:

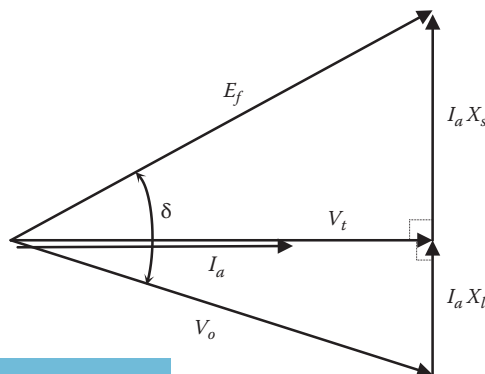


FIGURE 12.54 Phasor diagram of the system.

$$V_t = \sqrt{V_o^2 - (I_a X_l)^2} = \sqrt{\left(\frac{23}{\sqrt{3}}\right)^2 - (1 \times 1)^2} = 13.24 \text{ kV}$$

Similarly,

$$E_f = \sqrt{V_t^2 + (I_a X_s)^2} = \sqrt{(13.24)^2 + (1 \times 2)^2} = 13.4 \text{ kV}$$

The line-to-line equivalent excitation voltage is $\sqrt{3} \times 13.4 = 23.2 \text{ kV}$

b. The real power delivered to the infinite bus is

$$P = \frac{3V_o E_f}{X} \sin \delta$$

where

$$\delta = \sin^{-1}\left(\frac{I_a X_l}{V_o}\right) + \sin^{-1}\left(\frac{I_a X_s}{E_f}\right) = \sin^{-1}\left(\frac{1 \times 1}{23/\sqrt{3}}\right) + \sin^{-1}\left(\frac{1 \times 2}{13.4}\right) = 12.91^\circ$$

$$P = \frac{3V_o E_f}{X} \sin \delta = \frac{23 \times 23.2}{3} \sin 12.91^\circ = 39.7 \text{ MW}$$

c. Since we ignored the resistance of the transmission line, the real power at the terminals of the machine is the same as the real power at the infinite bus.

12.5.3 INCREASE TRANSMISSION CAPACITY

If we wish to increase the output electrical power of the synchronous machine, we must increase the mechanical power of the turbine. In addition, the transmission system must be able to transmit the extra power. The power system operates securely when the capacity of the transmission system is higher than the generated electric power. The capacity of the power system can be viewed as the maximum power that can be transmitted by the system. In Equation 12.100, the system capacity is the maximum power:

$$P_{\max} = \frac{3V_o E_f}{X} \quad (12.103)$$

The power plant cannot generate more than the transmission capacity P_{\max} . However, it is possible to increase the transmission capacity if we increase E_f or reduce the total inductive reactance X . There are two common methods to reduce X : (1) by inserting a capacitor in series with the transmission line and (2) by using parallel transmission lines.

12.5.3.1 Increasing Transmission Capacity by Using Series Capacitor

A capacitor can be connected in series with the transmission line, as shown in Figure 12.55, to reduce the total inductive reactance of the system. Recall that without the capacitor, $X = X_s + X_l$. Now with the capacitor, the total reactance is

$$\bar{X} = \bar{X}_s + \bar{X}_l + \bar{X}_c = jX_s + jX_l - jX_c = j(X_s + X_l - X_c) \quad (12.104)$$

$$X = X_s + X_l - X_c$$

where X_c is the capacitive reactance of the capacitor.

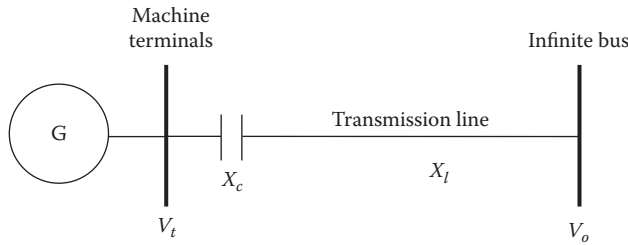


FIGURE 12.55 Capacitor in series with the transmission line.

Example 12.20

A synchronous generator is connected to an infinite bus through a transmission line. The infinite bus voltage is 230kV and the equivalent field voltage of the machine is 210kV. The transmission line’s inductive reactance is 10Ω, and the synchronous reactance of the machine is 2Ω:

1. Compute the capacity of the system.
2. If a capacitor is connected in series with the transmission line to increase the transmission capacity by 25%, compute its reactance.

Solution

1. The system capacity is

$$P_{\max} = \frac{3V_0E_f}{X} = \frac{230 \times 210}{(10 + 2)} = 4.025 \text{ GW}$$

2. The system capacity increases by 25% using a capacitor:

$$1.25 \times 4025 = \frac{3V_0E_f}{X_{\text{new}}} = \frac{230 \times 210}{(10 + 2 - X_c)}$$

Hence,

$$X_c = 2.4 \Omega$$

This is a large value of capacitive reactance, almost 1.1 mF. Since it carries large currents at high voltages, the capacitor is very large in size and can only be installed in major substations.

12.5.3.2 Increasing Transmission Capacity by Using Parallel Lines

Parallel lines are often used to increase the transmission capacity of the system. It is intuitive knowledge that two lines can transmit more power than any one line. Figure 12.56 shows a schematic of a system with two parallel lines (TL1 and TL2), and Figure 12.57 shows a photo of a transmission tower with two parallel circuits (each circuit consists of three-phase lines).

The equivalent circuit of the system is shown in Figure 12.58. In this system, the total reactance between the infinite bus and the equivalent field voltage is

$$X = X_s + \frac{X_{l1}X_{l2}}{X_{l1} + X_{l2}} \tag{12.105}$$

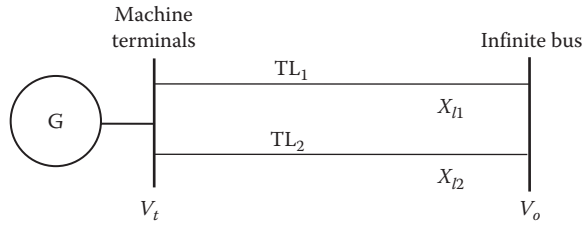


FIGURE 12.56 Two transmission lines in parallel.

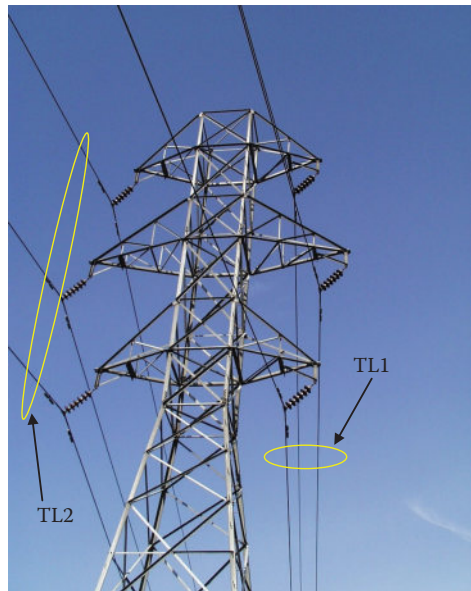


FIGURE 12.57 A tower with two transmission lines (the line is a three-phase circuit).

$$X = X_s + \frac{X_{l1} X_{l2}}{X_{l1} + X_{l2}}$$

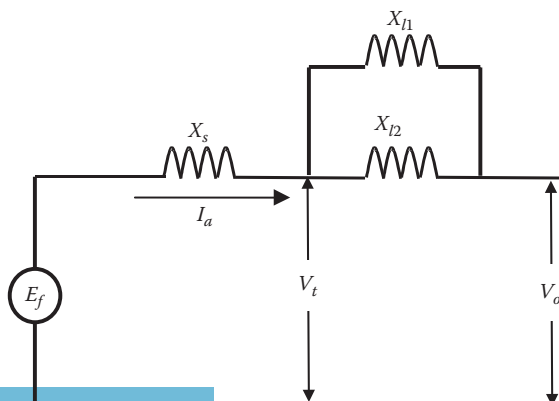


FIGURE 12.58 Equivalent circuit of power system with two parallel lines.

Example 12.21

A synchronous generator is connected to an infinite bus through a transmission line. The infinite bus voltage is 230 kV and the equivalent field voltage of the machine is 210 kV. The transmission line's inductive reactance is $10\ \Omega$, and the synchronous reactance of the machine is $2\ \Omega$:

1. Compute the capacity of the system.
2. Compute the capacity of the system if a second transmission line with a $10\ \Omega$ inductive reactance is connected in parallel with the first line.

Solution

- a. The system capacity is

$$P_{\max} = \frac{3V_0 E_f}{X} = \frac{230 \times 210}{(10 + 2)} = 4.025 \text{ GW}$$

- b. After the second line is added, the system capacity is

$$P_{\max} = \frac{3V_0 E_f}{X_{\text{new}}} = \frac{3V_0 E_f}{\left(X_s + \frac{X_{l1} X_{l2}}{X_{l1} + X_{l2}} \right)} = \frac{230 \times 210}{2 + \frac{10}{2}} = 6.9 \text{ GW}$$

The power capacity of the system increases by about 71% when the two parallel lines are used. Can you tell why the capacity is not doubled? Also, repeat the example for three parallel lines.

12.6 SYNCHRONOUS MOTOR

A synchronous machine is a dual action device; it can be used as a generator or motor. As a motor, the synchronous machine is very popular in applications that demand constant and precise speeds such as electric clocks, movie cameras, tractions, uniform actuators, gate and governor controls, constant feed industrial processes, and many others. Besides driving mechanical loads, the synchronous motor is also used to compensate for the reactive power of industrial loads. For small size synchronous motors, the rotor is often made of ferrite permanent magnet material. This is the most economic design for a fractional horsepower motor that does not experience repeated surges in stator currents. If repeatedly occurring, the inrush currents can demagnetize the rotor.

In more recent designs, the rotor is made of rare earth permanent magnet material such as the Samarium–Cobalt to produce stronger magnetic fields. The strong rare earth permanent magnet material can be used in motors as large as 100 hp. One great advantage of this rare earth motor is its high power/volume ratio that makes it one of the smallest machines. Furthermore, unlike the ferrite material, the rare earth permanent magnet cannot be easily demagnetized, so it can be used for applications that require heavy currents or inrush currents during starting and braking. Because of these advantages, the rare earth permanent magnet synchronous motor is used to actuate new commercial airplanes using fly-by-wire designs. It is also used in ground transportation; the hybrid electric vehicles in Figure 12.59 use this type of motor.

For large motors, the rotor is made of an electric magnet that is excited externally by a separate dc source. This is exactly the same rotor used for the synchronous generator; a photograph of its slipping arrangement is shown in Figure 12.36. The three-phase currents of the stator produce a rotating magnetic field at the synchronous speed n_s , exactly like the induction machine. The magnetic field of the rotor, which is stationary with respect to the rotor, aligns itself with the rotating field, thus spinning the rotor at the synchronous speed. This is similar to having two magnets; if one is moving, the



FIGURE 12.59 Hybrid electric vehicle uses PMSM.

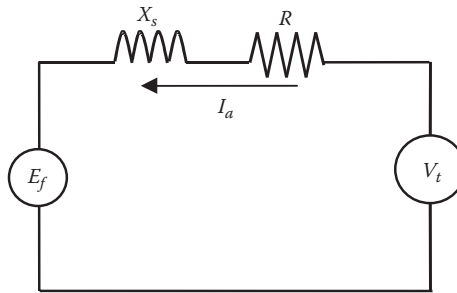


FIGURE 12.60 Equivalent circuit of synchronous motor.

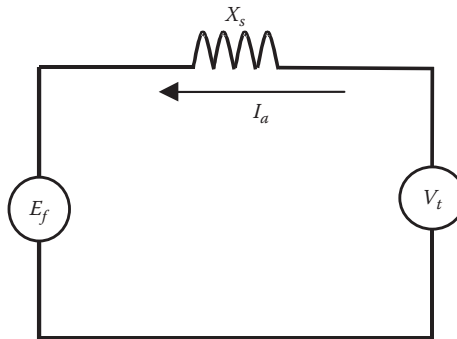


FIGURE 12.61 Simplified equivalent circuit of synchronous motor.

other follows at the same speed. The equivalent circuit of the synchronous generator, shown in Figure 12.42, is also applicable to the synchronous motor as seen in Figure 12.60. The only differences are: (1) the stator is excited by a three-phase source and (2) the armature current of the motor flows in the reverse direction when compared with the armature current of the generator. The equivalent circuit of the synchronous motor can be further simplified by ignoring the resistance of the armature winding. This is justified for large machines where the stator windings are made of large cross-section wires. The simplified equivalent circuit of the synchronous motor is shown in Figure 12.61.

The equation of the synchronous motor can be written as

$$\bar{V}_t = \bar{E}_f + \bar{I}_a \bar{X}_s \tag{12.106}$$

The phasor diagram of Equation 12.106 is shown in Figure 12.62. Note that for the synchronous motor, E_f lags V_t ; this is opposite to the synchronous generator. Also, note that the power factor angle θ is the angle between the armature current and the terminal voltage of the motor.

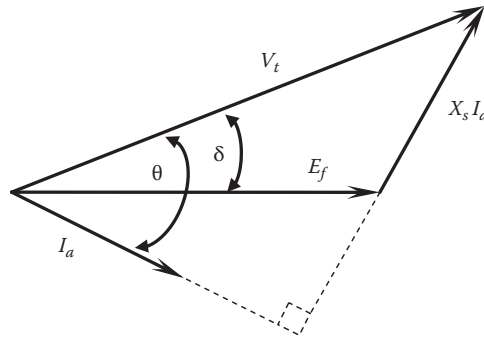


FIGURE 12.62 Phasor diagram of synchronous motor.

Example 12.22

A 30hp, four-pole, 480 V, 60Hz, three-phase, wye connected synchronous motor has a synchronous reactance of 2Ω . At full load, the armature current of the motor is 30 A and lags the terminal voltage. Ignore all losses and compute the following:

- a. Torque of the motor
- b. Equivalent field voltage
- c. Reactive power consumed by the motor

Solution

a. We can compute the torque of the motor if we know the output power and the speed of the motor. The output power at full load is 30 hp:

$$P_{out} = \frac{30}{1.34} = 22.39 \text{ kW}$$

$$n_s = 120 \frac{f}{p} = 120 \frac{60}{4} = 1800 \text{ rpm}$$

$$T = \frac{P_{out}}{\omega_s} = \frac{22390}{\frac{2\pi}{60} \times 1800} = 118.78 \text{ Nm}$$

b. Using the circuit in Figure 12.61, we can compute the equivalent field voltage. But first, we need to compute the phase angle of the current. Since the machine losses are ignored, the output power is equal to the input power. Hence,

$$P_{in} = P_{out} = \sqrt{3} V I_a \cos \theta$$

$$22390 = \sqrt{3} 480 \times 30 \times \cos \theta$$

$$\theta = 26.14^\circ$$

Using Equation 12.106, we can compute the equivalent field voltage. Select the terminal voltage to be the reference phasor:

$$\bar{E}_f = \bar{V}_t - \bar{I}_a \bar{X}_s = \frac{480}{\sqrt{3}} \angle 0^\circ - (30 \angle -26.14^\circ) \times 2 \angle 90^\circ = 256.4 \angle -12.13^\circ \text{ V}$$

The line-to-line value of E_f is 444 V.

c. The reactive power consumed by the motor is its input reactive power:

$$Q_{in} = \sqrt{3} V I_a \sin \theta = \sqrt{3} 480 \times 30 \times \sin(26.14) = 11 \text{ KVAR}$$

12.6.1 POWER OF SYNCHRONOUS MOTOR

The complex power of the synchronous motor is

$$\bar{S} = 3\bar{V}_t \bar{I}_a^* = P + jQ \quad (12.107)$$

where

\bar{I}_a^* is the conjugate of the current of the motor

V_t is the terminal voltage of the motor

Equation 12.91 can be rewritten in the form

$$\bar{S}^* = 3\bar{V}_t^* \bar{I}_a = P - jQ \quad (12.108)$$

where

$$\bar{I}_a = \frac{\bar{V}_t - \bar{E}_f}{\bar{X}_s} = \frac{V_t - E_f(\cos \delta - j \sin \delta)}{jX_s} \quad (12.109)$$

where δ is the angle between the terminal voltage and the equivalent field voltage E_f . δ is known as *power angle*.

In Equation 12.109, V_t , and E_f are phase quantities. Substituting Equation 12.109 into Equation 12.107 yields

$$\bar{S}^* = \frac{E_f V_t}{X_s} \sin \delta - j \frac{V_t}{X_s} (V_t - E_f \cos \delta) = P - jQ \quad (12.110)$$

The real power consumed by the motor is

$$P = \frac{E_f V_t}{X_s} \sin \delta \quad (12.111)$$

And the reactive power consumed by the motor is

$$Q = \frac{V_t}{X_s} (V_t - E_f \cos \delta) \quad (12.112)$$

12.6.2 REACTIVE POWER CONTROL AND SYNCHRONOUS CONDENSER

In Equations 12.106 and 12.112, the magnitude of V_t is often fixed since it is connected to the power system. However, E_f can be controlled by adjusting the dc field current in the rotor circuit. Hence, the armature current is dependent on the value of E_f . There are three possible scenarios for the current in Equation 12.106: lagging, leading, and in phase with the terminal voltage. The three possible phasor diagrams are shown in Figures 12.62 and 12.63. In Figure 12.62, E_f is adjusted so

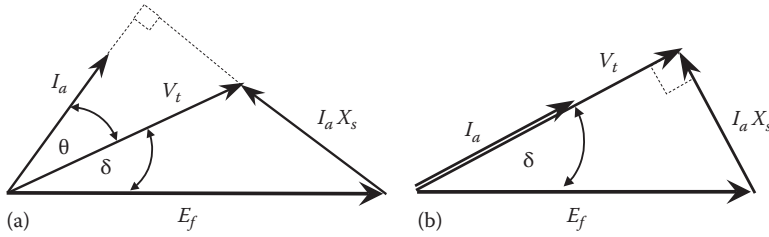


FIGURE 12.63 Phasor diagram of synchronous motor: (a) leading current and (b) unity power factor.

that $E_f \cos \delta < V_t$. In this case, the current I_a lags V_t , and the power factor measured at the terminals of the motor is lagging.

In Figure 12.63a, E_f is increased so that $E_f \cos \delta > V_t$. In this case, the current leads the terminal voltage and the power factor measured at the terminals of the motor is leading.

In Figure 12.63b, E_f is adjusted so that $E_f \cos \delta = V_t$. In this case, the current is in phase with the terminal voltage and the power factor measured at the terminals of the motor is unity.

The reactive power Q in Figure 12.62 is positive. This means that the motor is consuming reactive power. When Q is negative, the reactive power is produced by the motor.

Example 12.23

A 5 kV, 60 Hz synchronous motor has a synchronous reactance of 4 Ω. The motor runs unloaded and its equivalent field voltage is adjusted to 6 kV. Ignore all losses and compute the reactive power at the terminals of the motor.

Solution

Since the motor is unloaded, the output real power is zero; thus, the power angle is also zero. Hence, the current I_a is either leading or lagging V_t by 90°. However, since the power angle is zero and $E_f > V_t$, the current must be leading the terminal voltage as shown in the phasor diagram in Figure 12.64.

Using Equation 12.112, we can compute the reactive power as

$$Q = \frac{3V_t}{X_s} [V_t - E_f \cos \delta] = \frac{3 \times \frac{5000}{\sqrt{3}}}{4} \left[\frac{5000}{\sqrt{3}} - \frac{6000}{\sqrt{3}} \right] = -1.25 \text{ MVA}r$$

The negative value of the reactive power means the synchronous motor is acting as a capacitor delivering reactive power to the system. Therefore, the machine in this mode is often called *synchronous condenser*.

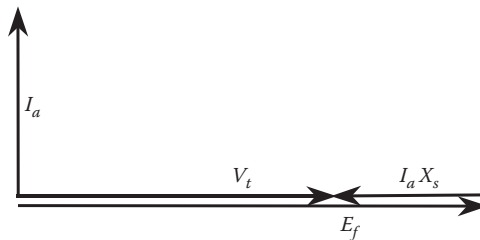


FIGURE 12.64 Phasor diagram of synchronous motor running at no load.

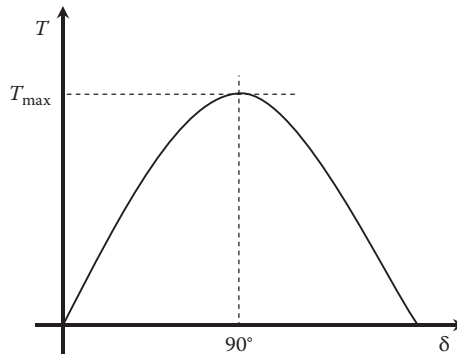


FIGURE 12.65 Torque curve of synchronous motor.

12.6.3 MOTOR TORQUE

The input real power is given in Equation 12.111. Since the synchronous machine rotates at synchronous speed, we can write the developed torque equation as

$$T = \frac{P}{\omega_s} = \frac{3V_t E_f}{\omega_s X_s} \sin \delta \quad (12.113)$$

Figure 12.65 shows the torque curve representing Equation 12.113. The maximum torque of the motor occurs at $\delta = 90^\circ$.

Example 12.24

A 3 kV, 60 Hz, six-pole synchronous motor is driving a load of 6 kN-m. The synchronous reactance of the motor is 5Ω . The equivalent field voltage as a function of the excitation current is $E_f = 40I_f$. Compute the following:

- Power consumed by the load
- Minimum excitation current of the machine
- Reactive power at the motor terminals

Solution

- The power of the motor is $P = T\omega_s$
where

$$\omega_s = \frac{2\pi}{60} \left(120 \frac{60}{6} \right) = 125.66 \text{ rad/s}$$

$$P = T\omega_s = 6000 \times 125.66 = 754 \text{ kW}$$

- The minimum excitation current is the value that makes the maximum torque of the motor in Equation 12.113 equal the load torque. Any excitation current less than this value will produce torque less than that needed by the load:

$$T_l = T_{\max} = \frac{3V_t E_{f \min}}{\omega_s X_s}$$

$$6000 = \frac{3 \frac{3000}{\sqrt{3}} E_{f \min}}{125.66 \times 5}$$

$$E_{f\min} = 725.5\text{V}$$

Hence, the minimum excitation current is

$$E_{f\min} = 40I_{f\min}$$

$$I_{f\min} = \frac{E_{f\min}}{40} = 18.14\text{ A}$$

c. The reactive power at the terminals of the motor is

$$Q = \frac{3V_t}{X_s} [V_t - E_f \cos \delta]$$

Since the machine is running under minimum excitation, the power angle is 90° :

$$Q = \frac{3V_t^2}{X_s} = 1.8\text{ MVA}$$

The positive sign of the reactive power means that the machine is consuming reactive power from the source.

12.7 DIRECT CURRENT MOTOR

The dc machine is one of the oldest electrical devices. The dc machine can operate as a motor or a generator without any change in its design. However, it is rarely used nowadays as a dc generator because of the wide use of power electronic converters.

The dc motor consists of a stator (called *field*) and a rotor (called *armature*). The stator is either a permanent magnet or an electric magnet. The winding of this electric magnet is excited by a dc source. Thus, the magnetic field is unidirectional from the north pole to the south pole as shown in Figure 12.66. A photo of the field winding in the stator circuit is shown in Figure 12.67.

The rotor of the dc motor is more complex than the rotor of the other motors. It consists of independent coils connected together in cascaded form. The terminals of each coil are connected to two copper strips (segments) mounted on the rotor shaft on opposite sides as shown in Figure 12.68. The copper segments of all coils form what is called *commutator*. The commutator rotates with the shaft. On the stator, two brushes are mounted on opposite sides of the commutator touching the terminals of one coil. The brush system consists of a spring and a carbon piece called *brush* as shown in Figure 12.69. The spring pushes the brush against the commutator to ensure connectivity with a coil. Because the position of the brush is fixed on the stator and the commutator is rotating, the carbon brushes make contact with the coil that moves under the two brushes. This way, the coils are switched on when they are under the brushes, and switched off when they move away from the brushes. To explain how the motor rotates, consider the Fleming's left-hand rule that explains the motion of electric motors. The rule states that if the y -axis is the direction of the magnetic field and the x -axis is the direction of current inside a conductor, then the z -axis is the direction of the force exerted on the conductor. Let us apply this rule for the conductor under the top brush in Figure 12.66. If the armature is excited by an external source whose voltage is V , the current I_a flows through the top brush to the top terminal of the coil and exits from the lower terminal of the same coil to the lower brush and back to the source. The current of the top terminal of the conductor enters the conductor. Since the magnetic field is moving from the top pole to the bottom pole, the force exerted on the top conductor F is to the left and the one on the lower conductor is to the right. These two forces create a torque

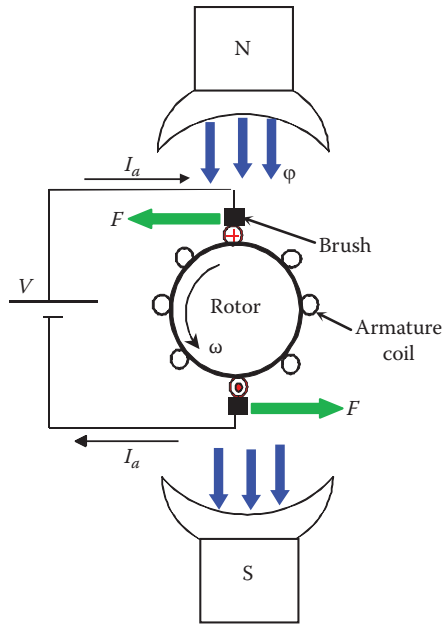


FIGURE 12.66 Main components of dc motor.



FIGURE 12.67 Stator windings (field) of dc motor.

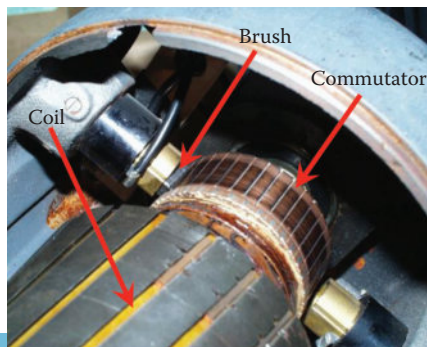


FIGURE 12.68 Rotor of dc motor.



FIGURE 12.69 Carbon brush.

causing the rotor to rotate in the counterclockwise direction. Once this coil moves away from under the brushes, the next one arrives under the brushes and the process is repeated. Thus, the motor is continuously rotating.

DC motors are popular because (1) they are simple to control by just adjusting the armature voltage or the field current; (2) they can deliver high starting torque, which makes them suitable for heavy loads such as elevators, forklifts, and transportations; and (3) their performance is almost linear, making them simple to stabilize.

12.7.1 THEORY OF OPERATION OF DC MOTOR

We can rewrite Equations 12.11 and 12.12 in the following forms

$$E_a = f(\varphi, \Delta n) = K\varphi\omega \quad (12.114)$$

$$T = f(\varphi, i_a) = K\varphi I_a \quad (12.115)$$

where

E_a is the voltage of the back electromagnetic force (emf) of the armature coil

I_a is the armature current

ω is the angular speed of the rotor

T is the torque of the rotor

φ is the magnetic field

K is a constant that accounts for a number of design parameters such as the number of turns in a coil and the length of the coil

The equivalent circuit of the dc motor is shown in Figure 12.70. The left part of the circuit is the field of the stator. If the stator is a permanent magnet, we do not need to consider it. However, most high-power motors have an electric magnetic field circuit in the stator. The field circuit is excited by a dc source. V_f causes a field current I_f to pass through the field windings. Since it is a dc circuit, the field winding is represented by its resistance R_f alone. The right side represents the armature (rotor). The circle with two brushes represents the voltage E_a , R_a is the resistance of the coil, V is the voltage of the source connected to the armature circuit, and I_a is the armature current.

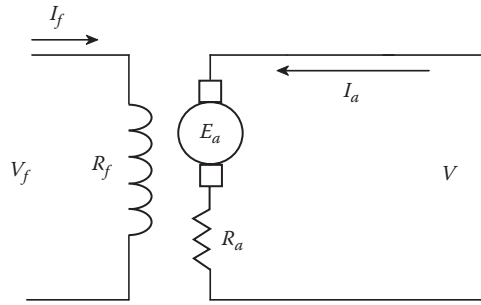


FIGURE 12.70 Representation of dc motor.

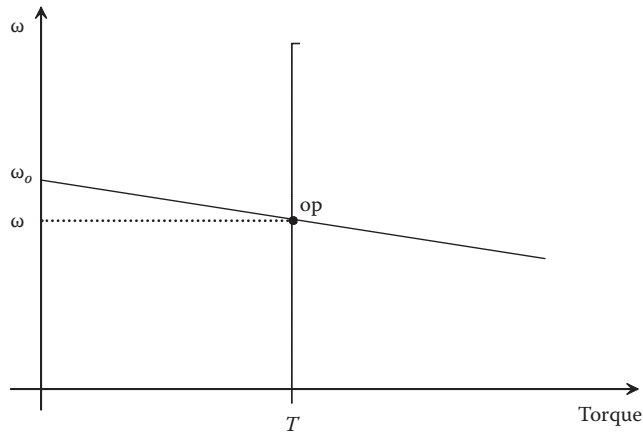


FIGURE 12.71 Speed–torque characteristics of dc motor.

The equation of the armature circuit is

$$V = E_a + I_a R_a \quad (12.116)$$

Substituting the value of E_a and I_a in Equations 12.114 and 12.115 into Equation 12.116, yields

$$V = K\phi\omega + \frac{T}{K\phi} R_a \quad (12.117)$$

Hence,

$$\omega = \frac{V}{K\phi} - \frac{R_a}{(K\phi)^2} T \quad (12.118)$$

Equation 12.118 can be used to sketch the speed–torque characteristics in Figure 12.71. At no load when the torque of the load $T=0$, the speed of the motor is called *no-load speed* ω_o :

$$\omega_o = \frac{V}{K\phi} \quad (12.119)$$

The actual speed of a loaded motor, as given in Equation 12.118, depends on the magnitude of the load torque, the value of the magnetic field, and the resistance of the armature winding.

Example 12.25

A 200 V dc motor has an armature resistance of 1Ω and an equivalent field voltage $K\phi = 3$ Vs. If the motor is driving a full load of 30 N-m, compute the speed of the motor.

Solution

Direct substitution in Equation 12.118, yields

$$\omega = \frac{V}{K\phi} - \frac{R_a}{(K\phi)^2} T = \frac{200}{3} - \frac{1}{9} 30 = 63.33 \text{ rad/s}$$

Or

$$n = \frac{\omega}{2\pi} = \frac{63.33}{2\pi} = 10.1 \text{ rev/s or } 606 \text{ rev/min}$$

12.7.2 STARTING OF DC MOTOR

The current of the dc motor can be computed using Equation 12.116:

$$I_a = \frac{V - E_a}{R_a} = \frac{V - K\phi\omega}{R_a} \quad (12.120)$$

At starting, the speed of the motor is zero; hence the starting current I_{st} is

$$I_{st} = \frac{V}{R_a} \quad (12.121)$$

This starting current is excessive as seen in Example 12.26.

Example 12.26

For the motor in Example 12.25, compute the armature current at full load and the current at starting.

Solution

The full load current can be computed using Equation 12.115:

$$I_a = \frac{T}{K\phi} = \frac{30}{3} = 10 \text{ A}$$

The starting current from Equation 12.121 is

$$I_{st} = \frac{V}{R_a} = \frac{200}{1} = 200 \text{ A}$$

The starting current is 20 times greater than the full load current.

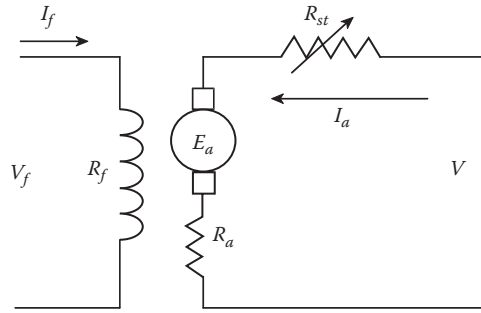


FIGURE 12.72 Starting of dc motor using starting resistance.

The high starting current is a major problem for dc motors. The large currents at starting can damage the armature winding due to the excessive heat they generate, especially if the motor is large and the inertia of the load is high, causing the motor to be slow at starting. From Equation 12.121, the starting current can be reduced by reducing the voltage at starting or inserting a resistance in the armature circuit at starting as shown in Figure 12.72.

Example 12.27

Compute the voltage at starting for the motor in Example 12.25 that leads to a starting current equal to three times the rated current.

Solution

Use Equation 12.121 to compute the starting voltage V_{st} :

$$V_{st} = I_{st} R_a = (3 * 10) * 1 = 30 \text{ V}$$

The voltage should be reduced to 30 V at starting.

Example 12.28

Compute the resistance that should be inserted in series with the armature of the motor in Example 12.25 to reduce the starting current to three times the rated current.

Solution

Use Equation 12.121 to compute the starting resistance R_{st} :

$$R_a + R_{st} = \frac{V}{I_{st}}$$

$$R_{st} = \frac{V}{I_{st}} - R_a = \frac{200}{30} - 1 = 5.67 \Omega$$

12.7.3 SPEED CONTROL OF DC MOTOR

If you examine Equation 12.118, you find that the speed of the dc motor can be controlled by increasing the armature resistance, by changing the voltage of the armature circuit, and by changing

the field ϕ . The field can be changed by adjusting the field current I_f . The first method requires the insertion of a resistance in the armature circuit, which reduces the efficiency of the motor. Adjustment of armature voltage is a very common method of speed control as it is highly efficient and simple to implement.

Example 12.29

For the motor in Example 12.25, compute the armature voltage that reduces the speed of the motor to 400 rpm.

Solution

Use Equation 12.117 to compute the new value of the voltage:

$$V = K\phi\omega + \frac{T}{K\phi} R_a = 3 \times 2\pi \frac{400}{60} + \frac{30}{3} \times 1 = 135.7 \text{ V}$$

Keep in mind that the voltage of the armature must be below the rated value of the motor. If the voltage exceeds the rated value, the armature winding insulation could be damaged, rendering the motor unusable. Hence, the armature voltage control reduces the speed of the motor below its full load speed.

To increase the speed of the motor higher than its full load speed, we can reduce the field voltage V_f . Doing so reduces the field current. Since the magnetic field ϕ is directly proportional to the field current I_f , the reduction of the field current reduces the field by the same percentage.

Example 12.30

For the motor in Example 12.25, compute the field voltage that increases the speed of the motor to 700 rpm. Assume that the field voltage at the full load speed is 300 V.

Solution

The magnetic field is proportional to the field current, and the field current is almost linearly proportional to the field voltage. Hence,

$$K\phi = CV_f$$

where C is a constant of proportionality; it can be computed using the data for the full load speed:

$$C = \frac{K\phi}{V_f} = \frac{3}{300} = 0.01 \text{ s}$$

Now compute $K\phi$ for the new speed:

$$V = K\phi\omega + \frac{T}{K\phi} R_a$$

$$K\phi V - (K\phi)^2 \omega - TR_a = 0$$

$$200 \times K\phi - (K\phi)^2 \left(2\pi \frac{700}{60} \right) - 30 \times 1 = 0$$

The solution of this equation leads to $k\phi = 2.57$.

The new value of the field voltage that rotates the motor at 700 rpm is

$$V_f = \frac{K\phi}{C} = \frac{2.57}{0.01} = 257 \text{ V}$$

12.8 STEPPER MOTOR

One major drawback of the motors discussed so far is their lack of simple and precise position control capability. However, the stepper motor is an excellent option for position control devices because it can control the position of the rotor and can hold the motor at this position for as long as needed. These features are essential in several applications that demand fine movements such as hard disk drives, printers, plotters, scanners, fax machines, medical equipment laser guiding systems, robots, and actuators. The stepper motors can achieve fine position control with a step resolution of one degree.

Stepper motors come in three basic types: (1) variable reluctance, (2) permanent magnet, and (3) hybrid. The stator of these three types is similar to that of the induction or synchronous machine. However, for a stepper motor, the phases could be any number, depending on the design preference and required resolution. Figure 12.73 shows a stator with four phases. The stator windings are not embedded inside the cylindrical stator, but are wrapped around salient poles extended inside the airgap.

When any of the stator windings ($a-a'$, $b-b'$, $c-c'$, or $d-d'$) is excited, the flux of the winding moves along the axis between the opposing poles of the same phase (e.g., a and a') as shown on the right side in Figure 12.73. The direction of the flux is dependent on the polarity of the applied voltage. Thus, the flow of the current determines the direction of the flux in the airgap.

The phases of the stator are switched by a power electronic converter; the most common one is the dc/ac converter such as the one shown in Figure 12.74. Each transistor switches one phase, and all phases are connected in a star configuration with the common neutral point providing the return path for all currents. The switching pattern of the transistors is a design parameter depending on the resolution of the step angle. A switching pattern in case of one phase is switched at a time is given at the bottom of Figure 12.74. The period of the switching cycle τ is the sum of the conduction period t_c of all phases.

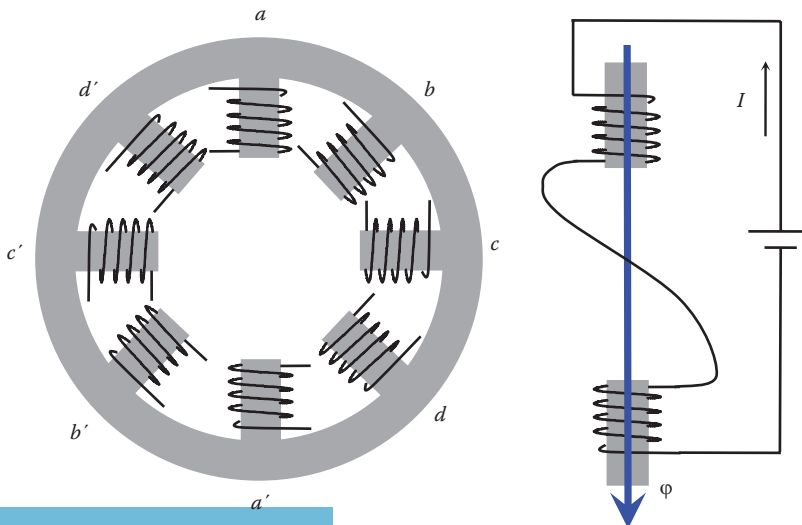


FIGURE 12.73 Stator of the stepper motor.

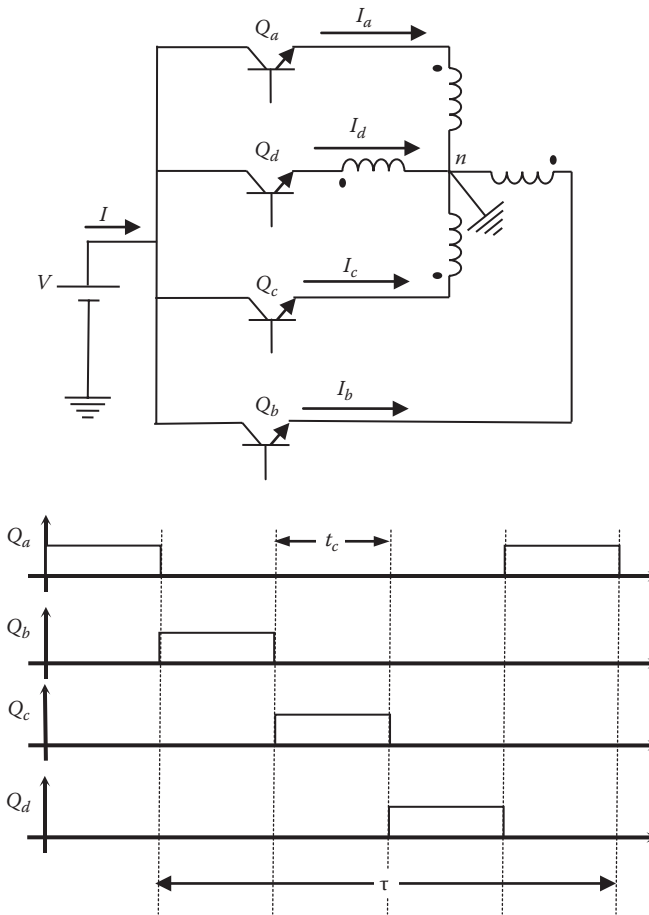


FIGURE 12.74 Switching of stepper motor winding.

12.8.1 VARIABLE RELUCTANCE STEPPER MOTOR

This is the oldest type of stepper motors. Unlike synchronous or induction motors, the rotor of the variable reluctance stepper motor (VRSM) is neither a magnet nor has any windings, but is made of a multi-tooth iron material. Stepper motors are described by their number of phases in the stator windings and the number of poles (or the number of teeth) in their rotors. Figure 12.75 shows a four-phase, six-tooth stepper motor.

When a tooth is aligned with the axis of a stator phase, the airgap distance between the tooth and the phase is called *tooth airgap*. Similarly, when a groove is aligned with the axis of a stator phase, the airgap distance between the groove and the phase is called *groove airgap*. The difference between the two airgaps develops a torque that aligns the rotor. To explain this, let us consider the force of attraction between an energized phase and the rotor, which is governed by the electromagnetic force equation

$$F = \frac{\mu_o}{4\pi d} I^2 \tag{12.122}$$

where

μ_o is the absolute permeability (1.257×10^{-6} H/m)

d is the airgap distance between the energized phase of the stator and the rotor

I is the current of the stator winding

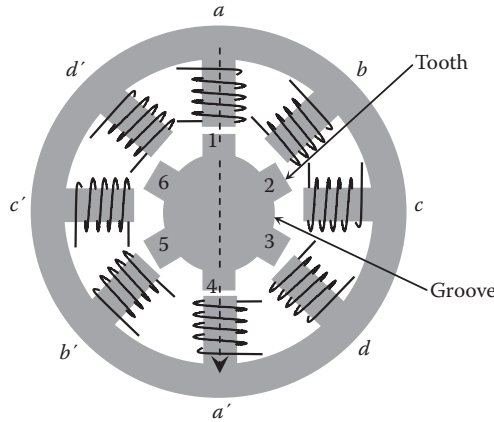


FIGURE 12.75 Variable reluctance stepper motor.

Since the tooth airgap is smaller than the groove airgap, the force of the attraction of the tooth is higher than that of the groove. Hence, a tooth is always aligned with the energized pole (in the figure, phase $a-a'$ is energized and teeth 1 and 4 are aligned along the axis of phase a). This attraction force is known as *detent force*.

If we disconnect phase a and energize phase b , the nearest teeth (2 and 5) move under poles $b-b'$, thus rotating one step in the counterclockwise direction. The movement angle is called *step angle* δ which is a function of the number of phases in the stator and the number of teeth in the rotor

$$\delta = \frac{360}{N_{ph}N_t} \tag{12.123}$$

where

- N_{ph} is the number of stator phases
- N_t is the number of teeth in the rotor

For the variable reluctance stepper, the rotor pole pair pp consists of one tooth and one groove. Thus, the relationship between the number of rotor poles p and number of rotor teeth is

$$\begin{aligned} pp &= N_t \\ p &= 2N_t \end{aligned} \tag{12.124}$$

Equation 12.123 can be written as a function of the rotor poles:

$$\delta = \frac{720}{N_{ph}p} \tag{12.125}$$

In the four-phase, six-tooth stepper motor, Figure 12.75, the number of rotor poles is 12 and the step angle is 15° . A finer step angle can be achieved if we increase the number of stator phases, increase the number of teeth, or energize more than one phase at a time.

The stepper motors are often rated by their number of steps per revolution (spr) s , which can be as high as 400:

$$s = \frac{360}{\delta} = \frac{N_{ph}p}{2} \tag{12.126}$$

To rotate the motor continuously, the switching of the phases must also be continuous. The motor speed n can be calculated in a process similar to that in Equation 12.9

$$n = \frac{120f}{p} = \frac{120}{\tau p} \quad (12.127)$$

where τ is the switching period in seconds. The unit of n in Equation 12.127 is rpm. The rotating stepper motor can also be rated by its step rate s_r , which is the number of steps per second (sps). Hence,

$$s_r = \frac{sn}{60} = \frac{N_{ph}}{\tau} \quad (12.128)$$

Example 12.31

A six-phase VRSM has a step angle of 10° . Compute the following:

- Number of teeth in the rotor.
- If the conduction period of each transistor is 2 ms, compute the continuous speed of the motor.

Solution

$$\begin{aligned} \text{a.} \quad \delta &= \frac{360}{N_{ph}N_t} \\ N_t &= \frac{360}{10N_{ph}} = \frac{360}{60} = 6 \text{ teeth} \end{aligned}$$

Hence, the motor is a 12-pole machine.

$$\text{b.} \quad \tau = t_c \times N_{ph} = 2 \times 6 = 12 \text{ ms}$$

$$n = \frac{120}{\tau p} = \frac{120}{12 \times 12} = 833.33 \text{ rpm}$$

12.8.2 PERMANENT MAGNET STEPPER MOTOR

Because its rotor has no magnet, the variable reluctance stepper develops little torque. Therefore, it is used only in applications such as disk drives, printers, or low torque actuations. For higher torque applications, the permanent magnet stepper motor (PMSM) is often selected. The rotor of the PMSM is cylindrical with several permanent magnets as shown in Figure 12.76. The magnet provides better holding force under the energized stator than the VRSM.

One common characteristic of permanent magnet motors is that they tend to cog as you turn the rotor manually without energizing the stator. This is because the rotor magnetic poles are attracted to the salient iron poles of the stator. This attraction force is known as *detent force*.

Equations 12.125 through 12.128 for the VRPM are also applicable to the PMSM. The only difference is that the PMSM has poles instead of teeth.

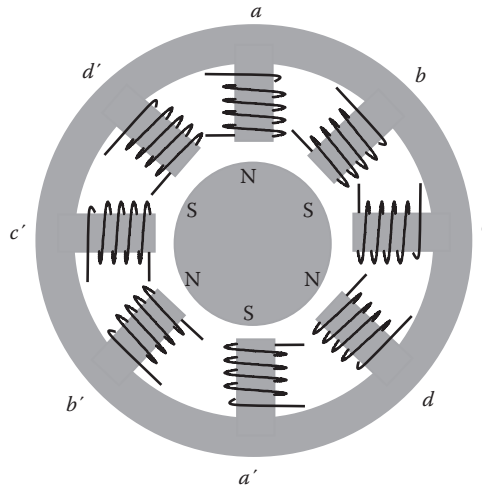


FIGURE 12.76 Permanent magnet stepper motor.

Example 12.32

A two-phase, four-pole PMSM is driven by 100Hz dc/ac converter. Compute the following:

- Speed of the motor
- Conduction period of each transistor in the converter

Solution

$$\text{a.} \quad n = \frac{120f}{p} = \frac{120 \times 100}{4} = 3000 \text{ rpm}$$

$$\text{b.} \quad \tau = t_c \times N_{ph}$$

$$t_c = \frac{\tau}{N_{ph}} = \frac{1}{f N_{ph}} = \frac{1}{100 \times 2} = 5 \text{ ms}$$

12.8.3 HYBRID STEPPER MOTOR

The hybrid stepper motor (HSM) provides the best resolution and the highest torque among all other types of stepper motors. The HSM can achieve a resolution of up to 400 spr. The rotor of the HSM is a multi-tooth rotor like the VRSM, but the teeth are also magnets (Figure 12.77). The attraction force of this motor is composed of two components; the attraction force due to the reluctance and the attraction force of the permanent magnet. Thus, a stronger attraction force is achieved.

12.8.4 HOLDING STATE OF STEPPER MOTOR

When the stepper motor is unloaded, the rotor is perfectly aligned with the energized phase as shown in Figures 12.75 through 12.77. In this case, there is no angle between the axes of the energized phase and the attracted poles of the rotor. If no other switching action is made, the rotor will maintain its holding position. During the holding state, when an external load torque T_l is applied on the stepper motor, the rotor may no longer be perfectly situated under the axis of the energized phase. Take for example, the

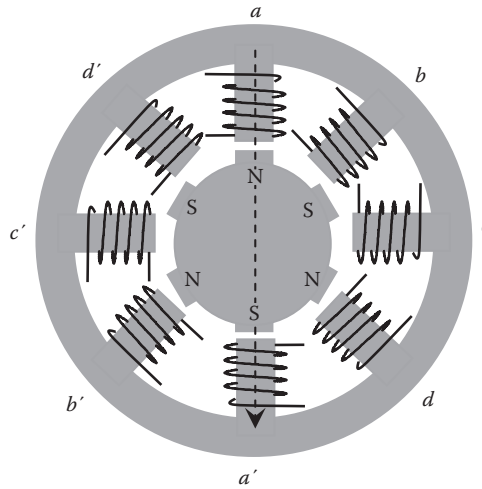


FIGURE 12.77 Hybrid stepper motor.

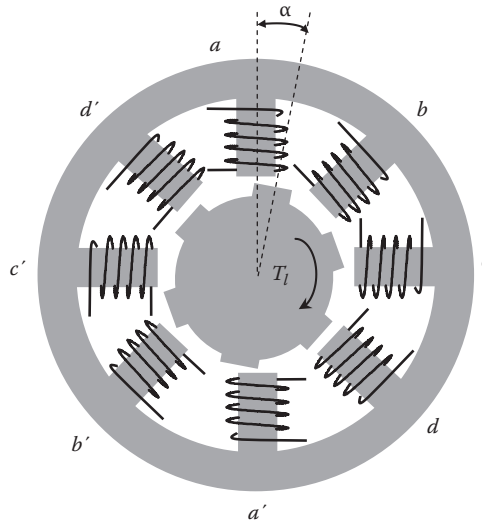


FIGURE 12.78 Displacement angle of stepper motor.

case in Figure 12.78 when phase $a-a'$ is excited and the load torque is in the clockwise direction. The load torque tends to move the rotor in the clockwise direction, thus causing the mechanical displacement angle α in Figure 12.78. The greater the torque applied, the larger the mechanical displacement angle. When the load torque exceeds the maximum static torque of the motor, which is called *holding torque* T_h , the motor enters an unstable state where the rotor can no longer maintain its holding state.

If the stepper motor is powered by one phase at a time, the developed torque of the motor can be computed using Faraday’s law in Equation 12.10. Hence,

$$T_d \sim \text{force} \sim I \tag{12.129}$$

$$T_d = KI$$

where K is a constant that depends on the motor geometry and the property of its windings. The unit of K is volt second. I is the current of the winding. When the axes of the stator windings and

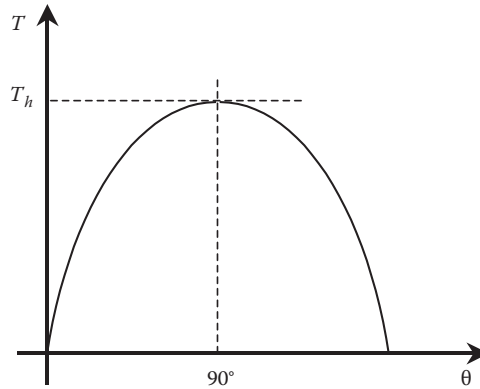


FIGURE 12.79 Torque curve of stepper motor.

the attracted poles are not perfectly aligned, the developed torque in the rotor that would align the axes can be written as

$$T_d = K I \sin \theta \quad (12.130)$$

where θ is called *electrical displacement angle*. In Figure 12.78, the electrical displacement angle θ is the same as the mechanical displacement angle δ . This is because the stepper is a two-pole machine. For any other number of poles, the relationship between the mechanical and electrical displacement angles is

$$\alpha = \frac{\theta}{p/2} = \frac{\theta}{N_t} \quad (12.131)$$

Equation 12.130 is plotted in Figure 12.79, and it shows that the maximum holding torque T_h occurs at $\theta = 90^\circ$. Hence,

$$T_h = K I \quad (12.132)$$

Example 12.33

A 10-teeth, two-phase VRSM is loaded by 10 mNm torque. The torque constant of the motor is 3 Vs and the holding torque is 30 mNm. Compute the following:

- Current of the stator windings
- Mechanical displacement angle
- Displacement error
- Stator current that reduces the mechanical displacement angle by 50%

Solution

- The holding torque is the maximum torque in Equation 12.130:

$$T_h = K I$$

$$I = \frac{T_h}{K} = \frac{30}{3} = 10 \text{ mA}$$

- b. The mechanical displacement angle of the rotor can be computed by Equation 12.130:

$$T_d = K I \sin(N_t \alpha)$$

$$10 = 30 \sin(10\alpha)$$

Hence, $\alpha = 2^\circ$

- c. The displacement error is the displacement angle with respect to the step angle. The step angle is

$$\delta = \frac{360}{N_{ph} N_t} = \frac{360}{2 \times 10} = 18^\circ$$

Displacement error = $(2/18) \times 100 = 11.11\%$

- d. For $\alpha = 1^\circ$,

$$T_d = K I \sin(N_t \alpha)$$

$$10 = 3I \sin(10)$$

Hence, $I = 19.2 \text{ mA}$

12.8.5 ROTATING STEPPER MOTOR

During the holding state, the stepper motor must develop enough torque to compensate for the load torque. When the motor rotates, the developed torque of the motor must compensate for three components: (1) load torque T_l , (2) friction and drag torque T_f , and (3) acceleration or deceleration torque T_j :

$$T_d = T_l + T_f + T_j \quad (12.133)$$

The acceleration and deceleration torque is also known as *inertia torque*

$$T_j = J \frac{d\omega}{dt} = \frac{2\pi}{60} J \frac{dn}{dt} \quad (12.134)$$

where J is the inertia of the rotor plus load (g m^2)

Example 12.34

A six-phase VRSM with a step angle of 7.5° and a step rate of 200 sps is driving an inertia load. The inertia of the load plus the rotor is 1 mg m^2 , and the friction torque is 15 mN m . Compute the following:

- Number of teeth in the rotor
- Switching period τ
- Speed of the motor
- Input power at steady-state (ignore electrical losses)
- Inertia torque to accelerate the motor at 40 rad/s^2

Solution

$$\begin{aligned} \text{a.} \quad \delta &= \frac{720}{N_{ph}p} \\ p &= \frac{720}{\delta N_{ph}} = \frac{720}{7.5 \times 6} = 16 \text{ poles} \end{aligned}$$

Hence, the number of teeth is 8.

$$\text{b.} \quad s_r = \frac{N_{ph}}{\tau} ; \quad \tau = \frac{6}{200} = 30 \text{ ms}$$

$$\text{c.} \quad n = \frac{120}{\tau p} = \frac{120}{30 \times 16} = 250 \text{ rpm}$$

d. Since the load is just inertia, the developed torque of the motor at steady-state compensates for only for the friction torque. Hence, the input power is

$$P = T_f \omega = 15 \times \frac{2\pi}{60} 250 = 392.7 \text{ mW}$$

$$\text{e.} \quad T_j = J \frac{d\omega}{dt} = 1 \times 40 = 0.04 \text{ Nm}$$

12.9 SINGLE-PHASE MOTORS

As discussed in Section 12.1, the three-phase source produces a naturally rotating magnetic field in the airgap of the induction and synchronous motors. This is the main advantage of using the three-phase system as it makes the heavy industrial motors start and rotate smoothly. However, for low-power applications, such as household and office equipment, we must rotate the motors without using a three-phase system. This is because the outlets in these places are only single-phase systems. To rotate the single-phase motors, we need to create a rotating magnetic field in the airgap by using various designs and circuits such as the ones discussed in this section.

12.9.1 SPLIT-PHASE MOTORS

A split-phase motor uses two stator windings as shown in Figure 12.80. The main winding is $M-M'$ and the auxiliary winding is $AU-AU'$. The auxiliary winding has less turns of smaller cross-section conductors than the primary winding. This makes the resistance of the auxiliary winding much higher than that for the primary winding ($R_{AU} > R_M$). Now consider the simple representation of the motor's windings in Figure 12.81. The figure shows a single-phase source connected to both windings. Each winding is represented by an equivalent resistance and an equivalent inductive reactance. The auxiliary winding is switched on at starting and switched off when the motor reaches its full speed. Assume that the switch is closed and the motor is energized, in this case the currents of the two windings are

$$\begin{aligned} \bar{I}_M &= \frac{\bar{V}_s}{Z_M \angle \theta_M} = \frac{\bar{V}_s}{Z_M} \angle -\theta_M \\ \bar{I}_{AU} &= \frac{\bar{V}_s}{Z_{AU} \angle \theta_{AU}} = \frac{\bar{V}_s}{Z_{AU}} \angle -\theta_{AU} \end{aligned} \tag{12.135}$$

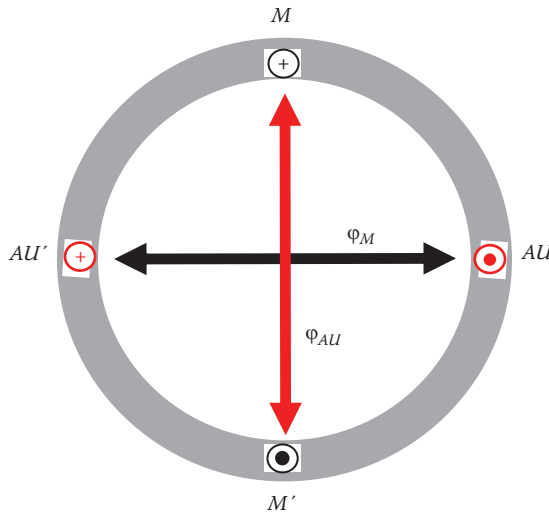


FIGURE 12.80 Winding arrangement of split-phase motor.

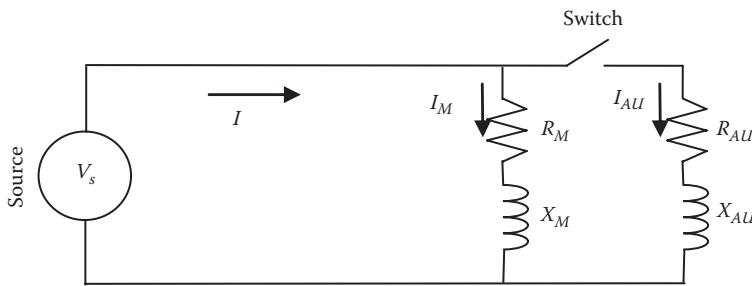


FIGURE 12.81 Windings representation of split-phase motor.

where

$$\bar{Z}_M = R_M + jX_M \tag{12.136}$$

$$\bar{Z}_{AU} = R_{AU} + jX_{AU}$$

Since $R_{AU} > R_M$ due to the thin wire, and $X_{AU} < X_M$ due to the smaller number of turns in the auxiliary winding, then

$$\theta_M > \theta_{AU} \tag{12.137}$$

The difference in these two angles creates a phase shift between the currents inside the two windings of as much as 30°. These two currents produce magnetic fields in the airgap that is rotating as explained in Example 12.35.

Example 12.35

The phase shift between the currents of the auxiliary and primary windings of a split-phase induction motor is 30°. Assume that the magnetic fields due to these currents are

$$\varphi_M = K \sin(377t)$$

$$\varphi_{AU} = 0.2K \sin(377t + 30)$$

where K is a constant value. Assume that the auxiliary winding is placed 90° from the main winding. Compute the magnetic field in the airgap at $t=1$, 4, and 8 ms.

Solution

As seen in Figure 12.80, the current of each winding produces its own magnetic field. The total magnetic field in the airgap is the phasor sum of both. Since they are placed 90° from each other, the total field in the airgap is

$$\bar{\varphi} = \sqrt{\varphi_M^2 + \varphi_{AU}^2} \angle \tan^{-1} \left(\frac{\varphi_{AU}}{\varphi_M} \right)$$

At $t=1$ ms,

$$\varphi_M = K \sin(377 \times 0.001) = 0.3681 K$$

$$\varphi_{AU} = 0.2K \sin \left(377 \times 0.001 + \frac{\pi}{6} \right) = 0.1567 K$$

$$\bar{\varphi} = \sqrt{\varphi_M^2 + \varphi_{AU}^2} \angle \tan^{-1} \left(\frac{\varphi_{AU}}{\varphi_M} \right) = 0.4 K \angle 23^\circ$$

At $t=4$ ms,

$$\varphi_M = K \sin(377 \times 0.004) = 0.998 K$$

$$\varphi_{AU} = 0.2K \sin \left(377 \times 0.004 + \frac{\pi}{6} \right) = 0.1791 K$$

$$\bar{\varphi} = \sqrt{\varphi_M^2 + \varphi_{AU}^2} \angle \tan^{-1} \left(\frac{\varphi_{AU}}{\varphi_M} \right) = 1.01 K \angle 10.2^\circ$$

At $t=8$ ms,

$$\varphi_M = K \sin(377 \times 0.01) = 0.1253 K$$

$$\varphi_{AU} = 0.2K \sin \left(377 \times 0.01 + \frac{\pi}{6} \right) = -0.0775 K$$

$$\bar{\varphi} = \sqrt{\varphi_M^2 + \varphi_{AU}^2} \angle \tan^{-1} \left(\frac{\varphi_{AU}}{\varphi_M} \right) = 0.15 K \angle -32^\circ$$

Note that the magnitude and the angle of the magnetic field in the airgap change with time as shown in Figure 12.82. The change in the angle is always in one direction causing the magnetic field to rotate in that direction, thus rotating the rotor of the motor. Because the magnitude of

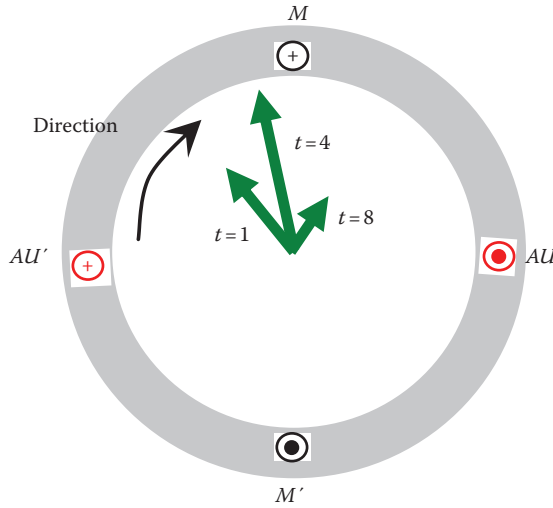


FIGURE 12.82 Rotating magnetic field of split-phase motor.

the rotating field is changing, the motor cannot be used to start heavy loads. Recall that the magnitude of the rotating field in three-phase systems is constant; thus, three-phase motors are more suitable for heavy loads.

The auxiliary winding is often switched by a centrifugal or solid-state switch. The centrifugal switch is normally closed and is opened only when the motor reaches its full speed. Thus, it activates the auxiliary windings at starting only. After the switch is opened, the motor continues rotating as the system inertia keeps the rotor spinning while it chases the magnetic field of the main winding.

12.9.2 CAPACITOR STARTING MOTORS

A capacitor starting motor is very similar to the split-phase motor. However, the phase shift between the main and auxiliary windings is achieved by inserting a capacitor in series with the auxiliary winding at starting as shown in Figure 12.83. The phase shift of the currents in both windings causes the magnetic field in the airgap to rotate much the same way as that explained in Example 12.35. After the motor starts, the capacitor and the auxiliary winding are switched off by a centrifugal switch or a solid-state device.

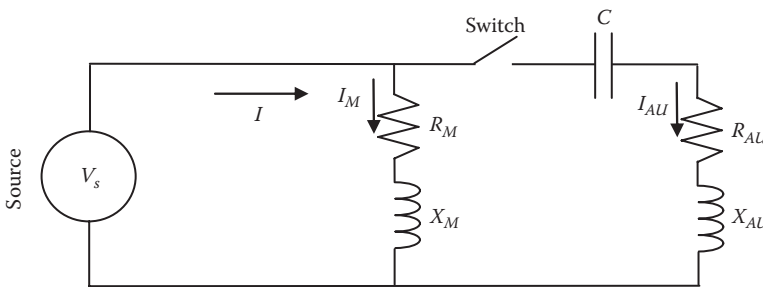


FIGURE 12.83 Representation of capacitor starting motor.

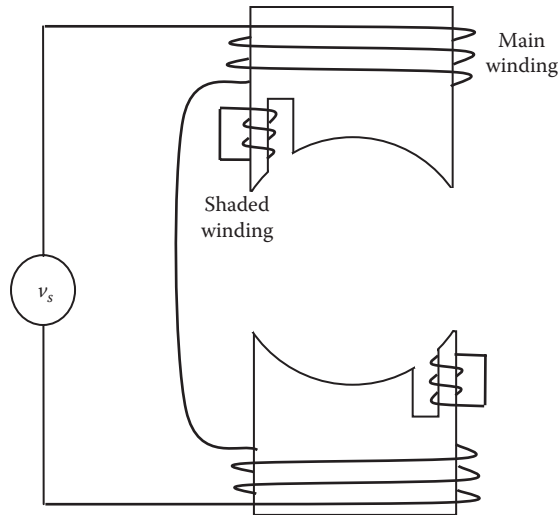


FIGURE 12.84 Structure of shaded-pole motor.

12.9.3 SHADED-POLE MOTORS

A shaded-pole motor has its stator core split into main and shaded cores as shown Figure 12.84. A small short-circuited winding composed of a few turns of thick wire is wrapped around the shaded leg of the core. The main winding is energized by a power source, thus producing the main magnetic field. This magnetic field in the core induces a current in the shaded winding, which creates its own magnetic field. The current in the shaded winding lags that of the main winding. Consequently, the airgap magnetic field of the shaded winding lags the magnetic field of the main winding. Since the shaded winding is displaced from the center axis of the main winding, a rotating magnetic field is produced in the airgap as explained in Example 12.35.

EXERCISES

- 12.1 The output power of a four-pole, three-phase induction motor is 100 hp. The motor operates at a slip of 0.02 and efficiency of 90%. Compute the following:
 - a. Input power of the motor in kW
 - b. Shaft torque (output torque)
- 12.2 The synchronous speed of a 60 Hz, three-phase induction motor is 1200 rpm. What is the synchronous speed of the motor if it is used in a 50 Hz system?
- 12.3 A 100 hp, 60 Hz, three-phase induction motor has a slip of 0.03 at full load. Compute the efficiency of the motor at full load when the friction and windage losses are 900 W, the stator core loss is 4200 W, and the stator copper loss is 2700 W.
- 12.4 A three-phase induction motor is rated at 50 hp, 480 V, 60 Hz, and 1150 rpm. If the motor operates at full load, compute the following:
 - a. Developed torque
 - b. Frequency of the rotor current
- 12.5 A three-phase, 480 V, 60 Hz, 12-pole, induction motor has the following parameters:

$R_1 = 1.0 \Omega$; $R_2' = 0.5 \Omega$; $X_{eq} = 10. \Omega$; $X_c = 100 \Omega$; $R_c = 800 \Omega$. Calculate the following:

- a. Slip at maximum torque
- b. Current at maximum torque

- c. Speed at maximum torque
 d. Maximum torque
- 12.6** A 480 V, three-phase, six-pole, slip-ring, 60 Hz *Y*-connected induction motor has $R_1 = R_2' = 0.1 \Omega$ and $X_{eq} = X_1 + X_2' = 0.5 \Omega$. The motor slip at full load is 3%, and its efficiency is 90%. Calculate the following:
- a. Starting current (you may ignore the magnetizing current)
 b. Starting torque
 c. Maximum torque
 d. Value of the resistance that should be added to the rotor circuit to reduce the starting current by 50%
 e. Starting torque of case (d)
 f. Value of the resistance that should be added to the rotor circuit to increase the starting torque to the maximum value
 g. Starting current of case (f)
- 12.7** A three-phase, four-pole, 480 V, 60 Hz, *Y*-connected slip-ring induction motor has the following parameters:

$$R_1 = R_2' = 0.5 \Omega; X_1 + X_2' = 5 \Omega; \text{ Compute the following:}$$

- a. Starting torque
 b. Inserted rotor resistance that increases the starting torque by a factor of 4
- 12.8** A three-phase, 2.2 kV, 60 Hz, *Y*-connected slip-ring induction motor has the following parameters:

$$R_1 = R_2' = 0.2 \Omega; X_1 + X_2' = 1.5 \Omega$$

The motor runs at 570 rpm. Ignore the rotational losses and calculate the full load torque.

- 12.9** A 480 V, 60 Hz, three-phase, induction motor has the following parameters:

$$R_1 = R_2' = 0.3 \Omega; X_{eq} = 1.0; X_c = 600 \Omega.$$

At full load, the motor speed is 1120 rpm, the rotational loss is 400 W, and the core loss is 1 kW. Calculate the following:

- a. Motor slip
 b. Developed torque at full load
 c. Developed power in hp
 d. Rotor current
 e. Copper losses
 f. Input power
 g. Reactive power consumed by the motor
 h. Power factor of the motor
- 12.10** The speed of a 12-pole, 480 V, 60 Hz three-phase induction motor at full load is 560 rpm. The motor has the following parameters:

$$R_1 = 0.1 \Omega; R_2' = 0.5 \Omega; X_1 + X_2' = 5 \Omega$$

- a. Compute the developed torque.
 b. While the torque is unchanged, the voltage is changed to reduce the speed of the motor to 520 rpm. Compute the new voltage.
- 12.11** A train is driven by a linear induction motor at 80 km/h when the frequency of the primary windings is 15 Hz. The frontal area of the train is 25 m² and its coefficient of drag is 0.9. The

- friction coefficient between the wheels of the train and the track is 0.1, and the weight of the train is 500,000 kg. The pole pitch of the vehicle is 3 m. Compute the following:
- Speed of the thrust force
 - Slip of the motor
 - Developed force of the motor at steady-state
 - Developed power in hp
- 12.12** A train with linear induction motor is traveling uphill at 80 km/h when the frequency of its primary windings is 15 Hz. The inclination of the hill is 5° . The frontal area of the train is 25 m^2 and its coefficient of drag is 0.9. The friction coefficient between the wheels of the train and the track is 0.1, and the weight of the train is 500,000 kg. The pole pitch of the vehicle is 3 m. Compute the following:
- Developed force of the motor at steady-state
 - Developed power in hp
- 12.13** A vehicle is powered by a linear induction motor with a pole pitch of 2 m. The primary circuit resistance R_1 is 0.5Ω , and the secondary resistance referred to the primary circuit R_2' is 1.0Ω . The equivalent inductance of the primary plus secondary circuits is 0.02 H. The frequency of the primary windings is 10 Hz. Assume that the drag force is 500 N and the friction force is 2 kN. Compute the voltage across the primary windings when the motor travels at 100 km/h.
- 12.14** A six-pole, 60 Hz, three-phase induction generator is receiving 500 hp from external mechanical source and is rotating at 1250 rpm. The rotational loss of the generator is 1 kW. Compute the following:
- Slip of the generator
 - Developed power
- 12.15** A wind turbine with eight-pole, 60 Hz, three-phase, Y-connected induction generator is delivering 500 kW to the grid at 0.7 pf lagging. The terminal voltage of the generator is 690 V. The electrical efficiency of the generator is 90% and the mechanical efficiency is 92%. The parameters of the machine are
- $$R_1 = R_2' = 0.02 \Omega; X_{eq} = 0.1 \Omega.$$
- Compute the following:
- Mechanical power received from wind
 - Developed power
 - Stator current
- 12.16** A wind turbine has 50 m long blades. The far stream wind speed is 15 m/s and the coefficient of performance C_p is 30% at the operational pitch angle. The induction generator is six-pole, 60 Hz machine and is rotating at 1260 rpm. The mechanical efficiency of the turbine is 85% and the electrical efficiency of the generator is 90%. Compute the following:
- Power captured by the blade
 - Slip of the generator
 - Power delivered to the stator
 - Output electric power of the wind turbine
 - Rotor copper loss
 - Stator losses
 - Total system efficiency
- 12.17** A synchronous generator connected directly to an infinite bus is generating at its maximum real power. The line-to-line voltage of the infinite bus is 480 V and the synchronous reactance of the generator is 5Ω . Compute the reactive power of the generator.
- 12.18** A 1 GW synchronous generator is connected to an infinite bus through a transmission line. The synchronous reactance of the generator is 9Ω and the inductive reactance of the transmission line is 3Ω . The infinite bus voltage is 110 kV. If the generator delivers its rated power at unity power factor to the infinite bus, compute the following:

- a. Terminal voltage of the generator
 - b. Equivalent field voltage
 - c. Real power output at the generator terminals
 - d. Reactive power output at the generator terminals
- 12.19** A synchronous generator is connected directly to an infinite bus. The voltage of the infinite bus is 15 kV. The excitation of the generator is adjusted until the equivalent field voltage E_f is 14 kV. The synchronous reactance of the machine is $5\ \Omega$. Compute the following:
- a. Pullover power (maximum power)
 - b. Equivalent excitation voltage that increases the pullover power by 20%
- 12.20** A 100 MVA synchronous generator is connected to a 25 kV infinite bus through two parallel transmission lines. The synchronous reactance of the generator is $2.5\ \Omega$, and the inductive reactance of each transmission line is $2\ \Omega$. The generator delivers 100 MVA to the infinite bus at 0.8 power factor lagging. Suppose a lightning strike causes one of the transmission lines to open. Assume that the mechanical power and excitation of the generator are unchanged. Can the generator still deliver the same amount of power to the infinite bus?
- 12.21** A synchronous generator is connected to an infinite bus through a transmission line. The infinite bus voltage is 15 kV and the equivalent field voltage of the machine is 14 kV. The transmission line inductive reactance is $4\ \Omega$, and the synchronous reactance of the machine is $5\ \Omega$.
- a. Compute the capacity of the system.
 - b. If a $2\ \Omega$ capacitor is connected in series with the transmission line, compute the new capacity of the system.
- 12.22** A synchronous motor excited by a 5 kV source has a synchronous reactance of $5\ \Omega$. The motor is running without any mechanical load (i.e., the output real power is zero). Ignore all losses and calculate the equivalent field voltage E_f that delivers 3 MVAR to the source. Also, draw the phasor diagram.
- 12.23** A six-pole, 60 Hz synchronous motor is connected to an infinite bus of 15 kV through a transmission line. The synchronous reactance of the motor is $5\ \Omega$, and the inductive reactance of the transmission line is $2\ \Omega$. When E_f is adjusted to 16 kV (line-to-line), the reactive power at the motor's terminals is zero:
- a. Draw the phasor diagram of the system.
 - b. Calculate the terminal voltage of the motor.
 - c. Calculate the developed torque of the motor.
- 12.24** A 12-pole, 480 V, 60 Hz synchronous motor has a synchronous reactance of $5\ \Omega$. The field current is adjusted so that the equivalent field voltage E_f is 520 V (line-to-line). Calculate the following:
- a. Maximum torque
 - b. Power factor at the maximum torque
- 12.25** An industrial load is connected across a three-phase, Y-connected source of 4.5 KV (line-to-line). The real power of the load is 160 kW, and its power factor is 0.8 lagging:
- a. Compute the reactive power of the load.
 - b. A synchronous motor is connected across the load to improve the total power factor to unity. The synchronous motor is running unloaded (no mechanical load). If the synchronous reactance of the motor is $10\ \Omega$, compute the equivalent field voltage of the motor.
- 12.26** A dc motor is driving a constant-torque load. If the armature voltage of the motor increases by 20%, calculate the percentage change in no load speed.
- 12.27** A dc motor is driving a constant-torque load. If the field voltage of the motor decreases by 20%, calculate the percentage change in no load speed.
- 12.28** A 150 V, dc motor drives a constant-torque load at a speed of 1200 rpm. The armature and field resistances are $2\ \Omega$ and $150\ \Omega$, respectively. The motor draws an armature current of 9 A and field current of 1 A. Assume that a resistance is added in the field circuit to reduce the field current by 20%. Calculate the armature current, motor speed, and value of the added resistance.

- 12.29** A 200 V dc motor is loaded by a constant torque of 10 Nm. The armature resistance of the motor is $2\ \Omega$, and the field constant $K\phi = 2.5\ \text{V s}$. Calculate the motor speed.
- 12.30** A 10-teeth VRSM is loaded by 10 mNm torque. The phase voltage is adjusted so that the winding current is 20 mA. The torque constant K of the motor is 3 V s. Compute the following:
- Holding torque of the motor
 - Mechanical displacement angle
- 12.31** An eight-pole, three-phase PMSM has a torque constant K of 2 V s. When the load torque is 20 mNm, the mechanical displacement angle is 10° . Compute the following:
- Holding torque
 - Current of the stator windings
 - Stator current that reduces the mechanical displacement angle to 4°
- 12.32** An eight-phase VRSM with a step angle of 4.5° and a step rate of 300 sps is driving an inertia load. The inertia of the load plus the rotor is $4.4\ \text{mgm}^2$, and the friction torque is 13 mNm. Compute the following:
- Number of teeth of the rotor
 - Switching period τ
 - Speed of the motor
 - Input power (ignore electric losses)
 - Inertia torque to accelerate the motor at $20\ \text{rad/s}^2$
- 12.33** Explain the rotation of the shaded-pole motor using your own words.
- 12.34** Write a computer program that shows how the capacitor in the auxiliary winding of a single-phase motor causes the airgap magnetic field to rotate.
- 12.35** For the split-phase motor, write a computer program to compute the magnetic field in the airgap.
- 12.36** Why do we need to switch off the auxiliary winding of the single-phase motor?

13 Power Quality

The ideal alternating current (ac) waveform has two important features: (1) it contains no harmonic component besides the fundamental frequency (50 or 60 Hz), and (2) its magnitude is constant over a long period. Figure 13.1 shows the shape of an ideal waveform that is symmetrical and cyclic with constant period. A deviation from any of these characteristics results in what is known as power quality problem.

Unfortunately, the ideal waveform in Figure 13.1 does not exist in the real world. The nonlinear characteristics of most power equipment and the switching of loads tend to distort the voltage and current waveforms. Devices such as transformers and motors can cause distortions due to the saturation of their magnetic cores. Power electronic converters can also cause distortions due to the continuous switching of their components as shown in Chapter 10. Cyclic load switching, such as that in sawmills and rock crushing plants, can cause flickers in voltage. Overloading distribution feeders can cause low voltage problems at customers' sites.

Most electrical equipment and devices tolerate small distortions in the alternating current waveforms. However, when the distortions are large enough to affect equipment or be perceived by the public as annoyances, they are power quality problems.

Although the use of modern power electronic converters cause some of the power quality problems due to their switching actions, power electronics can solve a large number of these problems as well. In the early 1980s, when personal computers were widely available, they were very susceptible to a wide range of power quality problems. Any dip in voltage, due to the use of heavy loads such as vacuum cleaners at starting, would result in freezing or rebooting computers. Nowadays, the advancement in power electronics allows us to build computers with power supplies that can ride through any voltage dip and most transients.

In this chapter, you will find that most of the power quality problems are created by some customers and can affect other customers on the same part of the grid. This situation creates a dilemma to utilities when it comes to identifying the parties responsible for the power quality problems, and who should bear the cost of fixing the problems. Utilities often argue that polluters of the waveforms must bear the costs of ensuring supply quality. Nevertheless, unless there are enforceable standards, utilities will continue to carry the burden of fixing the power quality problems on their grid.

The main power quality problems are related to voltage and frequency. Voltage problems include voltage flickers, voltage sags, voltage swells, stray voltages, voltage transients, and outages. Frequency problems include harmonic distortions and frequency variations. Electromagnetic interferences, whether from nearby energized circuits or from solar flares, are also considered power quality problems.

13.1 VOLTAGE PROBLEMS

Most of the voltage problems can be explained by the circuit in Figure 13.2. The figure shows two loads (Load₁ and Load₂) representing two customers connected to the same source via a feeder (cable, transmission line, etc.). The parallel impedance of the two loads can be computed by

$$\frac{1}{Z} = \frac{1}{Z_1} + \frac{1}{Z_2} \quad (13.1)$$

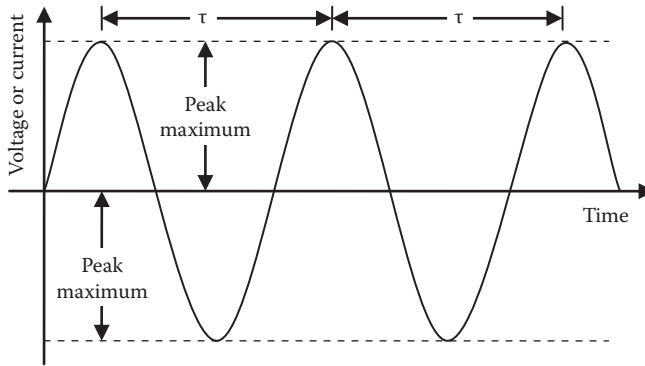


FIGURE 13.1 Ideal ac waveform.

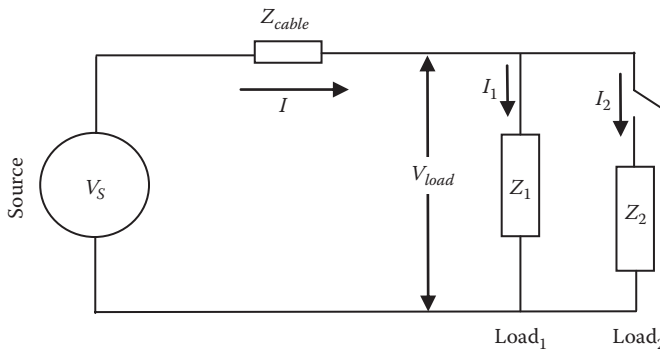


FIGURE 13.2 Loads connected to voltage source through cable.

The voltage at the load side can be computed by

$$\bar{V}_{load} = \bar{I}\bar{Z} = \frac{\bar{V}_s}{\bar{Z} + \bar{Z}_{cable}} \bar{Z} = \frac{\bar{V}_s}{1 + \left(\frac{\bar{Z}_{cable}}{\bar{Z}}\right)} \tag{13.2}$$

When Load₂ is switched on, the magnitude of the total impedances Z is smaller than the magnitude of any one of the two parallel impedances. Knowing this fact, let us examine Equation 13.2. The equation shows that when more loads are added, the total impedance Z is reduced, thus the load voltage is reduced. Therefore, the voltage at customer 1 depends on the load impedance of customer 2.

Example 13.1

For the system in Figure 13.2, assume $V_s = 120\text{ V}$, $Z_{cable} = 2 \angle 90^\circ \ \Omega$, $Z_1 = 10 \angle 0^\circ \ \Omega$, and $Z_2 = 5 \angle 0^\circ \ \Omega$. Compute the following:

- a. Load voltage when Load₂ is switched off
- b. Load voltage when Load₂ is switched on
- c. Voltage reduction on Load₁ due to the presence of Load₂

Solution

a. Without Load₂, the line current is

$$\bar{I} = \frac{\bar{V}_s}{\bar{Z}_1 + \bar{Z}_{cable}} = \frac{120\angle 0^\circ}{10 + j2} = 11.54 - j2.3 \text{ A}$$

The voltage on Load₁ without Load₂ is

$$\bar{V}_{load1} = \bar{Z}_1 \bar{I} = 10 \times (11.5 - j2.3) = 115.4 - j23 = 117.7\angle -11.3^\circ \text{ V}$$

b. With Load₂, the line current I is

$$\bar{I} = \frac{\bar{V}_s}{\frac{\bar{Z}_1 \bar{Z}_2}{\bar{Z}_1 + \bar{Z}_2} + \bar{Z}_{cable}} = \frac{120\angle 0^\circ}{3.33 + j2} = 31\angle -31^\circ \text{ A}$$

Hence, the load voltage is

$$\bar{V}_{load2} = \frac{\bar{Z}_1 \bar{Z}_2}{\bar{Z}_1 + \bar{Z}_2} \bar{I} = 3.33 \times 31\angle -31^\circ = 103\angle -31^\circ \text{ V}$$

c. The voltage reduction on Load₁ due to Load₂ is

$$\frac{\Delta V}{V_1} = \frac{V_{load2} - V_{load1}}{V_{load1}} = \frac{103 - 117.7}{117.7} = -12.5\%$$

The voltage on Load₁ is reduced by 12.5% when Load₂ is switched on. This is because Load₂ is twice as large as Load₁ (or $Z_1 = 2Z_2$). Repeat the example and assume Load₂ is smaller than Load₁ ($Z_2 > Z_1$). Can you draw a conclusion?

As seen in Example 13.1, the voltage at the customer side changes with the change in the overall loading of the feeder. However, it is normal for the voltage to change slightly and slowly. People perception and equipment are not affected by the small and slow changes in voltage. Actually if you measure the voltage in your home, you will find that its value changes slightly several times a day. In severe cases, when the changes are large, rapid, or cyclic, voltage problems could occur such as the following:

- *Fluctuations*: Small changes in voltage between 90% and 110% of the rated value. If the change is slow, every few hours, the fluctuations have no effect on people or equipment.
- *Flickers*: Fast and cyclic changes in voltage that are detected by human eyes. Although the magnitude of the flicker could be within the fluctuation range of the voltage, it is often fast enough, allowing human eyes to detect it.
- *Sags*: Voltage below 90% of the rated value for a short period (up to a few seconds).
- *Swells*: Voltage above 110% for a short period (up to a few seconds).
- *Undervoltage* (Brownout): Voltage drop below 90% for at least several minutes.
- *Overvoltage*: Voltage increase above 110% for at least several minutes.
- *Interruptions*: decrease in voltage below 10% for any period.

Most of these problems can be caused by similar scenarios but with different time scales and magnitudes. In this chapter, we shall cover the most common problems: flickers and sags. The analyses of the other problems are mostly extensions of the ones we cover.

13.1.1 VOLTAGE FLICKERS

The term “flicker” was originally used to describe visible modulation in light intensity of electric incandescent lamps. In general, flicker is the fluctuation of voltage at frequencies much lower than the power frequency.

One of the most irritating effects of voltage flickers is light flickers (fast variations in light intensity). Light intensity λ is a measure of the brightness of a light source which is roughly dependent on the power consumed by the light bulb. For incandescent lamps, which are essentially resistors, their light intensities or output powers are proportional to the square of the applied voltages:

$$\lambda_{incandescent} \propto P \propto V^2 \quad (13.3)$$

The ballasts in ballasted lamps (arc and fluorescent lamps), tend to make the light intensity proportional to the applied voltage:

$$\lambda_{ballast} \propto V \quad (13.4)$$

Thus, different lamps respond differently to voltage fluctuations. Incandescent lamps tend to be more sensitive to changes in voltage than ballasted lamps.

Example 13.2

A 120 V system experiences a 10% voltage drop. Compute the change in light intensity for incandescent and ballasted lamps.

Solution

For incandescent lamps the change in light intensity is

$$\Delta\lambda_{incandescent} = \frac{\lambda_2 - \lambda_1}{\lambda_1}$$

where

λ_1 is the light intensity at 120 V

λ_2 is the light intensity at 120 V – 10%

Hence,

$$\Delta\lambda_{incandescent} = \frac{V_2^2 - V_1^2}{V_1^2} = \frac{(0.9 \times 120)^2 - 120^2}{120^2} = 19\%$$

For ballasted lamps, the change in light intensity is proportional to the voltage:

$$\Delta\lambda_{ballast} = \frac{\lambda_2 - \lambda_1}{\lambda_1} = \frac{V_2 - V_1}{V_1} = \frac{(0.9 \times 120) - 120}{120} = 10\%$$

Notice that the light intensity reduction of the incandescent lamp is almost double that for the ballasted lamp.

The changes in light intensity can be easily perceived by the human eye which can detect variations in brightness as small as 1%. However, the human eye cannot normally detect light flickers above 35 Hz. Experimental studies show that the maximum sensitivity to light flickers is in the range of 8–10 Hz.

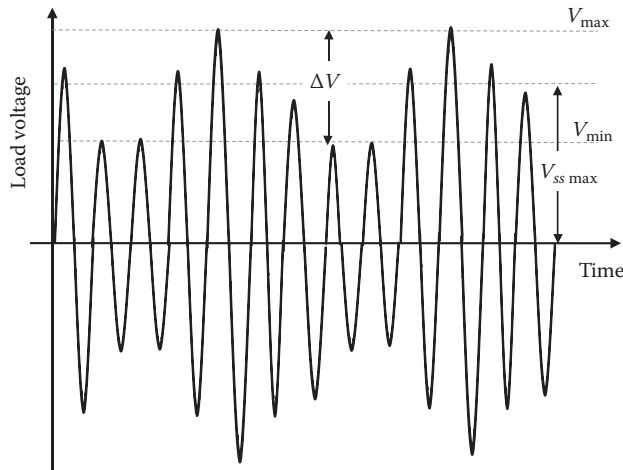


FIGURE 13.3 Cyclic flicker.

Besides the visual annoyance, voltage flickers can cause a wide range of problems, including computer freeze up (especially older computers), jitter of television pictures, faulty signals in electronic circuits, malfunction of sensitive equipment, and loss of information stored in electronic memories.

There are two types of flickers: cyclic flicker and noncyclic flicker. Cyclic flicker may occur at a regular frequency and may have a steady magnitude. It is caused by periodic heavy load fluctuations such as those in reciprocating compressors, automatic spot welders, arc furnaces, flashing signals, sawmills, group elevators, and cyclic electric hammers. An example of a cyclic flicker is shown in Figure 13.3. Noncyclic flicker may occur at random intervals and is caused by occasional heavy load switching.

A simple method to model the flicker in Figure 13.3 is to assume that the voltage is an amplitude modulated waveform similar to that used in radio broadcasting. In this case, the instantaneous value of the flicker voltage V_f that modulates the load voltage is

$$v_f = V_{ss\max} \sin(\omega t) \frac{\Delta V}{2} \sin(\omega_f t) \quad (13.5)$$

where

$V_{ss\max}$ is the peak value of the steady-state voltage without any flicker

$\Delta V/2$ is the modulation amplitude of the flicker

ω is the frequency of the supply voltage without the flicker

ω_f is the frequency of the flicker

The load voltage is the sum of the load voltage without the flicker v_{ss} and the flicker voltage. This is the well-known amplitude modulation equation:

$$v_{load} = v_{ss} + v_f = V_{ss\max} \left(1 + \frac{\Delta V}{2} \sin(\omega_f t) \right) \sin(\omega t) \quad (13.6)$$

The ratio of the modulation amplitude to the peak value of the source voltage without flicker is defined as the flicker factor F :

$$F = \frac{\Delta V/2}{V_{ss\max}} \quad (13.7)$$

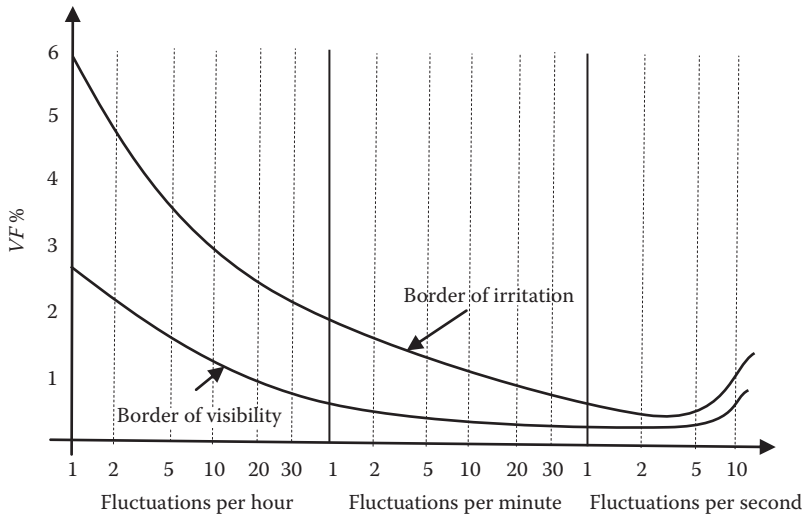


FIGURE 13.4 Effect of flickers on human.

If the flicker factor is zero, the voltage waveform is without any flicker. The larger the flicker factor, the more severe is the flicker problem.

Another term often used to quantify flicker is voltage fluctuation VF . It is the maximum flicker amplitude ΔV divided by the peak voltage without the flicker:

$$VF = \frac{\Delta V}{V_{ss\max}} = 2F \tag{13.8}$$

In the United States, General Electric Company did an extensive study on human tolerance to light flickers. In this study, a group of volunteers were subjected to different levels of VF at different frequencies. The result of the study is summarized in Figure 13.4. The study shows that the higher the frequency of the light flickers, the lower is the VF that induces irritation to the human eye. The human perception of repeated flicker is usually much more pronounced than the perception of infrequent flickers. However, above 35 Hz, people tend not to be affected by the flicker. Occasional voltage dips, not flickers, even if clearly perceptible, are not objectionable to the majority of individuals.

Example 13.3

A system with steady-state voltage of 120 V is connected to a cyclic load that fluctuates at a rate of 15 cycle/h. Compute the maximum allowable flicker ΔV .

Solution

The maximum allowable flicker is the value at the irritation level, not the level of perception. According to Figure 13.4, VF at the irritation level for 15 cycle/h is about 3%. In this case,

$$\Delta V = VF \times V_{ss\max} = 0.03 \times 120 \times \sqrt{2} = 5.1 \text{ V}$$

About 5 V variation in voltage can irritate people if the flicker is repeated 15 times/h.

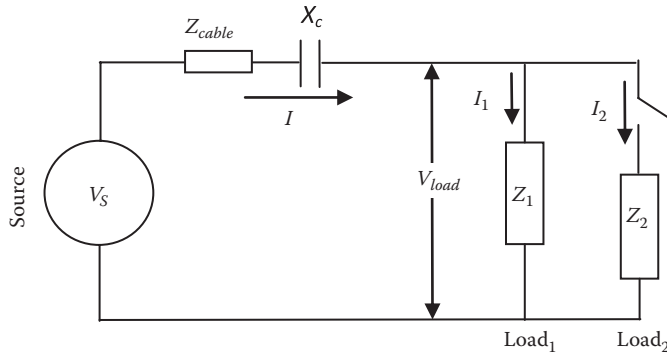


FIGURE 13.5 Loads connected to source by capacitor compensated cable.

There are a few methods to remedy flicker problems; among them is line compensation. As shown in Example 13.1, the voltage change is due to the large line impedance that feeds the loads. Since this impedance is predominantly inductive reactance, we can reduce the total reactive component of the line impedance by installing a series capacitor along the distribution feeder as shown in Figure 13.5. In this case, because the total impedance between the source and the load is substantially reduced, the voltage fluctuation is diminished as shown in Example 13.4.

Example 13.4

Repeat Example 13.1, but assume that the line is compensated by a series capacitor of 1.8Ω .

Solution

- a. With Load₂ switched off, the current of the cable is

$$\bar{I} = \frac{\bar{V}_s}{\bar{Z}_1 + \bar{Z}_{cable} + \bar{X}_c} = \frac{120\angle 0^\circ}{10 + j2 - j1.8} = 12 - j0.24$$

The steady-state voltage across Load₁ is

$$\bar{V}_{ss} = \bar{Z}_1 \bar{I} = 120 - j2.4 \approx 120\angle 0^\circ \text{ V}$$

- b. With Load₂ switched on, the line current is

$$\bar{I} = \frac{\bar{V}_s}{\frac{\bar{Z}_1 \bar{Z}_2}{\bar{Z}_1 + \bar{Z}_2} + \bar{Z}_{cable} + \bar{X}_c} = \frac{120\angle 0^\circ}{3.33 + j2 - j1.8} = 36\angle -3.44^\circ \text{ A}$$

Hence, the load voltage when Load₂ is switched on is

$$\bar{V}_{load} = \frac{\bar{Z}_1 \bar{Z}_2}{\bar{Z}_1 + \bar{Z}_2} \bar{I} = 3.33 \times 36\angle -3.44^\circ = 119.88\angle -3.44^\circ \text{ V}$$

- c. The voltage reduction of Load₁ due to the switching of Load₂ is

$$\frac{\Delta V}{V_{ss}} = \frac{V_{load} - V_{ss}}{V_{ss}} = \frac{119.88 - 120}{120} = -0.1\%$$

The voltage on Load₁ is reduced by just 0.1% when Load₂ is switched on *and* the line is compensated by the series capacitor. Without the series capacitor, the voltage reduction on Load₁ is 12.5% as computed in Example 13.1. According to Figure 13.4, the 0.1% flicker is unnoticeable.

13.1.2 VOLTAGE SAG

Voltage sag (also known as voltage dip) is the most common power quality problem. Voltage sag is a short duration of voltage reduction (see Figure 13.6) that is caused by switching on heavy electric loads such as elevators, cranes, pumps, air conditioners, refrigerators, and x-ray equipment. Voltage sags can also be caused by the disconnection of feeders and by faults in power system components. The difference between the sag and the flicker is that the flicker is repetitive or cyclic while the sag is not.

Motors continuously start and stop, causing transients in currents (called inrush current) due to the saturation of their magnetic cores and the inertia of their mechanical loads. Transformer switching also causes inrush current due to the saturation of its cores. The sudden applied voltage causes the flux in the core to briefly exceed its steady-state value, thus driving the core into saturation (refer to the hysteresis loop in Chapter 11). The inrush currents can reach values as high as 25 times the full-load ratings, and can last between 200 ms and 1 min. Typical starting current characteristics are shown in Figure 13.7. Figure 13.7a shows a symmetrical inrush current without any direct current (dc) component and Figure 13.7b shows the inrush current with a dc component that is often decayed very quickly. In both cases, when the voltage is applied, the inrush current ramps up quickly to its crest value, and then slowly decreases to its steady-state value.

The inrush currents of heavy equipment cause the voltage at the connection point to sag. You have probably noticed that when the vacuum cleaner in your home starts, the light intensity of lamps is reduced. Voltage sags can cause a variety of problems from interrupting controllers or relays to malfunction of sensitive medical equipment. They also cause some types of motors to run at lower speeds or take a longer time to start. Severe sags can cause major disruptions to assembly lines and central air-conditioning systems.

A voltage waveform with a voltage sag typically looks like the one in Figure 13.8 for the symmetrical inrush current without a dc component. The dip in voltage is due to the inrush current around its crest value, and the overshoot is often due to the inductive elements in the equipment.

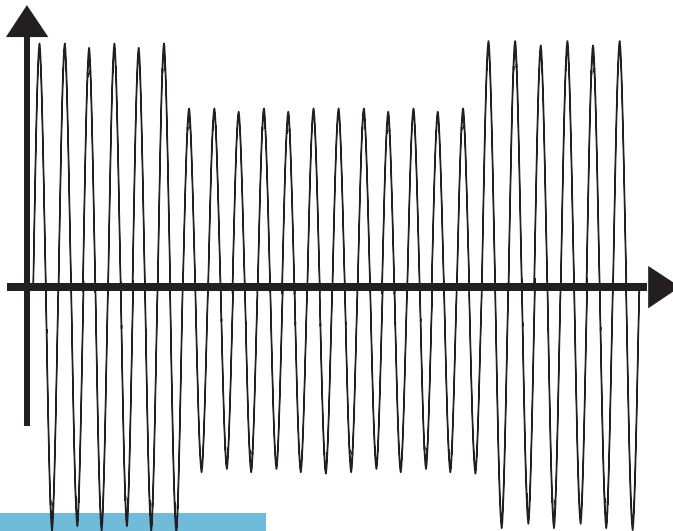


FIGURE 13.6 Voltage sag (dip).

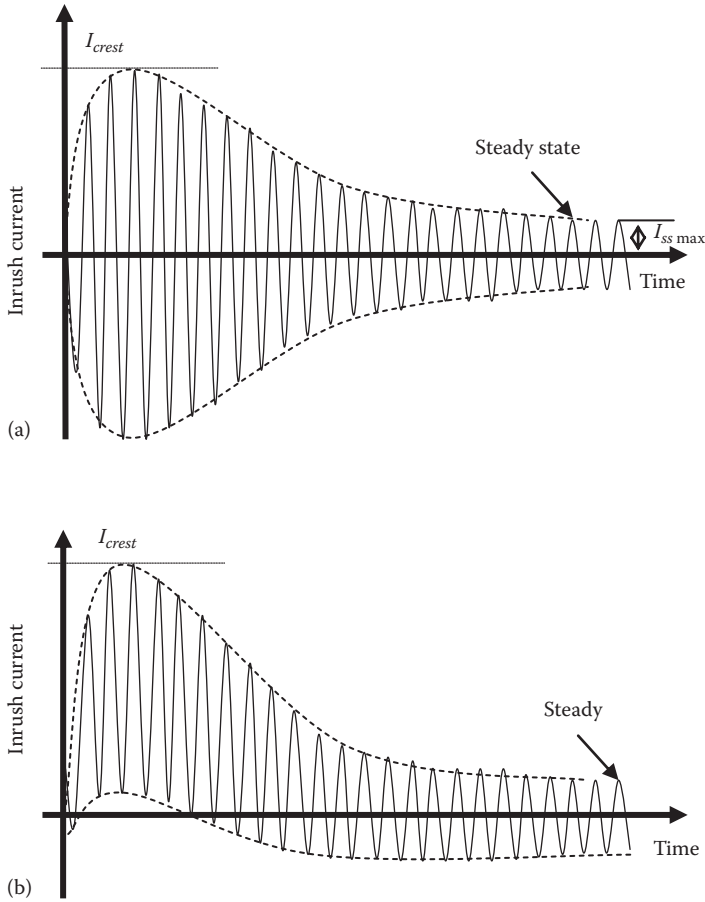


FIGURE 13.7 Typical inrush current waveforms at motor starting or transformer switching: (a) symmetrical inrush current and (b) asymmetrical inrush current.

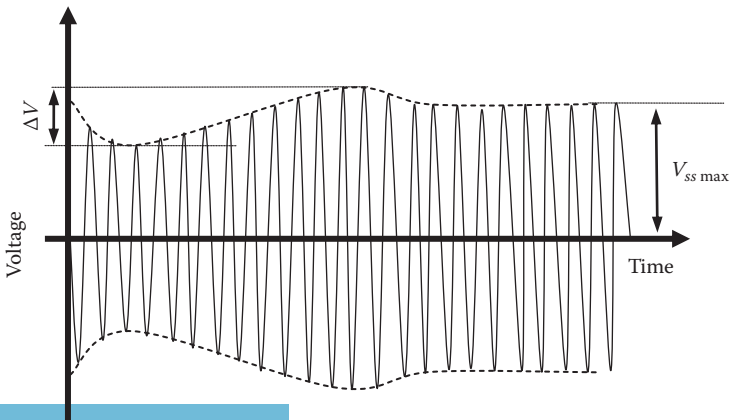


FIGURE 13.8 Flicker voltage due to symmetrical inrush current.

The symmetrical inrush current in Figure 13.7 can be expressed by the following generic equation:

$$i = I_{ss \max} \sin(\omega t) \left(1 - e^{-\frac{t}{\tau_1}} \right) \left(1 + k e^{-\frac{t}{\tau_2}} \right) \quad (13.9)$$

where

i is the instantaneous value of the inrush current

τ_1 is the rising time constant

τ_2 is the falling time constant (both τ_1 and τ_2 are functions of the parameters of equipment, especially magnetic circuit and system inertia)

k is a factor that determines the maximum crest of the inrush current I_{crest}

$I_{ss \max}$ is the peak value of the steady-state current

ω is the angular frequency of the source voltage

If the equipment is energized through a cable whose resistance is negligibly small and whose inductance is L , the voltage across the equipment v_{load} is

$$v_{load} = v_s - L \frac{di}{dt} \quad (13.10)$$

where v_s is the instantaneous voltage of the source

$$v_s = V_{\max} \sin(\omega t + \theta) \quad (13.11)$$

where θ is the angle of the source voltage with respect to the steady-state current. Solving Equation 13.10 numerically leads to the load voltage in Figure 13.8. To do this, we need to compute the derivative of the current in Equation 13.10, which is obtained by differentiating Equation 13.9:

$$\frac{di}{dt} = I_{ss \max} \left[\omega \cos(\omega t) \left(1 - e^{-\frac{t}{\tau_1}} \right) \left(1 + k e^{-\frac{t}{\tau_2}} \right) + \sin(\omega t) \left(\frac{e^{-\frac{t}{\tau_1}}}{\tau_1} \right) \left(1 + k e^{-\frac{t}{\tau_2}} \right) - \sin(\omega t) \left(1 - e^{-\frac{t}{\tau_1}} \right) \left(\frac{k e^{-\frac{t}{\tau_2}}}{\tau_2} \right) \right] \quad (13.12)$$

To compute the voltage sag by these equations is tedious and requires numerical solution. However, we can predict the approximate value of the sag if we make two reasonable assumptions:

1. Time constants (τ_1 and τ_2) are long enough with respect to one duration of the ac waveform. This would allow us to use root mean square (rms) calculations.
2. Inrush current is totally inductive until it reaches its crest value I_{crest} . This is a reasonable assumption as the inductive elements of the motors and transformers are predominant at starting.

In this case, we can compute the voltage across the load by the rms phasor calculations

$$\bar{V}_{load} = \bar{V}_s - \bar{X}_L \bar{I} \quad (13.13)$$

where

X_L is the inductive reactance of the line

I is the rms inrush current of the feeder (line)

In Equation 13.13, we ignored the resistance of the cable as it is often much smaller than the inductive reactance.

Since the current is predominantly inductive until it reaches its crest value, the current lags the source voltage by almost 90° . Hence, the source voltage, load voltage, and the drop across the line inductance are all in phase. In this case, we can use the magnitudes only for Equation 13.13:

$$V_{load} = V_s - X_L I \quad (13.14)$$

The voltage sag VS is defined as the change in voltage ΔV with respect to the steady-state voltage before the sag V_{ss} :

$$VS = \frac{\Delta V}{V_{ss}} = \frac{V_{load} - V_{ss}}{V_{ss}} \quad (13.15)$$

Example 13.5

The motor in Figure 13.9 has a crest current at starting of 20 A when the source voltage is 120 V. The inductive reactance of the cable is 2Ω . Estimate the voltage sag across the motor's terminals.

Solution

Keep in mind that the crest current is the peak value, not the rms value. Hence the crest current of the cable in rms is

$$\bar{I} = \frac{\bar{I}_{crest}}{\sqrt{2}} = \frac{-j20}{\sqrt{2}} = -j14.14 \text{ A}$$

The voltage across the motor at the crest of the starting current is

$$\bar{V}_{load} = \bar{V}_s - \bar{I} \bar{Z}_{cable} = 120 - (-j14.14)(j2) = 91.72 \angle -0^\circ \text{ V}$$

Before switching the motor, the voltage at the load side is equal to the source voltage. Hence, the voltage sag VS due to the start-up of the motor is

$$VS = \frac{\Delta V}{V_{ss}} = \frac{V_{load} - V_{ss}}{V_{ss}} = \frac{91.72 - 120}{120} = -23.6\%$$

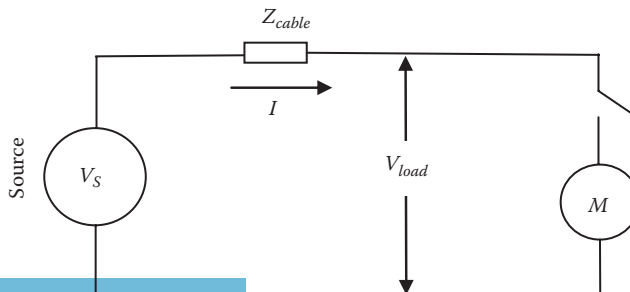


FIGURE 13.9 Motor connected to source via cable.

The voltage at the load side has dropped by 23.6%. This high level of voltage drop will be felt by any load connected in parallel with this motor.

Most of the methods used to remedy voltage sags are the same as the ones used for voltage flickers. We have discussed earlier the use of series capacitors to reduce the effect of voltage flickers. The same method can be used to reduce voltage sags. The capacitors can also be installed in parallel with the load.

Example 13.6

Repeat Example 13.5, but assume that a 6Ω capacitor is added in parallel with the motor at starting (Figure 13.10).

Solution

Since the crest inrush current is inductive, we can compute the equivalent reactance X_m of the motor at the crest point of the inrush current when the voltage is 91.72 V:

$$\bar{X}_m = \frac{\bar{V}_{load}}{\bar{I}_{crest}} = \frac{91.72\angle 0^\circ}{-j\frac{20}{\sqrt{2}}} = j6.5\ \Omega$$

The total load reactance X_{load} is the parallel combination of the motor equivalent inductive reactance X_m and the capacitive reactance of the capacitor X_c :

$$\bar{X}_{load} = \frac{\bar{X}_m \bar{X}_c}{\bar{X}_m + \bar{X}_c} = \frac{j6.5(-j6)}{j0.5} = -j78\ \Omega$$

The cable current at the crest of the inrush current is

$$\bar{I}_1 = \frac{\bar{V}_s}{\bar{X}_{load} + \bar{Z}_{cable}} = \frac{120\angle 0^\circ}{-j78 + j2} = j1.58\ \text{A}$$

Now, we can compute the load voltage:

$$\bar{V}_{load} = \bar{I}_1 \bar{X}_{load} = j1.58 \times (-j78) = 123.24\ \text{V}$$

The voltage sag at the start-up of the motor with the capacitor is

$$VS = \frac{\Delta V}{V_{ss}} = \frac{V_{load} - V_{ss}}{V_{ss}} = \frac{123.24 - 120}{120} = 2.7\%$$

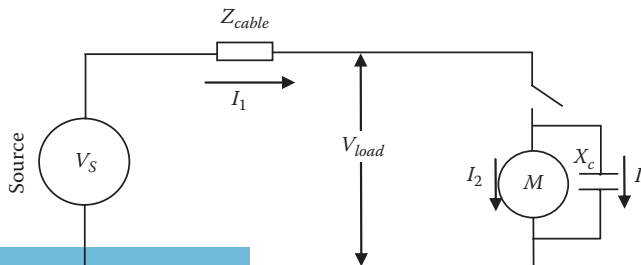


FIGURE 13.10 Motor with starting capacitor.

The voltage at the load side is actually increased by 2.7% at starting. A smaller increase in voltage can be obtained if the capacitance of the capacitor is reduced. Compare this change in voltage with the 23.6% drop without the capacitor. Can you find the size of the capacitor that reduces the VS to just 1%?

Faults in power systems can also cause voltage sags. The faults could be initiated by a number of scenarios such as falling trees on distribution feeders or failing insulations of power cables. Consider the simple system in Figure 13.11. The system at the top part of the figure consists of a voltage source whose magnitude is assumed constant, a feeder, and a load. The equivalent circuit of the system is shown at the bottom of the figure. V_s is the voltage of the source, X_{line} is the inductive reactance of the feeder per unit length, D is the length of the feeder, and Z_{load} is the impedance of the load. Assume that a fault occurs at a distance d from the load and the impedance of the fault is Z_{fault} as shown in Figure 13.12. Using Kirchoff's equations, we can develop the following relationships;

$$\begin{aligned} \bar{V}_s &= (D - d)\bar{X}_{line}\bar{I} + \bar{Z}_{fault}\bar{I}_{fault} \\ \bar{V}_s &= (D - d)\bar{X}_{line}\bar{I} + (d\bar{X}_{line} + \bar{Z}_{load})\bar{I}_{load} \\ \bar{I} &= \bar{I}_{fault} + \bar{I}_{load} \end{aligned} \tag{13.16}$$

Solving these equations for the load current yields

$$\bar{I}_{load} = \frac{\bar{V}_s}{\bar{Z}_{load} + D\bar{X}_{line} + \left(\frac{(D - d)\bar{X}_{line}(\bar{Z}_{load} + d\bar{X}_{line})}{\bar{Z}_{fault}} \right)} \tag{13.17}$$

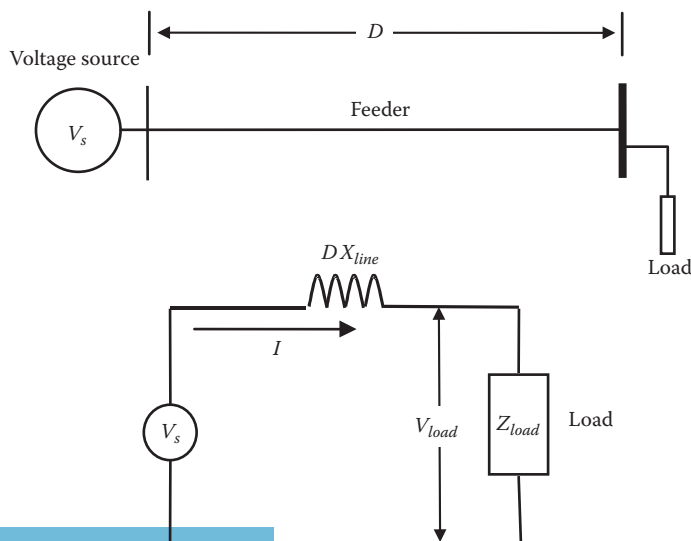


FIGURE 13.11 A representation of a simple power system.

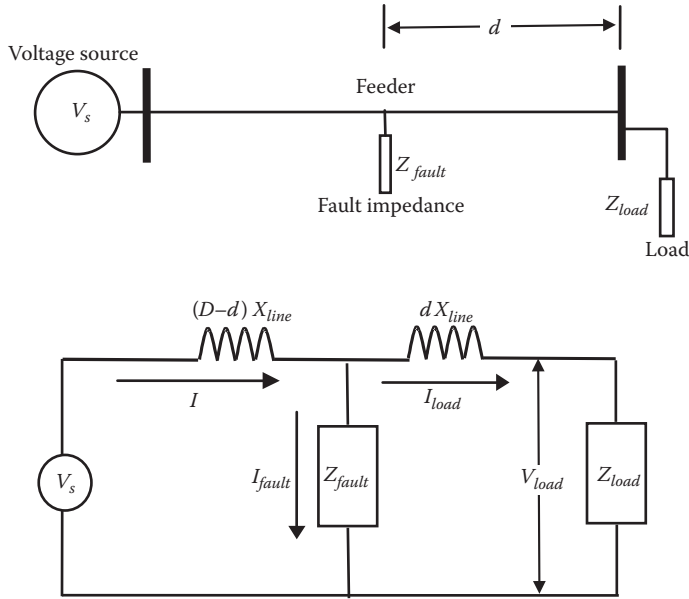


FIGURE 13.12 A representation of a simple power system with fault between source and load.

Hence, the load voltage is

$$\bar{V}_{load} = \bar{I}_{load} \bar{Z}_{load} = \frac{\bar{V}_s \bar{Z}_{load}}{\bar{Z}_{load} + D\bar{X}_{line} + \left(\frac{(D-d)\bar{X}_{line}(\bar{Z}_{load} + d\bar{X}_{line})}{\bar{Z}_{fault}} \right)} \tag{13.18}$$

As seen in Equation 13.18, the load voltage is lower when the fault impedance Z_{fault} is smaller.

Example 13.7

For the system in Figure 13.12, the source voltage is 67 kV (phase value), the feeder is 6 km in length, and its inductive reactance is 1.2 Ω/km. The impedance at the load side is 2∠30° kΩ. At 4 km from the source side, a falling tree causes a temporary fault. The impedance of the tree is 100∠75° Ω. Compute the voltage sag at the load side.

Solution

The first step is to compute the steady-state voltage V_{ss} at the load side before the fault. To do this, we can use Equation 13.18 when Z_{fault} is set to infinity:

$$\bar{V}_{ss} = \frac{\bar{V}_s \bar{Z}_{load}}{\bar{Z}_{load} + D\bar{X}_{line}} = \frac{67 \angle 0^\circ (2000 \angle 30^\circ)}{2000 \angle 30^\circ + 6 \times 1.2 \angle 90^\circ} = 66.88 \angle -0.18^\circ \text{ kV}$$

During the fault, the load voltage is

$$\bar{V}_{load} = \frac{\bar{V}_s \bar{Z}_{load}}{\bar{Z}_{load} + D\bar{X}_{line} + \left(\frac{(D-d)\bar{X}_{line}(\bar{Z}_{load} + d\bar{X}_{line})}{\bar{Z}_{fault}} \right)}$$

where

$$d = 6 - 4 = 2 \text{ km}$$

Hence,

$$\bar{V}_{load} = \frac{67 \angle 0^\circ (2000 \angle 30^\circ)}{2000 \angle 30^\circ + 6 \times 1.2 \angle 90^\circ + \left(\frac{4(1.2 \angle 90^\circ)(2000 \angle 30^\circ + 2 \times 1.2 \angle 90^\circ)}{100 \angle 75^\circ} \right)}$$

$$\bar{V}_{load} = 63.9 \angle -0.85^\circ \text{ kV}$$

The voltage sag at the load side during the fault is

$$VS = \frac{\Delta V}{V_{ss}} = \frac{V_{load} - V_{ss}}{V_{ss}} = \frac{63.9 - 67}{67} = -4.43\%$$

Notice that we assumed that the generator voltage is unchanged during the fault. In reality, the terminal voltage of the generator is reduced due to the actions of the various voltage regulators in the system as well as the changing internal impedance of the generator. Repeat the solution and assume the fault impedance is 10 Ω.

Example 13.8

For the system in Figure 13.13, the source voltage is 100 kV (phase value), the feeder reactance X_1 is 8 Ω and X_2 is 5 Ω. The load impedance is $3 \angle 20^\circ \text{ k}\Omega$. A temporary fault occurs at the location in the figure. The fault impedance is $50 \angle 80^\circ \Omega$. Compute the voltage sag at the load side. Assume the end of the feeder was unloaded before the fault.

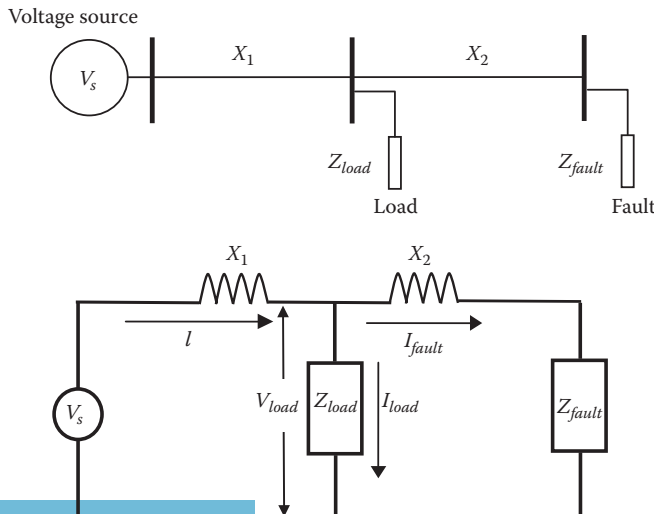


FIGURE 13.13 A representation of a simple power system with load between the fault and the source.

Solution

The steady-state voltage V_{ss} across the load before the fault is

$$\bar{V}_{ss} = \frac{\bar{V}_s \bar{Z}_{load}}{\bar{Z}_{load} + \bar{X}_1} = \frac{100 \angle 0^\circ (3000 \angle 20^\circ)}{3000 \angle 20^\circ + 8 \angle 90^\circ} = 99.9 \angle -0.14^\circ \text{ kV}$$

During the fault, you can easily compute the load current by writing the loop and nodal equations of the circuit in the matrix form:

$$\begin{bmatrix} \bar{V} \\ \bar{V} \\ 0 \end{bmatrix} = \begin{bmatrix} \bar{X}_1 & \bar{Z}_{load} & 0 \\ \bar{X}_1 & 0 & \bar{X}_2 + \bar{Z}_{fault} \\ -1 & 1 & 1 \end{bmatrix} \begin{bmatrix} \bar{I} \\ \bar{I}_{load} \\ \bar{I}_{fault} \end{bmatrix}$$

Hence,

$$\begin{bmatrix} \bar{I} \\ \bar{I}_{load} \\ \bar{I}_{fault} \end{bmatrix} = \begin{bmatrix} 8 \angle 90^\circ & 3000 \angle 20^\circ & 0 \\ 8 \angle 90^\circ & 0 & 5 \angle 90^\circ + 50 \angle 80^\circ \\ -1 & 1 & 1 \end{bmatrix}^{-1} \begin{bmatrix} 100 \angle 0^\circ \\ 100 \angle 0^\circ \\ 0 \end{bmatrix}$$

The solution of this equation leads to the load current during the fault:

$$\bar{I}_{load} = 27.13 - j10.56 \text{ A}$$

Then, the load voltage during the fault is

$$\bar{V}_{load} = \bar{Z}_{load} \bar{I}_{load} = 87.3 \angle -1.3^\circ \text{ kV}$$

The voltage sag at the load side during the fault is

$$VS = \frac{\Delta V}{V_{ss}} = \frac{V_{load} - V_{ss}}{V_{ss}} = \frac{87.3 - 99.9}{99.9} = -12.6\%$$

13.2 HARMONIC PROBLEMS

The alternating current waveform in its ideal shape is purely sinusoidal and its magnitude and frequency are constants. A waveform with any deviation from the ideal sinusoidal shape is considered distorted. An ideal waveform and an example of a distorted and periodic waveform are shown in Figure 13.14.

The reasons for the distortions of power system waveforms are many and include nonlinear loads and the switching of power electronic devices. But before we analyze harmonics, let us review the basic mathematics of harmonic analysis.

Any periodic waveform g that is not purely sinusoidal has a string of components at different frequencies. These components are called harmonics and can be represented by the well-known *Fourier series*

$$g = g_o + g_1(\omega t) + g_2(2\omega t) + g_3(3\omega t) + g_4(4\omega t) + \dots \quad (13.19)$$

where

g is the instantaneous value of the periodic waveform

g_o is the dc component in g

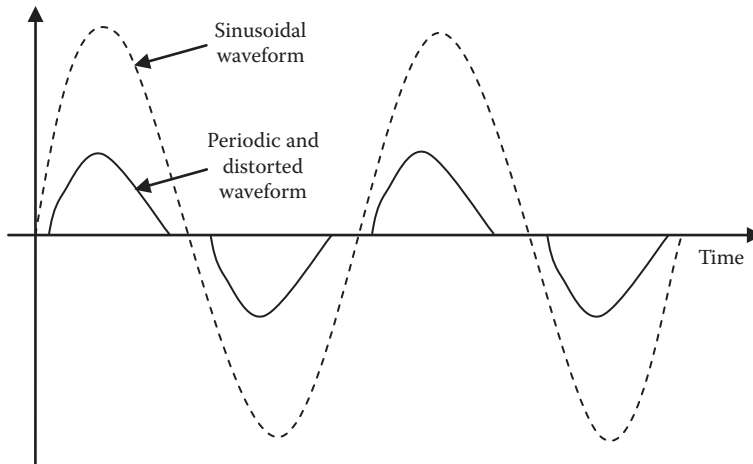


FIGURE 13.14 Sinusoidal and distorted waveforms.

g_1 is the instantaneous value of the sinusoidal component at the fundamental frequency ω
 g_2 is the sinusoidal component at double the fundamental frequency (second harmonic)
 g_3 is the third harmonic component at triple the frequency of the fundamental component,
 and so on

In its general form, the k th harmonic component can be written as

$$g_k = a_k \cos(k\omega t) + b_k \sin(k\omega t) \quad (13.20)$$

where

$$a_k = \frac{1}{\pi} \int_0^{2\pi} g \cos(k\omega t) d\omega t \quad (13.21)$$

$$b_k = \frac{1}{\pi} \int_0^{2\pi} g \sin(k\omega t) d\omega t$$

When g is in certain shapes, we can simplify the harmonic analysis. For instance, if g is an even waveform where $g(t) = g(-t)$, the sine term vanishes from Equation 13.20. For odd waveforms, such as the one in Figure 13.14 where $g(t) = -g(-t)$, the cosine term vanishes. For most distorted waveforms in power networks, odd functions are adequate representation. In this case, a current i that is periodic and distorted can be written as

$$i(\omega t) = I_{dc} + I_{1\max} \sin(\omega t) + I_{2\max} \sin(2\omega t) + I_{3\max} \sin(3\omega t) + \dots \quad (13.22)$$

where

I_{dc} is a dc component of i

$I_{1\max}$ is the peak value of the fundamental frequency component

$I_{2\max}$ is the peak value of the second harmonic current, and so on

The periodic current i in Equation 13.22 is hard to analyze in its instantaneous form. However, if we use rms quantities, we can simplify the analysis. The rms current is defined in Chapter 7 as

$$I = \sqrt{\frac{1}{2\pi} \int_0^{2\pi} [i(\omega t)]^2 d\omega t} \quad (13.23)$$

Hence, the rms current of a distorted waveform is

$$I = \sqrt{\frac{1}{2\pi} \int_0^{2\pi} [I_{dc} + I_{1\max} \sin(\omega t) + I_{2\max} \sin(2\omega t) + I_{3\max} \sin(3\omega t) + \dots]^2 d\omega t} \quad (13.24)$$

Before we continue with the analysis, you should know that the average value of cross-frequency components (two sinusoidal waveforms with different frequencies) is zero, that is,

$$\frac{1}{2\pi} \int_0^{2\pi} \sin(\omega t) \times \sin(k\omega t) d\omega t = 0; \quad \text{if } k \neq 1 \quad (13.25)$$

Using the fact in Equation 13.25, we can ignore all cross-frequency terms in Equation 13.24. Thus,

$$I = \sqrt{\frac{1}{2\pi} \left[\int_0^{2\pi} I_{dc}^2 d\omega t + \int_0^{2\pi} (I_{1\max} \sin(\omega t))^2 d\omega t + \int_0^{2\pi} (I_{2\max} \sin(2\omega t))^2 d\omega t + \dots \right]} \quad (13.26)$$

Keep in mind that the rms of any current harmonic is

$$I_k = \sqrt{\frac{1}{2\pi} \int_0^{2\pi} (I_{k\max} \sin(k\omega t))^2 d\omega t} \quad (13.27)$$

Then the rms current of a distorted waveform is

$$I = \sqrt{I_{dc}^2 + I_1^2 + I_2^2 + I_3^2 + \dots} \quad (13.28)$$

To quantify the distortion of a periodic function, two indices are often used: Individual harmonic distortion (IHD) and total harmonic distortion (THD). They are defined as follows:

$$\begin{aligned} \text{IHD}_k &= \frac{I_k}{I_1} \\ \text{THD} &= \frac{I_H}{I_1} \end{aligned} \quad (13.29)$$

where I_H is the harmonic current, which is the rms value of all harmonic components except the fundamental:

$$I_H = \sqrt{I_{dc}^2 + I_2^2 + I_3^2 + \dots} \quad (13.30)$$

The IHD_k is a measure of the contribution of the individual k th harmonic with respect to the fundamental component of the waveform. The THD is a measure of the total distortion in the waveform.

The THD has several other forms:

$$\text{THD} = \frac{\sqrt{I_{dc}^2 + I_2^2 + I_3^2 + \dots}}{I_1} = \sqrt{\frac{I_{dc}^2}{I_1^2} + \frac{I_2^2}{I_1^2} + \frac{I_3^2}{I_1^2} + \dots} \quad (13.31)$$

$$\text{THD} = \sqrt{\text{IHD}_{dc}^2 + \text{IHD}_2^2 + \text{IHD}_3^2 + \text{IHD}_4^2 + \dots}$$

Example 13.9

A distorted current waveform has four harmonic components represented by their rms values: the fundamental component is 50 A, the third harmonic component is 20 A, the fifth harmonic component is 5 A, and seventh harmonic component is 2 A. Compute the following:

- rms current of the distorted waveform
- IHD of the fifth harmonic
- THD

Solution

- Use Equation 13.28 to compute the rms current of the distorted waveform:

$$I = \sqrt{I_1^2 + I_3^2 + I_5^2 + I_7^2} = \sqrt{50^2 + 20^2 + 5^2 + 2^2} = 54.12 \text{ A}$$

- Use Equation 13.29 to compute IHD_5 :

$$\text{IHD}_k = \frac{I_k}{I_1} = \frac{5}{50} = 10\%$$

This result reveals that the fifth harmonic current is 10% of the fundamental component current.

- Use Equation 13.30 to compute the harmonic current:

$$I_H = \sqrt{20^2 + 5^2 + 2^2} = 20.71 \text{ A}$$

The total harmonic distortion is

$$\text{THD} = \frac{I_H}{I_1} = \frac{20.71}{50} = 41.42\%$$

This waveform contains 41.42% of its magnitude as harmonics.

13.2.1 HARMONIC DISTORTION OF ELECTRIC LOADS

The main question is why harmonics exist in a power system. If the source voltage is purely sinusoidal without any harmonics and the load impedance is linear, the current of the load is also

sinusoidal and free of harmonics. However, if the load is nonlinear, the load current is distorted as shown in the following example.

Example 13.10

A 120 V (rms) purely sinusoidal voltage source is feeding a nonlinear resistance. Assume that the value of the resistance is dependent on the applied voltage and can be expressed by

$$R = 10 + e^{(v^2/10^4)} \Omega$$

Draw the current waveform.

Solution

The current of the load is

$$i = \frac{v}{R} = \frac{V_{\max} \sin(\omega t)}{10 + e^{(V_{\max}^2 \sin^2(\omega t)/10^4)}} = \frac{169.7 \sin(\omega t)}{10 + e^{(169.7^2 \sin^2(\omega t)/10^4)}}$$

Using simulation software, you can obtain the current waveform in Figure 13.15.

Notice that the current seems to have two positive peaks and two negative peaks in one cycle. This is a typical shape of a waveform with large third harmonic component. Draw a fundamental frequency waveform and a third harmonic component on the same graph, then sketch the sum of the two waveforms.

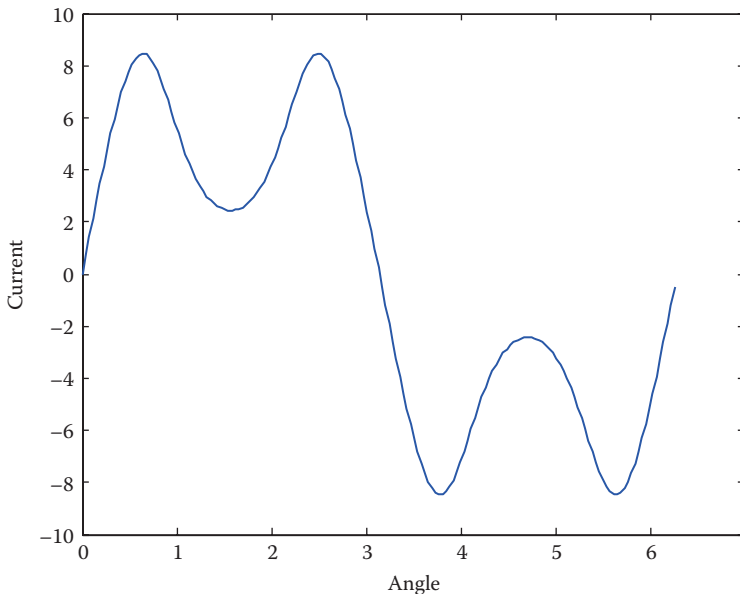


FIGURE 13.15 Current waveform of a nonlinear resistance.

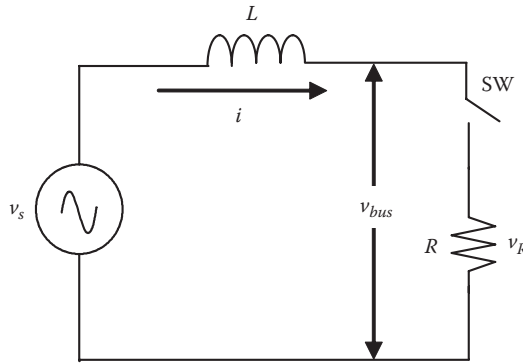


FIGURE 13.16 A representation of a simple system consists of source, cable, and switching load.

The distortion of the load current can result in distorted voltage across any other load connected to the same service circuit. To explain this important problem, consider the system in Figure 13.16. Assume that the voltage source is purely sinusoidal and the load is switched by a power electronic converter represented in the figure by the switch SW. This type of load includes household equipments such as computers, televisions, furnaces, washers, dryers, air conditioners, dimmers, and fans. However, since these household loads are relatively small with respect to the total loads on the utility feeders, their contribution to the THD is negligible. However, industrial loads such as arc furnaces and adjustable speed drives are large enough to produce significant harmonic distortions in the power grid. This results in distorted voltage waveforms at the load end of the feeder.

In Figure 13.16, the source voltage is v_s , the voltage across the resistance is v_R , and the voltage at the load end of the feeder is the bus voltage v_{bus} . Assume that the load is purely resistive and the cable (feeder) is purely inductive. When the switch SW is closed, the loop equation is

$$v_s = iR + L \frac{di}{dt} \tag{13.32}$$

where i is the current of the load. When the switch is open, the current in the circuit is zero. Since the status of the current is dependent on the switching status of SW, the current in Equation 13.32 can be computed much easier if we use the frequency domain. In this case, we can rewrite Equation 13.32 in the *Laplace* form

$$V_s(s) = RI(s) + sLI(s) \tag{13.33}$$

where $V(s)$ and $I(s)$ are the Laplace transformed voltage and current, respectively. Hence,

$$I(s) = \frac{V_s(s)}{(R + sL)} \tag{13.34}$$

Keep in mind that this equation is valid only when the switch is closed. When the switch is open, the current is zero. Assume that the voltage source is a purely sinusoidal waveform:

$$v_s = V_{max} \sin(\omega t) \tag{13.35}$$

Also, assume that the switch is closed at angle α and opened at an angle β . In this case, the source voltage in the Laplace form is

$$V_s(s) = \mathcal{L} v_s$$

$$V_s(s) = V_{\max} \left[\frac{s \sin \alpha + \omega \cos \alpha}{s^2 + \omega^2} e^{\left(\frac{-\alpha s}{\omega}\right)} - \frac{s \sin \beta + \omega \cos \beta}{s^2 + \omega^2} e^{\left(\frac{-\beta s}{\omega}\right)} \right] \quad (13.36)$$

Substituting Equation 13.36 into (13.34) and inverting the Laplace form back into time domain yield the current at the time the switch SW is closed

$$i = \frac{V_{\max}}{z} \left[\sin(\omega t - \varphi) + [\sin(\varphi - \alpha)] e^{-\left(\frac{\omega t - \alpha}{\omega \tau}\right)} \right] \quad (13.37)$$

where z , φ , and τ are the total impedance, the phase angle of the impedance, and the time constant of the system impedance, respectively. They are defined as follows:

$$\begin{aligned} z &= \sqrt{R^2 + (\omega L)^2} \\ \varphi &= \tan^{-1} \left(\frac{\omega L}{R} \right) \\ \tau &= \frac{L}{R} \end{aligned} \quad (13.38)$$

Notice that the current is not purely sinusoidal anymore due to the second term in Equation 13.37. Similarly, the voltage across the load resistance is distorted as shown in Equation 13.39:

$$v_R = R i = \frac{R V_{\max}}{z} \left[\sin(\omega t - \varphi) + [\sin(\varphi - \alpha)] e^{-\left(\frac{\omega t - \alpha}{\omega \tau}\right)} \right] \quad (13.39)$$

Now let us find out the bus voltage V_{bus} which is the voltage at the load end of the feeder. When the switch SW is closed, the bus voltage is equal to the voltage across the load resistance v_R . However, when the switch is opened, the bus voltage is equal to the source voltage v_s . The waveforms of the source voltage, current, and bus voltage are shown in Figure 13.17 for the case when the switch is an SCR. Notice the distorted shape of the bus voltage which does not resemble the pure sinusoidal waveform of the source voltage. This bus voltage is rich with harmonics. Therefore, when another customer is connected to the same bus, the distorted voltage is expected to be across that customer's load.

Different loads produce different harmonic distortions according to their operating environment or their power electronic designs. Table 13.1 shows a typical range of THD for some common loads. The THD of computers and monitors is very large. However, because their currents are small, their impact on the total system harmonics is relatively small. Ironically, some electrical contractors tend to power all computers in major installations by a dedicated feeder, thinking that they protect the computers from any harmonic that might exist if other equipment is allowed to be powered from the same feeder. In fact, these dedicated feeders are highly polluted with harmonics due to the aggregation of the harmonics of all computers. In such a feeder, the THD is actually very high. A better system is to allow other loads such as heaters and lights to be connected to the same feeder that powers the computers. This important point is further explained in Example 13.11.

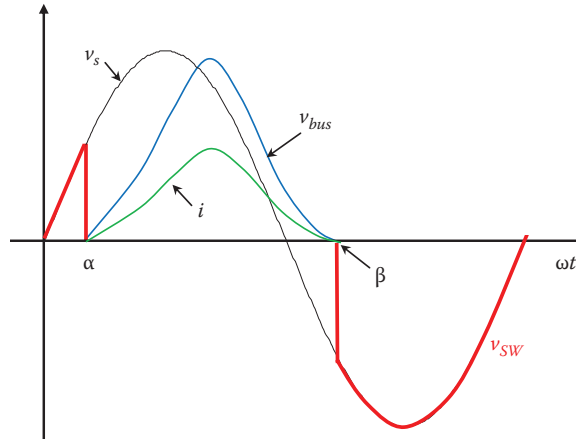


FIGURE 13.17 Waveforms of the circuit in Figure 13.16.

TABLE 13.1
THD of Common Load Currents

Type of Load	Typical THD (%)
Fluorescent lamp	15–25
Adjustable speed drives	30–80
Personal computer	70–120
Monitors	60–120

Example 13.11

A feeder is powering 100 computers. The total current of all computers can be represented by

$$i = 4 + 50 \sin(2\pi 60t) + 30 \sin(2\pi 180t) + 10 \sin(2\pi 300t) + 5 \sin(2\pi 420t) \text{ A}$$

Compute the THD of the feeder. Then, assume that a linear heating load of 100 A (rms) is connected to the same feeder, compute the new THD of the feeder.

Solution

First, compute the rms values of the harmonic components:

$$I_{dc} = 4 \text{ A}$$

$$I_1 = \frac{50}{\sqrt{2}} = 35.36 \text{ A}$$

$$I_3 = \frac{30}{\sqrt{2}} = 21.21 \text{ A}$$

$$I_5 = \frac{10}{\sqrt{2}} = 7.07 \text{ A}$$

$$I_7 = \frac{5}{\sqrt{2}} = 3.54 \text{ A}$$

Use Equation 13.30 to compute the rms value of the harmonic current:

$$I_H = \sqrt{4^2 + 21.21^2 + 7.07^2 + 3.54^2} = 23 \text{ A}$$

The total harmonic distortion is then

$$\text{THD} = \frac{I_H}{I_1} = \frac{23}{35.36} = 65\%$$

When the heating load is added, the fundamental component of the total current is the sum of the fundamental components of the computers' current and the current of the heating load. If we assume no phase shift between these two currents, then

$$I_1 = \frac{50}{\sqrt{2}} + 100 = 135.36 \text{ A}$$

The harmonic current when the heating load is added is unchanged as we assume that the heating load is linear:

$$I_H = \sqrt{4^2 + 21.21^2 + 7.07^2 + 3.54^2} = 23 \text{ A}$$

The total harmonic distortion with the heating load is

$$\text{THD} = \frac{I_H}{I_1} = \frac{23}{135.36} = 17\%$$

Notice that the same feeder now has a lower THD because the heating load increases the fundamental component of the total current.

Harmonic distortions can cause a wide range of problems in power grids as well as to other customers connected to the same feeders. These problems include the following:

- Resonance in power system that could stress the components beyond their designed ratings
- Increasing losses in transmission lines, transformers, and generators
- Damage to various compensation capacitor banks
- Creating drag forces inside motors that overheat the machine and reducing their torques
- Reducing the overall power factor (*pf*) of the system and producing inaccurate power measurements
- Increasing the electromagnetic interference to communication networks
- Premature aging of insulators in equipment and cables
- Causing picture jitters, and freezing or rebooting of computers and sensitive equipment

In the remainder of this chapter, we shall discuss some of the most important problems associated with harmonic distortions.

13.2.2 RESONANCE DUE TO HARMONICS

Capacitors are often used in power systems to improve the power factor and the voltage profile of the grid. These capacitors together with the inductances that exist in loads and feeders have a resonance

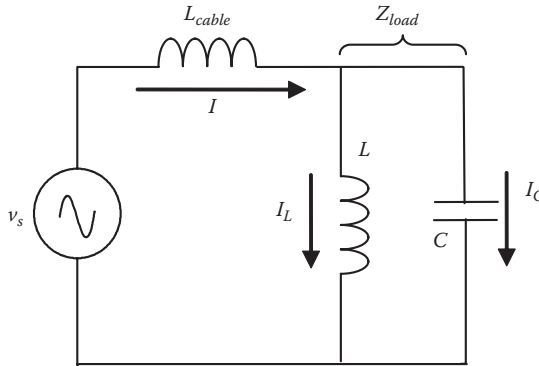


FIGURE 13.18 Compensated load.

frequency that is, by design, far away from the steady-state frequency of the system (50 or 60Hz). However, if a harmonic component exists with a frequency near the resonance frequency of the system, the current and voltage could oscillate at excessive magnitudes and could damage the power equipment.

Consider the system in Figure 13.18. It consists of voltage source v_s , cable impedance of inductance L_{cable} , and a compensated industrial load. The load consists of an inductive reactance L and a resistance. But for simplicity, we shall assume that the resistance is small with respect to the inductive reactance at the high frequency of the harmonics. The load is also compensated by a capacitor bank C .

The total load impedance Z_{load} is the parallel combination of the inductive reactance of the load and the compensation capacitor:

$$\bar{Z}_{load} = \frac{(j\omega L)(1/j\omega C)}{(j\omega L) + (1/j\omega C)} = \frac{j\omega L}{1 - \omega^2 LC} \tag{13.40}$$

The voltage across the load is then

$$\bar{V}_{load} = \bar{Z}_{load} \bar{I} \tag{13.41}$$

and the current of the circuit is

$$\bar{I} = \frac{\bar{V}_s}{\bar{Z}_{load} + \bar{Z}_{cable}} \tag{13.42}$$

where

$$\bar{Z}_{cable} = j\omega L_{cable} \tag{13.43}$$

Hence,

$$\bar{V}_{load} = \frac{\bar{Z}_{load}}{\bar{Z}_{load} + \bar{Z}_{cable}} \bar{V}_s \tag{13.44}$$

Substituting the impedances in Equations 13.40 and 13.43 into Equation 13.44 yields

$$\bar{V}_{load} = \frac{L}{(L + L_{cable}) - (L L_{cable} C)\omega^2} \bar{V}_s \tag{13.45}$$

As you see in Equation 13.45, the voltage across the load is a function of the frequency of source voltage v_s . This load voltage can reach a theoretical value of infinity if a frequency ω_o makes the denominator equal zero:

$$(L + L_{cable}) - (L L_{cable} C) \omega_o^2 = 0 \quad (13.46)$$

At this condition, the frequency is called resonance frequency f_o or ω_o . They are defined as

$$\begin{aligned} \omega_o &= \sqrt{\frac{L + L_{cable}}{L L_{cable} C}} \\ f_o &= \frac{1}{2\pi} \sqrt{\frac{L + L_{cable}}{L L_{cable} C}} \end{aligned} \quad (13.47)$$

Example 13.12

For the compensated load in Figure 13.18, assume that the load impedance is composed of 10Ω resistance in series with 0.1 H inductance. The transmission line inductance is 0.01 H and the compensation capacitor is $100 \mu\text{F}$. The voltage at the source side has a third harmonic component of 100 V at 180 Hz . Compute the third harmonic voltage across the load.

Solution

The total impedance on the load side is

$$\bar{Z}_{load} = \frac{(R + j\omega L)(1/j\omega C)}{(R + j\omega L) + (1/j\omega C)} = \frac{(10 + j0.1\omega)(10^4/j\omega)}{(10 + j0.1\omega) + (10^4/j\omega)}$$

where

$$\omega = 2\pi f = 2\pi \times (3 \times 60) = 1131 \text{ rad/s}$$

Hence, the total impedance at the load side is

$$\bar{Z}_{load} = 0.0713 - j9.58 \Omega$$

The source current of the system is

$$\bar{I} = \frac{\bar{V}_s}{\bar{Z}_{load} + \bar{Z}_{cable}} = \frac{100}{0.0713 - j9.58 + j11.31} = 2.39 - j57.9 \text{ A}$$

Hence, the voltage across the load is

$$\bar{V}_{load} = \bar{Z}_{load} \bar{I} = (0.0713 - j9.58)(2.39 - j57.9) = 555.2 \angle -177.2^\circ \text{ V}$$

Notice that the load voltage is more than five times the third harmonic source voltage. This high voltage may cause damage to equipment.

13.2.3 EFFECT OF HARMONICS ON TRANSMISSION LINES AND CABLES

There are two main transmission line problems associated with system harmonics: losses and excessive voltage. The harmonic currents produce line loss P_{line} in the form

$$P_{line} = \sum_k R I_k^2 \quad (13.48)$$

where

k is the harmonic number.

R is the resistance of the line. Its value increases with frequency due to skin effect.

These losses increase when the harmonic is of high magnitudes.

The second problem, the high voltage across lines and cables, is much more damaging than line losses. If the harmonic is close to the resonant frequency, the voltage across the cable or line is likely to be excessive and could damage cable insulations or even cause arcing between lines and nearby grounded objects. Examine Example 13.13.

Example 13.13

For the system in Example 13.12, compute the voltage across the feeder impedance.

Solution

The voltage across the line impedance V_{line} is

$$\bar{V}_{line} = \bar{Z}_{cable} \bar{I} = j11.31(2.39 - j57.9) = 655.2 \angle 2.4^\circ \text{ V}$$

The load across the line impedance is more than six times the source voltage at 180 Hz. This high voltage could damage the insulations of the cable.

13.2.4 EFFECT OF HARMONICS ON CAPACITOR BANKS

The most important problem for capacitors operating in a harmonic environment is the overvoltage across them. As seen in Example 13.12, the voltage across the capacitor, which is the same as the load voltage, could be excessive. This high voltage causes high current in the capacitor since

$$I_{capacitor} = \omega C V_{load} \quad (13.49)$$

When the harmonic frequency in Equation 13.49 is high and the load voltage for this harmonic component is also high, the capacitor current could be excessive and could damage the often expensive capacitor banks.

Example 13.14

For the system in Example 13.12, compute the capacitor current at 60 Hz and at the third harmonic voltage. Assume that the fundamental voltage is 240 V and the third harmonic voltage is 100 V.

Solution

At 60 Hz, the load impedance is

$$\bar{Z}_{load} = \frac{(R + j\omega L)(1/j\omega C)}{(R + j\omega L) + (1/j\omega C)} = \frac{(10 + j0.1 \times 377)(10^4/j377)}{(10 + j0.1 \times 377) + (10^4/j377)} = 31.3 + j61.5 \Omega$$

The 60 Hz current of the source is

$$\bar{I} = \frac{\bar{V}_s}{\bar{Z}_{load} + \bar{Z}_{cable}} = \frac{240}{10.0 + j37.7 + j3.77} = 1.74 + j3.21 \text{ A}$$

Hence, the voltage across the load is

$$\bar{V}_{load} = \bar{Z}_{load} \bar{I} = 252.2 \angle -1.5^\circ \text{ V}$$

and the current of the capacitor is

$$I_{capacitor} = \omega C V_{load} = 377 \times 10^{-4} \times 252.2 = 9.5 \text{ A}$$

Now repeat the solution for the third harmonic. In Example 13.12, the load voltage is 555.1 V. Hence, the current of the capacitor at 180 Hz is

$$I_{capacitor} = \omega C V_{load} = (3 \times 377) \times 10^{-4} \times 555.1 = 62.8 \text{ A}$$

This is almost 6.6 times the current at 60 Hz. Keep in mind that most capacitors are rated for the harmonic-free environment. In this case, it is expected that this capacitor would fail due to the excessive voltage across it and the excessive current through it. The excessive voltage damages the insulations inside the capacitor and the excessive current causes damaging internal heat.

13.2.5 EFFECT OF HARMONICS ON ELECTRIC MACHINES

Harmonics can cause a variety of problems to electrical machines including harmonic losses, excessive voltage, and drag torque (braking torque). The losses inside the machine are due to the losses in its windings and core. As shown in Chapter 11, the magnetic core loss is a function of how many times the hysteresis loop is completed—one loop is completed in one cycle. Hence, the higher the frequency of the harmonic, the higher is the core loss. In addition, the various resistances of the wires of the windings increase with the frequency due to the skin effect phenomenon, thus increasing the losses inside the machine.

If the machine is compensated by a capacitor bank, the frequency of the harmonic could cause the voltage of the machine to increase to damaging levels, as explained in the previous section.

Drag torque is related to the fact that the rotating field inside the machine is a function of the sequence of the three-phase waveform as explained in Chapter 12. At 60 cycle, the rotation of the magnetic field in the airgap follows the *abc* sequence where

$$\begin{aligned} v_a &= V_{\max} \sin(\omega t) \\ v_b &= V_{\max} \sin(\omega t - 120) \\ v_c &= V_{\max} \sin(\omega t + 120) \end{aligned} \quad (13.50)$$

In Equation 13.50, phase b lags phase a by 120° , and phase c leads phase a by 120° . Therefore, the magnetic field rotates in the abc sequence.

Now let us look at the fifth harmonic waveforms. The frequency of the fifth harmonic modifies Equation 13.50 to

$$\begin{aligned}v_a &= V_{\max} \sin 5(\omega t) \\v_b &= V_{\max} \sin 5(\omega t - 120) \\v_c &= V_{\max} \sin 5(\omega t + 120)\end{aligned}\tag{13.51}$$

Hence,

$$\begin{aligned}v_a &= V_{\max} \sin(5\omega t) \\v_b &= V_{\max} \sin(5\omega t + 120) \\v_c &= V_{\max} \sin(5\omega t - 120)\end{aligned}\tag{13.52}$$

In Equation 13.52, phase b leads phase a by 120° , and phase c lags phase a by 120° . So the magnetic field rotates in the acb sequence, which is opposite to the abc sequence of the fundamental frequency voltage. Therefore, the magnetic field rotation due to the fifth harmonic opposes the main magnetic field of the fundamental frequency. The torque produced by the fifth harmonic in this case is in opposite direction to the torque produced by the fundamental frequency. This fifth harmonic torque is therefore a dragging torque that causes the machine to run sluggishly, much like two people pushing a cart from opposite directions.

13.2.6 EFFECT OF HARMONICS ON ELECTRIC POWER

The instantaneous power is defined as

$$p(t) = v(t) i(t)\tag{13.53}$$

where

v is the instantaneous voltage

i is the instantaneous current

p is the instantaneous power

The active power P that produces work is the average value of the instantaneous power

$$P = \frac{1}{\tau} \int_0^{\tau} p(t) dt = \frac{1}{2\pi} \int_0^{2\pi} p(t) d\omega t\tag{13.54}$$

where τ is the time period. Assume that the voltage and current have different frequencies

$$\begin{aligned}v &= V_{\max} \sin(\omega t) \\i &= I_{\max} \sin(n\omega t + \theta)\end{aligned}\tag{13.55}$$

where

n is an integer number

θ is the phase shift of the current with respect to the voltage

The power P can be computed by

$$P = \frac{1}{2\pi} \int_0^{2\pi} V_{\max} \sin(\omega t) I_{\max} \sin(n\omega t + \theta) d\omega t$$

$$P = \frac{V_{\max} I_{\max}}{4\pi} \left[\int_0^{2\pi} \cos((n+1)\omega t + \theta) d\omega t + \int_0^{2\pi} \cos((n-1)\omega t + \theta) d\omega t \right] \quad (13.56)$$

$$P = \frac{V_{\max} I_{\max}}{4\pi} \left[\int_0^{2\pi} A d\omega t + \int_0^{2\pi} B d\omega t \right]$$

The integral of A is always zero regardless of the value of n , while the integral of B is nonzero only if $n=1$. This leads us to an important lemma for power, only voltages and currents of same frequency produce power. To apply this lemma, let us assume that the voltage and current have harmonic components:

$$v = V_{dc} + V_{1\max} \sin \omega t + V_{1\max} \sin 2\omega t + V_{3\max} \sin 3\omega t + \dots \quad (13.57)$$

$$i = I_{dc} + I_{1\max} \sin(\omega t - \theta_1) + I_{2\max} \sin(2\omega t - \theta_2) + I_{3\max} \sin(3\omega t - \theta_3) + \dots$$

According to the lemma, the power produced by these waveforms is

$$P = V_{dc} I_{dc} + \frac{V_{1\max} I_{1\max}}{2} \cos \theta_1 + \frac{V_{2\max} I_{2\max}}{2} \cos \theta_2 + \frac{V_{3\max} I_{3\max}}{2} \cos \theta_3 + \dots \quad (13.58)$$

$$P = V_{dc} I_{dc} + V_1 I_1 \cos \theta_1 + V_2 I_2 \cos \theta_2 + V_3 I_3 \cos \theta_3 + \dots$$

$$P = P_{dc} + P_1 + P_2 + P_3 + \dots$$

where

P_{dc} is the power of the dc component

P_1 is the power of the fundamental frequency

P_3 is the power of the third harmonic, and so on

An important term often used with power is the power factor (pf). It is a good indicator of how much of the apparent power is converted into work. For purely sinusoidal waveforms, the maximum value of pf is 1 when the load is purely resistive.

In circuits with harmonics, the power factor is defined in a similar way:

$$pf = \frac{P}{VI} = \frac{P_{dc} + P_1 + P_2 + P_3 + \dots}{\sqrt{(V_{dc}^2 + V_1^2 + V_2^2 + V_3^2 + \dots)} \sqrt{(I_{dc}^2 + I_1^2 + I_2^2 + I_3^2 + \dots)}} \quad (13.59)$$

Using the definition of the THD in Equation 13.31, we can rewrite Equation 13.59 as

$$pf = \frac{P_{dc} + P_1 + P_2 + P_3 + \dots}{V_1 I_1 \sqrt{(1 + \text{THD}_V^2)} \sqrt{(1 + \text{THD}_I^2)}} = \frac{P_{dc} + P_1 + P_2 + P_3 + \dots}{P_1 \sqrt{(1 + \text{THD}_V^2)} \sqrt{(1 + \text{THD}_I^2)}} \quad (13.60)$$

where

IHD_V is the total harmonic distortion of the voltage waveform

THD_I is the total harmonic distortion of the current

Regular power measurement devices and power factor meters are designed to produce accurate results in harmonic-free environments. The readings of these devices are often inaccurate when the system is polluted with severe harmonics. These devices are extensively installed in distribution systems all over the world. Replacing these meters with more sophisticated devices that account for the harmonics is extremely expensive. Most utilities opt for inaccurate readings instead of the prohibitive costs of upgrading the millions of meters in their system.

Example 13.15

An industrial load has the following rms harmonic components:

V	I	θ	
Dc component	10	1	
First harmonic	460	10	30°
Third harmonic	90	5	0°
Fifth harmonic	30	2	10°

- Assume that simple devices are used to measure the power and the power factor. Assume that the devices monitor only the fundamental components. What are their readings?
- What are the actual values of power and power factor?
- If the price of electricity is \$0.2/kWh, compute the losses for the utility in 1 year, assuming that the load is active for 10h daily.

Solution

- The power meter measures the fundamental frequency component only:

$$P_1 = V_1 I_1 \cos \theta_1 = 460 \times 10 \times \cos(30) = 4 \text{ kW}$$

$$pf_1 = \frac{P_1}{V_1 I_1} = \cos(30) = 0.866$$

- The actual value of power is

$$P = V_{dc} I_{dc} + V_1 I_1 \cos \theta_1 + V_3 I_3 \cos \theta_3 + V_5 I_5 \cos \theta_5$$

$$P = 10 \times 1 + 460 \times 10 \times \cos(30) + 90 \times 5 + 30 \times 2 \times \cos(10) = 4.52 \text{ kW}$$

The actual value of the power factor is

$$pf = \frac{P}{VI} = \frac{P_{dc} + P_1 + P_2 + P_3 + \dots}{\sqrt{(V_{dc}^2 + V_1^2 + V_2^2 + V_3^2 + \dots)} \sqrt{(I_{dc}^2 + I_1^2 + I_2^2 + I_3^2 + \dots)}}$$

$$pf = \frac{4520}{\sqrt{(10^2 + 460^2 + 90^2 + 30^2)} \sqrt{(1 + 10^2 + 5^2 + 2^2)}} = 0.844$$

c. The losses due to harmonics is

$$P_{\text{harmonics}} = P - P_1 = 4520 - 4000 = 520 \text{ W}$$

The annual energy unmonitored due to the harmonics is

$$E_{\text{harmonics}} = P_{\text{harmonics}} \times t = 520 \times 10 \times 365 = 1898 \text{ kWh}$$

The annual lost revenue of the utility is

$$\text{Lost revenue} = E_{\text{harmonics}} \times \text{cost of kWh} = 1825 \times \$0.2 = \$379.6$$

The lost revenue for this one load is probably high enough to justify the installation of more accurate meters.

13.2.7 EFFECT OF HARMONICS ON COMMUNICATIONS

Any wire carrying electrical current produces a magnetic field surrounding the wire. When the magnetic fields reach other wires or electronic circuits, they induce voltages that could interfere with the operation of circuits. Devices such as cellular phones or landline phones are designed to filter out the effect of power frequency. However, high-frequency harmonic components may not be filtered out and could interfere with communication signals.

EXERCISES

- 13.1** For the system in Figure 13.2, assume $V_S = 120 \text{ V}$, $Z_{\text{cable}} = 2 \angle 90^\circ \Omega$, $Z_1 = 10 + j5 \Omega$, and $Z_2 = 2 + j1 \Omega$. Compute the following:
- Load voltage when Load₂ is switched off
 - Load voltage when Load₂ is switched on
 - Voltage reduction on Load₁ due to the presence of Load₂
- 13.2** Repeat the previous problem but assume the line is fully compensated by a series capacitor.
- 13.3** A load voltage with flicker can be represented by the following equation:

$$v_{\text{load}} = 170(1 + 2 \cos(0.2t)) \cos(377t)$$

Compute the following:

- Flicker factor
 - Voltage fluctuation
 - Frequency of the fluctuation
 - Human tolerance to the flicker
- 13.4** A transformer is energized through a cable whose inductive reactance is 3Ω . The phase voltage at the source side of the cable is 8 kV . When the transformer is switched on (energized), the crest of the inrush current of the transformer can be modeled by an equivalent inductive reactance of 7Ω . Estimate the voltage flicker at the transformer side.
- 13.5** For the system in Figure 13.12, the source voltage is 100 kV (phase value), the feeder is 20 km in length, and its inductive reactance is $1.2 \Omega/\text{km}$. The impedance at the load side is $2 \angle 20^\circ \text{ k}\Omega$. A falling tree causes a temporary fault at the middle of the feeder. The fault impedance is $80 \angle 75^\circ \Omega$, assume the equivalent internal impedance of the source is 50Ω . Compute the voltage sag at the load side.

- 13.6** For the system in Figure 13.13, the source voltage is 50 kV (phase value), the feeder reactive reactance X_1 is $10\ \Omega$ and X_2 is $5\ \Omega$. The load impedance is $3\angle 20^\circ\ \text{k}\Omega$. A temporary fault occurs at the location in the figure. The fault impedance is $200\angle 80^\circ\ \Omega$. Compute the voltage sag at the load side. Assume the end of the feeder was unloaded before the fault.
- 13.7** Consider the current waveform:

$$i = 2 + 100\sin(377t) + 20\sin(1131t) + 10\sin(1885t) + 5\sin(2639t)\ \text{A}$$

Compute the following:

- Fundamental frequency
 - Harmonic frequencies
 - rms harmonic current
 - Total rms current
 - IHD of all harmonics
 - THD of the current
- 13.8** A harmonic voltage source is represented by $v_s = 340\sin(377t) + 100\sin(1131t) + 30\sin(1885t)\ \text{V}$. The voltage source is connected to a load impedance of $Z_l = (5 + j0.2\omega)\ \Omega$ through a cable whose inductive reactance is $Z_{cable} = j0.01\omega\ \Omega$. The load is compensated by a $200\ \mu\text{F}$ capacitor bank connected in parallel to the load. Compute the voltage across the load and the voltage across the cable impedance.
- 13.9** Compute the capacitor current in the previous problem.
- 13.10** For the compensated load in Figure 13.18, assume the load impedance is composed of $10\ \Omega$ resistance in series with $0.1\ \text{H}$ inductance. The transmission line inductance is $0.01\ \text{H}$ and the compensation capacitor is $100\ \mu\text{F}$. The source voltage contains several harmonics. Use any simulation software and find the frequency at which the voltage across the load is at its maximum value.
- 13.11** An industrial load is powered by purely sinusoidal voltage source. The load current has a THD of 20%, and the power factor of the fundamental waveforms is 0.8. Compute the power factor of the load.
- 13.12** An industrial load is powered by a purely sinusoidal voltage source of 277 V (rms). The load current has a THD of 20%, and the fundamental component of the current is $20\angle 30^\circ\ \text{A}$. Compute the load power.
- 13.13** An industrial load is powered by a voltage source whose fundamental component is 277 V (rms) and its THD is 10%. The load current has a fundamental component of 30 A and a THD of 20%. Assume no phase shift between the current components and their corresponding voltages. Compute the load power.

14 Power Grid and Blackouts

Electric power systems are probably the most complex systems ever built by man. In the United States, the power system contains several thousands of major generating units, tens of thousands of transmission lines, millions of transformers, and hundreds of millions of protection and control devices. Figure 14.1 shows the electric energy produced in the United States and worldwide. The power systems in 2009 produced over 20PWh (20×10^{15} Wh) of electrical energy worldwide and over 4.0PWh in the United States. The worldwide consumption, although already overwhelming, is expected to increase even more, primarily because of the rapid industrial development in Asia. To match the ever-growing demand for electrical energy, the capacity of power systems must continuously increase. In 2008, the United States had over 1TW of electrical energy capacity as shown in Figure 14.2.

Managing this staggering amount of energy is a daunting task indeed for engineers. It is remarkable that power engineers maintain the stable operation of these immense and complex power systems. Given the size and dynamic nature of the various components in the systems, it is incredible that only a few outages occur every year.

Power outages are often called *blackouts*, where loads in a given area are left without power. Blackouts, in general, occur due to the lack of power generation or the lack of transmission lines. The questions most people ask are whether we can predict the blackouts ahead of time, and whether we can prevent them from happening? These difficult questions have no general answers for all blackout scenarios. Although it is technically feasible to build a very robust power system by constructing a large number of distributed generations and multiple redundant transmission lines, the technical solution may not be cost effective and is often unacceptable to the public. The public views toward building new generations and new transmission lines are generally negative. Utilities often face a great deal of difficulties when expansions are proposed to meet new growth. The public, in general, prefers using renewable energy and conservation instead of building new fossil fuel or nuclear power plants near their towns. Furthermore, the utilities often face tremendous resistance when proposing new transmission lines, especially when the right of way is located near residential areas. Renewable energy and conservation are often stated as ways to reduce the frequency of blackouts and lessen their impacts. Given the current status of the technology, these ideas cannot really save power systems from blackouts as explained in the following discussion:

- Renewable energy cannot yet replace the large power plants (fossil, hydroelectric, and nuclear) we have today. However, in 10–20 years, the technology may provide us with high-energy-density renewable systems that can have impact on the generation portfolio.
- Conservation will help tremendously if it is implemented on large scales and conservation devices are imbedded in electrical equipment. Relying on individuals to reduce their energy consumptions has been proven less effective because most people buy comfort rather than electricity. Most of us do not think in terms of how many kilowatt hour we consume to make the home cool or warm. Rather, we set the temperature controllers to our comfort levels, and we let electricity flow to reach these levels.
- Besides renewable energy and conservation, blackouts can have lesser impact if distributed generations are used. Small generating units can be installed to provide electricity to an individual building or a group of buildings either continuously or as backup systems. These generating units have different design configurations ranging from a small natural gas power plant—the size of a household water heater (power plant in a box)—to large gas or renewable systems. The main obstacle facing these systems is their high costs, which can be justified only for sensitive loads such as hospitals.

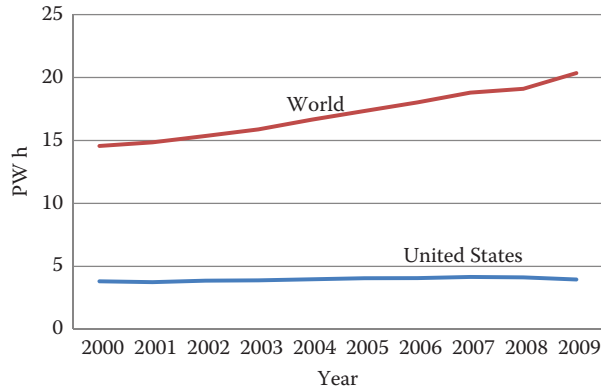


FIGURE 14.1 Net generation of electrical energy. (From U.S. Energy Information Administration, Washington, DC.)

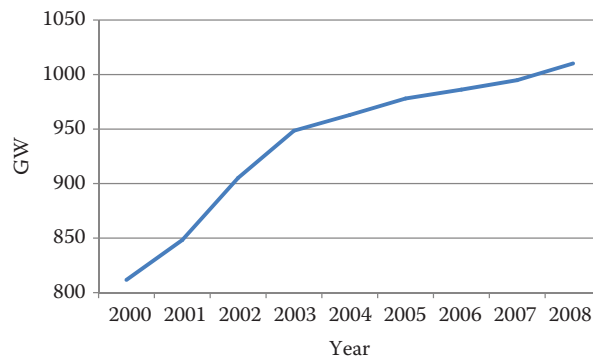


FIGURE 14.2 Generation capacity in the United States. (From U.S. Energy Information Administration, Washington, DC.)

Another question that is often asked after every blackout is why a power system cannot be controlled as phone and Internet networks are. After all, they are similarly large and complex. Actually, there are several reasons that make the control of power systems unique and different from all other large and complex networks, among them are the following:

- Power grid is not a programmable network like phone or Internet systems. Electricity cannot be sent from point to point in packages. The power grid is rather a giant reservoir where all generators deliver their energy to the reservoir and any load can tap from that reservoir. It is impossible to know which generator produces the energy you consume in your home at any given time.
- Since there is no effective way yet to store large amounts of electrical energy, the generated power must be consumed immediately by all loads as well as the various losses in the system. A deficiency or surplus in power may lead to a blackout if not corrected within seconds, or even milliseconds in some cases. For the Internet network, when the packets sent are at a higher rate than what is being processed by the user's node, the extra packets are often stored temporarily until the node is available. Even if the packets are dropped out at a busy or damaged node, the network can still function normally and future packets are rerouted through the rest of the network.
- Amount of energy that must be controlled at all times in the power system is immense. The Internet and phone networks process an infinitesimal amount of energy compared to

the power grid. The equipment for the power network is therefore heavy, bulky, and slow acting. The luxury of switching links and devices at a high rate in the phone and Internet networks is not applicable in power systems.

- Immense masses of generators, turbines, and motors in the power systems create relatively large delays in the control actions. Hence, instant correction is impossible for power systems. This problem is virtually nonexistent in phone and Internet networks.
- Overloaded equipment in power systems is often tripped to protect the equipment from being damaged. This could initiate outages. In phone or Internet networks, overloading the equipment often leads to just a delay in transmission.

Based on the earlier discussion and the status of the current technologies, the best option to reduce blackouts is to enhance the reliability of the existing power systems by building more generating plants, more transmission lines, and improving the monitoring and control systems. These are in addition to energy conservation and expanding renewable resources.

14.1 TOPOLOGY OF POWER SYSTEMS

Early power systems were simple in design but highly unreliable. They consisted mainly of generating units connected to load centers in *radial* fashion as shown in Figure 14.3. The generator is connected to a transformer (xfm_g) to raise the voltage to the transmission voltage level. The transmission lines connect the generating stations to the load centers; two of them are shown in the figure. At the load centers, transformers (xfm_1 and xfm_2) are used to step down the voltage to the users' level. Another form of the radial configuration is shown in Figure 14.4.

Both systems have reliability problems. In the first system, if $Line_1$ is tripped (opened) for any reason, both loads are left without power; hence, the system is in a *complete blackout* state. If instead $Line_2$ is tripped, only $Load_2$ is disconnected and the system is in a *partial blackout* state. The second

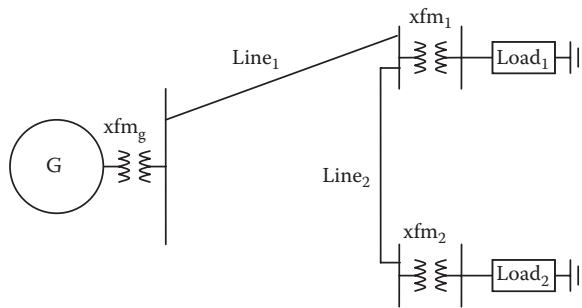


FIGURE 14.3 Radial power system.

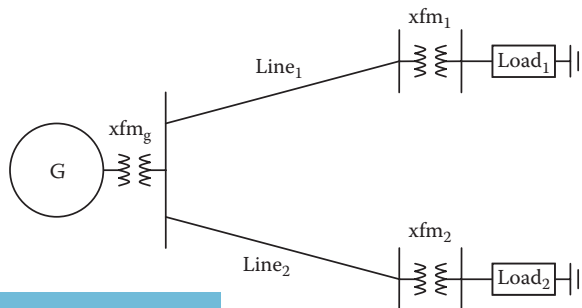


FIGURE 14.4 Another radial power system.

system is better designed because when any of the two lines is tripped, only the load being fed by that line is left without power. Hence, a single line tripping causes partial but not complete blackout.

14.1.1 ENHANCING POWER SYSTEM RELIABILITY BY ADDING TRANSMISSION LINES

For the radial systems in Figures 14.3 and 14.4, a loss of a single line can cause at least one load to be left without power. To correct this problem, a third line can be added as shown in Figure 14.5. In this new system, tripping any one line will not result in a power outage. The transmission system in this case is connected in a *network* configuration, where each load is fed by multiple lines. Thus, the network connection is more reliable than the radial connection.

14.1.2 ENHANCING POWER SYSTEM RELIABILITY BY ADDING GENERATION

The system in Figure 14.5 is unreliable in terms of generation—if the generator is tripped due to any reason, all loads will be left without power. The obvious solution to this problem is to add more generators to the system at different locations. An example is shown in Figure 14.6 for a two-generator, five-transmission-line system. Tripping out any one line, or one generator, may not result in loss of service to any load. However, there is no guarantee that the system is secure under any tripping scenario, as discussed in the following section. You may find scenarios where the system is insecure especially when the system is heavily loaded and the line with most current is tripped.

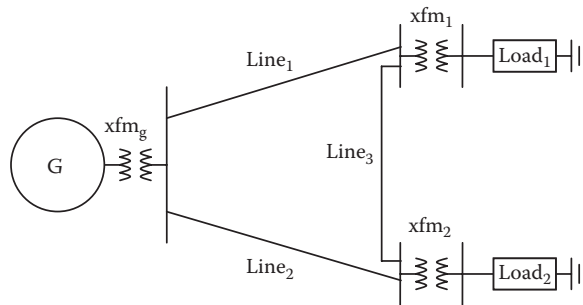


FIGURE 14.5 Network power system.

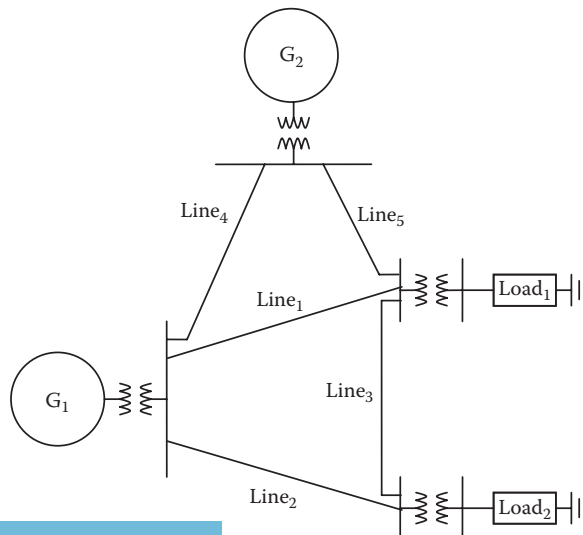


FIGURE 14.6 Network power system with multiple generators.

14.2 ANALYSIS OF POWER NETWORKS

To detect situations that may lead to blackouts (e.g., overcurrent, overvoltage, or undervoltage), a method known as load flow analysis is used to study the power network. The load flow is a circuit analysis tool that relates the structure of the power network and the load demands to the currents and voltages throughout the network. After performing the load flow analysis, the status of the power system can be determined. The power system is in a *secure state* if all currents and voltages of the major equipment (transmission lines, transformers, etc.) are within their design ranges. The system is *insecure* if any major equipment (transmission lines, transformers, etc.) is operating outside its normal voltage range or operating at current higher than its rating. If the load flow analysis identifies overloaded lines, the system is insecure and the operator must shift some of the loads to other lines, thus saving the system from a potential outage. For example, if the voltage at any load center is lower than its normal range, the load is probably served by insufficient number of lines and the operator must shift the flow of power through additional lines.

Because the power system is not fully monitored, the load flow analysis uses existing measurements of powers and various voltages to solve for the currents and voltages everywhere else in the network. The method, which is often numerical, uses a set of nonlinear equations relating the measurements to the unknowns. However, if we assume that all system impedances as well as the voltages of all generators are known, the load flow analysis turns into a solution of a set of linear equations. The procedure starts by developing the impedance diagram of the power system; the diagram for the system in Figure 14.5 is shown in Figure 14.7. Z_{11} is the impedance of load₁ plus its own transformer (xfm_1), Z_{22} is the impedance of load₂ including its transformer, and Z_{12} is the impedance of the transmission line between bus 1 and 2, and so on. The voltage at each bus is labeled according to the bus number, and the direction of the current can be chosen arbitrarily. The final solution of the current determines its direction; if the current is positive, the chosen direction is correct, and if it is negative the actual direction is opposite to the chosen one.

A convenient choice for the initial directions of the transmission line currents is to assume that the flow is from the larger numbered bus to the smaller numbered bus. In this case, the node equations at buses 1, 2, and 3 are

$$\begin{aligned} \bar{I}_1 &= \bar{I}_{12} + \bar{I}_{13} \\ \bar{I}_2 &= \bar{I}_{23} - \bar{I}_{12} \\ \bar{I}_3 &= \bar{I}_{13} + \bar{I}_{23} \end{aligned} \tag{14.1}$$

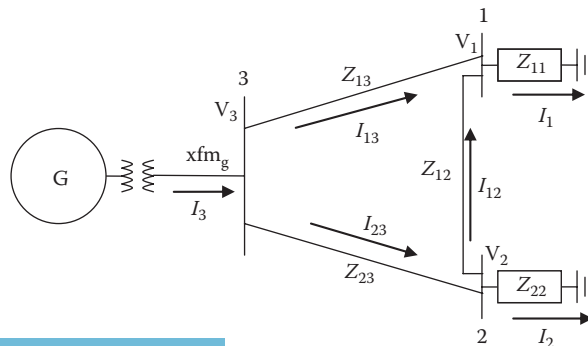


FIGURE 14.7 Current distribution of the system in Figure 14.5.

The load current can be written as a function of the bus voltage and the load admittance as follows:

$$\begin{aligned}\bar{I}_1 &= \bar{V}_1 \bar{Y}_{11} \\ \bar{I}_2 &= \bar{V}_2 \bar{Y}_{22}\end{aligned}\quad (14.2)$$

where $\bar{Y}_{ij} = 1/Z_{ij}$. The currents of the transmission lines can also be written as

$$\begin{aligned}\bar{I}_{12} &= (\bar{V}_2 - \bar{V}_1) \bar{Y}_{12} \\ \bar{I}_{13} &= (\bar{V}_3 - \bar{V}_1) \bar{Y}_{13} \\ \bar{I}_{23} &= (\bar{V}_3 - \bar{V}_2) \bar{Y}_{23}\end{aligned}\quad (14.3)$$

Substituting the currents in Equation 14.3 into Equation 14.1 yields

$$\begin{bmatrix} \bar{I}_1 \\ \bar{I}_2 \\ -\bar{I}_3 \end{bmatrix} = \begin{bmatrix} -(\bar{Y}_{12} + \bar{Y}_{13}) & \bar{Y}_{12} & \bar{Y}_{13} \\ \bar{Y}_{12} & -(\bar{Y}_{12} + \bar{Y}_{23}) & \bar{Y}_{23} \\ \bar{Y}_{13} & \bar{Y}_{23} & -(\bar{Y}_{13} + \bar{Y}_{23}) \end{bmatrix} \begin{bmatrix} \bar{V}_1 \\ \bar{V}_2 \\ \bar{V}_3 \end{bmatrix}\quad (14.4)$$

Substituting the load currents in Equation 14.2 into Equation 14.4 yields

$$\begin{bmatrix} \bar{I}_1 \\ \bar{I}_2 \\ -\bar{I}_3 \end{bmatrix} = \begin{bmatrix} -(\bar{Y}_{12} + \bar{Y}_{13}) & \bar{Y}_{12} & \bar{Y}_{13} \\ \bar{Y}_{12} & -(\bar{Y}_{12} + \bar{Y}_{23}) & \bar{Y}_{23} \\ \bar{Y}_{13} & \bar{Y}_{23} & -(\bar{Y}_{13} + \bar{Y}_{23}) \end{bmatrix} \begin{bmatrix} \bar{Z}_{11} \bar{I}_1 \\ \bar{Z}_{22} \bar{I}_2 \\ \bar{V}_3 \end{bmatrix}\quad (14.5)$$

Equation 14.5 can be written in the matrices form:

$$\begin{aligned}[I] &= [Y]([V] + [Z][I]) \\ [I] &= ([1] - [Y][Z])^{-1} [Y][V]\end{aligned}\quad (14.6)$$

Example 14.1

The power system in Figure 14.7 has the following data:

Impedance of load₁ plus its transformer is $\bar{Z}_{11} = 20 + j10 \Omega$.

Impedance of load₂ plus its transformer is $\bar{Z}_{22} = 30 + j5 \Omega$.

Impedance of Line₁ is $\bar{Z}_{13} = j0.5 \Omega$.

Impedance of Line₂ is $\bar{Z}_{23} = j0.6 \Omega$.

Impedance of Line₃ is $\bar{Z}_{12} = j0.4 \Omega$.

The voltage at the high voltage side of xfm_g is fixed at 230 kV (line-to-line).

The capacity of any line (maximum current the line can carry) is 6 kA.

The range of the voltage at any load bus is $230 \pm 5\%$.

All impedances are referred to the high-voltage side of the transformers. Assume that all connections are in wye.

- Compute the power delivered to each load and the power produced by the generator.
- Assume that transmission Line₃ is tripped; repeat part a.
- Is the system in part b secure?
- Assume that Line₁ is tripped while Line₂ and Line₃ are still in service; repeat part a.
- Is the system in part d secure?

Solution

- To compute the powers, we need to compute the currents of each load. We have five unknowns, I_1 , I_2 , I_3 , V_1 , and V_2 . Equation 14.5 can be used to solve for the currents

$$\begin{bmatrix} \bar{I}_1 \\ \bar{I}_2 \\ -\bar{I}_3 \end{bmatrix} = \begin{bmatrix} -(\bar{Y}_{12} + \bar{Y}_{13}) & \bar{Y}_{12} & \bar{Y}_{13} \\ \bar{Y}_{12} & -(\bar{Y}_{12} + \bar{Y}_{23}) & \bar{Y}_{23} \\ \bar{Y}_{13} & \bar{Y}_{23} & -(\bar{Y}_{13} + \bar{Y}_{23}) \end{bmatrix} \begin{bmatrix} \bar{Z}_{11}\bar{I}_1 \\ \bar{Z}_{22}\bar{I}_2 \\ \bar{V}_3 \end{bmatrix} \quad (14.7)$$

Equation 14.7 can be further rearranged as follows:

$$\begin{bmatrix} 1 + (\bar{Y}_{12} + \bar{Y}_{13})\bar{Z}_{11} & -\bar{Y}_{12}\bar{Z}_{22} & 0 \\ -\bar{Y}_{12}\bar{Z}_{11} & 1 + (\bar{Y}_{12} + \bar{Y}_{23})\bar{Z}_{22} & 0 \\ -\bar{Y}_{13}\bar{Z}_{11} & -\bar{Y}_{23}\bar{Z}_{22} & 1 \end{bmatrix} \begin{bmatrix} \bar{I}_1 \\ \bar{I}_2 \\ -\bar{I}_3 \end{bmatrix} = \begin{bmatrix} \bar{Y}_{13} \\ \bar{Y}_{23} \\ -(\bar{Y}_{13} + \bar{Y}_{23}) \end{bmatrix} \bar{V}_3 \quad (14.8)$$

By directly substituting the variables in this example into Equation 14.8, the currents of the system can be computed. Keep in mind that the phase voltage V_3 is $230/\sqrt{3}$.

$$\begin{bmatrix} \bar{I}_1 \\ \bar{I}_2 \\ \bar{I}_3 \end{bmatrix} = \begin{bmatrix} 5.9 \angle -27.7^\circ \\ 4.34 \angle -10.6^\circ \\ 10.12 \angle -20.44^\circ \end{bmatrix} \text{ kA}$$

The power consumed by Load₁ is

$$P_1 = 3I_1^2 R_{11} = 3 \times 5.9^2 \times 20 = 2.08 \text{ GW}$$

The power consumed by Load₂ is

$$P_2 = 3I_2^2 R_{22} = 3 \times 4.34^2 \times 30 = 1.7 \text{ GW}$$

The power produced by the generator is the sum of P_1 and P_2 since the lines have no resistance.

$$P_3 = P_1 + P_2 = 3.78 \text{ GW}$$

- If Line₃ is tripped, $Y_{12}=0$, and the current can be computed similar to part a.

$$\begin{bmatrix} \bar{I}_1 \\ \bar{I}_2 \\ \bar{I}_3 \end{bmatrix} = \begin{bmatrix} 5.87 \angle -27.7^\circ \\ 4.35 \angle -10.57^\circ \\ 10.12 \angle -20.42^\circ \end{bmatrix} \text{ kA}$$

The power consumed by Load₁ is

$$P_1 = 3I_1^2 R_{11} = 3 \times 5.87^2 \times 20 = 2.07 \text{ GW}$$

The power consumed by Load₂ is

$$P_2 = 3I_2^2 R_{22} = 3 \times 4.35^2 \times 30 = 1.7 \text{ GW}$$

The power produced by the generator is the sum of P_1 and P_2 .

$$P_3 = P_1 + P_2 = 3.77 \text{ GW}$$

- c. To check the security of the system, we need to compute the currents in the transmission lines and compare them with their capacities. But first, we need to compute the bus voltages.

$$\bar{V}_1 = \bar{Z}_{11}\bar{I}_1 = 131.42 - j 2.6 = 131.44 \angle -1.13^\circ \text{ kV}$$

$$\bar{V}_2 = \bar{Z}_{22}\bar{I}_2 = 132.31 - 2.56 = 132.33 \angle -1.11^\circ \text{ kV}$$

The upper limit of the voltage is 5% above or below the rated voltage. This makes the acceptable voltage in the range of 126.15–139.43 kV per phase. All the aforementioned voltages are within this range. Hence, the system is secured from the voltage point of view.

The line currents are

$$\begin{bmatrix} \bar{I}_{12} \\ \bar{I}_{13} \\ \bar{I}_{23} \end{bmatrix} = \begin{bmatrix} 0 \\ 5.87 \angle -27.7^\circ \\ 4.35 \angle -10.57^\circ \end{bmatrix} \text{ kA}$$

All the currents are lower than the line capacities, which is 6 kA. The system is also secured from the current point of view. The system can continue to provide power to all customers.

- d. If Line₁ is tripped, $Y_{13}=0$, and the currents are

$$\begin{bmatrix} \bar{I}_1 \\ \bar{I}_2 \\ \bar{I}_3 \end{bmatrix} = \begin{bmatrix} 5.8 \angle -29.9^\circ \\ 4.3 \angle -11.9^\circ \\ 9.97 \angle -22.25^\circ \end{bmatrix} \text{ kA}$$

The power consumed by Load₁ is

$$P_1 = 3I_1^2 R_{11} = 3 \times 5.8^2 \times 20 = 2.02 \text{ GW}$$

The power consumed by Load₂ is

$$P_2 = 3I_2^2 R_{22} = 3 \times 4.3^2 \times 30 = 1.66 \text{ GW}$$

The power produced by the generator is the sum of P_1 and P_2 :

$$P_3 = P_1 + P_2 = 3.68 \text{ GW}$$

- e. To check the security of the system, we need to compute the currents in the remaining lines:

$$\bar{V}_1 = \bar{Z}_{11}\bar{I}_1 = 129.37 - j 7.55 = 129.6 \angle -3.34^\circ \text{ kV}$$

$$\bar{V}_2 = \bar{Z}_{22}\bar{I}_2 = 130.53 - 5.54 = 130.65 \angle -2.43^\circ \text{ kV}$$

All the aforementioned voltages are within the acceptable voltage range. Hence, the system is secured from the voltage point of view. Now let us check the line currents:

$$\begin{bmatrix} \bar{I}_{12} \\ \bar{I}_{13} \\ \bar{I}_{23} \end{bmatrix} = \begin{bmatrix} 5.8 \angle -29.9^\circ \\ 0 \\ 9.97 \angle -22.25^\circ \end{bmatrix} \text{ kA}$$

Notice that Line₂ carries 9.97 kA, which is higher than the capacity of the line (6 kA). In this case, the system is insecure and Line₂ will eventually trip to prevent it from overheating and, thus, sagging too deeply and touching trees or structures. When this line is tripped, total blackout occurs and no load will be served.

14.3 ELECTRIC ENERGY DEMAND

The decision to construct new generation or transmission facilities is mainly based on reliability concerns as well as existing and predicted future load demands. However, the demand varies on hourly basis, and the maximum demand occurs probably a few times a year during heat waves or cold spills. Therefore, it is hard to justify the cost of new facilities based on the maximum demand alone. Instead, utilities regularly depend on neighboring utilities to provide support during the high demand periods.

During a typical day, the energy demand fluctuates widely. For most utilities, the peak energy consumptions occur twice in a typical day as shown in Figure 14.8: the first is around 9:00 AM when factories, shops, and offices are at their peak consumption; the second is around 6:00 PM when people are at their homes doing their normal activities such as preparing meals, turning on lights, and watching televisions.

To provide reliable service to its customers, every utility must be able to meet the daily peak demands. Since the high energy demand occurs for a few hours everyday, it is uneconomical to build generating plants to be used only during the peak loads. Instead, it would be more profitable for the utility to build its generating capacity to meet the average daily demand. But what should be done when the load is higher than the available generation? Consider, for example, the load profile in Figure 14.9. The dark areas represent the periods when the generating capacity is below the demand, and the dashed areas represent the periods when the generating capacity is higher than the demand.

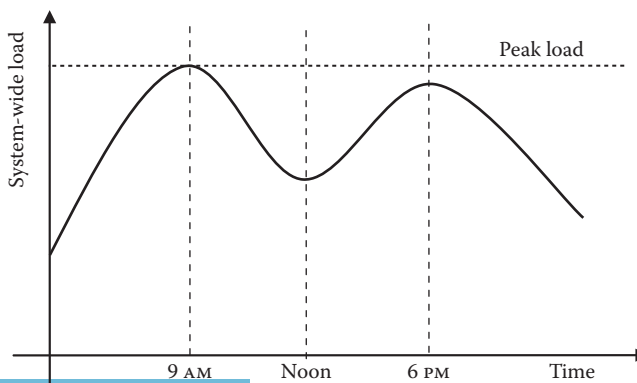


FIGURE 14.8 Daily system load.

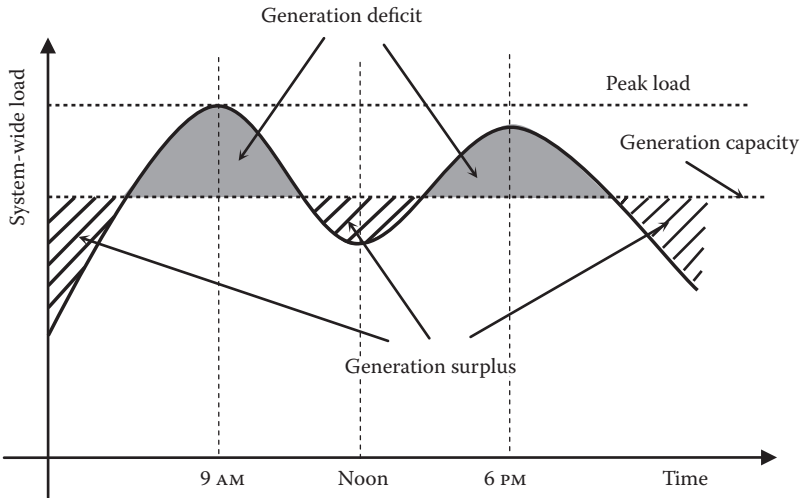


FIGURE 14.9 Setting the generation capacity.

The obvious economical solution to the deficit and surplus powers is to trade electricity with neighboring utilities. When a utility has surplus, it sells the excess power to another utility that needs it. When it has a deficit, the utility buys the extra power from another utility with surplus. This arrangement makes sense economically, but requires all utilities to be interconnected through a mesh of transmission lines.

Example 14.2

The load demand of a power system for a given day can be approximated by

$$P = 2 - 0.3 \times \cos(0.5417t - 1) \times e^{-0.01t} \text{ GW}$$

where t is the time of the day in hours using the 24 h clock. Compute the following:

- Times of the peak demands.
- Peak demands.
- Average demand.
- If the generation capacity of the utility is 2 GW, compute the power to be imported during the first peak.

Solution

- To compute the times of the peaks, we need to set the derivative of the power equation with respect to time to zero:

$$\frac{dP}{dt} = 0$$

$$0.01 \times \cos(0.5417t - 1) + 0.5417 \sin(0.5417t - 1) = 0$$

Hence,

$$\tan(0.5417t - 1) = -0.01846$$

$$t = \frac{1 + \tan^{-1}(-0.01846)}{0.5417}$$

Solving the aforementioned equation using the four quadrants of the tangent function, the first peak is at

$$t_1 = 7.6115 = 7:37 \text{ AM}$$

and the second peak is at

$$t_2 = 19.2 = 7:12 \text{ PM}$$

b. The first and second peaks are

$$P_{peak1} = 2 - 0.3 \times \cos(0.5417t_1 - 1) \times e^{-0.01 \times t_1} = 2.278 \text{ GW}$$

$$P_{peak2} = 2 - 0.3 \times \cos(0.5417t_2 - 1) \times e^{-0.01 \times t_2} = 2.2475 \text{ GW}$$

c. The average power during the 24 h period is

$$P_{ave} = \frac{1}{24} \int_0^{24} P dt$$

The power equation can be rewritten in the following form:

$$P = 2 - 0.162e^{-0.01t} \times \cos(0.5417t) - 0.2525e^{-0.01t} \times \sin(0.5417t)$$

Hence,

$$P_{ave} = \frac{1}{24} \int_0^{24} (2 - 0.162e^{-0.01 \times t} \times \cos(0.5417t) - 0.2525e^{-0.01 \times t} \times \sin(0.5417t)) dt$$

$$P_{ave} = 2 - \left[\frac{e^{-0.01t}}{0.01^2 + 0.5417^2} \left[(0.08523) \sin(0.5417t) - (0.1384) \cos(0.5417t) \right] \right]_0^{24}$$

$$P_{ave} = 1.7688 \text{ GW}$$

d. The power to be imported during the first peak is

$$P_{import} = P_{peak1} - P_{ave} = 2.278 - 1.7688 = 509.2 \text{ M}$$

14.4 TRADING ELECTRIC ENERGY

As mentioned earlier, the trading of energy between utilities makes great economic sense. For example, the two utilities in Figure 14.10 are connected by a transmission line often called *tie line*. Assume that the two utilities are located in two different longitudes (different time zones). The time zone of the western utility lags that of the eastern utility by 3 h. At 9:00 AM Eastern Time (ET), the eastern utility is at its peak demand while the western utility has surplus generation since it is 6:00 AM in the west. Hence, the extra power can be delivered to the eastern utility by the western utility. At noon ET, the western utility is at its peak demand, while the eastern utility has surplus. So the power can flow from east to west.

Another example of the power exchange occurs between utilities at different latitudes. Consider the case in Figure 14.11, where the northern area is assumed to be generally cooler than the southern area, for example, the Northwest region and California in the United States. Heating loads are dominant in the Northwest, while cooling loads are prevailing in California. In the summer, the temperature in the Northwest region is mild and the demand for electric energy is low. In California, however, it is generally hot and the energy demand is high because of the use of air-conditioning equipment. Hence, the Northwest has surplus energy, while California has a deficit. As a result, the power moves from north to south. In the winter, the scenario is reversed.

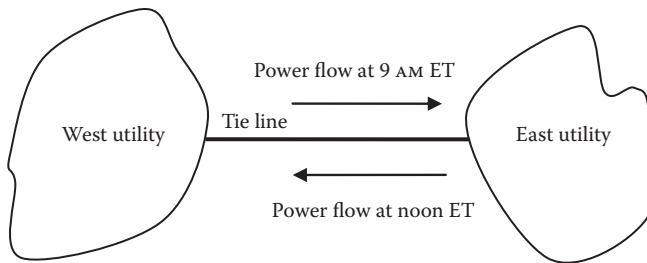


FIGURE 14.10 Two utilities at different time zones.

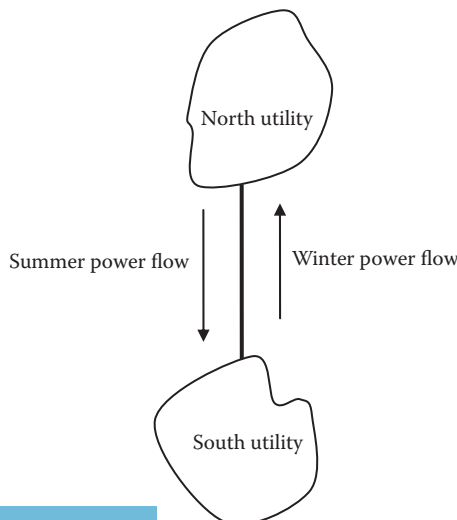


FIGURE 14.11 Trade between utilities at different latitudes.

Example 14.3

The load demand for a given utility can be approximated by

$$P = 4 - \cos(0.5t - 1.2) \text{ GW}$$

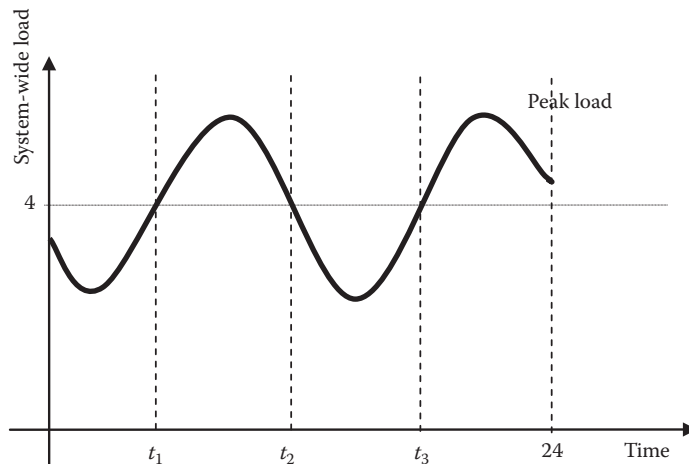
where t is the time of the day in hours using the 24 h clock. The generating capacity of the utility is 4 GW. Compute the following:

- Energy available for export
- Imported energy during the time of energy deficit
- Net energy trade

Solution

- The power available for trading is the difference between the actual demand and the generation capacity:

$$\Delta P = P_{ave} - P = \cos(0.5t - 1.2)$$



Before we compute the traded energy, we need to identify the times in the figure when the demand is equal to the capacity:

$$\Delta P = \cos(0.5t - 1.2) = 0$$

Hence,

$$t_1 = 5.542$$

$$t_2 = 11.825$$

$$t_3 = 18.108$$

The energy available for export is

$$E_{export} = \int_0^{t_1} \Delta P dt + \int_{t_2}^{t_3} \Delta P dt$$

$$E_{\text{export}} = 0.5 \sin(0.5t - 1.2) \Big|_0^{5.542} + 0.5 \sin(0.5t - 1.2) \Big|_{11.825}^{18.108} = 1.966 \text{ GWh}$$

b. The imported energy is

$$E_{\text{import}} = \int_{t_1}^{t_2} \Delta P dt + \int_{t_3}^{24} \Delta P dt$$

$$E_{\text{import}} = 0.5 \sin(0.5t - 1.2) \Big|_{5.542}^{11.825} + 0.5 \sin(0.5t - 1.2) \Big|_{18.108}^{24} = -1.99 \text{ GWh}$$

c. The net trade is

$$E_{\text{net}} = E_{\text{export}} - E_{\text{import}} = 1.966 - 1.99 = -24 \text{ MWh}$$

14.5 WORLD WIDE WEB OF POWER

In addition to the economic benefits, interconnecting utilities makes great sense with reference to system reliability. If some generators in certain areas are out of service, the generation deficit can be compensated by importing extra power from neighboring utilities. Also, if a key transmission line is tripped, other transmission lines in the grid can reroute the power to the customers. Because of these economic and reliability benefits, power systems are continuously merging with little regard to political or geographical borders.

Although interconnected, the operation, trade, and control functions for power systems are left to local pools, which are composed of several utilities in a geographical region. In the United States, Canada, and a small part of Mexico, the power grid is divided into the 10 power pools shown in Figure 14.12; the pools are called *reliability councils*. An example of a reliability council is the *Mid-Atlantic Area Council* (MAAC), which encompasses an area of nearly 130,000 km² and provides electricity to more than 23 million people in the northeastern region of the United States and eastern

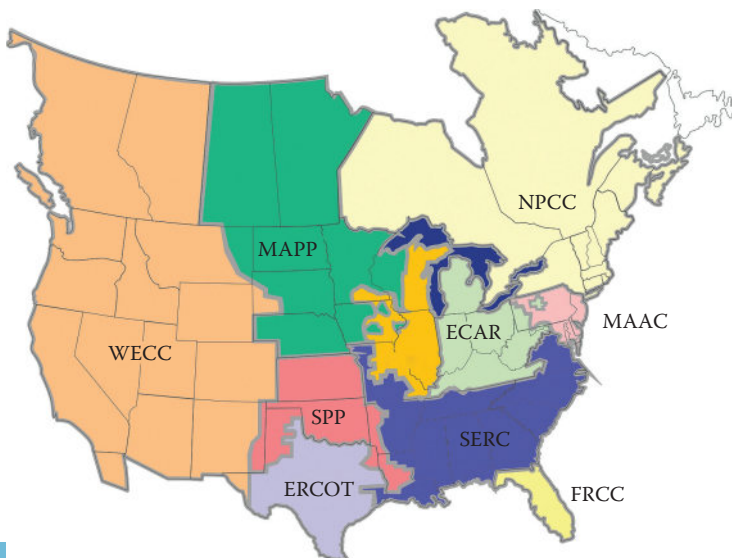


FIGURE 14.12 United States regional reliability councils.

Canada. The capacity of the MAAC is approximately 60 GW and it has over 13,000 km of bulk power transmission lines.

Another example of a pool is the *Western Electricity Coordinating Council* (WECC), which provides electricity to 71 million people in 14 western states, 2 Canadian provinces, and a portion of the Baja California State in Mexico. The WECC system consists of over 1000 generating units and tens of thousands of transmission lines. It has at least 600 generating units, each is rated at least 500 MW. The full WECC system is very complex and is hard to display in a single page. A small part of the WECC is shown in Figure 14.13.

All 10 coordinating councils form a nonprofit corporation called *North American Electric Reliability Council* (NERC). The NERC's mission is to ensure that the electric power system in North America is reliable, adequate, and secure by setting monitoring and enforcing standards for the reliable operation and planning of the electric grid.

The power systems are also fully interconnected in Western Europe, and their equivalent to NERC is called the *Union for the Co-ordination of Transmission of Electricity* (UCTE). UCTE covered about 20 European countries, while more countries from Eastern Europe are expected to be connected to the UCTE grid. Their service area includes 400 million people and its total annual consumption is approximately 2100 TWh. North Africa is also being connected with Europe through submarine cable systems under the Mediterranean Sea. In other regions of the world, the power systems are linked together whenever possible. Indeed, many consider that power engineers have succeeded in creating a borderless power grid that is truly unifying the world.

Although the interconnection of the power networks has many great advantages, it has two major drawbacks:

1. Power grid becomes incredibly complex, creating enormous challenges for monitoring, operation, protection, and control of the system.
2. Major failures in one area could affect other areas, thus creating wider blackouts. This was evident in the major blackouts in the United States in 1965, 1976, and 2003.

14.6 ANATOMY OF BLACKOUTS

Blackouts can be caused by a number of natural or man-made events as well as major component failure. The list is long, but the typical triggers for blackouts include the following:

- Faults in transmission lines could lead to excessive currents in the system. The faulted section of the network must be isolated quickly to prevent any thermal damage to the transmission lines, transformers, and other major power equipment. This is done by tripping (opening) the circuit breakers on both ends of the faulted line. The loss of the transmission line could result in outages.
- Natural calamities such as lightning, earthquake, strong wind, and heavy frost can damage major power system equipment. When lightning hits a power line, the line insulators can be damaged leading to short circuits (faults). Major earthquakes could damage substations, thus, interrupting power to the areas served by the substations. Heavy winds may cause trees to fall on power lines, creating faults that trip transmission lines.
- When major power system equipments such as generators and transformers fail, they may lead to outages.
- Protection and control devices may not operate properly to isolate faulty components. This is known as *hidden failure* and can cause the fault to affect a wider region in the system.
- Breaks in communication links between control centers in the power system may lead to the wrong information being processed, causing control centers to operate asynchronously, and probably negating each other.
- Human errors can lead to tripping of important equipment.

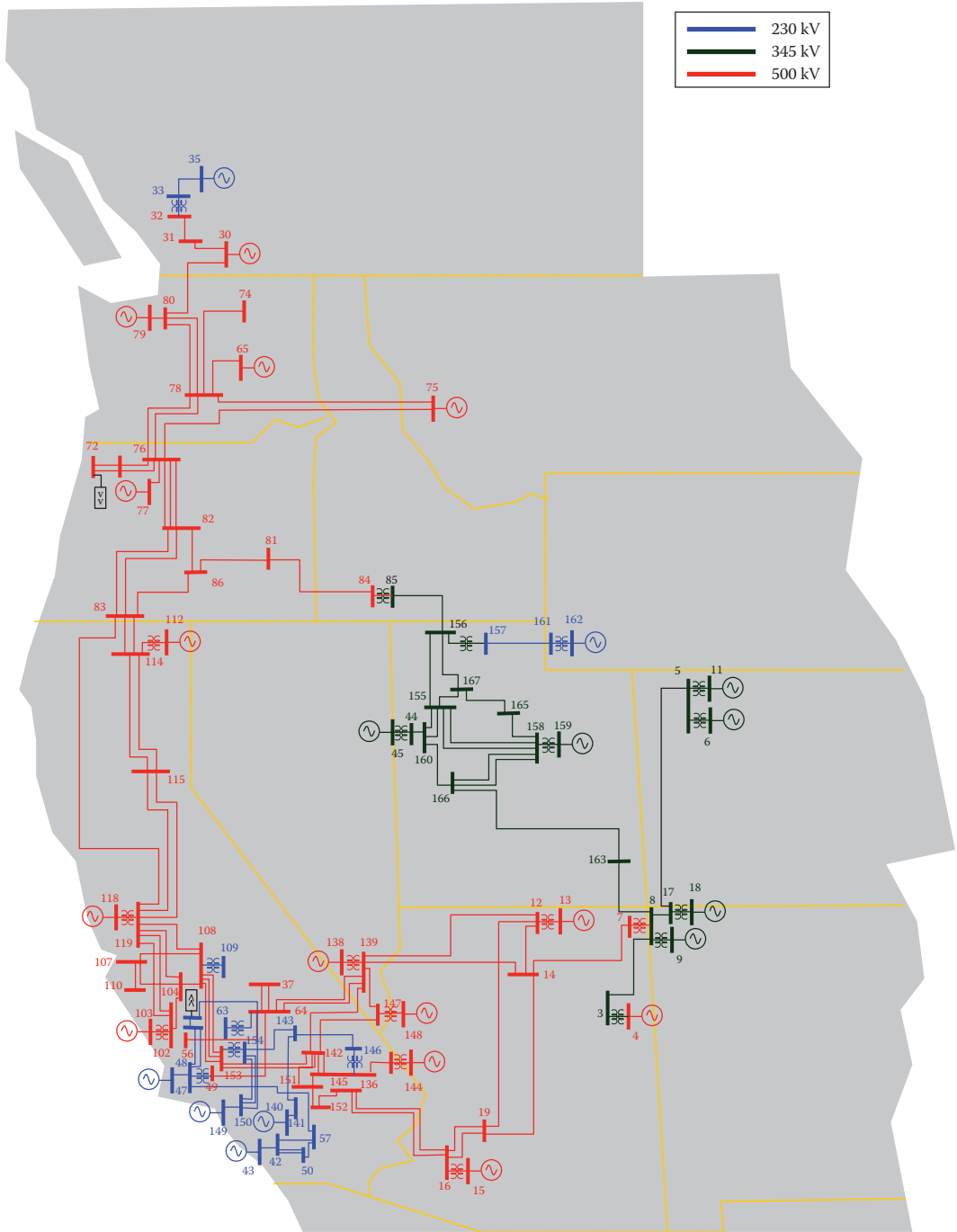


FIGURE 14.13 Major components of the WECC.

14.6.1 BALANCE OF ELECTRIC POWER

The power balance of the system must always be maintained to ensure its stable operation; that is, the sum of power from all generators must be equal to the sum of power of all loads plus all losses. This simple relationship must be preserved at the system-wide level, and at the power pool level.

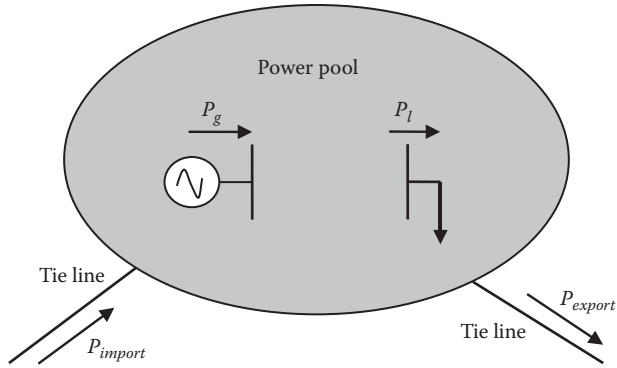


FIGURE 14.14 Power balance of a pool.

For example, the power pool in Figure 14.14 represents a geographical area or a service territory of a utility or a group of utilities. The power pool has a total power generation P_g from all its power plants, and a total system load P_l representing customers’ demand plus the losses in the system. The pool imports power P_{import} from neighboring utilities, and exports power P_{export} to other neighboring utilities. The balanced power equation of the pool is

$$P_g + P_{import} = P_l + P_{export} \tag{14.9}$$

Now let us assume that the tie line transmitting P_{import} is lost for some reason. Then, the power balance is not maintained, and

$$P_g < (P_l + P_{export}) \tag{14.10}$$

The fundamental question is how to balance the power in the pool. In this simple example, we have four options:

1. Reduce P_{export} , which may result in a power deficit in the neighboring utility.
2. If the generated power is below the capacity of the pool, increase the generation P_g .
3. Reduce the demand by disconnecting some loads. This is called *rolling blackouts*. If some loads are disconnected for some time, then other loads are disconnected afterward, and so on.
4. Find another utility that can transmit the needed power through other transmission routes.

All these solutions must be implemented within a short time (milliseconds in some cases), otherwise the system may collapse. Why? The answer is in the following sections.

14.6.2 BALANCE OF ELECTRICAL AND MECHANICAL POWERS

The synchronous generator is an electromechanical converter as depicted in Figure 14.15. Its input power is mechanical P_m and its output is electrical power P_g . If you ignore the internal losses, the balanced operation of the generator is achieved when

$$P_m = P_g \tag{14.11}$$

Keep in mind that the magnitude of the electrical power P_g is determined by customers’ actions. Although the utilities do not often know in advance their customers’ intentions, the utility must

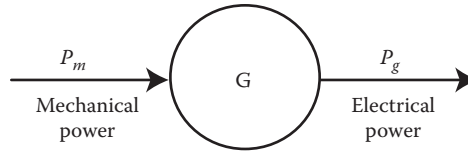


FIGURE 14.15 Power balance of synchronous generator.

continually adjust the mechanical power into its generators so that Equation 14.11 is satisfied at all times. As long as the balance is maintained, the system is stable and all loads are served.

Among the problems that lead to blackouts is the uncompensated imbalance between the mechanical and electrical powers of the generators. When the input power to the generator P_m is greater than the output power P_g , the excess power is stored in the rotating mass of the generator–turbine unit in the form of extra kinetic energy. If $P_m < P_g$, the electric power shortage is recovered from the kinetic energy in the rotating mass. The dynamic equation of the electromechanical powers of the generator can be written as

$$M_{eq} \frac{d\omega}{dt} = P_m - P_g \quad (14.12)$$

where

M_{eq} is the equivalent inertia of the rotating mass of the generator–turbine unit

ω is the angular speed of the rotor of the generator

$d\omega/dt$ is the angular acceleration of the rotor

$M_{eq} \frac{d\omega}{dt}$ is the kinetic power

As explained in Chapter 12, the speed of the synchronous machine ω_s is constant during the steady-state operation (stable operation) and is equal to

$$\omega_s = 2\pi \frac{n_s}{60} \text{ rad/s}$$

$$n_s = 120 \frac{f}{p} \text{ rpm} \quad (14.13)$$

where

f is the frequency of the output voltage of the generator

p is the number of poles inside the machine

n_s is the synchronous speed of the magnetic field, which is the same as the rotor speed in the steady state

Now let us assume that the synchronous machine is connected to an *infinite bus* as shown in Figure 14.16. As discussed in Chapter 12, the infinite bus is a term used to describe a large system that has constant frequency and constant voltage. The equivalent circuit of the synchronous generator, which is also given in Chapter 12, is depicted at the left side of Figure 14.17. E_f is the equivalent field voltage, V_t is the terminal voltage of the generator (the infinite bus voltage in our case), and X_s is the synchronous reactance of the generator.

As explained in Chapter 7, any phasor has three attributes: magnitude, angle, and frequency. Although we draw the phasor as a stationary vector, it is actually rotating at its own frequency.

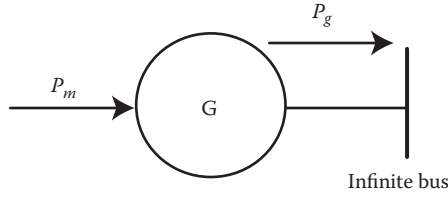


FIGURE 14.16 Phasor diagram of synchronous generator.

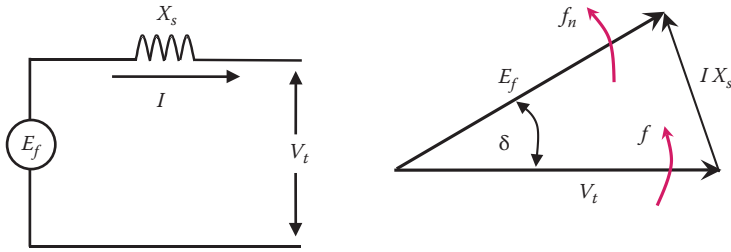


FIGURE 14.17 Model of synchronous generator.

In our example, and as shown at the right side of Figure 14.17, V_t rotates at the frequency of the infinite bus voltage f , which is constant (60Hz in the United States or 50Hz in Europe). E_f rotates at frequency f_n corresponding to the actual rotor speed n . As given in Chapter 12, f_n can be computed by using Equation 14.13.

$$f_n = \frac{P}{120} n \tag{14.14}$$

When the rotor of the generator rotates at the synchronous speed ($n = n_s$), the frequency of E_f is equal to the system frequency, that is, $f_n = f$, and the angle δ is constant.

Now let us use Equation 14.12 to discuss the three possible scenarios in Table 14.1. In scenario 1, the mechanical and electrical powers are equal. Hence, the acceleration $d\omega/dt = 0$, and

TABLE 14.1
Effects of Power Imbalance

Scenario	Power Equation	Rotor Acceleration $\frac{d\omega}{dt}$	Rotor Speed ω	Kinetic Energy of Rotating Mass
1	$P_m = P_g$	$\frac{d\omega}{dt} = 0$	$\omega = \omega_s$	Unchanged Machine is in synchronism. This is the steady-state operation
2	$P_m > P_g$	$\frac{d\omega}{dt} > 0$	$\omega > \omega_s$	Increases Machine is out of synchronism
3	$P_m < P_g$	$\frac{d\omega}{dt} < 0$	$\omega < \omega_s$	Decreases Machine is out of synchronism

the rotor speed ω is equal to the synchronous speed ω_s . Thus, $f_n = f$. Consequently, as shown in Figure 14.17, the power angle δ is constant. The difference between \bar{E}_f and \bar{V}_t , which is $\bar{I}_a \bar{X}_s$, is also constant. Since X_s is fairly constant, the current in the machine is constant. This is a balanced (steady-state) operation and the generator is said to be *in synchronism* with the rest of the power system.

For scenario 2 where $P_m > P_g$, the generator accelerates and the rotor speed becomes greater than the synchronous speed. Hence, $f_n > f$, and the machine in this case is said to be *out of synchronism* with the rest of the power system. Because of the difference in frequencies, δ keeps increasing, thus, the current inside the machine is continuously increasing. When the current reaches the thermal limit of the machine, the generator is disconnected from the grid to prevent any further damage to the machine. This can happen in just a few milliseconds.

In scenario 3 when $P_m < P_g$, the rotor decelerates and its speed goes below the synchronous speed. Hence, $f_n < f$, and the machine is *out of synchronism* with the rest of the power system. Unless corrected, E_f will eventually lag V_t , making the generator operate as a motor and reversing the flow of power. During this period, the current inside the machine will increase to a high level that shuts down the generator.

Based on the earlier discussion, we can conclude that every generator in the power network must operate under scenario 1, which satisfies Equation 14.11. Thus, the power plant controller must continuously adjust the mechanical power of the turbine to match the changes in the load demand to keep the generators of the plant in synchronism with the rest of the power network.

14.6.2.1 Control Actions for Decreased Demand

Substituting the value of P_g in Equation 14.9 into Equation 14.11 yields

$$P_m = P_l + P_{export} - P_{import} \quad (14.15)$$

Assume that P_{import} and P_{export} are constants. When the load demand P_l is reduced, the mechanical power into the generator must be reduced to match the new demand. This is a relatively simple process if the change in demands is slow (minutes or hours). For thermal power plants, the reduction of P_m is done by gradually reducing the steam entering the turbines. For hydroelectric power plants, the governor reduces the amount of water entering the turbine.

However, if the reduction in demand is sudden and large, the control action is stern and very fast. For thermal power plants, the steam is allowed to escape in the air, thus rapidly reducing the amount of steam entering the turbine. However, for hydroelectric power plants, changing the water flow is a slow process because rapid closure of the water valve can damage the penstock due to excessive water hammers. Instead, resistive loads, known as braking resistances, are connected to the system to consume the excess electric energy until the water flow is reduced.

14.6.2.2 Control Actions for Increased Demand

When the electrical demand P_l is greater than the output mechanical power of the turbine P_m , the steam of the thermal power plant, or the water of the hydroelectric power plant, must increase to match the new demand as explained in Equation 14.15. This is achievable if the change in demand is slow. However, matching a rapid increase in demand is a much difficult process as the increase in mechanical power is a slow process; for hydroelectric plants, the water time constant is about 7–10 s. Until the mechanical power increases, the hope is that enough kinetic energy is stored in the system to match the new demand for a short period. If not, one solution would be to increase the import power or decrease the export power. This must be coordinated with the other utilities to ensure that they are able to cope with the new changes. If none of these solutions is possible, the utility may have to resort to rolling blackouts to maintain the power balance in Equation 14.15.

To reduce the reliance on the rolling blackouts to balance the system powers, utilities install enough *spinning reserves* in each pool. The spinning reserves are rotating generators in power plants

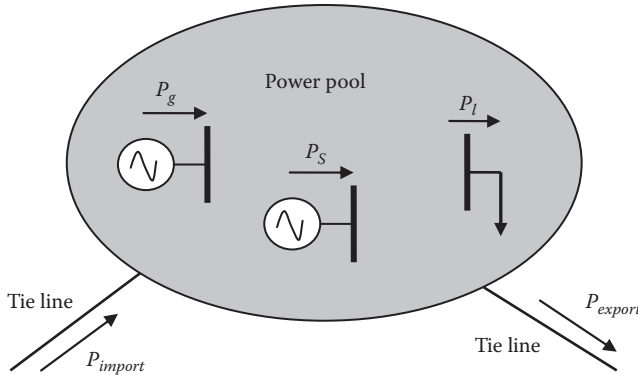


FIGURE 14.18 Power balance of a pool with spinning reserve.

that are on standby mode to generate electricity very quickly. These spinning reserves are normally steam power plants with their steam temperature and pressure kept at values necessary for generating electricity on a short notice. When the demand is rapidly increasing, the utility can use its own spinning reserve before it reaches out to neighboring utilities. This way, the reliability of the system is greatly enhanced. Figure 14.18 shows the modified power pool with the spinning reserve P_s .

With the spinning reserve, the stable operation of the power pool is when

$$(P_g + P_{import} + P_s) > (P_l + P_{export}) \tag{14.16}$$

Hence,

$$(P_g + P_{import} + P_s) = \lambda(P_l + P_{export}) \tag{14.17}$$

where λ is defined as *pool power margin*. For a robust system, the margin must be greater than 1.

Example 14.4

A power pool has a generation capacity of 1.5 GW. The trade commitments and forecasted load at four different times are given in the following table:

Time	P_l	P_{export}	P_{import}
t_1	800 MW	200 MW	0
t_2	1 GW	200 MW	0
t_3	1.2 GW	400 MW	100 MW
t_4	1.8 GW	600 MW	200 MW

Compute the spinning reserve at each of the four times to maintain a power pool margin of at least 110%.

Solution

Use Equation 14.17 to compute the spinning reserve.

At t_1 ,

$$P_s = \lambda(P_l + P_{export}) - (P_g + P_{import}) = 1.1(800 + 200) - (1500 + 0) = -400 \text{ MW}$$

There is no need for a spinning reserve at t_1 .

At t_2 ,

$$P_s = \lambda(P_l + P_{export}) - (P_g + P_{import}) = 1.1(1000 + 200) - (1500 + 0) = -180 \text{ MW}$$

There is no need for a spinning reserve at t_2 .

At t_3 ,

$$P_s = \lambda(P_l + P_{export}) - (P_g + P_{import}) = 1.1(1200 + 400) - (1500 + 100) = 160 \text{ MW}$$

At t_4 ,

$$P_s = \lambda(P_l + P_{export}) - (P_g + P_{import}) = 1.1(1800 + 600) - (1500 + 200) = 940 \text{ MW}$$

14.7 BLACKOUT SCENARIOS

Most major blackouts occur during heavy-loading conditions. The worst scenarios occur when the power plants are generating electricity close to their capacities, the transmission lines are heavily loaded, or the spinning reserves are low.

For example, consider the power pools shown in Figure 14.19. The pool in the middle is our system, which is connected to two neighboring pools (external pool 1 and external pool 2). Two tie lines connect our power pool to the external pools. Assume that our power pool is heavily loaded, and $P_l > P_g$. To compensate for the deficit in power, our power pool imports P_1 from external pool 1, and P_2 from external pool 2. Thus, our power pool is balanced. Hence,

$$P_g + P_1 + P_2 = P_l \tag{14.18}$$

If we add the spinning reserve P_s of our pool to Equation 14.18, we get

$$(P_g + P_1 + P_2 + P_s) > P_l \tag{14.19}$$

So far, the spinning reserve is not needed. Assume that all tie lines are heavily loaded (close to their capacities). Now, let us assume that tie line 2 is lost for some reason. In this case, our power pool has a deficit in power since

$$(P_g + P_1) < P_l \tag{14.20}$$

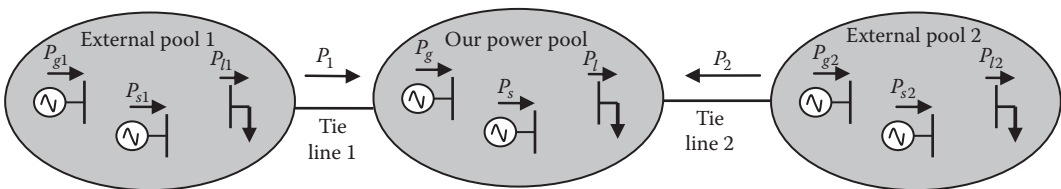


FIGURE 14.19 Blackout scenario.

To compensate for the deficit, our power pool uses its own spinning reserve. However, assume that the spinning reserve is not enough to compensate for the lost power P_2 ; that is,

$$(P_g + P_1 + P_s) < P_l \quad (14.21)$$

To correct the problem, tie line 1 needs to deliver more power to our pool. This requires two conditions: (1) external pool 1 can provide more power than what is scheduled and (2) tie line 1 can handle the extra currents. If these two conditions cannot be met, our power pool will be left with a deficit in generation and must quickly trip some of its loads (rolling blackout). Otherwise, its own generating plants will shut down to prevent them from being damaged and our power pool may experience a total blackout. Needless to say that unless they reduce their generation quickly, the other two external pools will also face blackouts after the tie lines are opened.

14.7.1 GREAT NORTHEAST BLACKOUT OF 1965

The Great Northeast Blackout of 1965 left 30 million people without electricity in New England, New York, and Ontario. Before the blackout, Ontario Hydro was exporting about 1.7GW to the United States through five tie lines including the Massena tie line. The blackout started in the following sequence:

1. A relay protecting one of the main transmission lines in the Ontario Hydro system was set too low. The line was heavily loaded and the relay tripped the transmission line. The line was directly connected to a hydroelectric plant on the Niagara River.
2. Because of the line tripping, the flow of power was shifted to the remaining four lines. These lines were heavily loaded before the power shift, and were overloaded after the shift.
3. Overloading the lines resulted in the tripping of the remaining lines successively.
4. The tripping of all lines resulted in a shortage of about 1.5 GW in the Canadian system, and the power reversed its flow to Canada from the United States.
5. The reversal of power overloaded the Massena tie line even further and it was tripped. The Canadian system was then completely isolated, and became deficient in generation and collapsed.
6. The U.S. system was also generation deficient since it was dependent on about 1.7GW from Canada. The New England and New York systems collapsed, and a total blackout occurred in their systems in a matter of seconds. It took 24 h to restore the system.

14.7.2 GREAT BLACKOUT OF 1977

This blackout affected eight million people mainly in New York City. The blackout was the second one for New York City in 12 years and lasted for 25 h.

On the hot evening of July 13, 1977, the electrical demand of New York City was very high at about 6GW. About 3GW of the power was imported from neighboring utilities. The area was also experiencing lightning storms. The blackout sequence was as follows:

1. One of the main tie lines serving Manhattan, the Bronx, Brooklyn, Queens, and Staten Island was stricken by lightning, which damaged the insulators, causing the line to trip.
2. The power was shifted to the other remaining lines feeding New York City, which were heavily loaded.
3. The spinning reserve of the New York City was used to alleviate the stress on the remaining tie lines. The solution was adequate and the system survived the loss of the line.

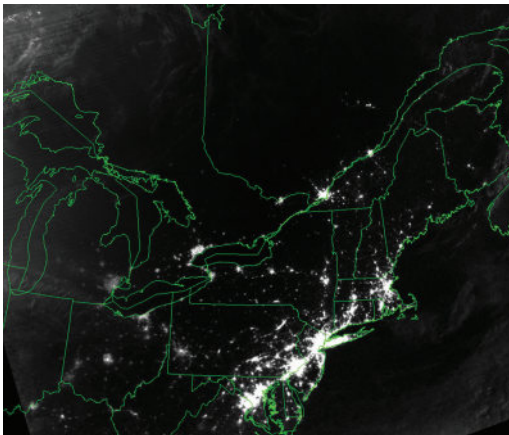
4. However, the storm was severe and after 20 min another lightning strike hit another major tie line and it was tripped.
5. All other lines carried currents beyond their thermal limits and sagged. One of the tie lines sagged too deeply and touched a tree causing a short circuit, and the line was tripped.
6. The New York area had a severe deficit in generation, and the system loads could not be served with the existing generations and transmission systems. The system collapsed in seconds.

14.7.3 GREAT BLACKOUT OF 2003

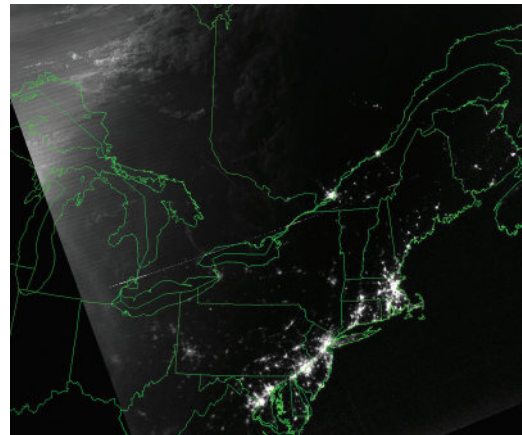
This blackout is the worst in history, so far. About 50 million people were affected by the blackout, and the power was out for several days. NASA published interesting Satellite photos of northeast United States before and after the blackout. These pictures are shown in Figure 14.20. Notice how dark Manhattan Island and the Midwest region are during the blackout.

On the hot summer day of August 14, 2003, the systems in the Eastern and Midwestern United States as well as Ontario, Canada, were heavily loaded and the blackout started in the following sequence:

1. A 680MW coal generation plant in Eastlake, Ohio, went off-line amid high energy demand.
2. An hour later, a transmission line in northeastern Ohio tripped because it was overloaded.
3. The outage put an extra strain on other transmission lines, and some lines sagged and came in contact with trees, causing short circuits that tripped the lines.
4. Utilities in Canada and the eastern United States experienced wild power swings causing stress on their systems. Power plants and high-voltage electric transmission lines in Ohio, Michigan, New York, New Jersey, and Ontario shut down.
5. In less than 3 min, 21 power plants were shut down including seven nuclear power plants. A total of 200 power plants eventually went off-line.



Just before the blackout



Just after the blackout

FIGURE 14.20 Satellite pictures of the northeast United States on August 14, 2003. (Courtesy of NASA, Washington, DC.)

EXERCISES

- 14.1** What is a spinning reserve?
- 14.2** State two advantages of interconnecting power pools.
- 14.3** State some differences between the power grid and the Internet.
- 14.4** What is the advantage of a network grid over a radial grid?
- 14.5** What is the advantage of connecting pools at different time zones?
- 14.6** Search the web and the literature to find the capacity of the ERCOT power pool in the United States. Find the area covered and the size of the population served.
- 14.7** Search the web and the literature and find the largest power pool in the United States.
- 14.8** The power system in Figure 14.5 has the following data:
- Impedance of Load₁ plus its transformer is $Z_{11} = 50 + j5 \Omega$
 - Impedance of Load₂ plus its transformer is $Z_{22} = 40 + j2 \Omega$
 - Impedance of Line₁ is $Z_{13} = 0 + j4 \Omega$
 - Impedance of Line₂ is $Z_{23} = 0 + j5 \Omega$
 - Impedance of Line₃ is $Z_{12} = 0 + j3 \Omega$
- All impedances are referred to the high-voltage side of the transformers. The voltage at the high-voltage side of xfm_g is fixed at 500kV (line-to-line). The capacity of any line (maximum current the line can carry) is 15kA. Assume that all connections are in wye. Compute the power delivered to each load, and the power produced by the generator.
- 14.9** For the system in the previous problem, assume that transmission Line₃ is tripped, repeat the solution. Is the system secure?
- 14.10** The load demand for a given day can be approximated by $P = 2 + 2e^{-\frac{(t-9)^2}{8}}$ GW where t is the time of the day in hour using the 24h clock. Compute the following:
- a. Peak demand
 - b. Time of the peak demands
 - c. Average daily demand
- 14.11** For the system in the previous problem, assume that the generation capacity is 1.9GW. Compute the imported energy to compensate for all demands higher than 1.9GW.
- 14.12** A power pool has a generation capacity of 1.5GW and a demand of 1000MW. The trade commitments of the pool are: $P_{import} = 500$ MW and $P_{export} = 800$ MW. Compute the spinning reserve that maintains the pool margin at 130%.

15 Future Power Systems

Thomas Edison and Nikola Tesla invented the early generation of power systems. Their system, however, has gone through tremendous developments and improvements over the past century. Today's power systems are probably the most complex systems known to man. They have immense capacities, are huge and complex, and are quick to respond to changes in the various parts of the system. Despite the blackouts we experience every few years, the reliability of modern power systems is very high, considering its complexity and enormous size.

A common question is what future power systems would look like. Is it going to remain the same, albeit in a more expanded and complex form? Will we use the same energy resources? Will the energy resources last for future generations? Will we keep locating our generating plants near cities? Will we continue polluting the environment? Will we be able to harvest electricity from the natural dynamics of earth? Will we be able to provide electricity to remote places on earth and space?

These are tough questions, which may require a crystal ball to answer. Nevertheless, researchers are working hard to develop what they perceive as the power system of the future. Following are some of the ideas and concepts that are being researched. Some of them are in the conceptual phase while others are currently being implemented.

15.1 SMART GRID

Distribution networks in today's utilities play passive roles as their function is limited to receiving electric power from transmission networks and delivering it to the loads (customers). Thus, the power flow in the distribution network is mostly unidirectional. The infrastructure of the current distribution networks, their protection and monitoring devices, as well as their control systems are all designed to operate in this passive environment. However, because renewable energy and distributed generation systems are often connected directly to the distribution networks, the network must be redesigned to allow for more vibrant bidirectional operations and control environments. One of the concepts for the future distribution network infrastructure is called *Smart Grid*.

The Smart Grid is the vision for future distribution networks that utilize newer and different technologies to allow for the integration of renewable energy systems and distributed generation systems into the distribution network. The concept of the smart grid was conceived at the end of the twentieth century by European and American researchers. It is an ambitious structure that embeds conventional and renewable energy generators, energy storage systems, demand-side management, wide-area monitoring, and intelligent control.

Figure 15.1 shows an artistic depiction of a smart grid. The renewable energy systems are connected directly into the distribution network. Renewable resources such as hydrogen have their own infrastructure to power loads and fuel cell vehicles. This requires safe and efficient storage systems for the hydrogen as well as underground pipe systems to transmit the gas. When the demand for electrical energy is low, renewable resources can be used to generate hydrogen through, for example, electrolysis processes. Surplus electric energy can be stored in, for example, supercapacitors (at the bottom left of the figure) for long periods with minimum losses. In addition, thermal storage can be used to directly heat buildings. This could be a simple system where rocks are heated when electricity is cheap or abundant. The heat is then extracted when electricity is expensive. The customers can also have their equipment controlled by the utility where at peak demands, the unessential loads

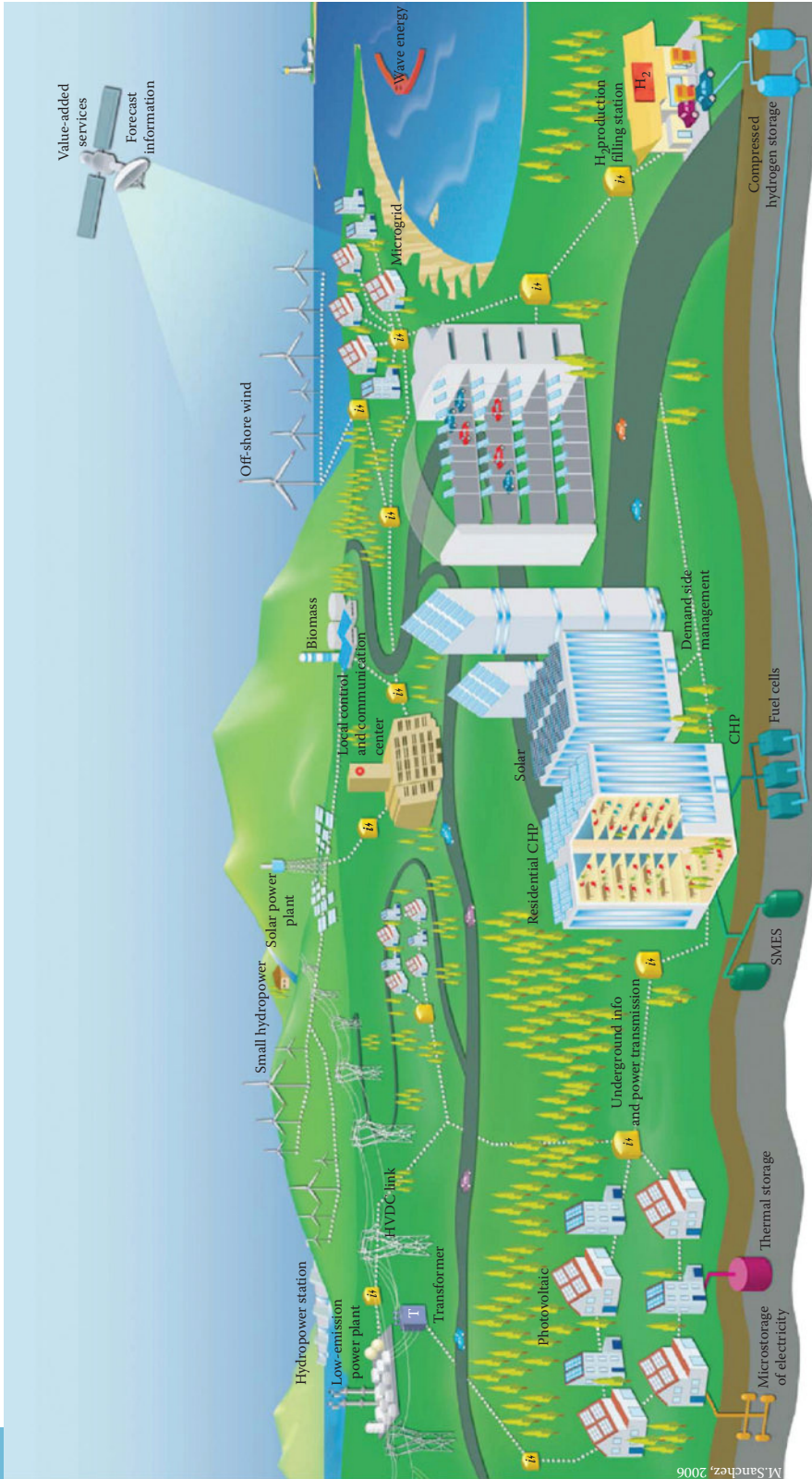


FIGURE 15.1 Concept of smart grid. (Courtesy of European Commission on Smart Grid, EUR22040 report.)

are disconnected. In this way, customers receive lower energy bills while the utility manages its resources much better. To optimize the operation of the smart grid, local and network information is collected and transmitted to a central control system where sophisticated algorithms operate the network efficiently and reliably at all times. As described by the visionaries, the smart grid has four major objectives:

1. *Improve accessibility* by granting access to all customers and allow bidirectional power flow to renewable resources.
2. *Increase system flexibility* by implementing technologies that respond to customers' needs while responding to changes and challenges in the grid.
3. *Enhance system reliability* by assuring the energy supplies and enhance system security.
4. *Reduce cost of energy* by providing the best values to the customers through innovation and efficient energy management.

By achieving these objectives, the smart grid can provide tremendous benefit to the power grid and energy customers, as follows:

- *Reduction in transmission congestion:* When renewable generation is located near load centers, the generated power can be consumed locally instead of hauling it from large power plants through transmission lines. This reduces the currents in the transmission lines, thus allowing for extra customers to be connected to the existing line instead of constructing new ones.
- *Reduced blackouts and forced outages:* The Department of Energy estimated that the "power outages and fluctuations cost U.S. businesses and consumers \$30 billion each year." The main cause for the outages is when the demand and generation are not equal, either because of inadequate generation or the lack of available transmission lines that can haul power to the customers. If more renewable generations are present near load centers, there is less dependency on generation from large utilities and less dependency on transmission lines.
- *Self-diagnosis:* The power system is extensively monitored, but the measurements do not cover the entire grid and the overwhelming data is extremely hard to process at the national grid level. The improvements in the capabilities of monitoring devices and their data communications as well as their data security will allow algorithms to better monitor the power grid and predict problems ahead of time. When problems occur, the system can quickly identify the source and location of the problems.
- *Self-healing:* With better monitoring systems and with more automation in power grids, it is possible for the grid to automatically reconfigure its network to restore power quickly.
- *Reduction in restoration time:* With self-healing, the grid can restore itself automatically instead of manual restoration.
- *Peak demand shaving:* Utilities purchase energy during peak times from other utilities as explained in Chapter 14. The cost of this energy is part of the rate structure of customers' bills. If technologies are developed to allow for customers to reduce their demands during these times without inconveniencing them, this can potentially save costs to utilities and customers.
- *Increased system capacity:* When generation resources and transmission lines are less used, the capacity of the grid increases. Thus, more customers and more demands can be added without elaborate expansion of the infrastructure.
- *Increased power system security and reduced vulnerability:* With local generation and less dependency on transmission infrastructure, the system security is improved. The loss of a transmission line feeding an area with local generation will have lesser impact than the case without local generation.

- *Hybrid and electric vehicles:* If electric vehicle (EV) penetration is high enough, it could cause a stability problem as a large number of vehicles could be plugged into the power grid after people arrive from work between 5 and 7 PM. This is because the load could rapidly increase beyond system limits. Adjustable charging techniques can address this problem.

To implement the smart grid, several technologies need to be developed, as follows:

1. *Energy storage:* This is the most important and the hardest goal to achieve. Large-scale energy storage has several advantages; the two key ones are the following:
 - a. *Reduces system instability:* As seen in Chapter 14, instability occurs when the generation does not meet the demands. With storage, the energy can come from the storage equipment until the grid normal operation is restored.
 - b. *Some renewable energy systems, such as wind, can generate large amounts of electricity during off-peak times.* In some Scandinavian countries with high wind penetration, the wind energy produced at night could be higher than the demand. With energy storage, this energy can be stored and used during high-demand periods.
2. *Advanced meters and sensors:* This technology is needed at all levels. At the customer level where meters can measure net energy, monitor house activities to identify problems within the service area, and perform self-diagnosis and self-healing functions. At the grid level, newer sensing technology allows operators to have a better understanding of the grid status and operation. With the aid of intelligent algorithms, the system can be better controlled.
3. *Grid-friendly plug-in hybrids:* If hybrid vehicles penetrate the market in a big way and are plugged into the grid within a short time, the grid could collapse. However, if the charging of the vehicle is controlled, the problem can be avoided. This requires a charging system that responds to grid conditions as well as price signals.
4. *Grid-friendly loads:* Loads can participate in lessening the problems the utilities face during peak times and during disturbance. If some loads within the house can be curtailed without inconveniencing customers, it can have a major impact on the reliability of the grid.
5. *Substation and distribution automation:* Until today, we still have a large numbers of control and protection devices operating manually. Disconnect switches and fuses are two examples. If these and other devices are replaced by automatically operating and controlling devices, the reliability of the grid can increase tremendously.
6. *Communications:* With more automation, the communication needs are very high. Standardized systems and protocols are needed to allow equipment to have plug and play capability, enhancing communication security and ensuring consumers' privacy.
7. *Data-intensive analysis:* Intensive data is hard to process, and its clues are hard to siphon. Algorithms and programs are needed to process the immense data and provide the user with the needed information on-demand and quickly.
8. *Visualization and human interface:* Technologies are needed to visualize the immense data being collected by the control centers of the grid. Raw numbers are proved to have little value. Using visualization and virtual reality technologies can make the data more understandable.
9. *Renewable energy integration:* To effectively integrate renewable energy resources, several technologies are needed.
 - a. *Weather prediction* is among the most important technologies. Two types of weather forecast are used: synoptic scale and mesoscale forecast. Synoptic scale (large-scale) meteorology is relatively accurate. It predicts air masses, fronts, and pressure systems. Mesoscale (local-scale) meteorology includes the effects of topography, bodies of water, urban heat island on wind speed. The mesoscale forecast is what is needed for renewable systems. Unfortunately, it is still less accurate for the reliable integration of renewable systems.

- b. *Control:* Renewable energy is still not controlled by grid control centers in most parts of the world. Any control of these facilities is often done locally. If their penetration into a power grid is high, they must be part of the grid control center to ensure the reliability of the grid.

Because of the extensive attention given to the smart grid and grid automation, several technologies have recently been developed or are in the final development phase. Some of these technologies are in the commercialization phase. A summary of selected ones is given in this chapter.

15.1.1 INTELLIGENT MONITORING

A critical task for controlling our massive power system is to sense and synchronize various signals measured at locations thousands of miles apart. Regular terrestrial communication networks have shortcomings with the exact synchronization of high-frequency signals. In ongoing research, engineers are considering using *geosynchronous* (e.g., GPS) and *low-earth orbit* (LEO) satellites for better monitoring and control of power systems. This is one of the intriguing ideas that will eventually lead to more effective and more reliable power system operation.

One of the most promising monitoring techniques is *phasor measurement unit* (PMU), which is also known as *synchrophasor*. But before we discuss the systems, we need to know some fundamental aspects of power flow between substations. In Figure 15.2, a long transmission line connects two major substations (Bus 1 and Bus 2). These two buses could be a few hundreds of miles apart. If the current flows from Bus 1 to Bus 2, the voltage of Bus 1 leads that of Bus 2 by an angle known as the *power angle* δ as shown in Figures 15.3 and 15.4.

The equation of the system in Figure 15.2 is

$$\bar{V}_1 = \bar{V}_2 + jx\bar{I} \tag{15.1}$$

where x is the inductive reactance of the line. We ignore the resistance of the line as it is often much smaller than the inductive reactance.

The line current in this case is

$$\bar{I} = \frac{\bar{V}_1 - \bar{V}_2}{jx} \tag{15.2}$$

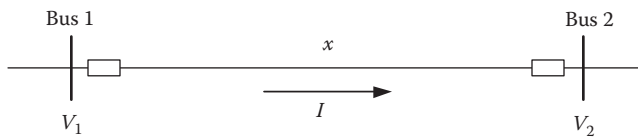


FIGURE 15.2 Flow between two buses.

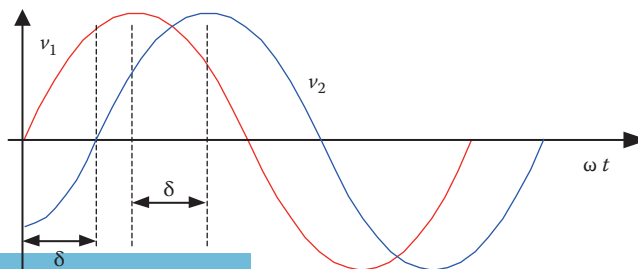


FIGURE 15.3 Voltage waveforms of two buses.

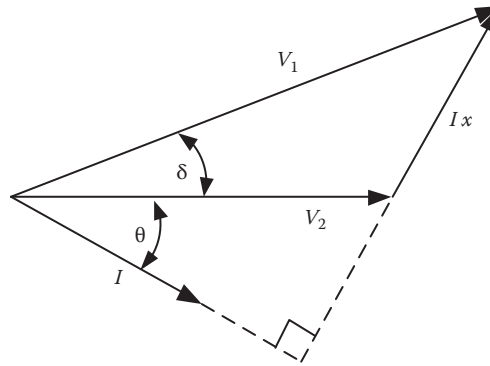


FIGURE 15.4 Phasor diagram of the two-bus system.

The current can be written as

$$\bar{I} = \frac{V_1 (\cos \delta + j \sin \delta) - V_2}{jx} \quad (15.3)$$

where the magnitude of the current is

$$I = \frac{\sqrt{(V_1 \sin \delta)^2 + (V_2 - V_1 \cos \delta)^2}}{x} \quad (15.4)$$

Equation 15.4 gives the magnitude of the line current, which in turn gives us information on how heavily the line is loaded. To obtain this information, we need three variables:

- Magnitude of voltages at Bus 1
- Magnitude of voltages at Bus 2
- Angle between the two voltages, which is the power angle δ .

In addition to the current, we can find the power delivered to Bus 2, both active and reactive. Consider the complex power equation

$$\bar{S}_2 = \bar{V}_2 \bar{I}^* \quad (15.5)$$

The conjugate of the current is used to make the reactive power of the inductance positive and that for the capacitor negative. This was the norm selected by our power system forefathers.

Conjugating both sides of Equation 15.5 leads to

$$\bar{S}_2^* = \bar{V}_2^* \bar{I} \quad (15.6)$$

Taking V_2 as a reference, Equation 15.6 can be written as

$$\bar{S}_2^* = V_2 \bar{I} = V_2 \frac{\bar{V}_1 - V_2}{jx} = V_2 \frac{(V_1 \cos \delta + j V_1 \sin \delta) - V_2}{jx} \quad (15.7)$$

The real and imaginary components in Equation 15.7 are

$$\bar{S}_2^* = \frac{V_1 V_2}{x} \sin \delta + j \frac{V_2}{x} (V_2 - V_1 \cos \delta) \quad (15.8)$$

Hence the real power delivered to Bus 2 is

$$P_2 = \frac{V_1 V_2}{x} \sin \delta \tag{15.9}$$

and the reactive power at Bus 2 is

$$Q_2 = \frac{V_2}{x} (V_2 - V_1 \cos \delta) \tag{15.10}$$

Equations 15.9 and 15.10 show that we can compute the real and reactive power at Bus 2 if we know the same three variables we need to compute the current: magnitude of voltages at both buses and the power angle δ . Obtaining these three variables would seem to be a simple task until we find that the measurements need to be synchronized in time. If the voltages at Bus 1 and Bus 2 are not sampled at exactly the same time, we cannot accurately compute the power angle. The time synchronization is difficult if local clocks at the buses are used. To solve this problem, the sampling must be time tagged by a single clock. This is what the PMU achieves. There are two scenarios for PMU systems. The first is based on ground communication and the other is based on satellite communication. In the first system shown in Figure 15.5, the satellite sends unified time signals to all buses. When received, the voltages at all buses are measured and time tagged. The samples are sent to a ground station that transmits the data to the control center where the waveforms are constructed

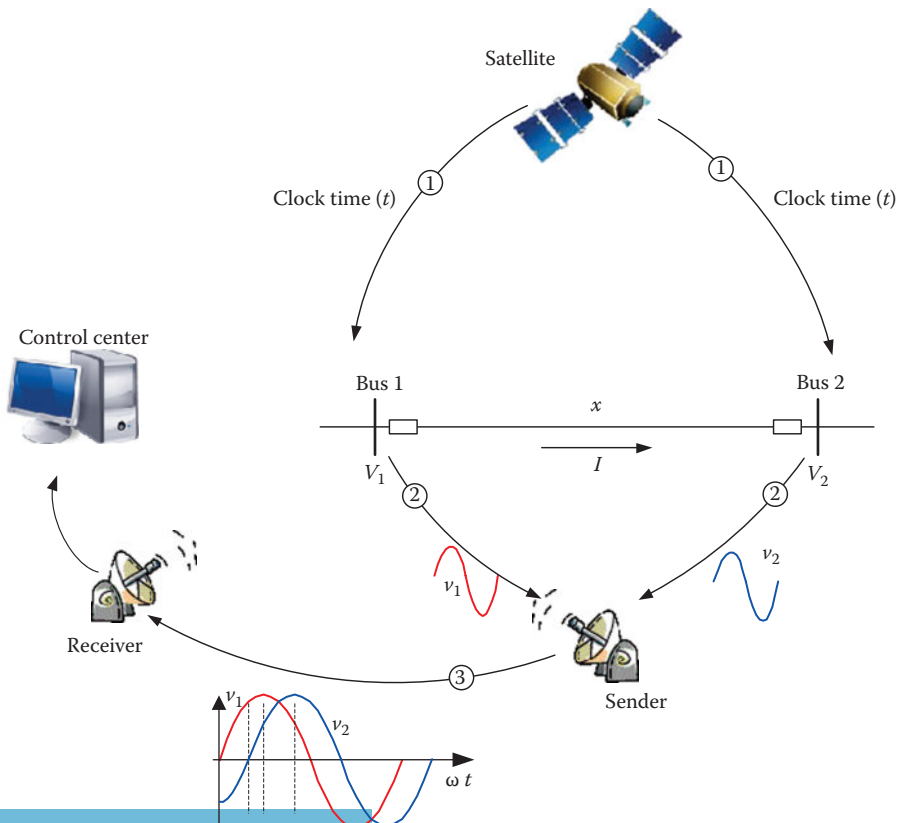


FIGURE 15.5 PMU with ground communication.

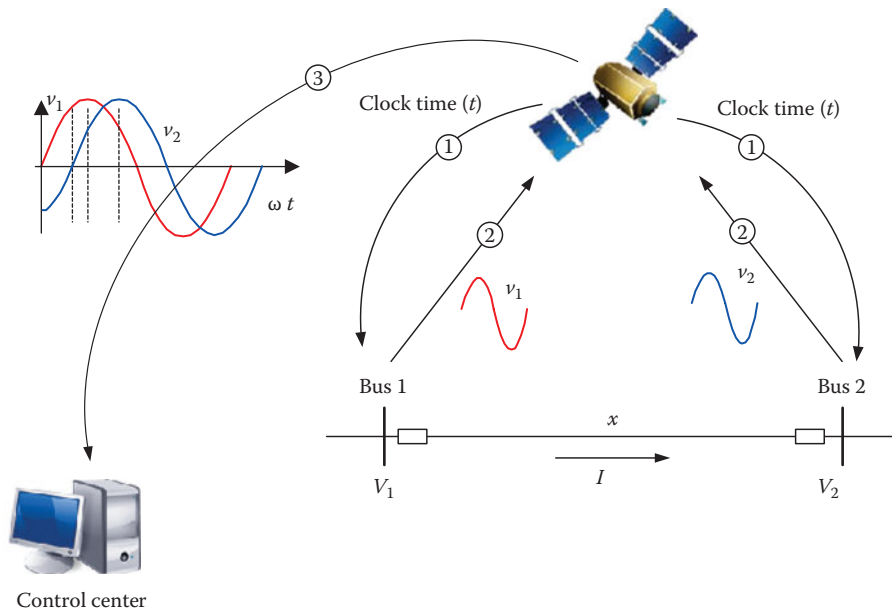


FIGURE 15.6 PMU with satellite communication.

and the power angle is computed. In the second system shown in Figure 15.6, the samples are sent to the satellite and then to the control center.

15.1.2 SMART HOUSE

The concept of smart house is not new; it dates back to the 1980s. Several utilities in the United States explored the idea and developed demonstration models. The technology at that time was limited, and most of the ideas did not evolve into commercial products. With smart grid activities, the smart house concept is back, and several operational devices have even been commercialized. The concept of the smart house is shown in Figure 15.7, where the owner of the smart house has access to a wide range of information, including all attractive energy contracts and their restrictions. The information is obtained through an aggregator who acts as a middleman between the owner and several utilities. The owner decides on the best option and the aggregator contacts the various utilities to execute the contract. The question is why do we need a middleman? Currently, all of our contracts are with the local distribution utility. The middleman actually plays an important role in keeping the energy cost low. When a single person negotiates with the utility, the person gets the individual rate. However, when an aggregator company negotiates with several utilities, the company gets the best bulk rate, and it can pass most of the saving to its customers. Moreover, if the aggregator is allowed to control the load consumption within the dwelling, the company can even get lower rates from the utility, which benefits the customers as well.

Because utility loads change continuously, the generation must also change continuously to meet the demand. This is known as *load tracking* or *load following*. Matching the demand at all times is an expensive process for utilities. With the smart house, it is possible to regulate the energy consumption of the dwelling without inconveniencing the customers. In any regular house in the United States and most of the world, there are appliances that consume large amounts of energy such as water heaters, stoves, refrigerators, washers, dryers, and air conditioners. During the time when the utility is short of energy, the house can reduce its consumption by either slowing down the process or turning off the appliances for a few minutes. Most customers would not even notice

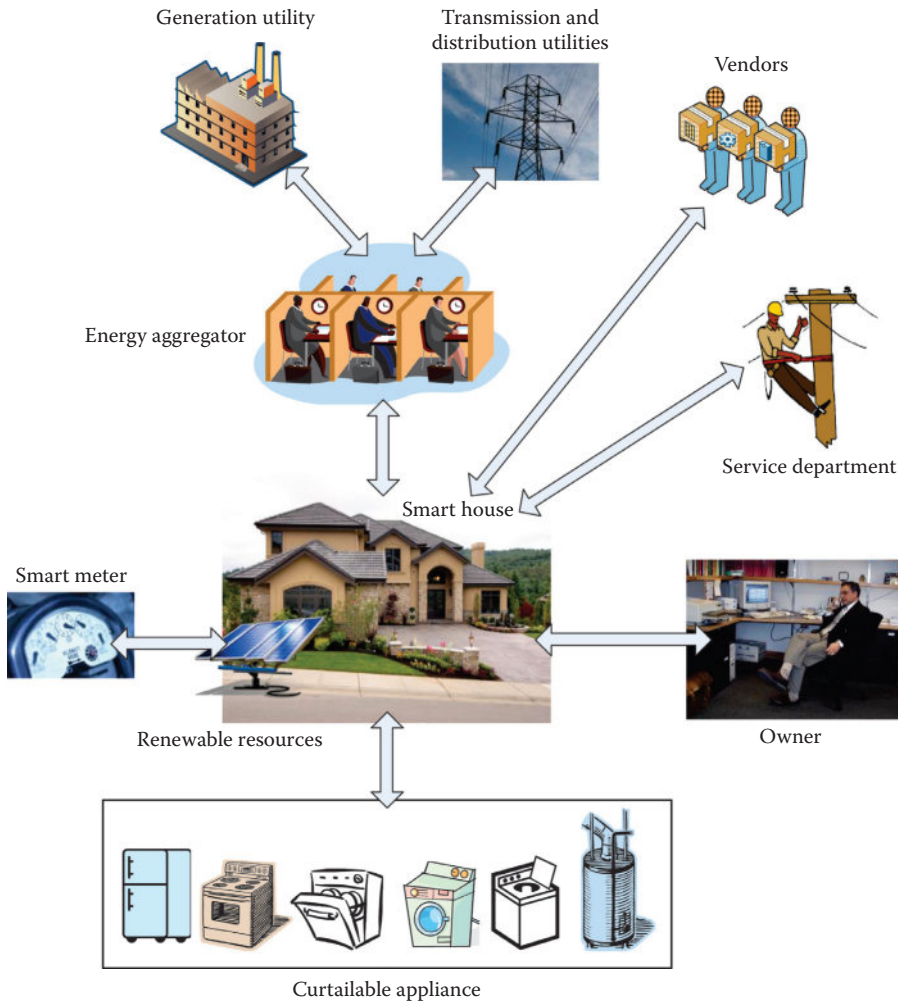


FIGURE 15.7 Concept of smart house.

that the appliance is being controlled. If this is done on a large scale, the demand in a wide area can relieve the utility from using expensive load-following or load-regulation processes. Some of this saving can be passed to the customers.

Furthermore, the smart house can communicate with vendors to select new products or services that increase efficiency. The smart house can also communicate directly with the maintenance department of the serving utility to inform them about any outage or disruption of service. The maintenance crew may even be able to remotely fix the problem or send the maintenance personnel to the exact location, thus fixing the problem much faster than is currently possible.

15.1.3 SELF-DIAGNOSIS AND SELF-HEALING

The concept of self-diagnosis and self-healing was initially developed for communication networks (phone, Internet, etc.). By this technology, the system can continuously monitor the operational status of its components and identifies areas of difficulties. When a failure occurs in a component, the system isolates the problem and reroutes the data through other paths. The user is often unaware of the problem when it occurs.

Unlike the Internet, the power grid operates in a more classical fashion. Often, the grid operator has no prior warning of brewing problems. This is partially due to the lack of adequate smart-monitoring devices throughout the system and the limitation of existing communication networks and data processing systems. When a problem occurs, it could cause major blackouts to large segments of utility customers. To fix the problem, utility personnel often use manual methods that may include driving around the system and inspecting the various components. This leads to long restoration times. For example, the failure of a critical transformer can result in power outages in the downstream network. To prevent the failure of transformers, utility personnel check the health status of the transformer by inspecting them periodically. The method includes extracting transformer oil for laboratory testing. Since the power grid has hundreds of thousands of these transformers, this job cannot be performed with adequate frequency. Therefore, problems inside transformers can be missed. However, if key variables in the transformer such as oil and gas levels, temperature, winding insulations, carbon concentration, and vibrations are monitored, potential transformer failure can be predicted.

15.2 ELECTRIC AND HYBRID ELECTRIC VEHICLES

EVs were invented before the diesel or Otto-cycle engines. In 1828, Ányos Jedlik from Hungary invented a small-scale prototype EV. The invention was followed by several developments in Europe and the United States. In 1899, Baker Motor Vehicle Company of Cleveland, Ohio, was the first manufacturer in the United States to produce EVs. Using electric motors to drive a vehicle was a simple concept that made the vehicle easy to design, build, and maintain. EVs required fewer components than the internal combustion engine vehicle (ICEV), and they did not use messy fluids or complex transmission systems. Unfortunately, the EV did not survive the competition from the ICEV. This was mainly because the ICEV had much longer range than the EV, and its refueling took just a few minutes. The range of the EV was limited to tens of miles, and the charging time of its batteries was very long. Therefore, the concept of EV died quickly. By the end of the twentieth century, the EV has resurfaced because of oil shortages and public awareness for a clean environment. During the last decade, we have seen several improvements to the EV. Battery technology has improved, allowing longer ranges and higher capacities. High-efficiency motors have been designed. Lighter material has been used to reduce the weight and energy consumption of the vehicles. Recovery systems have been implemented to capture energy during braking or slowing down. Smart controls have been developed to increase the efficiency of the EV during the various speed ranges.

The main components of an EV are shown in Figure 15.8. An ac source is used to charge the traction batteries of the EV. In modern designs, the ac source is just the household outlet. A charger is used to regulate the flow of current to the traction batteries to prevent them from overheating during charging. The voltage levels of the batteries vary from one manufacturer to another. The existing range is between 60 and 300 V. The traction batteries are connected to a high-voltage DC bus (HVDCB), which is similar to the substation of the power system. It distributes the power to the various components. Another charger can be used to charge the 12 V battery of various auxiliary services such as lights, instrumentation, radio and a startup switch (ignition switch). The electric drive system is a power electronic converter that regulates the speed of the electric motor as well as providing starting and braking functions. A microprocessor receives commands from the driver (speed change, acceleration, brakes, etc.) and controls the electric drive system accordingly.

In some EVs, the two front wheels are motors that are independently controlled to provide the traction needed as well as the differential task (when turning, the outside wheel spins faster than the inside wheel). In other designs, a single motor is used, and the power goes to the wheels through a transaxle.

Although today's battery technology is much better than the technology at the turn of the twentieth century, the still limited capacity of batteries led to the development of hybrid electric vehicles (HEV). The HEV has an electric motor as well as an internal combustion engine (ICE) as shown

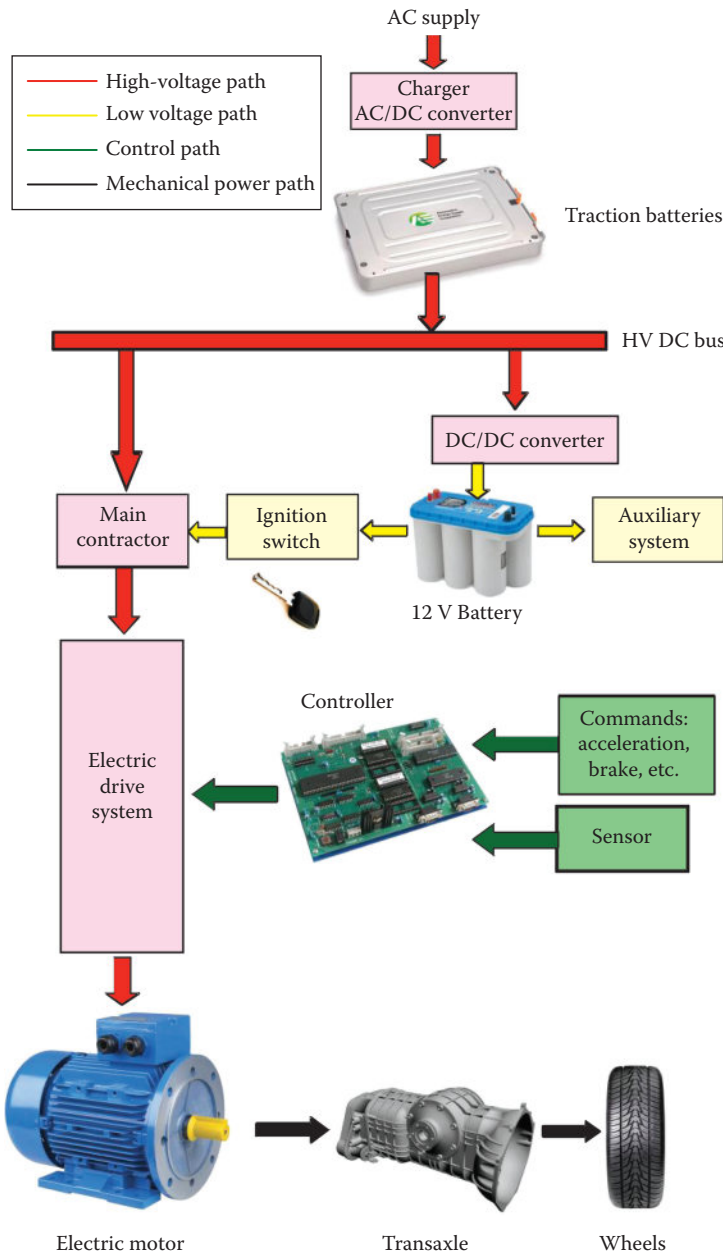


FIGURE 15.8 Main components of an EV.

in Figure 15.9. The controller of the vehicles switches between the two engines to achieve maximum efficiency and range. The control strategy depends on the manufacturer’s design philosophy. Some manufacturers switch between the two engines when one of them can provide higher efficiency. For example, during the stop-and-go traffic or during low speeds, the efficiency of the ICE is very low. The controller thus uses the electric motor to drive the vehicle. For highway driving, the efficiency of the ICE is relatively high, so the electric motor is turned off and the ICE drives the vehicle to increase its range. In another HEV design, the manufacturer installs batteries that have a range of 30–40 mile. This is enough range for most daily city commutes. The controller is always using the electric motor as long as there is enough charge in the battery. When the energy of the

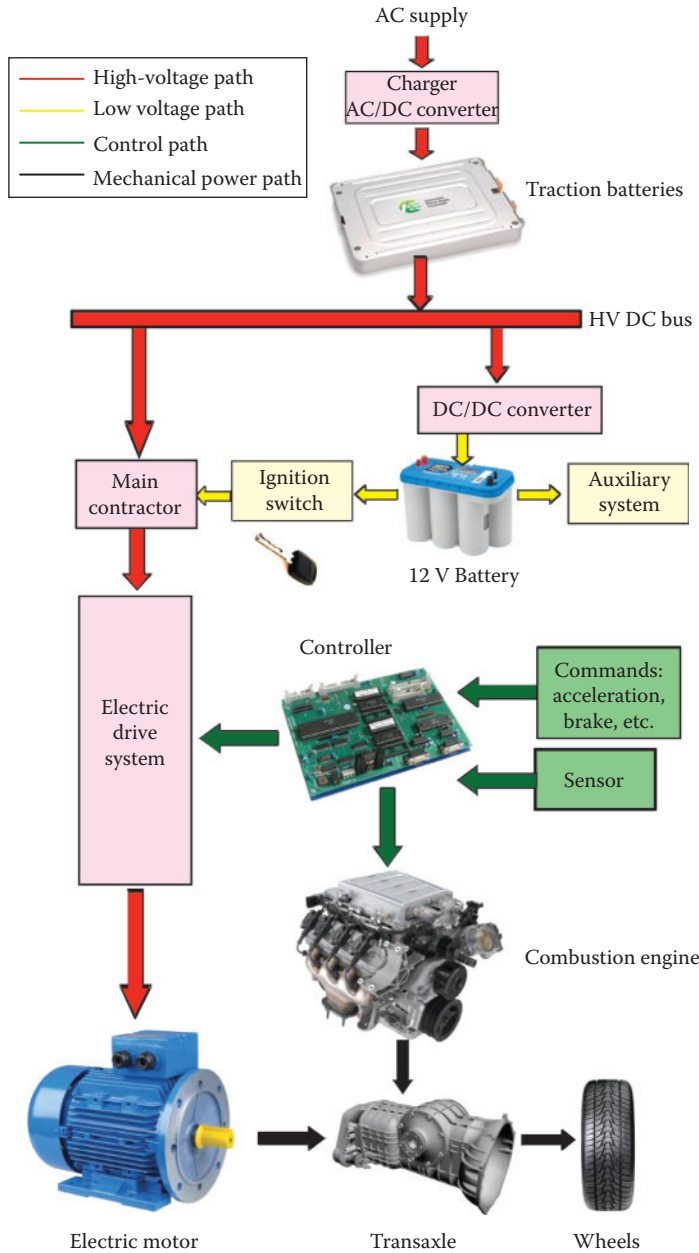


FIGURE 15.9 Main components of an HEV.

battery is depleted, an ICE is turned on to either drive the vehicle or drive a generator that charges the batteries. This design is simpler than the one discussed earlier, and it is conceivable that the owner will only use the gas engine during long trips. Most commuters drive less than 40 miles to work, so they can charge their cars daily and will not need to use the ICE.

There is a great deal of research and development needed to further the EV and the HEV. The areas include battery technology, power electronics, control, and material. In addition, the charging of the EV or HEV is an area of research. When people return from work late in the afternoon and plug their vehicles into the grid, the charging process adds sudden and large load during the already

peak load time. It is therefore conceivable for weak systems to experience stability problems. Smart charging is an area of research where the charging process can be controlled based on grid or price signal. In addition, the charger can also allow the modulation of the charging process to meet some utility functions such as load following (the charging rate is faster during slack time and lower during peak demand time).

15.3 ALTERNATIVE RESOURCES

Because of the environmental problems associated with the existing forms of energy resources (fossil, hydroelectric, and nuclear), researchers are looking for other resources that are less polluting and have less impact on the environment. Among the alternative resources are solar energy, wind energy, hydrokinetic energy, geothermal energy, biomass energy, hydrogen energy, and other forms of energies. Some of these technologies are in the early stages of development, and much work is needed to make them viable for serious consideration. Others are further along in their development, but more work is needed to increase their efficiency and reliability and make them cost-effective.

Recently, hydrogen has been proposed to generate electricity at a large scale. However, before hydrogen becomes competitive with other fossil fuels, serious technical challenges must be addressed to transform the oil-based economy to a hydrogen-based economy. Engineers need to develop systems that produce abundant amounts of hydrogen at affordable costs. They also need to develop extensive infrastructure to store and distribute hydrogen that is safe and economical.

15.4 LESS POLLUTING POWER PLANTS

Since Thomas Edison built the first power plant by the end of the eighteenth century, fossil fuel has been the main resource for generating electricity. As we have seen in this book, burning fossil fuels to produce the steam needed to generate electricity introduces polluting agents into the environment. The health effects and environmental damages due to industrial wastes are well studied, monitored, and documented in most parts of the world. By the middle of the twentieth century, these studies created strong awareness among the public, which led to the creation of several environmental advocacy groups and agents. The public no longer accepts industrial processes that harm the environment.

One of the most polluting fossil fuels is coal, which accounts for over 25% of the electricity generated worldwide and about 50% in the United States and China. The wide use of coal is due to its abundance and low cost; coal is probably the main reason for the low price of electricity in most parts of the world. However, because of the environmental concern regarding the burning of coal, the public are demanding that scientists and engineers improve the burning processes of fossil fuels to meet the various goals set by health and environmental organizations as well as international treaties. The research in the area of clean burning of fossil fuels is rapidly progressing. Scientists believe that it is possible in the future to make fossil fuels such as coal burn at near-zero emissions. To achieve this goal, several technologies are being developed to make future coal-burning systems more efficient and cleaner than they are today. Besides the technical challenges, the new processes must keep electricity affordable to ensure compliance in countries with growing economies. Among the new technologies are coal gasification, advanced combustion systems, and carbon sequestration.

Coal gasification is a process by which coal is converted into combustible gases known as synthesis gas (syngas). During the gasification process, coal reacts with pure oxygen and steam at an elevated pressure to produce gas with varying amounts of carbon monoxide, carbon dioxide, hydrogen, methane, and nitrogen. The various components of the syngas can be used as fuels or raw materials for chemical processes and fertilizers.

Carbon sequestration refers to the long-term storage of carbon dioxide (CO_2). Since CO_2 is one of the main greenhouse gases, it would seem reasonable to capture it and trap it in storage

facilities. Scientists are recommending storing the carbon dioxide underground or in oceans. Some researchers are even proposing that the CO_2 be stored in the terrestrial biosphere.

Hydroelectric power plants, which are renewable energy systems, have some negative environmental impacts as discussed in Chapter 5. In most countries, current hydroelectric systems and future developments must comply with several environmental laws. The main concern with hydroelectric systems is that they block water flow, which negatively affects the fish population and the biota of the river. To alleviate this problem, several techniques must be implemented. These techniques, though still under research, include building fish ladders to facilitate fish migration, redesigning the turbine blades to allow small fish to pass through without injuries, optimizing the operation of the power plant to maintain the water flow and reservoir height to the levels needed to protect spawning and incubation of fish, and compensating for fish habitat losses through restoration or replacement.

Besides solving the fish problem, research is needed to reduce the effects of coastline erosions stemming from the lack of silt on seashores. Silt management is also important to farmland on the banks of the rivers as silt revitalizes the soil. Oxygen depletion behind the dam and the increase of nitrogen downstream from the dam are two other areas of research to improve fish habitats.

It has been wrongly perceived that implementing rigid environmental enhancement measures may lead to higher costs and fewer jobs. In fact, studies have shown that the extra cost added to the products due to the compliance with environmental laws is offset by a reduction in medical expenses. Indeed, numerous studies have shown that health standards have improved in areas where pollution was reduced. Furthermore, reducing pollution is an industry by itself. It requires the skills of engineers, chemists, physicists, mathematicians, biologists, meteorologists, hydrologists, geologists, medical doctors, several government agencies, and many more. This field is wide open to new ideas and methods.

15.5 DISTRIBUTED GENERATION

The power plants we know today are located in areas where energy resources exist or can be easily accessed. This necessitates the construction of large regional generating plants, which is probably the most cost-effective arrangement. To transmit power to users, power lines hundreds of miles long are needed. The reliability of this power system is highly dependent on the transmission systems; if the line is tripped, the service could be interrupted. An alternative method is to install distributed generation systems where the power plants are located in neighborhoods or even at homes. For example, since natural gas reach a large number of homes, it can be used to generate electricity at homes by using water heater-sized thermal power plants. Another idea is to use fuel cells to generate electricity for home use. The concept of distributed generation should make electricity more reliable and more available. With this technology, blackouts that last for days will no longer affect large areas.

15.6 POWER ELECTRONICS

Electrical apparatus and equipment are often designed to provide optimum performance at a narrow range of loading conditions. When these devices operate at different conditions, their efficiency is normally reduced. To address this problem, the voltage and frequency must be adjusted continuously using semiconductor power electronic devices. Indeed, most of the appliances we use today are much more efficient than their predecessors. Every year, newer power electronic devices and circuits are introduced, which enhances the operation of various equipment and improves their overall efficiency.

In addition to the enhancement of the efficiency, power electronic devices make possible the development of technologies such as fuel cells, photovoltaic, superconducting magnetic energy

storage systems, and magnetic levitated systems. Power electronic devices allow us to use motors and actuators in applications that were never envisioned before, such as angio-surgeries, microtechnology, and mechatronics.

In high-power applications, power electronic devices are used to control the bulk power flow in transmission lines through devices such as the flexible alternating current transmission system (FACTS) and voltage compensators. In addition, power electronics allows us to monitor systems, process information, and take continuous control actions.

15.7 ENHANCED RELIABILITY

Although power systems are highly reliable, we tend to disagree with this notion when a blackout occurs. This is because we have become so dependent on electric power that blackouts are often costly and highly annoying. To totally eliminate blackouts is probably an unrealistic goal. However, reducing the frequency and impact of blackouts could be achieved. At any given moment, the power system moves enormous amounts of power through its various components. For stable operation, a delicate balance must always be maintained between demand and generation. If this balance is altered, blackouts could occur unless the balance is rapidly restored. The speed with which the energy balance is restored depends on the availability of fast and synchronized sensing, fast-acting relays and breakers, quick topology restoration, and effective system control. Although the research in these areas is advancing rapidly, predicting all possible scenarios for blackouts is a very challenging task. Furthermore, to be able to analyze and control the system online requires much more powerful computers and better knowledge of complex system techniques than we have attained so far. The reliability of the power system also depends on the redundancy of the transmission systems. However, due to public concern, fewer and fewer transmission systems are allowed to be constructed. Public resistance to the construction of new lines is based on ecstatic considerations and concerns regarding magnetic fields. Newer designs and technologies are needed to address these two issues.

15.8 INTELLIGENT OPERATION, MAINTENANCE, AND TRAINING

Human presence in hazardous environments, such as inside nuclear reactors, will eventually be replaced by intelligent autonomous robots. A swarm of these robots could provide the maintenance and operation inside the reactors where humans cannot be located. Robots can also be developed to crawl inside the millions of tubes to check the health status of power cables and equipment and even to perform maintenance work.

The power system will eventually benefit from the virtual reality technology as it will make it possible for experts located miles away to perform maintenance on high-voltage equipment while it is energized, much like the remote surgery approach that is being developed in the medical field. Virtual reality could also provide an excellent training system that could lead to more experienced operators. This is because various scenarios can be imposed on the system, and the operators could learn how to steer the system to a secure and stable region. This is similar to flight training simulators for aircraft pilots.

15.9 SPACE POWER PLANTS

Solar energy density in outer space is much higher than that at the surface of the earth. The U.S. government is pioneering the conceptual idea of having massive solar power plants orbiting the earth. The envisioned system consists of football-field-sized solar cells that could generate large amounts of power comparable to large terrestrial power plants. The generated electric power can be used to support spacecraft and long-space missions as well as beam the energy down to the

earth. The concept of a large-scale space solar power plant was considered improbable and silly in the 1970s. However, NASA and the National Science Foundation (NSF) revived the idea by the end of the twentieth century, and several research programs are working on developing the needed technologies. A space power plant is compatible with the environment, and it could lead to less dependency on conventional energy resources. The plant could potentially provide electric energy to remote and inaccessible areas all over the world. However, the idea of having satellites beaming their energy toward earth has remarkable technological challenges. Beaming the energy to earth may require the use of microwaves and highly accurate positioning systems. The health risks associated with the exposure to electric and magnetic fields generated by beaming the power to earth is a significant public concern. To make it possible to place football-field-sized solar arrays in space, the solar cell technologies must improve substantially. The solar cells must be lightweight, thin, flexible, highly efficient, and able to withstand the harsh environment of space. Today's solar cells are not adequate because they are heavy, bulky, and have low efficiency. However, nanotechnology offers a potential solution to this problem. Furthermore, space power stations located miles apart in orbits pose maintenance challenges. Among the ideas proposed is to use swarms of autonomous robots as maintenance crew. The research in this area is fascinating and highly challenging.

An example of a smaller-scale space power station can be found in the international space station (ISS) shown in Figure 15.10. The electrical energy in the ISS is used to operate the life support systems as well as allow the crew to operate the station and perform scientific experiments. The power system is integrated out of photovoltaic technology, which is much higher in efficiency and energy density than commercial devices. The system includes storing devices to provide continuous power during the eclipse part of the orbit. The system is highly efficient as the heat generated during the conversion of sunlight into electricity is used in various other processes on the ISS.



FIGURE 15.10 International space station. (Courtesy of NASA, Washington, DC.)

EXERCISES

- 15.1** What are the most important changes that need to be implemented to reduce the pollution associated with power plants?
- 15.2** Can coal be burned without polluting the environment? What are the latest technologies in reducing coal pollution?
- 15.3** If we replace all coal power plants in the world by wind energy systems, estimate how much reduction in CO₂ can be achieved.
- 15.4** What are the problems associated with the cyclic and stochastic nature of some renewable energy systems?
- 15.5** Find a diagram of a simple distribution network and compare it with the system in Figure 15.1. Identify the key differences.
- 15.6** Can you think of ways to store electrical energy besides batteries?
- 15.7** What are the major challenges associated with building infrastructure for hydrogen?
- 15.8** What is intelligent control?
- 15.9** What are the advantages and disadvantages of demand-side management?
- 15.10** Why is extensive monitoring needed for the smart grid?
- 15.11** Identify the major technical obstacles facing the development of the space power system.
- 15.12** Assume that the space power system is a reality and identify its benefits to society.
- 15.13** Can you direct microwaves and reduce their scattering?
- 15.14** Can you identify technologies that we need to develop for future power systems besides the ones discussed in this chapter?

Appendix A: Units and Symbols

Variable	Unit	Variable	Unit
Time t	Second (s)	Length l	Meter (m)
Electric current I	Ampere (A)	Electric potential (E or V)	Volt (V)
Electric resistance R	Ohm (Ω)	Resistivity ρ	Ω -m
Capacitance C	Farad (F) or s/ Ω	Inductance L	Henry (H) or Ω -s
Charge q	Coulomb or A-s	Frequency f	Hertz (Hz or cycles/s)
Magnetic flux ϕ	Weber or V-s	Magnetic field density B	Tesla or V-s/m ²
Magnetic field intensity H	A/m	Reluctance \mathfrak{R}	A turn/weber
Magnetomotive force \mathfrak{F}	A turn	Permeability μ	H/m or N/A ²
		Electric real power P	Watt (W)
Electric reactive power Q	VA	Electric apparent power S	VA
Mechanical power P	Horse power (hp)	Energy or work	W-s or Joule (J)
Linear speed v	m/s	Angular speed ω	Revolution per second (r/s)
Linear acceleration	m/s ²	Angular acceleration	r/s ²
Force	Newton (N)	Torque	N-m
Weight w	Gram (g)	Volume	m ³
Temperature	°C or Kelvin		

Appendix B: Conversions

Prefix

Prefix	Value	Symbol	Prefix	Value	Symbol
Yotta	10^{24}	Y	Deci	10^{-1}	d
Zetta	10^{21}	Z	Centi	10^{-2}	c
Exa	10^{18}	E	Milli	10^{-3}	m
Peta	10^{15}	P	Micro	10^{-6}	μ
Tera	10^{12}	T	Nano	10^{-9}	n
Giga	10^9	G	Pico	10^{-12}	p
Mega	10^6	M	Femto	10^{-15}	f
Kilo	10^3	k	Atto	10^{-18}	a
Hector	10^2	h	Zepto	10^{-21}	z
Deka	10^1	da	Yocto	10^{-24}	y

Distance

- 1 mile = 1.609 km
- 1 yard = 0.91440 m
- 1 foot = 0.30480 m
- 1 inch = 0.02540 m

Area

- 1 mile² = 2.59 km²
- 1 hectare = 0.01 km²
- 1 acre = 4046.9 m²

Volume

- 1 cu foot = 0.02832 m³
- 1 m³ = 1.308 yd³
- 1 m³ = 1000 L
- 1 fluid ounce = 0.02957 L
- 1 US gallon = 3.78540 L
- 1 liter of water = 1 kg in weight
- 1 US gallon of water = 3.7854 kg in weight

Mass

- 1 pound = 0.45360 kg
- 1 ounce = 28.35 g
- 1 ton = 1000 kg

Force

- 1 Pound/in² = 7.03×10^2 kg/m²
- 1 Pound/in² = 6.89 kPa

Speed

Speed of light = 299,792,458 m/s
1 Knot = 1.151 mile/h
1 Knot = 1.852 km/h

Energy

British thermal unit (BTU) = 252 cal
British thermal unit (BTU) = 1.0548 kJ (kW-s)
1 N-m = 1 W-s

Power

1 kW = 1.34 hp

Temperature

Kelvin = Celsius + 273.15
Celsius = (Fahrenheit - 32) × 5/9

Magnetic fields

Tesla = 10^4 Gauss

Appendix C: Key Parameters

Elementary charge constant (q) = 1.602×10^{-19} C

Boltzmann's constant k = 1.380×10^{-23} J/K

One mole of a substance contains 6.002214×10^{23} entities (molecules, ions, electrons, or particles)

Avogadro number N_A = 6.002214×10^{23} /mol

Extraterrestrial solar power density = 1.353 kW/m²

Standard atmospheric pressure at sea level = $101,325$ Pa or N/m²

Specific gas constant for air = 287 W-s/(kg K)

Air permittivity ϵ_0 = 8.85×10^{-12} Farad/m

Table of Resistivity

Aluminum	4.0×10^{-8} Ω -m
Copper	1.673×10^{-8} Ω -m
Nickel	10^{-7} Ω -m
Steel	7.2×10^{-7} Ω -m

Appendix D: Inductors

The inductor used in the power electronics chapter can be designed using a ring core (toroid). The toroid is made of a magnetic material and a copper wire is wrapped around the core as shown in Figure D.1. The inductance of the toroid is directly related to the number of turns of the winding, the geometry of the core, and the material used to build the core.

The inductance L is defined as the flux linkage λ produced by the current I

$$L = \frac{\lambda}{I} = \frac{N\varphi}{I}$$

where

N is the number of turns of the coil

I is the current of the coil

φ is the magnetic flux

λ is the flux linkage

Since the reluctance \mathfrak{R} of the core is defined as

$$\mathfrak{R} = \frac{NI}{\varphi}$$

hence,

$$L = \frac{N^2}{\mathfrak{R}}$$

The reluctance can be calculated using the geometry of the core and its permeability

$$\mathfrak{R} = \frac{l}{\mu_o\mu_r A}$$

where

A is the cross section of the core

l is the circumference of the core

μ_o is the absolute permeability ($\mu_o = 4\pi \times 10^{-7}$)

μ_r is the relative permeability of the core material

Hence, the inductance of the toroid is

$$L = \mu_o\mu_r \frac{A}{l} N^2$$

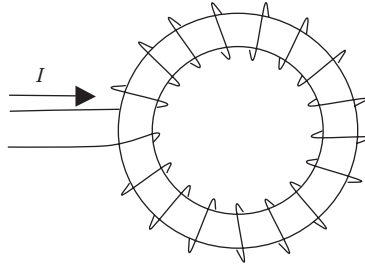


FIGURE D.1 Toroid.

Appendix E: Key Integrals

$$V_{average} = \frac{1}{2\pi} \int_0^{2\pi} v \, d\omega t$$

$$V_{rms} = \sqrt{\frac{1}{2\pi} \int_0^{2\pi} v^2 \, d\omega t}$$

$$\int e^{ax} \cos(bx) = \frac{e^{ax}}{a^2 + b^2} [a \cos(bx) + b \sin(bx)]$$

$$\int_{t=0}^{24} e^{-\frac{(t-t_0)^2}{2\sigma^2}} dt \approx \sqrt{2\pi}\sigma$$

$$\int e^{ax} [c \times \cos(bx) + k \times \sin(bx)] dx = \frac{e^{ax}}{a^2 + b^2} [(ka + cb) \sin(bx) + (ca - kb) \cos(bx)]$$

Electric Energy

An Introduction, Third Edition

"El-Sharkawi's book is an excellent introduction to electric power. ... Particularly valuable are the color pictures showing power plants, transmission lines and other hardware. The operation principles of the system are also clearly described ... Particularly important are the clear discussion of renewable energy generation and the explanation of emerging generation techniques like fuel cells."

— **George G. Karady**, Arizona State University, Tempe, USA

"This is a great piece of work. It combines a diverse set of materials creatively in a single text."

— **Peter Idowu**, Penn State Harrisburg, Middletown, USA

"The strength of this book is in its broad treatment of electric energy components and systems in a way that is both useful to engineering students as a stand-alone course and provides background for more advanced study in these topics."

— **Paul Hines**, The University of Vermont, Burlington, USA

The search for renewable energy, the societal impact of blackouts, and the environmental impact of generating electricity, along with the new ABET criteria, continue to drive a renewed interest in electric energy. Keeping pace with these changes, **Electric Energy: An Introduction, Third Edition** restructures the traditional introductory course to better meet the needs of engineering students.

What's New in This Edition

- Color illustrations
- Substation and distribution equipment
- Updated data on energy resources
- Expanded coverage of power plants
- Expanded material on renewable energy
- Expanded material on electric safety
- Three-phase system and pulse width modulation for DC/AC converters
- Induction generator
- More information on smart grids
- Additional problems and solutions

Now in color, this third edition of a bestseller combines the fundamentals of traditional energy conversion with contemporary topics, giving students the broad background they need to meet future challenges.

K14454



CRC Press
Taylor & Francis Group
an **informa** business

www.crcpress.com

6000 Broken Sound Parkway, NW
Suite 300, Boca Raton, FL 33487
711 Third Avenue
New York, NY 10017
2 Park Square, Milton Park
Abingdon, Oxon OX14 4RN, UK

ISBN: 978-1-4665-0303-8



9 781466 503038